

GRILLAGE PUSH-DOWN ANALYSIS OF FRACTURE CRITICAL STEEL TWIN

TUB GIRDER BRIDGES

A Dissertation

by

NATASHA COLLEEN BOGER

Submitted to the Office of Graduate and Professional Studies of
Texas A&M University
in partial fulfillment of the requirements for the degree of

DOCTOR OF PHILOSOPHY

Chair of Committee,	Stefan Hurlebaus
Committee Members,	Anna Birely
	Robert Lytton
	Cliff Spiegelman
Head of Department,	Robin Autenrieth

December 2019

Major Subject: Civil Engineering

Copyright 2019 Natasha Colleen Boger

ABSTRACT*

Twin steel tub girder bridges are an aesthetically pleasing structural option, offering long span solutions in tight radii direct connectors. However, these bridges require a routine two-year inspection frequency, as well as a thorough hands-on inspection, because of their fracture critical designation. The heightened inspection requirements for fracture-critical bridges come at a significant cost to the Department of Transportations (DOTs). Recent research has shown that tangent, or nearly tangent, twin steel tub girder sections can redistribute load to the intact girder after fracture of one of the girder bottom flanges. Additional research is required to develop recommendations for practical analysis of typical twin steel tub span configurations with the degree of curvature common to twin steel tub direct connectors.

A key objective of this research is to develop more rigorous modeling and analysis methods. These analysis and modeling methods shall take into account the capacity of the fractured girder, especially at support locations, and realistically model the load distribution between the intact girder and the fractured girder. However, the modeling and analysis methods need to be sufficiently straightforward to be applied on a large scale to the inventory of steel tub bridges. The analysis method developed should meet the

* Reprinted with permission from “Fracture Critical Steel Twin Tub Girder Bridges Technical Report” 0-6937-R1 by Hurlebaus S., Mander J., Terzioglu T., Boger N., Fatima A., 2018. Texas A&M Texas Transportation Institute, Copyright 2018 by Texas A&M Texas Transportation Institute

requirements outlined in the Federal Highway Administration (FHWA) Memorandum (FHWA 2012).

DEDICATION

I would like to dedicate this dissertation to my loving mother and father who have supported me along my educational journey along with the friends, family, and educators who aided me along the way.

ACKNOWLEDGEMENTS

I would like to thank my committee chair, Dr. Stefan Hurlebaus, for his unwavering leadership and guidance over the course of my doctoral candidacy. I would also like to thank my committee members Dr. Anna Birely, Dr. Robert Lytton, and Dr. Cliff Spiegelman for their support and assistance during this time.

A special thanks to other members of the research team, Dr. John Mander, Dr. Tevfik Terzioglu, and Amreen Fatima, for their comradery and work ethic during the duration of the project.

Thanks also to all of my friends, professors, colleagues, and department staff for their support and fellowship during my time at Texas A&M University.

Last but not least, thanks to my mother and father for their unending encouragement and to my friends and family back home, their support has been invaluable.

CONTRIBUTORS AND FUNDING SOURCES

Contributors

The research presented in this dissertation was supervised by a dissertation committee consisting of Professor Stefan Hurlebaus (the candidate's advisor), Professor Anna Birely, and Professor Robert Lytton of the Zachry Department of Civil and Environmental Engineering and Professor Cliff Spiegelman of the Department of Statistics.

The data analyzed and analysis conducted in Chapter 3 and Chapter 5 was provided by Dr. Tevfik Terzioglu of the Zachry Department of Civil Engineering and were published in 2018.

All other work conducted for the dissertation was completed by the student independently

Funding Sources

Graduate studies was supported by fellowships from Texas A&M University and the Zachry Department of Civil Engineering.

The work was also made possible in part by Texas Transportation Institute and the Texas Department of Transportation.

TABLE OF CONTENTS

	Page
ABSTRACT	ii
DEDICATION	iv
ACKNOWLEDGEMENTS	v
CONTRIBUTORS AND FUNDING SOURCES.....	vi
TABLE OF CONTENTS	vii
LIST OF FIGURES.....	x
LIST OF TABLES	xv
1. INTRODUCTION.....	1
1.1. Background and Motivation.....	1
1.2. Objectives of Research.....	4
1.3. Structure of Dissertation	4
2. LITERATURE REVIEW.....	5
2.1. Introduction	5
2.2. Approaches to Analyzing the Behavior of Bridge Structures	6
2.2.1. Elastic Structural Analysis	7
2.2.2. Plastic Methods of Analysis (Limit Analysis)	11
2.2.3. Computational Nonlinear Finite Element Solutions	14
2.3. Fatigue and Fracture in Bridges	15
2.3.1. Fatigue and Fracture Failures in Bridge Structures.....	15
2.3.2. Addressing Fatigue Problems by Design	20
2.4. Redundancy	22
2.5. Fracture Critical Investigations on Slab-on-Steel Girder Bridges	30
2.6. Fracture Critical Steel Twin Tub Girder Bridges.....	31
2.7. Research Questions Arising	37
3. PARAMETRIC STUDY FOR STEEL TWIN TUB GIRDER BRIDGES USING NONLINEAR FINITE ELEMENT ANALYSIS	39

3.1. Introduction	39
3.2. Evaluation of TxDOT Steel Twin Tub Bridge Inventory	39
3.2.1. General	39
3.2.2. Distribution of Texas STTG Bridges	40
3.2.3. Selection of Fifteen Representative Steel Twin Tub Girder Bridges	43
3.3. Nonlinear Finite Element Model of a Steel Twin Tub Girder Bridges	47
3.3.1. Validation of Finite Element Model.....	47
3.3.2. FEM Parametric Study of Fifteen Bridges	49
4. PARAMETRIC STUDY FOR STEEL TWIN TUB GIRDER BRIDGES USING GRILLAGE METHOD PUSH-DOWN ANALYSIS	53
4.1. Introduction	53
4.2. Grillage Method Push-Down Analysis	55
4.2.1. Introduction	55
4.2.2. Material Models	56
4.2.3. Grillage Beam Elements.....	59
4.2.4. Grillage Plastic Hinges	62
4.2.5. Simulating HL93 Loading.....	64
4.3. Grillage Analysis of selected STTG Bridges	67
4.3.1. Grillage Analysis of Bridge 0- FSEL: TxDOT Project # 0-6937.....	68
4.3.2. Grillage Analysis of Bridge 1-NBI #12-102-3256-01-403	71
4.3.3. Grillage Analysis of Bridge 2-NBI #12-102-0271-17-530	73
4.3.4. Grillage Analysis of Bridge 3-NBI #12-102-0508-01-294	76
4.3.5. Grillage Analysis of Bridge 4-NBI #12-102-0271-07-637	79
4.3.6. Grillage Analysis of Bridge 5-NBI #14-227-0-0015-13-452.....	82
4.3.7. Grillage Analysis of Bridge 6-NBI #12-102-0271-07-575	85
4.3.8. Grillage Analysis of Bridge 7-NBI #12-102-0177-07-394	88
4.3.9. Grillage Analysis of Bridge 8-NBI #12-102-0271-06-661	92
4.3.10. Grillage Analysis of Bridge 9-NBI #12-102-0177-07-394	96
4.3.11. Grillage Analysis of Bridge 10-NBI #14-227-0-0015-13-450.....	100
4.3.12. Grillage Analysis of Bridge 11-NBI #12-102-0271-07-593	104
4.3.13. Grillage Analysis of Bridge 12-NBI #12-102-0271-07-639	108
4.3.14. Grillage Analysis of Bridge 13-NBI #14-227-0-0015-13-452.....	112
4.3.15. Grillage Analysis of Bridge 14-NBI #18-057-0-0009-11-460.....	115
4.3.16. Grillage Analysis of Bridge 15-NBI #12-102-0271-06-689	119
4.4. Conclusion.....	122
4.5. Grillage Analysis: Additional Parametric Study	125
4.5.1. Concrete Strengths	125
4.5.2. Reinforcing Bar Area	126
4.5.3. Concrete Deck Thickness	127
5. GRILLAGE METHOD AND FEM COMPARISON.....	129

5.1. Introduction	129
5.2. Single Span Bridges	129
5.3. Interior Spans	133
5.4. Exterior Spans	138
6. GRILLAGE METHOD DESIGN GUIDE.....	152
6.1. Procedure.....	152
6.1.1. Define Cylindrical Coordinate System.....	153
6.1.2. Define Non-Linear Material Properties.....	154
6.1.3. Define Section Properties	154
6.1.4. Defining Hinge Properties.....	156
6.1.5. Assign Members to Grid	157
6.1.6. Assign Hinges to Frame Members	158
6.1.7. Assign Boundary Conditions.....	159
6.1.8. Define Load Patterns and Cases	160
6.1.9. Assign Frame Loads.....	160
6.1.10. Assign Data Collection Points.....	161
6.1.11. Run Analysis for Dead Load Only	162
6.1.12. Run Analysis for All Load Cases (Intact Bridge)	162
6.1.13. Replace Hinges at Fracture.....	163
6.1.14. Run Analysis for All Load Cases (Fractured Bridge)	163
6.1.15. Post Process Data	164
7. CONCLUSION AND FINDINGS	166
7.1. Conclusion.....	166
7.2. Findings	168
7.3. Future Work	168
REFERENCES	171
APPENDIX A STRUCTURAL DRAWINGS	178
APPENDIX B GRILLAGE HINGE PROPERTIES	304
APPENDIX C GRILLAGE DESIGN EXAMPLES.....	347

LIST OF FIGURES

	Page
Figure 2.1: Silver Bridge after the collapse in 1967 (Reprinted from NTSB 1971)	16
Figure 2.2: Collapse of the Mianus River Bridge (Reprinted from Fisher 1997)	18
Figure 2.3: Cracked girder of the I-79 Glenfield Bridge in 1977 (Reprinted from Fisher 1984)	19
Figure 2.4 Steel Twin Tub Girder Bridge I 35/US 290 Interchange, Austin, Texas.....	32
Figure 2.5. External bracing types: (a) K-type cross-frames; (b) solid diaphragms (Reprinted from Hunley and Harik 2012).	34
Figure 2.6. FSEL Bridge test: (a) Surveyed deflections and assumed yield line; (b) Damaged deck after test (Reprinted from Samaras et al. 2012).	36
Figure 3.1. Distribution of Texas STTG Bridges by Maximum Span Length.....	40
Figure 3.2. Distribution of Texas STTG Bridges by Curvature.....	41
Figure 3.3. Distribution of Texas STTG Bridges by Number of Continuous Spans	42
Figure 3.4. Span vs Curvature Scatter of Simple Span STTG Bridges in Texas	44
Figure 3.5. Span vs Curvature Scatter of Two-Span STTG Bridges in Texas.....	45
Figure 3.6. Span vs Curvature Scatter of Three-Span STTG Bridges in Texas.....	45
Figure 3.7 Comparison of FEM deflection profile with test results after web fracture (Reprinted from Hurlebaus, 2018).....	49
Figure 4.1 Constitutive Model for Steel Members (from SAP2000).....	57
Figure 4.2 Constitutive Model of Concrete (from SAP2000).....	58
Figure 4.3 Representative Longitudinal Grillage Members.....	60
Figure 4.4 Representative Transverse Grillage Members.....	61
Figure 4.5 Representative Grillage Schematic	61
Figure 4.6 Representative Plastic Hinge Property (SAP2000)	63

Figure 4.7 HL93 Loading Diagram for Two-Lane Loaded Case.....	65
Figure 4.8 Grillage Deflection Profile of Bridge FSEL (0) with Activated Hinges	70
Figure 4.9 Grillage Analysis Results of Bridge FSEL (0)	70
Figure 4.10 Grillage Deflection Profile of Bridge 1 with Activated Hinges	72
Figure 4.11 Grillage Analysis Results of Bridge 1	73
Figure 4.12 Grillage Deflection Profile of Bride 2 with Activated Hinges	75
Figure 4.13 Grillage Analysis Results of Bridge 2	75
Figure 4.14 Grillage Deflection Profile for Bridge 3 with Activated Hinges	78
Figure 4.15 Grillage Analysis Results of Bridge 3	78
Figure 4.16 Grillage Deflection Profile for Span 2 of Bridge 4 with Activated Hinges..	81
Figure 4.17 Grillage Analysis Results of Bridge 4-Span 1	81
Figure 4.18 Grillage Analysis Results of Bridge 4-Span 2	82
Figure 4.19 Grillage Deflection Profile for Span 1 of Bridge 5 with Activated Hinge ...	84
Figure 4.20 Grillage Analysis Results of Bridge 5-Spans 1&2	85
Figure 4.21 Grillage Deflection Profile for Spans 1 & 2 of Bridge 6 with Activated Hinges	87
Figure 4.22 Grillage Analysis Results of Bridge 6-Spans 1&2	88
Figure 4.23 Grillage Deflection Profile for Span 2 of Bridge 7 with Activated Hinges..	91
Figure 4.24 Grillage Analysis Results of Bridge 7-Span 1	91
Figure 4.25 Grillage Analysis Results of Bridge 7-Span 2	92
Figure 4.26 Grillage Deflection Profile for Span 2 of Bridge 8 with Activated Hinges..	94
Figure 4.27 Grillage Analysis Results of Bridge 8-Span 1	95
Figure 4.28 Grillage Analysis Results of Bridge 8-Span 2	95
Figure 4.29 Grillage Deflection Profile for Span 2 of Bridge 9 with Activated Hinges..	98

Figure 4.30 Grillage Analysis Results of Bridge 9-Span 1	98
Figure 4.31 Grillage Analysis Results of Bridge 9-Span 2	99
Figure 4.32 Grillage Analysis Results of Bridge 9-Span 3	99
Figure 4.33 Grillage Deflection Profile for Span 2 of Bridge 10 with Activated Hinges	102
Figure 4.34 Grillage Analysis Results of Bridge 10-Span 1	102
Figure 4.35 Grillage Analysis Results of Bridge 10-Span 2	103
Figure 4.36 Grillage Analysis Results of Bridge 10-Span 3	103
Figure 4.37 Grillage Deflection Profile for Span 2 of Bridge 11 with Activated Hinges	106
Figure 4.38 Grillage Analysis Results of Bridge 11-Span 1	106
Figure 4.39 Grillage Analysis Results of Bridge 11-Span 2	107
Figure 4.40 Grillage Analysis Results of Bridge 11-Span 3	107
Figure 4.41 Grillage Deflection Profile for Span 2 of Bridge 12 with Activated Hinges	110
Figure 4.42 Grillage Analysis Results of Bridge 12-Span 1	110
Figure 4.43 Grillage Analysis Results of Bridge 12-Span 2	111
Figure 4.44 Grillage Analysis Results of Bridge 12-Span 3	111
Figure 4.45 Grillage Deflection Profile for Span 2 of Bridge 13 with Activated Hinges	114
Figure 4.46 Grillage Analysis Results of Bridge 13-Spans 1&3	114
Figure 4.47 Grillage Analysis Results of Bridge 13-Span 2	115
Figure 4.48 Grillage Deflection Profile for Span 2 of Bridge 14 with Activated Hinges	117
Figure 4.49 Grillage Analysis Results of Bridge 14-Spans 1&3	118
Figure 4.50 Grillage Analysis Results of Bridge 14-Span 2	118

Figure 4.51 Grillage Deflection Profile for Span 2 of Bridge 15 with Activated Hinges	121
Figure 4.52 Grillage Analysis Results of Bridge 15-Spans 1&3	121
Figure 4.53 Grillage Analysis Results of Bridge 15-Span 2	122
Figure 5.1. Results for Short Single Span (Simply Supported) Fractured Twin Tub Bridges	131
Figure 5.2. Results for Long Single Span (Simply Supported) Fractured Twin Tub Bridges	132
Figure 5.3. Results for Shorter Interior Spans of Fractured Twin Tub Bridges	134
Figure 5.4. Results for Average Interior Spans of Fracture Twin Tub Bridges	135
Figure 5.5. Results for Long Interior Spans of Fracture Twin Tub Bridges	136
Figure 5.6. Results for Very Long Interior Span of Fracture Twin Tub Bridges	137
Figure 5.7. Results for Short Exterior Spans of Fracture Twin Tub Bridges	140
Figure 5.8. Results for Short Exterior Spans of Fracture Twin Tub Bridges	141
Figure 5.9. Results for Short Exterior Spans of Fracture Twin Tub Bridges	142
Figure 5.10. Results for Short Exterior Spans of Fracture Twin Tub Bridges	143
Figure 5.11. Results for Short Exterior Span of Fracture Twin Tub Bridges	144
Figure 5.12. Results for Average Exterior Spans of Fracture Twin Tub Bridges	145
Figure 5.13. Results for Average Exterior Spans of Fracture Twin Tub Bridges	146
Figure 5.14. Results for Average Exterior Spans of Fracture Twin Tub Bridges	147
Figure 5.15. Results for Long Exterior Spans of Fracture Twin Tub Bridges	148
Figure 5.16. Results for Long Exterior Spans of Fracture Twin Tub Bridges	149
Figure 5.17. Results for Very Long Exterior Spans of Fracture Twin Tub Bridges	150
Figure 6.1 Grillage Grid System for a Single Span Bridge	153
Figure 6.2 Constitutive Material Models (SAP2000)	154

Figure 6.3 Representative Longitudinal Members	155
Figure 6.4 Representative Transverse Members	156
Figure 6.5 Representative Hinge Property	157
Figure 6.6 Screenshot of SAP2000 Post Frame Section Assignment	158
Figure 6.7 Representative Hinge Assignments	159
Figure 6.8 Spring Boundary Conditions	160
Figure 6.9 Grillage HS20 Truck and Lane Load.....	161
Figure 6.10 Location of Grillage Data Collection Points.....	162
Figure 6.11 Fractured Hinge Pattern	163
Figure 6.12 Spreadsheet of Grillage Data	165

LIST OF TABLES

	Page
Table 3.1 Range of Parameters Considered for the Bridge Selection	43
Table 3.2 Main Geometric Properties of Selected Texas STTG Bridges	46
Table 3.3 FEM Overstrength Factors for Single Span STTG Bridges (Reprinted Hurlebaus et al. 2018).....	50
Table 3.4 FEM Overstrength Factors for Interior Spans of STTG Bridges (Reprinted from Hurlebaus et al. 2018).....	51
Table 3.5 FEM Overstrength Factor for Exterior Spans of STTG Bridges (Reprinted from Hurlebaus et al. 2018).....	52
Table 4.1 Geometric Details of Steel Tub Girders for Bridge FSEL (0)	68
Table 4.2 General Geometric Properties of Bridge FSEL (0).....	69
Table 4.3 Geometric Details of Steel Tub Girders for Bridge 1	71
Table 4.4 General Geometric Properties of Bridge 1	71
Table 4.5 Geometric Details of Steel Tub Girders for Bridge 2	73
Table 4.6 General Geometric Properties of Bridge 2.....	74
Table 4.7 Geometric Details of Steel Tub Girders for Bridge 3	76
Table 4.8 General Geometric Properties of Bridge 3.....	77
Table 4.9 Geometric Details of Steel Tub Girders for Bridge 4	79
Table 4.10 General Geometric Properties of Bridge 4.....	80
Table 4.11 Geometric Details of Steel Tub Girders of Bridge 5.....	83
Table 4.12 General Geometric Properties of Bridge 5.....	84
Table 4.13 Geometric Details of Steel Tub Girders of Bridge 6.....	86
Table 4.14 General Geometric Properties of Bridge 6.....	86

Table 4.15 Geometric Details of Steel Tub Girders of Bridge 7.....	89
Table 4.16 General Geometric Properties of Bridge 7.....	90
Table 4.17 General Geometric Properties of Bridge 8.....	93
Table 4.18 Geometric Details of Steel Tub Girders of Bridge 8.....	94
Table 4.19 General Geometric Properties of Bridge 9.....	96
Table 4.20 Geometric Details of Steel Tub Girders of Bridge 9.....	97
Table 4.21 Geometric Details of Steel Tub Girders of Bridge 10.....	100
Table 4.22 General Geometric Properties of Bridge 10.....	101
Table 4.23 Geometric Details of Steel Tub Girders of Bridge 11.....	104
Table 4.24 General Geometric Properties of Bridge 11.....	105
Table 4.25 Geometric Details of Steel Tub Girders of Bridge 12.....	108
Table 4.26 General Geometric Properties of Bridge 12.....	109
Table 4.27 Geometric Details of Steel Tub Girders of Bridge 13.....	112
Table 4.28 General Geometric Properties of Bridge 13.....	113
Table 4.29 Geometric Details of Steel Tub Girders of Bridge 14.....	116
Table 4.30 General Geometric Properties of Bridge 14.....	117
Table 4.31 Geometric Details of Steel Tub Girders of Bridge 15.....	119
Table 4.32 General Geometric Properties of Bridge 15.....	120
Table 4.33 Overstrength Factors for Single Span Bridges utilizing Grillage Analysis .	124
Table 4.34 Overstrength Factors for End Spans utilizing Grillage Analysis	124
Table 4.35 Overstrength Factors for Interior Spans utilizing Grillage Analysis	125
Table 4.36 Bridge 2: Overstrength Factors (Ω) with Varied Concrete Strengths	126
Table 4.37 Bridge 9 (Mid-Span): Overstrength Factors (Ω) with Varied Concrete Strengths	126

Table 4.38 Bridge 2: Overstrength Factors (Ω) with Varied Reinforcing Bar Areas	127
Table 4.39 Bridge 9 (Mid-Span): Overstrength Factors (Ω) with Varied Reinforcing Bar Areas	127
Table 4.40 Bridge 2: Overstrength Factors (Ω) with Varied Concrete Thicknesses.....	128
Table 4.41 Bridge 9 (Mid-Span): Overstrength Factors (Ω) with Varied Concrete Thicknesses.....	128
Table 5.1 Results for Simple Spans	130
Table 5.2 Results for Interior Spans.....	133
Table 5.3 Exterior Span Results	139

1. INTRODUCTION*

1.1. Background and Motivation

Twin tub girder bridges have the potential to serve as an engineering solution to the problem of long-span, curved bridges with tight radii of curvature. These bridges are becoming an alternative in lieu of the curved I-girder bridges. However, the major deterrent in the widespread reliance of these bridges is the classification of these bridges as fracture critical by the Federal Highway Administration (FHWA). The fracture critical designation leads to long term costs associated with hands-on inspections and fabrication of the fracture critical members (FCMs) according to the American Welding Society (AWS) Fracture Control Plan (FCP). There have been disastrous consequences in cases of failure of fracture critical bridges that have elicited the need for rigorous hands-on inspections to avoid such terrible losses of life and property in the future. The American Association of State Highway and Transportation Officials (AASHTO) Load and Resistance Factor Design (LRFD) Bridge Design Specifications (AASHTO 2017) defines a FCM as a “component in tension whose failure is expected to result in the collapse of the bridge or the inability of the bridge to perform its function.” Therefore, hands-on inspections are required to ensure the structure is safeguarded against fracture and fatigue failures. The hands-on inspection of these bridges are costing the Department of Transportations (DOTs) large sums of funds that could be allocated to address other

* Part of this chapter is reprinted with permission from “Fracture Critical Steel Twin Tub Girder Bridges Technical Report” 0-6937-R1 by Hurlebaus S., Mander J., Terzioglu T., Boger N., Fatima A., 2018. Texas A&M Texas Transportation Institute, 1-4, Copyright 2018 by Texas A&M Texas Transportation Institute

problems since not all the twin tub girder bridges are truly fracture critical. The current definition of FCMs, based on only load path redundancy, is highly conservative, which deems all bridges as requiring elaborate and expensive inspections that deplete money and time. Instead of an elastic analysis that may be grossly underestimating the reserve capacity of the redundant structural members, a more realistic and exact elasto-plastic analysis is recommended for this research. It is imperative to initiate an investigation to assess the relevance of the current classification of the twin tub girder bridges as fracture critical. A thorough analysis is needed to carry out the investigation aimed at reclassifying a bridge from its fracture critical status by proving sufficient reserve strength due to the structural redundancy of the superstructure. To execute an investigation, it is proposed that researchers conduct two independent analyses and compare the results to comprehend the behavior of these bridge superstructure systems in detail. The aim of the two methods is to find the overstrength of the twin tub girder bridges selected from the bridge inventory. The overstrength reflects the amount of reserve capacity the structural members possess when applied with factored design loads. The decision regarding the reclassification from the fracture critical status may be conclusively drawn if the scope of this research both methods converge to a reasonable degree. Once it is identified that the two methods consistently predict sufficient reserve capacity, one or more methods may be recommended for implementation in the industry depending on the trends, if any, emerging from this research project. The two methodologies that are implemented are:

- An accurate and thorough computational finite element analysis.
- A lower-bound computational grillage method.

The finite element analysis implements the use of advanced elasto-plastic nonlinear elements to accurately simulate the material behavior and loading. The results generated from this method are considered the most accurate because the program utilizes advanced computational accuracy to model the system with high precision. Consequently, the procedure requires time and sophisticated computational resources. The plastic method is employed to develop a lower-bound (strip method) solution to calculate the reserve capacity manually. This gives a range of the overstrength factors to quickly compare with the computational methods. The grillage analysis (based on a lower-bound strip method) is conducted using nonlinear elasto-plastic material and hinge properties to model the behavior of the bridge under design vehicular loading. The computational push-down grillage analysis is carried out using the matrix methods of structural analysis in SAP2000. The grillage analysis can be considered as a practical blend of the advanced computational finite element analysis and the plastic method due to its nonlinear elasto-plastic modeling approach and its evolution from the lower-bound strip method.

The two methods are independently studied via extensive parametric studies and the veracity of each method is checked by validating the analytical results with those obtained experimentally. The next stage of analyses involve the assessment of the overstrength factors of these bridges when analyzed under AASHTO load and resistance factor design (LRFD) loading. This research was aimed at equipping professional bridge engineers to apply the analytical methods to investigate the inherent reserve strength of the twin tub girder bridges so as to eliminate the FCM designation of the steel tub girders

and reclassify them as system redundant members (SRMs) as defined by Federal Highway Administration (FHWA) memorandum HIBT-10 FHWA (2012).

1.2. Objectives of Research

A key objective of this research is to develop more rigorous modeling and analysis methods. These analysis and modeling methods shall take into account the capacity of the fractured girder, especially at support locations, and realistically model the load distribution between the intact girder and the fractured girder. However, the modeling and analysis methods need to be sufficiently straightforward to be applied on a large scale to the inventory of steel tub bridges. The analysis method developed should meet the requirements outlined in the Federal Highway Administration (FHWA) Memorandum (FHWA 2012).

1.3. Structure of Dissertation

The structure of this dissertation is as follows. Chapter 2 details the background knowledge gleaned on the subject matter. Chapter 3 details the parametric selection of bridges to be evaluated in this study as well as accompanying Finite Element Analysis (FEM) results for the 15 bridges. Chapter 4 contains the Grillage Push-Down Analysis of the 15 selected bridges in the parametric study. A comprehensive comparison of the FEM and Grillage Analysis results is located in Chapter 5. A detailed Grillage Analysis Design Guide is located in Chapter 6. Finally the conclusion of the study and findings going forward are located in Chapter 7.

2. LITERATURE REVIEW*

2.1. Introduction

Steel twin tub girder bridges have become increasingly popular in Texas because they offer a solution for long-span and/or curved highway bridges in addition to providing an aesthetic structural option. Steel twin tub girder bridges appear in many different designs and they vary in number of spans, span length and degree of horizontal curvature. The twin box bridge superstructure has become more common due to construction problems with curved I-girders. However the choice of twin steel tub superstructure comes with additional maintenance and fabrication cost due to their “fracture critical” designation according to the American Association of State Highway and Transportation Officials (AASHTO) *Guide Specification for Fracture Critical Non-Redundant Steel Bridge Members* (2012). Fracture critical or non-redundant designation requires strict fatigue consideration, substantial testing during fabrication and more periodic maintenance compared to non-fracture critical structures because they consist of nonredundant structural systems that could collapse or partially collapse due to the loss of a single structural member. In particular, rigorous frequent inspection requirement increases the life cycle cost of this class of bridge superstructure significantly.

Steel twin tub girder bridges require hands-on inspection every two years, which costs the Texas Department of Transportation (TxDOT) about \$2 million every two years

* Reprinted with permission from “Fracture Critical Steel Twin Tub Girder Bridges Technical Report” 0-6937-R1 by Hurlebaus S., Mander J., Terzioglu T., Boger N., Fatima A., 2018. Texas A&M Texas Transportation Institute, 5-30, Copyright 2018 by Texas A&M Texas Transportation Institute

including the traffic control costs. Therefore, removing the fracture critical designation of some or all of these bridges may significantly lower the cost of this bridge system, leading to more economic inspection requirements. In order to be able to designate a two-girder bridge as redundant, it is necessary to show that the bridge has sufficient reserve capacity after the fracture of one of the girders. This can be achieved through rigorous analysis techniques.

This chapter documents the state of the art and practice for the analysis of bridges and redundancy studies of fracture critical bridges. This opening subsection introduces the fracture critical twin tub girder bridges and describes the motivation. In the second subsection, different methods of analysis are listed and briefly summarized. The third subsection presents the definition of fatigue and fracture, and several bridge failures due to fatigue and fracture. The fourth subsection introduces the concept of redundancy and the motivation for the initiation of fracture critical protocol. Different definitions provided in the design codes and specifications along with different sources of redundancy are also discussed in this subsection. In the final subsection relevant research about fracture critical bridges and modeling approaches for evaluating the redundancy of steel twin tub bridges are presented.

2.2. Approaches to Analyzing the Behavior of Bridge Structures

In structural engineering, physical phenomena are simulated using mathematical models which can represent the actual behavior of a structural system. Over the previous centuries, methods of structural analysis have developed and become more sophisticated as the ability to compute solutions has also improved. Indeterminate structural systems

require solutions that concurrently deal with both equilibrium and compatibility of deformations. In contrast, if the compatibility condition is violated due to inelastic behavior but equilibrium maintained, plastic solutions that provide collapse loads may be obtained. This subsection first describes historic through to modern methods of elastic structural analysis. Second, plastic methods for both frames and slabs are discussed. In the third and final part to this subsection, nonlinear methods of analysis are described whereby computational solutions can give the entire solution from the initial elastic behavior through to the plastic collapse load.

2.2.1. Elastic Structural Analysis

Linear analysis simply assumes that the load is proportional to displacement. This principle was first introduced by Robert Hooke and remains well-known due to Hooke's law (1678). As force is related to stress and displacement to strains, they are also proportional to each other. Linear elastic analysis is based on the original undeformed geometry and elastic material properties. Analysis of structures using mechanics of materials approach or theory of elasticity are analytical formulations using linear elastic behavior and therefore closed-form solutions may be obtained. Although most structural systems involve material and geometric nonlinearity, elastic analysis has been widely used due to its simplicity. Engineers still use linear elastic methods by some modification to consider nonlinearities. When predicting the ultimate strength or in-service deformations, the results of linear elastic analysis are adjusted permitting a prescribed amount of moment redistribution. While it remains valid to use superposition for linear elastic analysis and then apply a measure of moment redistribution, it is not possible to assess the actual

collapse load. However, if the provided capacity is greater than the load demands some reserve capacity remains. Elastic solutions together with a limited amount of moment redistribution are lower bound limit state solutions.

Linear elastic analysis may be used to estimate the actions and deflections of reinforced concrete structures under service loads but care must be taken for reduced stiffness due to cracking resulting from loading or restraint to thermal and shrinkage effects. These additional reasons of material nonlinearity complicate the design process using linear elastic methods.

2.2.1.1. Beams and Frames

The simplified approach of using linear elastic behavior defined by Hooke's law enabled scientists to formulate mathematical models for many engineering problems. Bernoulli and Euler (1750) formulated differential equations for the deflection calculation of a beam. Euler has derived equations to calculate deflection of beams, buckling load of beams and his approach could be extended to calculate flexural stresses. Euler-Bernoulli beam theory (EBT) for flexural behavior and stiffness was developed and evolved over some 400 years. In EBT, it is assumed plain sections transverse to the longitudinal axis of the beam remain plane (straightness) and perpendicular to the axis after deformation (normality). In this so-called straight line theory, the transverse deflection of a beam is governed by a fourth order differential equation. Although the derivation of analytical formulas originated back in 1700s the results of EBT were not commonly used until the 19th century when the wrought iron and later on steel was started to be used in large structures (Timoshenko 1953).

The theory of elasticity developed throughout the second half of 18th and 19th century. These developments made it possible to design and build relatively simple structures such as bridges. However, finding analytical solutions for mathematical models for complicated (indeterminate) structures had led to large numbers of equations, which was not easy to manage without modern computational methods. One of the early methods for analyzing statically indeterminate elastic structures is the force method or flexibility method which was initially developed by James Clerk Maxwell in 1874 and later improved by Heinrich Müller-Breslau. A breakthrough was made when Hardy Cross (1932) first introduced the iterative “moment distribution” method.

A significant development which led to computational analysis of structural systems was the development of Matrix structural analysis (MSA). MSA was first used in aerospace industry in 1930s through the formulation of Duncan and Collar (1934). Turner (1959) proposed direct stiffness method (DSM) which created the framework for the finite element method. Later Argyris and Kelsey (1960) described contrasting force and displacement based matrix methods. These methods became solvable with early digital computers and were popularized in the 1960`s and beyond. MSA basically discretize the mathematical model and create the matrix formulation for an assembly of bar, beam and/or beam-column members, which is then solved by computational tools.

2.2.1.2. Plates and Shells

In two-dimensional elasticity the most basic member behavior is membrane which has in-plane stiffness only. This behavior is analogous to bar element in one-dimension. This means membrane cannot resist any bending moment. A plate is defined as a structural

member which is thin and its thickness is much smaller than its length or width. Similar to the beams the transverse loads are carried by the bending actions of the plate. Plate behavior models out-of-plane bending stiffness only and the member can resist bending moments. There are various plate theories which differ by their simplifying assumptions. Most commonly used one is the classical plate theory (Kirchhoff theory of plates), which is a generalization of Euler-Bernoulli beam theory. There are three main assumptions; sections perpendicular to mid-surface remain straight (straightness), these sections also remain perpendicular to the mid-surface (normality), and the thickness does not change during deflection (inextensibility). Based on these assumptions the normal stresses in the transverse direction vanishes (plane stress), and the transverse shear strains are neglected. However, for thick plates there may be significant shear strains that contributes to transverse stresses. Mindlin plate theory includes the effect of transverse shear strains by removing the normality assumption, which is analogous to the Timoshenko beam theory (Timoshenko and Woinowsky-Krieger 1959). Shell behavior considers both in-plane stiffness (membrane behavior) and out-of-plane stiffness (plate bending) for modeling a two-dimensional structural member.

It is possible to simulate the behavior of a bridge superstructure as an orthotropic plate in order to get analytical solution for the displacements and stresses as well as eigenfrequencies (Hurlebaus 2007; Hurlebaus et al. 2001). An orthotropic plate is the common name for plates that have uniform but different elastic properties in the two orthogonal directions. In this method the bridge superstructure is represented by an equivalent orthotropic plate with uniform thickness. Longitudinal stiffnesses are

calculated based on the composite beam and slab section. Transverse stiffnesses are calculated based on the deck stiffness alone. This geometric simplification requires that the beams are equally spaced, which is generally the case in practice (Sanders and Elleby 1970). Considering these assumptions the orthotropic plate behavior satisfies a fourth order partial differential equation (Timoshenko and Woinowsky-Krieger 1959). Although this is a way of obtaining the solution, this method requires many approximations to reduce the three-dimensional complex bridge superstructure to a two-dimensional constant thickness plate.

2.2.2. Plastic Methods of Analysis (Limit Analysis)

Traditionally theory of elasticity has been widely used because it is relatively simple due to the assumption of proportional stress and strains, however, this approach cannot estimate the real behavior or safety at the limit state. Structural materials, especially steel, may withstand considerable strains beyond their initial yield strain. As a structural member is loaded beyond yield, the material behaves in a plastic fashion. Once a section reaches its load capacity it deforms at almost constant load. This ultimate load capacity of the section is calculated from the material properties in the plastic range. The first critical section reaches the yield moment while other sections of the structure remain elastic. This state of the structure results in elastic-plastic deformations that eventually reaches full plasticity as the loads are increased. When a full mechanism is achieved the collapse load is reached.

In formulating plastic methods of analysis, there are two main theorems: (1) lower bound theorem that commonly uses graphical means or simplifying assumptions; and (2)

upper bound theorem where various mechanisms are assumed with the correct mechanism having the lowest load (least energy).

2.2.2.1. Beams and Frames

In using the LRFD (load and resistance factor design) approach, beams and frames are analyzed using elastic methods while the reinforcement for beams and frames is calculated by strength methods which considers the inelastic properties at the ultimate load. Limit analysis does not have this inconsistency, and accounts for redundancies and redistribution allowing more practical reinforcement design. Limit analysis of beams and frames can be achieved through lower bound graphical methods. All plastic hinges must have adequate rotation capacity.

The lower-bound analysis implies that the estimated capacity is smaller or equal to the true load capacity. The starting point of lower bound graphical methods consists of: (i) drawing moment diagrams for a statically determinate structure; (ii) assigning fixing moments (the redundant actions); (iii) determining the required plastic capacity which is the largest moment. Note this may not lead to a complete mechanism hence the solution is said to be a lower bound.

2.2.2.2. Slabs

Plastic analysis methods for estimating the ultimate capacity of beam and slab bridges have been used by many designers and researchers in the past. For example, the use of elastic analysis for estimating highly ductile reinforced concrete bridge deck results in very conservative ultimate load predictions. The application of plastic analysis for slabs is

relatively less tedious compared to beams and frames because slabs are generally under-reinforced and consequently have large rotational capacity. Several practical techniques have been developed for application of plastic method to slabs such as lower bound strip methods (Park and Gamble 2000).

Plastic methods of analysis for analysis and design of bridge decks have long been available but rarely used in US. Limit analysis is particularly useful for investigating the possible failure modes, behavior beyond yielding, and residual capacity of in-service or deficient bridges. By investigating certain collapse mechanism, it is possible to detect undesirable collapse mechanisms such as shear failure, which is a sudden brittle failure mode, and adjust the design to get a more ductile behavior and get flexure mechanism at the ultimate load.

Strip methods for slabs were first developed by Hillerborg (1956). Strip methods provide lower bound solutions which satisfy equilibrium and yield conditions (moments are always smaller than or equal to the plastic moment) everywhere in the slab. In contrast to yield line analysis, strip methods provide conservative (safe) capacity predictions. The strip method is a practical design method where the reinforcement can be designed without any iterative process. Wood et al. (1968) later evaluated and improved the method regarding continuity conditions. Armer (1968) conducted an experimental study where half-scale slab specimens designed using strip method were tested. It was concluded that the strip methods consistently produce safe designs.

2.2.3. Computational Nonlinear Finite Element Solutions

Physical systems are generally modeled using differential equations and corresponding boundary conditions. For real world problems, such as complex structural shapes including material nonlinearity, it is most of the time impossible to get a closed form analytical solution. It is a common practice to seek solution using approximate and computational methods such as finite difference, finite volume and finite elements. Finite element method (FEM) is the most widely used technique due to its generality, versatility and applicability to various differential equations. FEM is particularly useful for analyzing complex geometries, loadings and material properties, which is generally the case in real physical problems. In FEM modeling approach the structure is approximated with set of elements having simple geometries such as triangles and rectangles. Each element satisfies the differential equation of the problem in hand and has the material properties of structure, which forms the element stiffness relation. These elements are connected at their nodes to form the global stiffness relation for the whole structure creating set of algebraic relations.

Although it is not possible to clearly identify the inventor of FEM, (Turner et al. 1956) generalized the direct stiffness method and created FEM that was used in everyday engineering problems starting in aerospace engineering. Later Ed Wilson developed the first open source computer program in FOR-TRAN II (1958) using IBM 704. Wilson's work provided the basis for most of the early FEM programs. In 1950s and 1960s the FEM technology was transferred from aerospace engineering to wide range of engineering applications by J. H. Argyris (1960), R. W. Clough (1956), and H. C. Martin (1956).

2.3. Fatigue and Fracture in Bridges

Traffic loads on bridges causes stress cycling. Repeated stress cycling accumulates damage that may initiate fatigue cracks. If left unattended the fatigue induced cracks grow and lead to unstable growth and eventually fracture the material. Fatigue damage is prevalent in metal structures and particularly steel bridges. High cycle fatigue failure is common in or near the connection of metal bridge components. Older metal bridges, whether they be constructed from wrought iron or steel commonly show signs of distress at riveted connections. More modern steel bridge structures have a propensity for fatigue failure at or nearby welded connections. This subsection commences by outlining some classical fatigue and fracture failures. Then goes on to describing how fatigue problems are categorized by design in accordance with AASHTO LRFD Specifications (2014). In particular, fracture critical structural systems and how such systems are dealt with, by design is discussed.

2.3.1. Fatigue and Fracture Failures in Bridge Structures

Scheffey (1971) investigated the failure of the collapse of the Point Pleasant Bridge (Figure 2.1) in December 1976 and reported that the collapse was due to failure of a single eye-bar connecting the suspension chain. The Point Pleasant Bridge, also known as Silver Bridge because of her silvery painted aluminum color, in West Virginia over the Ohio River was opened in 1928. The Silver Bridge was “nearly 2,235 ft long, including a main span of 700 ft and two side spans of 380 ft each” (Witcher 2017). The bridge design first called for conventional wire cables but was later modified to use eye-bar chains since they were less expensive. The Silver Bridge was the first eye-bar suspension bridge in the

United States and after nearly 40 years in use and a significant change of the vehicle loads, the bridge collapsed during the evening rush-hour with the result that 46 people died and 9 were injured. (Witcher 2017). Although the bridges that were constructed before 1985 did not have strict fatigue and fracture requirements, there are very few examples of failure in US and the Silver Bridge was one of them.



Figure 2.1: Silver Bridge after the collapse in 1967 (Reprinted from NTSB 1971)

Barker and Puckett (2013) describes two critical bridge collapses that led to the development of more strict code provisions. All the other crashed bridges since 1950 collapsed because of other unforeseen events such as accidents of vehicles, ships or natural disasters. The total collapse of the Silver Bridge had a big influence on the design, selecting materials and fabrication on future bridges and the inspection of non-redundant bridges in the United States. In 1968, the National Bridge Inspection Standards (NBIS)

were inaugurated under the Federal-Aid Highway Act which prescribes, that the time lag of an inspection of a bridge should not exceed two years.

The Mianus River Bridge, seen in Figure 2.2, was the second bridge which collapsed (1983) due to fatigue of the material. The Mianus River Bridge was a “pin and hanger” design bridge, which was commonly used in the year of construction because of the cheaper construction costs and collapsed after 25 years of service. Due to corrosion of storm drains which were installed ten years before the collapse, the pin and hanger assemblies moved and shifted the weight to the outside hanger which had to carry all the weight, resulting a fatigue crack. This fatigue crack caused the hanger to separate from the upper pin and subsequent the span of the bridge collapsed and the span fell down into the river. The Mianus River Bridge disaster could have been avoided because it had regular, but insufficient inspections. After the collapse of the Silver Bridge over the Ohio River, the Mianus River Bridge was inspected 12 times with the last inspection only 1 year before the collapse, but the inspectors only inspected the bridge visually from the ground with binoculars so that they could not identify the lateral displacement of the hangers. They noted “heavy rust on the top pins from water leaking through the expansion joints”, but this was not relevant enough to foresee the collapse.



Figure 2.2: Collapse of the Mianus River Bridge (Reprinted from Fisher 1997)

After the publication of AASHTO guidelines for fracture critical members (FCM), the steel manufacturing industry and structural engineers adopted them successfully. Therefore, fatigue and fracture failures are very rare in the last 35 years (Connor et al. 2005). Note however, that both the Point Pleasant Bridge and the Mianus River Bridge, were constructed before the implementation of FCB inspection program. There have been several FCBs that have experienced partial or full depth fracture in the last 40 years. They were generally identified during periodic inspection but did not result in a collapse or loss of life. Apparently secondary elements such as the deck, cross bracing, or diaphragm helped to particularly redistribute the load to other members.

Several total member failures of twin girder bridges indicated that two girder bridges offer somewhat of a redundant load path while they are all declared as fracture critical because of their composition. In May 1975, one of the main girders of the Lafayette Street Bridge over the Mississippi River in St. Paul, Minnesota was discovered by the Minnesota Department of Highways inspection personnel (now Minnesota Department of

Transportation) to have a full depth fracture (Fisher et al. 1977). The crack was due to a fatigue crack and as a result the bridge did sag 6.5 in. (165 mm) but did not collapse (Connor et al. 2005).

In January 1977, a tugboat captain discovered a large crack in a girder of the I-79 Glenfield Bridge over the back channel of the Ohio River. After spotting the damage, the crack was observed to move up the web to the bottom of the flange in about one hour. Figure 2.3 shows the full depth fracture of the girder. Obviously, the bridge had a redundant member which carried the load of the broken girder.



Figure 2.3: Cracked girder of the I-79 Glenfield Bridge in 1977 (Reprinted from Fisher 1984)

A similar case was spotted in 2003 by a bird watcher who discovered a crack in a girder of one of the six girders of the I-95 Brandywine River Bridge. The last full inspection was less than half a year before the crack was discovered and at the time “no

evidence of fatigue cracks on the fascia girder was reported” (Chajes 2005). Directly after the confirmation of the crack, the Delaware Department of Transportation closed the bridge. However, all the three given examples of girder bridges did not result in a collapse and provide evidence, that two-girder bridges feature some redundancy in load path even though they are classified as fracture critical.

2.3.2. Addressing Fatigue Problems by Design

Fatigue is the structural damage of the material due to repeatedly applied loads. The damage occurs, when the material is exposed to cyclic loadings and the maximum load which initiate such a damage may be much less than the capacity of the material which is usually called yield stress limit. The material may experience progressive brittle cracking far below its yield stress due to the cyclic loadings. Cyclic loading is the repeated loading and unloading of the material and the first microscopic brittle cracks develop where there are stress concentrations.

Much experimental research has been conducted to identify crack initiation (fatigue) and fracture propagation (fracture mechanics). However, all research and simulations on crack initiation are modeled on a macroscopic scale and the first voids become visible at the size of 1 μm (Belak 1998). That indicates that the nucleation of tiny voids during the fatigue process is microscopic start before they may be identified. Fatigue has a significant influence on the life time of the structure because if the crack reaches a critical size, the crack size may increase rapidly and the structure will fracture.

Fracture is the separation of a structural member into two or more independent pieces due to excessive stress or fatigue. The ductile fracture is the extensive permanent

plastic deformation ahead of the crack and the deformation is stable during the applied stress unless the load is increased. Most metal fractures may exhibit ductile characteristics when the applied load is increased continuously. First the metal will deform elastically and will return to its original state, when the applied load is removed until the yield point is reached. After exceeding the yield point, the curve typically decreases due to dislocation (Cottrell and Bilby 1949) and then the material will deform plastically until the ultimate strength is attained. The rupture of structural steel occurs after reaching the ultimate strength and passing the necking period where the strain concentrates disproportionately in a small region of the material. The second type of fracture is the brittle fracture and that is how ceramics, cold metals or ice break. Brittle fractures are characterized by possessing little or no plastic deformation. The crack appears quickly without an increase of the applied load and is unstoppable.

A fracture initiated via fatigue stress cycling may also mean that brittle failure has progressed through to unstable fracture propagation with the maximum (average) stress well below the yield stress limit. Therefore, fatigue design specifications for steel bridges were developed in 1970s as a result of research studies conducted as part of an NCHRP project (Fisher 1970; Fisher et al. 1974). The use of floor beams or diaphragm plates connected to the flanges became the requirement in fatigue design specifications by 1985. These fatigue design specifications were adopted in AASHTO LRFD Specifications in 1998 (AASHTO 1998). Modern steel bridges that were built after 1985 possess high level of reliability in terms of fatigue due to current design and detailing requirements according to fatigue design specifications. Fatigue problems in bridges that were built according to

current fatigue design provisions were typically due to design errors or unintended behavior.

AASHTO fracture control plan has two main aspects; (1) strict controls during the design and construction to prevent structural flaws and to assure sufficient material toughness, (2) detailed inspection requirements to ensure that the defects are detected and repaired on time. The requirements for the manufacturing of steel girders and material toughness specifications assures high standards for modern bridges. In addition, high performance steel offers superior toughness, which could reduce the need for some strict provisions for FCMs (Dexter et al. 2004). On the other hand, the second aspect of AASHTO fracture control plan for the hands-on inspection highly restrictive provisions even for newly built steel bridges. Although this strict inspection protocol may be necessary for older bridges that were built before 1985, current fracture control plan does not differentiate between the modern bridges and old bridges. A lot of the modern steel twin I-girder or twin tub girder bridges fall into a “fracture critical” category.

2.4. Redundancy

The structural engineering community has realized the importance of redundancy in steel bridges after the total collapse of the Silver Bridge in West Virginia in 1967 due to failure of a single eye-bar connecting the suspension chain (Scheffey 1971). Code provisions and safety requirements were then modified for bridges susceptible to a fracture critical condition, where the failure of one member may lead to total collapse of the bridge. The concept of redundancy and definition of fracture critical members (FCM) was first introduced into the AASHTO *Standard Specifications for Highway Bridges* (1979) after

the release of AASHTO *Guide Specification for Fracture Critical Non-Redundant Steel Bridge Members* (1978). However, the definition of redundancy and fracture critical members was vague and there remains no clear guidance on quantifying the level of redundancy. A fracture critical member is defined as a “component in tension whose failure is expected to result in the collapse of the bridge or the inability of the bridge to perform its function” in the current AASHTO *LRFD Bridge Design Specification* (2012) but there are many other definitions such as “a steel member in tension, or with a tension element, whose failure would probably cause a portion of or the entire bridge collapse.” in the National Bridge Inspection Standards (NBIS) (Lwin 2012).

Most of the US and Canadian DOTs use the AASHTO or the NBIS definition for redundancy (Connor et al. 2005). In general, slab-on-girder type bridge superstructures are considered redundant when they have at least three girders, which is based on a load-path consideration. This approach is quite conservative and does not take into account lateral distribution of loads through secondary elements from a damaged member to an undamaged member. In addition, internal redundancy and structural redundancy has not been taken into account for redundancy assessment. Early redundancy studies between the 1970’s and late 90’s were conducted to develop tools for evaluating and measuring the redundancy levels in structural systems. The following summarizes several early studies conducted following the release of the AASHTO Guide Specifications (1978) in which non-redundant bridges were defined as “structures where the failure of one member could cause collapse.” However, no objective way of measuring redundancy was introduced to define redundancy.

Some twin girder bridges are likely to withstand service loads after the fracture of one member due to internal redundancy or alternate load paths such as bracings. One of the earliest studies about the internal redundancy was carried out by Sweeney (1979). The author points out that riveted built-up members may provide internal redundancy; riveted members are not as critical as welded members in case of a fracture. Therefore, these differences should be identified to better quantify post-fracture redundancy. Sweeney (1979) suggested that providing a redundant load path or a component redundant structure, such as in the case of riveted built-up structures, may be required to avoid fracture failures.

Numerous other studies have focused on post-fracture behavior by considering the alternative load path provided by bracing. Heins and Hou (1980) and Heins and Kato (1982) evaluated two girder steel bridge behavior after the major fracture of a girder. The findings suggest lateral bottom bracing and cross bracing effectively transfer load to intact members creating additional post-fracture redundancy.

In the 1980's researchers tried to develop guidelines and provisions to better define the redundancy of a bridge in the event of a full-depth fracture of a member. One of the early attempts was the study by Parmelee and Sandberg (1987). Their study suggested a more objective criteria and provisions should be developed to define redundant live load levels, allowable stress and deflection limits after the fracture of a member in a non-redundant system.

Frangopol and Curley (1987) performed an analytical study in an effort to identify the effect of redundancy on the reliability of a bridge system. The authors defined

redundant factors, or math mode, for intact and damaged structures in order to quantify residual capacity.

$$R_2 = \frac{L_{intact}}{L_{design}} \quad (2.1)$$

$$R_3 = \frac{L_{damaged}}{L_{intact}} \quad (2.2)$$

$$\Omega = R_2 R_3 = \frac{L_{damaged}}{L_{design}} \quad (2.3)$$

Where R_2 = reserve redundant factor; R_3 = residual redundant factor; L_{intact} = load carrying capacity of the intact structure; L_{design} = design load; and $L_{damaged}$ = load carrying capacity of the damaged structure. The product of the reserve capacity and the residual capacity is a measure of the structure's reliability. It was suggested that math mode-factors may provide a deterministic way of measuring overall system strength.

Daniels et al. (1989) carried out a detailed analytical study investigating the redundancy of simple span and continuous steel twin girder bridges with bracing systems. A fracture was assumed emanating from the bottom flange up the entire depth of the webs, but not into the compression flange. The post-fracture behavior of twin girder steel bridges was evaluated in significant detail, guidelines provided for assessing the redundancy through 3D analytical models or finite element method (FEM) analysis of an as-built structure with properly modeled bracings. It was concluded that twin girder steel bridges with properly designed bracing are capable of providing significant redundancy following

a near full-depth failure of one of the girders. Although the bracing may not be designed for redundancy, the bracing may provide a secondary load path following the fracture of one girder. The authors suggested that a redundancy rating based on 3D analytical models or computational FEM analysis may be used to develop a redundancy rating.

Ghosn and Moses (1998) defined redundancy as “the capability of a bridge superstructure to continue to carry loads after the damage or the failure of one of its members.”. A bridge system may be declared as safe if it satisfies four criteria. First, the system has to provide an appropriate safety level against member failure. Second, the system capacity of the bridge may not reach its maximum under extreme loading conditions. Third the bridge may not deform largely under expected loading conditions and last the bridge has to be able to carry some traffic loads after the failure of one of its members.

Ghosn and Moses (1998) also set objective criteria for estimating the residual capacity of bridges and provide guidelines accordingly. Their proposed approach utilizes statistical system factors to assess the level of redundancy of a member. Therefore, the overall system behavior is considered rather than individual components. Current code requirements generally ignore the system effect and considers load-path redundancy resulting in a conservative consideration. This research suggested system factors that provide sufficient level of redundancy for structural safety under service load conditions when the system reserve ratio for damaged condition is greater than 0.5 which means that the bridge capacity must be more than 50% of the capacity of the critical member.

$$R_d = \frac{Lf_d}{LF_1} \quad (2.4)$$

Where R_d = system reserve ratio for the damaged condition; LF_1 = the capacity of the bridge before failure of any member using elastic analysis; and Lf_d = the capacity of the damaged bridge before reaching ultimate load. Although the proposed approach has been used by different agencies and bridge designers, it has not been adopted into national bridge design specifications.

Connor et al. (2005) carried out a synthesis study as part of National Cooperative Highway Research Program (NCHRP) Report 354, which focused on the inspection and maintenance of fracture critical bridges since the manufacturing costs were found to be small compared to mandated fracture critical inspection. As of 2005, they noted that around 76 percent of all FCBs were built prior to 1978. Eleven percent of all bridges in United States have FCM designation and 83% of these bridges are two-girder-bridges or two-line-trusses and 43% of the FCM are riveted members (Connor et al. 2005). The authors suggest that designers focus on a target reliability level rather than a redundancy level. They suggested that it is possible to achieve target reliability for a non-redundant bridge by providing about 17% conservatism in the design. One of the major contributions of this synthesis study was the compiled field information about the fracture incidents. Only two bridges, the Point Pleasant Bridge (constructed in 1928) and Mianus River Bridge (constructed in 1957) had a total collapse due to fracture.

A technical memo with the subject “*Clarification of Requirements for Fracture Critical Members*,” (Lwin 2012) points out the shortcomings of current redundancy definitions and recognizes the system level performance as a way of evaluating

redundancy. The concept of redundancy is critical for bridges because non-redundant bridges are classified as fracture critical. Although the term “redundant” is very intuitive for most structural engineers, there is no clear definition for measuring the redundancy level of a bridge superstructure. AASHTO LRFD describes redundancy as “the quality of a bridge that enables it to perform its design function in a damaged state.”

Three different types of redundancy are defined (FHWA NBIS 2012):

- a) Load Path Redundancy
- b) Structural Redundancy
- c) Internal Redundancy

A structure may be classified as redundant if it satisfies one or more of these redundancy criteria. Each of these are discussed in the following paragraphs:

Load-path redundancy is relatively easy to identify because these bridges having more than two girders are designated redundant, but some agencies even require four or more load carrying girders to be contemplated as load-path-redundant. If one of the girders would completely fracture or may not perform its task, the load would be redistributed to the neighboring girders and the bridge would be safe from a total collapse. Load-path redundancy simply considers parallel primary load carrying members, which may be girders or trusses.

Structural redundancy is a function of static indeterminacy of the entire structure, which may be due to continuity of the bridge over interior supports or sometimes due to secondary members such as the deck. Continuous multiple span-bridges possess structural

redundancy and in case of a failure of one beam member, some load is redistributed from one span to another for which reason a total collapse of the bridge may be minimized.

Internal redundancy may be provided by member detailing to prevent fracture propagation through the entire cross-section. Internal redundancy exists in built-up members which have multiple parallel plates and other structural components within a member. A member is internally redundant if it has three or more similar elements connected together. If one of the elements fail, the load may be redistributed to the other elements and the member will not fail. Internal redundancy may be abolished when the member has to be repaired by welding the elements together. Welded members carry the load path from one member to the other and may be considered as one single member. In general, redundancy is determined considering alternative load paths for the purpose of identifying fracture critical bridges (FCB). However recent experimental and analytical research has shown that certain bridges identified as non-redundant may have sufficient reserve capacity due to 3D system behavior and transverse load distribution through secondary load paths, such as the deck slab and/or cross-frames.

FCB designation have two main aspects: (1) design/fabrication requirement; and (2) inspection protocol. Currently FCM`s require 24-month inspection criteria and stricter fabrication requirements to meet the American Welding Society (AWS) *Bridge Welding Code* requirements. These requirements are collectively called the Fracture Control Plan (FCP). Although FHWA (2012) allows the use of rigorous analysis and consideration of system level redundancy for the inspection of in-service bridges, this approach is not allowed for fabrication protocols of steel twin tubs. Therefore, for fabrication, redundancy

should be decided based on load-path redundancy and non-redundant tension members should conform to AASHTO LRFD, FCP and AWS. This new classification is defined as a System Redundant Member (SRM): “A member that requires fabrication according to the AWS FCP, but need not be considered a FCM for in-service inspection.”

2.5. Fracture Critical Investigations on Slab-on-Steel Girder Bridges

Steel twin I-girder bridges are a popular system of construction used for both straight and curved bridges; this bridge system is designated as fracture critical due to lack of load path redundancy (having less than three girder lines). Fasl et al. (2016) investigated the fatigue response of a fracture critical steel twin I-girder bridge, which was built in 1935 over Medina river on IH-35. The bridge has been featuring fatigue cracks along the weld at the top flange and lateral beam connections. The bridge was instrumented using strain gage and crack propagation gauges along the existing fatigue cracks. The behavior and crack propagation was monitored during rush hours. Due to extent of the fatigue cracks the girders were strengthened by installing bolted cover plates at critical locations. The behavior was also monitored after the installation of bolted cover plates. The authors monitored the bridge for more than two months before strengthening and estimated the residual fatigue life of the structure. The bridge was also monitored during and after the strengthening. The authors reported that the built-up sections provide some level of internal redundancy because the fatigue cracks did not propagate into the webs. They also concluded that the strengthening method reduced the fatigue damage by providing composite action with the deck and this may be a potential rehabilitation for old bridges that exceed their original design life expectancy.

2.6. Fracture Critical Steel Twin Tub Girder Bridges

Figure 2.4 presents a typical steel twin tub girder bridge of the type that has become popular in Texas because they offer a solution for long-span and/or curved highway bridges in addition to providing an aesthetic structural option. Steel twin tub girder bridges consist of two steel girders which are the primary members for transmitting the dead load and live load to the substructure. On the other hand concrete deck and stringers are secondary members that create a load path between girders (Daniels et al. 1989). Because of their fracture critical designation, steel twin tub girder bridges require a hands-on inspection every 2-years. This rigorous inspection may include the testing of welds, nondestructive evaluation and visual assessment. Procedures of nondestructive evaluation of steel members may “include dye penetrant, magnetic particle, or ultrasonic techniques” (TxDOT 2013).

Most bridges in the Texas FCB inventory are steel twin tub girders, which automatically fall into the fracture critical category because of two girder lines. Field testing of in-service bridges and experimental testing of full-scale bridges under controlled loading help to build up experimental data in order to assess the reliability level after the fracture of a load carrying member. Furthermore, this data enables researchers to verify different modeling approaches and develop modeling standards for evaluating redundancy levels due to internal redundancy, structural redundancy or alternative load distributions through secondary members.

Coletti et al. (2005) provided guidelines and preliminary design suggestions for the design of steel tub girder bridges including preliminary sizing and spacing

considerations. They also discussed possible design issues, available analysis tools and detailing of tub girders. The authors stated that steel twin tub girders are economical between a span range of 150 to 500 ft, permitting also tight radius of curvature solutions and good aesthetics owing to the simple clean lines.



**Figure 2.4 Steel Twin Tub Girder Bridge I 35/US 290 Interchange, Austin, Texas
(Reprinted from Coletti 2005)**

Hunley and Harik (2012) investigated the effect of various secondary structural components for developing load transfer paths for one member of a twin steel tub bridge fails using a parametric non-linear finite element analysis. The variables that were studied in this investigation included location of damage, continuity, and span length. A load transfer mechanism from a fractured girder to the intact girder should develop in order to have a measure of redundancy. Figure 2.5 shows that for steel twin tub superstructures, it

is only possible through concrete deck and/or external cross-frames. If the deck fails progressively following the failure of a girder, one should not rely only on the deck for lateral load transfer.

Hunley and Harik (2012) analyzed 33 bridge configurations to investigate reserve load capacities following fracture of one member. The fracture of one of the girders was modeled by reducing the stiffness of bottom flange line element and the web shell element. The damaged condition of the deck was modeled by reducing the stiffness of individual finite element when they reach crushing strain. Redundancy levels of the analyzed bridges were calculated using the damaged condition capacity, R_d , as defined in NCHRP Report 406. The authors determined the capacity of the damaged bridge should be at least 50% of the capacity of the undamaged bridge to be classified as “redundant.” Based on the assessment of redundancy levels of all analyzed bridge geometries, the authors concluded that a progressive failure of a bridge deck results in insufficient load capacity to meet the minimum redundancy level. It was also noted that girder continuity increases redundancy. The authors also concluded that the external bracing is the key parameter for providing sufficient redundancy as seen in Figure 2.5.

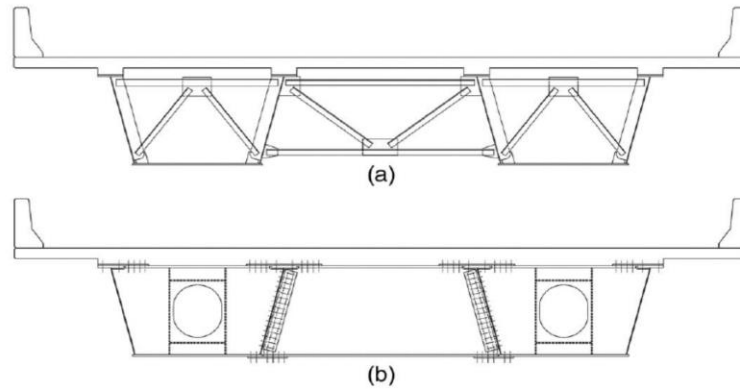


Figure 2.5. External bracing types: (a) K-type cross-frames; (b) solid diaphragms (Reprinted from Hunley and Harik 2012).

Barnard et al. (2010) recently investigated steel twin tub girders performance as part of TxDOT Project 9-5498. The study included extensive laboratory testing, with the experimental investigation of a full-scale box-girder bridge together with comprehensive computational modeling. The major objective of the research was to evaluate the behavior of twin box girder bridges after the fracture of one girder and provide guidelines for modeling the post-fracture response. The tested bridge was simply supported; therefore, it did not have the structural redundancy that often exists for continuous multiple span (indeterminate) bridges. External braces that could contribute to load distribution in the damaged bridge were removed based on TxDOT practices. The authors conducted three tests at different damage states using different loading conditions. During the first test a sudden fracture was created at the mid-span of bottom flange of the exterior girder using charge explosives while an equivalent HS20 load was placed directly above the fractured girder. The bridge deflected less than one-inch. The second test was conducted under similar loading but this time a sudden full-depth fracture was created on the external

girder. The fractured external girder deflected 7 in. but could still support the service load. The third test was the ultimate load test while the exterior girder had full-depth fracture. The bridge could still carry more than five times the legal truck load. It was concluded that the prominent failure mode was initiated by pull-out of shear studs in the deck followed by crushing of the reinforced concrete deck.

The effect of different parameters including radius of curvature, railing and continuity were also considered in the tests and analysis. The effect of the railing significantly reduced the deflection while increasing the tensile forces on the stud connections. Therefore, ignoring the railing is not necessarily conservative in a redundancy analysis. The results also showed that the decrease in the radius of curvature resulted in an increase in the vertical deflection of the damaged girder. Based on experimental testing it was observed that the damaged bridge performed with sufficient redundancy to redistribute and continue to carry the very high applied loads.

Samaras et al. (2012) proposed a simplified method for evaluating the redundancy of twin steel box-girder bridges based on the work conducted as part of TxDOT Project 9-5498. The suggested method proposes initial strength check and yield line analysis for evaluating the remaining strength of the damaged bridge. A three level redundancy check was recommended:

(i) The initial strength check (ISC) of the bridge with intact girder is conducted. If the moment and shear strength is adequate and the deck has adequate shear capacity, the bridge can be called redundant.

(ii) If the initial strength check is not satisfied, a yield line analysis (YLA) can be performed. ISC cannot be used if the shear studs pull out from the deck concrete. Figure 2.6 depicts the surveyed deck deflections and assumed elastic plate displacements based on the actual failure shape. A yield line pattern was developed based on the observed failure shape. It was concluded that the assumed yield line could be used for fractured steel twin box girder bridges for estimating the ultimate load if shear studs pull out. Both ISC and YLA are conservative and convenient methods to quickly evaluate the redundancy level of fracture critical bridges. It was concluded this method can provide information about the mode of failure that can help identifying the remaining capacity of the bridge with a fractured girder.

(iii) If YLA also shows inadequate capacity then more sophisticated nonlinear computational methods such as finite element must be used.

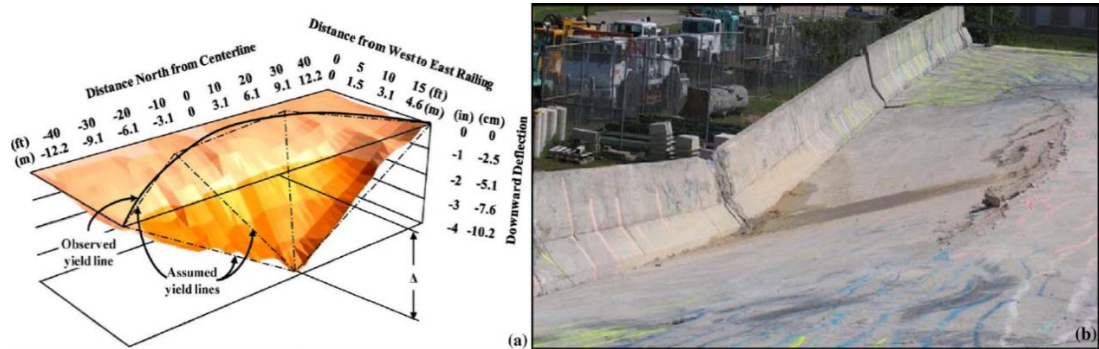


Figure 2.6. FSEL Bridge test: (a) Surveyed deflections and assumed yield line; (b) Damaged deck after test (Reprinted from Samaras et al. 2012).

Kim and Williamson (2014) developed finite-element modeling guidelines for evaluating the redundancy level of steel-twin tub bridges. This study was also conducted as part of TxDOT Project 9-5498. Their proposed modeling approach considers nonlinearity due to concrete cracking and crushing, as well as steel yielding. In addition, shear stud connection failure mechanism was also considered in the FEM model as stud connection failure may significantly affect redundancy. The pullout behavior of the embedded shear studs was evaluated through laboratory tests (Mouras et al. 2008; Sutton et al. 2014). A shear stud failure mode was observed during the second test where the girder had full depth fracture. The FEM models successfully estimated the bridge component failures. Both the test and FEM analysis suggested that the bridge had greater redundancy than defined by current code provisions.

After verifying the modeling approach, Kim and Williamson (2014) analyzed several other bridge configurations using the same modeling approach to investigate the remaining load capacity following a full-depth failure of one member. They concluded that the shear stud connection behavior is one of the important parameters for capturing the failure mode correctly and evaluating the redundancy level.

2.7. Research Questions Arising

In light of the foregoing survey of the state-of-the-art and state-of-the practice for fracture critical bridges in general and steel twin tub girder bridges in particular, certain lingering questions remain that will be addressed in this research as follows:

1. Is it possible to identify redundancy levels of existing and future steel twin tub girder bridges in order to classify them as non-fracture critical?

2. Do existing steel twin tub girder bridges have adequate capacity following the fracture of one box member?
3. Is it possible to develop reliable and easy to implement analysis criteria using grillage analysis?
4. It is possible to develop reliable an easy to implement analysis criteria using grillage analysis?

3. PARAMETRIC STUDY FOR STEEL TWIN TUB GIRDER BRIDGES USING NONLINEAR FINITE ELEMENT ANALYSIS*

3.1. Introduction

The chapter deals with a parametric study that includes the selection of 15 typical steel twin tub girder (STTG) bridges from the Texas bridge inventory, validating a FEM model to results obtained in TxDOT project 9-5498 (Barnard et al. 2010), and computational modeling of selected bridges using finite element method (FEM).

The current study investigates the performance of existing fracture critical steel twin tub girder bridges in the case of a full depth fracture of one of the girders. Therefore, a total of 15 steel twin tub girder bridges were selected by considering different span lengths, different degrees of curvature, and the effect of continuity. These parameters are considered to be critical geometric parameters for evaluating the bridges' response in terms of load distribution between girders.

The subsequent section presents the Texas steel twin tub girder bridge inventory and shows distribution of span lengths and curvatures for all STTG bridges.

3.2. Evaluation of TxDOT Steel Twin Tub Bridge Inventory

3.2.1. General

It is important to select the bridges that are representative of existing STTG bridge inventory. This selection is done using range of critical parameters that represent current

* Part of this chapter is reprinted with permission from "Fracture Critical Steel Twin Tub Girder Bridges Technical Report" 0-6937-R1 by Hurlebaus S., Mander J., Terzioglu T., Boger N., Fatima A., 2018. Texas A&M Texas Transportation Institute, 33-142, Copyright 2018 by Texas A&M Texas Transportation Institute

STTG bridges in Texas. The critical parameters were identified as span length, radius of curvature and continuity based on literature and input from TxDOT. The distribution of these three key parameters were investigated while selecting the 15 bridges for the parametric study.

3.2.2. Distribution of Texas STTG Bridges

The span length is one of the key parameters that can affect post-fracture behavior, overall flexural demand, and load distribution. The relatively high flexural strength of steel tub girders offers long span ranges up to 500 ft. An efficient lower span length is limited to 150 ft due to the 5 ft minimum web depth suggestion, which is for providing accessibility during inspection. Although very long spans have been achieved, most of the steel twin tub bridges are typically between 150 – 300 ft in length. Figure 3.1 presents the histogram of maximum span lengths for Texas STTG bridges. Majority of STTG bridges have between 150-300 ft span lengths with a median value of 210 ft.

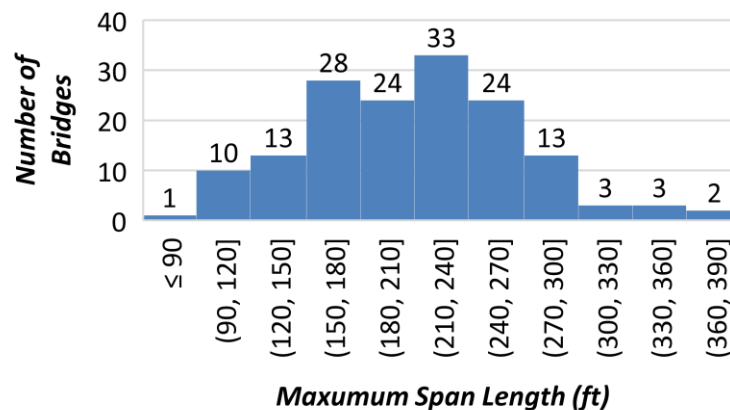


Figure 3.1. Distribution of Texas STTG Bridges by Maximum Span Length

Another important parameter is the horizontal curvature. Although steel tub girders can be used for straight bridges, they offer a great advantage for curved bridges due to their superior torsional stiffness. They can achieve extremely tight curvatures, up to 0.0067. The range of horizontal curvature may be considered from tangential to 150 ft radius. The flexural bending load demand on the outside girder increases as the curvature increases. Therefore, curvatures of STTG bridges were considered as one of the key parameters for the bridge selection process. Figure 3.2 shows the distribution of Texas STTG bridges by curvature. Most STTG bridges in Texas have curvature values between 0.0007 and 0.0016 with a mean curvature of 0.00123.

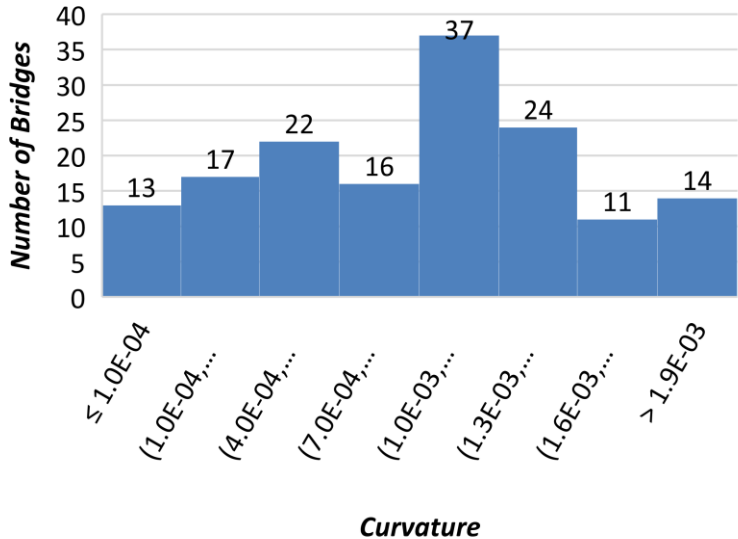


Figure 3.2. Distribution of Texas STTG Bridges by Curvature

The third parameter of importance is continuity, which generally improves residual capacity due to structural redundancy inherent to continuous bridges. Most STTG bridges are classified as fracture critical based on load-path redundancy which only considers lateral load distribution hence, categorizing bridges with less than three girders as fracture critical. However, structural redundancy due to continuity can contribute significantly to longitudinal distribution of the load hence, improving the flexural capacity. Therefore, different numbers of continuous spans including simply supported, two span continuous, and three span continuous bridges were considered in order to assess the effect of continuity on the level of redundancy. Figure 3.3 provides a histogram for the distribution of STTG bridges in terms of number of continuous spans. Most STTG bridges have three continuous spans followed by two span continuous bridges.

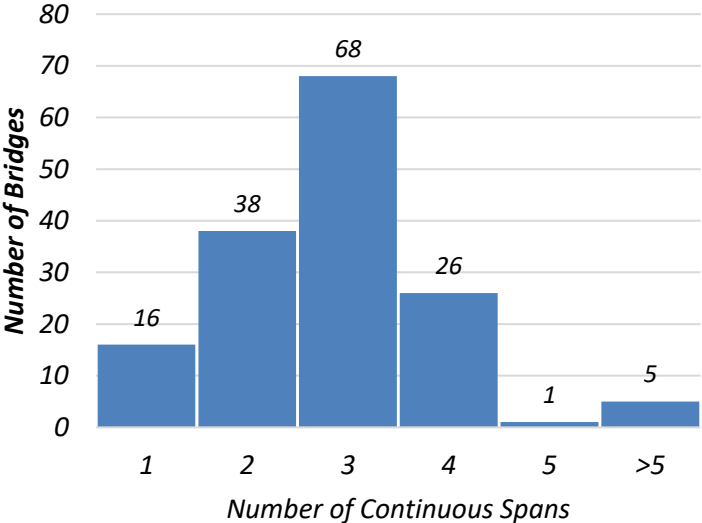


Figure 3.3. Distribution of Texas STTG Bridges by Number of Continuous Spans

The above listed three key parameters were evaluated to come up with a range of radii of curvatures, span lengths, and number of continuous spans that represent most Texas STTG bridges. Table 3.1 lists the range of selected parameters that are considered for the FEM models for the parametric study.

Table 3.1 Range of Parameters Considered for the Bridge Selection

Parameter	Range
Span Length, L	100 – 300 ft
Curvature, R	0 – 0.006
Continuity	Simple, Two and Three Spans

3.2.3. Selection of Fifteen Representative Steel Twin Tub Girder Bridges

The investigation of the histogram for number of continuous spans suggests that majority of selected bridges should be three-span continuous followed by two-span continuous and simple span bridges. These three groups represent all that is necessary to evaluate the structural behavior as they cover simple span, exterior and interior spans of continuous bridges. A total of 7 three-span continuous, 5 two-span continuous, and 3 simple span bridges were selected based on the distribution of Texas STTG bridges by number of spans.

Span length versus curvature scatter plots were created for simple, two-span, and three-span bridges (Figure 3.4, Figure 3.5 and Figure 3.6). The scatter plots were then grouped using k-means clustering which groups data points using the squared Euclidean distance measured. Clustering scattered data points helps to identify different data groups

with multi parameters. The solid red line shows where the span length to radius ratio is equal to 0.3 ft. For closed box and tub girders the effect of curvature may be ignored in the analysis for determination of the major-axis bending moments and bending shears if for all spans the arc span divided by radius is less than 0.3 radians, girders are concentric and bearings are not skewed (AASHTO 2014). The black circled points are the selected bridges for that specific category. The selection procedure followed two main criteria; (1) bridges from different clusters having similar curvature values but different span lengths, (2) bridges from same cluster having similar span length but different curvature.

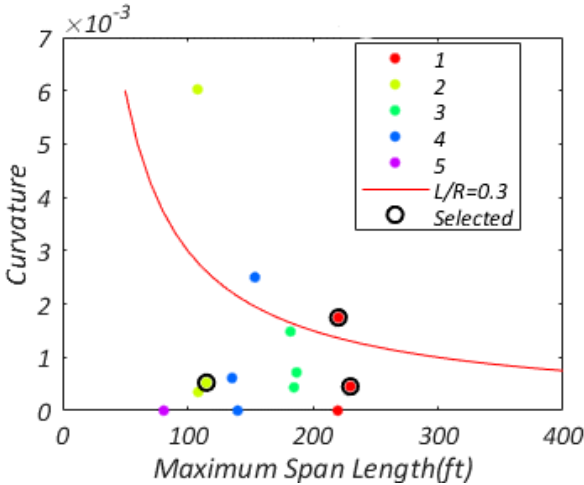


Figure 3.4. Span vs Curvature Scatter of Simple Span STTG Bridges in Texas

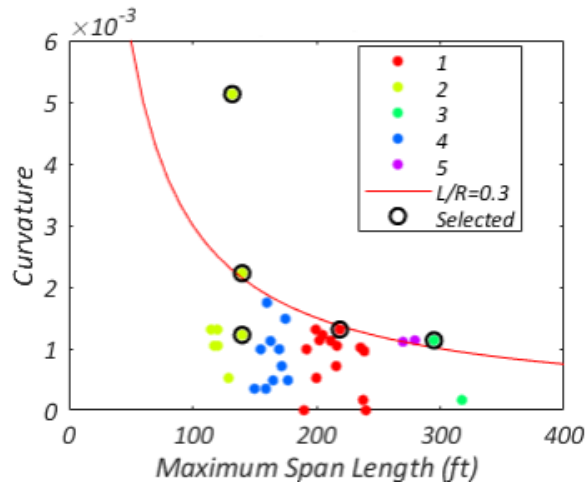


Figure 3.5. Span vs Curvature Scatter of Two-Span STTG Bridges in Texas

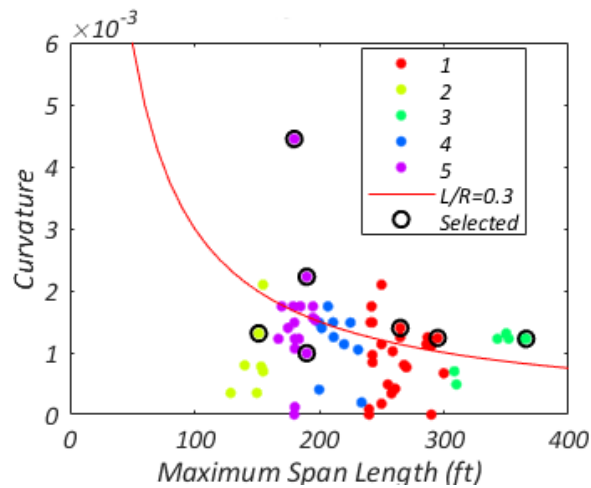


Figure 3.6. Span vs Curvature Scatter of Three-Span STTG Bridges in Texas

Figure 3.4 shows the scatter plot with selected bridges for simple span STTG bridges. Three simple span bridges were selected for parametric study; one bridge with small curvature from the short span cluster, another two bridges with small and large curvatures from the long span cluster. Similarly, Figure 3.5 presents the scattered

distribution of span length-curvature data and selected bridges for two span STTG bridges. A total of five two span bridges were selected for the parametric study; from different span length groups having various curvature values. Figure 3.6 presents clustered scatter of span-curvature data and selected bridges for three span STTG bridges. Four bridges from different span clusters ranging from short to long spans, and another three bridges from the medium span cluster having small medium and large curvatures were selected. Table 3.2 lists the selected Texas STTG bridges with their span length radius of curvature and continuity information. Full plans for all 15 bridges are located in Appendix A.

Table 3.2 Main Geometric Properties of Selected Texas STTG Bridges

Bridge No.	Bridge ID	Span 1 (ft)	Span 2 (ft)	Span 3 (ft)	Radius of Curvature (ft)
1	12-102-3256-01-403	220.5	-	-	573.0
2	12-102-0271-17-530	115.0	-	-	1909.9
3	12-102-3256-01-403	230.0	-	-	2207.3
4	12-102-0271-07-637	132.0	128.2	-	195.0
5	14-227-0-0015-13-452	140.0	139.6	-	450.0
6	12-102-0271-07-575	140.0	140.0	-	818.5
7	12-102-0177-07-394	218.9	189.7	-	763.9
8	12-102-0271-06-661	265.0	295.0	-	881.5
9	12-102-0177-07-394	139.5	151.4	125.6	763.9
10	14-227-0-0015-13-450	148.0	265.0	189.6	716.2
11	12-102-0271-07-593	223.0	366.0	235.0	818.5
12	12-102-0271-07-639	140.0	180.0	145.0	225.0
13	14-227-0-0015-13-452	151.5	190.0	151.5	450.0
14	18-057-0-0009-11-460	150.0	190.0	150.0	1010.0
15	12-102-0271-06-689	200.0	295.0	200.0	809.0

3.3. Nonlinear Finite Element Model of a Steel Twin Tub Girder Bridges

3.3.1. Validation of Finite Element Model

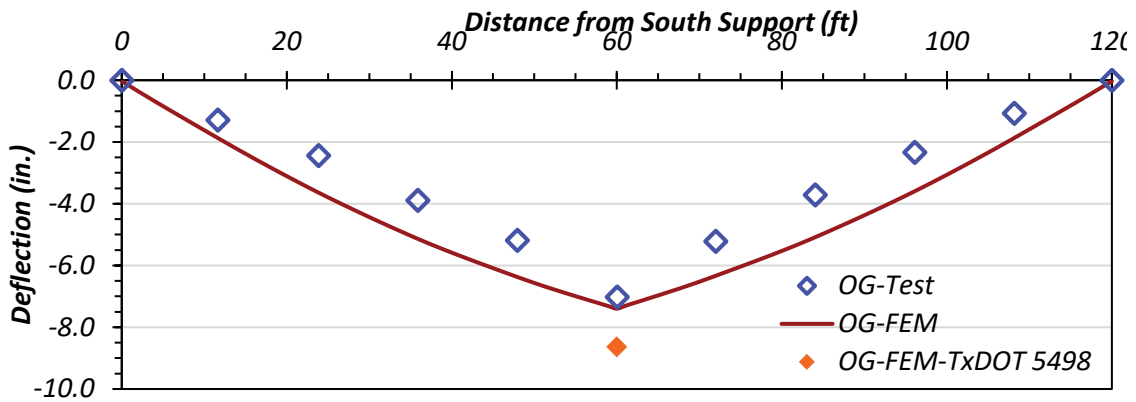
In conjunction with the grillage analysis of the bridges selected from the parametric study, an accompanying FEM analysis was conducted by Dr. Tevfik Terzioglu as part of the work completed in TxDOT project 0-6937 (Hurlebaus et al. 2018).

Terzioglu used Abacus to generate a FEM model of the FSEL test bridge in TxDOT project 9-5498 (Barnard et al. 2010). The FSEL test bridge was 120 foot long twin tub girder bridge, with a deck width of 23 feet 4 inches and a radius of curvature of 1365 feet. Four different loading conditions were applied to the test bridge. The first load case was a HS-20 truck load with a fully intact tension flange and web. The second load case was a HS-20 truck load with a fractured tension flange but intact web. The third load case was an HS-20 truck load with fractured tension flange and web. The final load case was at ultimate loading conditions. Loads were simulated using concrete girders for load cases 1 thru 3 and sand was additionally used in load case 4.

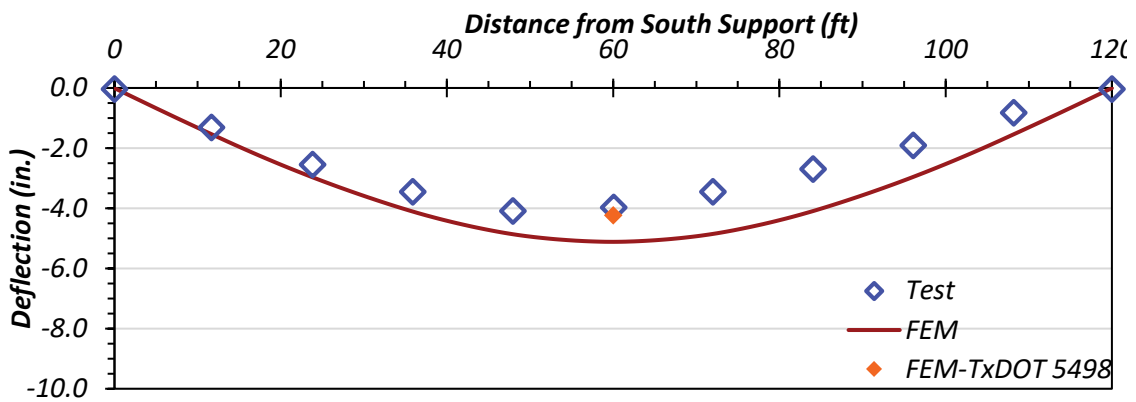
Elasto-plastic material models were chosen for the for FEM model as to capture full material nonlinearity of concrete crushing and steel yielding. Appropriate shear stud and haunch constitutive mechanical models were used to accurately model the behavior. Compatible finite elements were used to model the various components of the bridge. The concrete deck and railing was modeled by three dimensional 8-node linear continuum elements (C3D8). Reinforcing bars were modeled using 2-node truss elements (T3D2). Steel tub members and intermediate diaphragms were modeled using 8-node quadrilateral shell elements (S8R). Internal bracing was modeled using first order three dimensional

beam elements (B31). The boundary conditions were simply supported elastomeric bearing pads.

The FEM was validated for load cases 2 thru 4. The results for load case 3 can be seen in Figure 3.7. It should be noted that there is close agreement with the FEM model and the deflection profile of both the fractured outside girder as well at the intact interior girder. In TxDOT report 0-6937 it was concluded that the FEM accurately represented the bridge behavior.



(a) Fractured East Girder



(b) Intact West Girder

Figure 3.7 Comparison of FEM deflection profile with test results after web fracture (Reprinted from Hurlebaus, 2018)

3.3.2. FEM Parametric Study of Fifteen Bridges

Terzlioglu generated an FEM model for each of the 15 preselected bridged from the TxDOT inventory and obtained the results for the both the intact and complete exterior girder failure cases. From the results of the bridge models a redundancy level or overstrenght factor was determined for each bridge and is defined as

$$\Omega = R_d/Q_u \quad (3.1)$$

where R_d = capacity of the damaged bridge, and Q_u = factored load demand. The bridge can be considered redundant with sufficient reserve capacity when $\Omega > 1.0$.

HL-93 loading conditions were applied to bridges which consist of 1.25DL+1.75(HS20+IM)+1.75LL as per AASHTO LRFD Bridge Design Specifications (2014) where DL, LL and IM represent dead load, lane load, and impact factor, respectively. Failure is defined by two limit states: ultimate limit state and deflection limit state. Ultimate limit state is defined by a load at which the fractured bridge drops below 5 percent of the initial stiffness of the intact bridge. The deflection limit state is defined by two different criteria: (1) a cord rotation of 2 degrees for simply supported and interior spans; and 3 degrees for exterior spans in the longitudinal direction; and (2) a transverse deck rotation of 5 degrees. The lowest of the three failure modes controls. The overstrength factors, as determined by FEM, for all the single span, interior spans, and exterior spans are located in Table 3.3, Table 3.4, and Table 3.5 respectively.

Table 3.3 FEM Overstrength Factors for Single Span STTG Bridges (Reprinted Hurlebaus et al. 2018)

ID	Span	R (ft)	L (ft)	B (ft)	S (ft)	5% SF	5° Trans.	2° Long.
0	1	1300	120	23	6.0	0.86	-	0.91
1	1	573	220	32	9.5	0.88	0.82	0.82
2	1	1910	115	26	6.1	1.75	1.70	1.65
3	1	2207	230	39	12.6	0.88	0.85	0.87

Note: L= length, B=breadth, R=radius of curvature, S=spacing between interior top flanges

**Table 3.4 FEM Overstrength Factors for Interior Spans of STTG Bridges
(Reprinted from Hurlebaus et al. 2018)**

ID	Span	R (ft)	L (ft)	B (ft)	S (ft)	5% SF	5° Trans.	2° Long.
9	2	764	151	28	7.0	2.45	2.55	2.50
10	2	716	265	30	7.7	2.05	1.60	1.45
11	2	819	366	28	7.0	2.45	1.20	1.55
12	2	225	180	28	7.6	2.10	2.05	1.80
13	2	450	190	30	9.3	1.75	-	1.40
14	2	1010	190	28	6.5	2.00	-	1.80
15	2	809	295	28	8.0	1.40	1.70	1.50

Note: L= length, B=breadth, R=radius of curvature, S=spacing between interior top flanges

**Table 3.5 FEM Overstrength Factor for Exterior Spans of STTG Bridges
(Reprinted from Hurlebaus et al. 2018)**

ID	Span	R (ft)	L (ft)	B (ft)	S (ft)	5% SF	5° Trans.	2° Long.
4	1	195	132	28	7.6	2.00	2.30	1.65
4	2	195	128	28	7.6	2.03	-	1.73
5	1	450	140	30	9.7	1.50	-	1.20
5	2	450	140	30	9.7	1.50	-	1.20
6	1	819	140	38	9.8	1.90	2.10	1.80
6	2	819	140	38	9.8	1.90	2.10	1.80
7	1	764	219	28	7.4	1.40	1.20	1.20
7	2	764	190	28	7.4	1.75	-	1.45
8	1	882	265	28	8.4	0.99	-	-
8	2	882	295	28	8.4	0.88	-	0.91
9	1	764	140	28	7.4	1.80	2.00	1.70
9	3	764	126	28	7.4	1.90	2.15	1.80
10	1	716	148	30	7.7	1.70	-	1.70
10	3	716	190	30	7.7	1.60	-	1.45
11	1	819	223	28	7.0	1.60	-	1.70
11	3	819	235	28	7.0	1.60		1.65
12	1	225	140	28	7.6	1.90	1.95	1.60
12	3	225	145	28	7.6	1.90	1.90	1.60
13	1	450	152	30	9.3	1.50	-	1.00
13	3	450	152	30	9.3	1.50	-	1.00
14	1	1010	150	28	6.5	1.80	-	1.65
14	3	1010	150	28	6.5	1.80	-	1.65
15	1	809	200	28	8.0	1.80	-	1.70
15	3	809	200	28	8.0	1.80	-	1.70

Note: L= length, B=breadth, R=radius of curvature, S=spacing between interior top flanges

4. PARAMETRIC STUDY FOR STEEL TWIN TUB GIRDER BRIDGES USING GRILLAGE METHOD PUSH-DOWN ANALYSIS*

4.1. Introduction

The task at hand consist of a parametric study involving a selection of 15 preselected typical steel twin tub girders (STTG) bridges from the Texas bridge inventory utilizing a Grillage Method Push-down Analysis. These 15 bridges are the same bridges evaluated using the Finite Element Method (FEM) in Chapter 3. The Grillage method employed was verified using the static ultimate load test results of the STTG bridge tested in Texas Department of Transportation (TxDOT) research project (Barnard et al. 2010). The TxDOT project 9-5498 consisted of testing a full scale fracture critical steel box girder bridge under simulated HS-20 truck loading and at ultimate loading with a full depth fracture on the exterior girder.

This task evaluates the performance of existing fracture critical steel twin tub girder bridges in the event of a full depth web fracture of one of the girders. The 15 bridges that are under evaluation vary with respect to span lengths, degree of curvature, and continuity. These variables are considered to be the most critical geometric properties for determining the response of a bridge in reference to load distribution between girders.

Grillage models have been created using the commercial software package SAP2000 which is a structural analysis program that utilizes the matrix structural analysis

* Part of this chapter is reprinted with permission from “Fracture Critical Steel Twin Tub Girder Bridges Technical Report” 0-6937-R1 by Hurlebaus S., Mander J., Terzioglu T., Boger N., Fatima A., 2018. Texas A&M Texas Transportation Institute, 195-259, Copyright 2018 by Texas A&M Texas Transportation Institute

approach to solve and evaluate structural engineering problems. All of the Grillage bridge models have used nonlinear elasto-plastic material and hinge properties due to the nonlinear behavior of the reinforcing bars, steel plate, and concrete during concrete crushing and steel yielding under ultimate loading conditions. The Grillage models were analyzed under the factored HL93 live loading model. This loading pattern consists of HS20 truck loading as well as a uniformly distributed lane load. Per AASHTO LRFD Bridge Design Specifications (AASHTO 2017), the load demands were $1.25DL+1.75(LL+IM)$, where DL, LL, and IM represent respectively dead load, live load, and impact factor.

The bridges evaluated utilizing the Grillage method were analyzed twice: (1) analysis of the bridge with the intact girder condition, (2) analysis of the bridge with full depth girder fracture for one of the tub girders. The intact bridge analysis provides information about the initial stiffness of the intact bridge as well as the overstrength factor for the nonfractured case. The second analysis is for simulating the ultimate load behavior when one of the girders are fractured. A predefined overstrength factor was determined for both the fully intact case and one fractured girder case to assess the load carrying capacity of both cases under critical loading. The Grillage method allows for load redistribution from the fractured girder through the lateral deck slab members.

The following section describes the Grillage method and material models used for all evaluated bridges. The third section gives the load displacement results of the Grillage models as well as their respective overstrength factor results.

4.2. Grillage Method Push-Down Analysis

4.2.1. Introduction

The grillage method is a computational variation of the strip method, both of which are conservative lower bound solutions. The strip method has been employed by designers due to its ability to quickly generate solutions by hand. Like the strip method the grillage method models the bridge deck and beam elements as a “grillage” of beams. The longitudinal grillage members consists of the steel tub girders, the concrete deck with longitudinal reinforcement, and the guardrail. The transverse grillage members are bridge deck components with transverse reinforcement.

The grillage method was originally developed in the 1950’s by Lightfoot and Sawko (1959). Created in the primitive days of matrix structural analysis, the grillage method was utilized to divide a bridge deck into equivalent longitudinal and transverse beam members which resembled a grillage. Due to the increase in technological abilities, through programs such as SAP2000, this method has increased in accuracy. Surana and Agrawal (1998) studied the grillage method of analysis as it applies to various bridge types. It was discovered that, when compared with other method of analysis, including FEM, that the grillage method of analysis was an accurate and valid modeling technique.

Grillage models of the preselected 15 bridges were created and analyzed using the structural analysis software SAP2000 version 19 (Computers and Structures 2017). The grillage models should capture the constitutive material behavior and boundary condition to be able to accurately predict load displacement behavior and the ultimate load capacity of the analyzed bridge. For all 15 bridges, the support conditions were modeled using

springs with a lateral stiffness of 6 kip/in. and a vertical stiffness of 3050 kip/in. These values are conducive with the stiffness values used in the elastomeric bearing pads at the support locations in the bridge. Appropriate steel and concrete nonlinear material models were used to ensure appropriate modeling of the bridge behavior under the ultimate loading conditions.

4.2.2. Material Models

Grillage models generated for the 15 bridges in the parametric study were created using similar material models utilized in FEM modeling approach. Nonlinear material models were used for the Grillage analysis of the bridges due to the concrete crushing and yielding of the steel plates and reinforcing bars. The steel model used for both reinforcing bars and steel plates assume nonlinear elastic-plastic behavior with strain hardening. The mechanical constitutive model of concrete considers nonlinear inelastic behavior up to peak stress level without damage mechanics. Therefore it assumes perfectly plastic behavior beyond peak compressive and tensile stress.

4.2.2.1. Steel Material Model

The built-up plate components of the STTG bridges are comprised of grade 50 structural steel. The constitutive behavior of both the steel members and reinforcing bars use the classical metal plasticity models with strain hardening. The nonlinear steel models assume a perfectly plastic behavior once the yield stress is reached. The reinforcing bar in both the longitudinal and transverse directions as well as railings consist of grade 60 ASTM A615 steel.

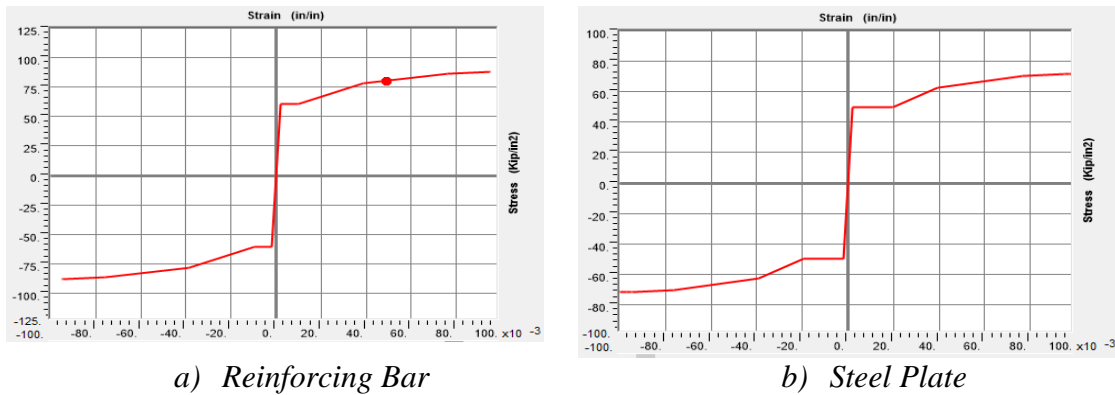


Figure 4.1 Constitutive Model for Steel Members (from SAP2000)

Figure 4.1 shows the stress-strain relationship of both the plate steel and reinforcing bars. Both steel plate and rebar constitutive behavior were obtained from material test conducted on actual coupons as part of TxDOT project 9-5498 (Barnard et al. 2010).

4.2.2.2. Concrete Material Model

The constitutive concrete behavior was defined using the Kent and Park (1971) model, the same model used in the FEM analysis with a design strength of 4000 psi. After reaching ultimate compressive and tensile forces the concrete behavior is assumed to be perfectly plastic.

Figure 4.2 shows the stress-strain behavior of the concrete used for the grillage models. The tensile strength of the concrete was calculated using the empirical equation in AASHTO (2017) Article 5.4.2.6 as:

$$f_r = 0.2\sqrt{f'_c} \quad (4.1)$$

where, f_r = the modulus of rupture (ksi) and f'_c = compressive strength of concrete (ksi). The modulus of elasticity of concrete for different was calculated using an empirical equation from AASHTO (2017) Article 5.4.2.4 as:

$$E_c = 33000K_1w_c^{1.5}\sqrt{f'_c} \quad (4.2)$$

where, K_1 =correction factor for aggregate source and assumed to be 1.0 unless determined by physical test; w_c =unit weight of concrete (kcf), 0.145 is assumed for normal weight concrete; f'_c =compressive strength of concrete (ksi).

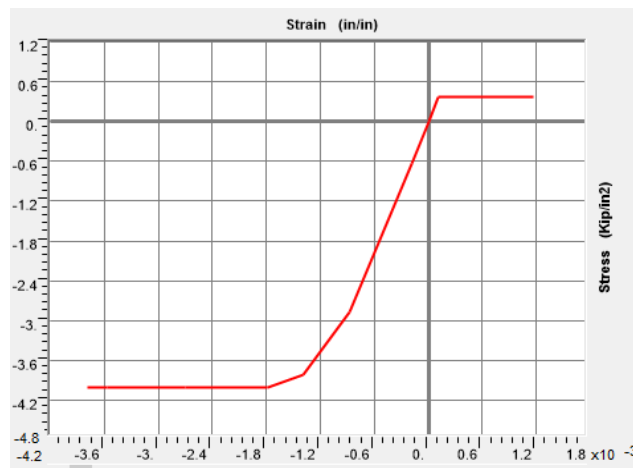


Figure 4.2 Constitutive Model of Concrete (from SAP2000)

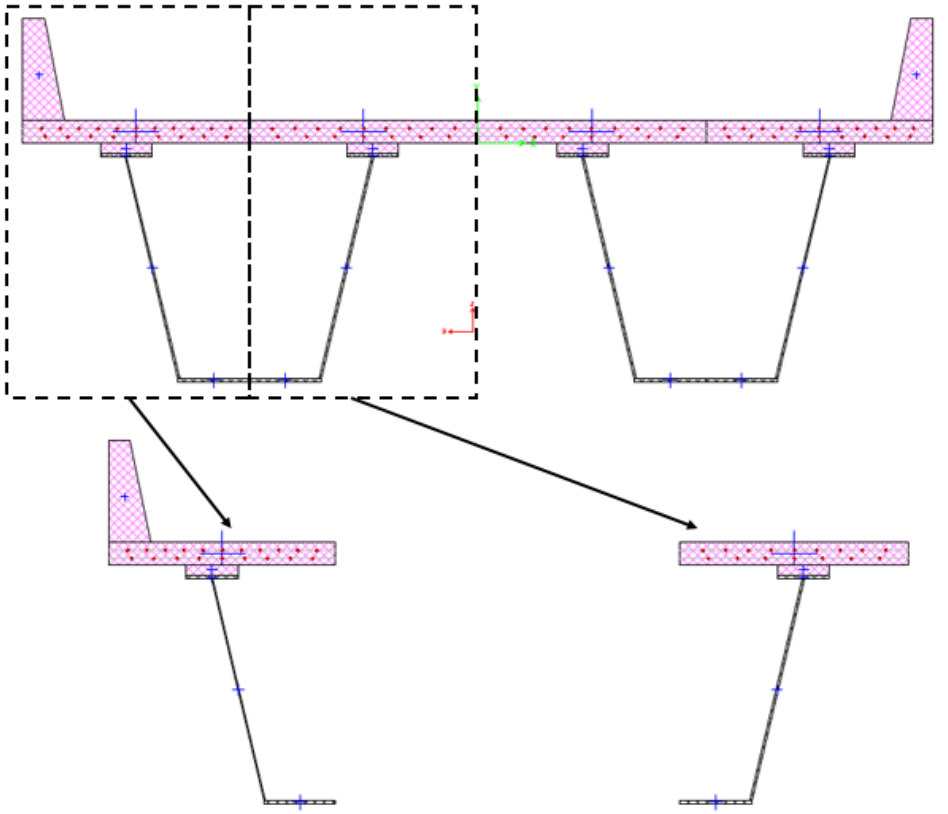
The constitutive model from SAP2000 indicates that beyond compressive crushing and tensile rupturing the strength is maintained. This behavior was utilized to be consistent with the FEM modeling approach and to avoid convergence issues in SAP2000.

4.2.3. Grillage Beam Elements

Hambly and Pennells (1975) and Barker and Puckett (2007) have established guidelines for the construction and location placement of beam elements. It is recommended that for each grillage member to take on the same bending and torsional properties of their representative bridge sections. For the case of slab-on-girder bridges, the longitudinal beam element should be placed along the centerline of the girder. Since the twin tub girders are so wide, in this grillage analysis they were divided in half and the centerline of the top flange was used as the centerline for the placement of grillage elements. This maintains the stiffness at the appropriate location within the bridge structure, and appropriate load distribution. Lateral beam members should be placed at appropriate locations. Grillage members should be positioned in locations of high stress and forces. High force and stress locations could include interior and exterior supports and point load locations. In order to assure accurate load distribution it is important that the longitudinal and transverse members are equally gaged in both directions.

The exterior longitudinal members (Figure 4.3a) consist of the guardrail, the deck from the outside edge to the center of the tub girder including corresponding reinforcing bars, and half of the tub girder. The interior longitudinal members (Figure 4.3b) consists of the deck from the center of the tub girder to the centerline of the bridge with corresponding reinforcing bars and half of the tub girder. The transverse members (Figure 4.4a-b) consist of deck slab and transverse reinforcing bars. The longitudinal members are placed along the centerline of each of the four top flange members of the tub girders. The

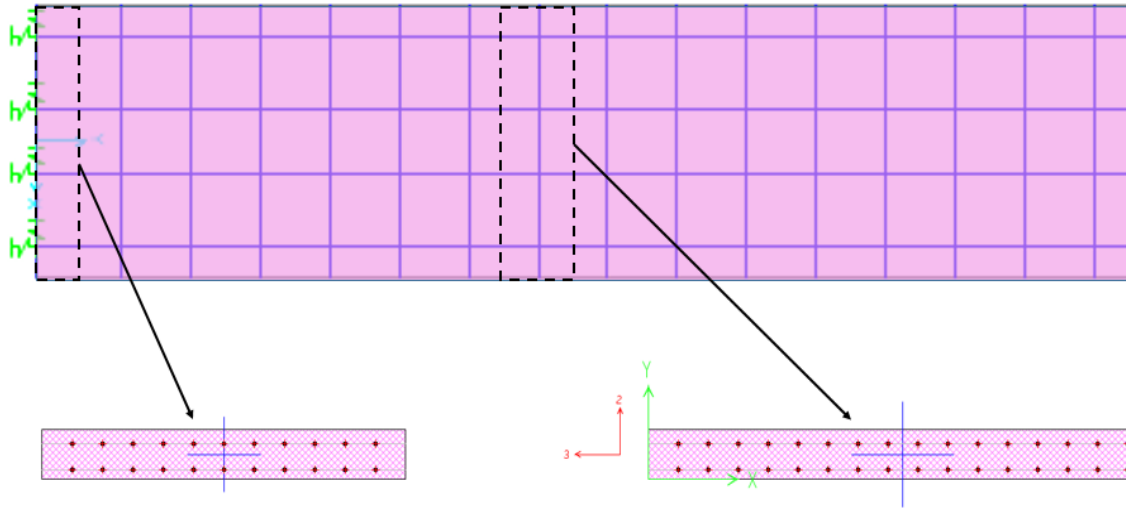
transverse members are placed at 7 ft increments along the interior with varying spacing at the end supports. Figure 4.5 is a representative grillage schematic of a grillage model.



a) Exterior Longitudinal Member

b) Interior Longitudinal Member

Figure 4.3 Representative Longitudinal Grillage Members



a) Exterior Transverse Member

b) Interior Transverse Member

Figure 4.4 Representative Transverse Grillage Members

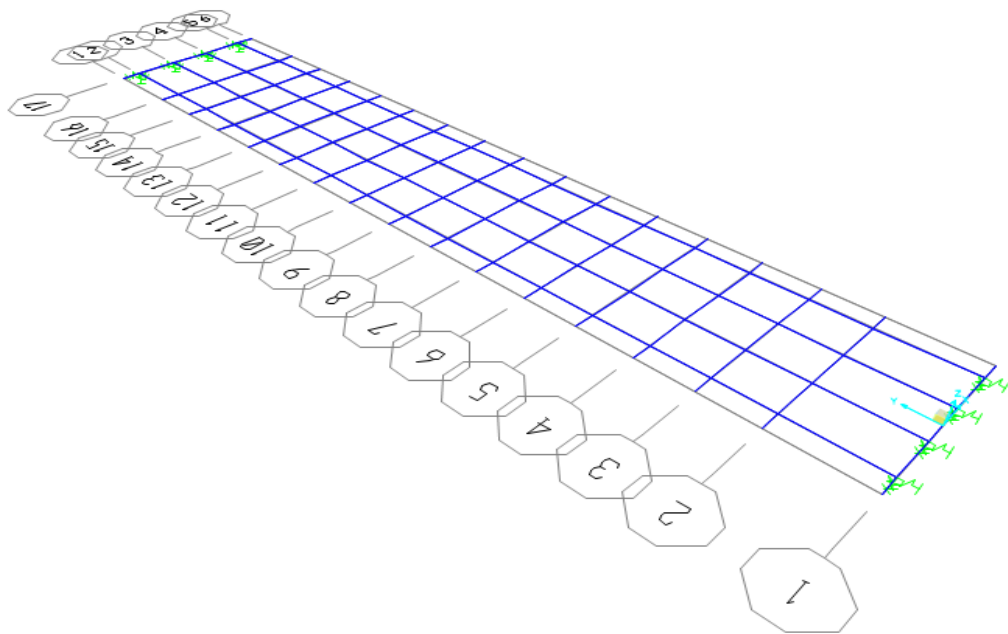


Figure 4.5 Representative Grillage Schematic

4.2.4. Grillage Plastic Hinges

In order to capture the nonlinear behavior of the bridge at ultimate loading conditions the nonlinear static analysis approach, which is also known as “push down analysis”, was used. Incorporating this approach reduces the uncertainty and conservatism inherently existing in elastic analysis. Since the bridge superstructure is modeled as grillage of beam elements the inelastic behavior is achieved by using plastic hinges at the anticipated hinge locations. The hinges used are moment controlled (M3) in the global Z (or gravitational) direction. Longitudinal and transverse hinges were developed using the moment curvature responses of the individual cross-sections. The individual cross-sections were generated using the section designer tool in SAP2000 which allows the user to combine the concrete, reinforcing bars, and steel plates into one composite grillage member. Once the member is created, SAP2000 has a moment curvature feature within the section designer which generates the moment curvature response of the composite section. In the case of the fractured longitudinal plastic hinge the bottom flange and web were removed prior to generating the moment curvature diagram.

The length of the plastic hinge was taken to be half of the depth of the member both in the transverse and longitudinal directions. Two of the most prominent hinge length expressions for reinforced concrete beam elements in flexure were developed by Corley (1966) and Mattock (1967) represented as:

$$l_p = 0.5d + 0.5\sqrt{d}(z/d) \quad (4.3)$$

$$l_p = 0.5d + 0.05(z) \quad (4.4)$$

where, l_p = plastic hinge length, d = member depth, and z = distance from hinge to node location. For the purposes of this section the hinge is located at the point of contra flexure therefore driving the value of z to 0. The remaining portions of both expressions reduces to half the member depth value.

A representative external longitudinal intact plastic hinge is shown in Figure 4.6. For convergence requirements, once the maximum moment value was reached, a perfectly plastic assumption was made and the maximum moment was maintained for all further rotation. Perfectly plastic assumption is acceptable as the aim was to identify the ultimate load, not the post peak load degradation of the structure.

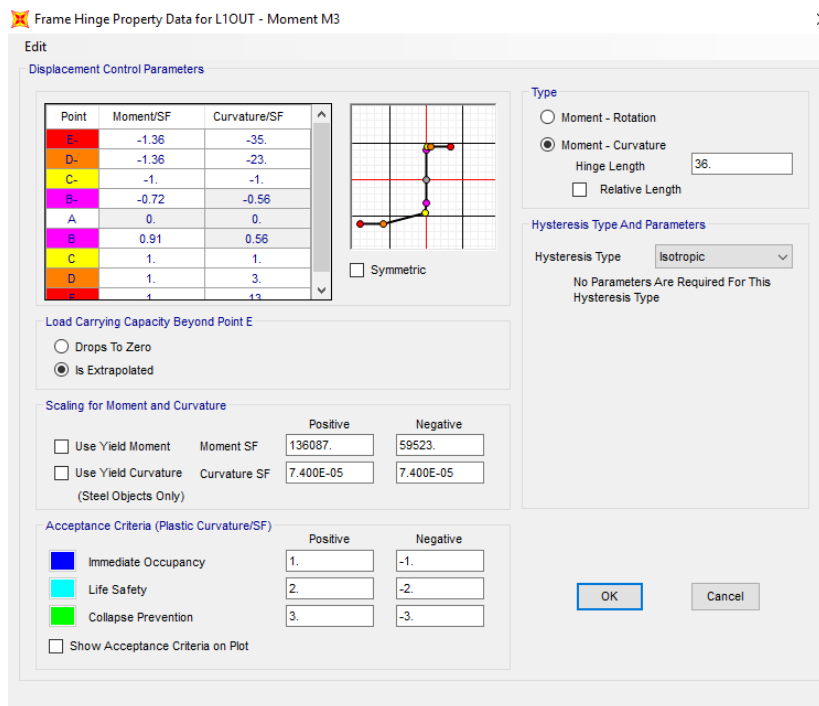


Figure 4.6 Representative Plastic Hinge Property (SAP2000)

For the longitudinal members the hinges were placed at both ends of the longitudinal beam elements. For the transverse members the hinges were placed at the edge of the top flanges or a distance of half a flange length from each node. All plastic hinge properties are located in Appendix B.

4.2.5. Simulating HL93 Loading

In simulating the HL93 loading it was critical to place the HS20 truck load and the uniform lane load at the appropriate critical locations shown in Figure 4.7. The interior transverse grillage beams were placed at 7 ft increments to have a grillage member at locations corresponding to the axles of HS20 truck that has axle spacing of 14 ft. The center axle of the truck load was placed at the midspan. HS20 truck consists of 32 kips middle and rear axles and 8 kips front axle for a total of 72 kips. The distance between wheel lines of the truck is 6 ft.

When analyzing two lane bridges the first lane, which is 12 ft wide, was defined as close as possible to the outside edge of the curved bridge to create most adverse loading condition when outside girder has full depth web fracture. AASHTO LRFD (2017) requires that a design lane should be at least 2 ft away from the nominal rail face which is generally one foot away from the edge of the deck. To create most adverse loading conditions both the HS20 truck and the uniform lane load was placed starting at the outside edge of the design lane. For the first lane loading, the first wheel line of the truck was placed at 3 ft from the edge of the deck (at the outside edge of the first lane) and per the HS20 definition the second wheel line is located 6 ft from the first wheel line. The standard uniform lane load is distributed to 10 ft width and starts at 3 ft from the outside edge of

the deck and ends at 13 ft from the deck edge. Therefore the uniform lane load for the first lane was modeled by a line load of 0.64 kip/ft along the longitudinal members located at 8 ft from the outer edge of the bridge. Since the line load generally occurred between two grillage members, an equivalent load was distributed appropriately to each of the grillage members. The second lane loading is the same as the first one, however, it begins at the edge of the second lane, which is 15 ft away from the outer edge of the deck.

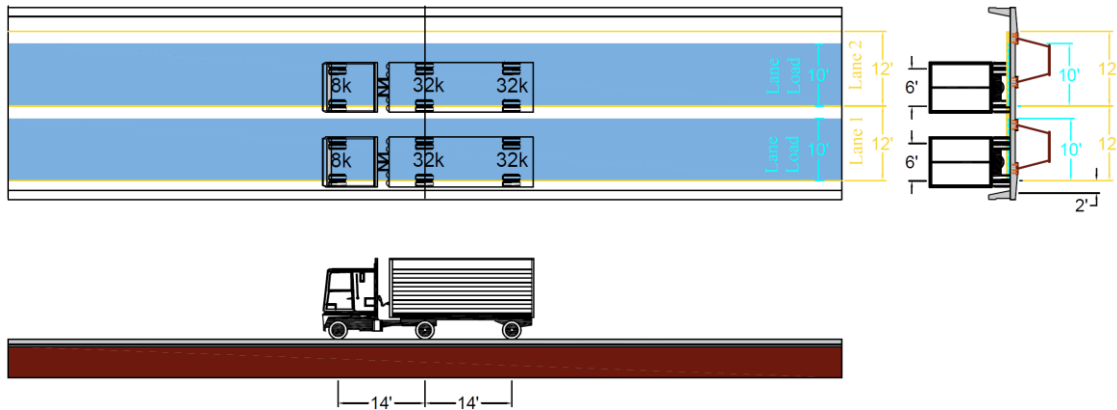


Figure 4.7 HL93 Loading Diagram for Two-Lane Loaded Case

Each bridge was first analyzed in its intact condition with no fractures. Subsequently, the fractured model for each bridge was analyzed. Load steps were generated for two lanes loaded case as follow: $1.25DL+1.75LL+1.75(HS20+IM)$ where, DL is dead load, LL is lane load, IM = 33% impact load, and HS20 is the HS20 truck load.

The intact bridge was analyzed first. The grillage members were generated in SAP2000's section designer. Using the moment curvature feature within the section designer moment curvature output was produced for each of the transverse and

longitudinal members in the bridge. Plastic hinges were developed for each of the intact members based on the moment curvature criteria produced from the section designer. The longitudinal and transverse grillage members were then arranged in a grillage array that adequately represented the geometry for the bridge. End spring supports were then added to represent the elastomeric bearing pads. Appropriate section hinges were added to each node, or crossing of longitudinal and transverse members. HS20 truck loads and lane loads were appropriately defined and assigned to the correct grillage elements. The standard load case was then defined as $1.25\text{DeadLoad}+1.75\text{LaneLoad}+2.33\text{HS20Load}$. The first loading step began at zero stress state, each additional load case began at the final loading and displacement of the preceding load case. Each load step was applied to the bridge in 20 increments. Load steps were continually applied to the bridge until the stiffness reduces to 5% of the initial stiffness of the intact bridge.

After the analysis of the intact bridge, the bridge in its fractured state was evaluated. Once the analysis of the intact bridge was complete, a copy of both the exterior and interior longitudinal sections at midspan were created. The bottom flanges and webs were removed in both sections to mimic a full web fracture. Using section designer, moment curvature plots were generated for each of the sections as well as compatible hinges. At midspan of the intact bridge, the exterior and interior longitudinal hinges were then replaced, on the heavily loaded side of the bridge, with the representative fractured hinges. The bridge was then analyzed under the same loading sequence as the intact bridge starting from a state of zero stress with continuous additions of the standard load case in 20th increments until the stiffness was reduced to 5% of the stiffness of the intact bridge,

the transverse rotation was greater than 5°, or the longitudinal rotation for the exterior spans was greater than 3° and interior spans is greater than 2°.

SAP2000 has a load case feature called staged loading which allow certain loads to be applied to certain members during various stages of construction. An example of this would be applying the dead load of the tub girder and the weight of the concrete slab to only the tub girder of the composite member, while applying the live loads and impact loads to the composite deck and tub girder member. Staged loading would have allowed for a more accurate representation as to the true load displacement nature of both the intact and fractured bridge spans. However, this could not be utilized in the fractured bridge case due to the fact that staged loading does not allow for frame section or plastic hinge substitutions during mid loading. For comparative purposes of the intact and fractured bridges were loaded from a zero stress state in complete composite action.

4.3. Grillage Analysis of selected STTG Bridges

In order to successfully gage the redundancy of the 15 STTG bridges it was important to establish a quantitative measurement of the remaining strength in the bridge beyond the factored design load demand. An overstrength factor was established to measure the residual strength and is defined as:

$$\Omega = R_d/Q_u \quad (4.5)$$

where, R_d =capacity of the damaged bridge, and Q_u =factored load demand. Bridges where, $\Omega > 1.0$, are considered redundant and have enough reserve capacity post fracture. In this section, redundancy levels are established via the Grillage results using design material properties. The loading condition, as per AASHTO LRFD Bridge Design

Specifications (AASHTO 2017), used was $1.25DL+1.75(HS20+IM)+1.75LL$, where DL, LL, and IM are dead load, uniform lane load, and impact factor, respectively.

4.3.1. Grillage Analysis of Bridge 0- FSEL: TxDOT Project # 0-6937

FSEL Tests Bridge, included in TxDOT project number 0-6937, is a simple span straight bridge used for research purposes and for method verification earlier on this project. The FSEL test bridge has span length of 120 ft, a bridge width of 23 ft 4 in, and an 8 inch deck. Full bridge details are located in Table 4.1 and Table 4.2. The FSEL test bridge was evaluated using the established grillage method. It should be noted that, due to the narrow road width, only one lane of HL93 loading was use to evaluate the post fracture redundancy.

Table 4.1 Geometric Details of Steel Tub Girders for Bridge FSEL (0)

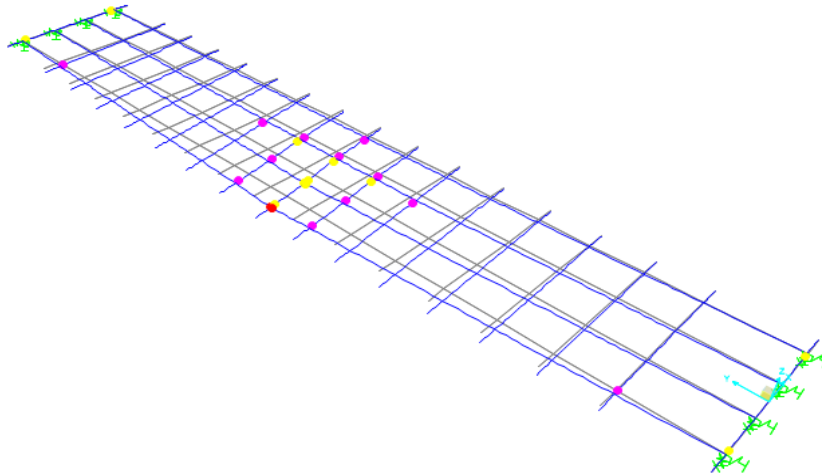
Location ft	Top Flange		Web		Bottom Flange	
	Width in.	Thickness in.	Width in.	Thickness in.	Width in.	Thickness in.
0-120	12	0.625	57	0.5	47	0.75

Table 4.2 General Geometric Properties of Bridge FSEL (0)

Location	Parameter	Description/Value
Bridge	Length, ft	120
	Spans, ft	120
	Radius of Curvature, ft	-
	Width, ft	23.333
Deck	Thickness, in.	8
	Haunch, in.	4
	Rail Type	T501
Rebar	# of Bar Longitudinal Top Row (#4)	32
	# of Bar Longitudinal Bottom Row (#5)	30
	Transverse Spacing Top Row (#5)	6
	Transverse Spacing Bottom Row (#5)	6

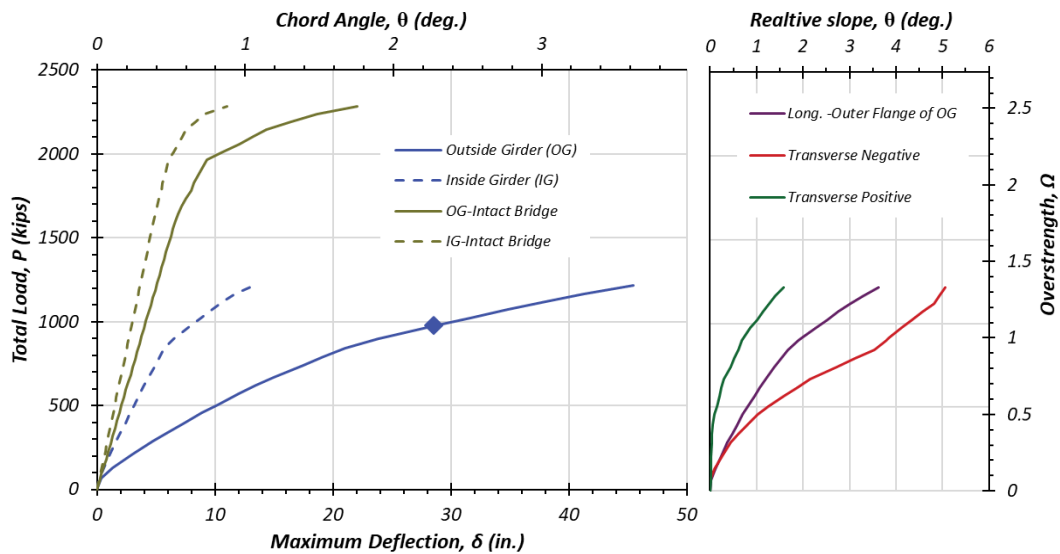
Figure 4.8 depicts the displacement profile with activated hinges of Bridge FSEL (0). Figure 4.9 shows the grillage analysis results of the FSEL Bridge. The solid lines indicate the behavior of the outside girder and the dashed lines indicate the behavior of the inside girder. The blue color represents the load displacement results for fractured model and the color green represents the load-displacement results of the intact model. The ultimate load capacity of the fracture bridge model is indicated by a blue diamond symbol. The ultimate load capacity of the bridge is defined as the lowest of the following: when the stiffness of the bridge falls below 5% of the initial stiffness of the intact outside girder, or the transverse rotation is greater than 5°, or the longitudinal rotation is greater than 2°.

The fractured FSEL Bridge fails under HL93 loading at an overstrength factor of 1.07 via longitudinal rotation. While the intact bridge fails under stiffness control at an overstrength value of 2.55.



Note: The colors represent achieved curvature limits (Magenta=yielding, Yellow=beyond yielding, Orange=beyond yielding close to failure, Red=Failure) Additional Hinge Data Located in Appendix

Figure 4.8 Grillage Deflection Profile of Bridge FSEL (0) with Activated Hinges



(a) Load-displacement

(b) Deck rotations

Note: δ is along the centerline of the girder, Ω is the load normalized by factored design load

Figure 4.9 Grillage Analysis Results of Bridge FSEL (0)

4.3.2. Grillage Analysis of Bridge 1-NBI #12-102-3256-01-403

Simple span, 220.5 ft long, 32 ft 5 in. wide Bridge 1 is primarily supported by two steel tub girders, built along the IH 10 connector in 2007, located in Houston, TX, and has 8 in. thick deck. Table 4.3 and Table 4.4 contain the necessary geometric information for generating an adequate Grillage model.

Table 4.3 Geometric Details of Steel Tub Girders for Bridge 1

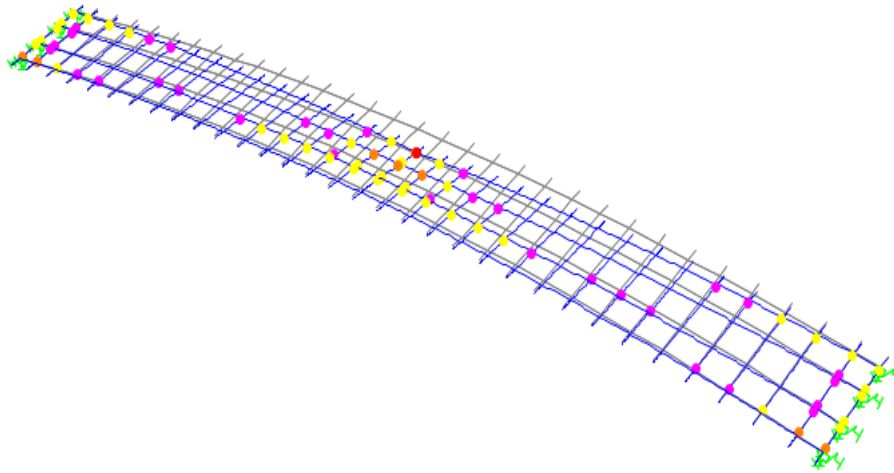
Location ft	Top Flange		Web		Bottom Flange	
	Width in.	Thickness in.	Width in.	Thickness in.	Width in.	Thickness in.
0-52	18	1.50	84	0.625	72	1.00
52-167	18	2.25	84	0.625	72	1.50
167-220	18	1.50	84	0.625	72	1.00

Table 4.4 General Geometric Properties of Bridge 1

Location	Parameter	Description/Value
Bridge	Location	Harris County, I610
	Year Designed/Year Built	2004/2007
	Design Load	HS20
	Length, ft	220.46
	Spans, ft	220.46
	Radius of Curvature, ft	572.96
Deck	Width, ft	32.417
	Thickness, in.	8
	Haunch, in.	5
	Rail Type	SSTR
Rebar	# of Bar Longitudinal Top Row (#5)	38
	# of Bar Longitudinal Bottom Row (#5)	44
	Transverse Spacing Top Row (#5) in.	5
	Transverse Spacing Bottom Row (#5) in.	5

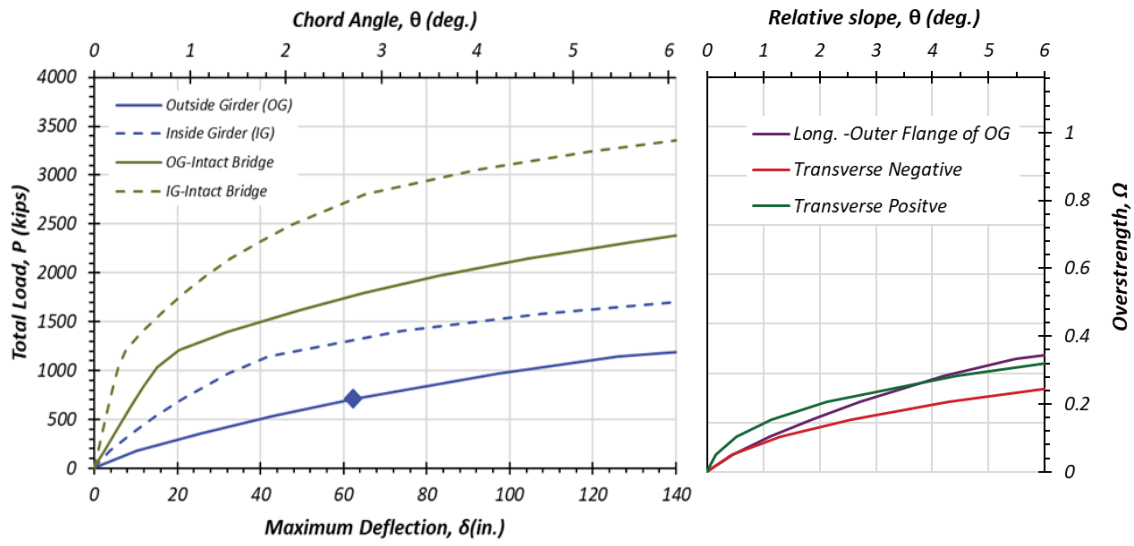
Figure 4.10 shows the grillage deflection profile of Bridge 1 with activated plastic hinges at the ultimate loading condition. Figure 4.11 depicts the load displacement plot at of the bridge at the center of both the interior and exterior girders.

The intact bridge has an overstrength factor of 1.00 and the fractured bridge has an overstrength factor of 0.21, controlled by longitudinal rotation. Under the fractured condition, Bridge 1 is not considered redundant due to its overstrength factor being less than 1.



Note: The colors represent achieved curvature limits (Magenta=yielding, Yellow=beyond yielding, Orange=beyond yielding close to failure, Red=Failure) Additional Hinge Data Located in Appendix

Figure 4.10 Grillage Deflection Profile of Bridge 1 with Activated Hinges



(a) Load-displacement

(b) Deck rotations

Note: δ is along the centerline of the girder, Ω is the load normalized by factored design load

Figure 4.11 Grillage Analysis Results of Bridge 1

4.3.3. Grillage Analysis of Bridge 2-NBI #12-102-0271-17-530

Bridge 2 is a simple span bridge 115 ft in length, with a deck width of 26.6 ft and thickness of 8 in. built on the I160 connector in 2004 located in Harris County. The nonlinear model for Bridge 2 was developed using a similar process as Bridge 1. Table 4.5 and Table 4.6 contain the relative geometry information for Bridge 2 necessary to create a grillage model.

Table 4.5 Geometric Details of Steel Tub Girders for Bridge 2

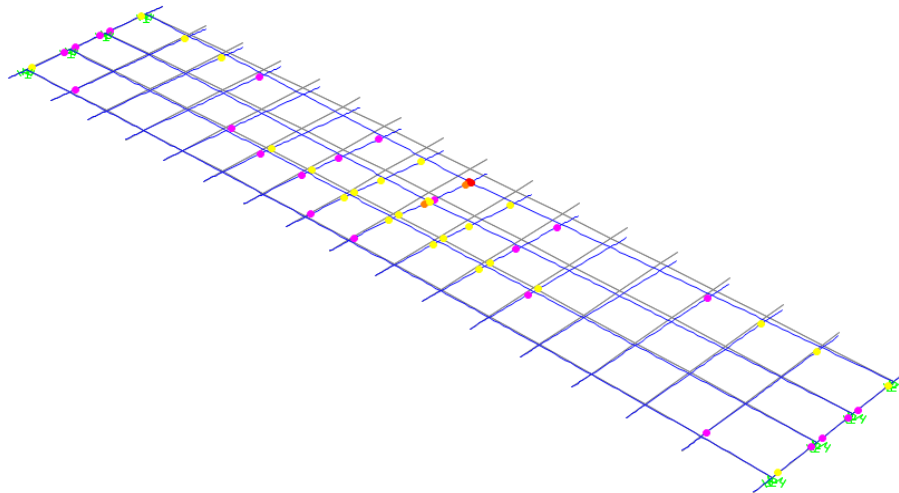
Location ft	Top Flange		Web		Bottom Flange	
	Width in.	Thickness in.	Width in.	Thickness in.	Width in.	Thickness in.
0-115	18	1.00	79	0.625	50	1.00

Table 4.6 General Geometric Properties of Bridge 2

Location	Parameter	Description/Value
Bridge	Location	Harris County, I610
	Year Designed/Year Built	2002/2004
	Design Load	HS25
	Length, ft	115
	Spans, ft	115
	Radius of Curvature, ft	1909.86
Deck	Width, ft	26.625
	Thickness, in.	8
	Haunch, in.	4
	Rail Type	SSTR
Rebar	# of Bar Longitudinal Top Row (#5)	40
	# of Bar Longitudinal Bottom Row (#5)	32
	Transverse Spacing Top Row (#5) in.	5
	Transverse Spacing Bottom Row (#5) in.	5

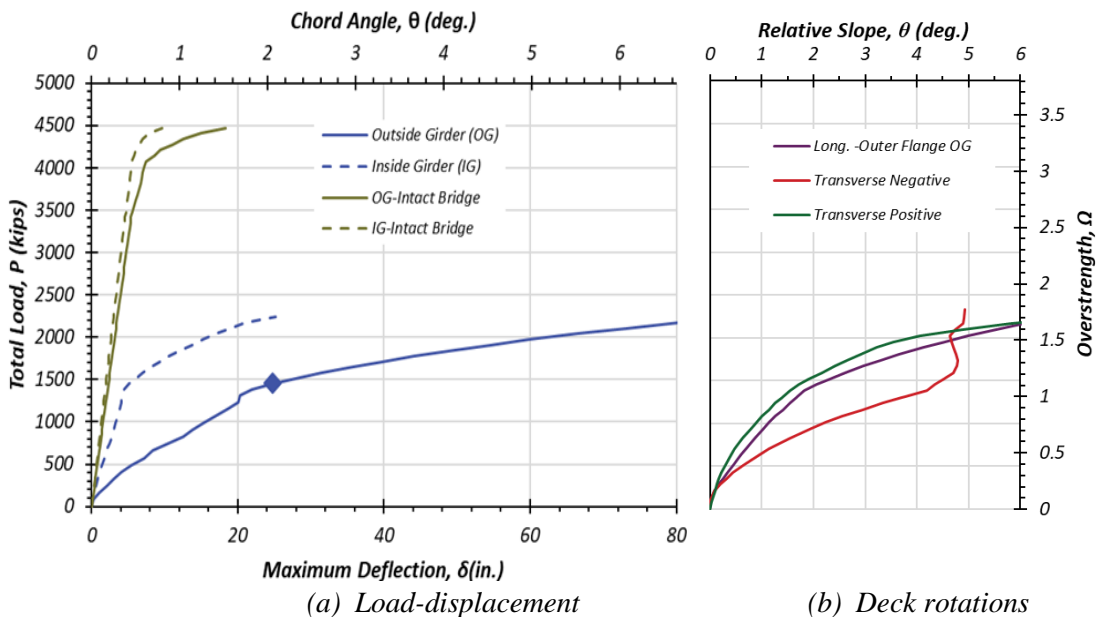
Figure 4.12 depicts the deflection profile of Bridge 2 at the ultimate loading condition with activated hinges. Figure 4.13 illustrates the load displacement along the centerline of the girders.

The fractured grillage model of Bridge 2 was ran with a full web fracture at midspan of the bridge. Under HL93 loading, Bridge 2 has an intact overstrength factor of 3.42 and a fractured overstrength factor of 1.11, controlled by stiffness reduction. Since the overstrength value is greater than 1, Bridge 2 is considered to be redundant however, there is a significant strength reduction caused by the fracture of the outside girder.



Note: The colors represent achieved curvature limits (Magenta=yielding, Yellow=beyond yielding, Orange=beyond yielding close to failure, Red=Failure) Additional Hinge Data Located in Appendix

Figure 4.12 Grillage Deflection Profile of Bride 2 with Activated Hinges



Note: δ is along the centerline of the girder, Ω is the load normalized by factored design load

Figure 4.13 Grillage Analysis Results of Bridge 2

4.3.4. Grillage Analysis of Bridge 3-NBI #12-102-0508-01-294

Bridge 3 has a span length of 230 ft with a roadway width of 38.8 ft and a 9 in. deck slab thickness and was built in 2002 in Harris County. Table 4.7 and Table 4.8 both contain geometric information of Bridge 3 which is necessary to create an accurate grillage model. The processes by which the grillage model was created is same by which preceding bridges were built.

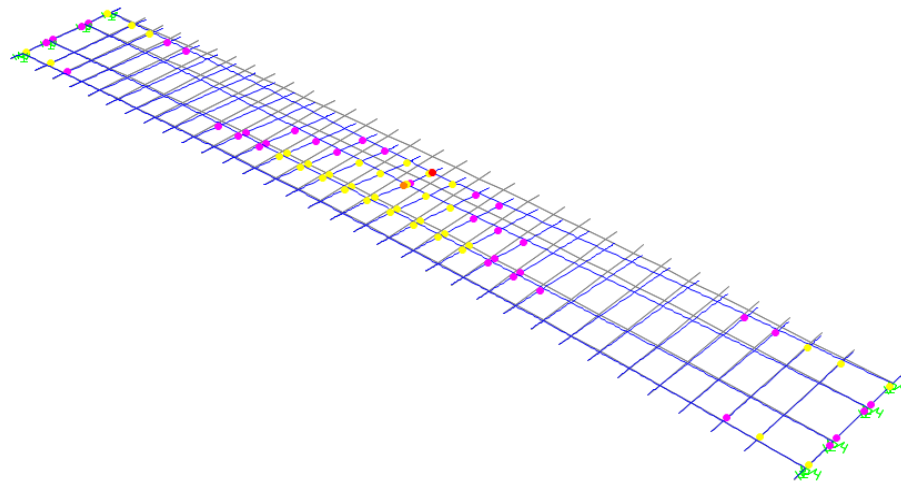
Table 4.7 Geometric Details of Steel Tub Girders for Bridge 3

Location ft	Top Flange		Web		Bottom Flange	
	Width in.	Thickness in.	Width in.	Thickness in.	Width in.	Thickness in.
0-21	24	1.5	102	0.75	63.5	1.25
21-42	24	2.5	102	0.75	63.5	1.75
42-185	24	3	102	0.75	63.5	2.75
185-207	24	2.5	102	0.75	63.5	1.75
207-230	24	1.5	102	0.75	63.5	1.25

Table 4.8 General Geometric Properties of Bridge 3

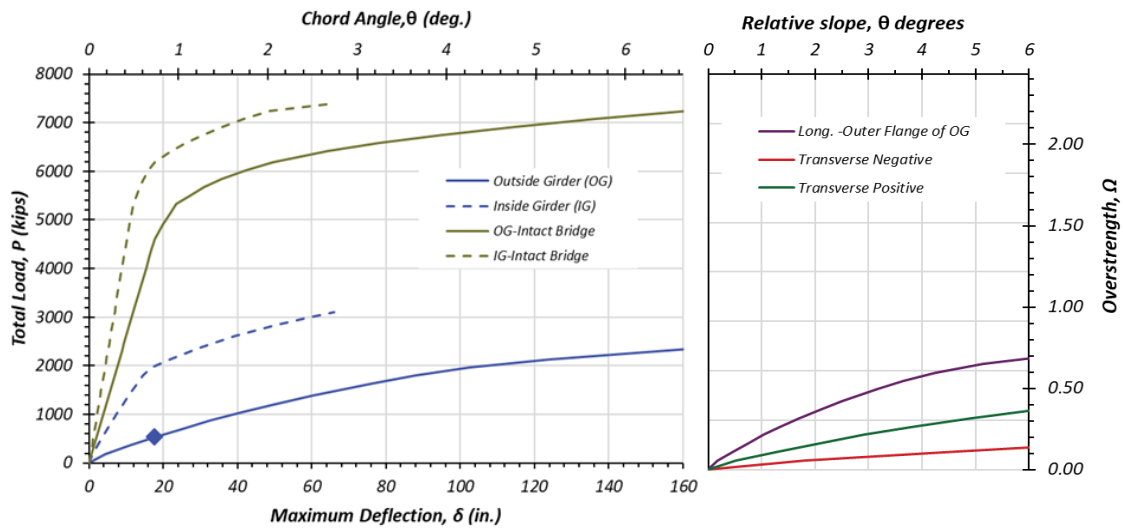
Location	Parameter	Description/Value
Bridge	Location	Harris County, FWY
	Year Designed/Year Built	1997/2002
	Design Load	HS20
	Length, ft	230
	Spans, ft	230
	Radius of Curvature, ft	2207.3
Deck	Width, ft	38.833
	Thickness, in.	9
	Haunch, in.	4
	Rail Type	T-501
Rebar	# of Bar Longitudinal Top Row (#5)	46
	# of Bar Longitudinal Bottom Row (#5)	64
	Transverse Spacing Top Row (#5), in.	5
	Transverse Spacing Bottom Row (#5), in.	5

Figure 4.14 shows the deflection profile of Bridge 3 along with the activated plastic hinges. The load displacement results from Bridge 3 are located in Figure 4.15. Post fracture, the bridge has an overstrength factor of 0.16 controlled by transverse rotation, and varies significantly from the intact overstrength factor of 2.00. In its fractured state, Bridge 3 has an overstrength less than 1 therefore not a redundant structure.



Note: The colors represent achieved curvature limits (Magenta=yielding, Yellow=beyond yielding, Orange=beyond yielding close to failure, Red=Failure) Additional Hinge Data Located in Appendix

Figure 4.14 Grillage Deflection Profile for Bridge 3 with Activated Hinges



(a) Load-displacement

(b) Deck rotations

Note: δ is along the centerline of the girder, Ω is the load normalized by factored design load

Figure 4.15 Grillage Analysis Results of Bridge 3

4.3.5. Grillage Analysis of Bridge 4-NBI #12-102-0271-07-637

Bridge 4 is a two span continuous STTG bridge built in 2007 in Harris County. Span 1 of Bridge 4 is 132 ft long and Span 2 is 128 ft long. Bridge 4 has a deck width of 28.4 ft and a thickness of 8.5 in. Table 4.9 and Table 4.10 give the geometric properties for Bridge 4. It should be noted that although the top and bottom flanges do not vary in width they do vary in thickness. It should also be noted that over the intermediate support and negative moment region there is additional top reinforcing bar.

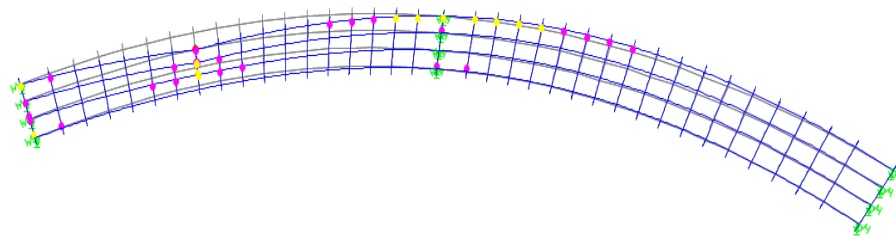
Table 4.9 Geometric Details of Steel Tub Girders for Bridge 4

Location ft	Top Flange		Web		Bottom Flange	
	Width in.	Thickness in.	Width in.	Thickness in.	Width in.	Thickness in.
0-82	20	1.00	54	0.5	72	0.875
82-110	20	.50	54	0.5	72	1.750
110-130	20	2.75	54	0.5	72	1.750
130-150	20	2.75	54	0.5	72	1.750
150-177	20	1.50	54	0.5	72	1.750
177-260	20	1.00	54	0.5	72	0.875

Figure 4.16 shows the deflection profile of Bridge 4 with fracture at $0.4 \cdot L$ of Span 2. Figure 4.17 and Figure 4.18 shows the load vs. displacement diagram for Spans 1 and 2 respectively of Bridge 4. Following a $0.4 \cdot L$ fracture the overstrength factors are 1.30 for Span 1 and 1.32 for Span 2. Prior to fracture Span 1 has an overstrength factor of 2.60 and Span 2 has an overstrength factor of 2.88. Under HL93 loading both spans are redundant under the fractured condition and are controlled by longitudinal rotation.

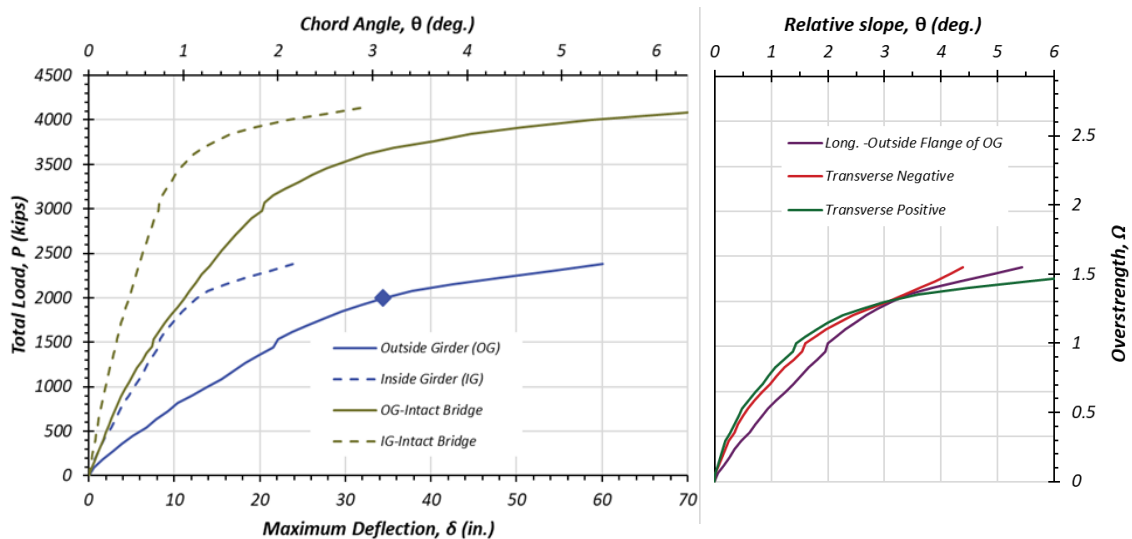
Table 4.10 General Geometric Properties of Bridge 4

Location	Parameter	Description/Value
Bridge	Location	Harris County, FWY
	Year Designed/Year Built	2004/2007
	Design Load	HS25
	Length, ft	260.27
	Spans, ft	132.03, 128.24
	Radius of Curvature, ft	195
Deck	Width, ft	28.417
	Thickness, in.	8.5
	Haunch, in.	3.5
	Rail Type	SSTR
Rebar	# of Bar Longitudinal Top Row (#5)	38
	# of Bar Longitudinal Bottom Row (#5)	30
	# of Bar Longitudinal Top Row (#5) @support	78
	# of Bar Longitudinal Bottom Row (#5) @support	30
	Transverse Spacing Top Row (#5), in.	5
	Transverse Spacing Bottom Row (#5), in.	5



Note: The colors represent achieved curvature limits (Magenta=yielding, Yellow=beyond yielding, Orange=beyond yielding close to failure, Red=Failure) Additional Hinge Data Located in Appendix

Figure 4.16 Grillage Deflection Profile for Span 2 of Bridge 4 with Activated Hinges

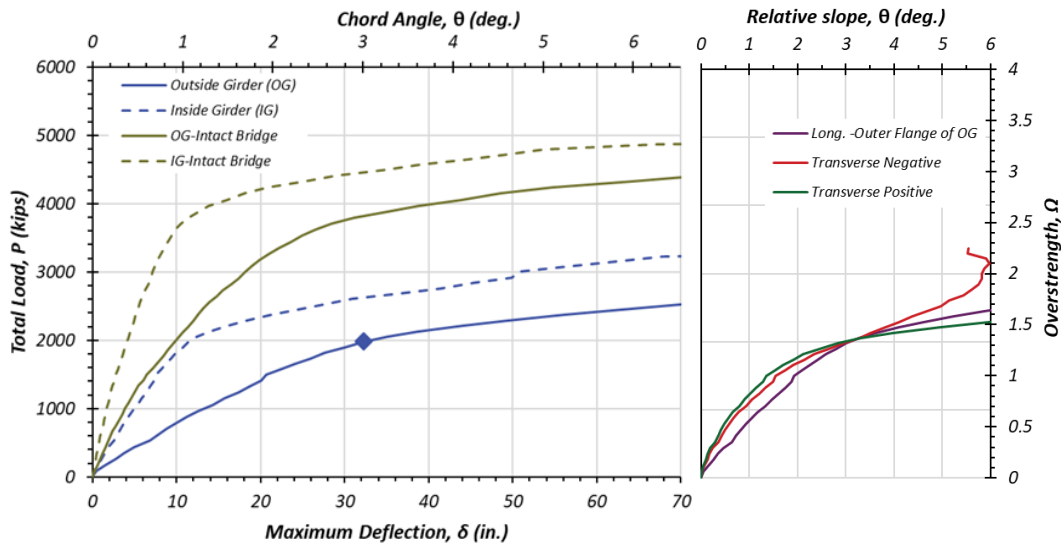


(a) Load-displacement

(b) Deck rotations

Note: δ is along the centerline of the girder, Ω is the load normalized by factored design load

Figure 4.17 Grillage Analysis Results of Bridge 4-Span 1



(a) Load-displacement

(b) Deck rotations

Note: δ is along the centerline of the girder, Ω is the load normalized by factored design load

Figure 4.18 Grillage Analysis Results of Bridge 4-Span 2

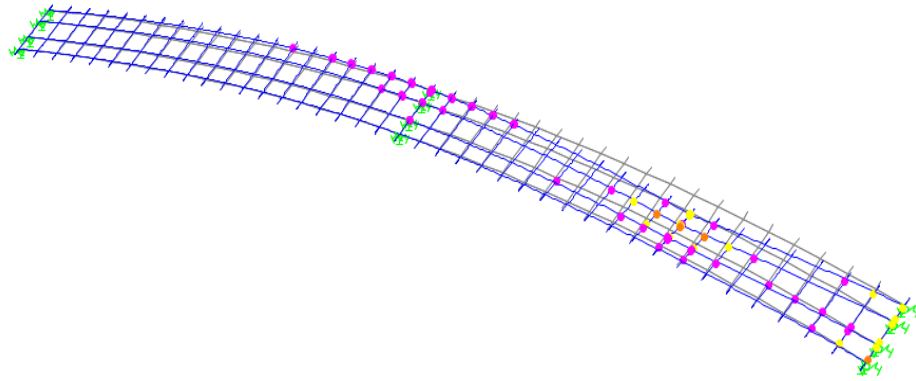
4.3.6. Grillage Analysis of Bridge 5-NBI #14-227-0-0015-13-452

Bridge 5 was built in 2002 in Travis County along I-35. It is a continuous two-span twin tub girder bridge. The first span of Bridge 5 has a span length of 140 ft with the second span length of 139.6 ft. The bridge deck is 30 ft wide with a thickness of 8 in. Table 4.11 and Table 4.12 contain the geometric properties of Bridge 5 needed to construct an appropriate grillage model. Note that top flange, web and bottom flange thickness as well as the rebar configuration change along the length.

Table 4.11 Geometric Details of Steel Tub Girders of Bridge 5

Location ft	Top Flange		Web		Bottom Flange	
	Width in.	Thickness in.	Width in.	Thickness in.	Width in.	Thickness in.
0-105	18	1.00	54	0.5	56	0.75
105-122	18	1.00	54	0.5625	56	1.250
122-140	18	1.75	54	0.5625	56	1.250
140-157	18	1.75	54	0.5625	56	1.250
157-174	18	1.57	54	0.5625	56	1.250
174-192	18	1.00	54	0.5625	56	0.75
192-280	18	1.00	54	0.5	56	0.75

Figure 4.19 shows the deflection profile of Span 1 of Bridge 5. Figure 4.20 depicts the load-displacement results for Spans 1 and 2 of Bridge 5. Prior to fracture, Bridge 5 has an overstrength factor of 2.15. With a controlling fractured overstrength value of 1.10, Bridge 5 is considered redundant. Since the bridge contained spans of almost equal lengths, there was no need to run a second analysis on Span 2. The fracture failure of Bridge 5 is controlled by longitudinal rotation.

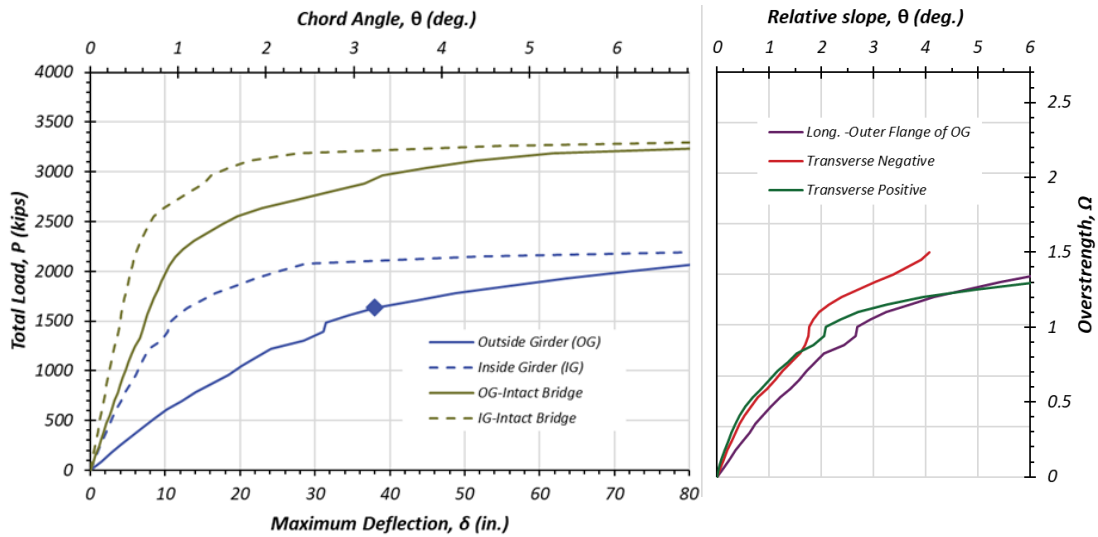


Note: The colors represent achieved curvature limits (Magenta=yielding, Yellow=beyond yielding, Orange=beyond yielding close to failure, Red=Failure) Additional Hinge Data Located in Appendix

Figure 4.19 Grillage Deflection Profile for Span 1 of Bridge 5 with Activated Hinge

Table 4.12 General Geometric Properties of Bridge 5

Location	Parameter	Description/Value
Bridge	Location	Travis County, I35
	Year Designed/Year Built	1998/2002
	Design Load	HS20
	Length, ft	279.58
	Spans, ft	140, 139.58
	Radius of Curvature, ft	450
Deck	Width, ft	30
	Thickness, in.	8
	Haunch, in.	4
	Rail Type	T4(S)
Rebar	# of Bar Longitudinal Top Row (#4)	41
	# of Bar Longitudinal Bottom Row (#5)	36
	# of Bar Longitudinal Top Row (#4) @support	41
	# of Bar Longitudinal Top Row (#5) @support	40
	# of Bar Longitudinal Bottom Row (#5) @support	36
	Transverse Spacing Top Row (#5), in.	5
	Transverse Spacing Bottom Row (#5), in.	5



(a) Load-displacement

(b) Deck rotation

Note: δ is along the centerline of the girder, Ω is the load normalized by factored design load

Figure 4.20 Grillage Analysis Results of Bridge 5-Spans 1&2

4.3.7. Grillage Analysis of Bridge 6-NBI #12-102-0271-07-575

Bridge 6 is a two-span continuous twin tub girder bridge located in Harris County constructed along IH 10 in 2005. Both spans of Bridge 6 have a length of 140 ft, and it has a deck width of 30 ft with a thickness of 8.25 in. Table 4.13 contains the geometric details of the steel tubs. It should be noted that along the length of the girder the top flange thickness changes. Table 4.14 provides general information about the overall geometric properties of the bridge. Bridge 6 was created using the same principles as all the preceding bridges.

Table 4.13 Geometric Details of Steel Tub Girders of Bridge 6

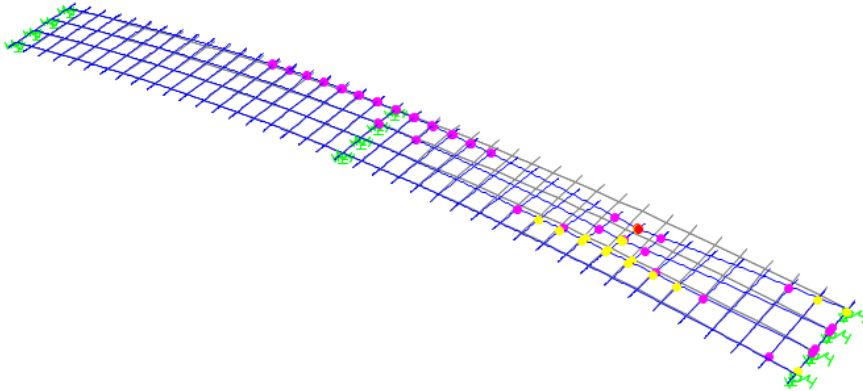
Location ft	Top Flange		Web		Bottom Flange	
	Width in.	Thickness in.	Width in.	Thickness in.	Width in.	Thickness in.
0-110	18	1.000	76	0.6875	60	1.000
110-130	22	1.000	76	0.6875	60	1.875
130-150	22	1.875	76	0.6875	60	1.875
150-170	22	1.000	76	0.6875	60	1.875
170-280	18	1.000	76	0.6875	60	1.000

Table 4.14 General Geometric Properties of Bridge 6

Location	Parameter	Description/Value
Bridge	Location	Harris County, IH10
	Year Designed/Year Built	2003/2005
	Design Load	HS25
	Length, ft	280
	Spans, ft	140,140
	Radius of Curvature, ft	818.51
Deck	Width, ft	38.417
	Thickness, in.	8.25
	Haunch, in.	4.5
	Rail Type	SSTR
Rebar	# of Bar Longitudinal Top Row (#5)	54
	# of Bar Longitudinal Bottom Row (#5)	48
	# of Bar Longitudinal Top Row (#5) @support	99
	# of Bar Longitudinal Bottom Row (#5) @support	48
	Transverse Spacing Top Row (#5), in.	4
	Transverse Spacing Bottom Row (#5), in.	4

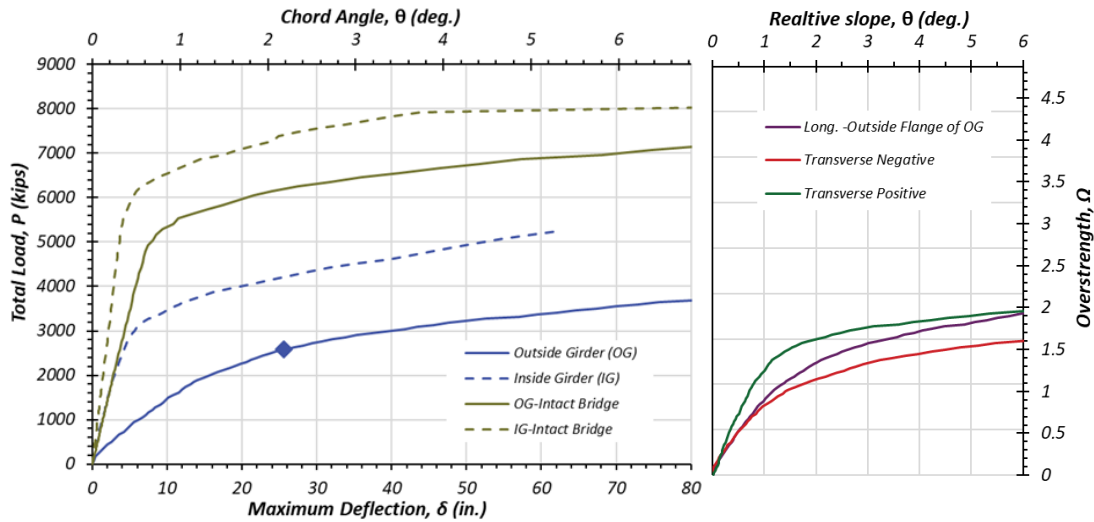
Figure 4.21 depicts the deflection profile of Spans 1&2 of Bridge 6 under ultimate loading condition with activated plastic hinges. Figure 4.22 shows the load deflection data at $0.4*L$ of Bridge 6. Both spans of Bridge 6 have an intact overstrength factor of 3.38. Post fracture of the outside girder, the overstrength factor is 1.43. Yet, the fracture

overstrength factor is still greater than 1. This implies that the bridge is redundant and fails under the stiffness criteria.



Note: The colors represent achieved curvature limits (Magenta=yielding, Yellow=beyond yielding, Orange=beyond yielding close to failure, Red=Failure) Additional Hinge Data Located in Appendix

Figure 4.21 Grillage Deflection Profile for Spans 1 & 2 of Bridge 6 with Activated Hinges



(a) Load-displacement

(b) Deck rotation

Note: δ is along the centerline of the girder, Ω is the load normalized by factored design load

Figure 4.22 Grillage Analysis Results of Bridge 6-Spans 1&2

4.3.8. Grillage Analysis of Bridge 7-NBI #12-102-0177-07-394

Bridge 7 is a two span continuous twin tub bridge with two spans of length 219 ft and 190 ft, built in 2004 along IH10 in Harris County. This bridge has an overall deck width of 28.4 ft and a thickness of 8 in. Table 4.15 contains the geometric information for the steel tub girder. It should be noted that the top and bottom flanges change thickness along length of the girder as well as the top flange width. Further geometric details of Bridge 7 are located in Table 4.16. This table includes details of the concrete deck including reinforcing bars.

Figure 4.23 shows the grillage profile of Bridge 7 under ultimate loading condition on Span 2 with a fracture located midspan of Span 2 with activated plastic hinges. Figure

4.24 and Figure 4.25 contain the load displacement results for both Spans 1 and 2, respectively for Bridge 7.

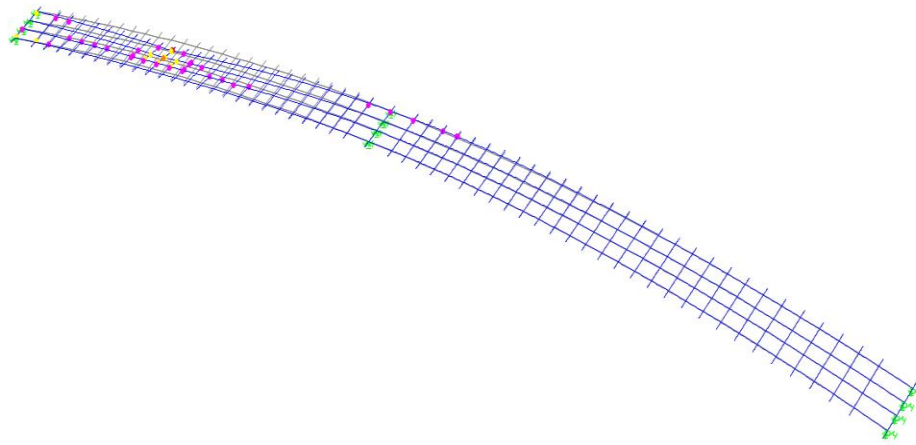
Table 4.15 Geometric Details of Steel Tub Girders of Bridge 7

Location ft	Top Flange		Web		Bottom Flange	
	Width in.	Thickness in.	Width in.	Thickness in.	Width in.	Thickness in.
0-17	20	1.100	63	0.625	60	1.000
17-141	20	2.360	63	0.625	60	2.362
141-162	20	1.770	63	0.625	60	1.772
162-193	30	1.770	63	0.625	60	1.772
193-219	30	3.150	63	0.625	60	3.150
219-247	30	3.150	63	0.625	60	3.150
247-292	30	1.770	63	0.625	60	1.772
292-381	20	1.100	63	0.625	60	1.102
381-408	20	1.100	63	0.625	60	1.000

Table 4.16 General Geometric Properties of Bridge 7

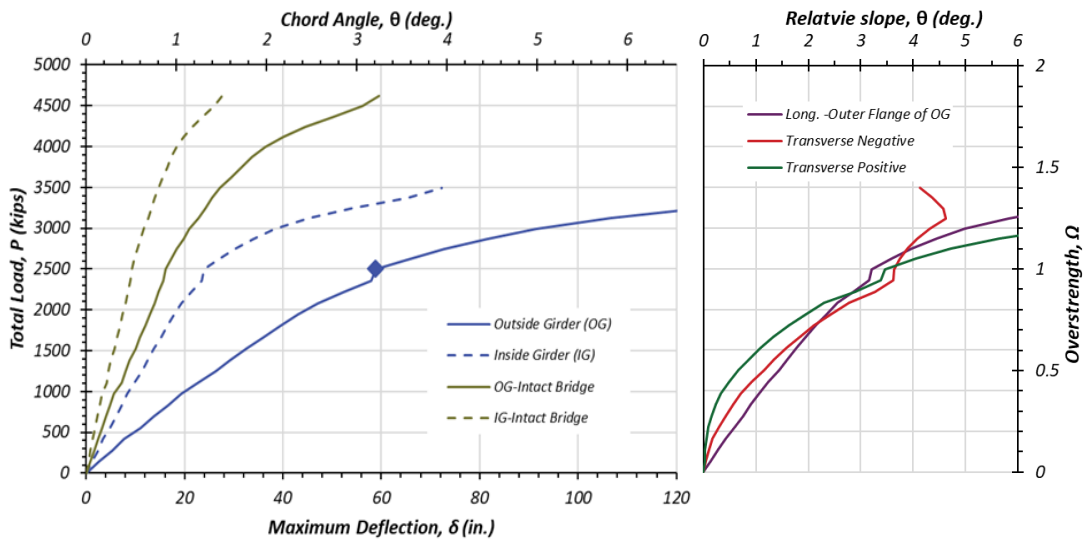
Location	Parameter	Description/Value
Bridge	Location	Harris County, IH10
	Year Designed/Year Built	2002/2004
	Design Load	HS20
	Length, ft	408.62
	Spans, ft	218.92,189.7
	Radius of Curvature, ft	763.96
Deck	Width, ft	28.417
	Thickness, in.	7.9
	Haunch, in.	5.5
	Rail Type	T501
Rebar	# of Bar Longitudinal Top Row (#5)	30
	# of Bar Longitudinal Bottom Row (#5)	40
	# of Bar Longitudinal Top Row (#5) @support	59
	# of Bar Longitudinal Bottom Row (#5) @support	40
	Transverse Spacing Top Row (#5), in.	6
	Transverse Spacing Bottom Row (#5), in.	6

Span 1 and 2 have intact overstrength factors of 1.85 and 2.15. Span 1 has a fractured overstrength factor of 0.94, and Span 2 has a fractured overstrength factor of 1.25. Span 1 having an Ω less than 1 is not considered redundant but, Span 2 is redundant post fracture. Both Span 1 and Span 2 fail due to excess longitudinal rotation.



Note: The colors represent achieved curvature limits (Magenta=yielding, Yellow=beyond yielding, Orange=beyond yielding close to failure, Red=Failure) Additional Hinge Data Located in Appendix

Figure 4.23 Grillage Deflection Profile for Span 2 of Bridge 7 with Activated Hinges

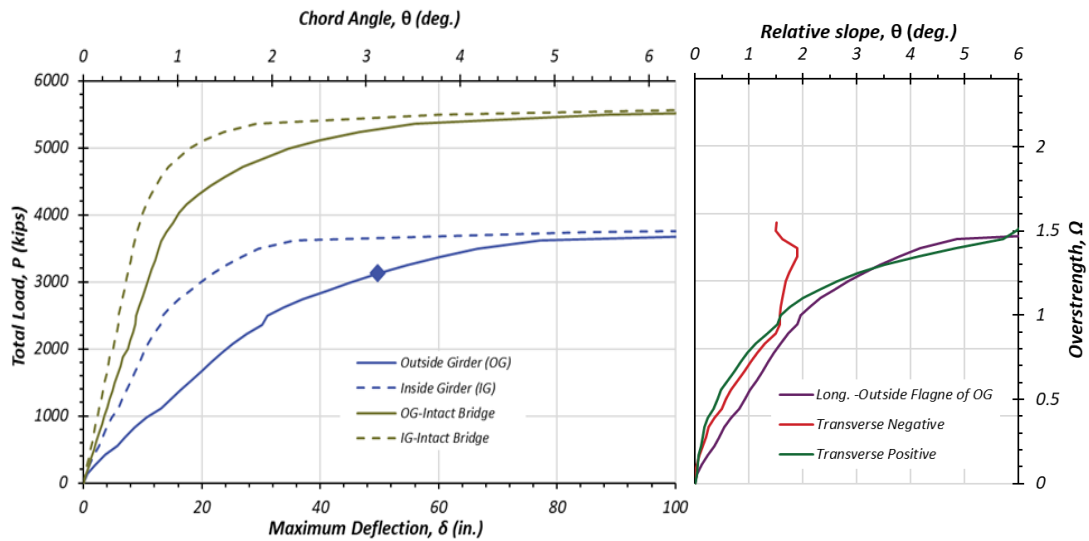


(a) Load-displacement

(b) Deck rotation

Note: δ is along the centerline of the girder, Ω is the load normalized by factored design load

Figure 4.24 Grillage Analysis Results of Bridge 7-Span 1



(a) Load-displacement

(b) Deck rotation

Note: δ is along the centerline of the girder, Ω is the load normalized by factored design load

Figure 4.25 Grillage Analysis Results of Bridge 7-Span 2

4.3.9. Grillage Analysis of Bridge 8-NBI #12-102-0271-06-661

Bridge 8 is a two span twin tub girder continuous bridge built in Harris County along IH 10 in 2011. Bridge 8 is composed of a 265 ft span and a 295 ft span with a 28.4 ft wide and 8 in. thick deck. Table 4.18 contains the geometric information for the steel tub portion for Bridge 8. It should be observed that the top flange and bottom flange of the tubs vary with thickness along the length of the girder. Table 4.17 provides further geometric information for Bridge 8 including, concrete deck information and reinforcing bar.

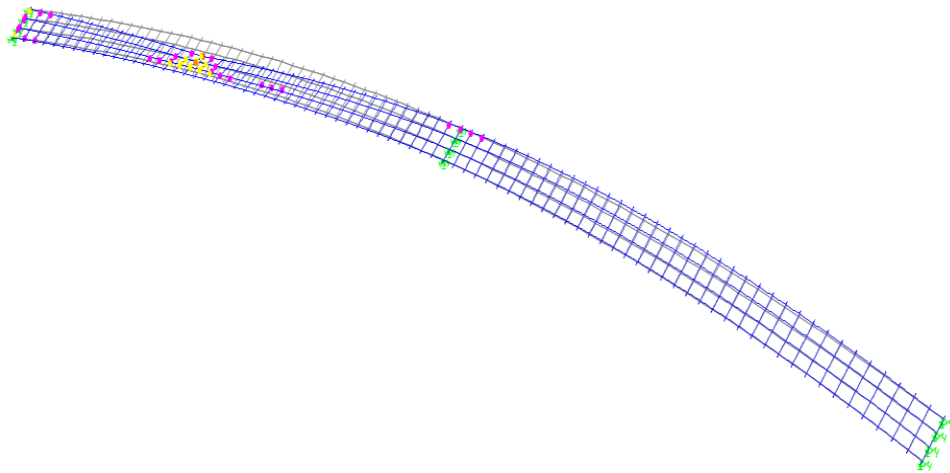
Table 4.17 General Geometric Properties of Bridge 8

Location	Parameter	Description/Value
Bridge	Location	Harris County, IH10
	Year Designed/Year Built	2011/NA
	Design Load	NA
	Length, ft	560
	Spans, ft	265, 295
	Radius of Curvature, ft	881.47
Deck	Width, ft	28.417
	Thickness, in.	8
	Haunch, in.	4
	Rail Type	SSTR
Rebar	# of Bar Longitudinal Top Row (#5)	38
	# of Bar Longitudinal Bottom Row (#5)	38
	# of Bar Longitudinal Top Row (#5) @support	76
	# of Bar Longitudinal Bottom Row (#5) @support	38
	Transverse Spacing Top Row (#5), in.	5
	Transverse Spacing Bottom Row (#5), in.	5

Figure 4.26 depicts the grillage displacement profile of a fractured Span 1 under ultimate loading conditions. Figure 4.27 and Figure 4.28 contain the load vs. displacement behavior of Span 1 and Span 2. Span 1 has an intact overstrength factor of 1.75 and a fractured overstrength factor of 0.88. Span 2 has an intact overstrength factor of 1.45 and a fractured overstrength factor of 0.60. Both spans do not exhibit redundant behavior having controlling overstrength factors less than 1, and are controlled by transverse and longitudinal rotation.

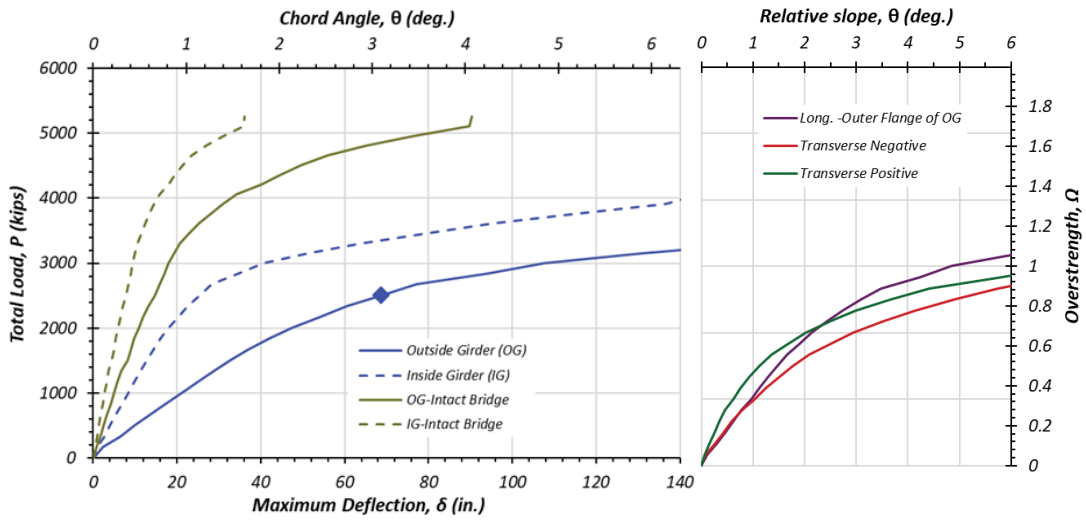
Table 4.18 Geometric Details of Steel Tub Girders of Bridge 8

Location ft	Top Flange		Web		Bottom Flange	
	Width in.	Thickness in.	Width in.	Thickness in.	Width in.	Thickness in.
0-30	24	1.25	93	0.75	53.5	1.250
30-71	24	1.50	93	0.75	53.5	1.500
71-142	24	1.50	93	0.75	53.5	2.000
142-183	24	1.50	93	0.75	53.5	1.500
183-214	24	1.25	93	0.75	53.5	1.500
214-234	24	2.00	93	0.75	53.5	2.000
234-307	24	2.50	93	0.75	53.5	2.500
307-338	24	1.25	93	0.75	53.5	1.500
338-370	24	1.50	93	0.75	53.5	1.500
370-391	24	1.50	93	0.75	53.5	2.000
391-496	24	2.00	93	0.75	53.5	2.500
496-528	24	1.50	93	0.75	53.5	2.000
528-560	24	1.25	93	0.75	53.5	1.250



Note: The colors represent achieved curvature limits (Magenta=yielding, Yellow=beyond yielding, Orange=beyond yielding close to failure, Red=Failure) Additional Hinge Data Located in Appendix

Figure 4.26 Grillage Deflection Profile for Span 2 of Bridge 8 with Activated Hinges

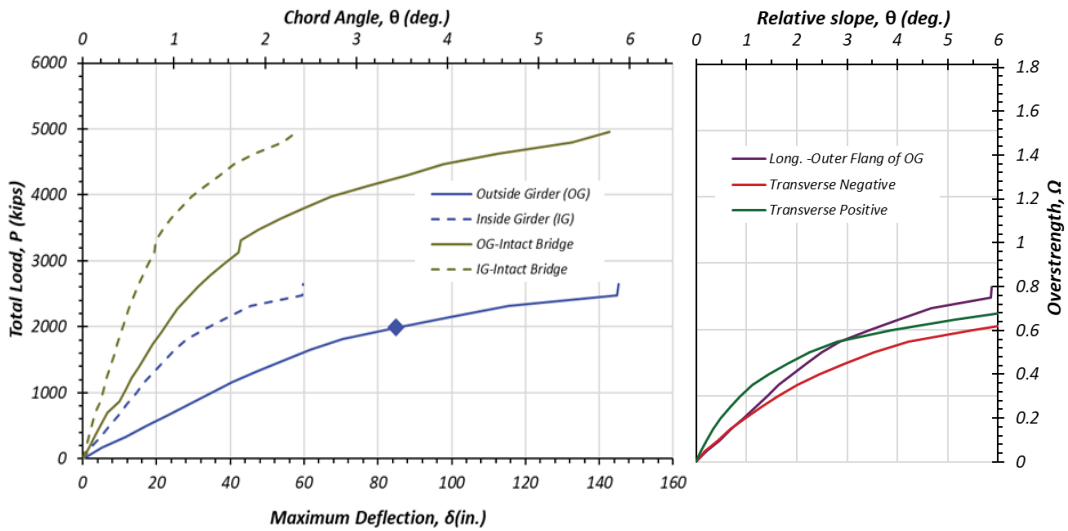


(a) Load-displacement

(b) Deck rotation

Note: δ is along the centerline of the girder, Ω is the load normalized by factored design load

Figure 4.27 Grillage Analysis Results of Bridge 8-Span 1



(a) Load-displacement

(b) Deck rotation

Note: δ is along the centerline of the girder, Ω is the load normalized by factored design load

Figure 4.28 Grillage Analysis Results of Bridge 8-Span 2

4.3.10. Grillage Analysis of Bridge 9-NBI #12-102-0177-07-394

The first three span continuous bridge evaluated in this study is Bridge 9. Bridge 9 has spans of length 139.5 ft, 151.4 ft, and 125.5 ft. The overall deck width is 28.4 ft wide with a thickness of 8 in. It should be noted that Bridge 9 is the in the same segment of bridges which contain Bridge 7. Table 4.19 and Table 4.20 contain relevant geometric properties to produce a grillage model for Bridge 9. It should be noted that the top and bottom flange thicknesses change along the length of the tub girder.

Table 4.19 General Geometric Properties of Bridge 9

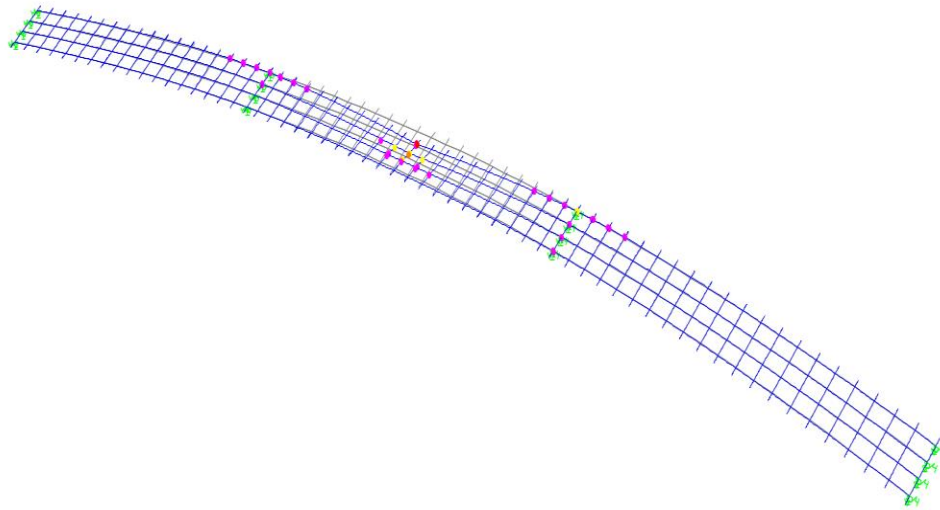
Location	Parameter	Description/Value
Bridge	Location	Harris County, IH10
	Year Designed/Year Built	2002/2004
	Design Load	HS20
	Length, ft	416.66
	Spans, ft	139.5,151.44,125.62
	Radius of Curvature, ft	763.93
Deck	Width, ft	28.417
	Thickness, in.	8
	Haunch, in.	4
	Rail Type	T501
Rebar	# of Bar Longitudinal Top Row (#5)	30
	# of Bar Longitudinal Bottom Row (#5)	40
	# of Bar Longitudinal Top Row (#5) @support	59
	# of Bar Longitudinal Bottom Row (#5) @support	30
	Transverse Spacing Top Row (#5), in.	5
	Transverse Spacing Bottom Row (#5), in.	5

Figure 4.29 depicts the displacement profile of Bridge 9 with HL93 loading on the fractured Span 2. Figure 4.30, Figure 4.31, and Figure 4.32 depict the load displacement

results of all three spans in Bridge 9. Span 1 has an intact overstrength factor of 2.82 and a fractured overstrength factor of 1.35. Span 2 has an intact overstrength factor of 3.10 and a fractured factor of 2.10. Span 3 has an intact overstrength factor of 3.05 and a fractured overstrength factor of 1.53. All spans of Bridge 9, even with the exterior girder fractured, have overstrength factors greater than 1 and considered to be redundant and are controlled by stiffness.

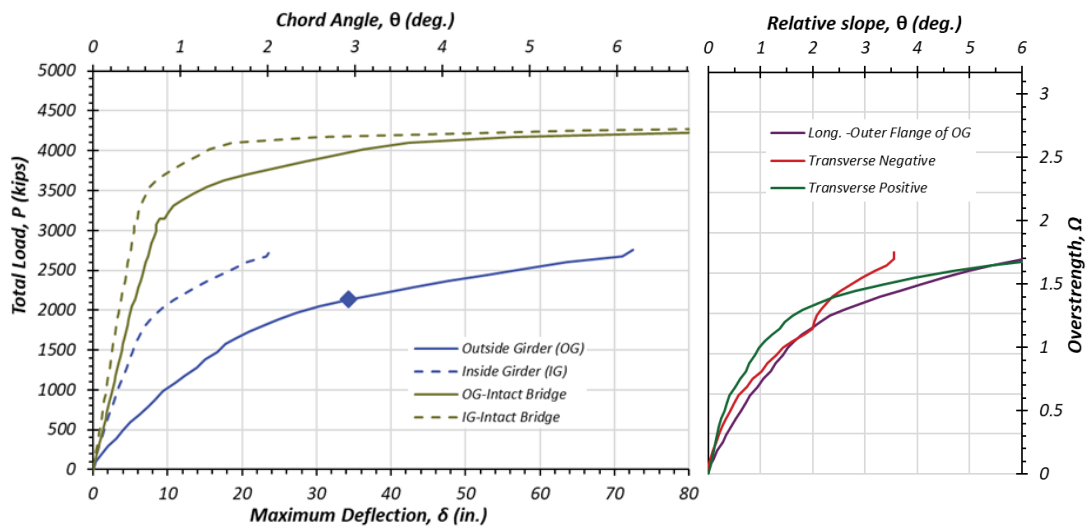
Table 4.20 Geometric Details of Steel Tub Girders of Bridge 9

Location ft	Top Flange		Web		Bottom Flange	
	Width in.	Thickness in.	Width in.	Thickness in.	Width in.	Thickness in.
0-104	20	1.10	63	0.625	59	1.000
104-127	20	1.10	63	0.625	59	1.250
127-152	20	1.58	63	0.625	59	1.500
152-177	20	1.10	63	0.625	59	1.250
177-240	20	1.10	63	0.625	59	1.000
240-265	20	1.10	63	0.625	59	1.250
265-278	20	1.10	63	0.625	59	1.500
278-316	20	1.58	63	0.625	59	1.500
316-341	20	1.10	63	0.625	59	1.250
341-416	20	1.10	63	0.625	59	1.000



Note: The colors represent achieved curvature limits (Magenta=yielding, Yellow=beyond yielding, Orange=beyond yielding close to failure, Red=Failure) Additional Hinge Data Located in Appendix

Figure 4.29 Grillage Deflection Profile for Span 2 of Bridge 9 with Activated Hinges

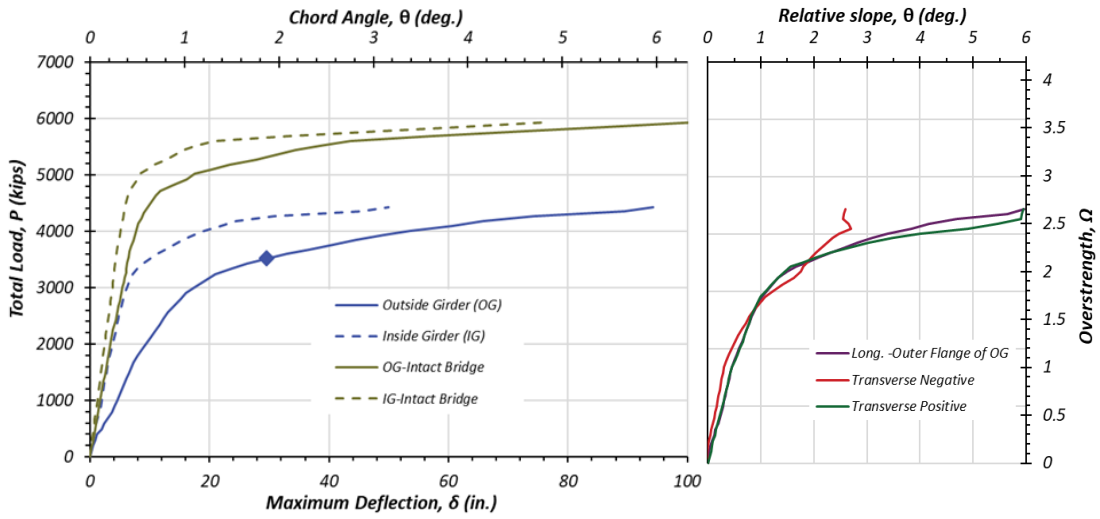


(a) Load-displacement

(b) Deck rotation

Note: δ is along the centerline of the girder, Ω is the load normalized by factored design load

Figure 4.30 Grillage Analysis Results of Bridge 9-Span 1

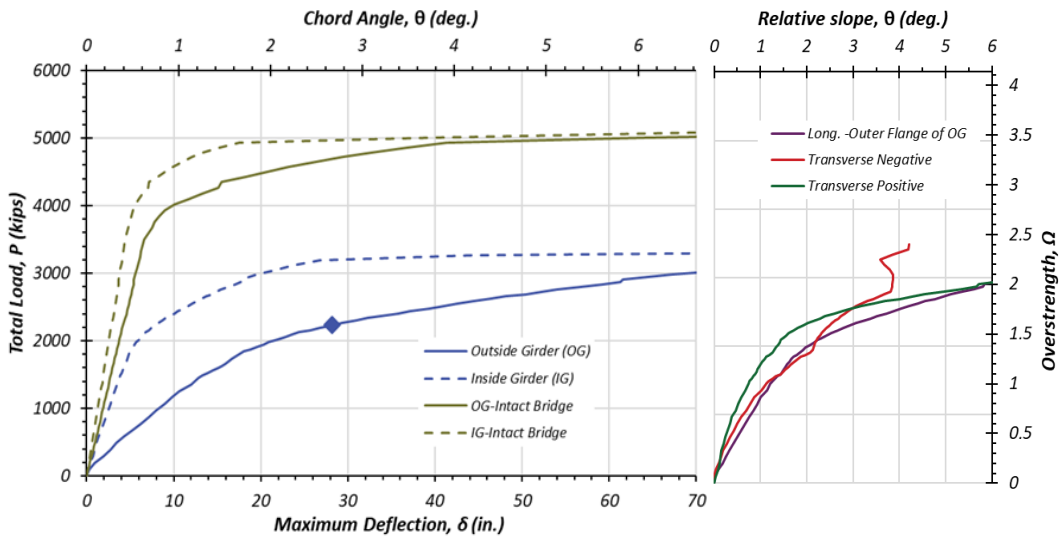


(a) Load-displacement

(b) Deck rotation

Note: δ is along the centerline of the girder, Ω is the load normalized by factored design load

Figure 4.31 Grillage Analysis Results of Bridge 9-Span 2



(a) Load-displacement

(b) Deck rotation

Note: δ is along the centerline of the girder, Ω is the load normalized by factored design load

Figure 4.32 Grillage Analysis Results of Bridge 9-Span 3

4.3.11. Grillage Analysis of Bridge 10-NBI #14-227-0-0015-13-450

Bridge 10, built in 2002 in Harris County along IH 10, is a continuous three span bridge with span lengths of 148 ft, 265 ft, and 189.6 ft. It has a total deck width of 30 ft and thickness of 8 in. Table 4.21 and Table 4.22 contain the geometric property details of Bridge 10. It should be noted that the top flange, web, and bottom flange thicknesses change over the length of the girders. The top reinforcing bars are a mixture of number 4 and 5 bars over the support.

Table 4.21 Geometric Details of Steel Tub Girders of Bridge 10

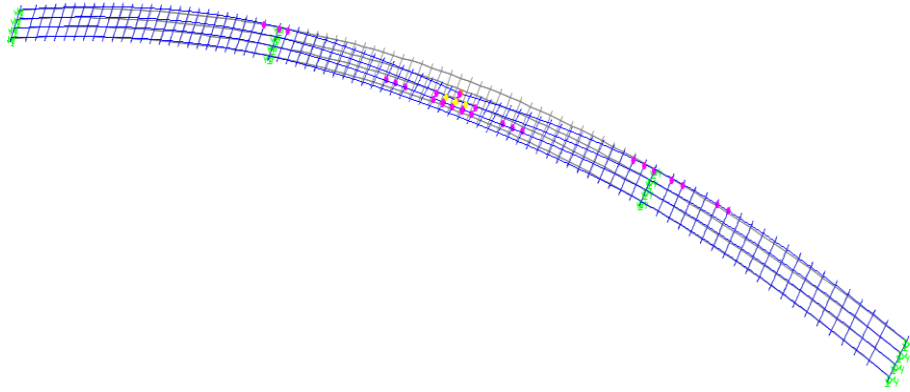
Location ft	Top Flange		Web		Bottom Flange	
	Width in.	Thickness in.	Width in.	Thickness in.	Width in.	Thickness in.
0-50	24	1.00	78	0.625	59	0.750
50-98	24	1.00	78	0.625	59	1.250
98-131	24	2.00	78	0.75	59	2.000
131-181	24	3.00	78	0.875	59	2.000
181-230	24	1.00	78	0.875	59	1.250
230-247	24	1.00	78	0.75	59	1.000
247-297	24	1.00	78	0.75	59	1.250
297-330	24	1.00	78	0.75	59	1.000
330-380	24	1.00	78	0.875	59	1.250
380-396	24	2.00	78	0.875	59	1.250
396-430	24	3.00	78	0.875	59	2.000
430-447	24	3.00	78	0.875	59	2.000
447-464	24	2.00	78	0.75	59	1.250
464-499	24	1.00	78	0.75	59	1.250
499-602	24	1.00	78	0.625	59	0.750

Figure 4.33 depicts the displacement profile of Bridge 10 with HL93 loading a fracture in Span 2. Figure 4.34, Figure 4.35, and Figure 4.36 illustrates the load

displacement results for all spans of Bridge 10. Span 1 has a fractured overstrength factor of 1.71. Span 2 has a fractured overstrength factor of 1.25 and an intact overstrength factor of 1.85. Span 3 has a fractured factor of 1.25 and an intact factor of 2.10. Each of the spans has an overstrength factor greater than one and are therefore exhibiting a necessary level of redundancy for load redistribution post fracture. Span 1 is controlled by stiffness, however Span 2 and Span 3 are controlled by longitudinal chord rotation.

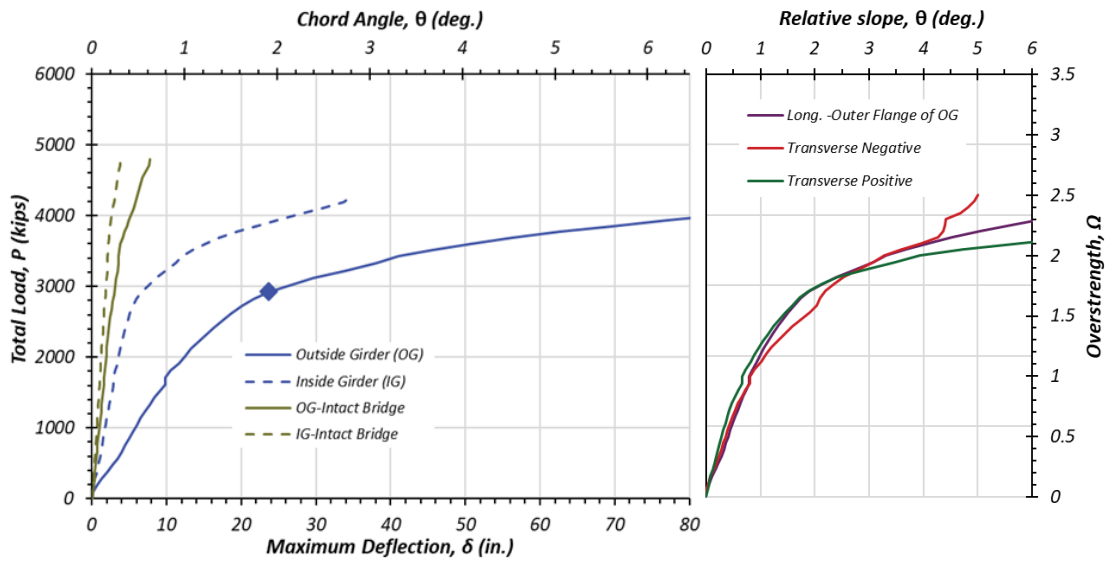
Table 4.22 General Geometric Properties of Bridge 10

Location	Parameter	Description/Value
Bridge	Location	Harris County, IH10
	Year Designed/Year Built	1998/2002
	Design Load	HS20
	Length, ft	602.58
	Spans, ft	148, 265, 189.58
	Radius of Curvature, ft	716.2
Deck	Width, ft	30
	Thickness, in.	8
	Haunch, in.	5
	Rail Type	T4(s)
Rebar	# of Bar Longitudinal Top Row (#4)	42
	# of Bar Longitudinal Bottom Row (#5)	32
	# of Bar Longitudinal Top Row (#4) @support	42
	# of Bar Longitudinal Top Row (#5) @support	40
	# of Bar Longitudinal Bottom Row (#5) @support	32
	Transverse Spacing Top Row (#5), in.	6
	Transverse Spacing Bottom Row (#5), in.	6



Note: The colors represent achieved curvature limits (Magenta=yielding, Yellow=beyond yielding, Orange=beyond yielding close to failure, Red=Failure) Additional Hinge Data Located in Appendix

Figure 4.33 Grillage Deflection Profile for Span 2 of Bridge 10 with Activated Hinges

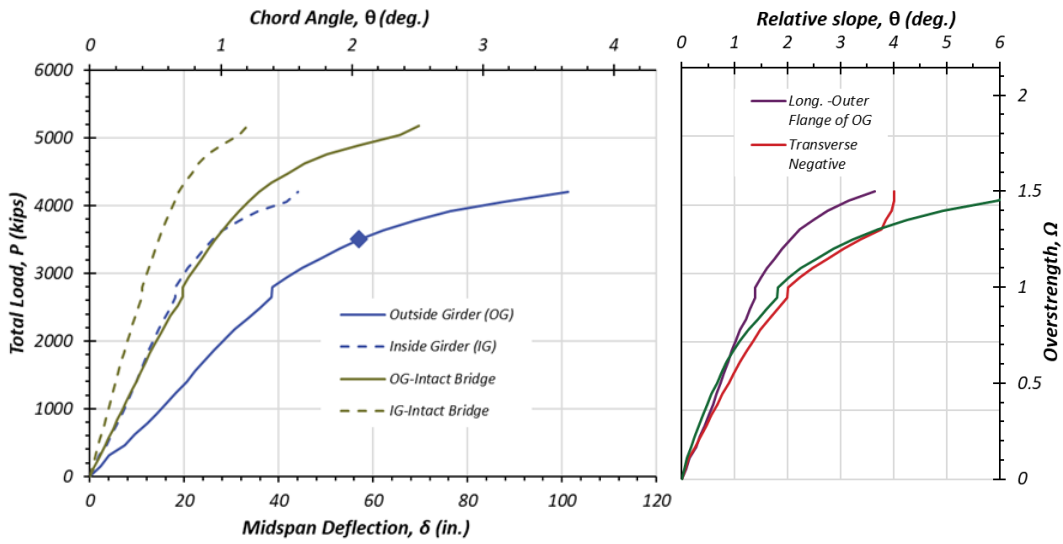


(a) Load-displacement

(b) Deck rotation

Note: δ is along the centerline of the girder, Ω is the load normalized by factored design load

Figure 4.34 Grillage Analysis Results of Bridge 10-Span 1

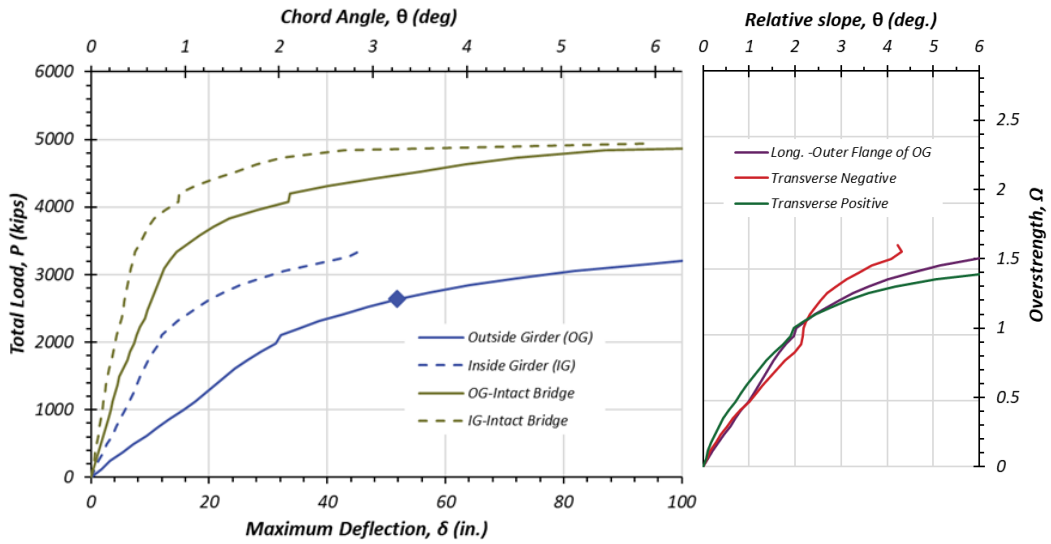


(a) Load-displacement

(b) Deck rotation

Note: δ is along the centerline of the girder, Ω is the load normalized by factored design load

Figure 4.35 Grillage Analysis Results of Bridge 10-Span 2



(a) Load-displacement

(b) Deck rotation

Note: δ is along the centerline of the girder, Ω is the load normalized by factored design load

Figure 4.36 Grillage Analysis Results of Bridge 10-Span 3

4.3.12. Grillage Analysis of Bridge 11-NBI #12-102-0271-07-593

Bridge 11, compared to Bridge 10, is a longer three span continuous bridge located along IH 10 in Harris County. Bridge 11 consist of three spans with span lengths of 223 ft, 366 ft, and 235 ft with an overall deck width of 28.4 ft and a deck thickness of 8 in. Table 4.23 and Table 4.24 contain the necessary geometric information to generate an accurate grillage model. It should be noted that both the top flange width and thickness changes over the length of the girder as well as the bottom flange thickness.

Table 4.23 Geometric Details of Steel Tub Girders of Bridge 11

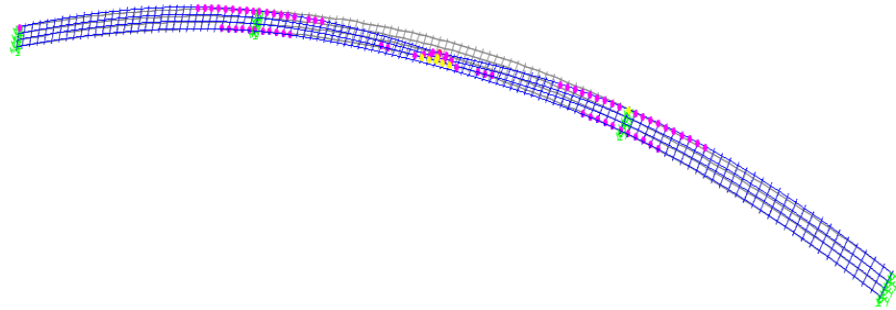
Location ft	Top Flange		Web		Bottom Flange	
	Width in.	Thickness in.	Width in.	Thickness in.	Width in.	Thickness in.
0-128	18	1.00	102	0.875	66	1.000
128-154	18	1.00	102	0.875	66	1.500
154-180	30	1.75	102	0.875	66	1.500
180-247	30	3.00	102	0.875	66	3.000
247-256	30	3.00	102	0.875	66	1.500
256-281	30	1.75	102	0.875	66	1.500
281-522	18	1.75	102	0.875	66	1.500
522-555	30	1.75	102	0.875	66	1.500
555-630	30	3.00	102	0.875	66	3.000
630-647	30	1.75	102	0.875	66	1.500
647-681	18	1.00	102	0.875	66	1.500
681-824	18	1.00	102	0.875	66	1.000

Figure 4.37 illustrates the deflection profile of Span 2 for an HL93 load. Figure 4.38, Figure 4.39, and Figure 4.40 show the load displacement response of all three spans of Bridge 11. Span 1 has a fractured overstrength factor of 1.35. Span 2 has a fractured

overstrength factor of 1.00. Span 3 has a fractured overstrength factor of 1.30. Span 1 fails via stiffness, Span 2 fails via longitudinal rotation, and Span 3 is controlled by transverse rotation.

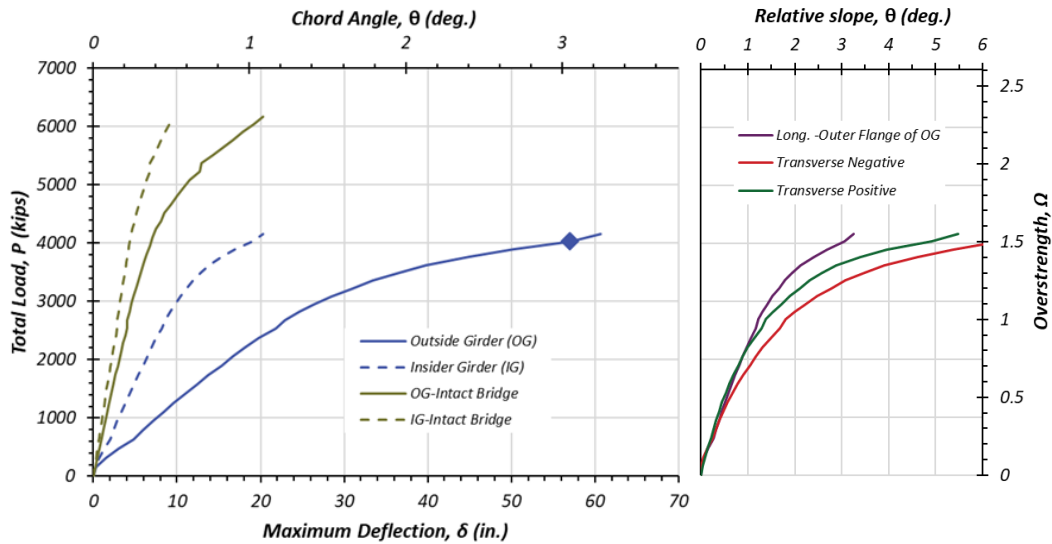
Table 4.24 General Geometric Properties of Bridge 11

Location	Parameter	Description/Value
Bridge	Location	Harris County, IH10
	Year Designed/Year Built	2004/2007
	Design Load	HS25
	Length, ft	824
	Spans, ft	223, 366, 235
	Radius of Curvature, ft	818.51
Deck	Width, ft	28.417
	Thickness, in.	8
	Haunch, in.	4
	Rail Type	SSTR
Rebar	# of Bar Longitudinal Top Row (#5)	30
	# of Bar Longitudinal Bottom Row (#5)	38
	# of Bar Longitudinal Top Row (#5) @support	59
	# of Bar Longitudinal Bottom Row (#5) @support	38
	Transverse Spacing Top Row (#5), in.	6
	Transverse Spacing Bottom Row (#5), in.	6



Note: The colors represent achieved curvature limits (Magenta=yielding, Yellow=beyond yielding, Orange=beyond yielding close to failure, Red=Failure) Additional Hinge Data Located in Appendix

Figure 4.37 Grillage Deflection Profile for Span 2 of Bridge 11 with Activated Hinges

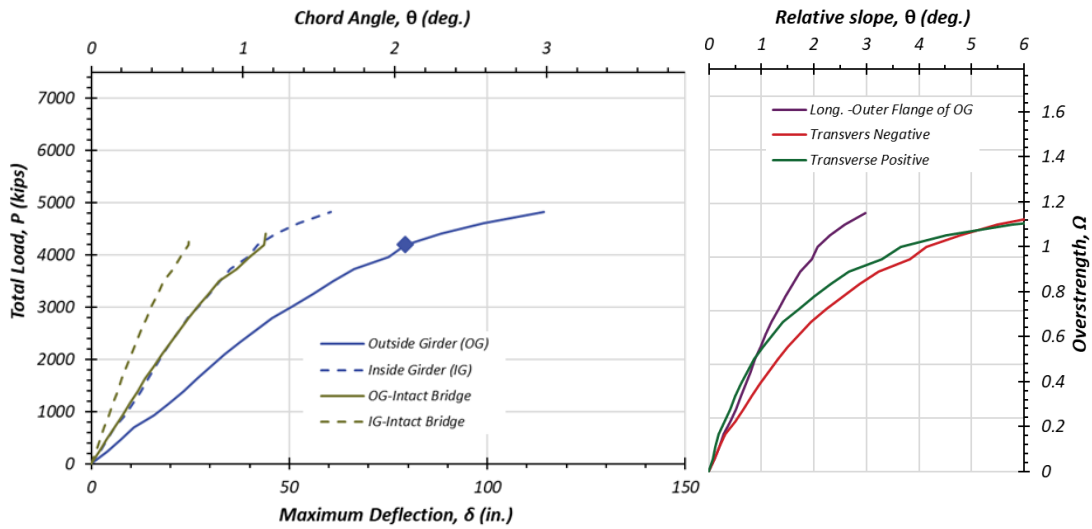


(a) Load-displacement

(b) Deck rotations

Note: δ is along the centerline of the girder, Ω is the load normalized by factored design load

Figure 4.38 Grillage Analysis Results of Bridge 11-Span 1

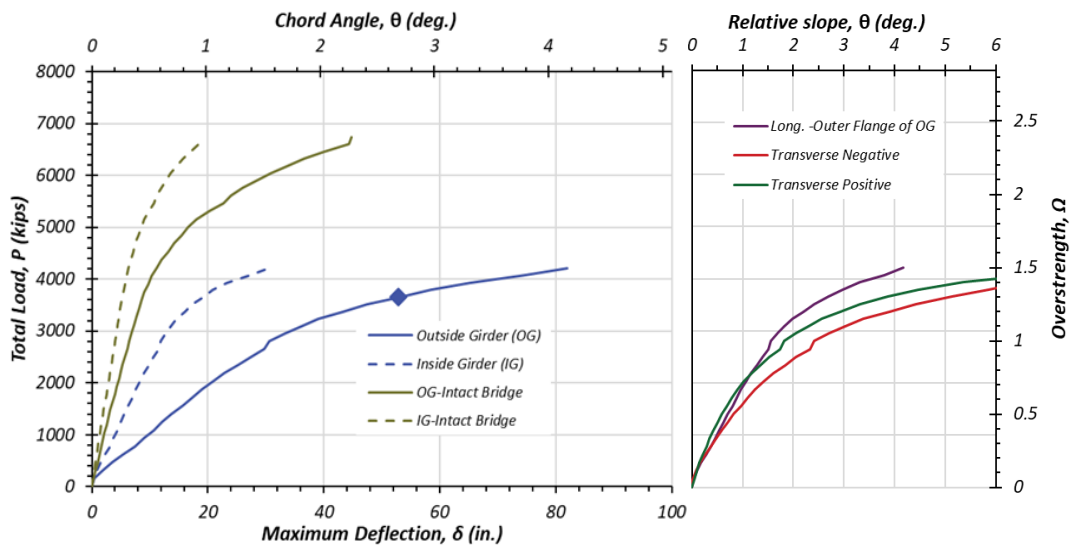


(a) Load-displacement

(b) Deck rotation

Note: δ is along the centerline of the girder, Ω is the load normalized by factored design load

Figure 4.39 Grillage Analysis Results of Bridge 11-Span 2



(a) Load-displacement

(b) Deck rotation

Note: δ is along the centerline of the girder, Ω is the load normalized by factored design load

Figure 4.40 Grillage Analysis Results of Bridge 11-Span 3

4.3.13. Grillage Analysis of Bridge 12-NBI #12-102-0271-07-639

Bridge 12, built in 2007 in Harris County along IH10, is a three span continuous bridge. The lengths of the spans which comprise Bridge 12 are as 140 ft, 180 ft, and 145 ft respectively. The overall bridge deck width of 28.4 ft and deck thickness of 8.5 in. Table 4.25 and Table 4.26 contain the geometric properties and information necessary for appropriately generating a grillage model to represent Bridge 12. Note, both the top and bottom flanges vary in thickness along the length of the member.

Table 4.25 Geometric Details of Steel Tub Girders of Bridge 12

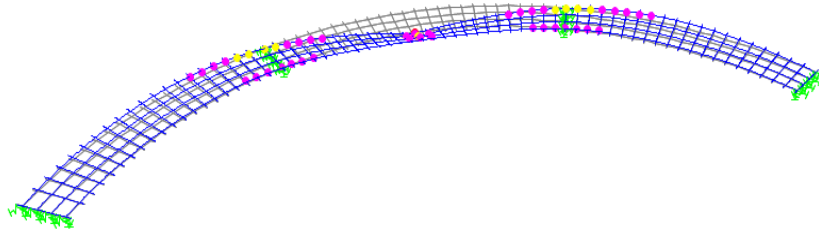
Location ft	Top Flange		Web		Bottom Flange	
	Width in.	Thickness in.	Width in.	Thickness in.	Width in.	Thickness in.
0-90	20	1.00	54	0.5	72	0.875
90-116	20	1.75	54	0.5	72	1.750
116-138	20	3.25	54	0.5	72	1.750
138-160	20	3.25	54	0.5	72	1.750
160-189	20	1.75	54	0.5	72	1.750
189-267	20	1.00	54	0.5	72	0.875
267-296	20	1.75	54	0.5	72	1.750
296-318	20	3.25	54	0.5	72	1.750
318-340	20	3.25	54	0.5	72	1.750
340-377	20	1.75	54	0.5	72	1.750
340-465	20	1.00	54	0.5	72	0.875

Figure 4.41 depicts the displacement profile for Bridge 12 under the ultimate HL93 loading state. Figure 4.42, Figure 4.43, and Figure 4.44 illustrates the load displacement behavior of all spans of Bridge 12 under HL93 loading. Span 1 has a fractured overstrength factor of 1.20 and an intact factor of 2.50. Span 2 has a fractured overstrength of 1.56 and

an intact factor of 2.60. Span 3 has a fractured overstrength factor of 1.15 and an intact factor of 2.35. Once again, the longer spans have lower overstrength factors. Span 1 fails due to transverse rotation while Spans 2 and 3 fail due to longitudinal rotation.

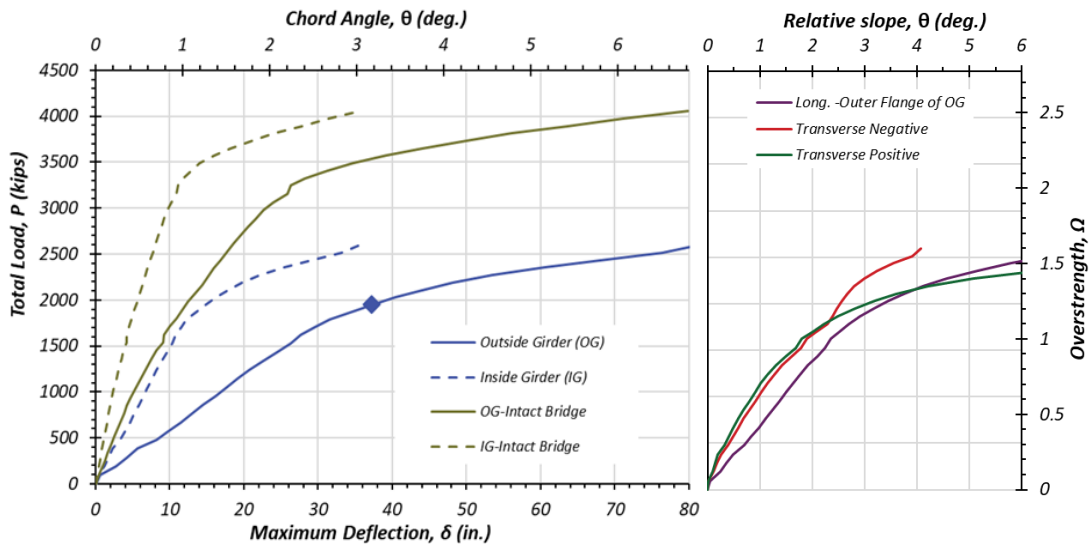
Table 4.26 General Geometric Properties of Bridge 12

Location	Parameter	Description/Value
Bridge	Location	Harris County, IH10
	Year Designed/Year Built	2004/2007
	Design Load	HS25
	Length, ft	465
	Spans, ft	140, 180, 145
	Radius of Curvature, ft	225
Deck	Width, ft	28.417
	Thickness, in.	8.5
	Haunch, in.	3.5
	Rail Type	SSTR
Rebar	# of Bar Longitudinal Top Row (#5)	40
	# of Bar Longitudinal Bottom Row (#5)	30
	# of Bar Longitudinal Top Row (#5) @support	79
	# of Bar Longitudinal Bottom Row (#5) @support	30
	Transverse Spacing Top Row (#5), in.	5
	Transverse Spacing Bottom Row (#5), in.	5



Note: The colors represent achieved curvature limits (Magenta=yielding, Yellow=beyond yielding, Orange=beyond yielding close to failure, Red=Failure) Additional Hinge Data Located in Appendix

Figure 4.41 Grillage Deflection Profile for Span 2 of Bridge 12 with Activated Hinges

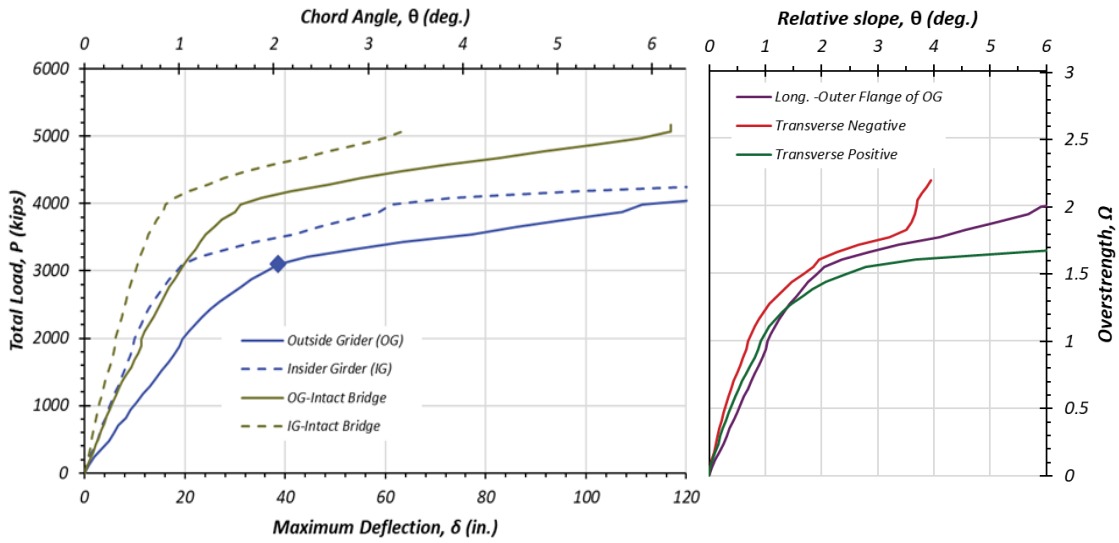


(a) Load-displacement

(b) Deck rotation

Note: δ is along the centerline of the girder, Ω is the load normalized by factored design load

Figure 4.42 Grillage Analysis Results of Bridge 12-Span 1

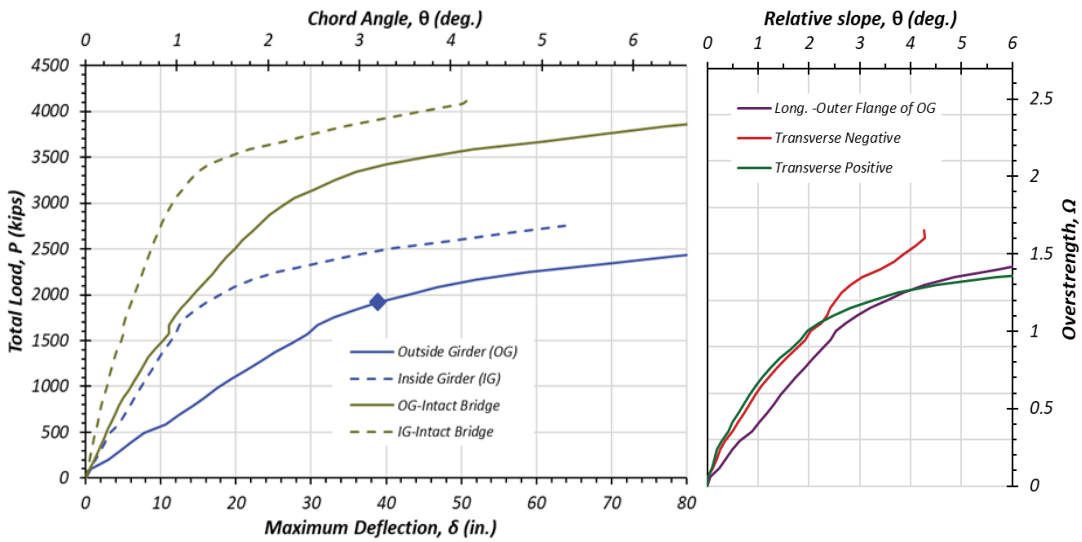


(a) Load-displacement

(b) Deck rotation

Note: δ is along the centerline of the girder, Ω is the load normalized by factored design load

Figure 4.43 Grillage Analysis Results of Bridge 12-Span 2



(a) Load-displacement

(b) Deck rotation

Note: δ is along the centerline of the girder, Ω is the load normalized by factored design load

Figure 4.44 Grillage Analysis Results of Bridge 12-Span 3

4.3.14. Grillage Analysis of Bridge 13-NBI #14-227-0-0015-13-452

Bridge 13, located in Travis County along IH 35, is a three span continuous bridge built in 2002. Bridge 13 has an overall deck width of 30 ft with a deck thickness of 8 in. and has 151.5 ft, 190 ft, and 151.5 ft long spans. Table 4.27 contains the geometric property details for the tub girders for Bridge 13. Table 4.28 details further geometric properties necessary for constructing an appropriate grillage model.

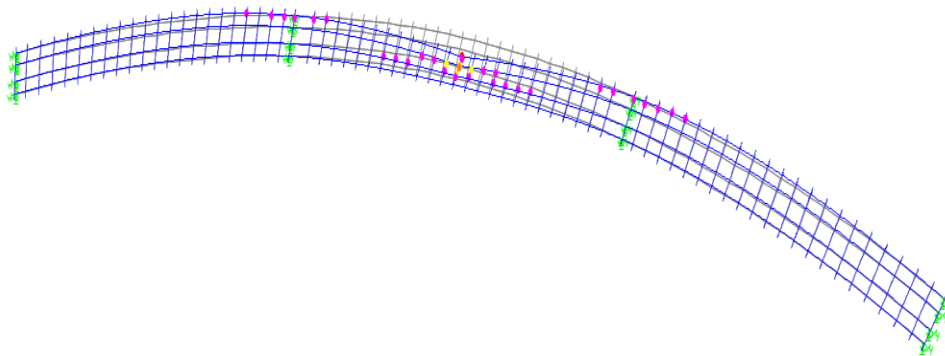
Table 4.27 Geometric Details of Steel Tub Girders of Bridge 13

Location ft	Top Flange		Web		Bottom Flange	
	Width in.	Thickness in.	Width in.	Thickness in.	Width in.	Thickness in.
0-18	24	1.25	54	0.625	60	0.750
18-94	24	1.25	54	0.625	60	0.750
94-113	24	1.25	54	0.625	60	0.750
113-132	24	1.25	54	0.625	60	1.250
132-151	24	1.75	54	0.625	60	1.500
151-170	24	2.75	54	0.625	60	2.000
170-189	24	1.75	54	0.625	60	1.500
189-208	24	1.25	54	0.625	60	1.250
208-284	24	1.25	54	0.625	60	0.750
284-303	24	1.25	54	0.625	60	0.750
303-322	24	1.25	54	0.625	60	1.250
322-341	24	1.75	54	0.625	60	1.500
341-360	24	2.75	54	0.625	60	2.000
360-379	24	1.75	54	0.625	60	1.500
379-398	24	1.25	54	0.625	60	1.250
398-474	24	1.25	54	0.625	60	0.750
474-493	24	1.25	54	0.625	60	0.750

Figure 4.45 illustrates the deflection profile of Bridge 13 with a fractured second span and with the HL93 load case. Figure 4.46 and Figure 4.47 depict the load displacement behavior of each span of Bridge 13. Span 1 and 3 has an intact overstrength factor of 2.10 with fractured overstrength factor of 1.10. Span 2 has an intact overstrength factor of 2.20 and a fractured overstrength factor of 1.35. All spans of Bridge 13 fail due to longitudinal rotation.

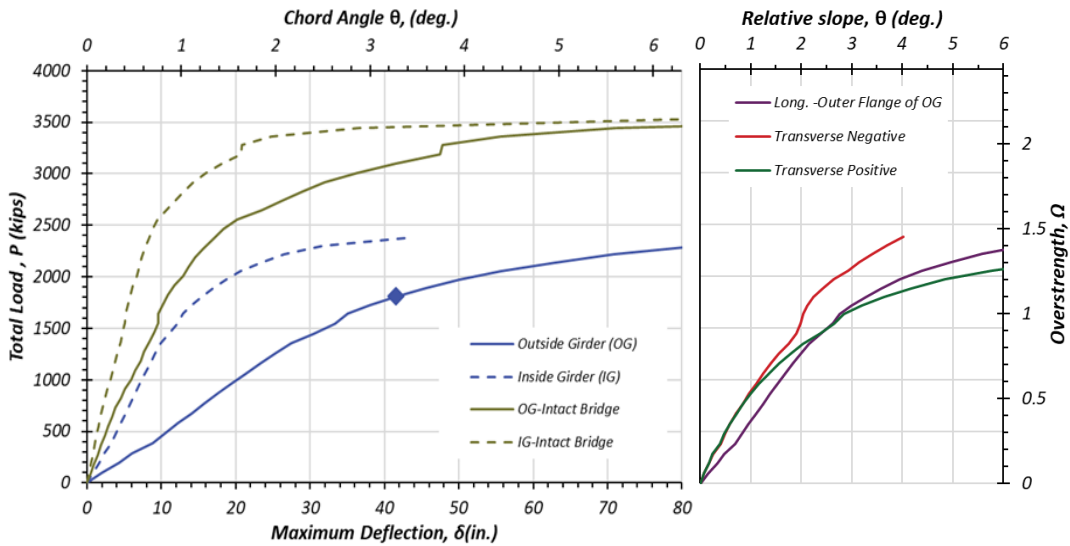
Table 4.28 General Geometric Properties of Bridge 13

Location	Parameter	Description/Value
Bridge	Location	Travis County, IH35
	Year Designed/Year Built	1998/2002
	Design Load	HS20
	Length, ft	493
	Spans, ft	151.5, 190, 151.5
	Radius of Curvature, ft	450
Deck	Width, ft	30
	Thickness, in.	8
	Haunch, in.	4
	Rail Type	T4(S)
Rebar	# of Bar Longitudinal Top Row (#4)	40
	# of Bar Longitudinal Bottom Row (#5)	32
	# of Bar Longitudinal Top Row (#4) @support	39
	# of Bar Longitudinal Top Row (#5) @support	40
	# of Bar Longitudinal Bottom Row (#5) @support	32
	Transverse Spacing Top Row (#5), in.	6
	Transverse Spacing Bottom Row (#5), in.	6



Note: The colors represent achieved curvature limits (Magenta=yielding, Yellow=beyond yielding, Orange=beyond yielding close to failure, Red=Failure) Additional Hinge Data Located in Appendix

Figure 4.45 Grillage Deflection Profile for Span 2 of Bridge 13 with Activated Hinges

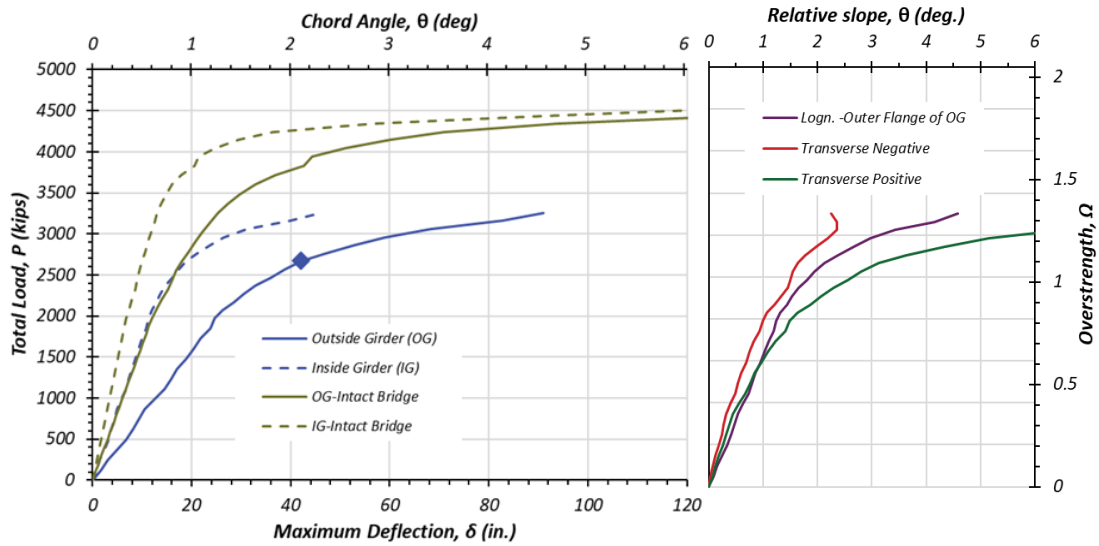


(a) Load-displacement

(b) Deck rotation

Note: δ is along the centerline of the girder, Ω is the load normalized by factored design load

Figure 4.46 Grillage Analysis Results of Bridge 13-Spans 1&3



(a) Load-displacement

(b) Deck rotation

Note: δ is along the centerline of the girder, Ω is the load normalized by factored design load

Figure 4.47 Grillage Analysis Results of Bridge 13-Span 2

4.3.15. Grillage Analysis of Bridge 14-NBI #18-057-0-0009-11-460

Bridge 14, built in Dallas County in 2012, is a three span continuous bridge built along IH30. Bridge 14 consists of three spans with lengths of 150 ft, 190 ft, and 150 ft. It has a deck with an overall width of 28 ft and a thickness 8 in. Table 4.29 contains the geometric information of the steel tub girders for Bridge 14. Note that the top flanges, web, and bottom flange vary in thickness along the length of the girder. Table 4.30 contains additional information needed to construct an accurate grillage model of Bridge 14.

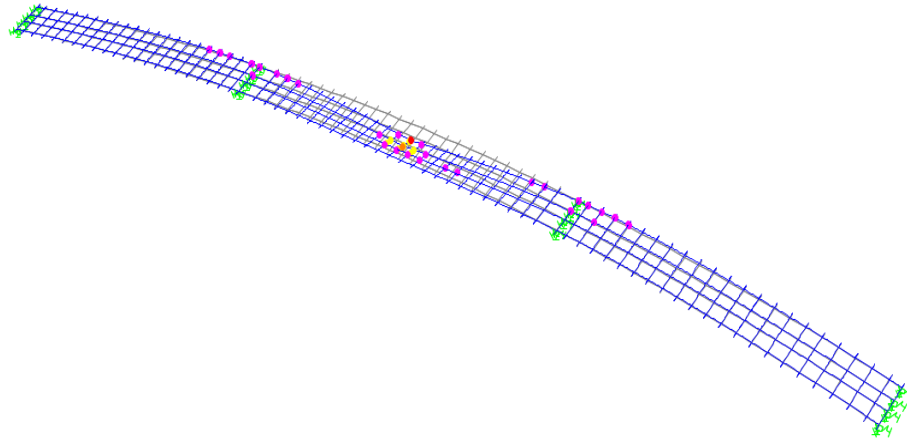
Table 4.29 Geometric Details of Steel Tub Girders of Bridge 14

Location ft	Top Flange		Web		Bottom Flange	
	Width in.	Thickness in.	Width in.	Thickness in.	Width in.	Thickness in.
0-103	22	1.00	60	0.5625	70	0.750
103-112	22	1.00	60	0.5625	70	1.125
112-131	22	1.00	60	0.625	70	1.125
131-169	22	1.75	60	0.625	70	1.500
169-198	22	1.00	60	0.625	70	1.125
198-302	22	1.00	60	0.5625	70	0.750
302-321	22	1.00	60	0.625	70	1.125
321-358	22	1.75	60	0.625	70	1.500
358-386	22	1.00	60	0.625	70	1.125
386-490	22	1.00	60	0.5625	70	0.750

Figure 4.48 shows the deflection profile of Span 2 under the ultimate HL93 loading with a midspan fracture and activated plastic hinge. Figure 4.49 and Figure 4.50 illustrate the load displacement behavior of all spans of Bridge 14. Spans 1 and 3 have an intact overstrength factor of 2.15 fractured overstrength factor of 1.25. Span 2 has an intact overstrength factor of 2.05 fractured overstrength factor of 1.35. All spans of Bridge 14 have fractured overstrength factors greater than 1 and are therefore redundant. All spans of Bridge 14 are controlled by the longitudinal rotation limit.

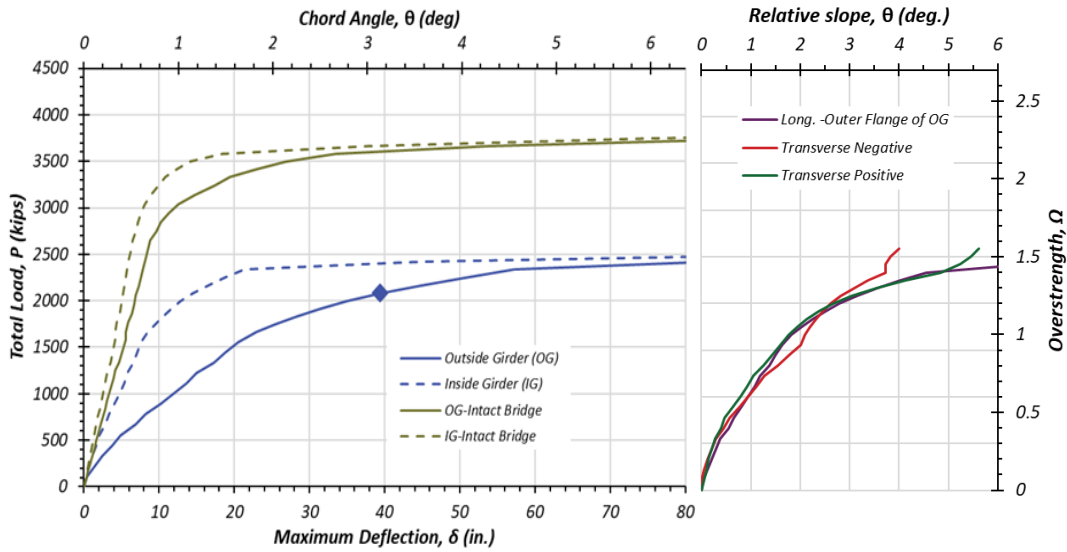
Table 4.30 General Geometric Properties of Bridge 14

Location	Parameter	Description/Value
Bridge	Location	Dallas County, IH30
	Year Designed/Year Built	2008/2012
	Design Load	HS20
	Length, ft	490
	Spans, ft	150,190,150
	Radius of Curvature, ft	1010
Deck	Width, ft	28
	Thickness, in.	8
	Haunch, in.	4
	Rail Type	SSTR
Rebar	# of Bar Longitudinal Top Row (#4)	38
	# of Bar Longitudinal Bottom Row (#5)	32
	# of Bar Longitudinal Top Row (#4) @support	38
	# of Bar Longitudinal Top Row (#5) @support	38
	# of Bar Longitudinal Bottom Row (#5) @support	32
	Transverse Spacing Top Row (#5), in.	6
	Transverse Spacing Bottom Row (#5), in.	6



Note: The colors represent achieved curvature limits (Magenta=yielding, Yellow=beyond yielding, Orange=beyond yielding close to failure, Red=Failure) Additional Hinge Data Located in Appendix

Figure 4.48 Grillage Deflection Profile for Span 2 of Bridge 14 with Activated Hinges

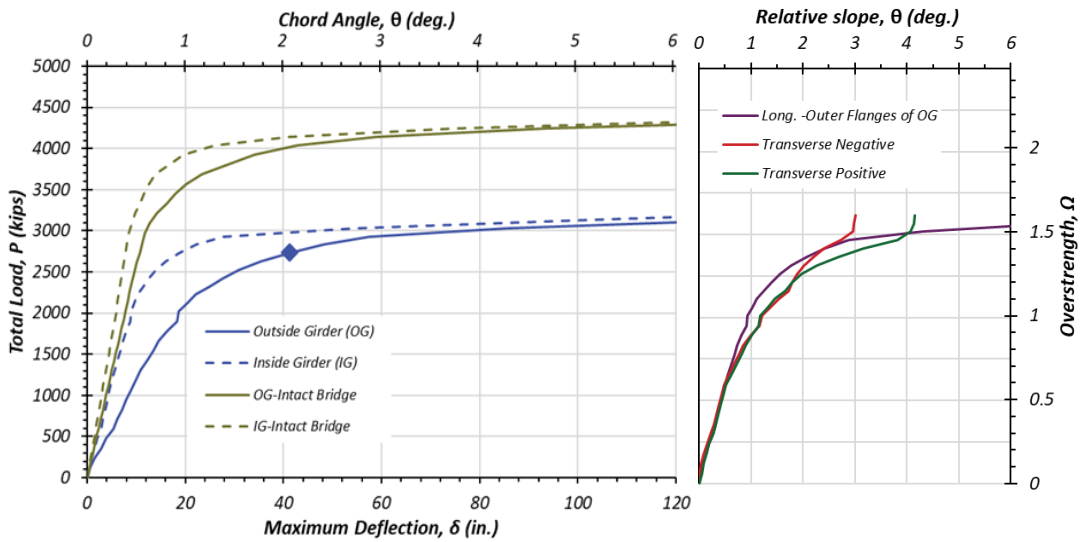


(a) Load-displacement

(b) Deck rotation

Note: δ is along the centerline of the girder, Ω is the load normalized by factored design load

Figure 4.49 Grillage Analysis Results of Bridge 14-Spans 1&3



(a) Load-displacement

(b) Deck rotation

Note: δ is along the centerline of the girder, Ω is the load normalized by factored design load

Figure 4.50 Grillage Analysis Results of Bridge 14-Span 2

4.3.16. Grillage Analysis of Bridge 15-NBI #12-102-0271-06-689

The final bridge investigated in this study is Bridge 15. It is a three span continuous bridge. Bridge 15 contains 200 ft, 295 ft, and 200 ft long spans with an overall deck width 28.4 ft and a thickness of 8 in. Table 4.31 details the geometric details of the tub girders in Bridge 15. It should be noted that the top and bottom flanges vary in thickness along the length of the girder. Table 4.32 outlines additional information regarding the geometric configuration of Bridge 15 need to generate an appropriate grillage model.

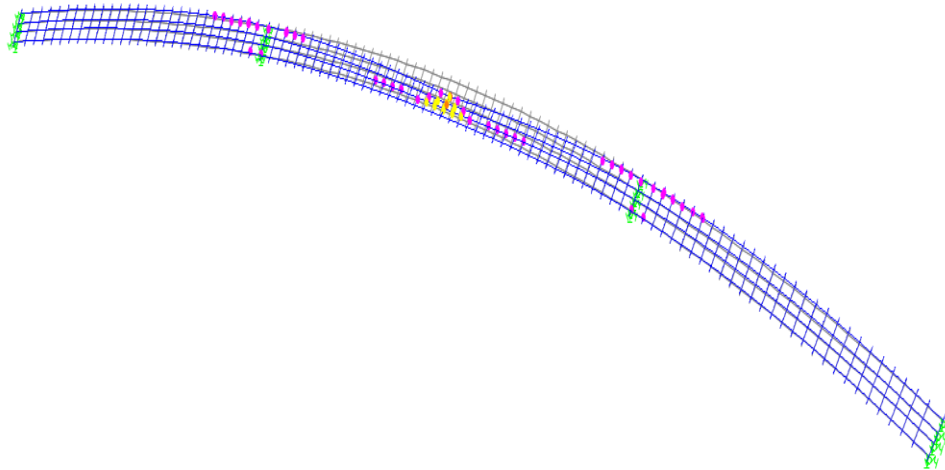
Table 4.31 Geometric Details of Steel Tub Girders of Bridge 15

Location ft	Top Flange		Web		Bottom Flange	
	Width in.	Thickness in.	Width in.	Thickness in.	Width in.	Thickness in.
0-126	24	1.25	84	0.6875	53.5	1.250
126-147	24	1.50	84	0.6875	53.5	1.750
147-168	24	1.75	84	0.6875	53.5	2.000
168-189	24	2.25	84	0.6875	53.5	2.250
189-210	24	2.25	84	0.6875	53.5	2.250
210-231	24	2.50	84	0.6875	53.5	2.500
231-252	24	1.75	84	0.6875	53.5	2.000
252-284	24	1.25	84	0.6875	53.5	1.250
284-410	24	1.50	84	0.6875	53.5	1.750
410-422	24	1.25	84	0.6875	53.5	1.250
422-463	24	1.75	84	0.6875	53.5	2.000
463-484	24	2.25	84	0.6875	53.5	2.250
484-505	24	2.50	84	0.6875	53.5	2.500
505-526	24	2.25	84	0.6875	53.5	2.250
526-547	24	1.75	84	0.6875	53.5	2.000
547-568	24	1.50	84	0.6875	53.5	1.750
568-698	24	1.25	84	0.6875	53.5	1.250

Figure 4.51 depicts the displacement profile of the fractured Span 2 under the ultimate HL93 loading case. Figure 4.52 and Figure 4.53 shows the load displacement response of all spans in Bridge 15. Spans 1 and 3 have an intact overstrength factor of 2.45 and a fractured overstrength factor of 1.40. Span 2 has a fractured overstrength factor of 1.25. All three spans of Bridge 15 have fractured Ω factors greater than 1 and considered redundant. Every span in Bridge 15 is controlled by longitudinal rotation.

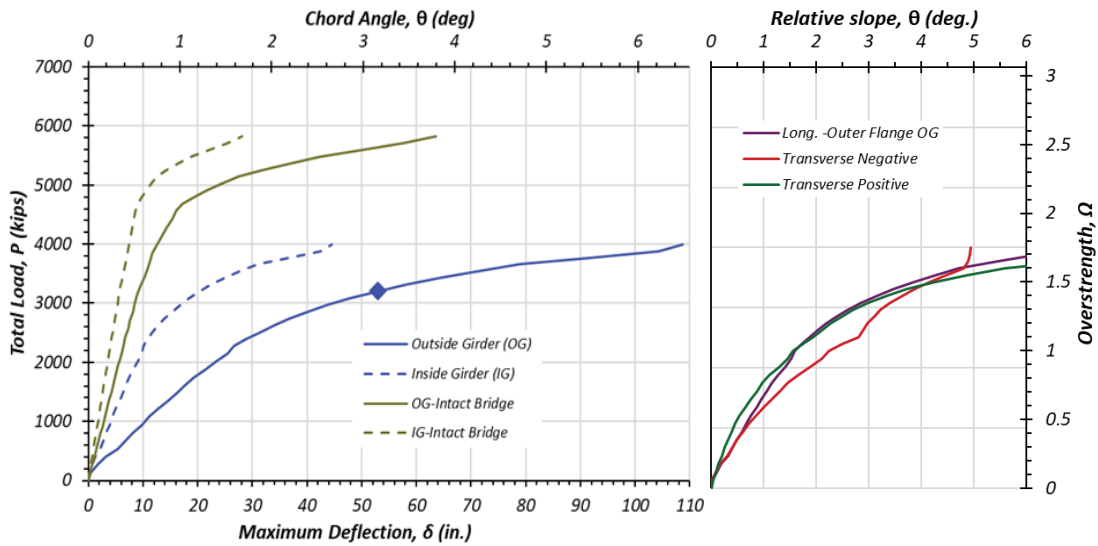
Table 4.32 General Geometric Properties of Bridge 15

Location	Parameter	Description/Value
Bridge	Location	Dallas County, IH30
	Year Designed/Year Built	2008/2012
	Design Load	HL93
	Length, ft	695
	Spans, ft	200,295,200
	Radius of Curvature, ft	809
Deck	Width, ft	28.417
	Thickness, in.	8
	Haunch, in.	4.5
	Rail Type	SSTR
Rebar	# of Bar Longitudinal Top Row (#5)	38
	# of Bar Longitudinal Bottom Row (#5)	36
	# of Bar Longitudinal Top Row (#5) @support	78
	# of Bar Longitudinal Bottom Row (#5) @support	36
	Transverse Spacing Top Row (#5), in.	5
	Transverse Spacing Bottom Row (#5), in.	5



Note: The colors represent achieved curvature limits (Magenta=yielding, Yellow=beyond yielding, Orange=beyond yielding close to failure, Red=Failure) Additional Hinge Data Located in Appendix

Figure 4.51 Grillage Deflection Profile for Span 2 of Bridge 15 with Activated Hinges

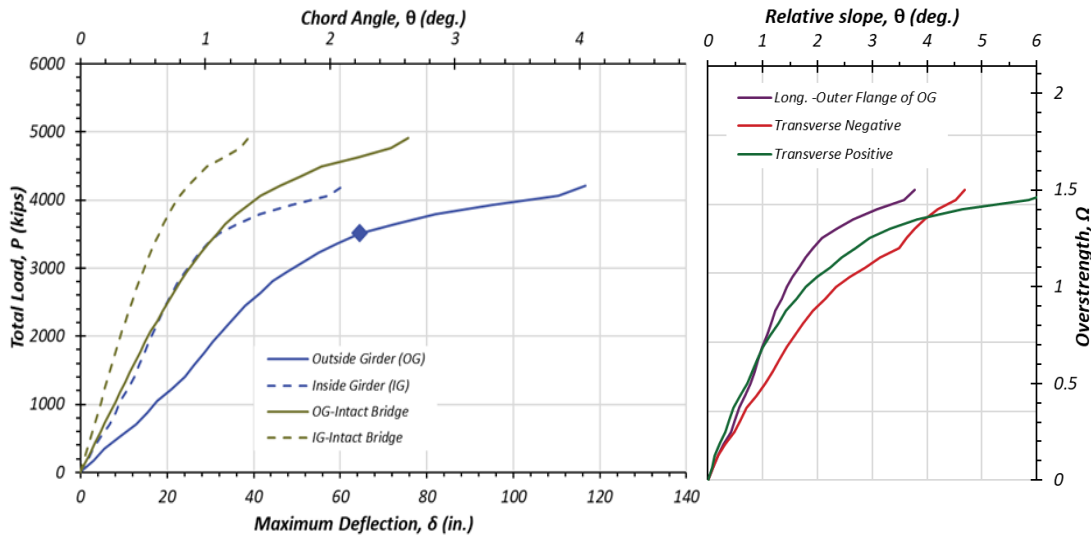


(a) Load-displacement

(b) Deck rotation

Note: δ is along the centerline of the girder, Ω is the load normalized by factored design load

Figure 4.52 Grillage Analysis Results of Bridge 15-Spans 1&3



(a) Load-displacement

(b) Deck rotation

Note: δ is along the centerline of the girder, Ω is the load normalized by factored design load

Figure 4.53 Grillage Analysis Results of Bridge 15-Span 2

4.4. Conclusion

In this portion of this STTG study, 15 bridges from the Texas Bridge inventory were evaluated to determine their strength and redundancy before and after a simulated fracture under HL93 design load. The 15 bridges were modeled using the state of the art structural analysis program SAP2000, based on matrix analysis methods and principles. These bridges were evaluated in manner outlined in Chapter 6. Table 4.33 offers a summary of the grillage analysis results gathered and includes the normalized load for the fractured and nonfractured cases for each bridge. From the grillage analysis results, the following observations were seen:

- Overall, simple span bridges have much lower fractured overstrength factors than their continuous span counterparts. The fractured overstrength factors range from

0.16 to 1.11 while their intact overstrength factors range from 3.42 to 1.00. On average, after simulating a full web fracture, simple span bridges experience a strength reduction of nearly 74%.

- In the case of exterior spans of continuous bridge (all spans in two span bridges and exterior span in three span bridges) fractured overstrength factors range from 0.60 to 1.71. Their intact overstrength factors range from 1.45 to 3.38. However, as a whole, exterior spans lose an average of 46% of their initial strength post web fracture, which, is significantly less than that of the single span bridges.
- When compared to single span bridges and the exterior spans, the interior spans of the three span continuous bridge had the lowest strength reduction post full web fracture. This can be seen by looking at the results of the continuous bridges. The intact overstrength factors range from 1.85 to 3.10. The fractured overstrength factors range from 1.00 to 2.10. Yet, the average strength reduction of the interior spans is only 35%. This is significantly lower than that of the simple spans and exterior spans.
- From the results it is clear that there is some redundancy due to continuity due to the fact that as the degree of continuity increases, the average strength reduction decreases. These results demonstrate that, even though there exist transverse redundancy between the two girders, there is some longitudinal redundancy and load redistribution between the spans of the same bridge.

Table 4.33 Overstrength Factors for Single Span Bridges utilizing Grillage Analysis

ID	Span	R (ft)	L (ft)	B (ft)	S (ft)	5% SF	5° Trans.	2° Long.
0	1	1300	120	23	6.0	1.33	1.33	1.07
1	1	573	220	32	9.5	0.46	0.28	0.21
2	1	1910	115	26	6.1	1.11	1.65	1.11
3	1	2207	230	39	12.6	0.60	0.16	0.37

Note: L= length, B=breadth, R=radius of curvature, S=spacing between interior top flanges

Table 4.34 Overstrength Factors for End Spans utilizing Grillage Analysis

ID	Span	R (ft)	L (ft)	B (ft)	S (ft)	5% SF	5° Trans.	3° Long.
4	1	195	132	28	7.6	1.50	1.45	1.30
4	2	195	128	28	7.6	1.58	1.53	1.32
5	1	450	140	30	9.7	1.25	1.30	1.10
5	2	450	140	30	9.7	1.25	1.30	1.10
6	1	819	140	38	9.8	1.43	1.58	1.58
6	2	819	140	38	9.8	1.43	1.58	1.58
7	1	764	219	28	7.4	1.30	1.15	0.94
7	2	764	190	28	7.4	1.50	1.45	1.25
8	1	882	265	28	8.4	0.94	0.88	0.83
8	2	882	295	28	8.4	0.80	0.60	0.60
9	1	764	140	28	7.4	1.35	1.65	1.40
9	3	764	126	28	7.4	1.53	1.95	1.61
10	1	716	148	30	7.7	1.71	2.10	1.94
10	3	716	190	30	7.7	1.40	1.35	1.25
11	1	819	223	28	7.0	1.35	1.45	1.50
11	3	819	235	28	7.0	1.40	1.30	1.40
12	1	225	140	28	7.6	1.55	1.20	1.40
12	3	225	145	28	7.6	1.50	1.35	1.15
13	1	450	152	30	9.3	1.40	1.25	1.10
13	3	450	152	30	9.3	1.40	1.25	1.10
14	1	1010	150	28	6.5	1.35	1.45	1.25
14	3	1010	150	28	6.5	1.35	1.45	1.25
15	1	809	200	28	8.0	1.55	1.60	1.40
15	3	809	200	28	8.0	1.55	1.60	1.40

Note: L= length, B=breadth, R=radius of curvature, S=spacing between interior top flanges

Table 4.35 Overstrength Factors for Interior Spans utilizing Grillage Analysis

ID	Span	R (ft)	L (ft)	B (ft)	S (ft)	5% SF	5° Trans.	2° Long.
9	2	764	151	28	7.0	2.10	2.50	2.15
10	2	716	265	30	7.7	1.50	1.45	1.25
11	2	819	366	28	7.0	1.15	1.10	1.00
12	2	225	180	28	7.6	2.05	1.67	1.56
13	2	450	190	30	9.3	1.60	1.50	1.35
14	2	1010	190	28	6.5	1.45	1.60	1.35
15	2	809	295	28	8.0	1.50	1.45	1.25

Note: L= length, B=breadth, R=radius of curvature, S=spacing between interior top flanges

4.5. Grillage Analysis: Additional Parametric Study

In addition to the parametric study involving the 15 selected bridges from the TxDOT inventory, a parametric study was completed on two of the bridges varying multiple parameters of the bridge. Bridge 2, a single span bridge, and the middle span of Bridge 9, a three span bridge, were selected to analyze in the parametric study. A single span bridge and a middle span were selected to see the varying effect with the greatest degree of continuity difference. Three parameters: concrete strength, reinforcing bar area, and deck thickness, were varied for both spans involved in the parametric study.

4.5.1. Concrete Strengths

TxDOT's design strength of all off the bridges involved in the parametric study was 4000 psi. In this study the bridges were analyzed with the design strength of 4000 psi as well as concrete strengths of 5000 psi and 6000 psi.

The results for Bridge 2 and the middle span of Bridge 9 are located in Table 4.36 and Table 4.37 respectively. Both bridge spans failure overstrength factors increase

relatively similar amounts from 4000 psi to 5000 psi (0.05 for Bridge 2, and 0.02 for Bridge 9) and from 4000 psi to 6000 psi (0.08 for Bridge 2 and Bridge 9). Not only did increasing the concrete strength increase the overstrength factor, but it also shifted the failure mode from structural failure to longitudinal rotation failure for both bridges when transitioning from a concrete strength of 5000 psi to 6000 psi.

Table 4.36 Bridge 2: Overstrength Factors (Ω) with Varied Concrete Strengths

f'c (psi)	5% S.F	5° Trans	2° Long
<i>4000</i>	1.11	1.65	1.11
<i>5000</i>	1.16	1.36	1.16
<i>6000</i>	1.30	1.24	1.19

Table 4.37 Bridge 9 (Mid-Span): Overstrength Factors (Ω) with Varied Concrete Strengths

f'c (psi)	5% S.F	5° Trans	2° Long
<i>4000</i>	2.10	2.50	2.15
<i>5000</i>	2.12	2.62	2.15
<i>6000</i>	2.18	2.63	2.18

4.5.2. Reinforcing Bar Area

Reinforcing bar area was another variable altered in the parametric study. The design reinforcing bar area was analyzed for both Bridge 2 and the middle span of Bridge 9. The percentage of reinforcing bar area was increased 25% and 50% and analyzed using the grillage method. Both transverse and longitudinal reinforcing bar areas were increased in this study.

Table 4.38 and Table 4.39 contain the overstrength factor results from increasing the reinforcing bar areas in the slab of bridge deck of Bridge 2 and the middle span of Bridge 9. The overstrength factors of Bridge 2 and mid-span of Bridge of 9 increased as the percentage of reinforcing increased and the failure mode consistently remained structural failure. However, the amount by which the overstrength factors increased varied significantly between the bridges for the both the 25% increase (0.01 for Bridge 2 and 0.05 for Bridge 9) and the 50% increase (0.03 for Bridge 2 and 0.14 for Bridge 9). This could be accounted for by the increase in continuity.

Table 4.38 Bridge 2: Overstrength Factors (Ω) with Varied Reinforcing Bar Areas

% rebar	5% S.F	5° Trans	2° Long
<i>100</i>	1.11	1.65	1.11
<i>125</i>	1.12	1.77	1.18
<i>150</i>	1.14	1.80	1.21

Table 4.39 Bridge 9 (Mid-Span): Overstrength Factors (Ω) with Varied Reinforcing Bar Areas

% rebar	5% S.F	5° Trans	2° Long
<i>100</i>	2.10	2.50	2.15
<i>125</i>	2.15	2.80	2.21
<i>150</i>	2.24	3.00	2.29

4.5.3. Concrete Deck Thickness

Another key parameter investigated in this study is concrete deck thickness. The design concrete deck thickness for both Bridge 2 and Bridge 9 is 8 inches. The parametric study

increased the deck thickness by 1 and 2 inches, which takes the total deck thicknesses to 9 and 10 inches respectively.

Table 4.40 and Table 4.41 contains the overstrength results for Bridge 2 and the mid-span of Bridge 9 with increased deck thicknesses. Bridge 2 and Bridge 9 have overstrength factors which increase as deck thickness increase. However, Bridge 2 changes failure modes from structural failure with a 9 inch thickness to a longitudinal rotation failure at 10 inches. Bride 9 has a consistent failure mode of structural failure. Overstrength values increased more rapidly for Bridge 2 than for the mid-span of Bridge 9. This indicates that deck thickness may influence less continuous structures more than bridge spans with greater continuity.

Table 4.40 Bridge 2: Overstrength Factors (Ω) with Varied Concrete Thicknesses

Deck (in.)	5% S.F	5° Trans	2° Long
8	1.11	1.65	1.11
9	1.19	1.74	1.24
10	1.66	1.86	1.39

Table 4.41 Bridge 9 (Mid-Span): Overstrength Factors (Ω) with Varied Concrete Thicknesses

Deck (in.)	5% S.F	5° Trans	2° Long
8	2.10	2.50	2.15
9	2.13	2.88	2.19
10	2.23	N/A	2.35

5. GRILLAGE METHOD AND FEM COMPARISON*

5.1. Introduction

From the FEM results in Section 3.3.2 and the Grillage results in Section 4.4 it can be clearly seen that for some bridge spans the two methods are in good agreement and for other bridge spans the results seem to diverge. This section will discuss the observed similarities and differences between the two analysis methods and the impact of these results on potential industry use of the grillage method to adequately assess failure capacity of steel twin tub girder bridges. This section will break down bridge spans for comparison by number of fixed supports. First, spans with no fixed supports, or single span Bridges 0 to 3 will be looked at. Then, bridge spans with two fixed supports, or the middle spans of Bridges 9 to 15 will be evaluated. Finally, bridge spans with one fixed support, or the end spans of Bridges 4 to 15 will be compare and contrasted. Note: All of the FEM data came from TxDOT Report 0-6937 (Hurlebaus et al. 2018).

5.2. Single Span Bridges

Single span bridges have the least amount of support redundancy and it is expected that their overstrength factors will be lower than that of the interior spans and end spans. In all of the simply sported bridge cases the location of fracture was assumed to be at the center of the span along the exterior girder. Table 5.1 contains the overstrength factor results from both FEM analysis and Grillage Push-Down analysis. The table is organized in

* Part of this chapter is reprinted with permission from “Fracture Critical Steel Twin Tub Girder Bridges Technical Report” 0-6937-R1 by Hurlebaus S., Mander J., Terzioglu T., Boger N., Fatima A., 2018. Texas A&M Texas Transportation Institute, 259-282, Copyright 2018 by Texas A&M Texas Transportation Institute

increasing order in accordance with span length. It should be noted that span length increases the overstrength factor decreases for both the FEM and Grillage analysis methods.

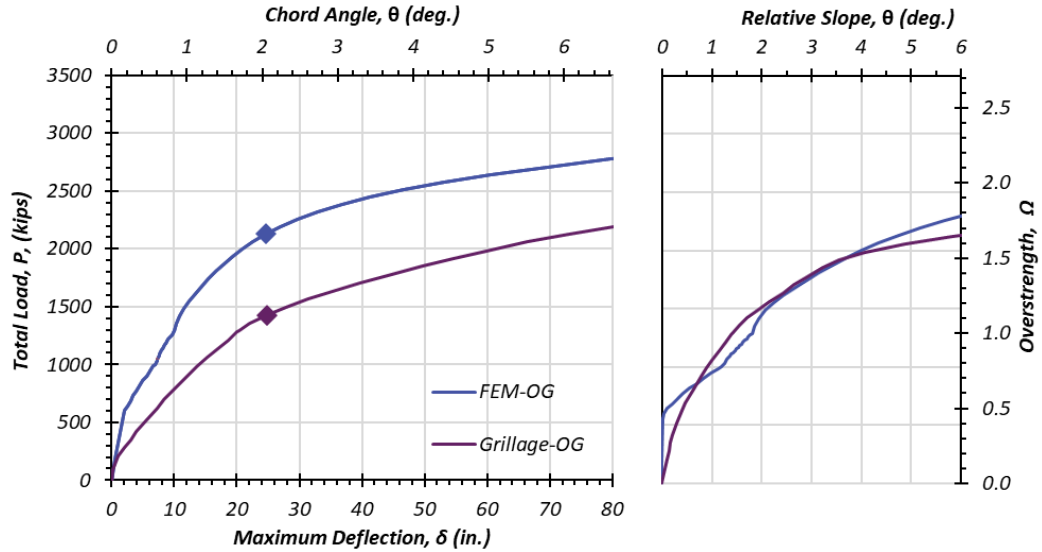
Table 5.1 Results for Simple Spans

ID	Span	R (ft)	L (ft)	B (ft)	S (ft)	FEM	Grillage
2	1	1910	115	26	6.1	1.65	1.11
0	1	1300	120	23	6	0.86	1.07
1	1	573	220	32	9.5	0.82	0.21
3	1	2207	230	39	12.6	0.85	0.16

The single span bridges are divided into two categories: short single span bridges (spans less than or equal to 120 feet) and long single span bridges (spans greater than or equal to 220 feet). The single span bridges can be considered redundant if the overstrength factor is greater than 1. For the shorter span bridges, there is some, however not conclusive, agreement between the FEM and Grillage methods. However, there is greater disparity between FEM and Grillage for the longer span bridges. The Grillage method of analysis does not incorporate some of the internal redundancies such as: cross bracing, diaphragms, and shear stud connectors, which the FEM analysis accounts for. This is a probable explanation for the magnification of difference between the overstrength factors for the FEM and Grillage methods.

Figure 5.1 demonstrates that the shorter span bridges have the potential to reach an overstrength factor of at least 1 and quite possibly be considered redundant. Figure 5.2 illustrates the vast difference in the FEM and Grillage analysis results for longer simple

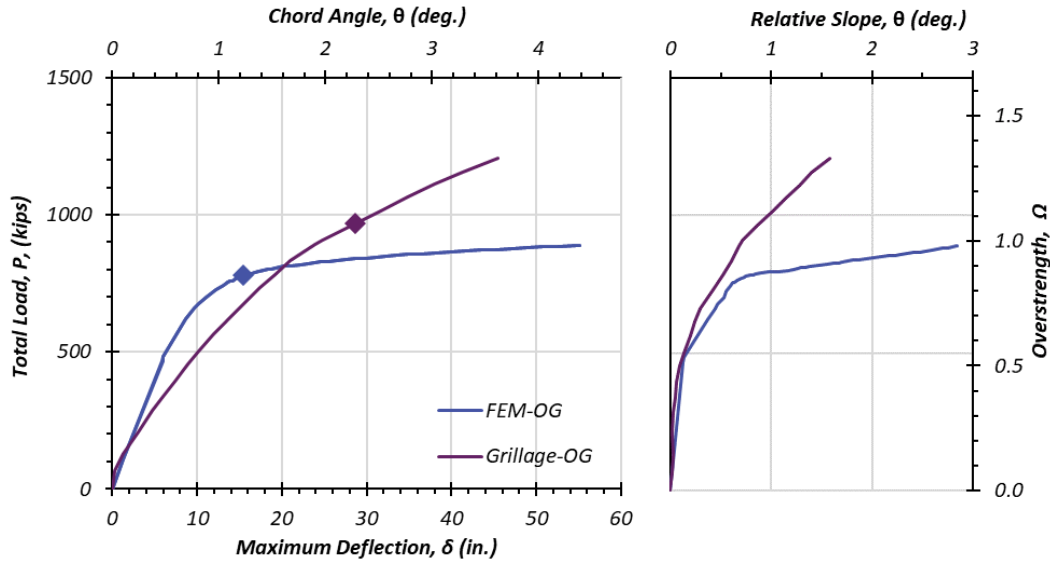
span bridges. However, both methods conclude that longer span simply supported bridges are unable to meet the criteria of a redundant structure.



(i) Load displacement

(ii) Deck rotations

(a) Comparison of the Results for Bridge 2, $L=115$ ft

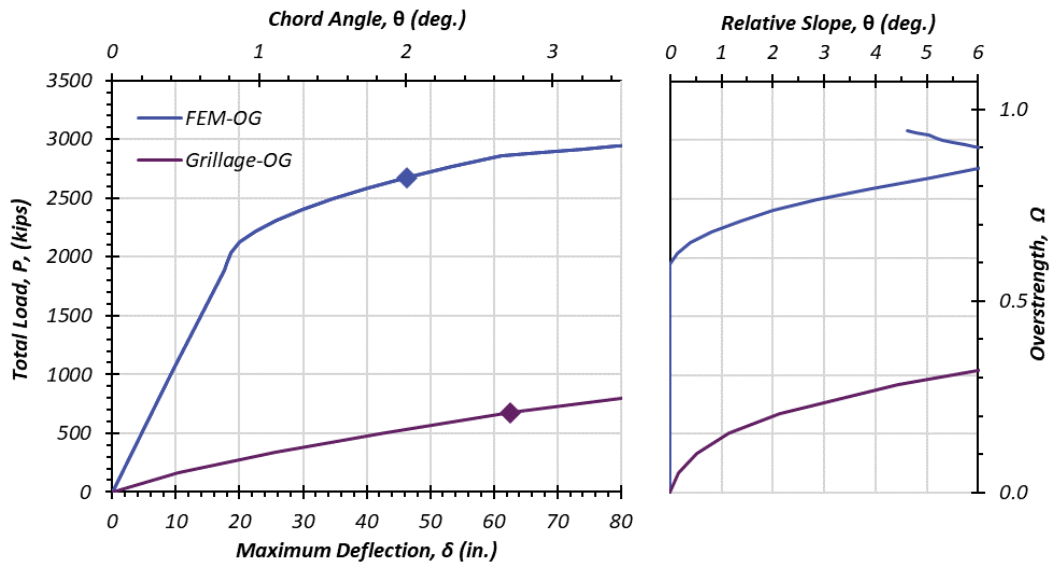


(i) Load displacement

(ii) Deck rotations

(b) Comparison of the Results for Bridge 0, $L=120$ ft

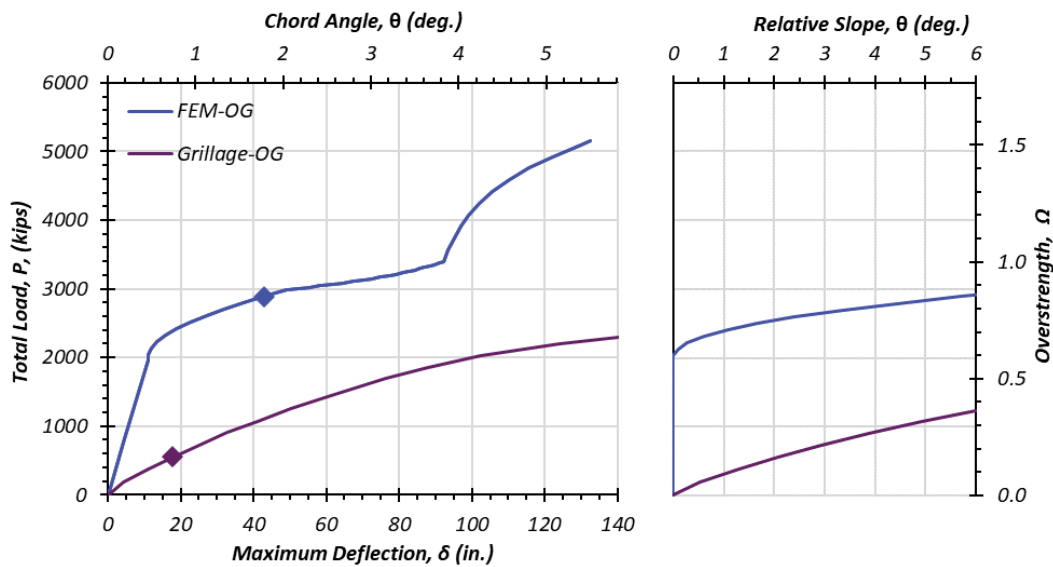
Figure 5.1. Results for Short Single Span (Simply Supported) Fractured Twin Tub Bridges



(i) Load displacement

(ii) Deck rotations

(a) Comparison of the Results for Bridge 1, L=220 ft



(i) Load displacement

(ii) Deck rotations

(b) Comparison of the Results for Bridge 3, L=230 ft

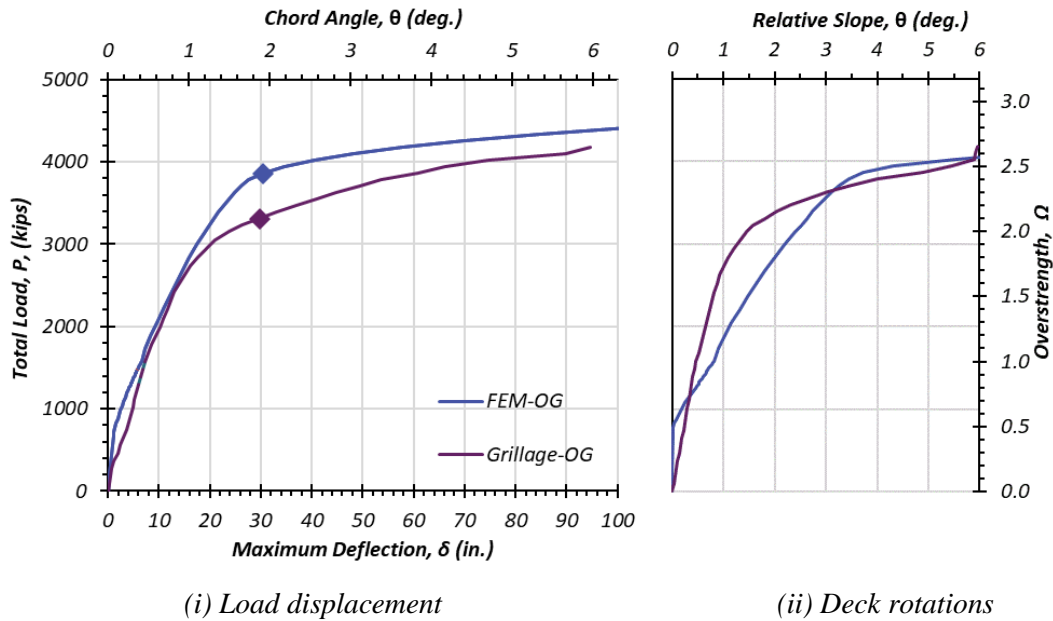
Figure 5.2. Results for Long Single Span (Simply Supported) Fractured Twin Tub Bridges

5.3. Interior Spans

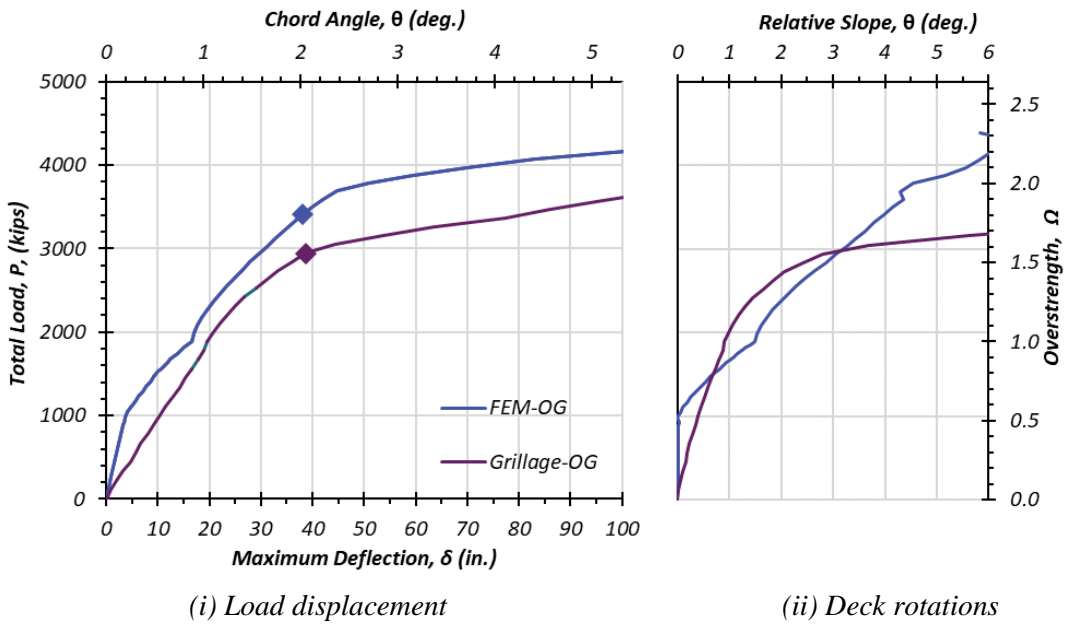
Interior spans, or the middle spans on three span bridges, have the greatest amount of structural support redundancy and are expected to have the highest overstrength factors when compared to their single span and end span counterparts. Table 5.2 below lists the overstrength factors for the interior span bridges sorted by span length in ascending order. It should be noted that all of the interior spans have overstrength factors greater than or equal to one, all are redundant. Grillage analysis results are consistently lower than the FEM analysis results. This correlation can be explained by the fact that Grillage analysis method is a conservative simplified lower bound strip method and the FEM adequately models and the 3-D components. Grillage and FEM overstrength factors values for the interior spans are in closer agreement than the simple span bridges. Detailed results for all of the interior spans are located in Figure 5.3, Figure 5.4, Figure 5.5, and Figure 5.6 are presented according to bridge length.

Table 5.2 Results for Interior Spans

ID	Span	R (ft)	L (ft)	B (ft)	S (ft)	FEM	Grillage
9	2	764	151	28	7	2.45	2.10
12	2	225	180	28	7.6	1.80	1.56
13	2	450	190	30	9.3	1.40	1.35
14	2	1010	190	28	6.5	1.80	1.35
10	2	716	265	30	7.7	1.45	1.25
15	2	809	295	28	8	1.40	1.25
11	2	819	366	28	7	1.20	1.00

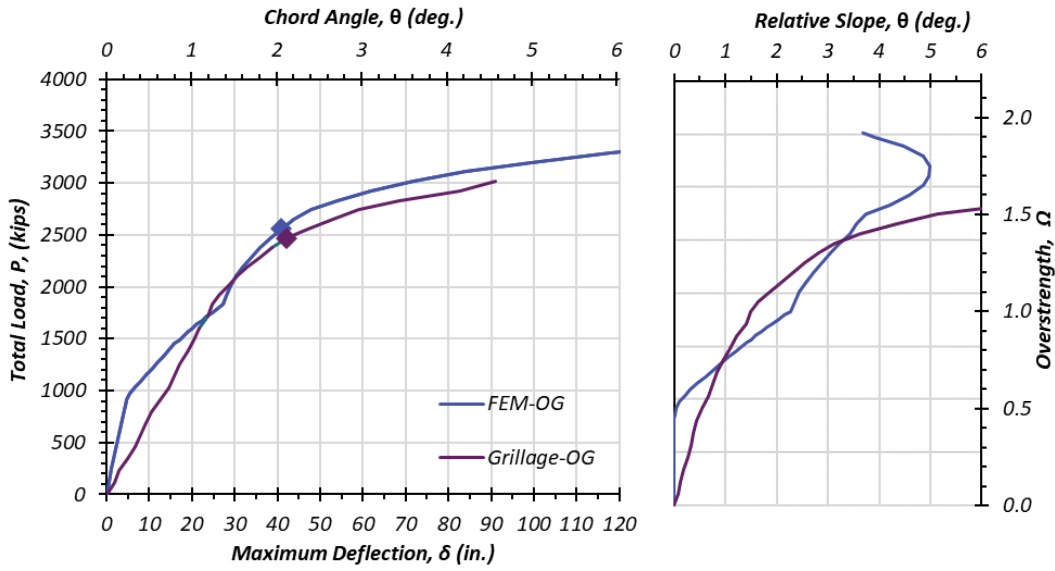


(a) Comparison of the Results for Bridge 9 Span 2, L=151 ft



(b) Comparison of the Results for Bridge 12 Span 2, L=180 ft

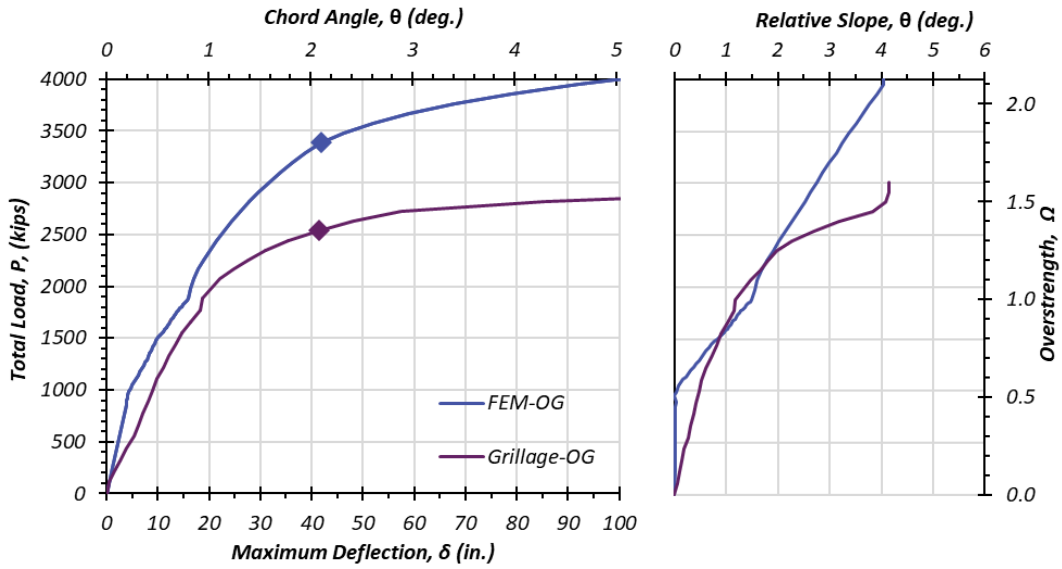
Figure 5.3. Results for Shorter Interior Spans of Fractured Twin Tub Bridges



(i) Load displacement

(ii) Deck rotations

(a) Comparison of the Results for Bridge 13 Span 2, $L=190$ ft

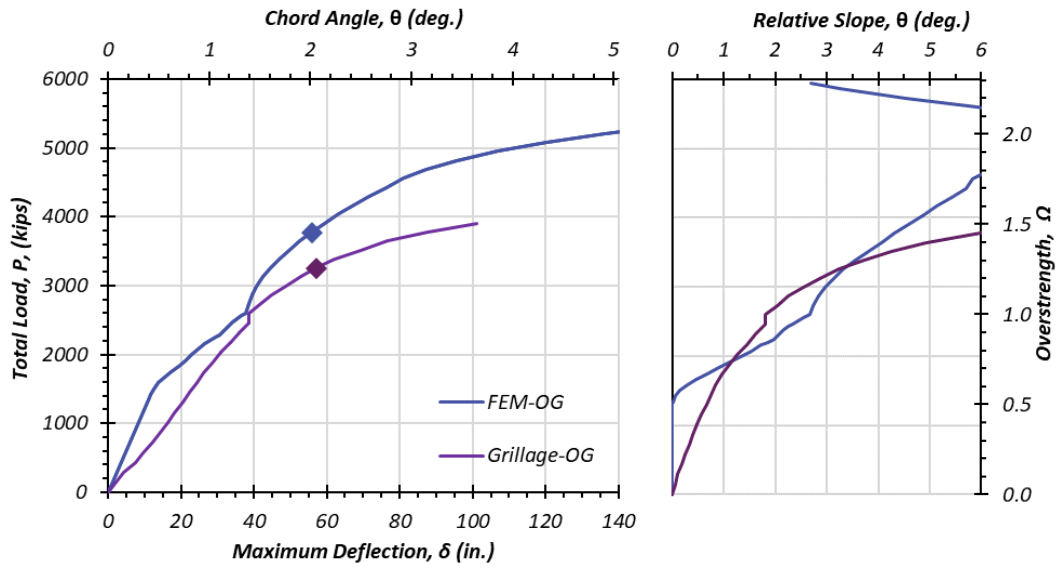


(i) Load displacement

(ii) Deck rotations

(b) Comparison of the Results for Bridge 14 Span 2, $L=190$ ft

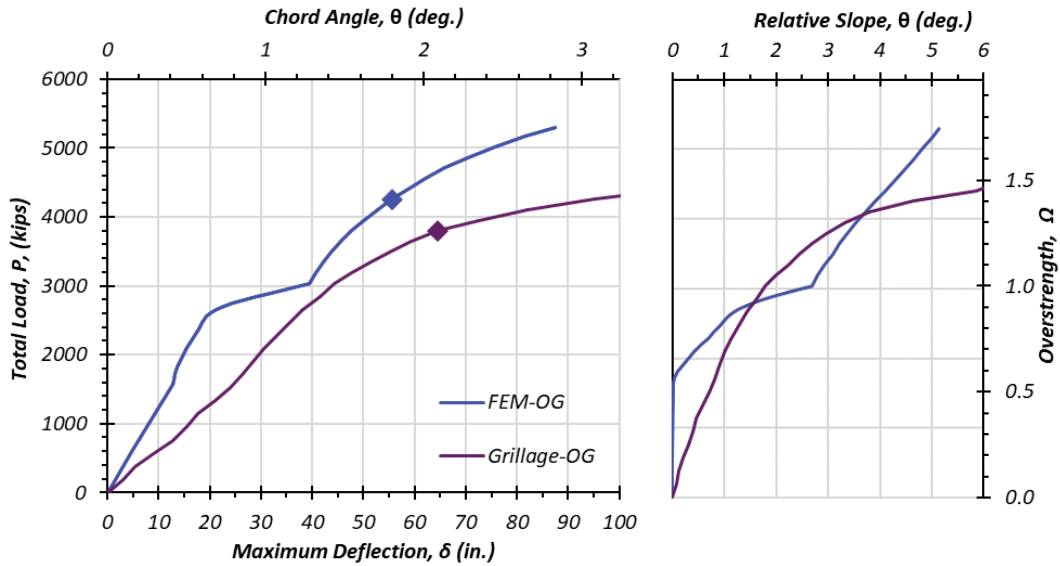
Figure 5.4. Results for Average Interior Spans of Fracture Twin Tub Bridges



(i) Load displacement

(i) Deck rotations

(a) Comparison of the Results for Bridge 10 Span 2, $L=265$ ft

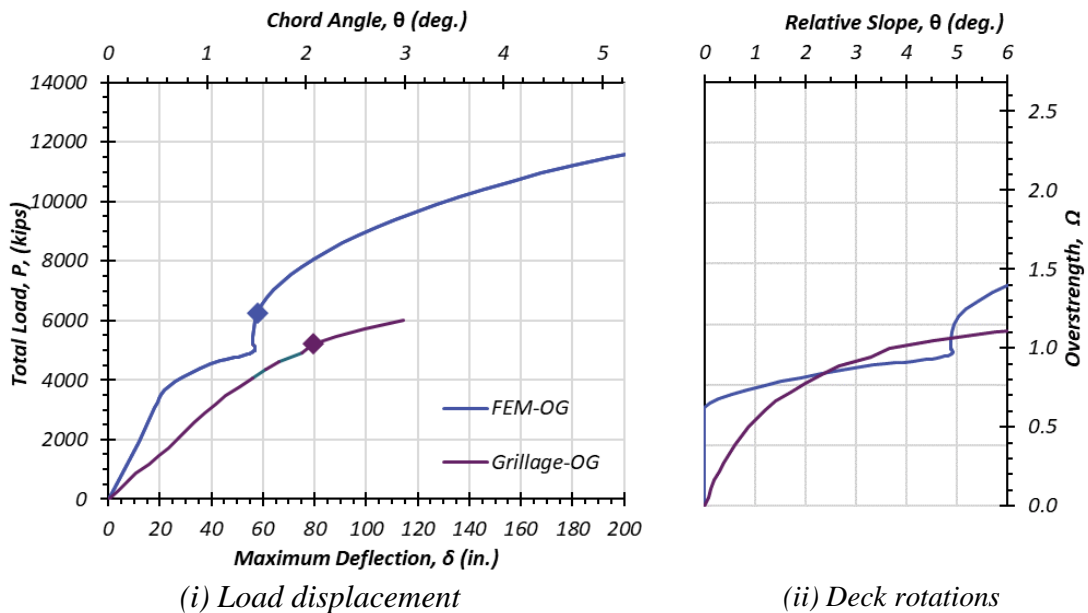


(i) Load displacement

(ii) Deck rotations

(b) Comparison of the Results for Bridge 15 Span 2, $L=295$ ft

Figure 5.5. Results for Long Interior Spans of Fracture Twin Tub Bridges



(i) Load displacement (ii) Deck rotations
Comparison of the Results for Bridge 11 Span 2, L=366 ft
Figure 5.6. Results for Very Long Interior Span of Fracture Twin Tub Bridges

Figure 5.3 illustrates the FEM and Grillage analysis results for shorter interior spans (span lengths ≤ 180 feet) as shows great agreement amongst the analysis methods. Figure 5.4 shows the results for average interior spans ($180 \text{ feet} < \text{span lengths} \leq 250 \text{ feet}$). Both interior spans from Bridge 14 and 13 are 190 feet but differ in overstrength values, with Bridge 13 having a lower value. One significant reason is due to the fact that the radius of curvature for Bridge 13 is nearly half of that of Bridge 14. However both have overstrength factors greater than one. Figure 5.5 depicts the results for longer interior spans ($250 \text{ feet} < \text{span length} \leq 300 \text{ feet}$). Interior spans from Bridge 10 and 15 are longer interior spans have overstrength values greater than one and excellent agreement between the two analysis methods. Very long interior span (span lengths ≥ 300 feet) results can be seen in Figure 5.6. There is slight disparity between the two analysis methods the very

long interior span of Bridge 11 with FEM yielding a result of 1.2 and Grillage Method an overstrength factor of 1.0. However, since Grillage Method is a conservative analysis approach, Bridge 11 can safely be classified as a redundant structure.

Overall, interior spans of three span bridges, are more redundant than single span bridges and exterior span with all overstrength factors being greater than one. As the span length increased, the overstrength values decreased. It is also notable that as the radius of curvature increases so does the overstrength value.

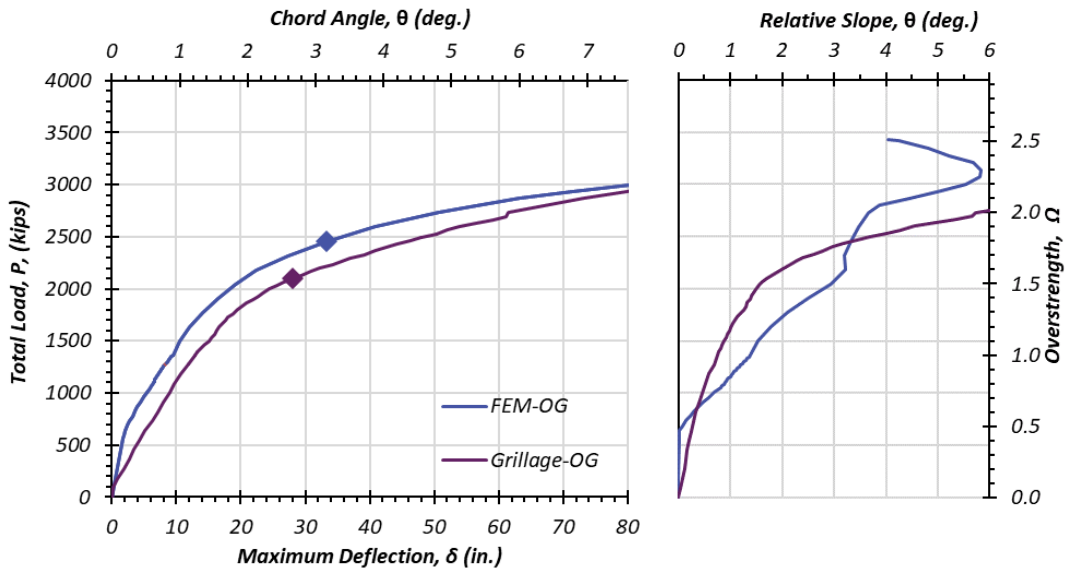
5.4. Exterior Spans

Exterior spans, all spans of two span bridges and end spans of three span bridges, have greater overstrength values than single span bridges but lower overstrength factors than the interior spans. Unlike the interior and single spans, the exterior spans fail at approximately $0.4*L$ distance away from the free support due to indeterminate behavior. Table 5.3 presents both the Grillage and FEM overstrength factor results in increasing span length order. All but 3 of the 24 exterior spans are redundant according to FEM and Grillage analysis methods; and 1 of the 3 spans is considered redundant under FEM analysis. Increasing span length and decreased radii of curvatures yields lower overstrength factors in exterior spans and is complementary to trend seen in single spans and interior spans. Majority of the exterior spans (all but 3) the Grillage overstrength factors are less than the FEM analysis results, which was expected. Figure 5.7, Figure 5.8, Figure 5.9, Figure 5.10, and Figure 5.11 depict detailed FEM and Grillage analysis results for shorter (span lengths < 150 feet) exterior spans. Figure 5.12, Figure 5.13, and Figure 5.14 compare the results for average ($150 \text{ feet} \leq \text{span length} \leq 200 \text{ feet}$) exterior

span lengths. Figure 5.15 and Figure 5.16 illustrates the results for FEM and Grillage analysis of longer (200 feet < span lengths <250 feet) exterior spans. Finally, Figure 5.17 displays the results for very long (span length \geq 250 feet) exterior spans.

Table 5.3 Exterior Span Results

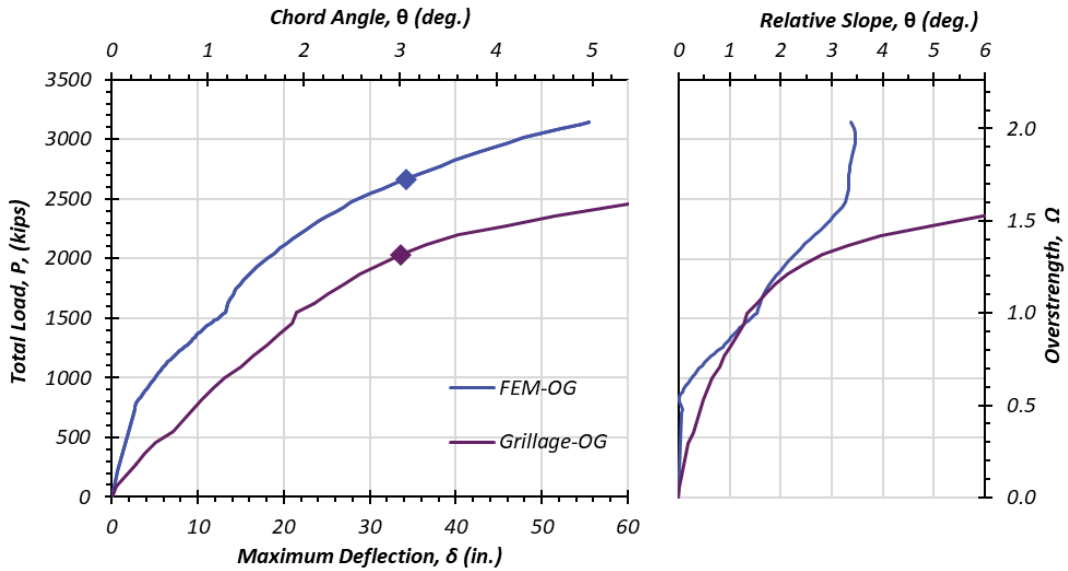
ID	Span	R (ft)	L (ft)	B (ft)	S (ft)	FEM	Grillage
9	3	764	126	28	7.4	1.80	1.53
4	2	195	128	28	7.6	1.73	1.32
4	1	195	132	28	7.6	1.65	1.30
9	1	764	140	28	7.4	1.70	1.35
6	1	819	140	38	9.8	1.80	1.43
6	2	819	140	38	9.8	1.80	1.43
5	1	450	140	30	9.7	1.20	1.10
5	2	450	140	30	9.7	1.20	1.10
12	1	225	140	28	7.6	1.60	1.20
12	3	225	145	28	7.6	1.60	1.15
10	1	716	148	30	7.7	1.70	1.71
14	1	1010	150	28	6.5	1.65	1.25
14	3	1010	150	28	6.5	1.65	1.25
13	1	450	152	30	9.3	1.00	1.10
13	3	450	152	30	9.3	1.00	1.10
7	2	764	190	28	7.4	1.45	1.25
10	3	716	190	30	7.7	1.45	1.25
15	1	809	200	28	8	1.70	1.40
15	3	809	200	28	8	1.70	1.40
7	1	764	219	28	7.4	1.20	0.94
11	1	819	223	28	7	1.60	1.35
11	3	819	235	28	7	1.60	1.30
8	1	882	265	28	8.4	0.99	0.83
8	2	882	295	28	8.4	0.88	0.60



(i) Load displacement

(ii) Deck rotations

(a) Comparison of the Results for Bridge 9 Span 3, $L=126$ ft

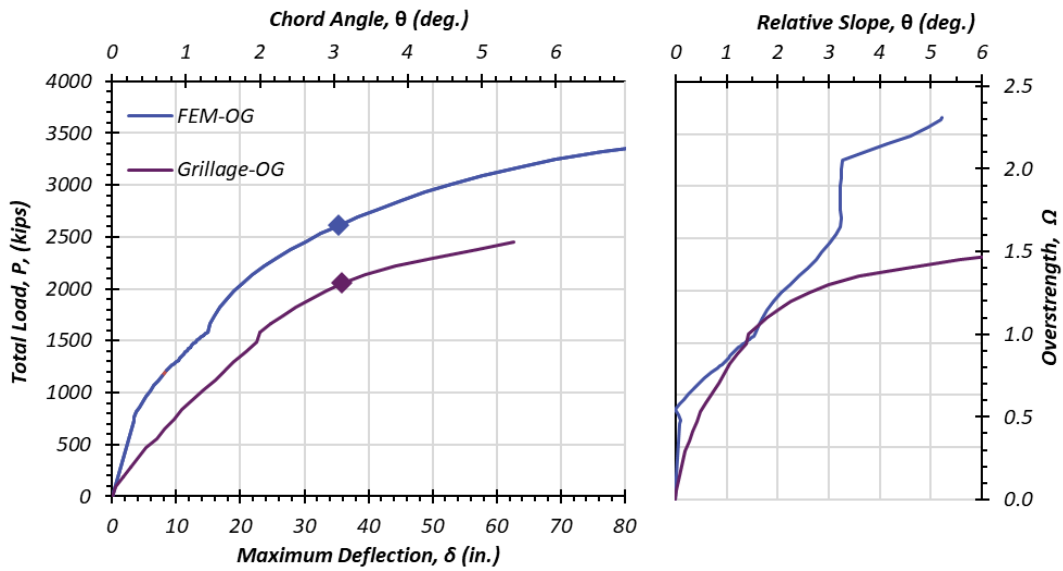


(i) Load displacement

(ii) Deck rotations

(b) Comparison of the Results for Bridge 4 Span 2, $L=128$ ft

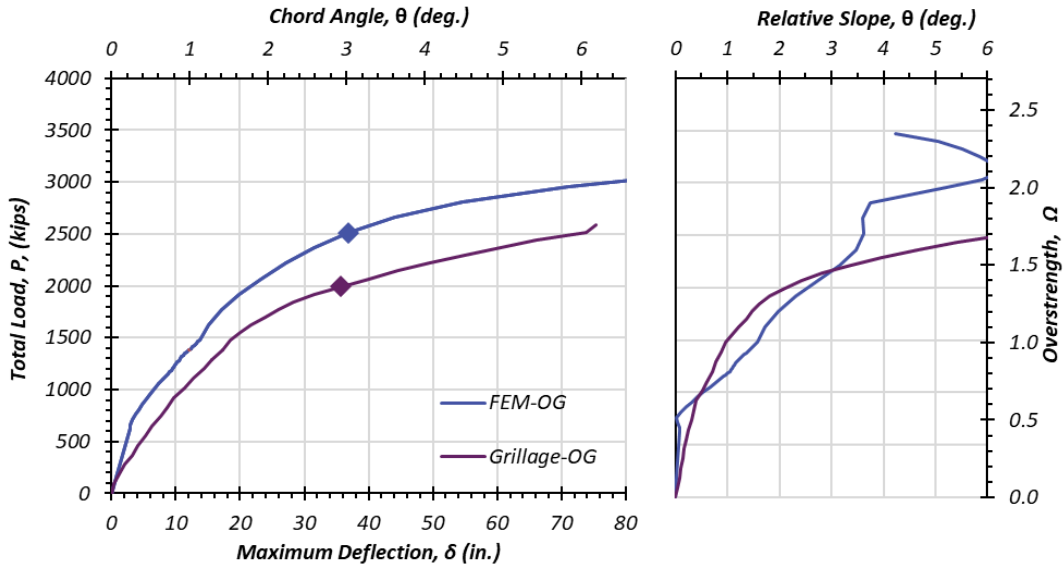
Figure 5.7. Results for Short Exterior Spans of Fracture Twin Tub Bridges



(i) Load displacement

(i) Deck rotations

(a) Comparison of the Results for Bridge 4 Span 1, $L=132$ ft

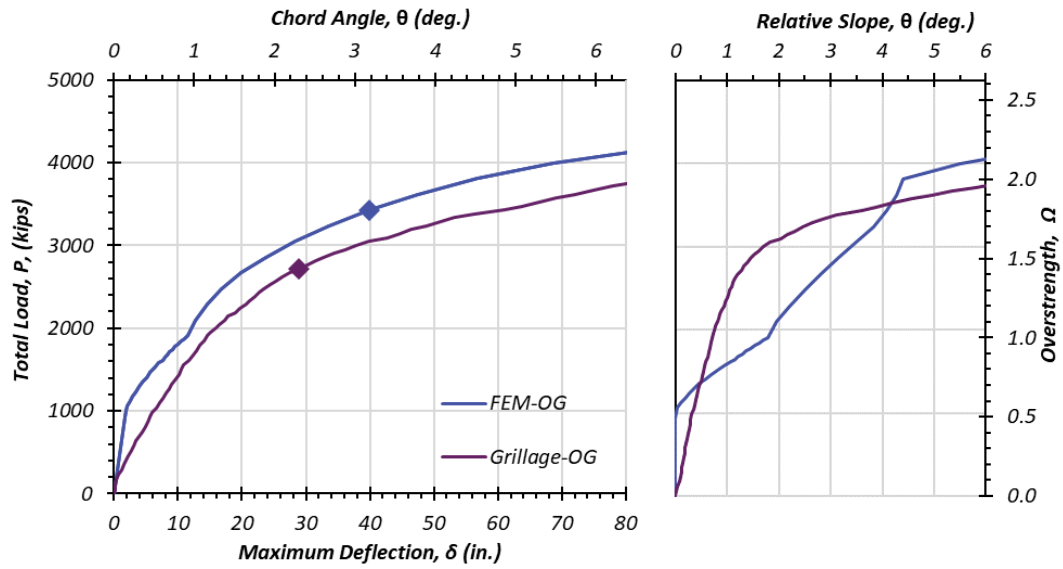


(i) Load displacement

(ii) Deck rotations

(b) Comparison of the Results for Bridge 9 Span 1, $L=140$ ft

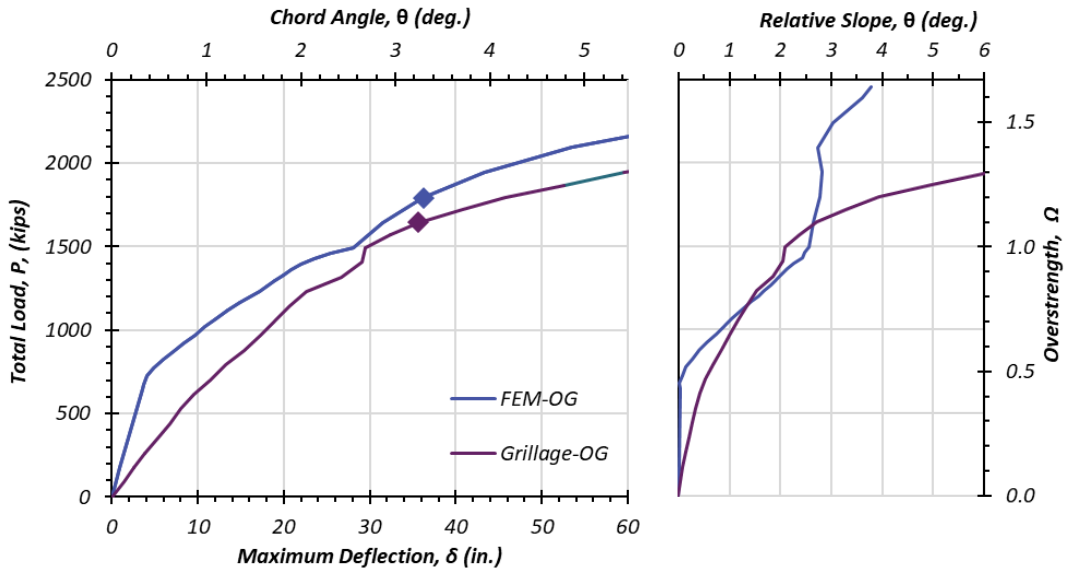
Figure 5.8. Results for Short Exterior Spans of Fracture Twin Tub Bridges



(i) Load displacement

(ii) Deck rotations

(a) Comparison of the Results for Bridge 6 Span 1 and 2, $L=140$ ft

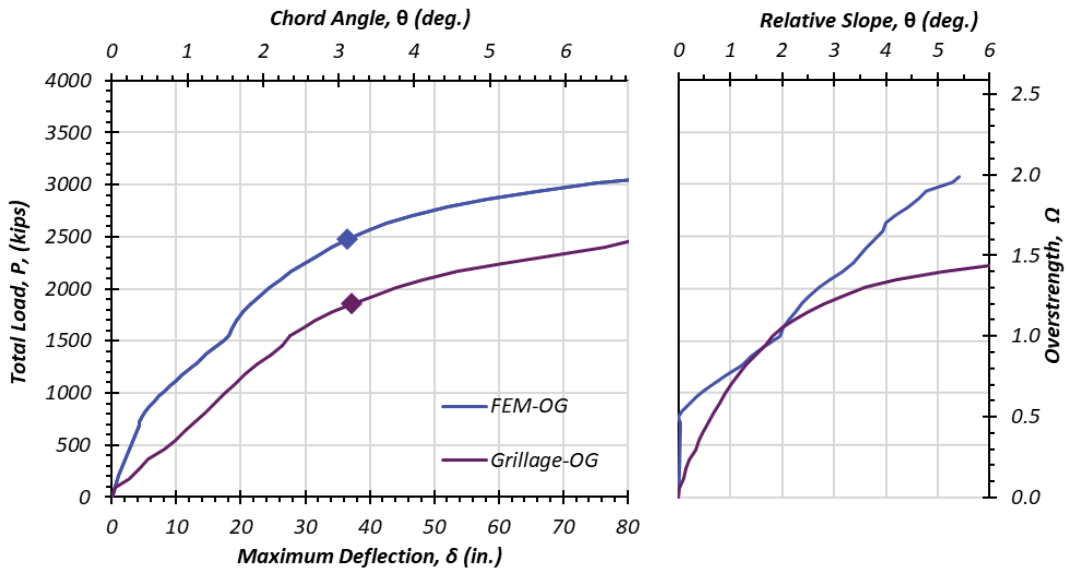


(i) Load displacement

(ii) Deck rotations

(b) Comparison of the Results for Bridge 5 Span 1 and 2, $L=140$ ft

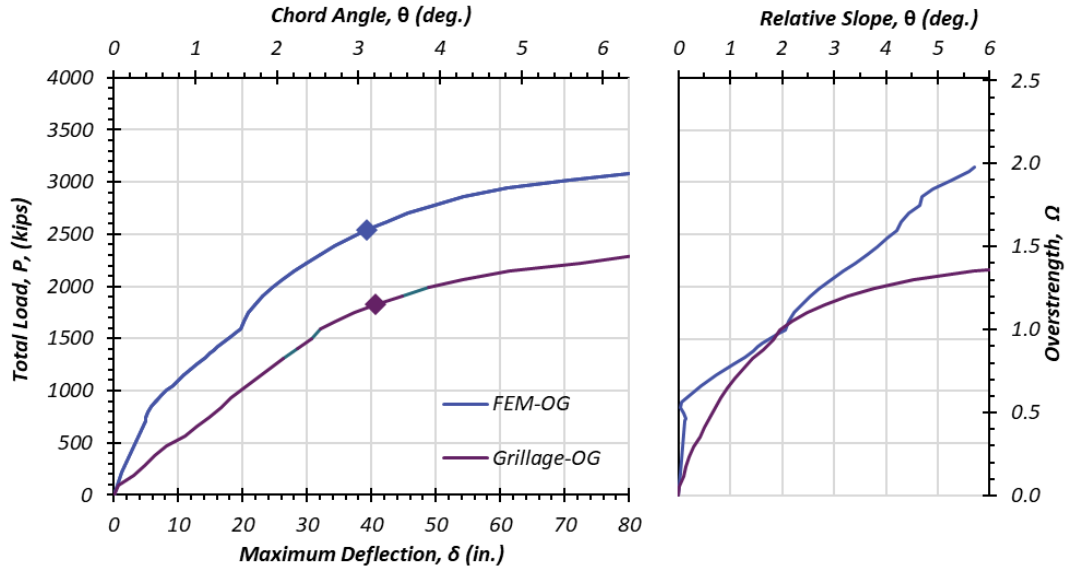
Figure 5.9. Results for Short Exterior Spans of Fracture Twin Tub Bridges



(i) Load displacement

(ii) Deck rotations

(a) Comparison of the Results for Bridge 12 Span 1, $L=140$ ft

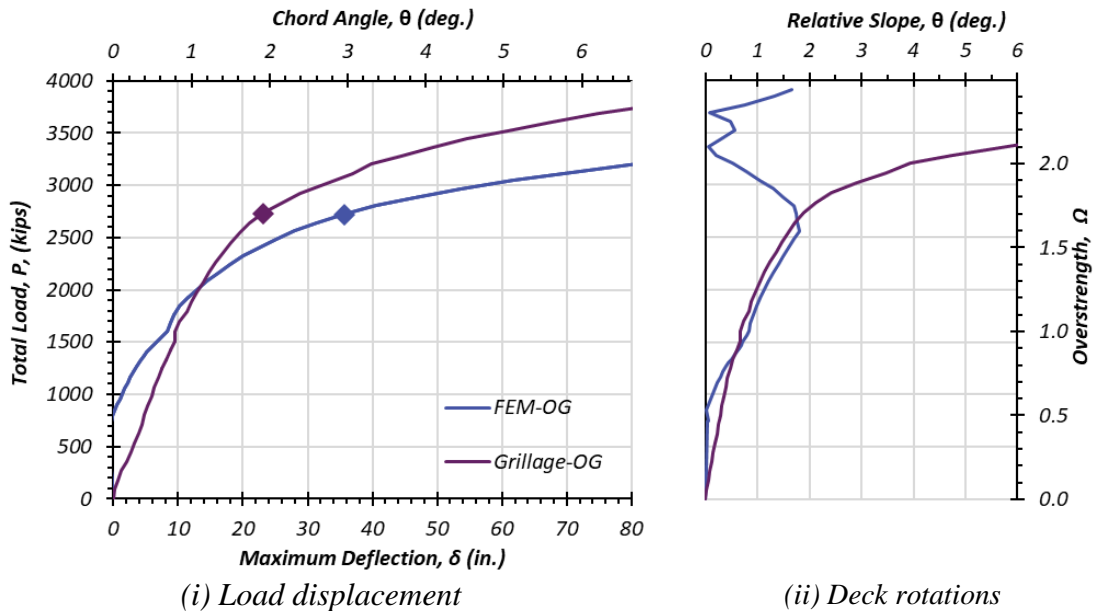


(i) Load displacement

(ii) Deck rotations

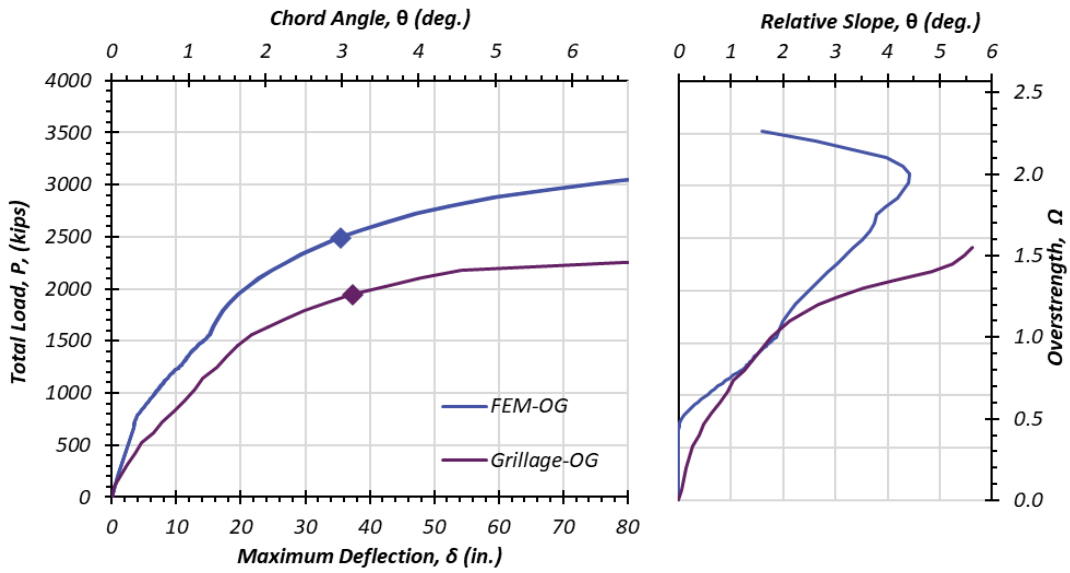
(b) Comparison of the Results for Bridge 12 Span 3, $L=145$ ft

Figure 5.10. Results for Short Exterior Spans of Fracture Twin Tub Bridges



(i) Load displacement (ii) Deck rotations
Comparison of the Results for Bridge 10 Span 1, $L=148$ ft
Figure 5.11. Results for Short Exterior Span of Fracture Twin Tub Bridges

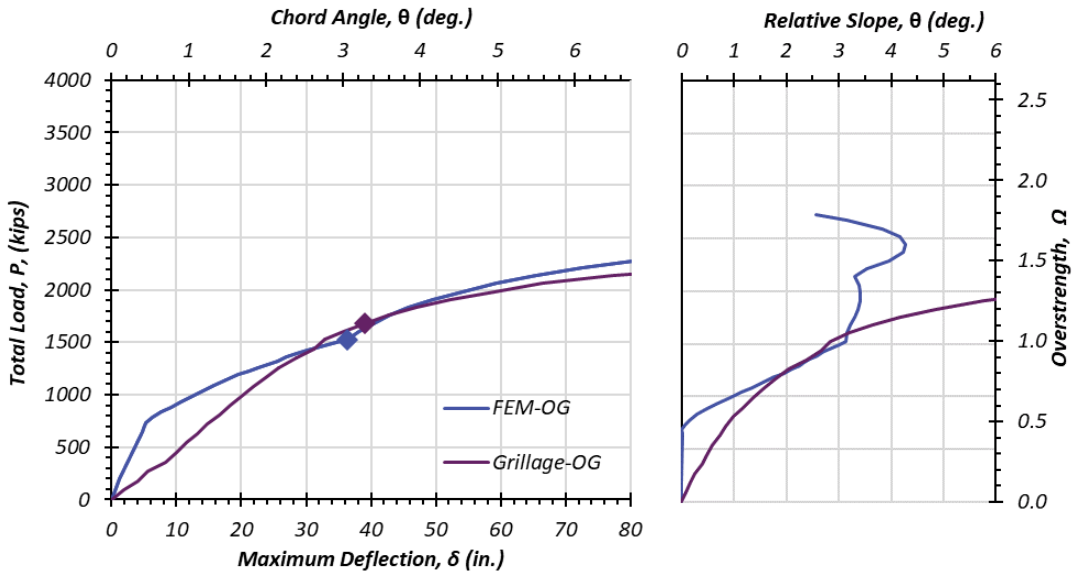
FEM and Grillage Analysis results are in acceptable agreement for short exterior spans, and all short exterior spans in this study are considered redundant. The Grillage and FEM results for exterior spans from Bridge 4, located in Figure 5.8, and Bridge 12, located in Figure 5.10, vary more than the other spans short span category. This difference can be accounted for by their tight radius of curvatures (195 feet for Bridge 4 and 225 feet for Bridge 12) and is conservatively accounted for in the Grillage analysis method. Span 1 of Bridge 10 is another note worth short exterior span due to the Grillage overstrength factor (1.71) being greater than the FEM value (1.70). This can potentially be accounted for by the lack of elastic representation in the FEM data. However, since both methods provide overstrength values significantly greater than one, Span 1 of Bridge 10 can be considered redundant.



(i) Load displacement

(ii) Deck rotations

(a) Comparison of the Results for Bridge 14 Span 1 and 3, $L=150$ ft

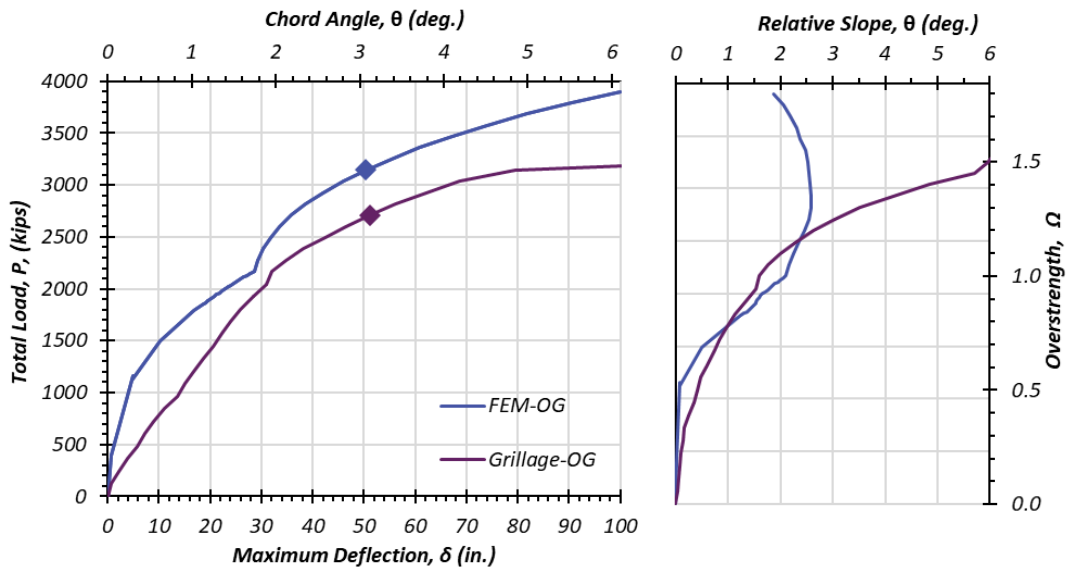


(i) Load displacement

(ii) Deck rotations

(b) Comparison of the Results for Bridge 13 Span 1 and 3, $L=152$ ft

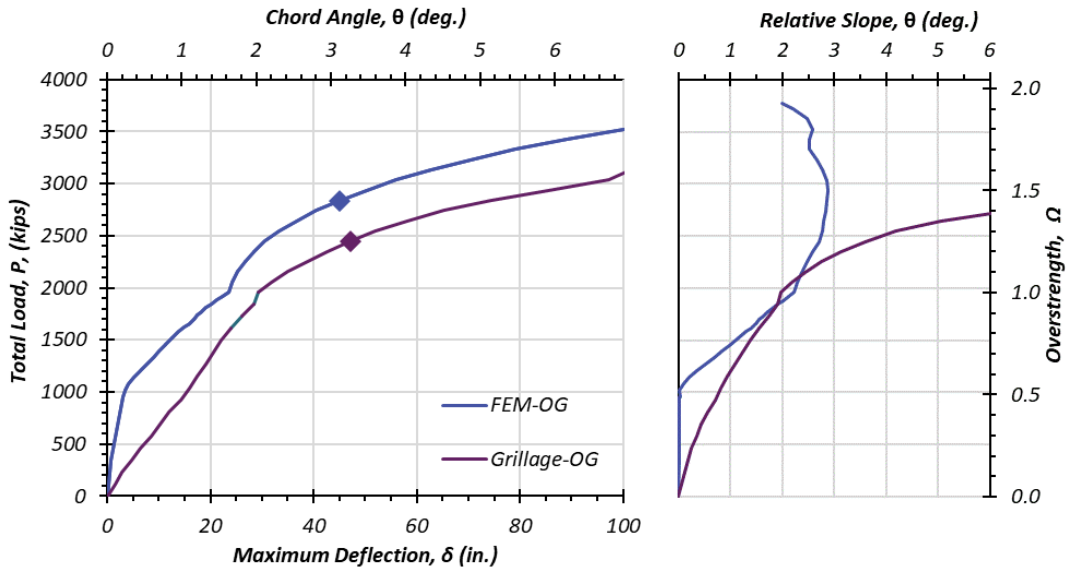
Figure 5.12. Results for Average Exterior Spans of Fracture Twin Tub Bridges



(i) Load displacement

(ii) Deck rotations

(a) Comparison of the Results for Bridge 7 Span 2, $L=190$ ft

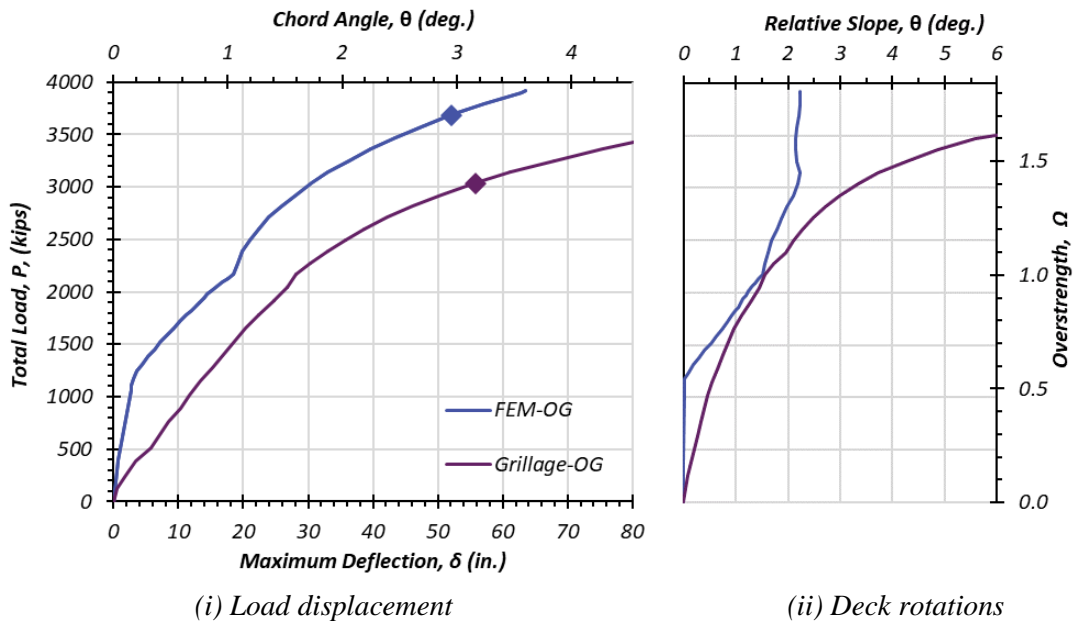


(i) Load displacement

(ii) Deck rotations

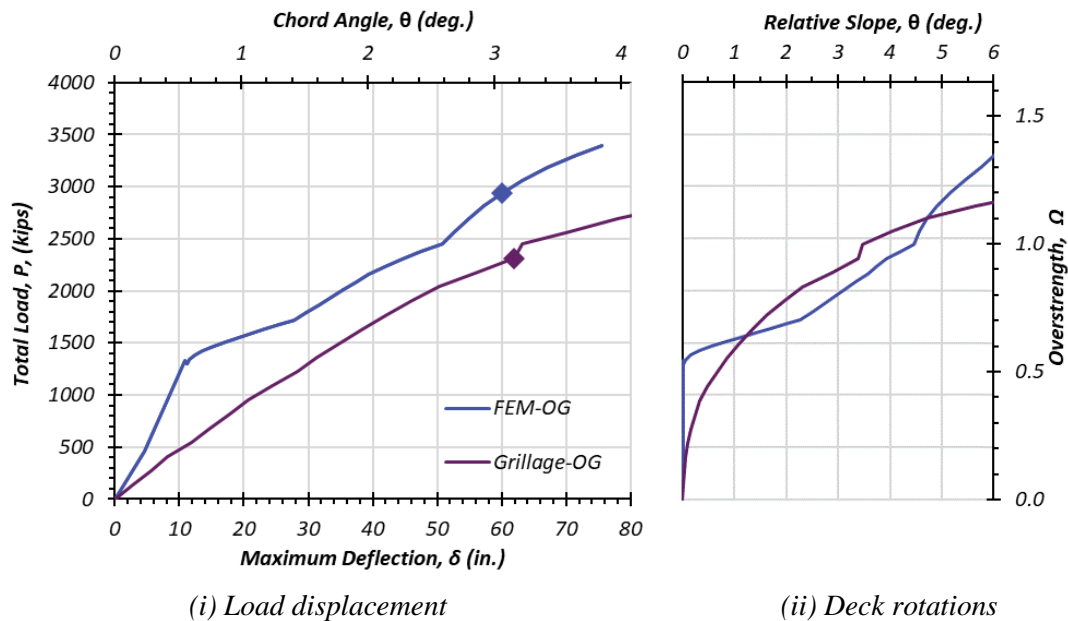
(b) Comparison of the Results for Bridge 10 Span 3, $L=190$ ft

Figure 5.13. Results for Average Exterior Spans of Fracture Twin Tub Bridges



(i) Load displacement *(ii) Deck rotations*
Comparison of the Results for Bridge 15 Span 1 and 3, L=200 ft
Figure 5.14. Results for Average Exterior Spans of Fracture Twin Tub Bridges

Grillage analysis and FEM results for average length exterior spans are complementary to one another. In all cases but one, Spans 1&2 of Bridge 13, the Grillage overstrength factors for average length exterior spans are lower than the FEM overstrength factors, which is expected. Bridge 13, Spans 1&2, present a minor contradiction to the trend of FME and Grillage results but both methods present overstrength values greater than or equal to one, and therefore redundant. Another observable trend of average exterior spans is that as the length of the span increases the disparity between the FEM and Grillage results increases slightly. The slight increase can be attributed by the increasingly conservative approach of Grillage analysis.

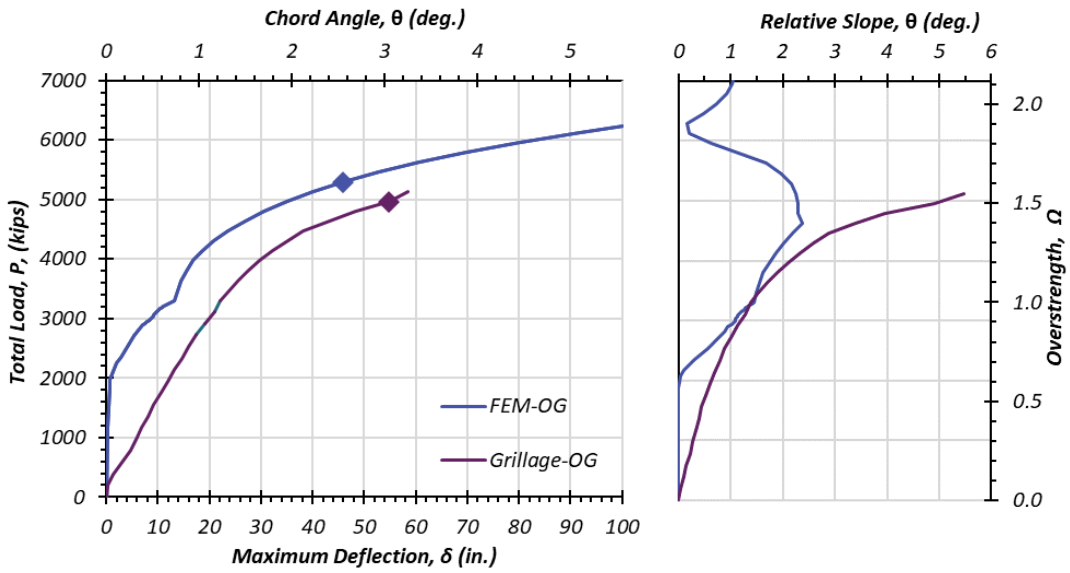


(i) Load displacement (ii) Deck rotations

Comparison of the Results for Bridge 7 Span 1, $L=219$ ft

Figure 5.15. Results for Long Exterior Spans of Fracture Twin Tub Bridges

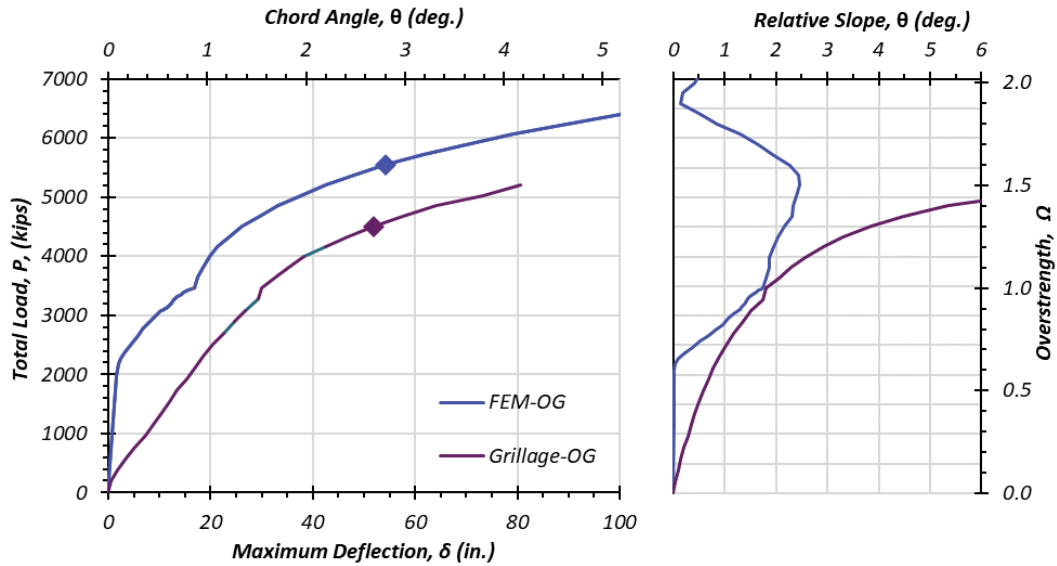
Grillage and FEM results for long exterior spans are in close agreement with the Grillage analysis results offering a more conservative outcome. Span 1 of Bridge 7 presents a discrepancy in redundancy when comparing the two methods having an FEM overstrength of 1.20 and a Grillage overstrength factor of 0.94 (less than 1). However, with the Grillage method being a conservative approach, if the Grillage method provides a result marginally close to 1 it is advisable to use a more rigorous method of analysis. Other spans of the long exterior span category are classified as redundant by both analysis methods.



(i) Load displacement

(ii) Deck rotations

(a) Comparison of the Results for Bridge 11 Span 1, $L=223$ ft

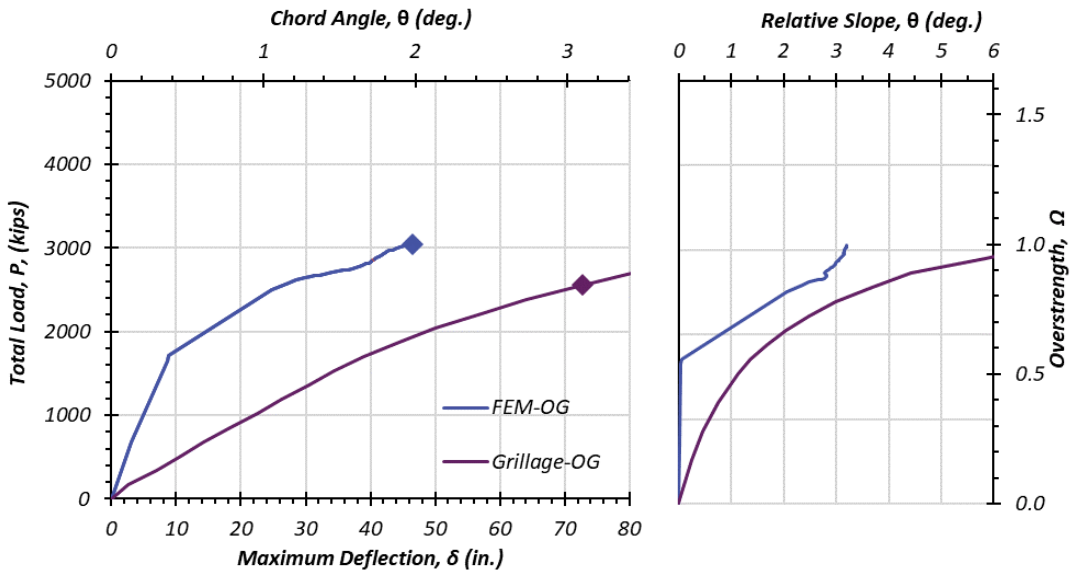


(i) Load displacement

(ii) Deck rotations

(b) Comparison of the Results for Bridge 11 Span 3, $L=235$ ft

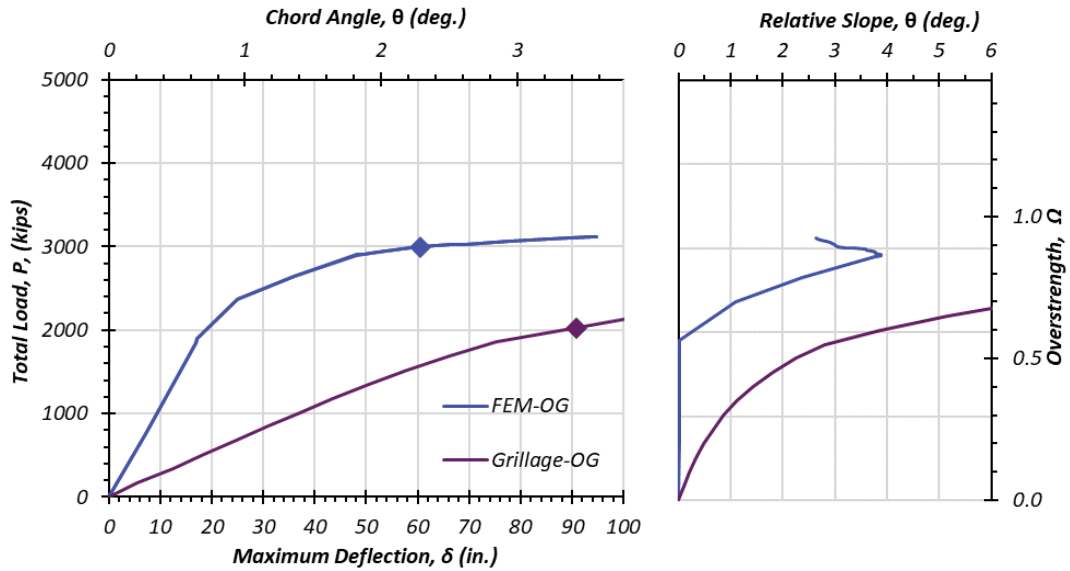
Figure 5.16. Results for Long Exterior Spans of Fracture Twin Tub Bridges



(i) Load displacement

(ii) Deck rotations

(a) Comparison of the Results for Bridge 8 Span 1, $L=265$ ft



(i) Load displacement

(ii) Deck rotations

(b) Comparison of the Results for Bridge 8 Span 2, $L=295$ ft

Figure 5.17. Results for Very Long Exterior Spans of Fracture Twin Tub Bridges

Spans 1&2 of Bridge 8 are both considered very long exterior span (span length ≥ 250 feet). FEM and Grillage analysis results are in agreement with one another with

the Grillage analysis being more conservative. None of the very long exterior spans are considered redundant as both spans have overstrength factors less than one utilizing both analysis methods. Due to a lack of redundancy of the very long spans, there may be a length limit at which exterior spans may no longer be considered redundant.

6. GRILLAGE METHOD DESIGN GUIDE*

6.1. Procedure

The computational analysis of the Fracture Critical Twin Tub Girder Bridges (TTGB) may be implemented using commercial nonlinear structural analysis software. Programs such as SAP2000 may be useful to carry out the following steps. Detailed design examples for Bridge 2, Bridge 5, and Bridge 10 are located in Appendix C. The steps detailed in this section are as follows:

1. Define cylindrical coordinate system
2. Define non-linear material properties
3. Define member section properties
4. Define section hinge properties
5. Assign frame members to grid
6. Assign hinges to frame members
7. Assign boundary conditions
8. Define load patterns and load cases
9. Assign frame loads to frames
10. Assign data collection points along frame members
11. Run analysis for dead load case
12. Run analysis for all load cases

* Part of this chapter is reprinted with permission from “Analysis Guidelines and Examples for Fracture Critical Steel Twin Tub Girder Bridges” 0-6937-P1 by Hurlbaeus S., Mander J., Terzioglu T., Boger N., Fatima A., 2018. Texas A&M Texas Transportation Institute, 11-20, Copyright 2018 by Texas A&M Texas Transportation Institute

13. Replace hinges at fracture location
14. Run analysis for all load cases
15. Post process the data

6.1.1. Define Cylindrical Coordinate System

For the TTGB, the longitudinal grids need to be located at the location of the two exterior edges of the bridge, the centerline of the two exterior top flanges, and the two interior top flanges. The transverse grillage grids need to be located at ends, at 7 ft spacing increments in the middle of the bridge (for easier assignment of the HS20 truck load), and at pier locations for the case of a multi-span bridge. An illustration of the grid system for a single span bridge is located in Figure 6.1. The transverse spacing increments will need to be converted to a radial spacing in the cylindrical coordinate system using Equation (6.1).

$$Radial\ Spacing\ (deg.) = \left(\frac{Spacing\ Length}{Radius\ of\ bridge} \right) * \left(\frac{180}{\pi} \right) \quad (6.1)$$

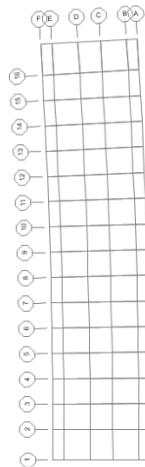
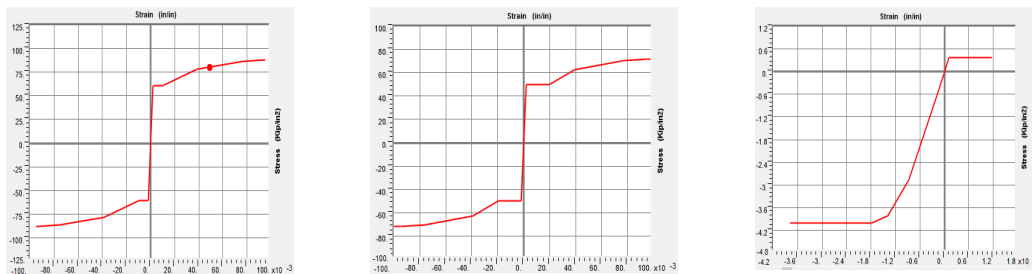


Figure 6.1 Grillage Grid System for a Single Span Bridge

6.1.2. Define Non-Linear Material Properties

The fractured TTGB will be analyzed at ultimate loading conditions therefore the steel and concrete components of the bridge will be taken beyond their elastic capacity. The composite girder and deck system is composed of concrete that will reach cracking and crushing strains and rebar and steel plate that will reach strains beyond yielding. The material models to be used are represented in Figure 6.2. Nonlinear constitutive material behavior is defined in the advanced properties within the material definition.



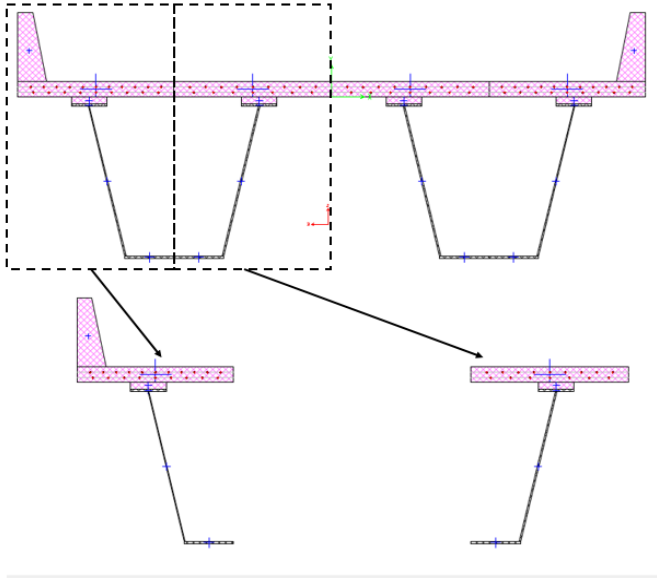
(a) Reinforcing Bar (b) Steel Plate (c) Concrete

Figure 6.2 Constitutive Material Models (SAP2000)

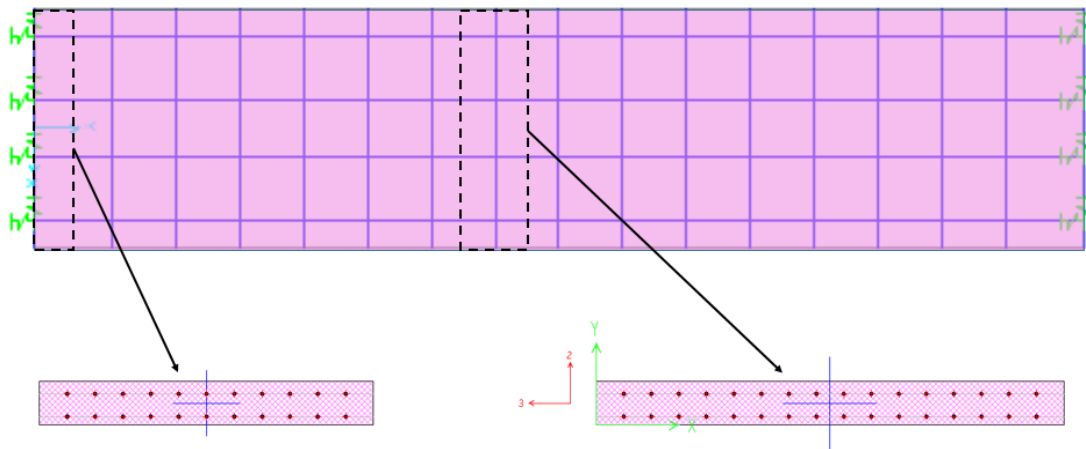
6.1.3. Define Section Properties

Using the section designer feature in SAP2000 a composite tub, deck, and railing section can be generated. The exterior longitudinal member, in Figure 6.3, consist of: the railing, the deck from the centerline of the girder to the exterior edge with corresponding reinforcing bar, one top flange, one web, and half of the bottom flange. The interior longitudinal member consist of: the deck from the centerline of the bridge to the centerline of the girder with corresponding longitudinal reinforcing bar, one top flange, one web, and

one half of the bottom flange. The transverse members, in Figure 6.4, consists of concrete deck and transverse reinforcing bar. However, it is critical to set the weight modifier to zero of the transverse section as to not double count the concrete deck weight. It should be noted that as the steel plate members change dimensions and the reinforcing pattern changes throughout the length of the bridge new sections will need to be created to represent the new dimensions.



a) Exterior Longitudinal Member b) Interior Longitudinal Member
Figure 6.3 Representative Longitudinal Members



a) End Transverse Member

b) Interior Transverse Member

Figure 6.4 Representative Transverse Members

The fractured girder can be modeled by simply copying the exterior and interior longitudinal sections and removing the bottom flange, web, and top flange steel plate components.

6.1.4. Defining Hinge Properties

Following the creation of the necessary longitudinal and transverse members, plastic hinges need to be created for each section. The grillage push down analysis will generate plastic hinge formation under the ultimate loading condition. Within the section designer of SAP2000, there is a moment curvature response tool which allow the user to generate moment curvature data for each of the members created in Step 3. The data form SAP2000 is then exported into an Excel spreadsheet. Then the angle on the Moment Curvature window can be changed to 180 to get the negative moment curvature and once again the data is exported to the same Excel spreadsheet. The moment curvature response is then normalized against the maximum positive and negative moments and their corresponding

curvatures and plotted. The hinge definition window in SAP2000 will only allow four normalized positive and negative moment curvature data points per section hinge. Therefore, a best fit plot for each moment curvature response needs to be generated in Excel using only 9 points (4 positive, 4 negative, and 1 zero). The hinge length is assigned as half the member depth. A representative hinge property is depicted in Figure 6.5. For ease of convergence nonnegative slopes are recommended for the hinge properties.

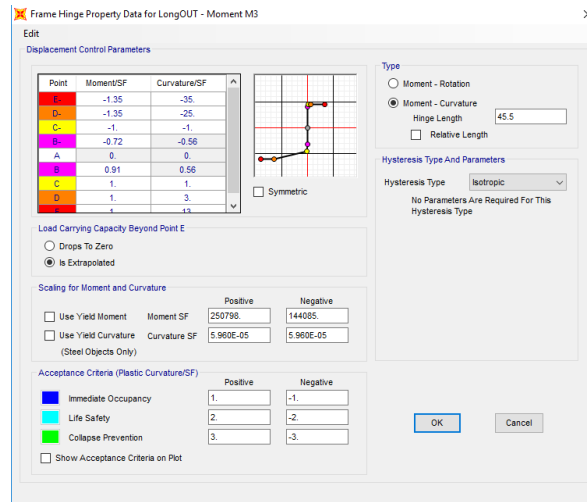


Figure 6.5 Representative Hinge Property

6.1.5. Assign Members to Grid

Using the “quick draw” frame section tool in SAP2000 the various longitudinal and transverse frame sections can be assigned to the grillage grid that was established in Step 1 by merely selecting the desired section from the drop down menu and clicking on the

appropriate grillage grid. Figure 6.6 shows a screenshot from SAP2000 after all members have been assigned to a simple span bridge.

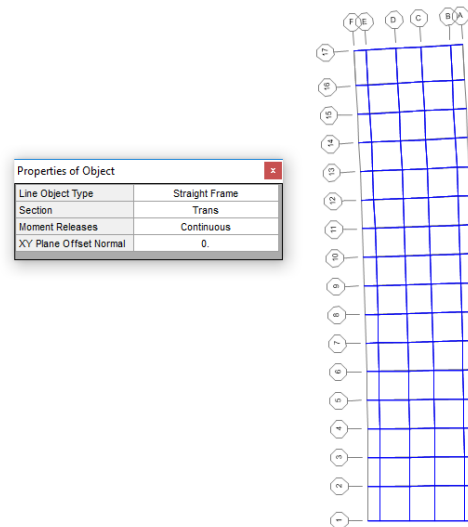


Figure 6.6 Screenshot of SAP2000 Post Frame Section Assignment

6.1.6. Assign Hinges to Frame Members

At this stage, the longitudinal and transverse members are already assigned to the grillage grid. To allow for plastic hinge formation hinges need to be assigned at the nodal intersection of all members as represented in Figure 6.7. Longitudinal hinges need be placed at both joints at the end of each member. Transverse hinges need to be assigned at a distance of half a top flange width away from each node.

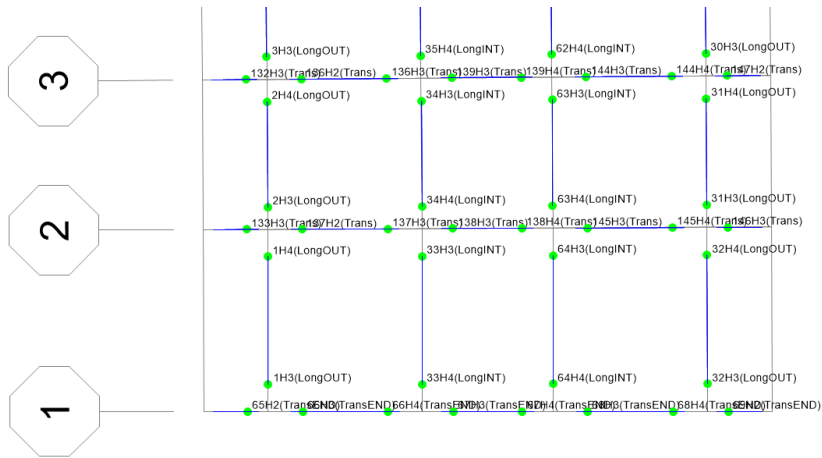


Figure 6.7 Representative Hinge Assignments

6.1.7. Assign Boundary Conditions

The support conditions of the physical bridge are elastomeric bearing pads. These will be represent by springs with a lateral stiffness of 6 kip/in. and a vertical stiffness of 3050 kip/in. in the grillage model as represented in Figure 6.8. For the single span bridges, springs will be assigned at each of end longitudinal joints. For the two and three span bridges, springs are also assigned to the ends longitudinal joints as well as the joints at the pier location.

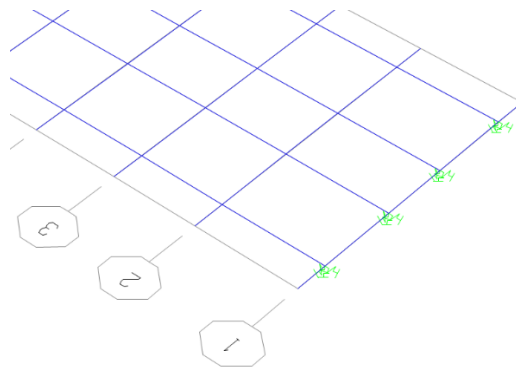


Figure 6.8 Spring Boundary Conditions

6.1.8. Define Load Patterns and Cases

For the single span bridges, two additional load patterns need to be created: the HS20 truck load and the lane load for lane load. For the two and three span bridges a HS20 truck load pattern needs to be defined for each span and the same follows for lane load. Once, load patterns are established load cases need to be created. Each load case represents a load combination of $1.25*DL+1.75(LL+IM)$ where DL=dead load, LL=live load, and IM=impact load or $1.25*DL+1.75*LL+2.33*HS20$ where DL=dead load, LL=lane load, and HS20=truck load. Each load case should be set to nonlinear behavior. The first load case should start from a zero initial conditions. Each proceeding load case should start from the end of the previous load case. Each span should have its own set of load cases. Also, each load case should be divided into 20 or more steps.

6.1.9. Assign Frame Loads

Two lanes of HS20 truck loading should be assigned as a series of point loads; and the two lines of lane loads should be distributed as line loads to the longitudinal members (as depicted in Figure 6.9) . A HS20 truck load consists of two sets of 16 kip axle loads and

one set of 4 kip axle loads spaced 14 feet longitudinally and 6 feet in transversely. The first line of axels will be placed 3 ft from the curved edge, the second 9 ft from the edge, the third 15 ft from the edge, and the fourth 21 ft from the edge. The middle axle load of each truck should be place at have the span length on the single span bridges and interior middle spans of three span bridges. The middle axle should be placed at approximately $0.4*L$ from the end of the end spans of two span and three span bridges. Two lanes of lane loading (0.64 kip/in. each) located at 8 ft from the edge, and the second line located at 20 ft from the edge. However, since the longitudinal members are placed according to the girder placement, the lane loads have to be distributed according to tributary area.

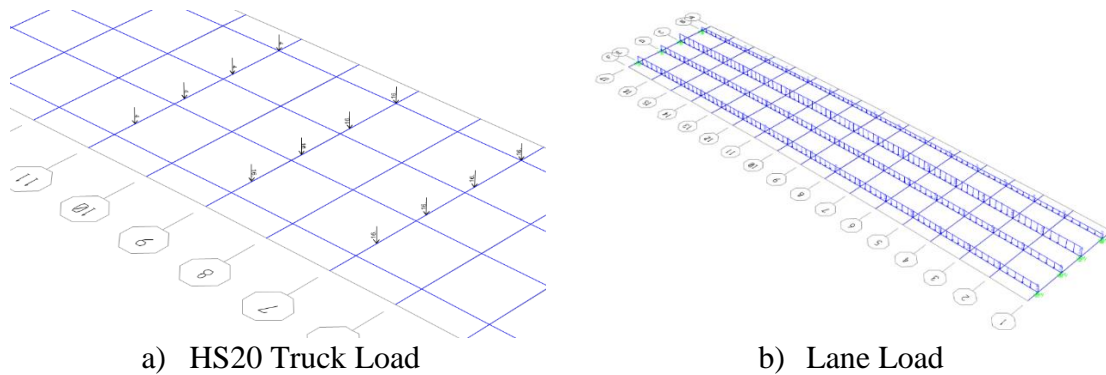


Figure 6.9 Grillage HS20 Truck and Lane Load

6.1.10. Assign Data Collection Points

At the location of each of the center axles, the transverse members between the outer longitudinal member and the interior longitudinal member need to be divided it two pieces

using the divide lines feature in SAP2000. This allow for the collection of data at the centerline of the member.

6.1.11. Run Analysis for Dead Load Only

In order to get to dead load value of the data the intact bridge should be ran solely under the dead load case. The reactions should be recorded for all supports.

6.1.12. Run Analysis for All Load Cases (Intact Bridge)

For the intact bridge run all HL93 load cases for the span being evaluated. Once the program has ran, collect the displacement data for points 1 thru 4 (seen in Figure 6.10) and the centerline points of the inside and outside girder at the location of the center axle. Be sure to obtain the results in the step-by-step format so that the load case and step for each displacement point can be collected as well. This process will be completed once for each span.

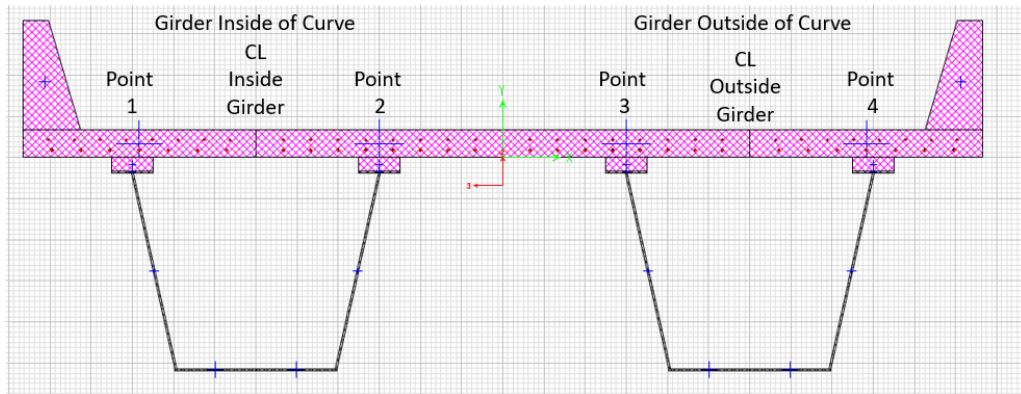


Figure 6.10 Location of Grillage Data Collection Points

6.1.13. Replace Hinges at Fracture

At the location of the center axle for the span being evaluated, replace the longitudinal hinges on the outside girder with their fractured counterparts. The hinge assignment is depicted in Figure 6.11.



Figure 6.11 Fractured Hinge Pattern

6.1.14. Run Analysis for All Load Cases (Fractured Bridge)

For the fractured bridge run all HL93 load cases for the span being evaluated. Once the program has ran, collect the displacement data for points 1 thru 4 (seen in Figure 6.10) and the centerline points of the inside and outside girder at the location of the center axle. Be sure to obtain the results in the step-by-step format so that the load case and step for each displacement point can be collected as well. This process will be completed once for each span, making certain to replace intact hinges in the preceding span before assigning fractured hinges in the following span.

6.1.15. Post Process Data

For both the intact and fractured bridge the following calculations need to be made:

- Omega (Ω)
 - $\Omega_i = \Omega_{i-1} + \left(\frac{1}{\# \text{ of Steps in Load case}} \right)$
- Longitudinal Chord Rotation of Interior and Exterior Girder
 - $\text{Chord Rot.}_{\text{Single Span or Interior Span}} = -1 * \left(\frac{\delta_{CL}}{0.5 * L} \right)$
 - $\text{Chord Rot.}_{\text{Exterior Span}} = -1 * \left(\frac{\delta_{CL}}{0.4 * L} \right)$
 - The above equations are in radians
- Transverse Deck Rotation
 - Relative rotation of deck at inside flange of inside girder
 - $\alpha_{2-3} = \left(\frac{\delta_3 - \delta_2}{s} \right) - \left(\frac{\delta_2 - \delta_1}{w} \right)$
 - $\alpha_{3-2} = \left(\frac{\delta_3 - \delta_2}{s} \right) - \left(\frac{\delta_4 - \delta_3}{w} \right)$
 - Where s=spacing between the interior top flanges of the inside and outside girders and w=spacing between the top flanges of the same girder
 - The above rotations are in radians.
- Applied load
 - Calculate unit applied load or applied load at 1 Ω
 - $\text{Unit Applied Load}_{\text{single span}} = 1.25 * \text{Total Reaction from Dead Load Case} + 2 * (2.33 * \text{HS20 truck} + 1.75 * \text{Lane Load})$
 - $\text{Unit Applied Load}_{\text{multi span}} = 1.25 * \text{Total Reaction from Dead Load Case} * \left(\frac{L_{\text{span}}}{L_{\text{Total}}} \right) + 2 * (2.33 * \text{HS20 truck} + 1.75 * \text{Lane Load})$
 - $\text{Applied Load} = \text{Unit Applied Load} * \Omega$
- Intact Stiffness of Intact Bridge

$$\circ \text{Initial Stiffness}_{Intact \text{ at } \Omega=0.4} = \frac{0.4}{Abs(\delta_{OG-CL})}$$

- Instantaneous Stiffness for Fracture Bridge

$$\circ \text{Instantaneous Stiffness}_{OG-Frac. i} = \frac{\Omega_i - \Omega_{i-1}}{\delta_i - \delta_{i-1}}$$

The criteria above can be organized into an Excel spreadsheet noted in Figure 6.12.

	A	B	C	D	E	F	G	H	I	J	K	L	M	V	X	Y	Z	AA	AB	AC	AD	
1	Intact			OG-CL		IG-CL		Point 4	Point 3	Point 2	Point 1			Applied Load (kip)	OG	IG						
2	Load Case	Load Step	Ω	Delta (in)	Chord (rad)	Delta (in)	Chord (rad)	Delta (in)	Delta (in)	Delta (in)	Delta (in)	$\alpha 23$ (rad)	$\alpha 32$ (rad)		Ω (cal)	Delta (in)	Chord (deg)	Delta (in)	Chord (deg)	$\alpha 23$ (deg)	$\alpha 32$ (deg)	
3	LC1	0	0	0	0.00000	0	0.00000	0	0	0	0	0	0	0	0.00	0.00	0.00000	0.00	0.00000	0	0	
4	LC1	1	0.05	-0.1037	0.00015	-0.087926	0.00013	-0.10541	-0.10129	-0.0942	-0.07905	7.89E-05	4.94E-05		66	0.05	0.10	0.00861	0.09	0.00730	0.004522	0.002831
5	LC1	2	0.1	-0.2074	0.00030	-0.175851	0.00025	-0.21081	-0.20259	-0.18839	-0.15809	0.000158	9.88E-05		132	0.10	0.21	0.01722	0.18	0.01460	0.009043	0.005662

Figure 6.12 Spreadsheet of Grillage Data

Failure Criteria:

- The instantaneous stiffness for the fractured outside girder is less than 5% of the initial stiffness of intact outside girder.
- The chord angle of the outside girder for simple spans or interior spans is greater than 2°. The chord angle for exterior spans in multi-span bridges is greater than 3°.
- The transverse deck rotation is greater than 5°.

7. CONCLUSION AND FINDINGS*

7.1. Conclusion

The Grillage Push-Down Analysis has proven to be an accurate lower bound solution to modeling fracture twin tub girder bridges in this research and shown that it can be an effective tool for declassifying twin tub girder bridges as non-redundant structures. The Grillage results, in vast majority of the bridge spans analyzed, is conservative and in good agreement with the FEM results.

Single span bridges presented the greatest amount of difference between FEM and Grillage analysis results. Shorter single span bridge Grillage results have better agreement than the longer single spans with FEM results however the results were still not consistent. Long single span bridges show very little consistency between FEM and Grillage analysis with an average 77% difference in the results, where the shorter single span bridges have 28.7% agreement. However, both FEM and Grillage analysis demonstrate a lack of redundancy of long single span bridges. This is understandable due to the lack of structural redundancy at a fixed support.

Interior spans of three span bridges show the greatest amount of similarity between the Grillage and FEM results of any of the bridge categories, with an average 13.9% difference between results. All of the interior spans demonstrate redundancy, having overstrength factors greater than one. However, it should be noted that the longest interior

* Part of this chapter is reprinted with permission from “Fracture Critical Steel Twin Tub Girder Bridges Technical Report” 0-6937-R1 by Hurlebaus S., Mander J., Terzioglu T., Boger N., Fatima A., 2018. Texas A&M Texas Transportation Institute, 283-285, Copyright 2018 by Texas A&M Texas Transportation Institute

span, Span 2 of Bridge 11, having a length of 366 feet approached an overstrength factor of 1, implying that there may exist a limit on span length at which interior spans can no longer be considered redundant structures.

Exterior spans, like the interior spans, show satisfactory compatibility between the Grillage analysis results and those gathered from FEM. There is only an average 17.8% difference between the two analysis methods with the Grillage analysis being conservative. Span 1 of Bridge 7, is the only bridge that presents a conflict of results as to the classification of redundancy. The Grillage Analysis yields an overstrength value of 0.94 whereas, the FEM analysis calculates the overstrength factor to be 1.2. However, as discussed in Chapter 5 with spans that present overstrength values marginally close to 1 under Grillage analysis, may warrant the use of a more rigorous approach (such as FEM) to reclassify them as redundant spans. It should also be noted that the two very long exterior spans, Spans 1&2 of Bridge 8 (265 feet and 295 feet respectively), fail prior to reaching an overstrength value of 1 under both analysis methods. This is indicative that a span length limit exists for exterior spans to be considered redundant structures.

An additional parametric was conducted to evaluate the effect of increasing concrete strength, reinforcing bar area, and deck thickness on the overstrength factor of the fractured bridge. The results demonstrated that increasing all three variables increases the overstrength factor for both the single span bridge and the interior span evaluated (Bridge 2 and Span 2 of Bridge 9). Increasing the deck thickness was most effective in increasing the overstrength value for the single span bridge. However, increasing the percentage of reinforcing bar was most effective for increasing the overstrength value of

the interior span analyzed. The outcomes of this portion of the research demonstrates there are ways to improve the bridges that are marginally close to being redundant in a way to reclassify them.

7.2. Findings

- 1) Bridges can be declassified a non-redundant structures if determined by the Grillage method of having a satisfactory overstrength value ($\Omega > 1$). Or if they have a Grillage overstrength value marginally close to 1 and determined by a more rigorous method to be sufficient (such as FEM).
- 2) Due to the inconsistency of the Grillage and FEM results for single span bridges, it is advisable to continue to classify all single span bridges as fracture critical unless the span length is ≤ 120 feet.
- 3) If a bridges span has structural redundancy, as provided by continuity of a girder over interior supports bridges may be declassified so long as the following conditions are met
 - a. Exterior Spans ≤ 250 feet
 - b. Interior Span ≤ 350 feet
 - c. Achieve an acceptable overstrength value ($\Omega \geq 1$) under Grillage Analysis
- 4) If all the above conditions are not met a more rigorous analysis method should be utilized (such as FEM).

7.3. Future Work

The research results presented in this dissertation provide substantial information and data to support grillage analysis as an acceptable analysis method for steel twin tub girder

bridge post fracture of the exterior girder. However, there are many areas where this research could be supplemented with further research. Areas of additional research include the following:

1. Improving compatibility between FEM and Grillage analysis results for single span bridges by altering grillage method. The greatest amount of variation between the two analysis methods occurred in the simple span bridges. Many times the grillage analysis was significantly lower than that of the FEM analysis. This could simply be due to the simplicity of the model but improvements to the model to should be investigate to see if greater compatibility could be achieved between the two methods for simple span bridges.
2. Strive to generate hinge moment curvature behavior more compatible with cross section moment curvature response. The moment curvature behavior of hinges in the grillage analysis are fairly accurate. However, due to limitations within SAP2000, no regions with negative slope could be represented in the hinge properties without crashing the program due to convergence issues. Investigating how to incorporate the regions of negative sloping moment curvature response into the hinge properties would be valuable.
3. Conducting a more comprehensive assessment of the effects of various variables such as deck thickness, reinforcing bar area, and concrete strength on the redundancy of the bridges. A brief study was completed as part of this research but a more in depth assessment is warranted. It may be of value to change plate thicknesses of the steel as another variable.

4. Adjusting time of fracture initiation in grillage models. The FEM analysis initiates the fracture of the exterior girder after all construction loads are applied. However, due to software limitations, the grillage analysis method initiates the complete girder fracture before construction loads are applied. This scenario does not adequately represent how the bridge is loaded in the field. More time should be invested into determining how to represent a more accurate fracture sequence in the software.

REFERENCES

- AASHTO (1978). "Guide Specification for Fracture Critical Nonredundant Steel Bridge Members." American Association of State Highway and Transportation Officials, Washington, DC.
- AASHTO (1979). "Standard Specifications for Highway Bridges, 14th Edition." American Association of State Highway and Transportation Officials, Washington, DC.
- AASHTO (1998). "AASHTO LRFD Bridge Design Specifications, 2nd Edition." American Association of State Highway and Transportation Officials, Washington, DC.
- AASHTO (2012). "AASHTO LRFD Bridge Design Specifications." American Association of State Highway and Transportation Officials (AASHTO), Washington, DC.
- AASHTO (2014). "AASHTO LRFD Bridge Design Specifications." American Association of State Highway and Transportation Officials (AASHTO), Washington, DC.
- Argyris, J. H., and Kelsey, S. (1960). *Energy theorems and structural analysis*, Springer.
- Armer, G. (1968). "Ultimate load tests of slabs designed by the strip method." *Proceedings of the Institution of Civil Engineers*, 41(2), 313-331.

- Barker, R. M., and Puckett, J. A. (2013). *Design of highway bridges: An LRFD approach*, John Wiley & Sons.
- Barnard, T., Hovell, C. G., Sutton, J. P., Mouras, J. M., Neuman, B. J., Samaras, V. A., Kim, J., Williamson, E. B., and Frank, K. H. (2010). "Modeling the Response of Fracture Critical Steel Box-Girder Bridges." *Report No. FHWA/TX-10/9-5498*, Center for Transportation Research at the Univ. of Texas at Austin, Austin, TX.
- Belak, J. (1998). "On the nucleation and growth of voids at high strain-rates." *Journal of computer-aided materials design*, 5(2-3), 193-206.
- Chajes, M. (2005). *Steel Girder Fracture on Delaware's I-95 Bridge over the Brandywine River*, PROCEEDINGS OF THE STRUCTURES CONGRESS AND EXPOSITION.
- Coletti, F., Holt, Vogel (2005). "Practical Steel Tub Girder Design." *TRB 2006 Annual Meeting CD-ROM*, 15.
- Computers and Structures, I. 2017. SAP2000, version 19.1.1Computers and Structures Inc., Berkeley, CA.
- Connor, R. J., Dexter, R. J., and Mahmoud, H. (2005). "Inspection and Management of Bridges with Fracture-Critical Details." *NCHRP Synthesis 354*, National Cooperative Highway Research Program, Transportation Research Board, Washington, DC.
- Corley, W. (1966). "Rotational capacity of reinforced concrete beams." *Journal of the Structural Division*, 92(5), 121-146.

- Cottrell, A. H., and Bilby, B. (1949). "Dislocation theory of yielding and strain ageing of iron." *Proceedings of the Physical Society. Section A*, 62(1), 49.
- Cross, H. (1932). "Analysis of continuous frames by distributing fixed-end moments." *American Society of Civil Engineers Transactions*.
- Daniels, J. H., Kim, W., and Wilson, J. L. (1989). "Recommended Guidelines for Redundancy Design and Rating of Two-Girder Steel Bridges." *NCHRP Report 319*, National Cooperative Highway Research Program., Transportation Research Board, Washington, DC.
- Dexter, R. J., Wright, W. J., and Fisher, J. W. (2004). "Fatigue and fracture of steel girders." *Journal of Bridge Engineering*, 9(3), 278-286.
- Duncan, W., and Collar, A. (1934). "LXXIV. A method for the solution of oscillation problems by matrices." *The London, Edinburgh, and Dublin Philosophical Magazine and Journal of Science*, 17(115), 865-909.
- Fasl, J., Helwig, T., and Wood, S. L. (2016). "Fatigue Response of a Fracture-Critical Bridge at the End of Service Life." *Journal of Performance of Constructed Facilities*, 04016019.
- FHWA (2012). "Clarification of Requirements for Fracture Critical Members." *Memorandum from Office of Bridge Technology*, Federal Highway Administration, Washington, DC.
- FHWA NBIS (2012). *Bridge Inspector's Reference Manual*, U.S. Department of Transportation.

- Fisher, J. (1997). "Evolution of fatigue-resistant steel bridges." *Transportation Research Record: Journal of the Transportation Research Board*(1594), 5-17.
- Fisher, J. W. (1970). *Effect of weldments on the fatigue strength of steel beams*, TRB. Washington, D.C.: Highway Research Board National Academy of Science
- Fisher, J. W. (1984). *Fatigue and fracture in steel bridges. Case studies*. New York, N.Y.: Wiley.
- Fisher, J. W., Albrecht, P., Yen, B. T., Klingerman, D. J., and McNamee, B. M. (1974). "Fatigue strength of steel beams with welded stiffeners and attachments." *NCHRP report*(147).
- Fisher, J. W., Pense, A. W., and Roberts, R. (1977). "Evaluation of fracture of Lafayette Street bridge." *Journal of the Structural Division*, 103(ASCE 13051 Proceeding).
- Frangopol, D. M., and Curley, J. P. (1987). "Effects of damage and redundancy on structural reliability." *Journal of Structural Engineering*, 113(7), 1533-1549.
- Ghosn, M., and Moses, F. (1998). "Redundancy in highway bridge superstructures." *NCHRP Report 406*, National Cooperative Highway Research Program, Transportation Research Board, Washington, DC.
- Heins, C. P., and Hou, C. K. (1980). "Bridge redundancy: Effects of bracing." *Journal of the Structural Division*, 106(6), 1364-1367.
- Heins, C. P., and Kato, H. (1982). "Load redistribution of cracked girders." *Journal of the Structural Division*, 108(8), 1909-1915.

- Hillerborg, A. (1956). "Equilibrium theory for reinforced concrete slabs." *Betong*, 41(4), 171-182.
- Hunley, C. T., and Harik, I. E. (2012). "Structural Redundancy Evaluation of Steel Tub Girder Bridges." *Journal of Bridge Engineering*, 17(3), 481-489.
- Hurlebaus, S., Mander, J., Terzioglu, T., Boger, N., and Fatima, A. (2018). "Fracture Critical Steel Twin Tub Girder Bridges." *Research Report No. FHWA/TX-12/0 6937*, Texas A&M Transportation Institute and Texas Department of Transportation.
- Hurlebaus, S. (2007). "Calculation of eigenfrequencies for rectangular free orthotropic plates—An overview." *ZAMM-Journal of Applied Mathematics and Mechanics/Zeitschrift für Angewandte Mathematik und Mechanik*, 87(10), 762-772.
- Hurlebaus, S., Gaul, L., and Wang, J.-S. (2001). "An exact series solution for calculating the eigenfrequencies of orthotropic plates with completely free boundary." *Journal of Sound and Vibration*, 244(5), 747-759.
- Kim, J., and Williamson, E. B. (2014). "Finite-Element Modeling of Twin Steel Box-Girder Bridges for Redundancy Evaluation." *Journal of Bridge Engineering*, 20(10), 04014106.
- Lwin, M. M. (2012). "Action: Clarification of Requirements for Fracture Critical Members." *HIBT-10*, FHWA, 5.

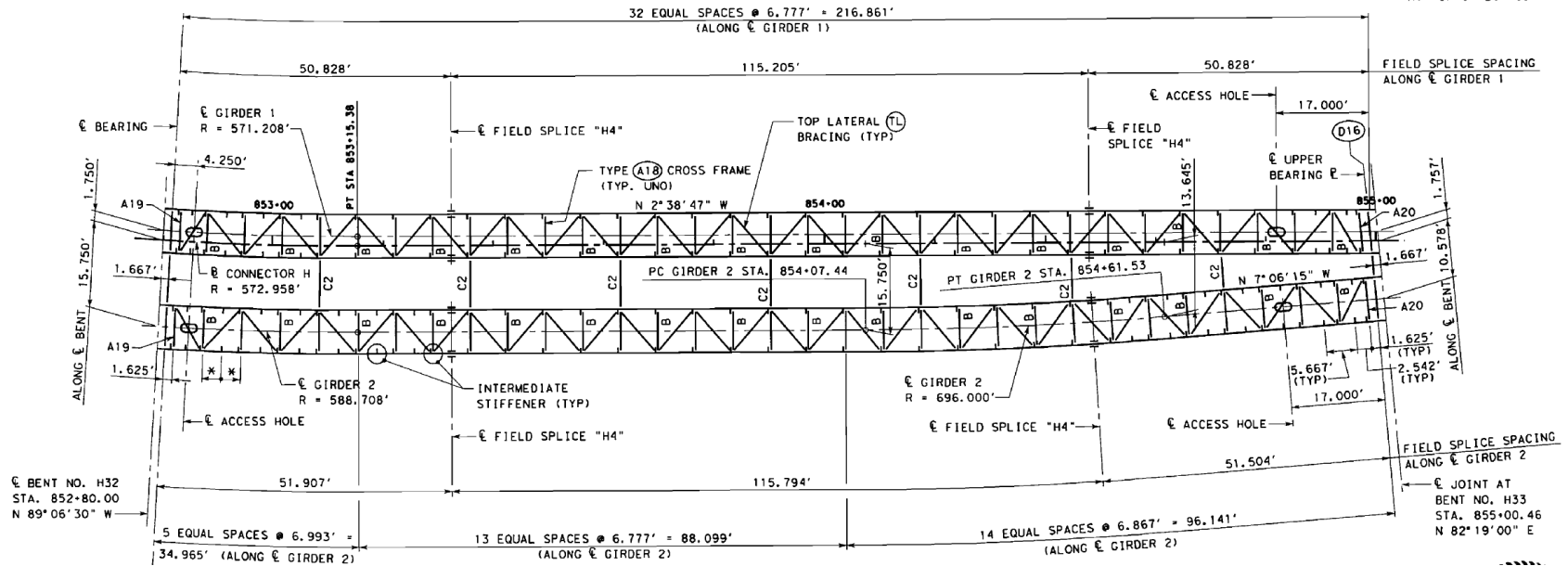
- Mouras, J. M., Sutton, J. P., Frank, K. H., and Williamson, E. B. (2008). "The tensile capacity of welded shear studs." *Report No. FHWA/TX-09/9-5498-2*, Center for Transportation Research at the Univ. of Texas at Austin, Austin, TX.
- NTSB (1971). "Collapse of U.S. 35 Bridge, Point Pleasant, West Virginia, December 15, 1967." National Transportation Safety Board, Washington, D.C.
- Park, R., and Gamble, W. L. (2000). *Reinforced concrete slabs*, New York, N.Y.: Wiley.
- Parmelee, R. A., and Sandberg, H. R. (1987) "Redundancy - A Design Objective." *Proc., AISC National Engineering Conference and Conference of Operating Personnel Proceedings*. New Orleans, L.A., 39-1 to 39-12
- Samaras, V. A., Sutton, J. P., Williamson, E. B., and Frank, K. H. (2012). "Simplified method for evaluating the redundancy of twin steel box-girder bridges." *Journal of Bridge Engineering*, 17(3), 470-480.
- Sanders, W. W., and Elleby, H. A. (1970). "Distribution of Wheel Loads on Highway Bridges." National Cooperative Highway Research Program, Highway Research Board.
- Scheffey, C. F. (1971). "Point Pleasant Bridge Collapse: Conclusions of Federal Study." *Civil Engineering*, 41(7), 41.
- Sutton, J. P., Mouras, J. M., Samaras, V. A., Williamson, E. B., and Frank, K. H. (2014). "Strength and ductility of shear studs under tensile loading." *Journal of Bridge Engineering*, 19(2), 245-253.

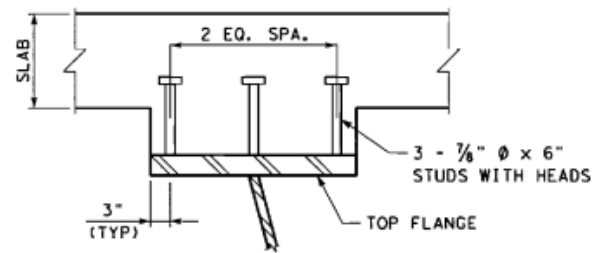
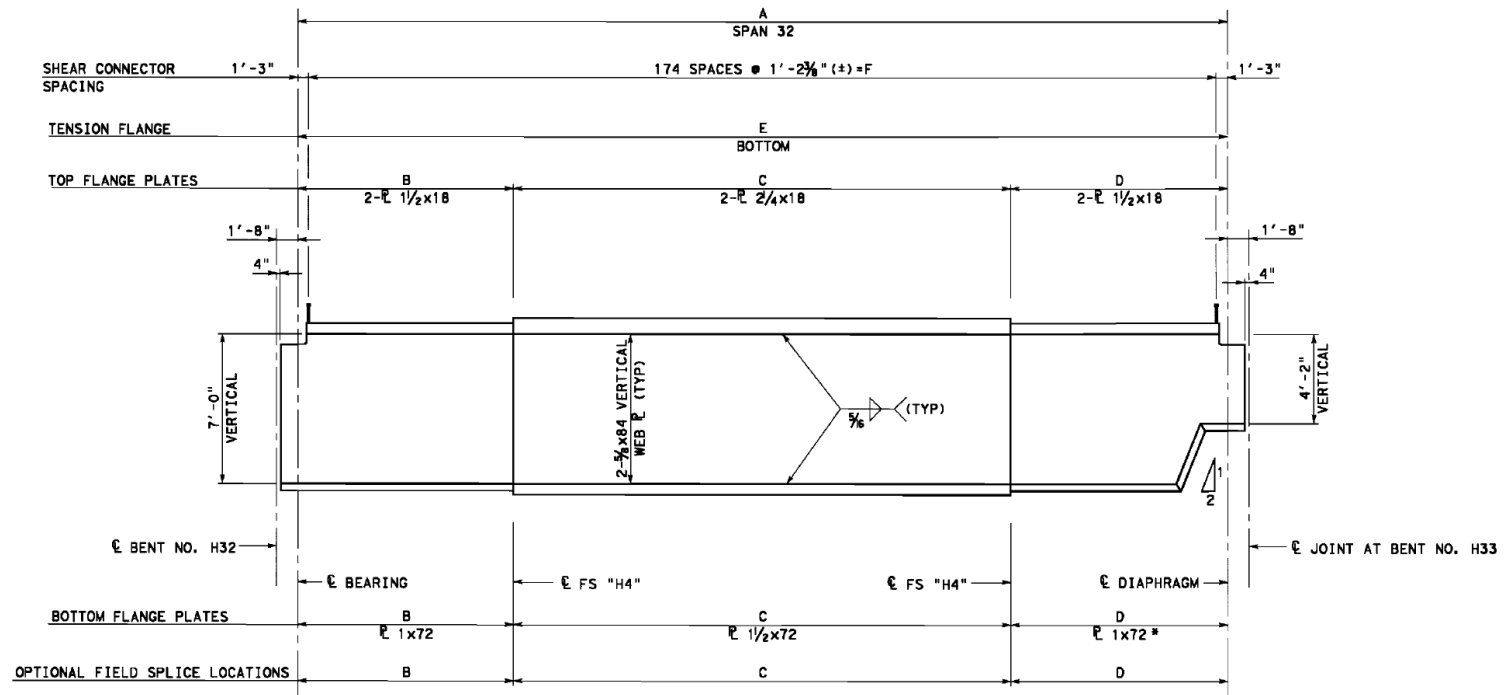
- Sweeney, R. (1979). "Importance of redundancy in bridge-fracture control." *Transportation Research Record*(711).
- Timoshenko, S. (1953). *History of strength of materials: with a brief account of the history of theory of elasticity and theory of structures*, McGraw Hill, New York, N.Y.
- Timoshenko, S. P., and Woinowsky-Krieger, S. (1959). *Theory of Plates and Shells*, McGrawHill, New York. N.Y.
- Turner, M. (1959). *The Direct Stiffness Method of Structural Analysis*, Structural and Materails Panel Paper, AGARD Meeting, Aachen, Germany
- Turner, M. J., Clough, R. W., Martin, H. C., and Topp, L. J. (1956). "Stiffness and deflection analysis of complex structures." *Journal of the Aeronautical Sciences*, 23(9), 805-823.
- TxDOT (2013). *Bridge Inspection Manual - Revised August 2013*, Texas Department of Transportation.
- TxDOT (2015). *Preferred Practices for Steel Design, Fabrication, and Erection*, Texas Department of Transportation.
- Witcher, T.R., (2017)"From Disaster to Prevention: The Silver Bridge." *Civil Engineering*, 87(11), 44-47
- Wood, R., Armer, G., and Hillerborg, A. (1968). "The Theory of the Strip Method for Design of Slabs.(Includes Appendix)." *Proceedings of the Institution of Civil Engineers*, 41(2), 285-311.

APPENDIX A
STRUCTURAL DRAWINGS

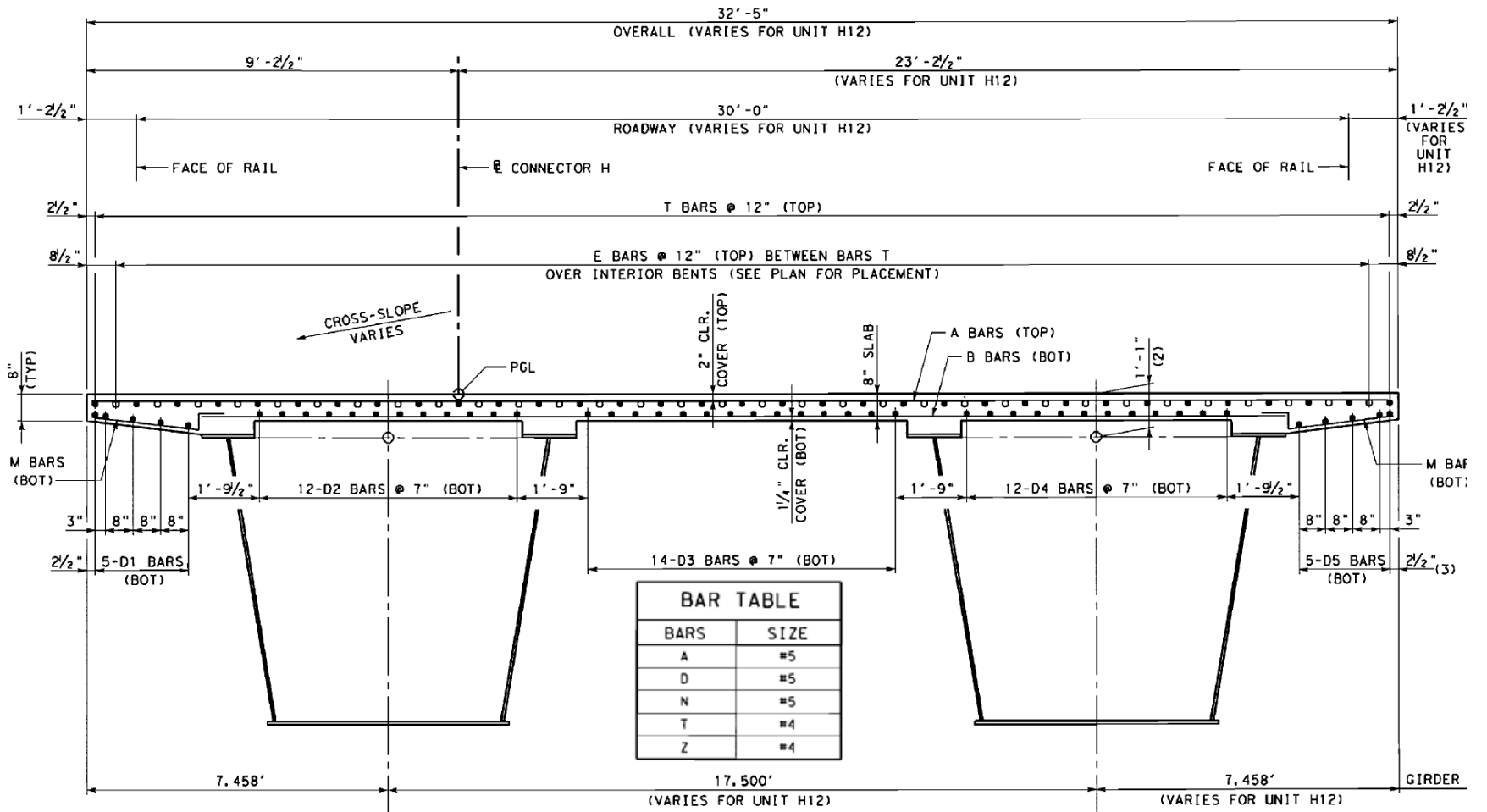
BRIDGE 1: 12-102-3256-01-403

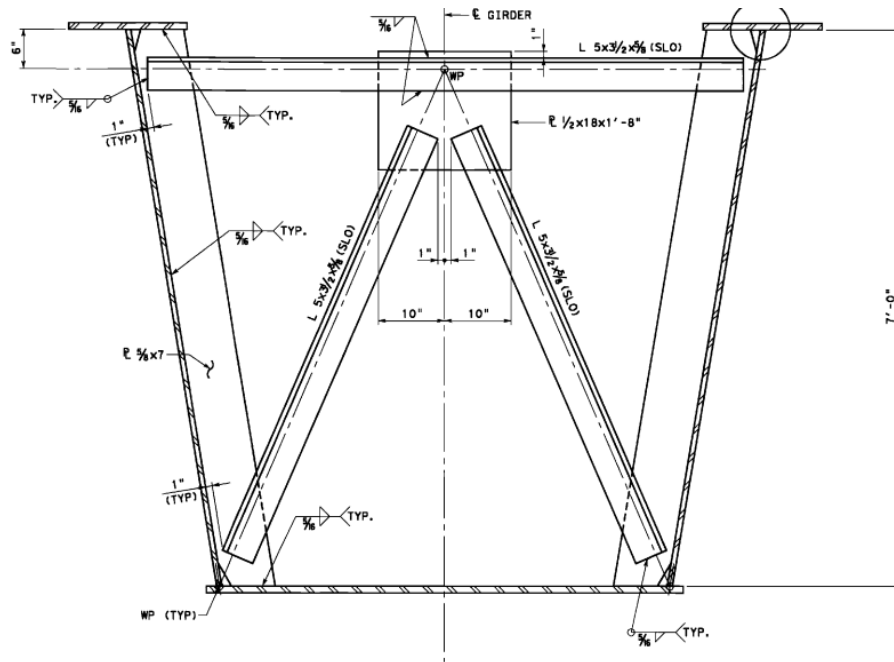
NOTE: GIRDER RADIUS IS MEASURED AT TOP OF BOX GIRDER WEB.



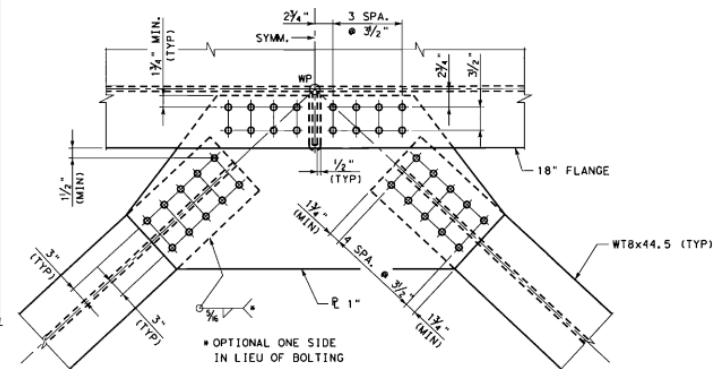


SHEAR CONNECTOR STUD DETAIL

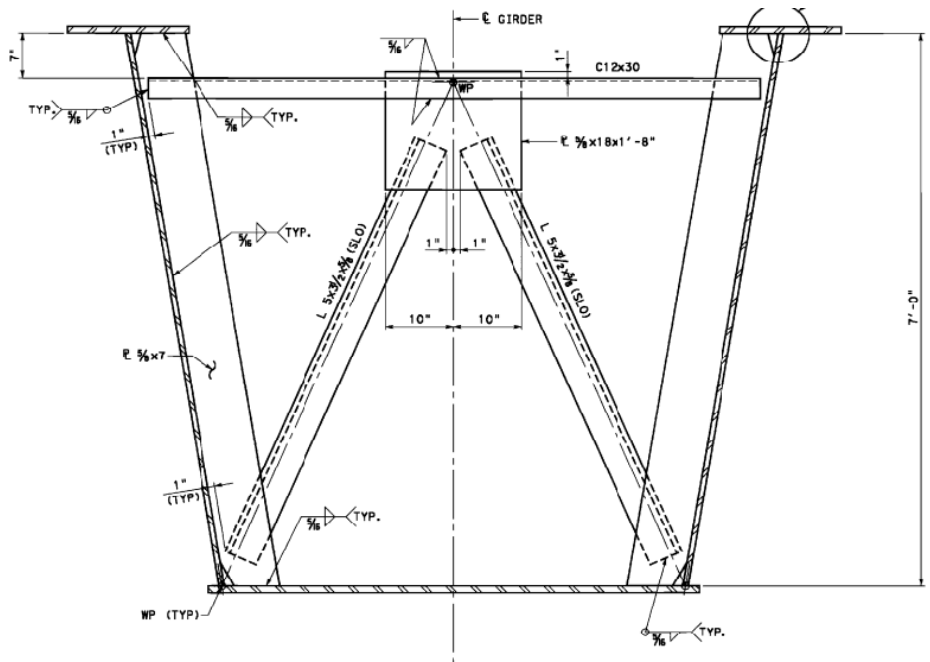




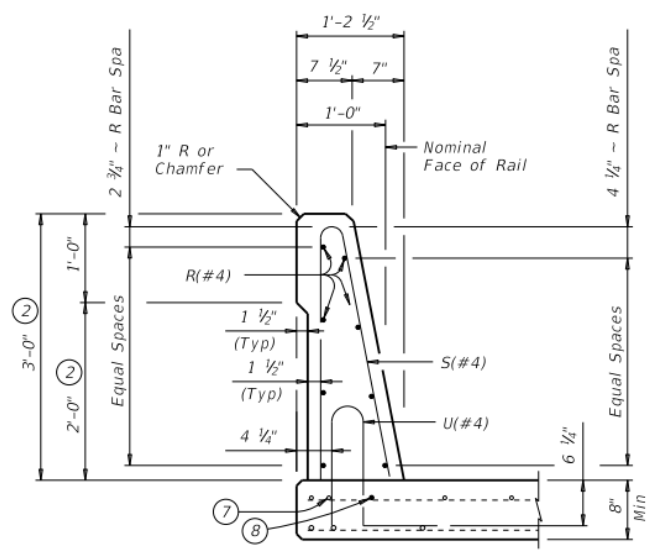
CROSS FRAME - TYPE A18

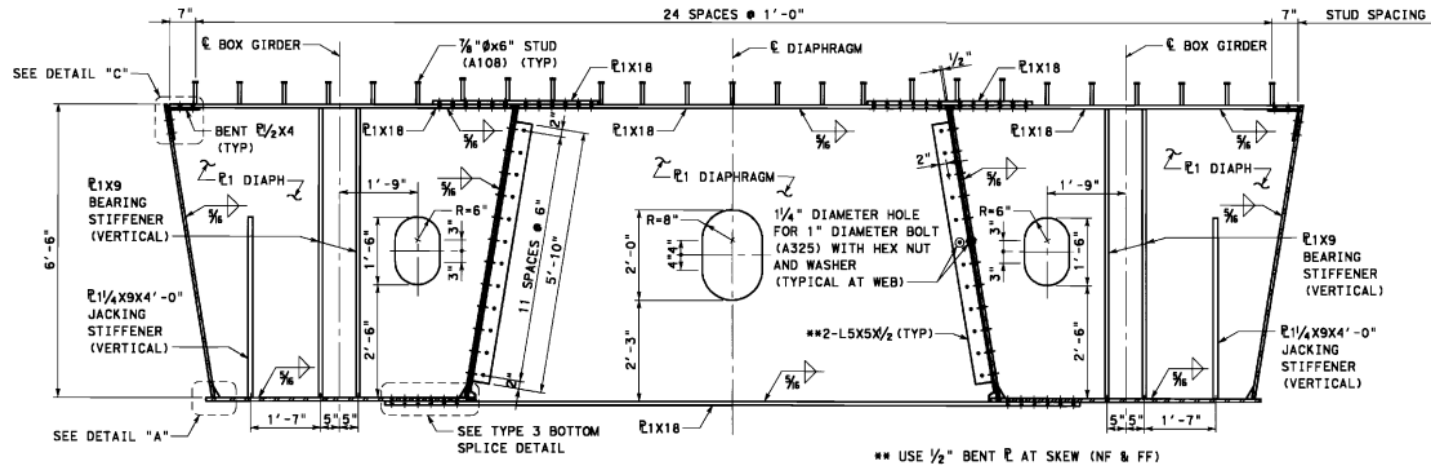


TOP LATERAL BRACING CONNECTION
DETAIL - UNIT H12
 (18" TOP FLANGE)

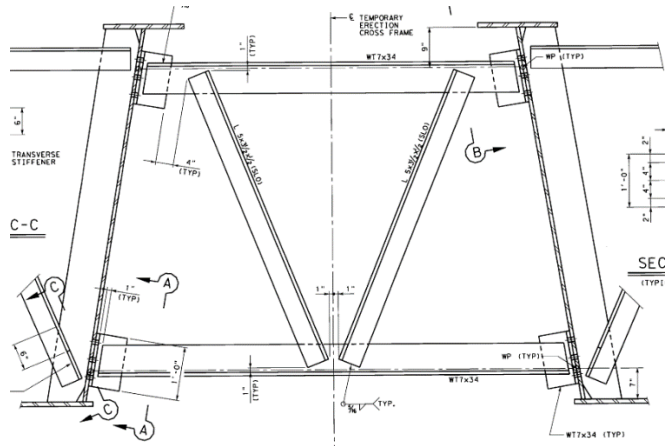


CROSS FRAME - TYPE A19



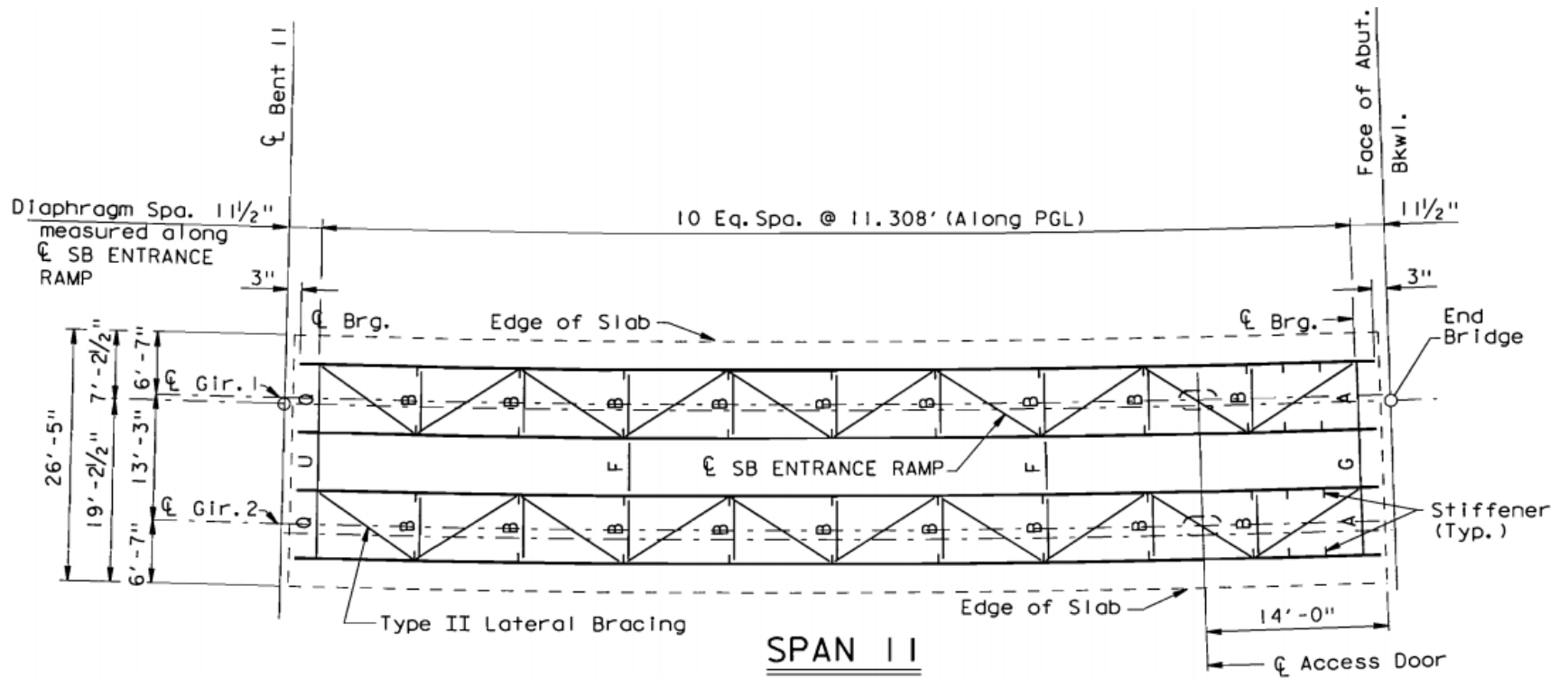


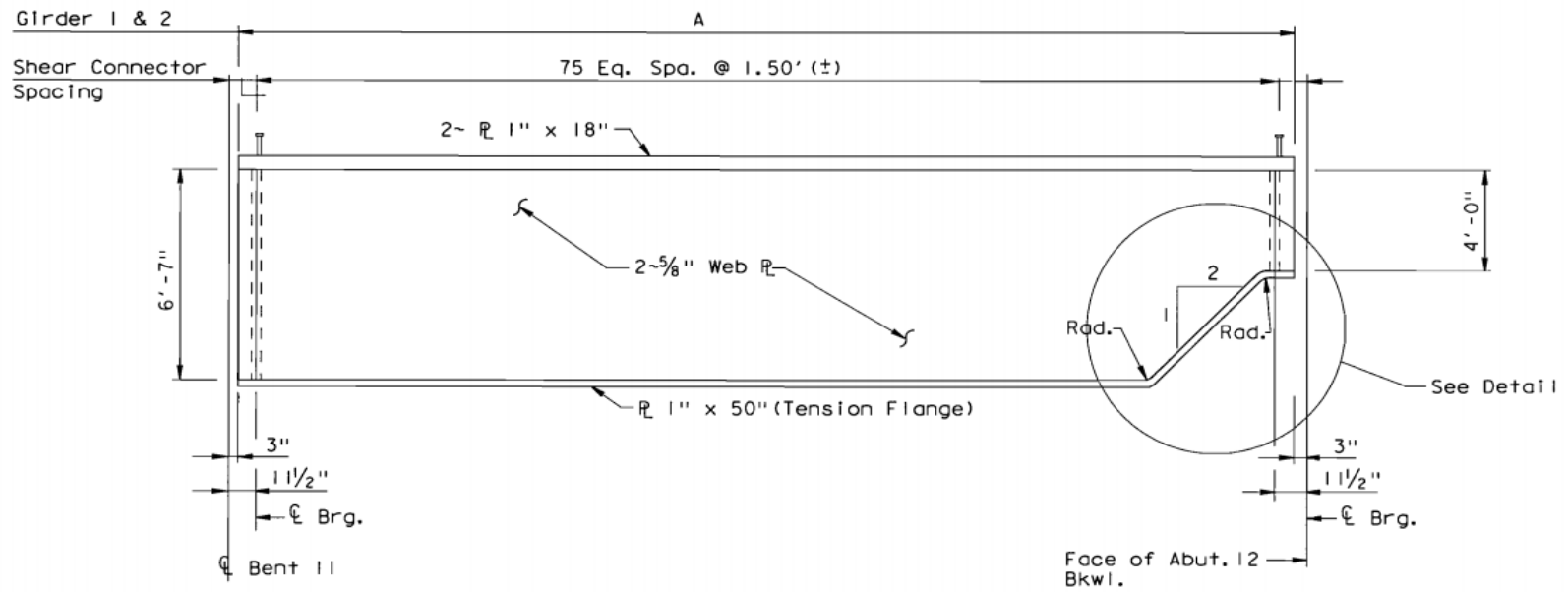
DIAPHRAGM - TYPE D13



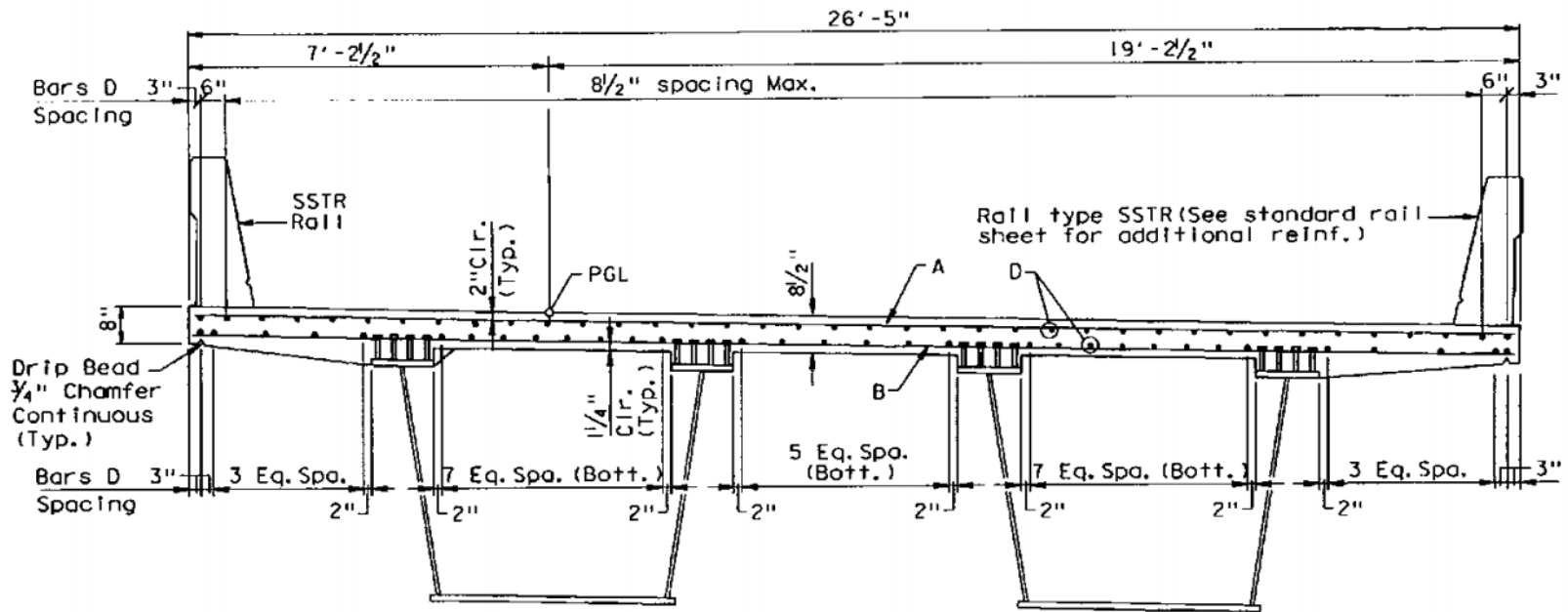
TEMPORARY ERECTION CROSS FRAME TYPE C2

BRIDGE 2: 12-102-0271-17-530



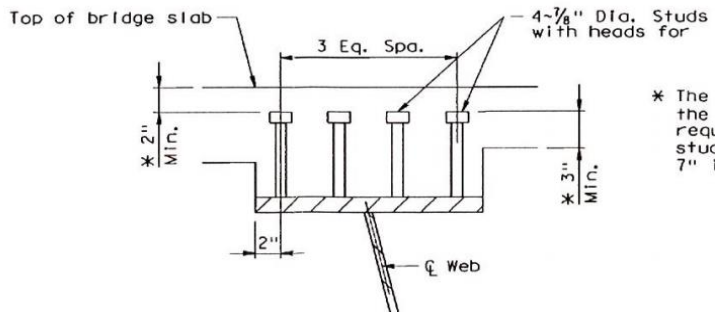


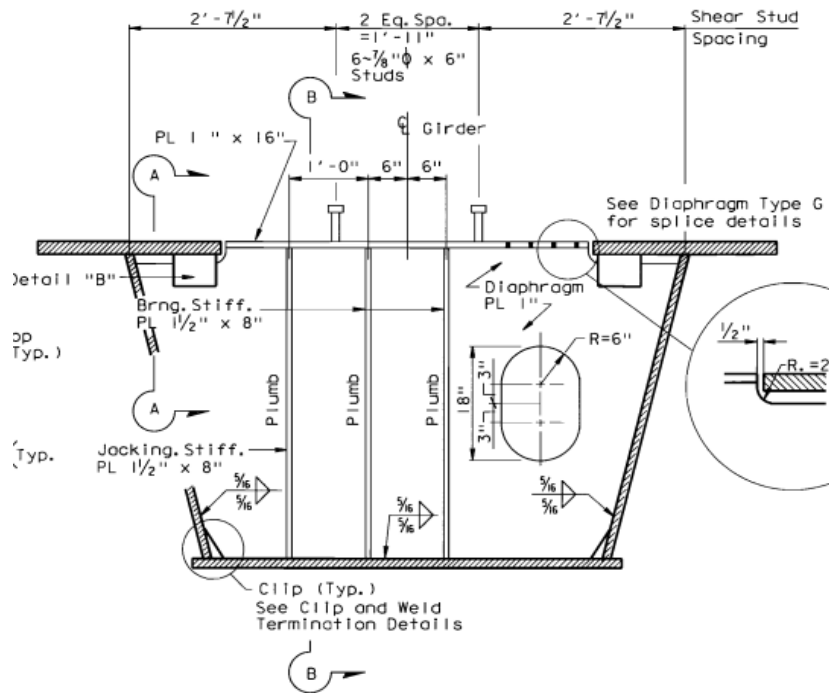
BOX GIRDER ELEVATION (TYP)
 (DIMENSIONS SHOWN ARE ALONG CL GIRDER)



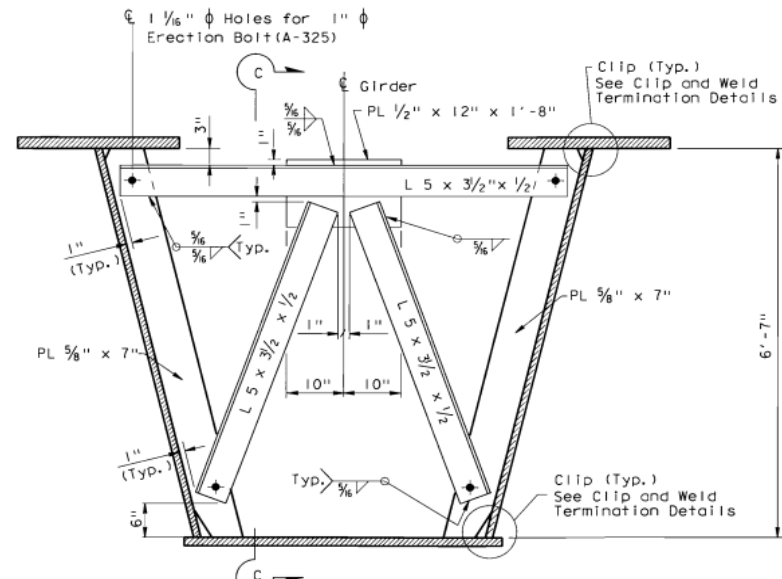
BOX GIRDER ELEVATION (TYP)

(DIMENSIONS SHOWN ARE ALONG ϕ GIRDER)

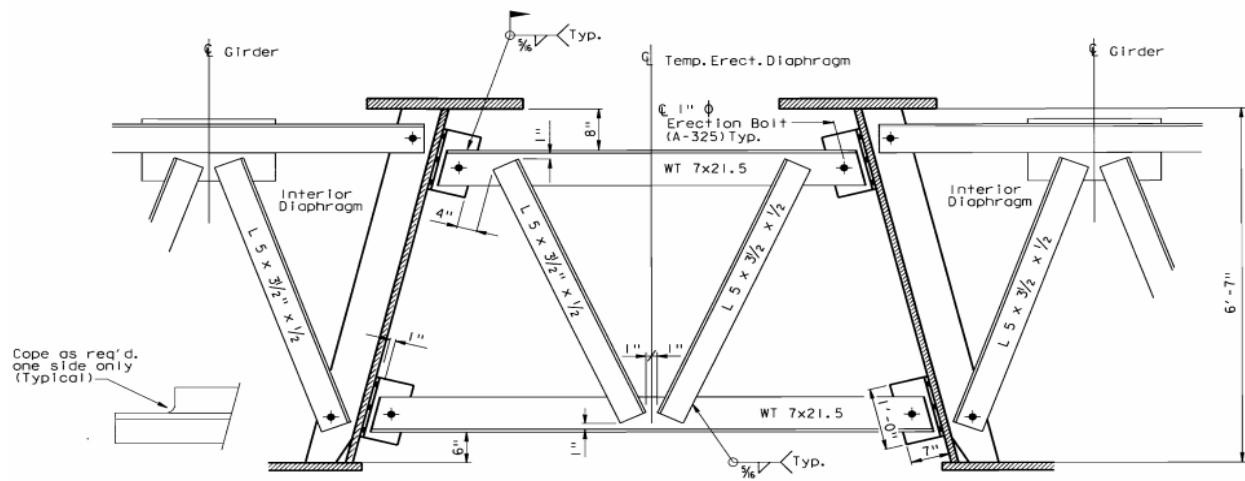




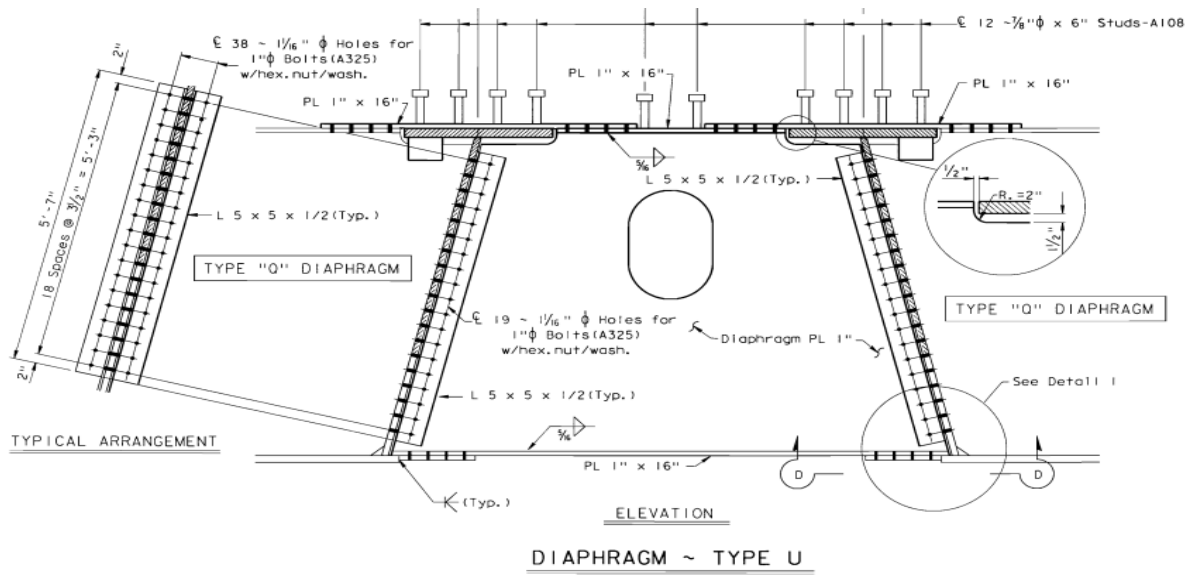
DIAPHRAGM ~ TYPE A

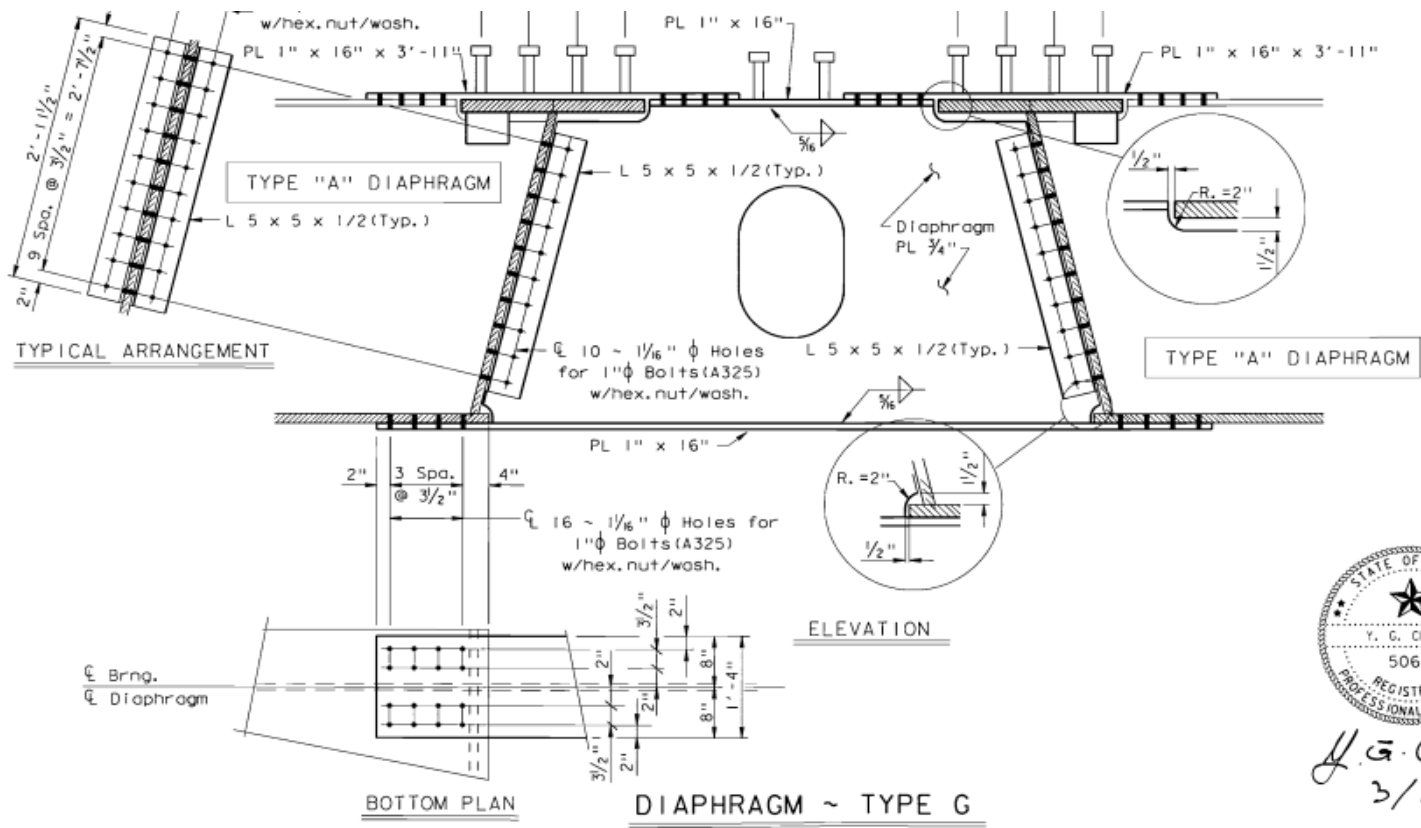


DIAPHRAGM ~ TYPE B

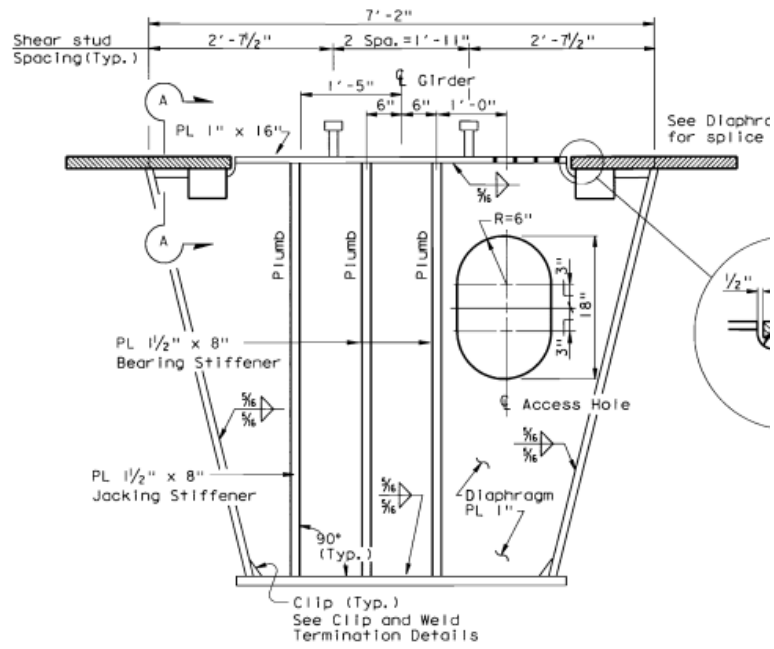


DIAPHRAGM ~ TYPE F (Temporary)

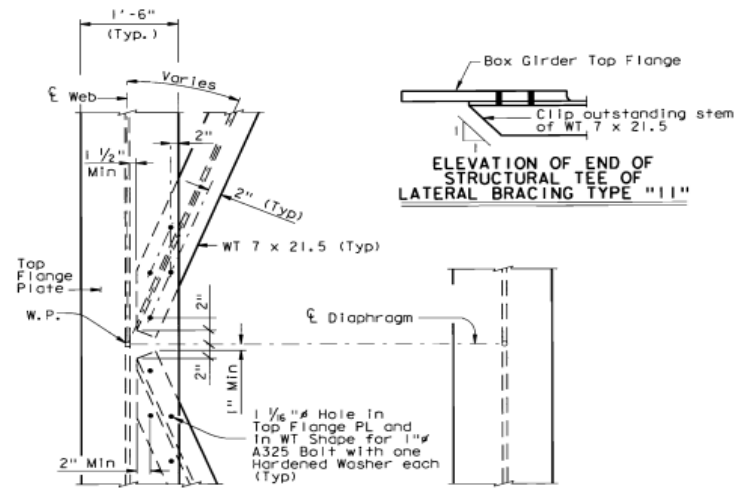




Y. G. C.
3/1



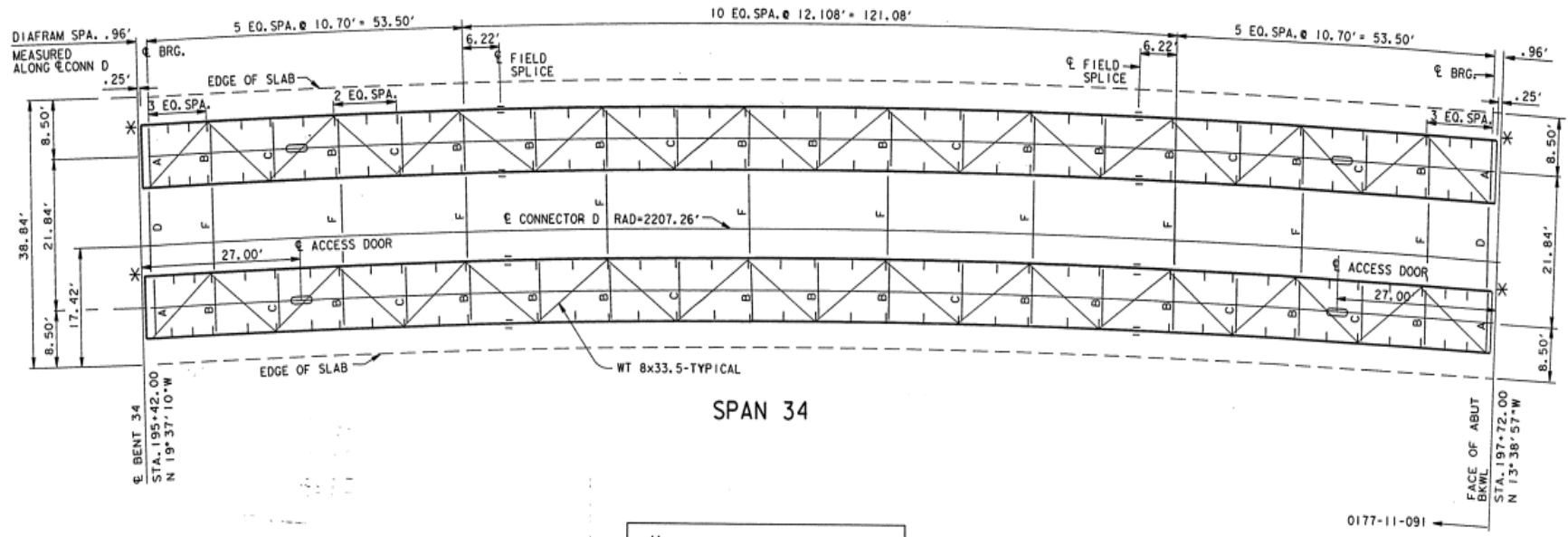
DIAPHRAGM ~ TYPE Q

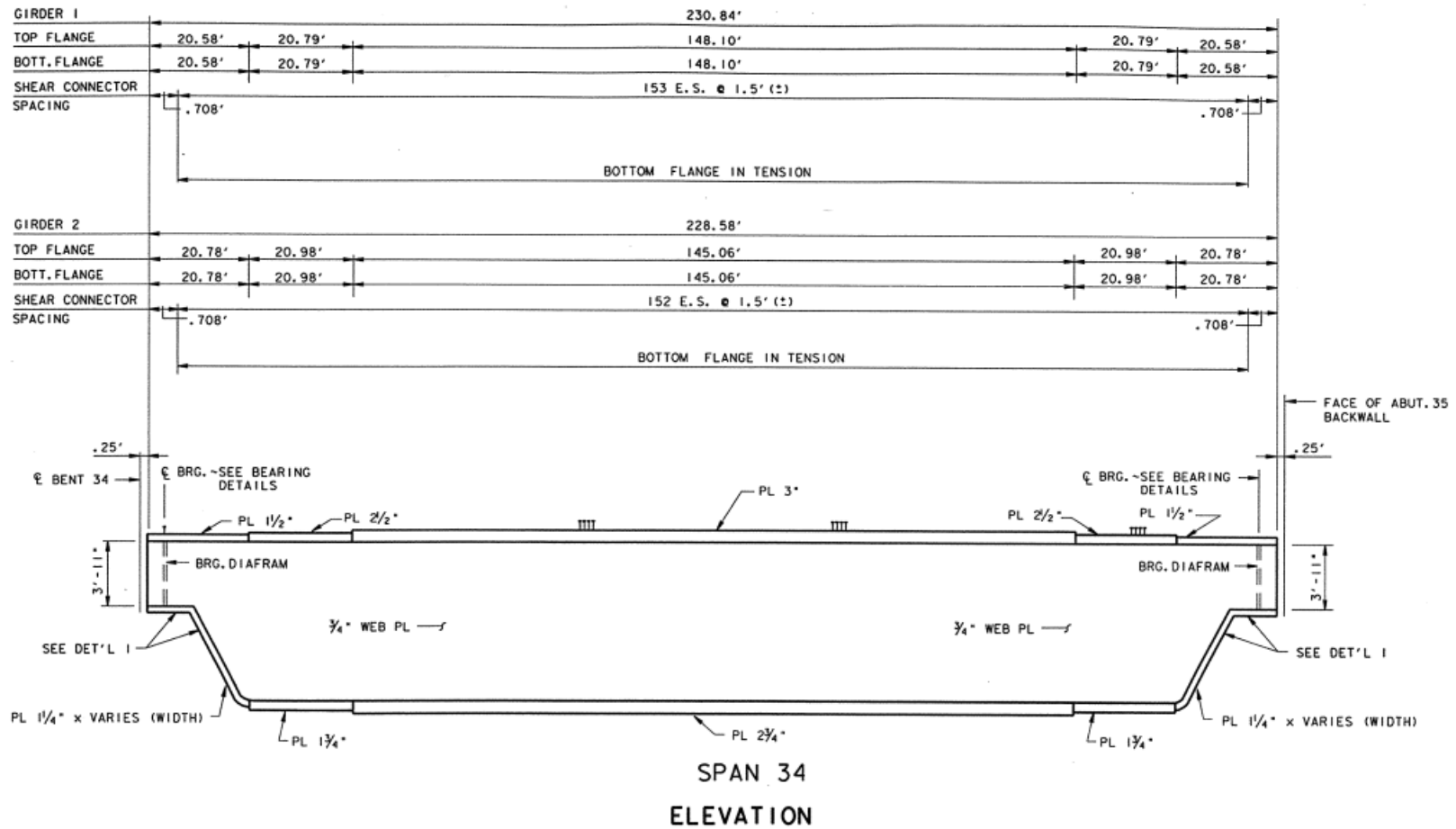


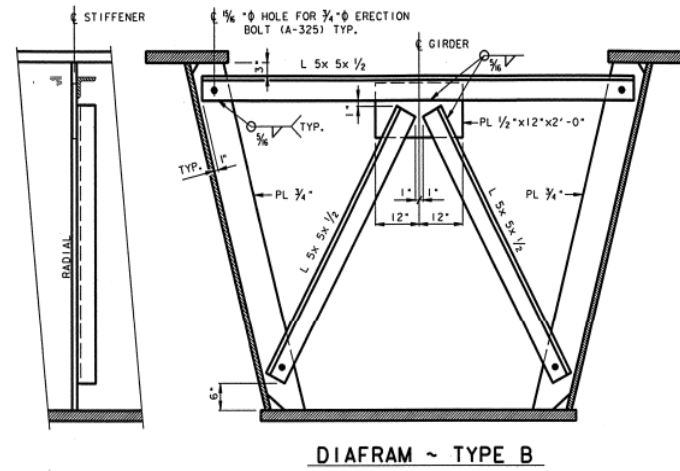
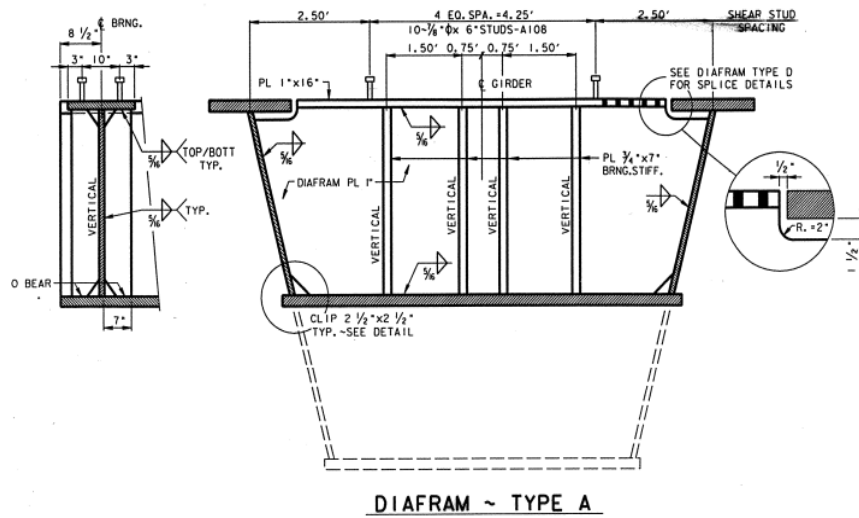
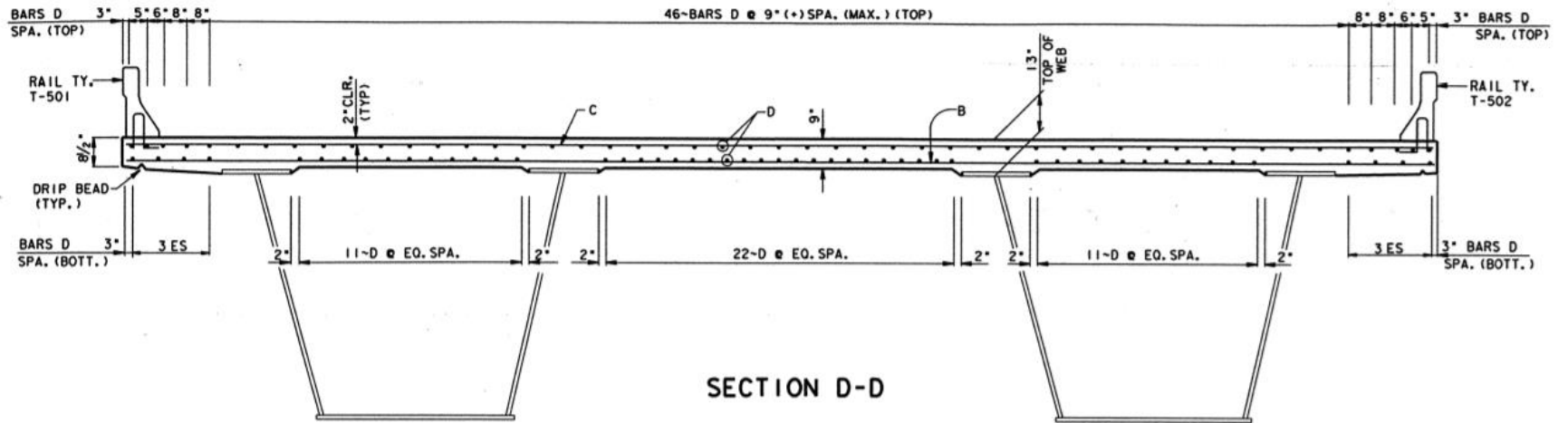
TYPICAL PLAN VIEW OF LATERAL BRACING TYPE "111"

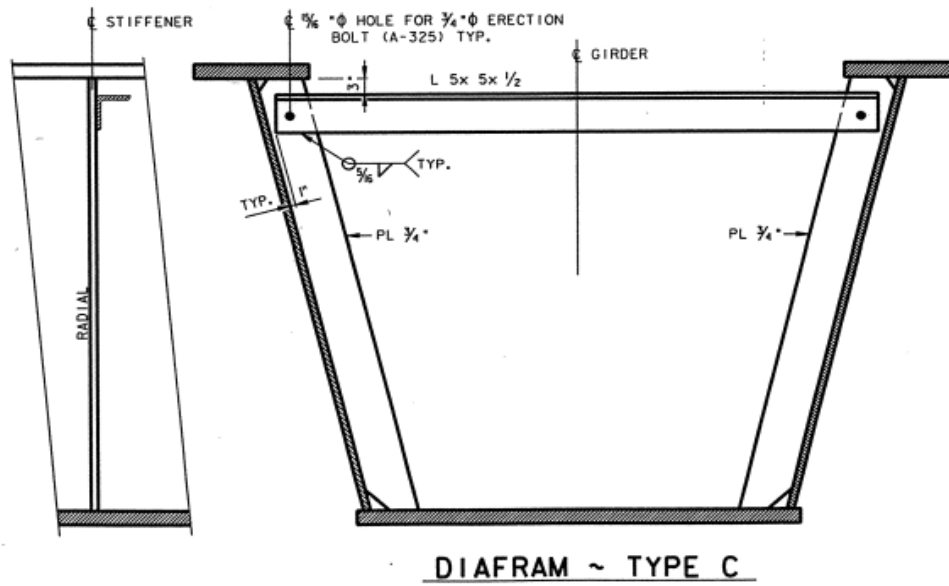
Installed in shop except at locations spanning a field splice, which shall be installed in the field.

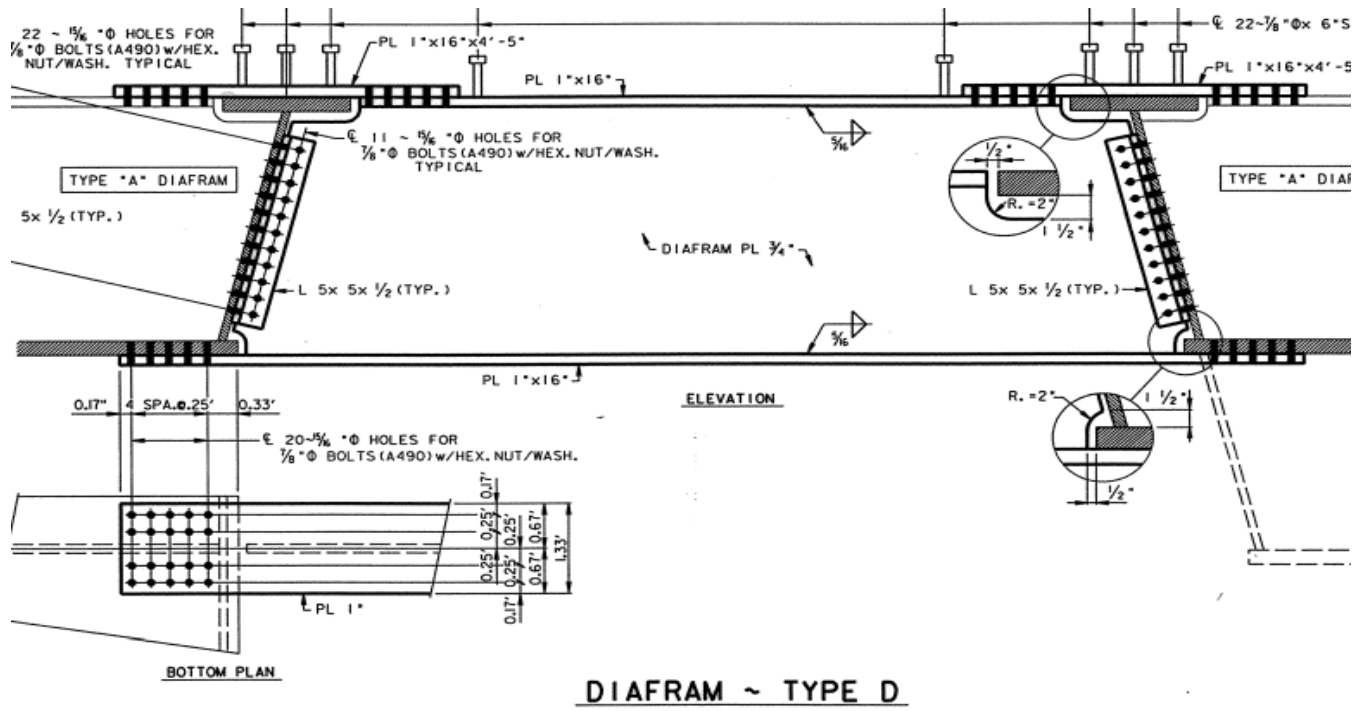
BRIDGE 3: 12-102-0508-01-294

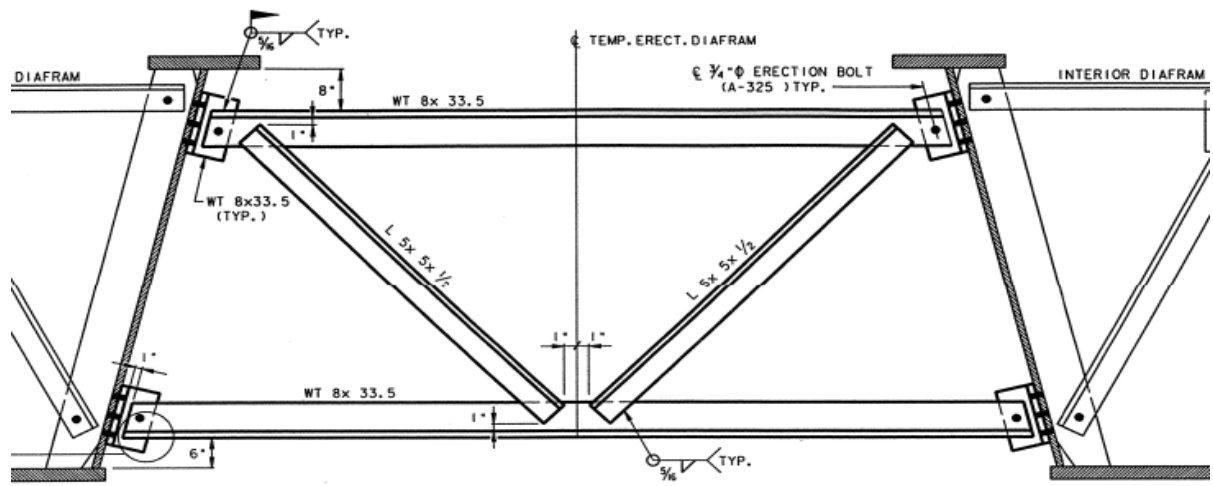




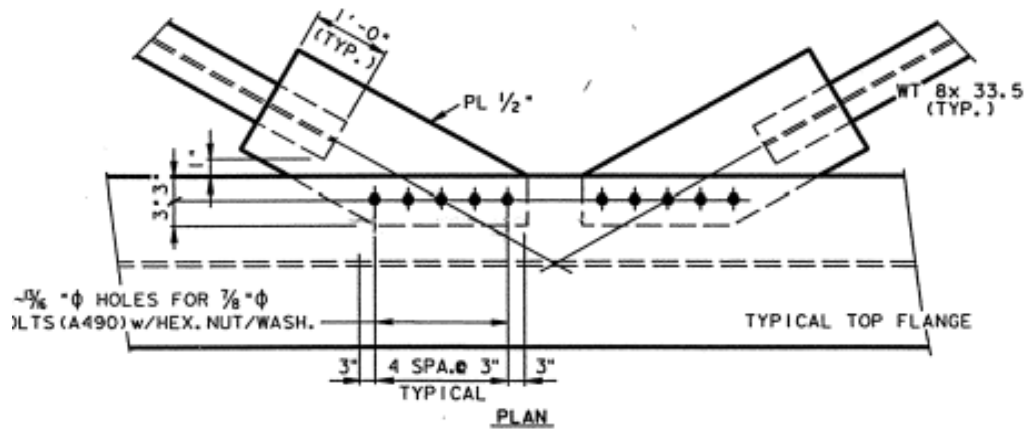




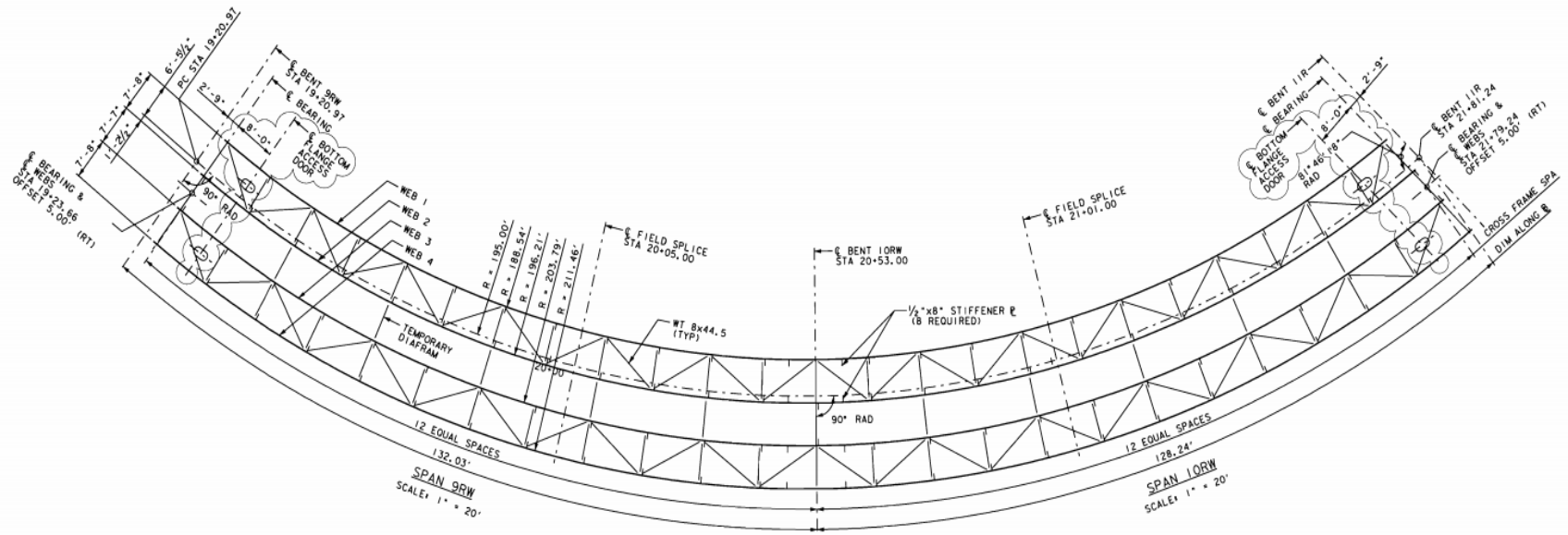


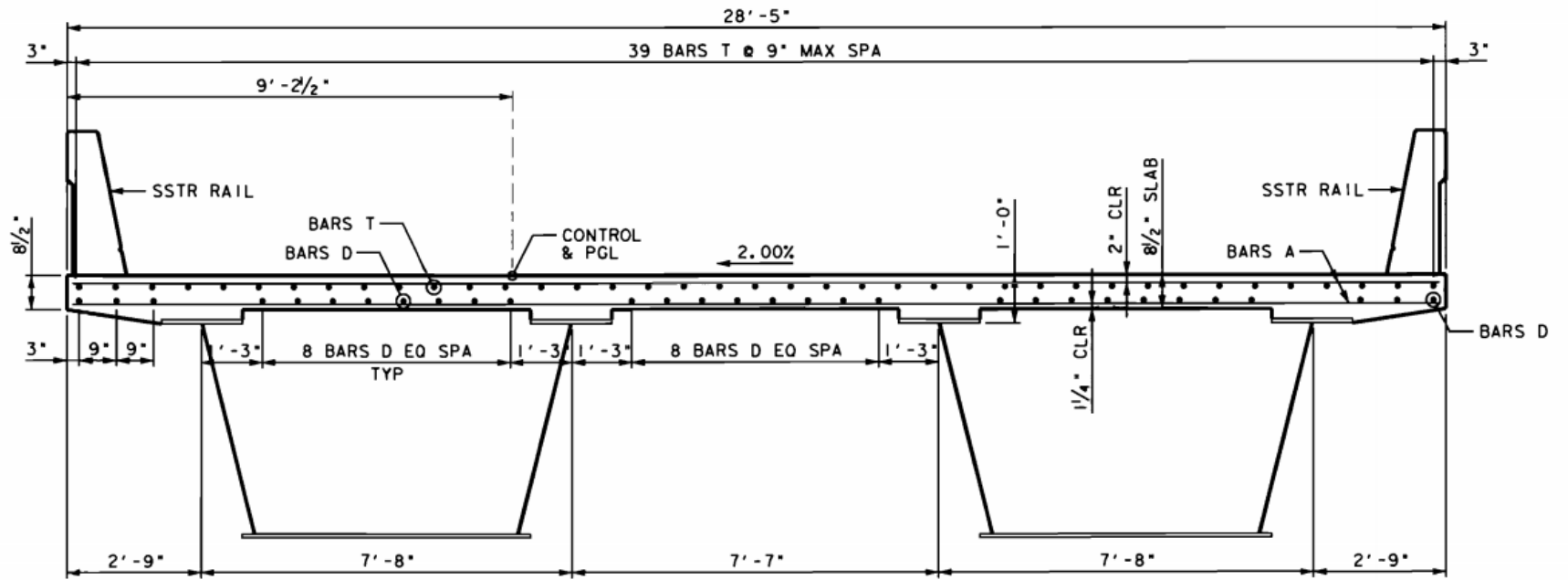


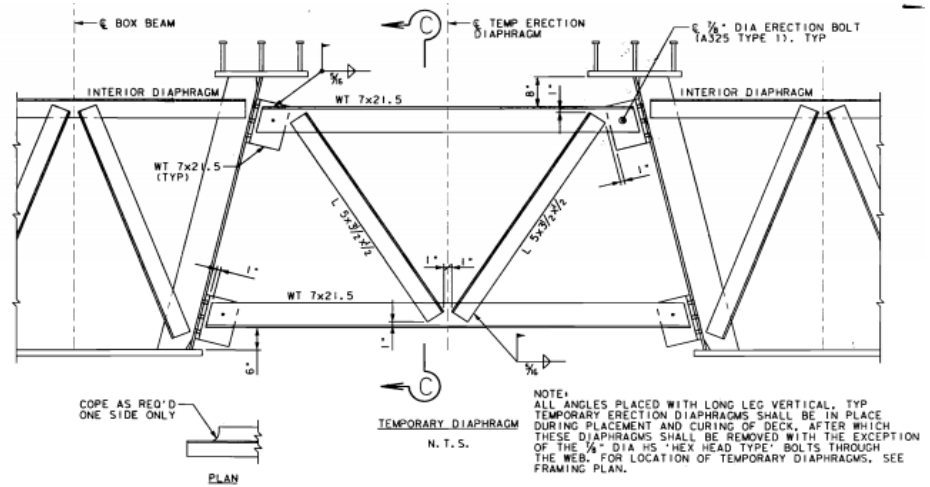
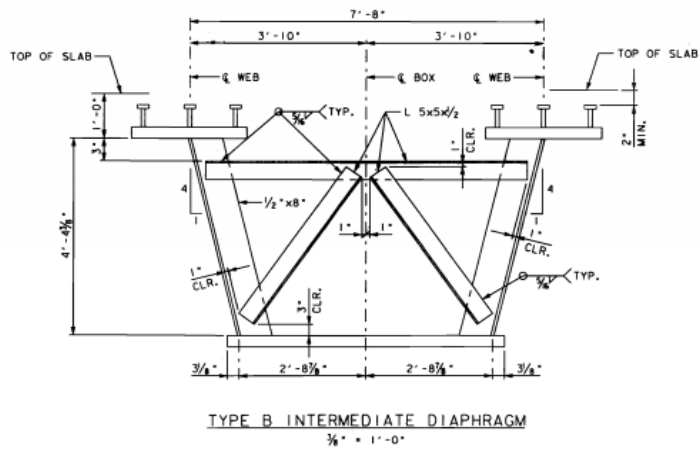
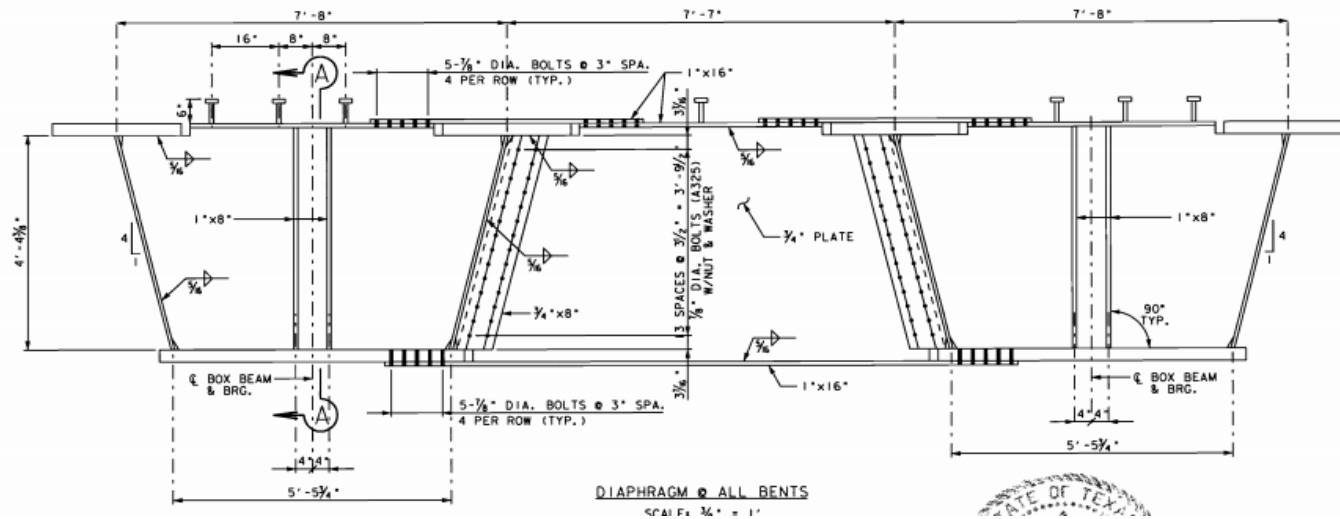
DIAFRAM ~ TYPE F (TEMPORARY)



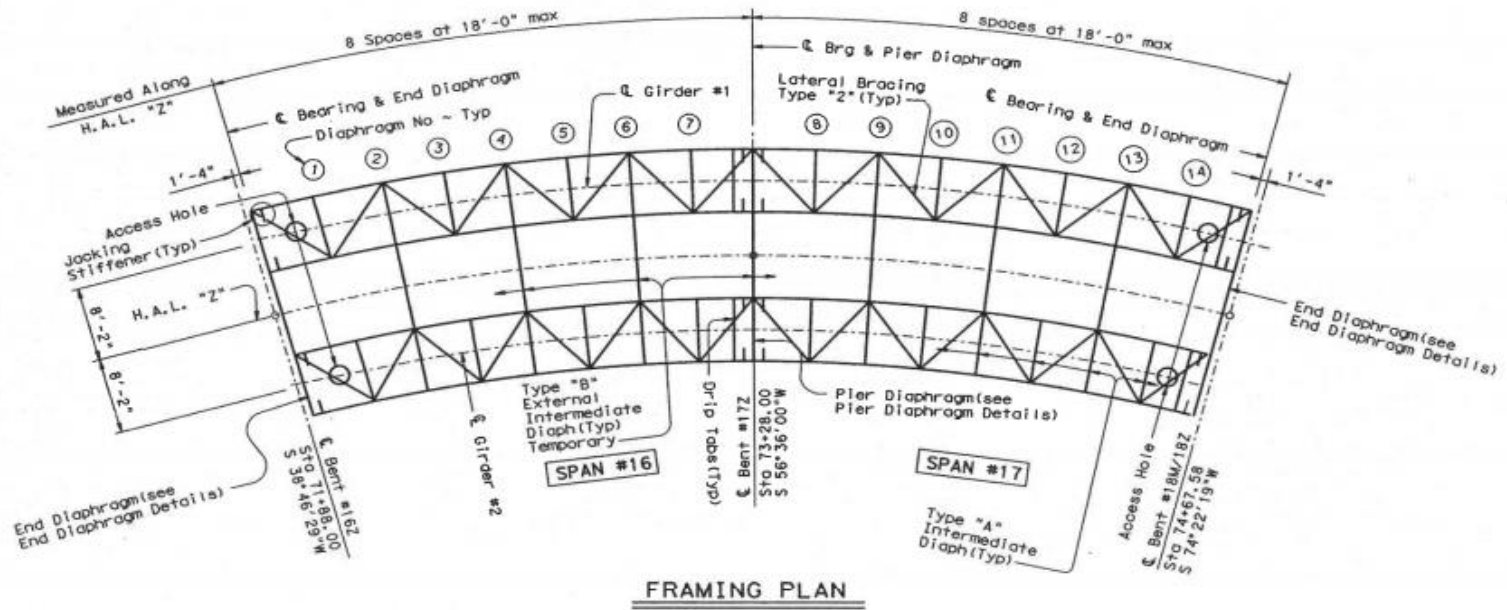
BRIDGE 4: 12-102-0271-07-637

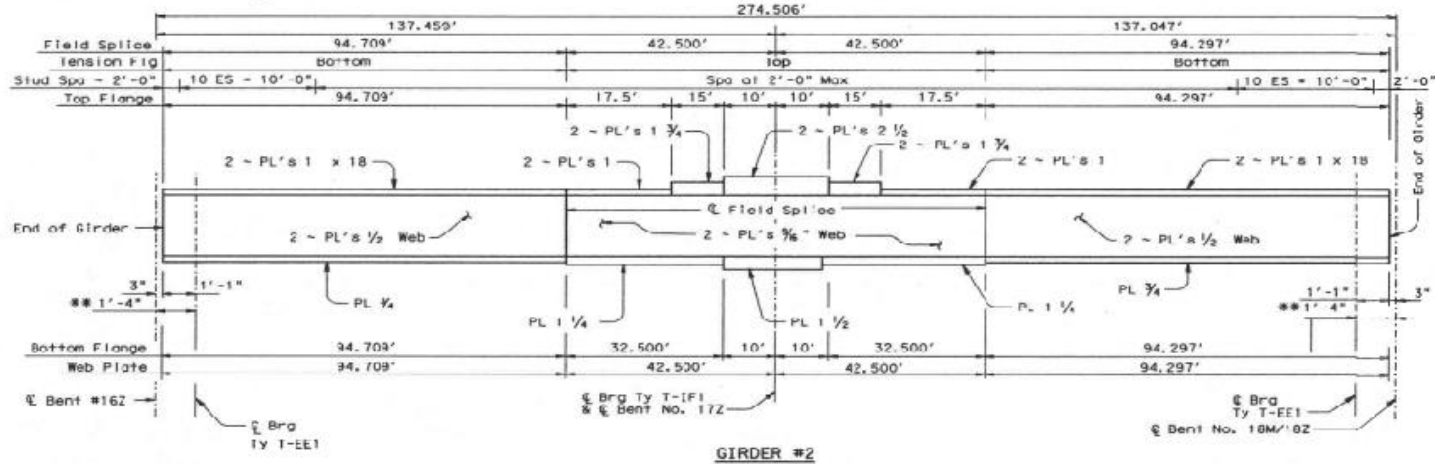
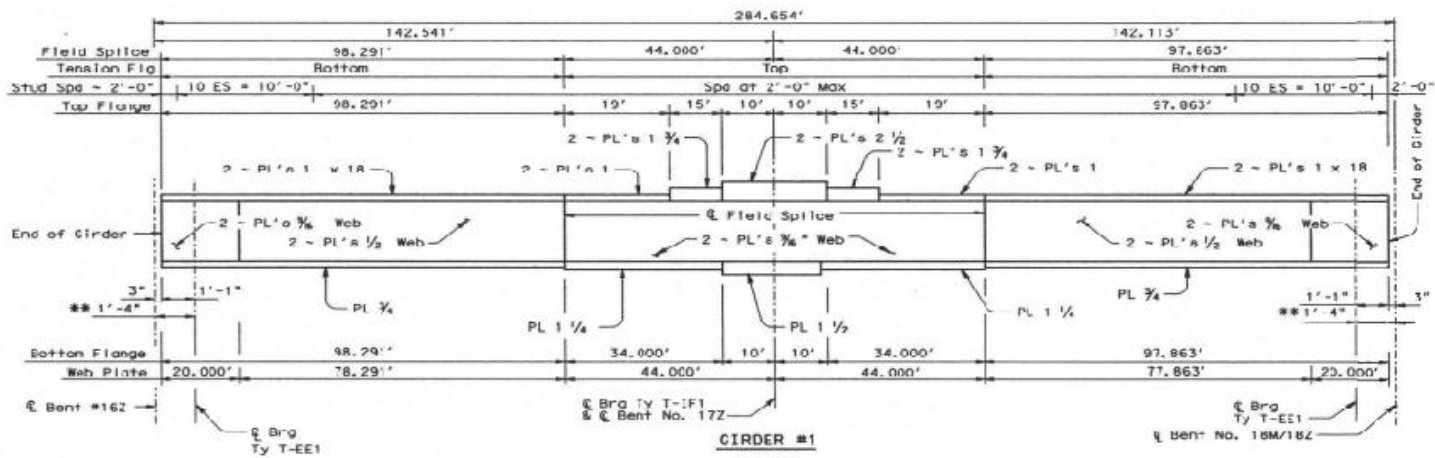


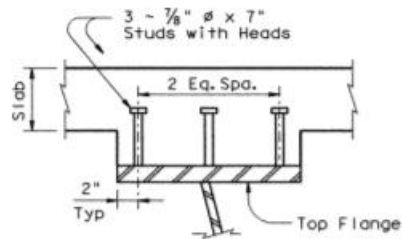
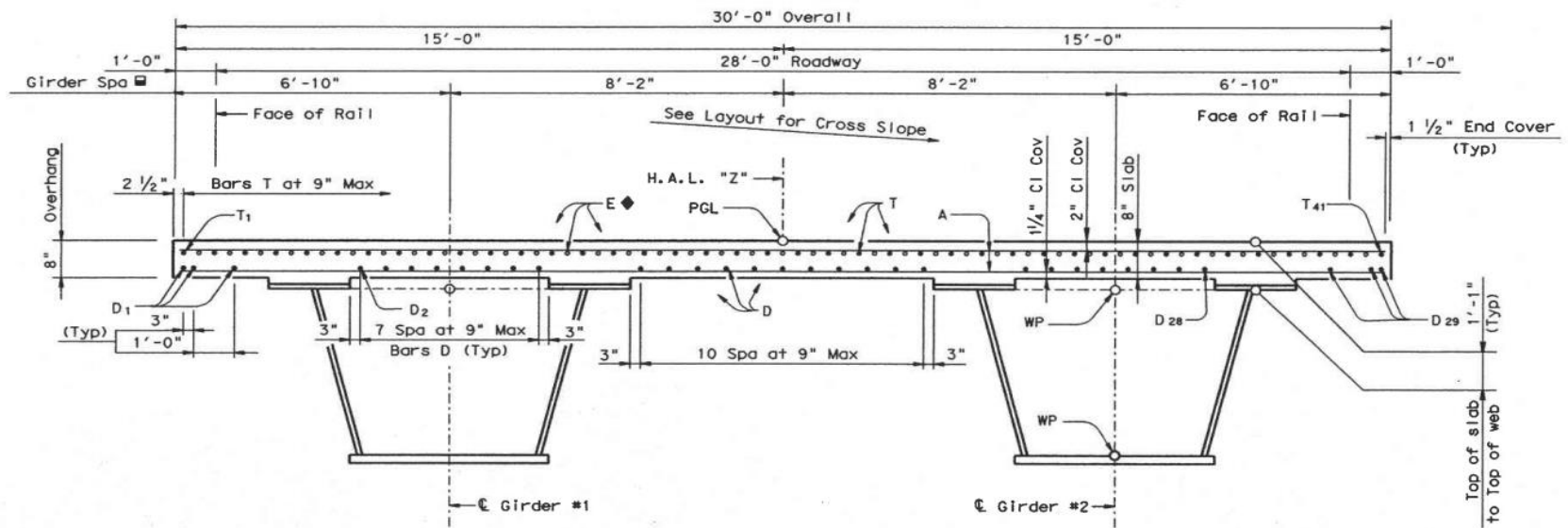




BRIDGE 5: 14-227-0-0015-13-452

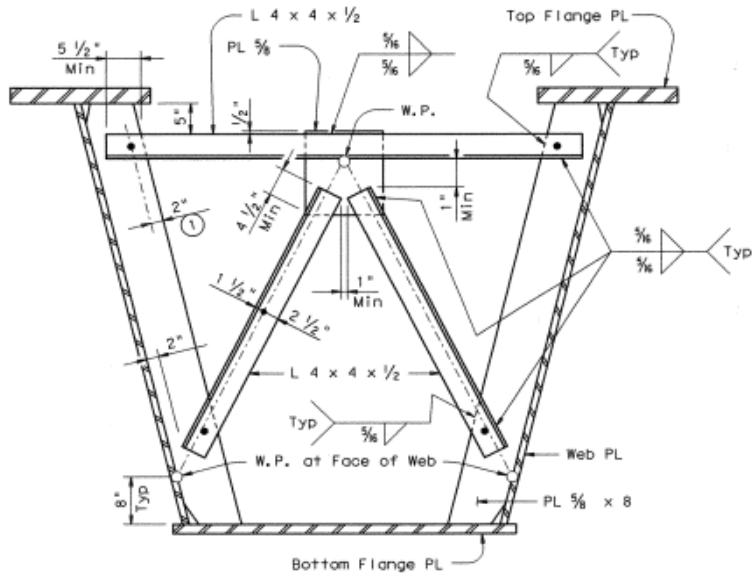






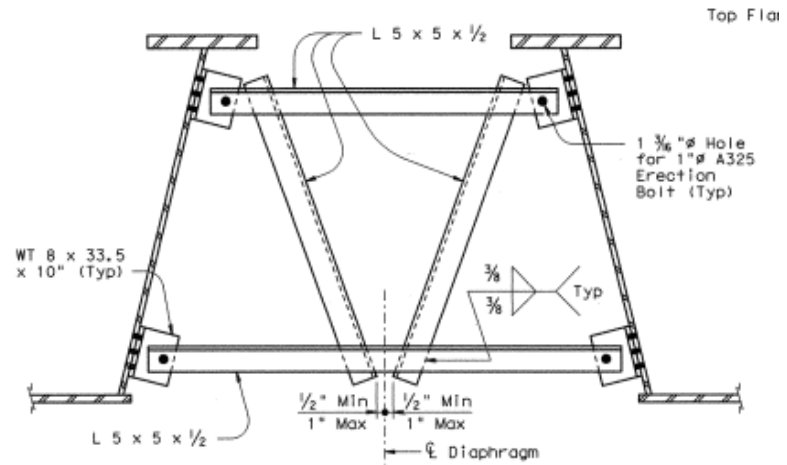
SHEAR CONNECTOR STUD DETAIL

Studs shall be Electric arc end-welded to the flanges with complete fusion. (See Span details for spacing along girder.)

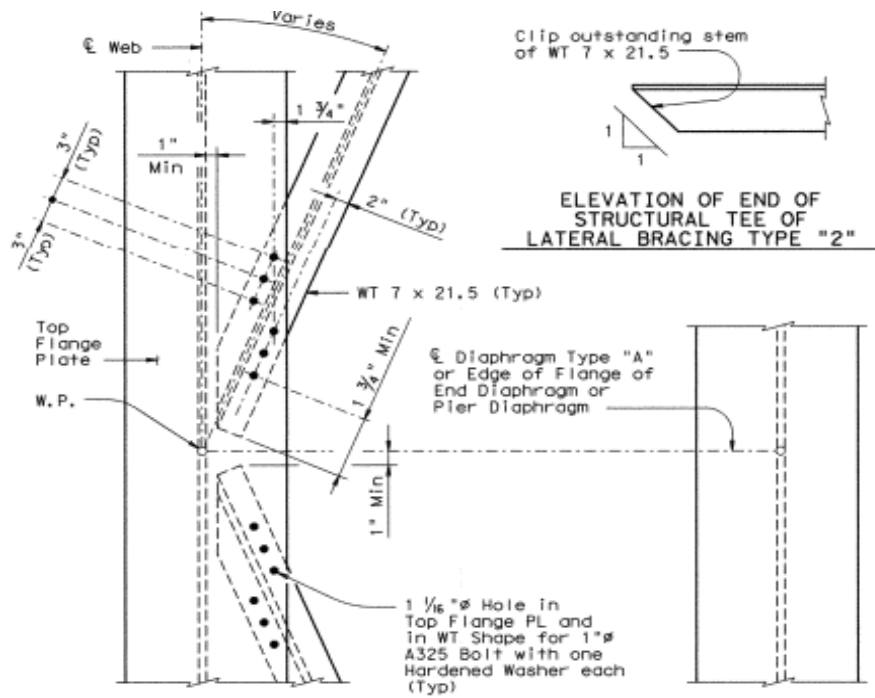


TYPICAL SECTION AT TYPE "A" INTERNAL INTERMEDIATE DIAPHRAGM

To be fully installed in the shop.



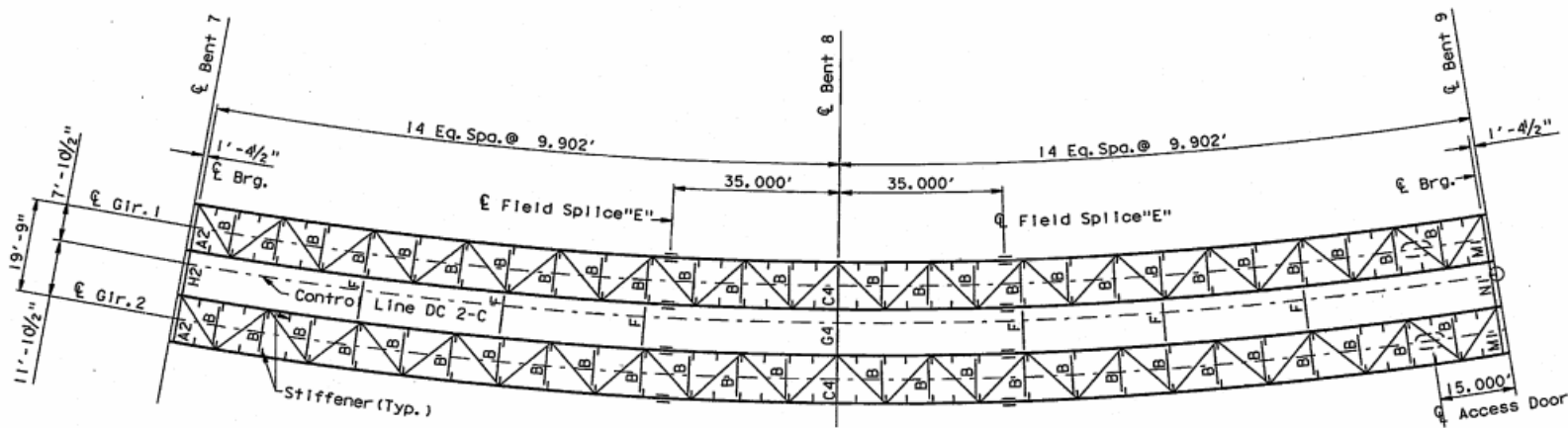
TYPICAL SECTION AT TYPE "B" EXTERNAL INTERMEDIATE DIAPHRAGM (TEMPORARY)



**TYPICAL PLAN VIEW OF
LATERAL BRACING TYPE "2"**

Installed in shop except at locations spanning a field splice, which shall be installed in the field.

BRIDGE 6: 12-102-0271-07-575

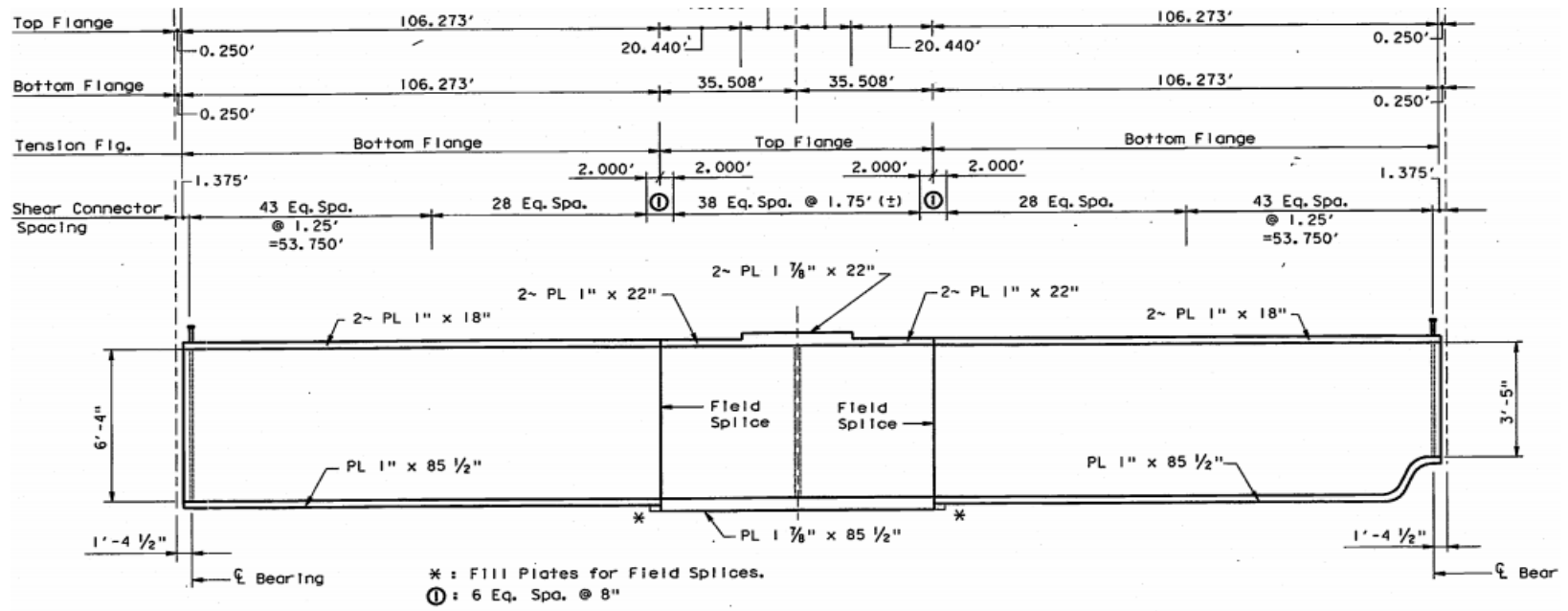


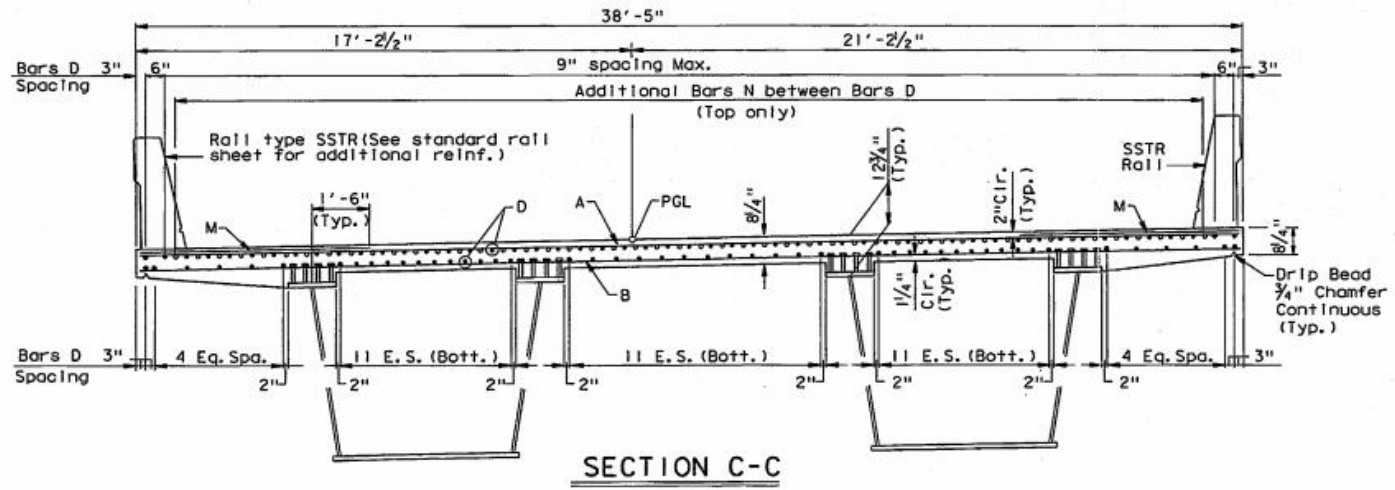
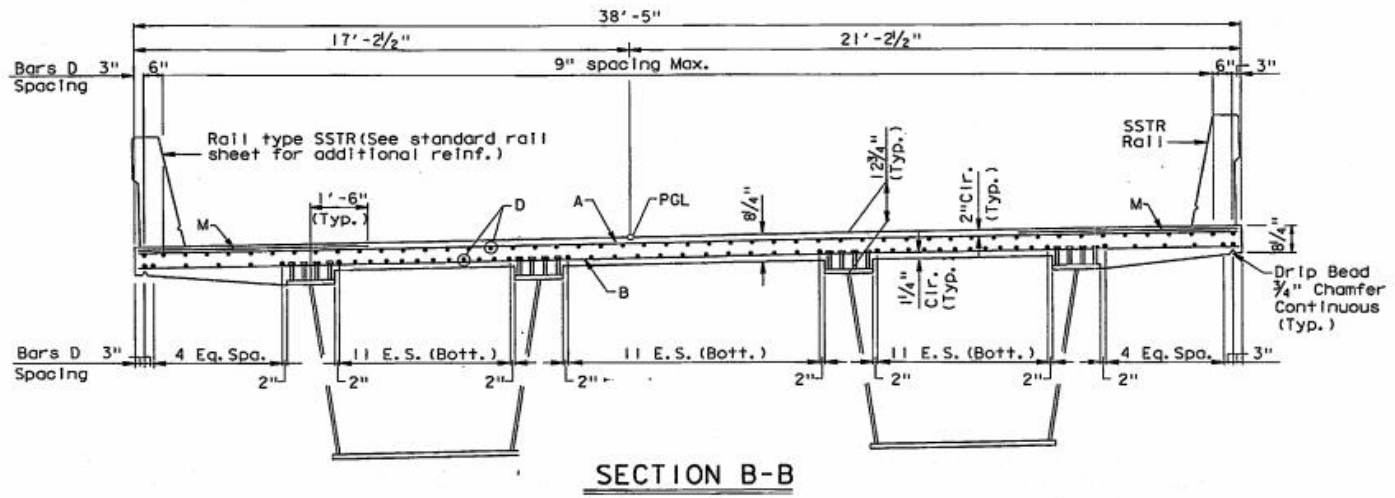
SPAN 7

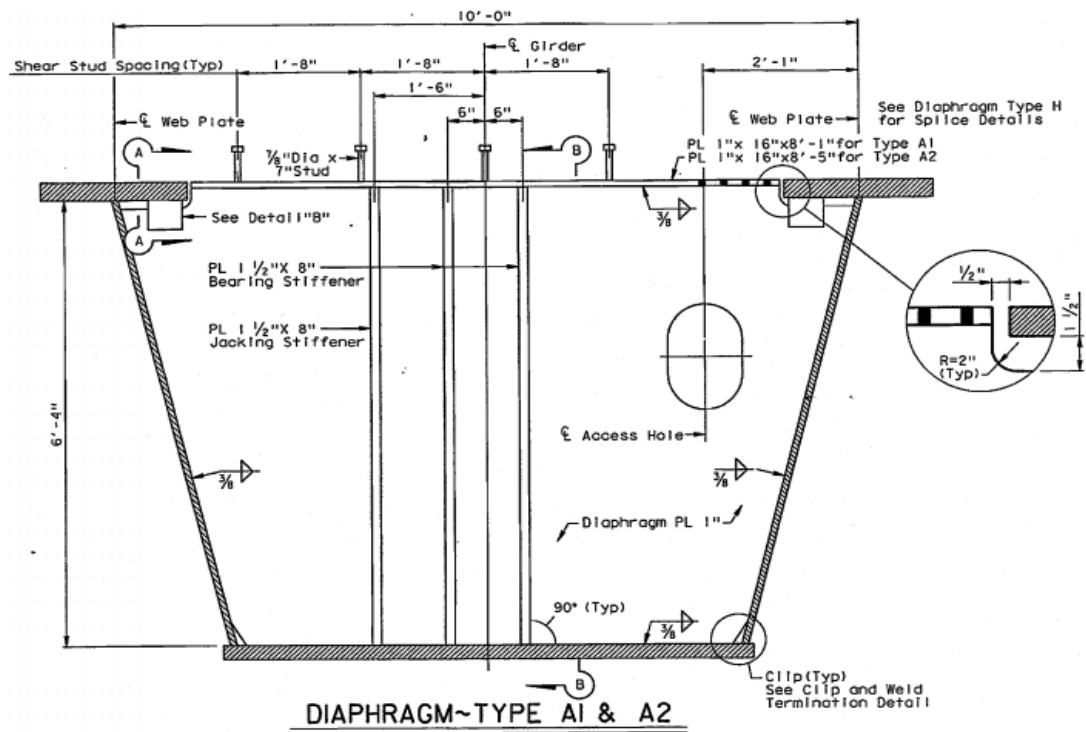
SPAN 8

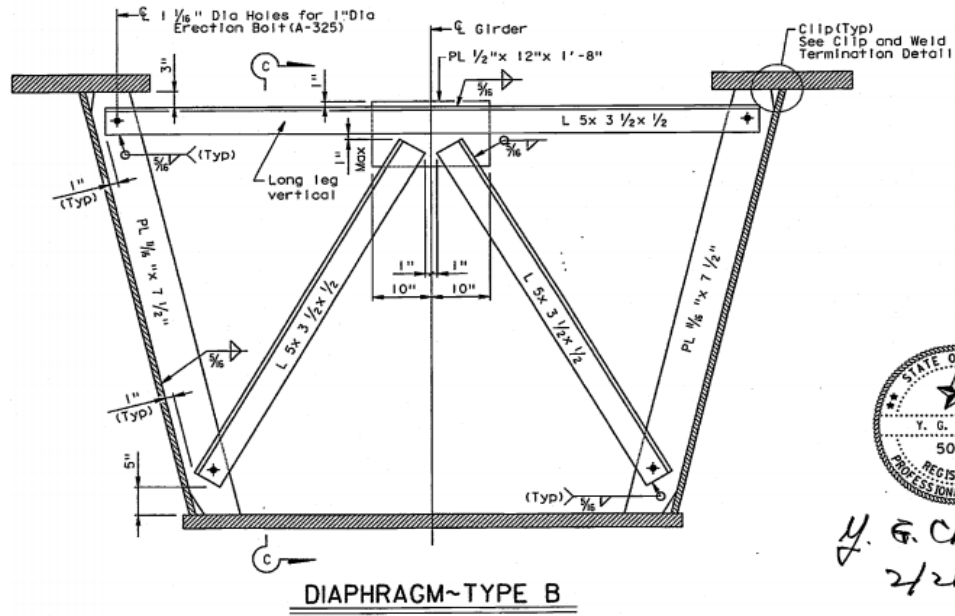
LATERAL BRACING INFORMATION		
SPAN	MEMBER SIZE	CONNECTION DETAIL #
5	WT 8 x 38.5	7, 8, or 9
6	WT 8 x 38.5	7, 8, or 9
7	WT 7 x 21.5	10, 11, or 12
8	WT 7 x 21.5	10, 11, or 12

J.G.
2/2

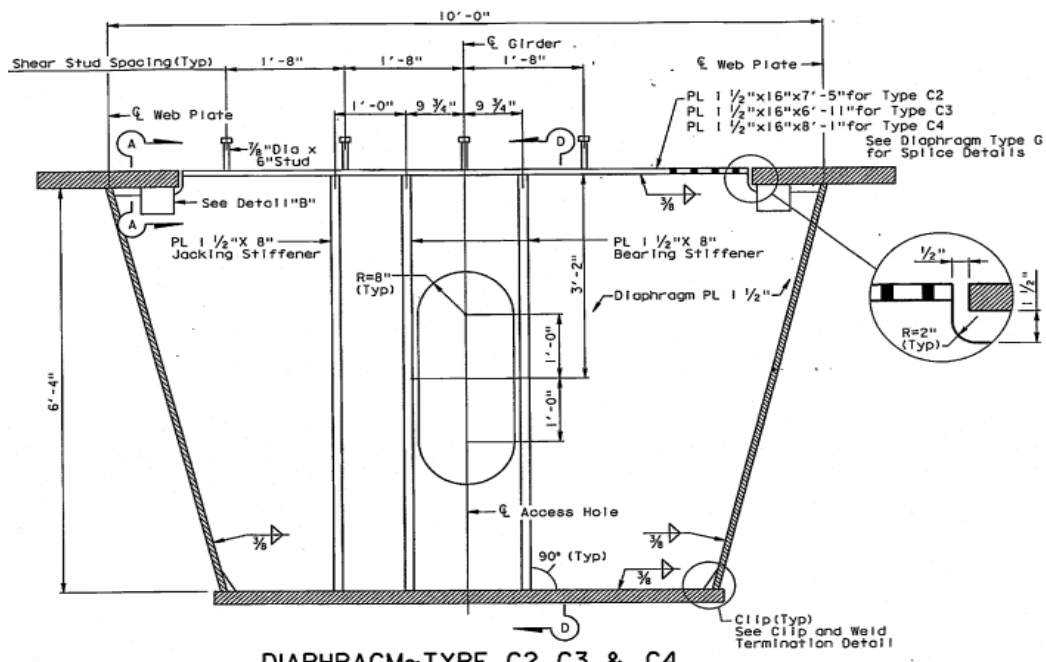




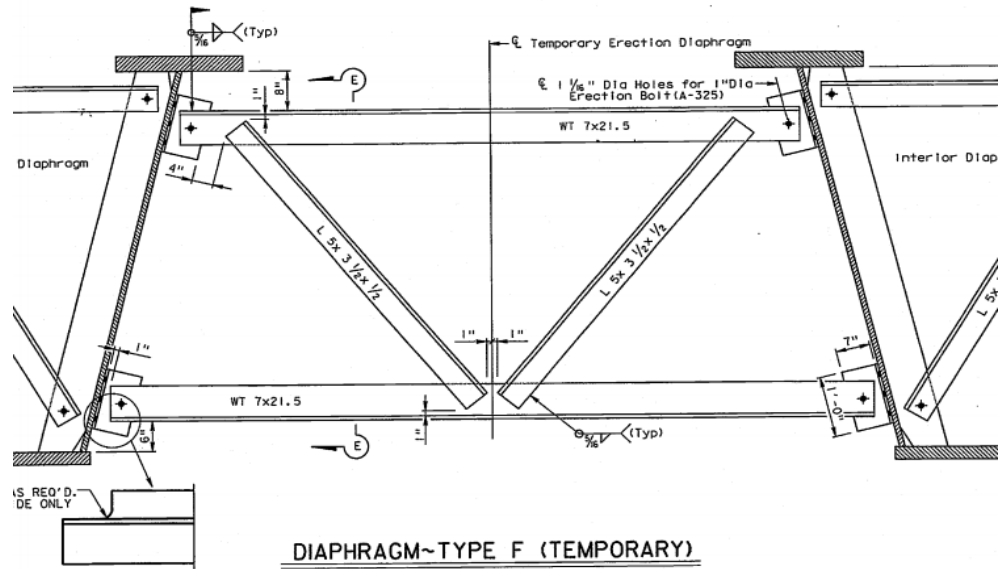


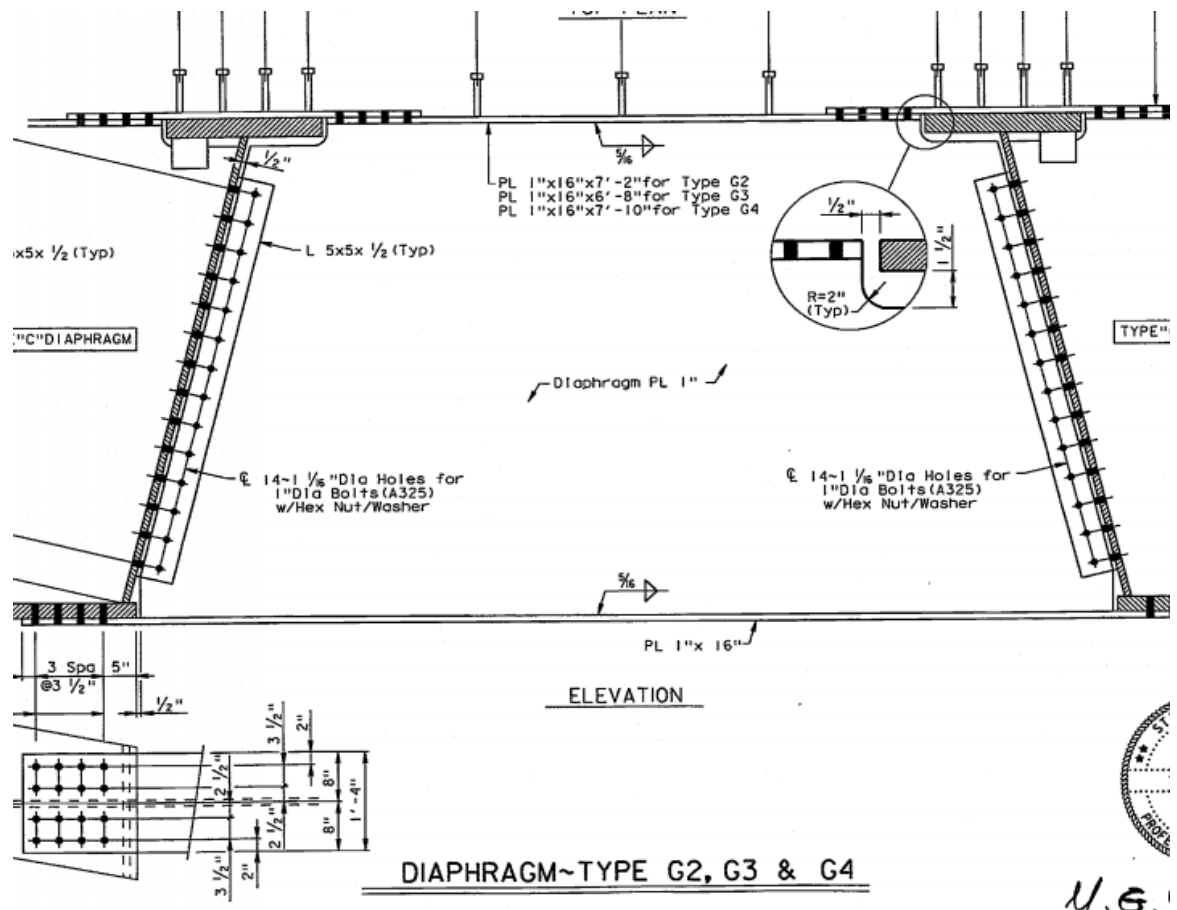


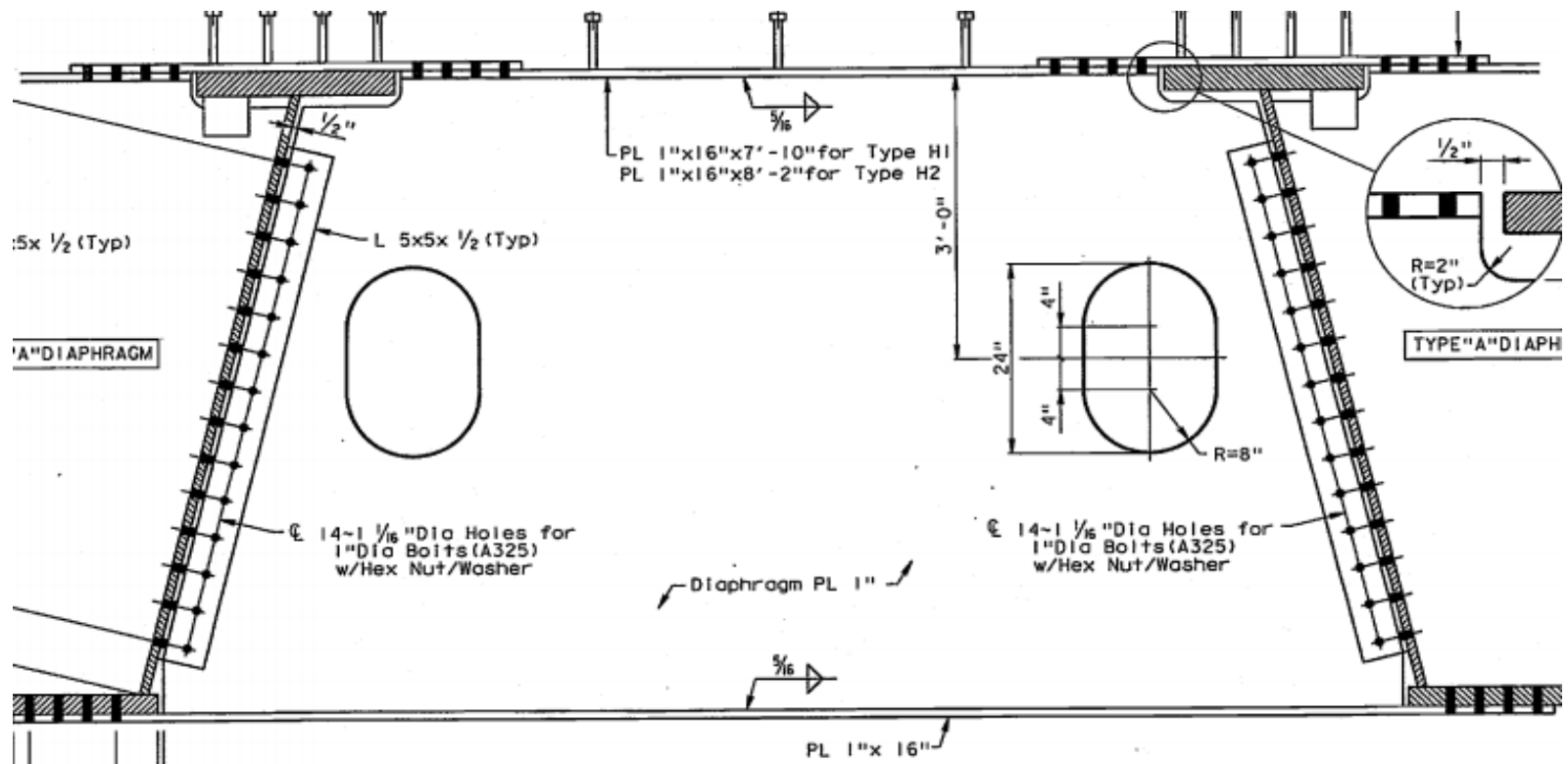
Y. G. C.
2/20



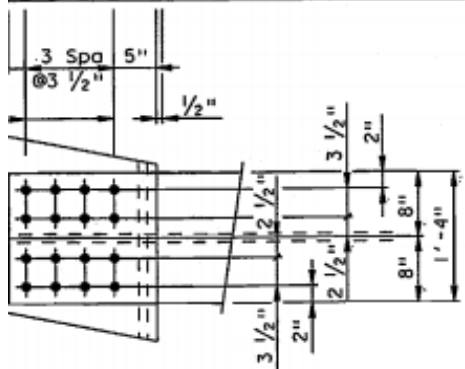
DIAPHRAGM~TYPE C2, C3 & C4







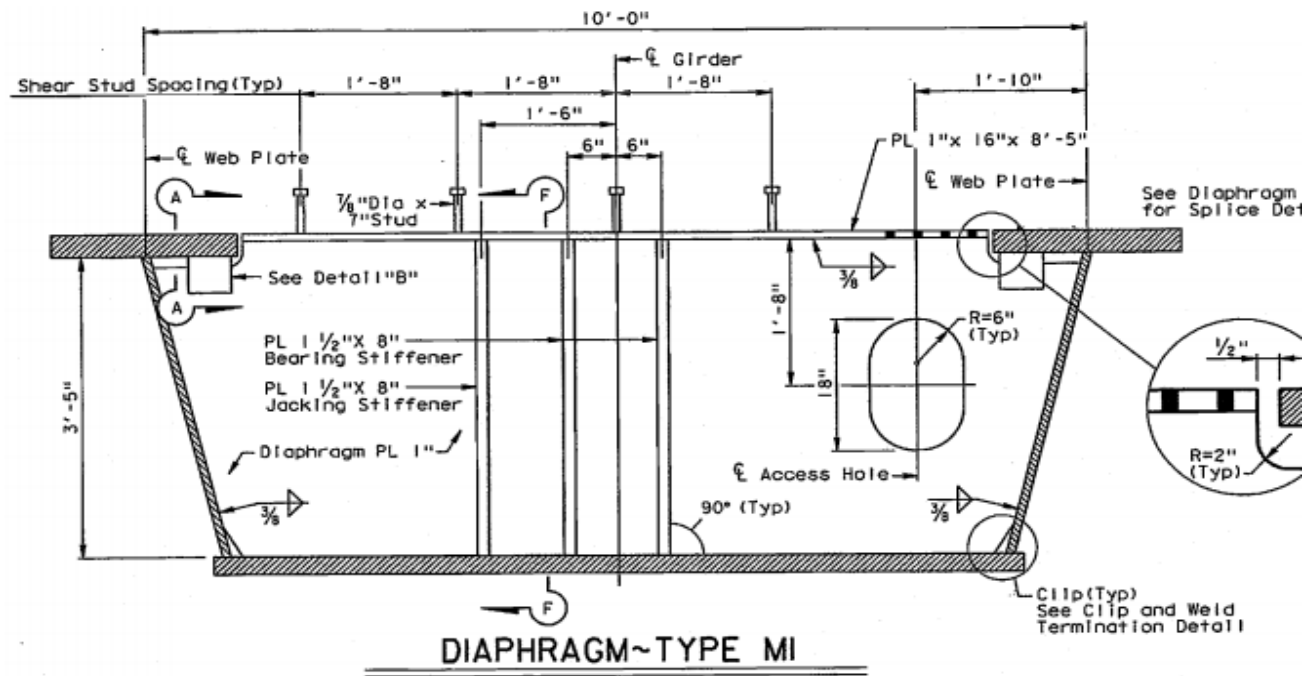
ELEVATION

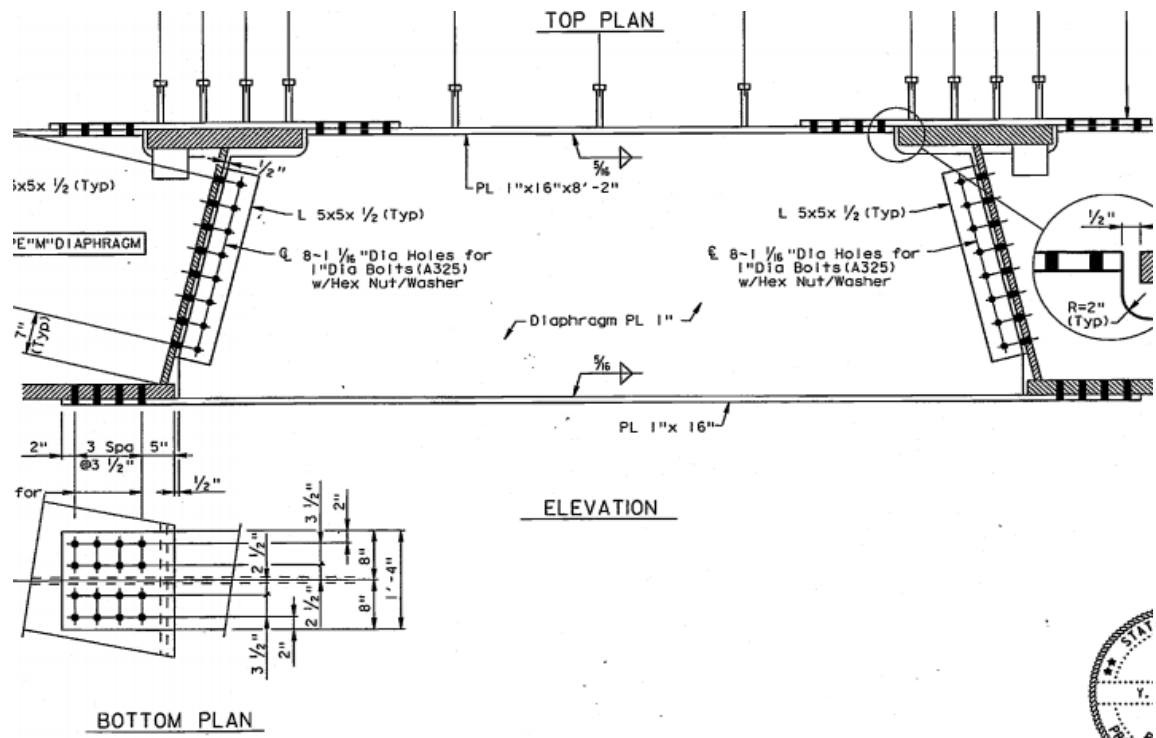


DIAPHRAGM~TYPE HI & H2

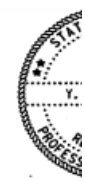


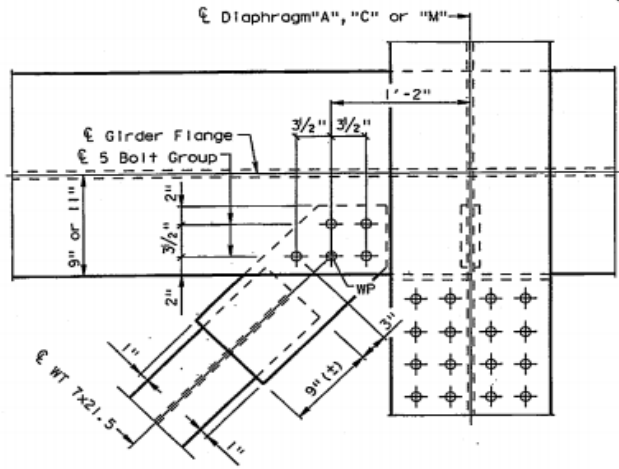
11204





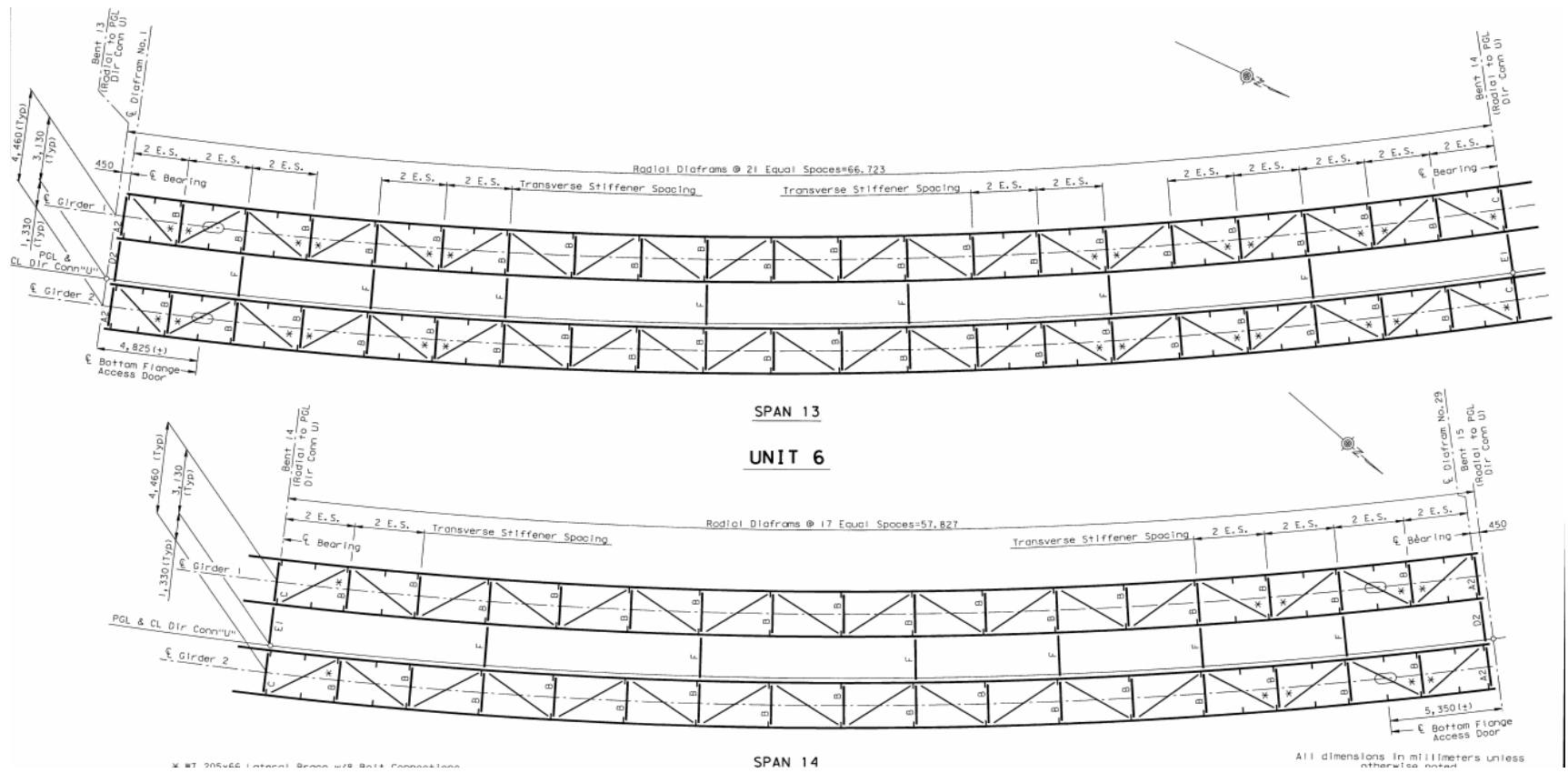
DIAPHRAGM~TYPE NI

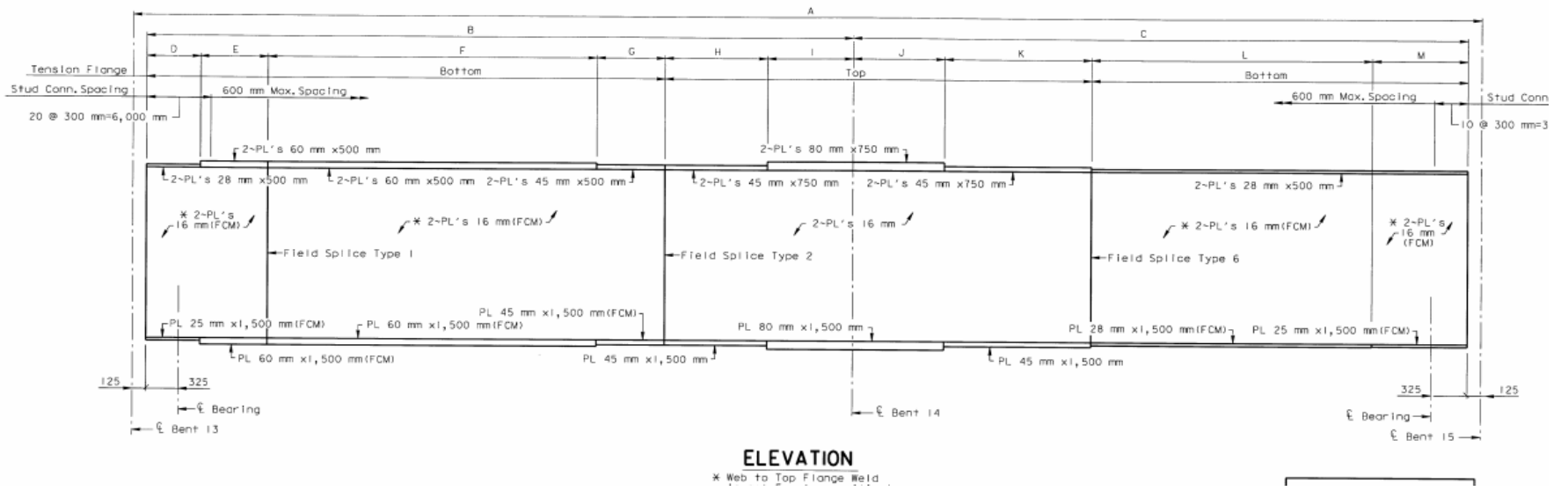


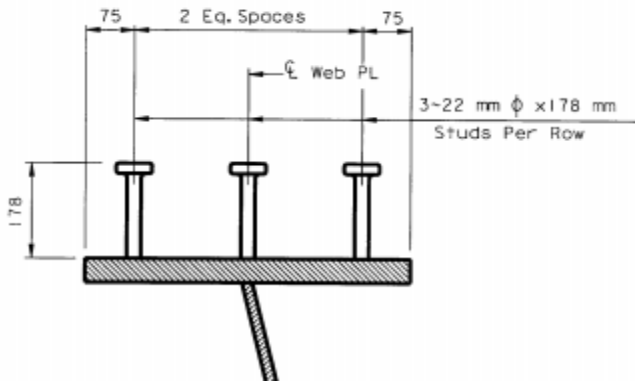
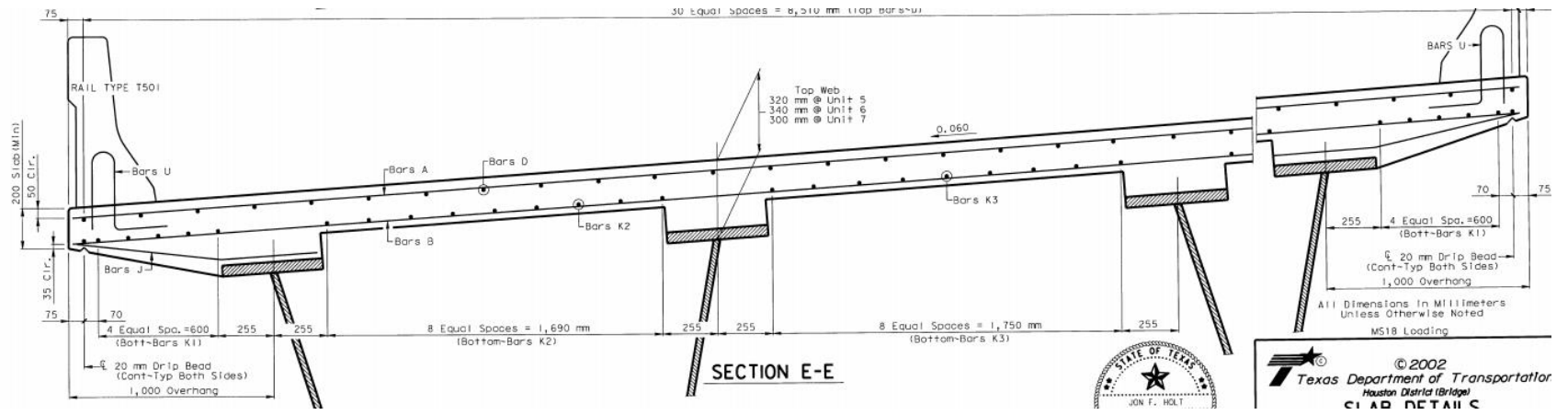


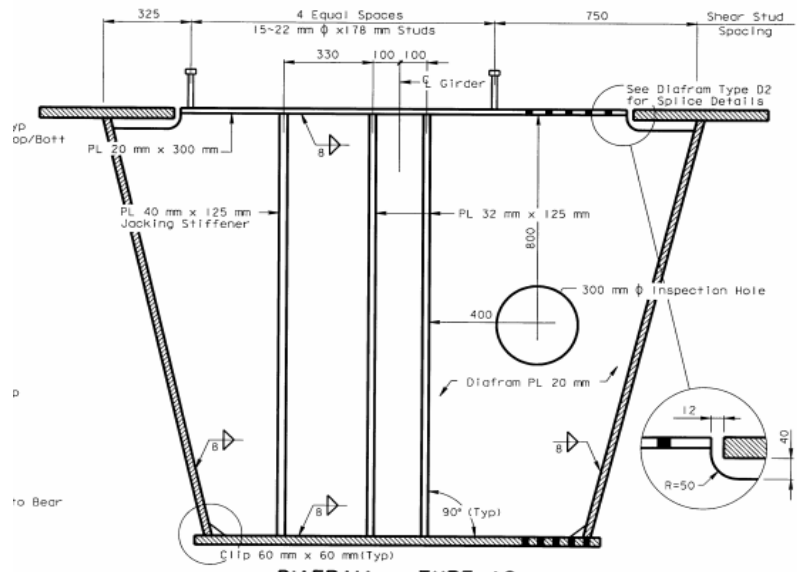
LATERAL BRACING CONNECTION DETAIL "12"

BRIDGE 7: 12-102-0177-07-394

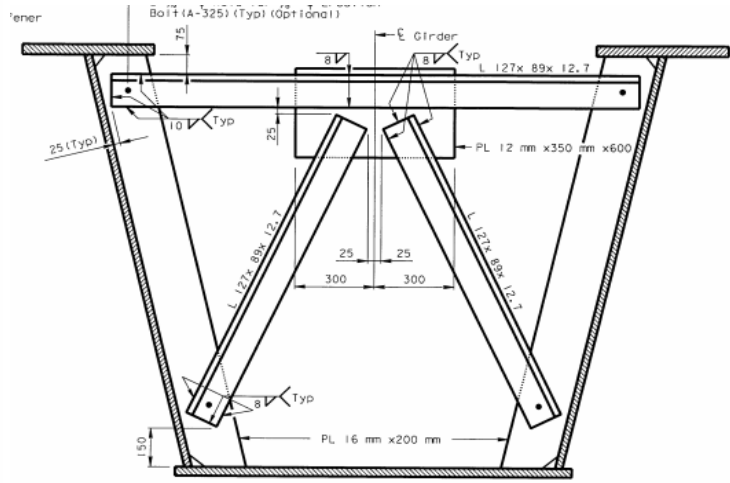






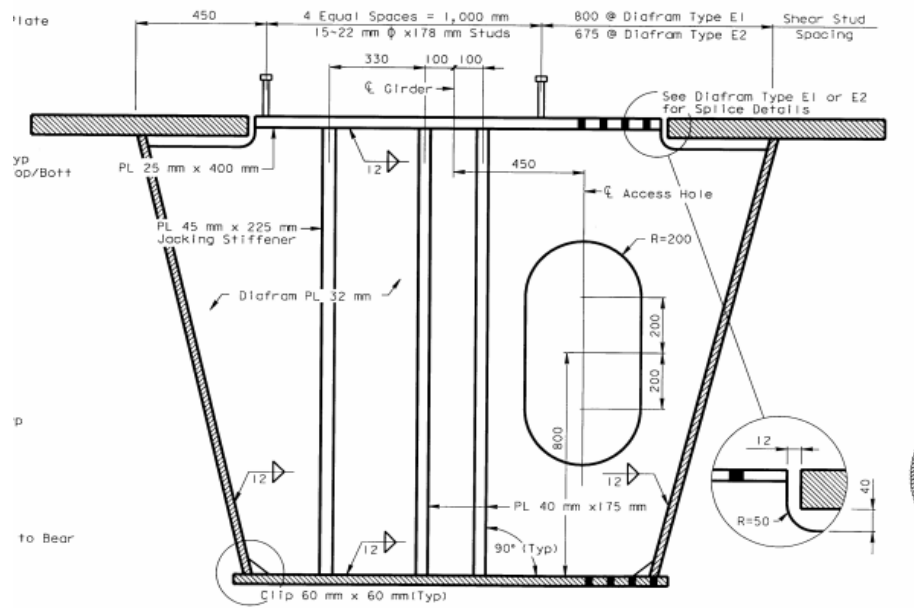


DIAFRAM ~ TYPE A2

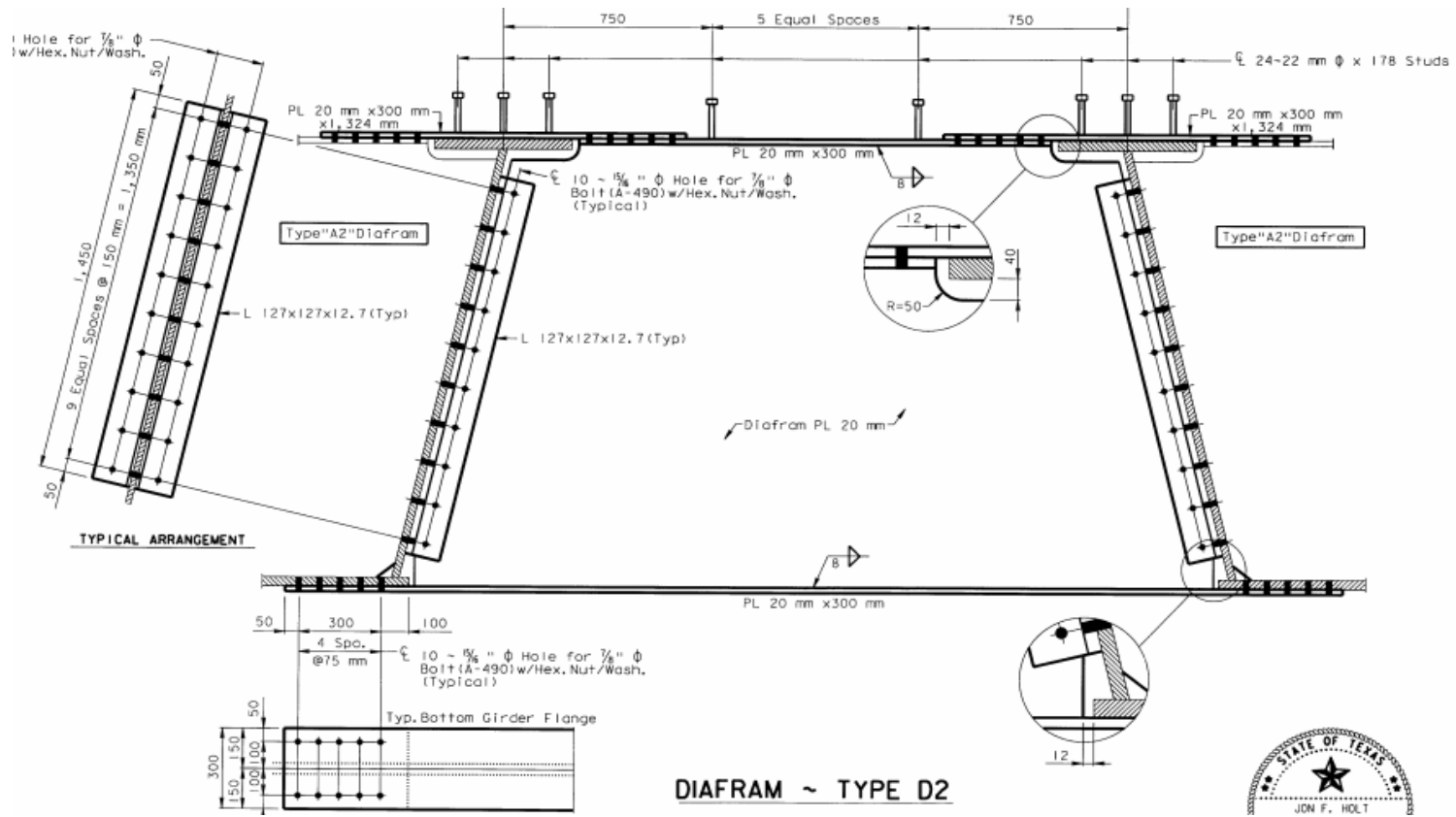


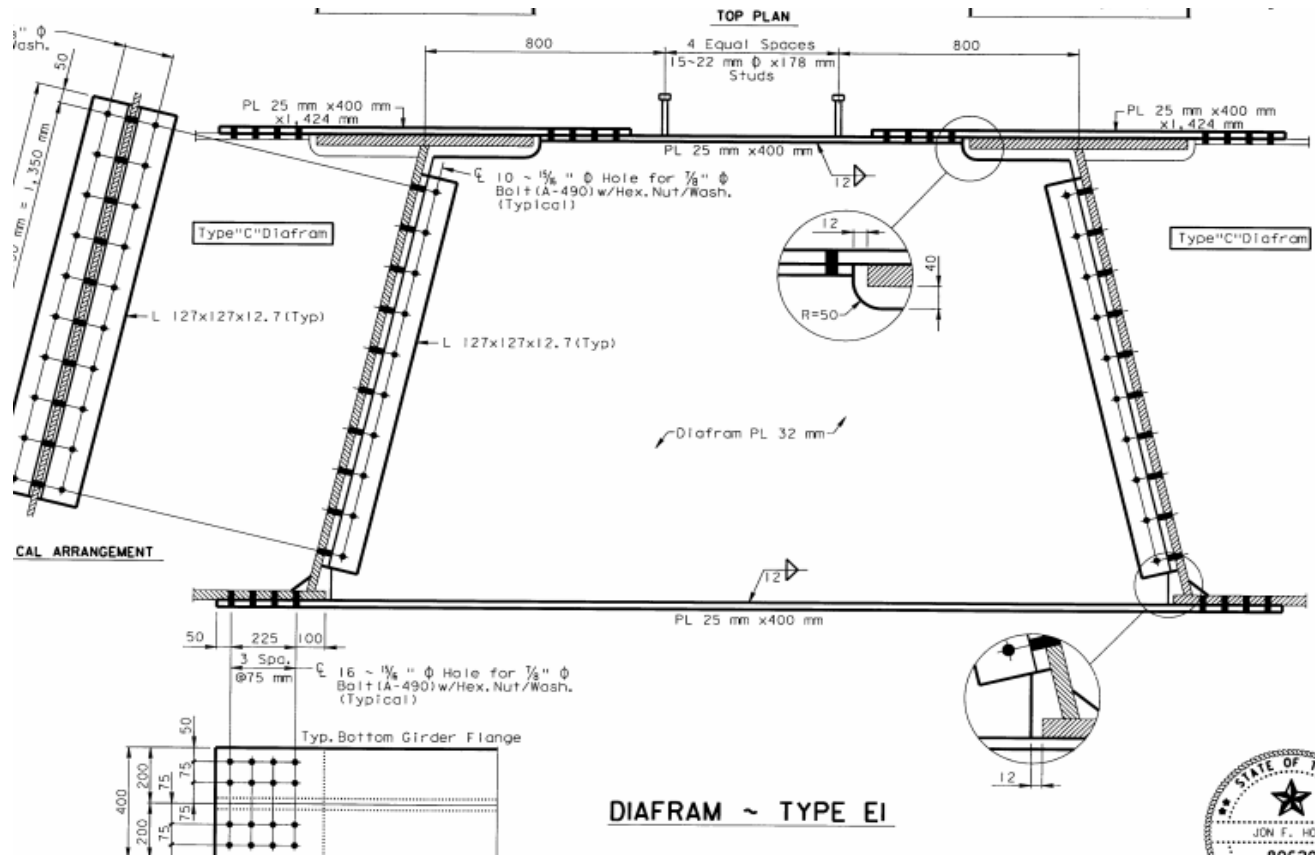
DIAFRAM ~ TYPE B

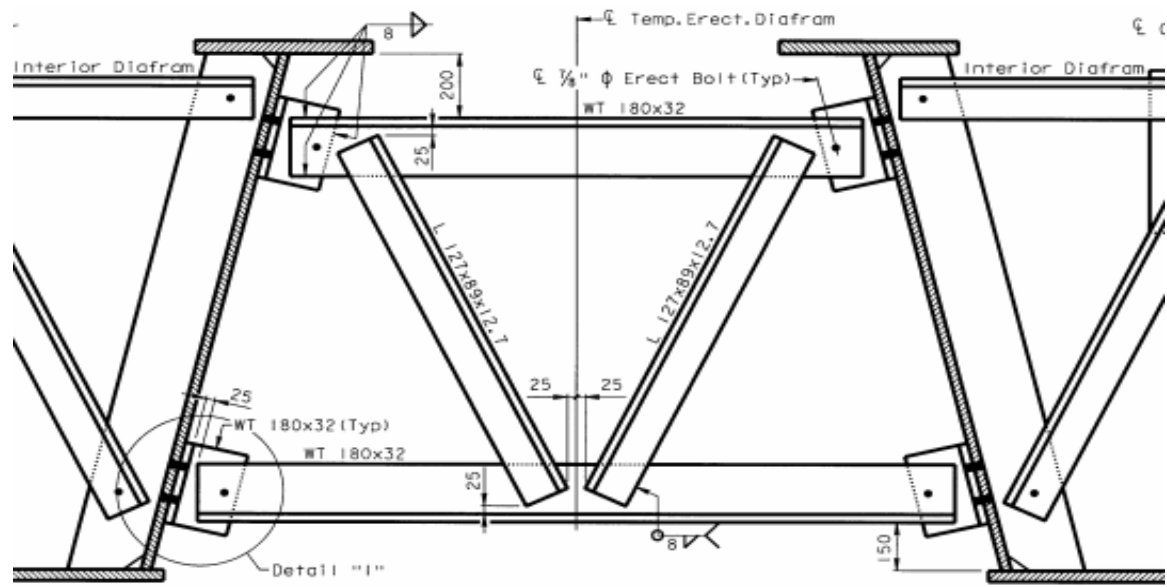
Note: All Angles Placed with Long Leg Vertical (Typ)



DIAFRAM ~ TYPE C

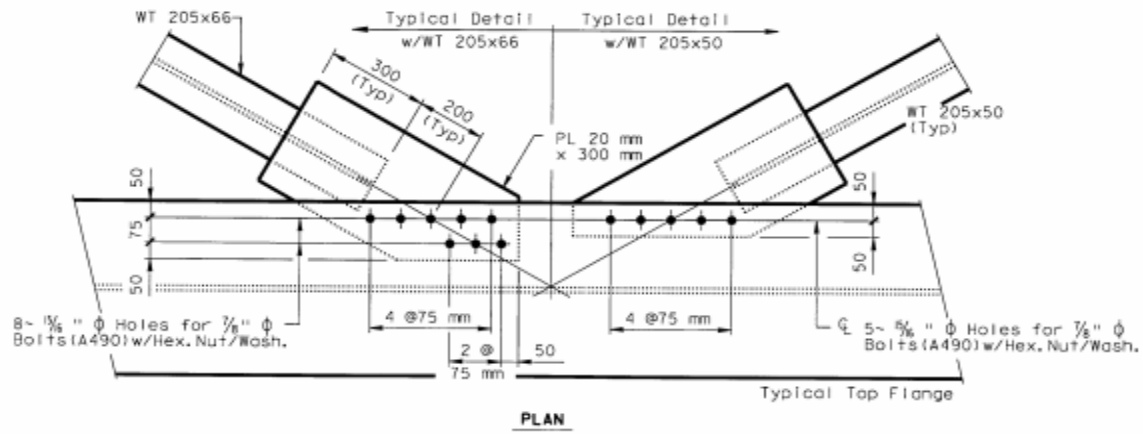




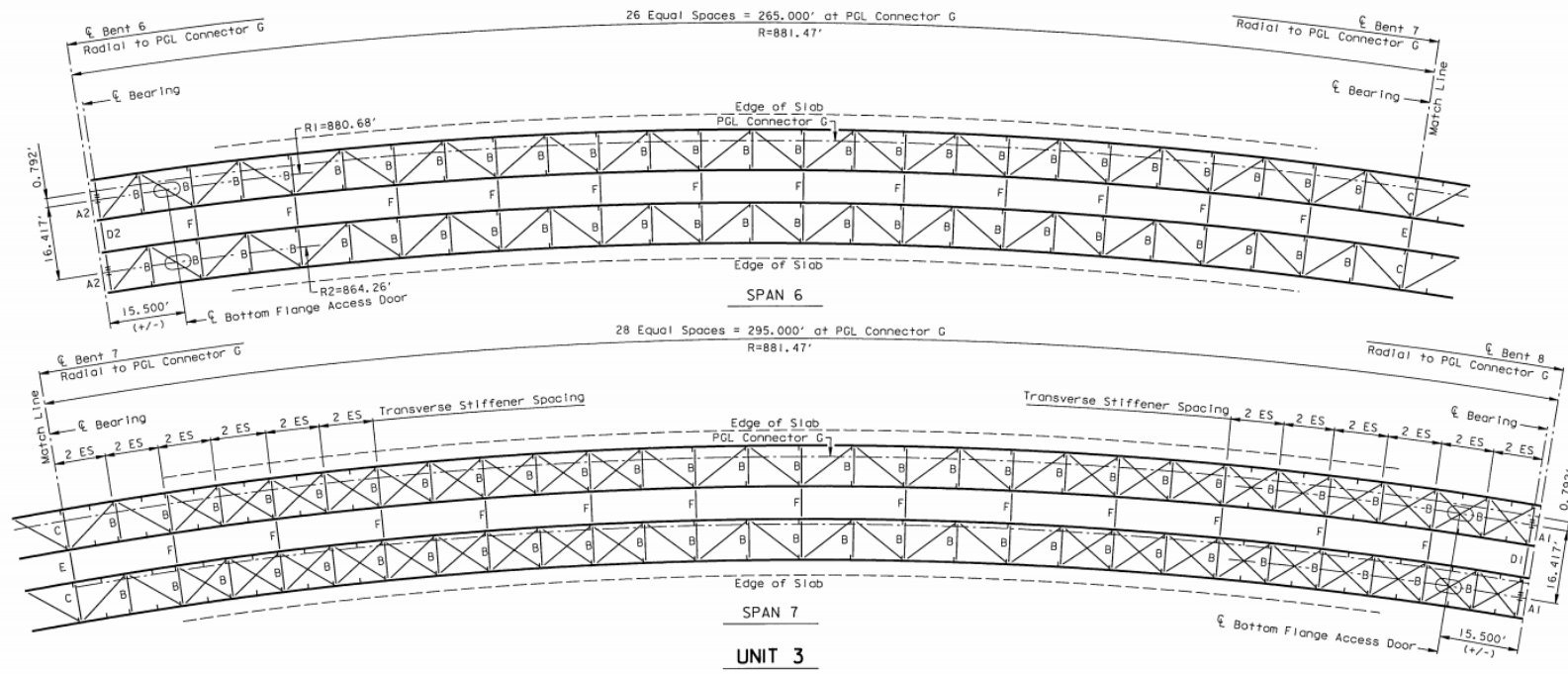


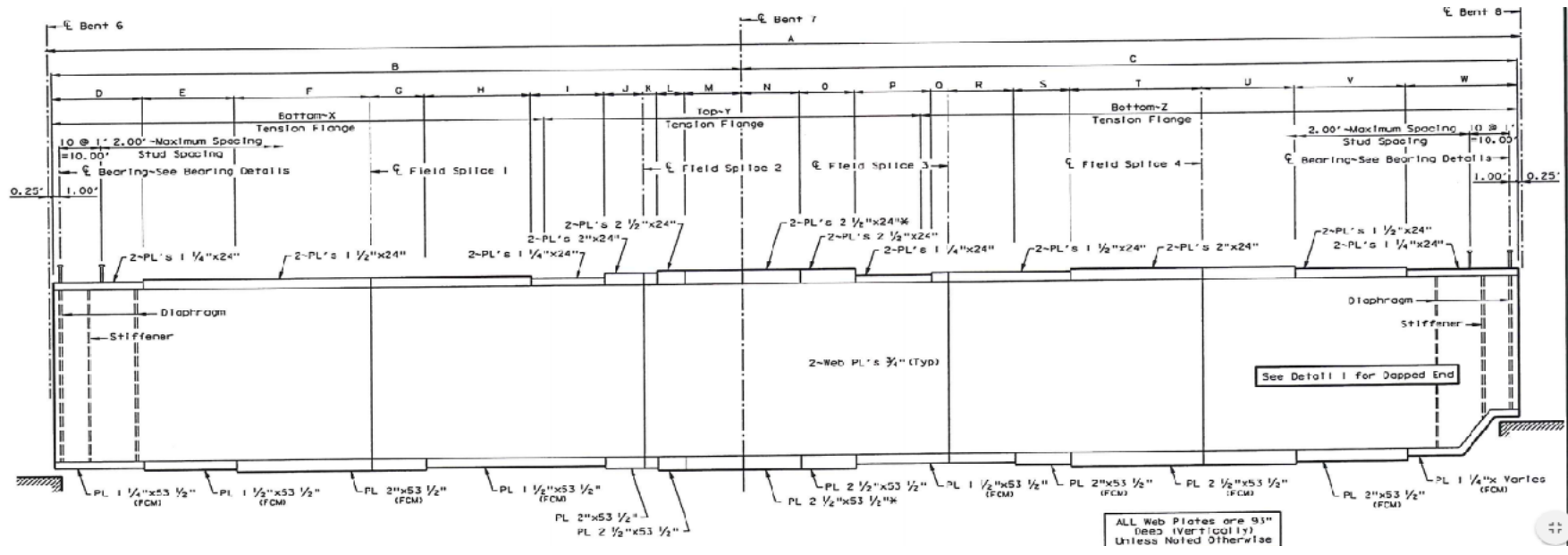
DIAFRAM ~ TYPE F (TEMPORARY)

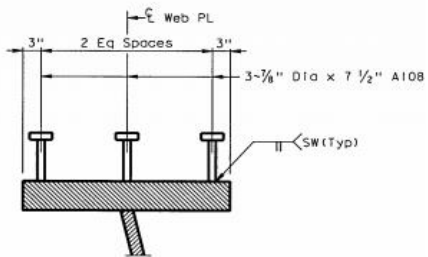
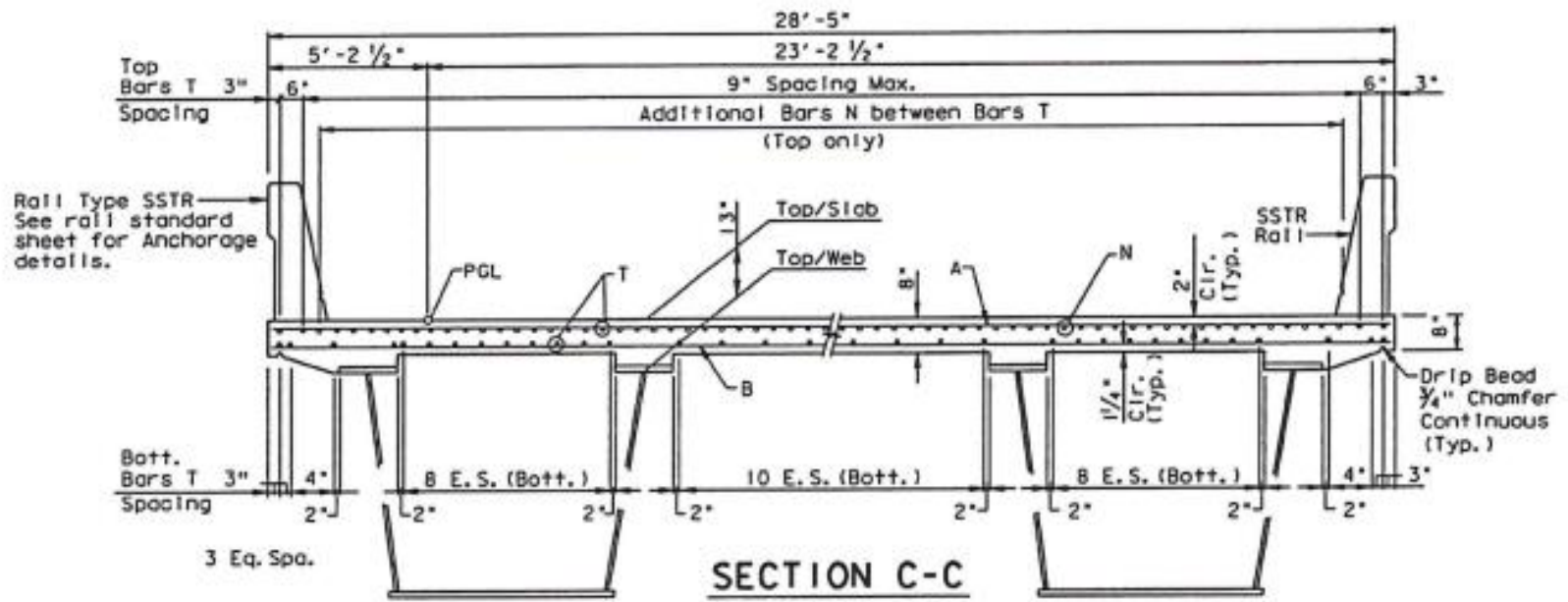
GENERAL NOTES:



BRIDGE 8: 12-102-0271-06-661

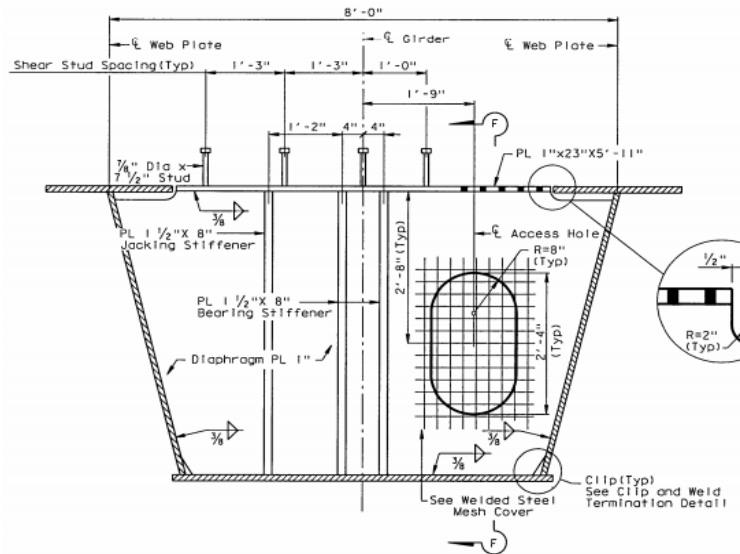






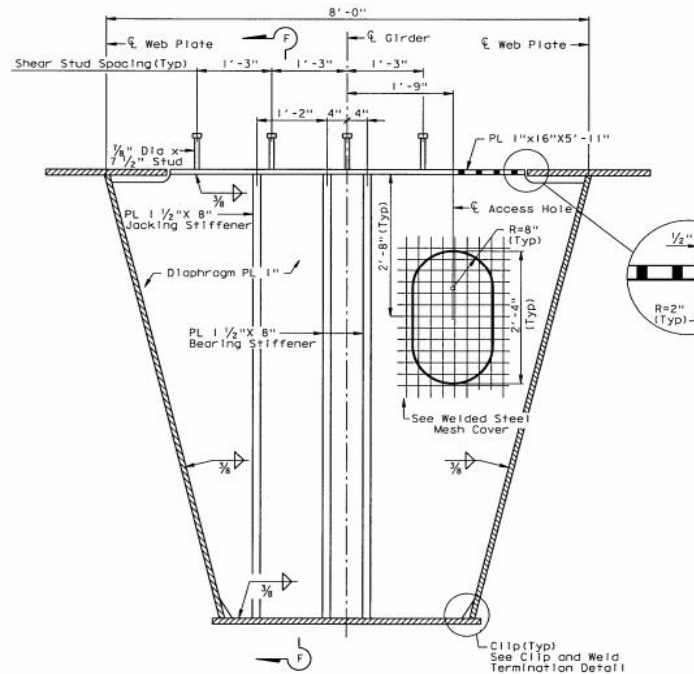
SHEAR CONNECTOR DETAIL

NOTE:



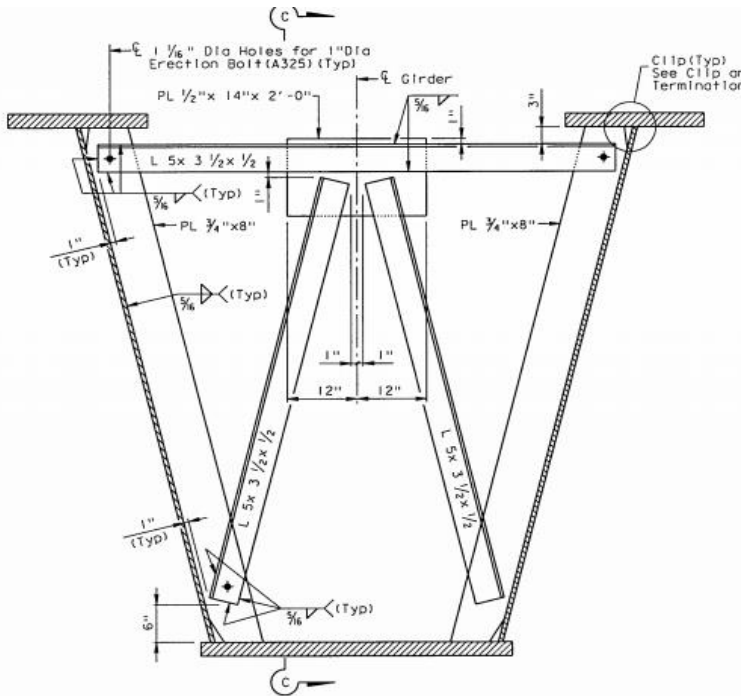
DIAPHRAGM~TYPE A1

Girder 1 Shown, Girder 2 Similar w/Opposite Hand Access Hole



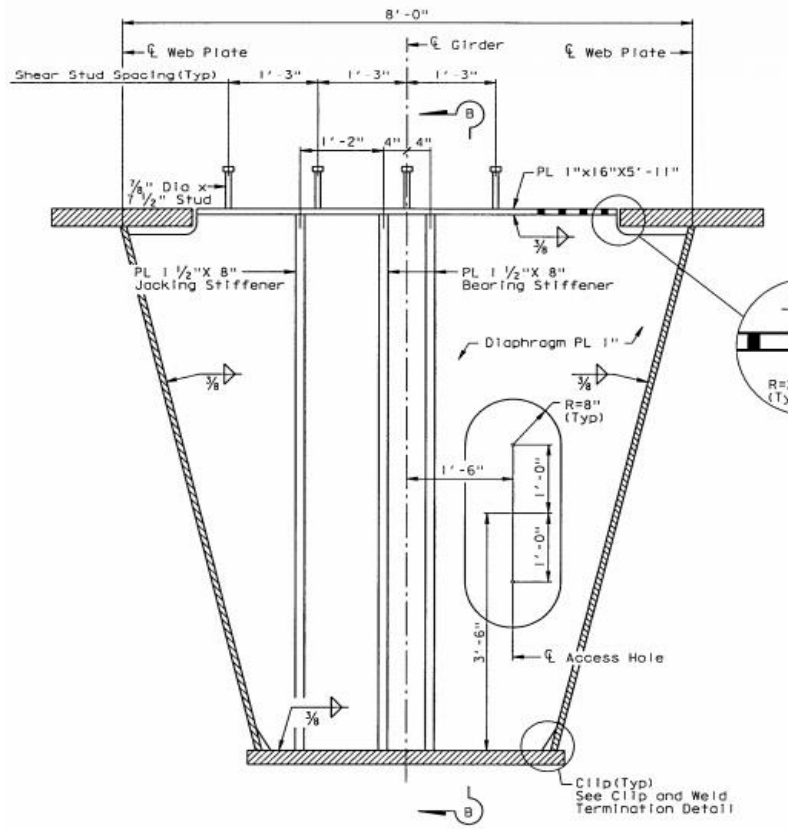
DIAPHRAGM~TYPE A2

Girder 1 Shown, Girder 2 Similar w/Opposite Hand Access Hole



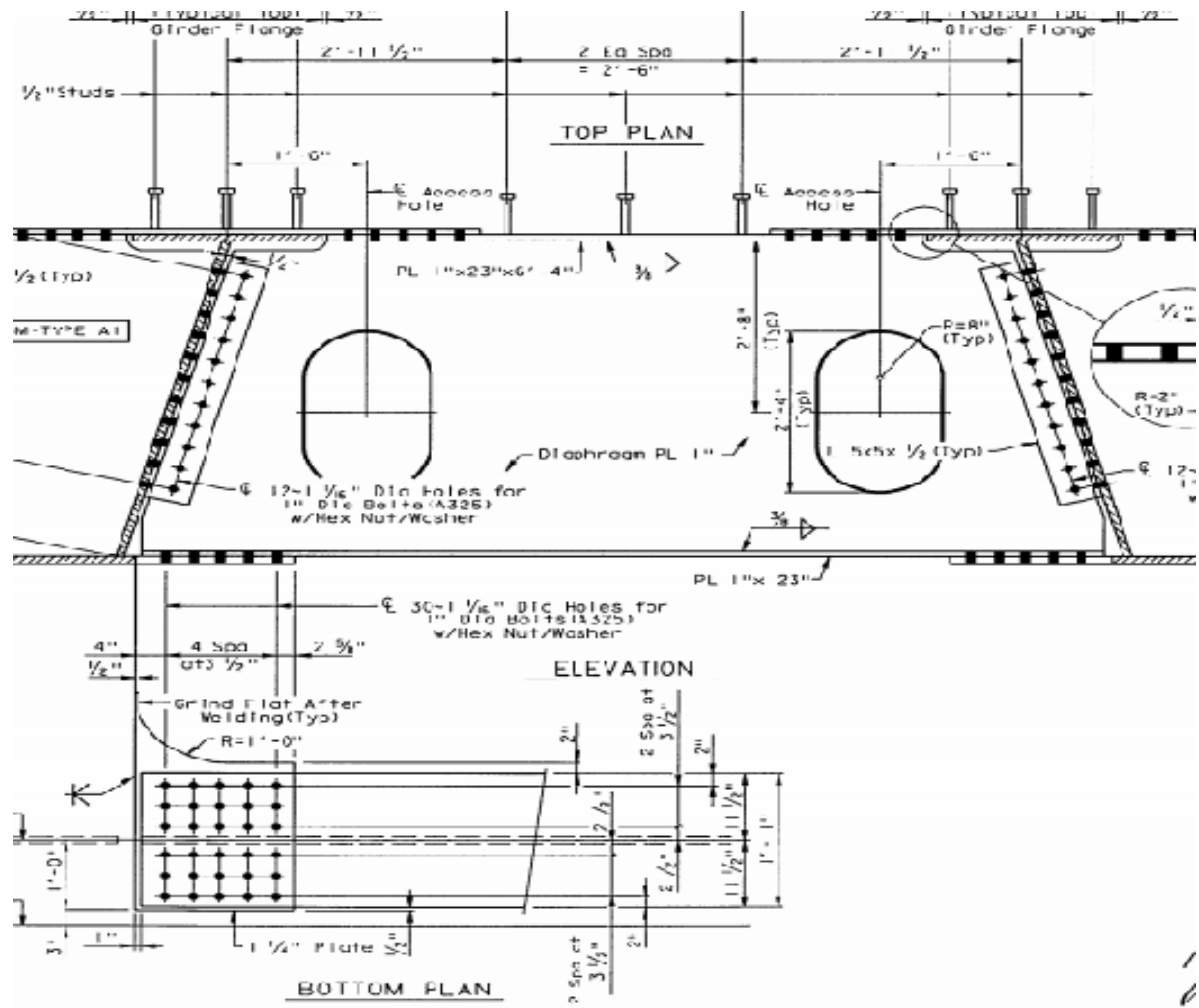
DIAPHRAGM~TYPE B

Note: All Angles Placed with Long Leg Vertical

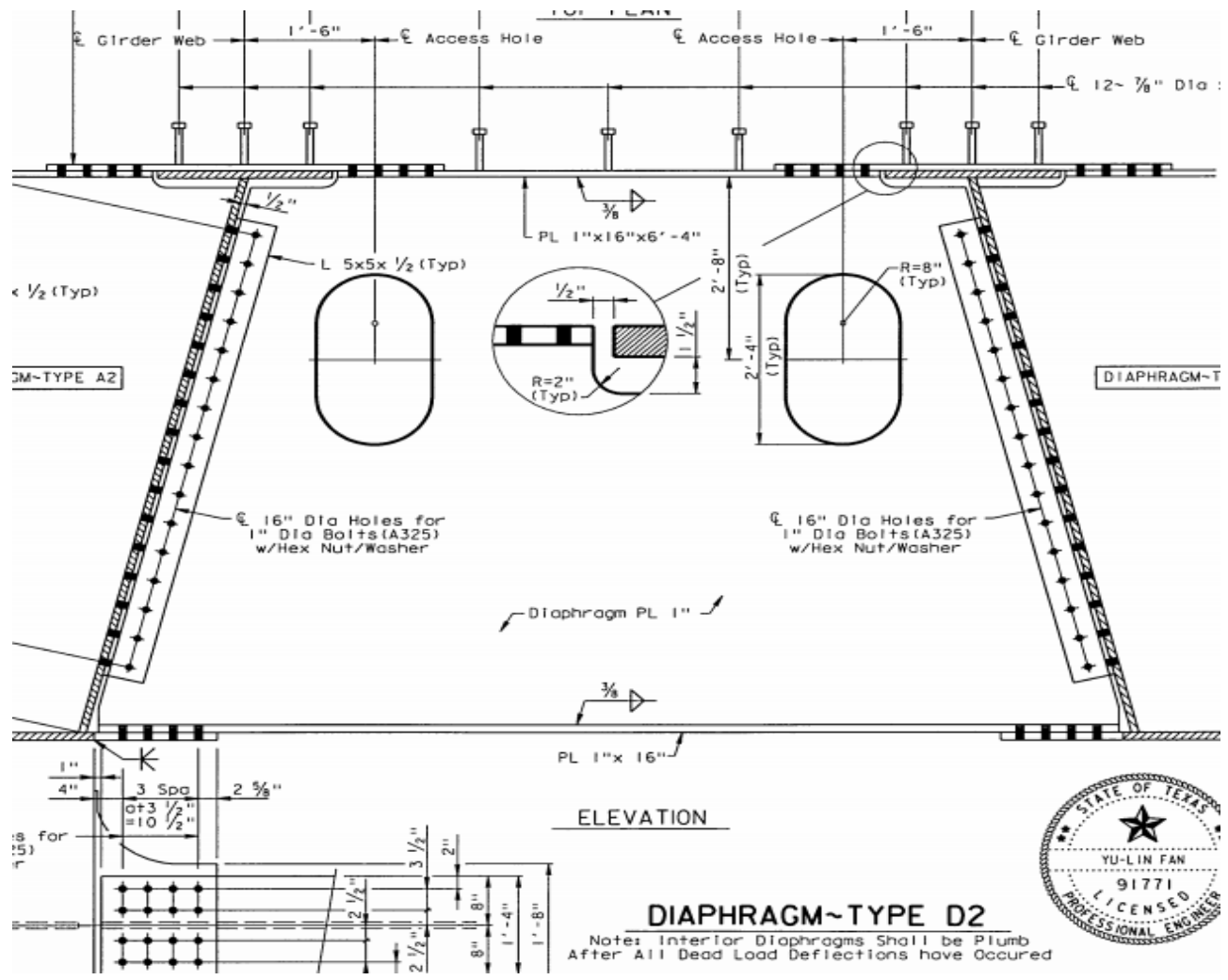


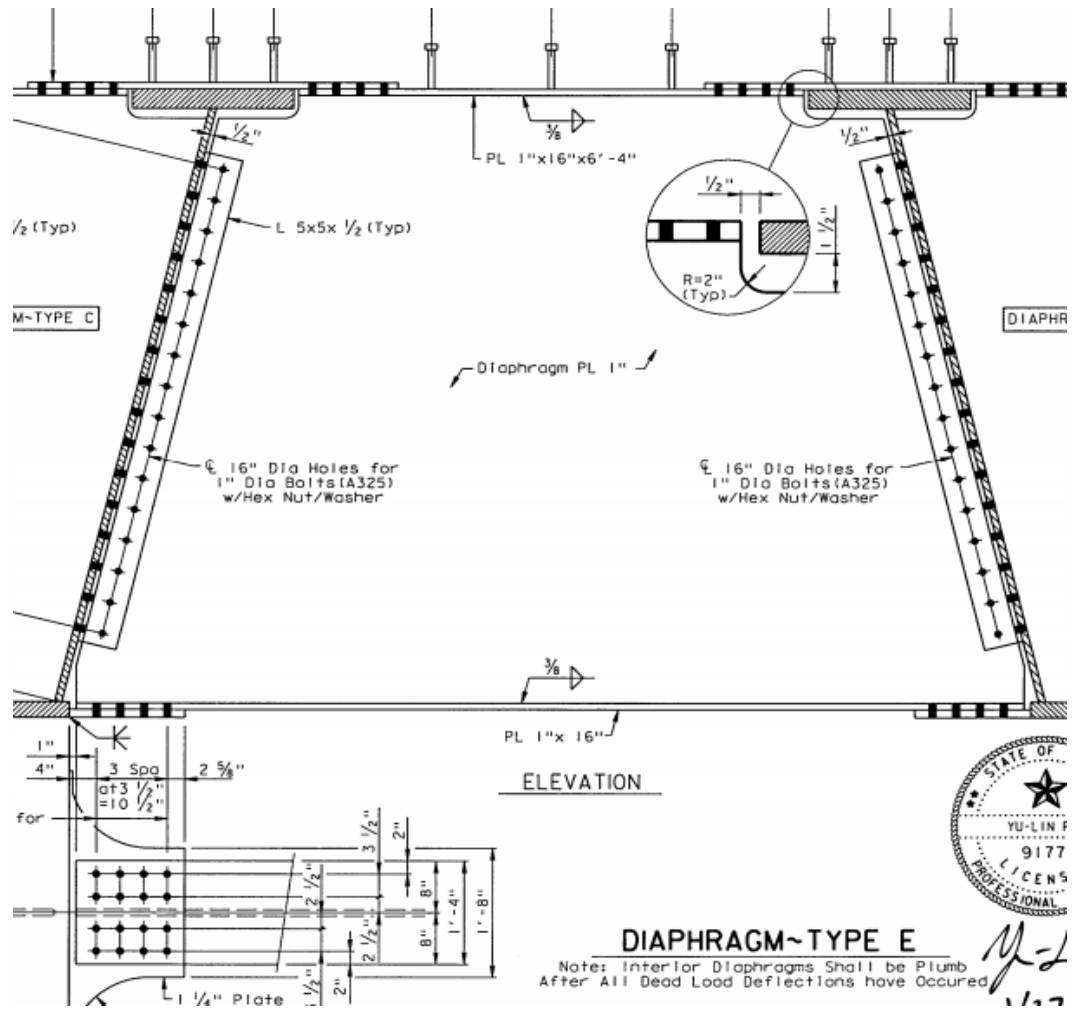
DIAPHRAGM~TYPE C

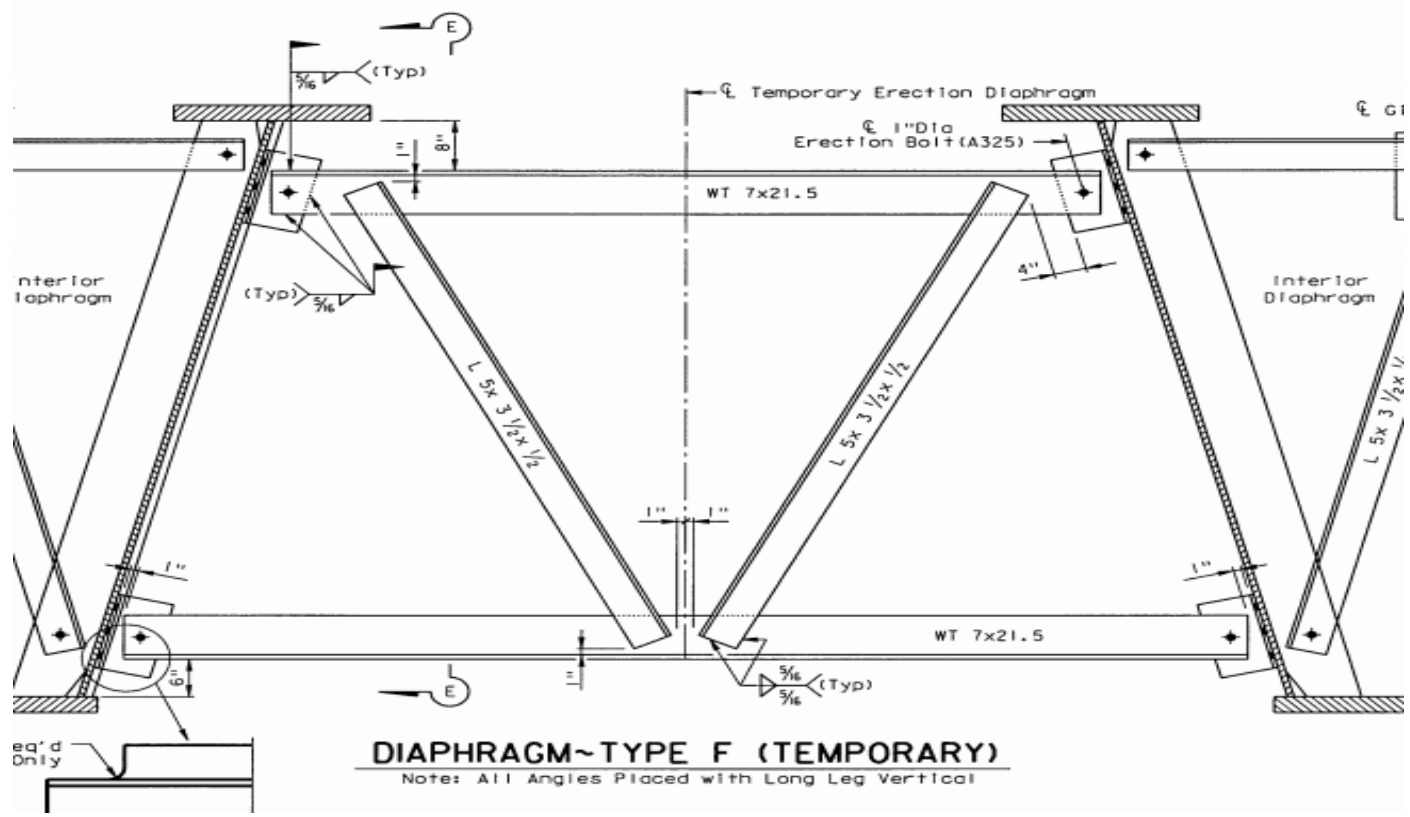
Girder 1 Shown, Girder 2 Similar w/Opposite Hand Access Hole

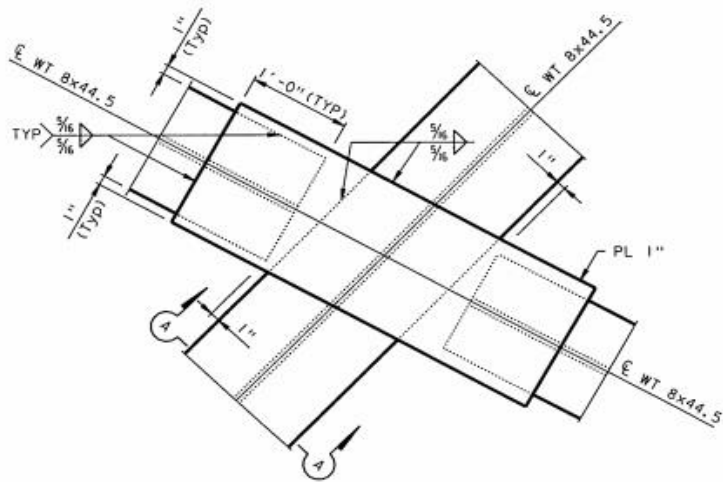


DIAPHRAGM~TYPE DI



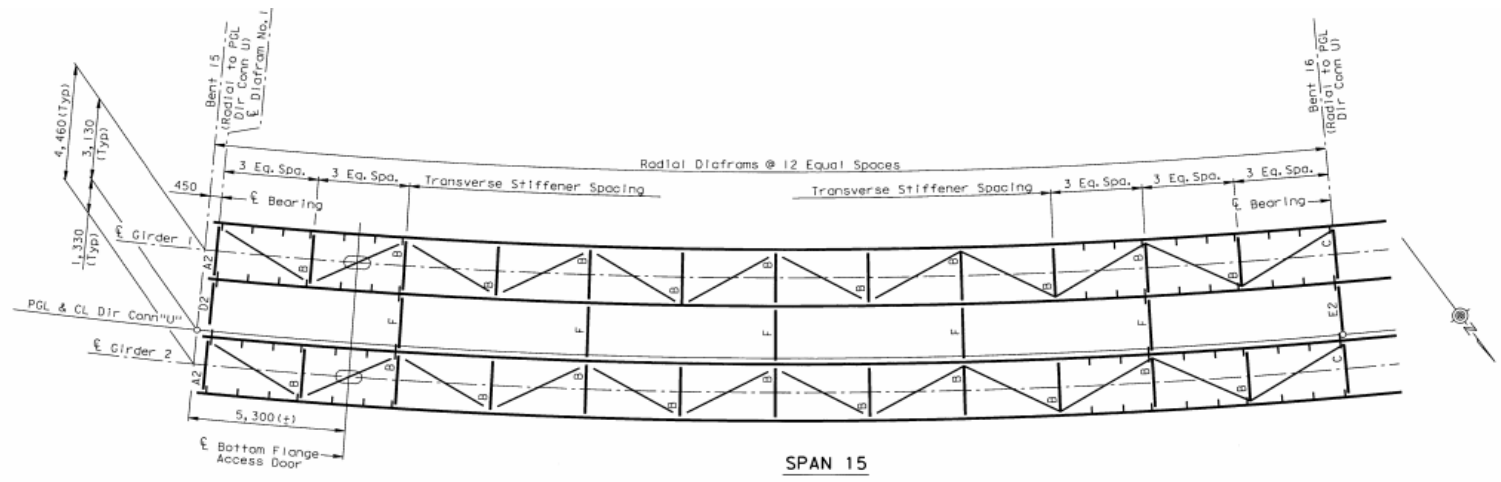




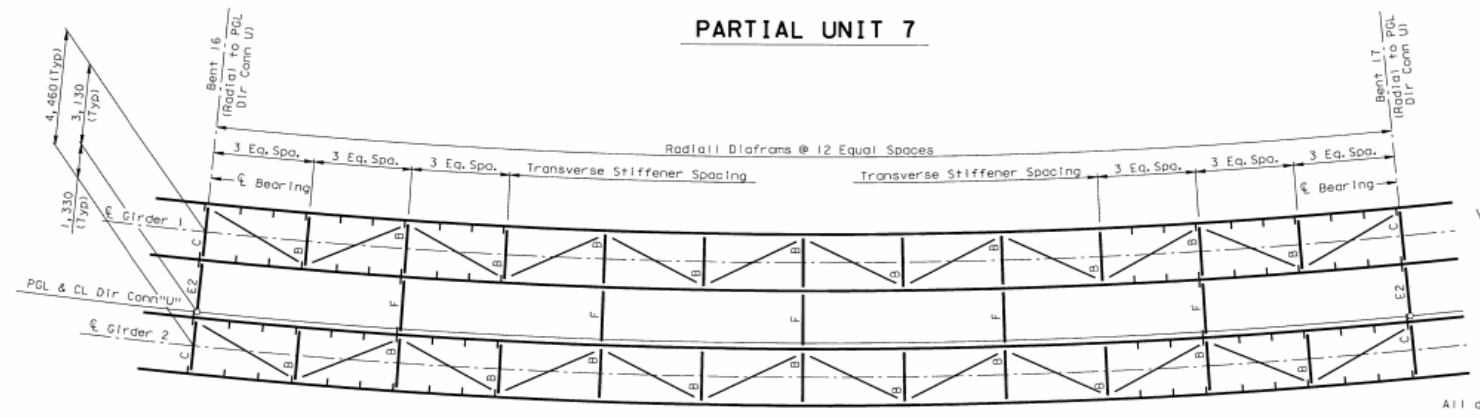


LATERAL BRACING DETAIL "3"
 (FOR X-BRACING)

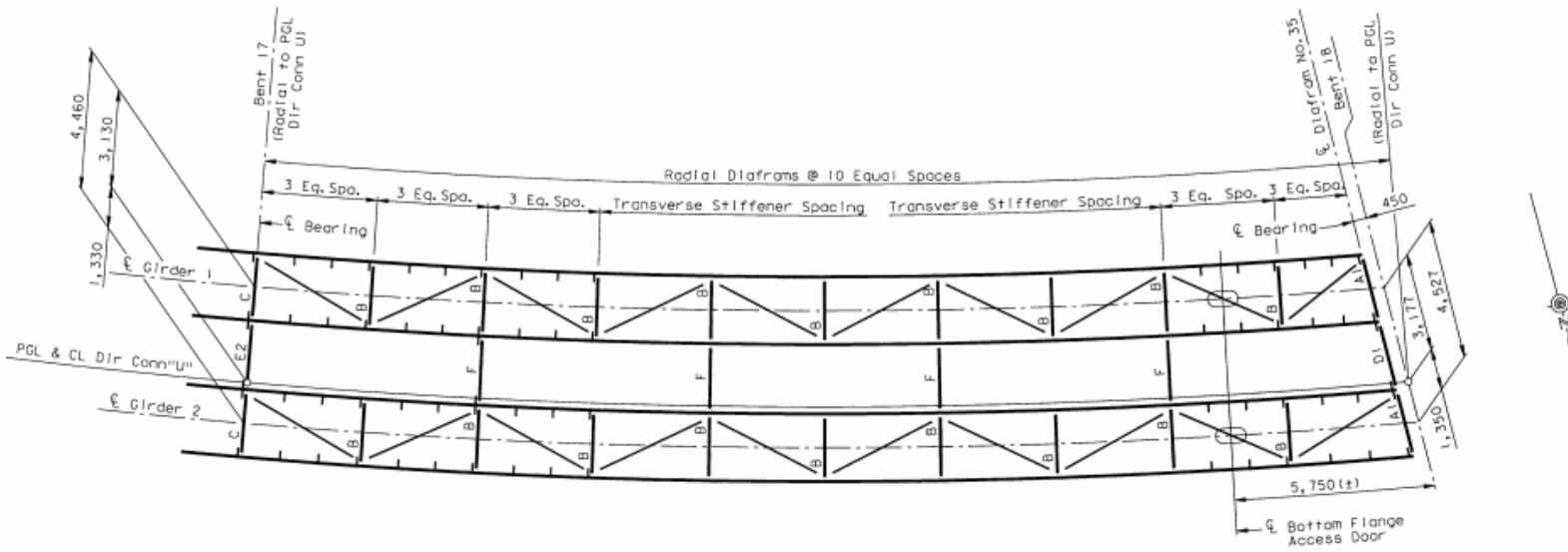
BRIDGE 9: 12-102-0177-07-394



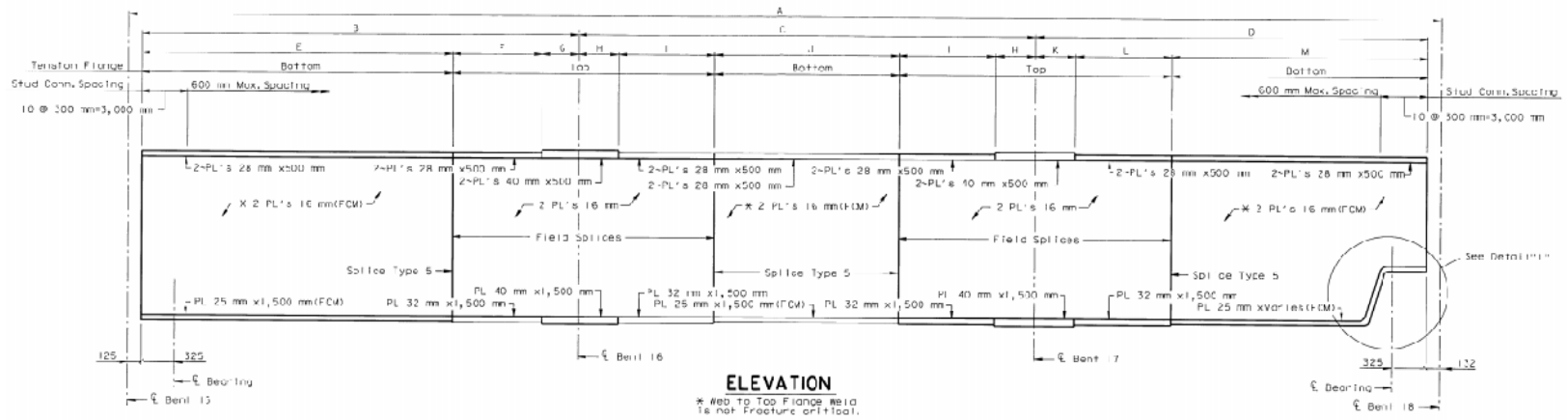
PARTIAL UNIT 7



All dimensions in feet unless otherwise noted
MS18

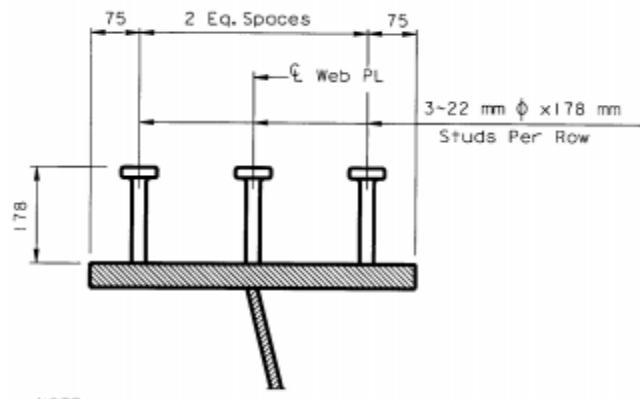
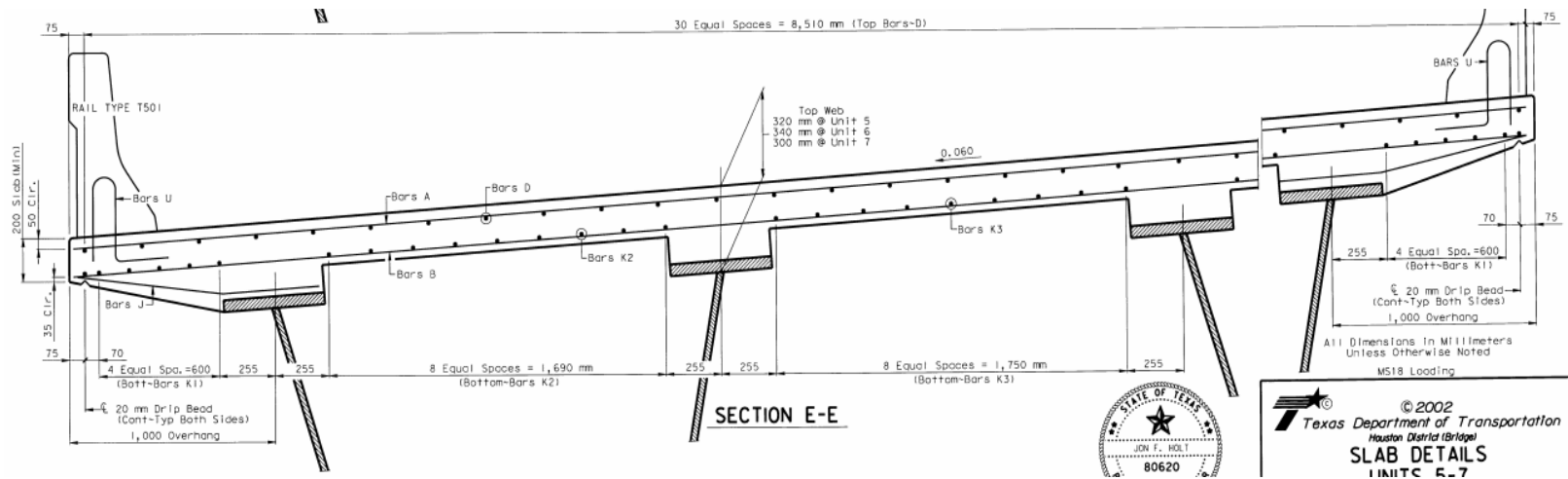


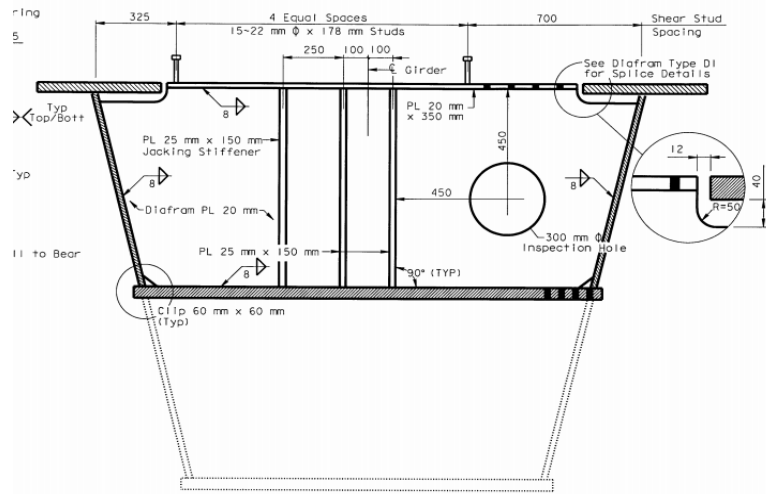
SPAN 17



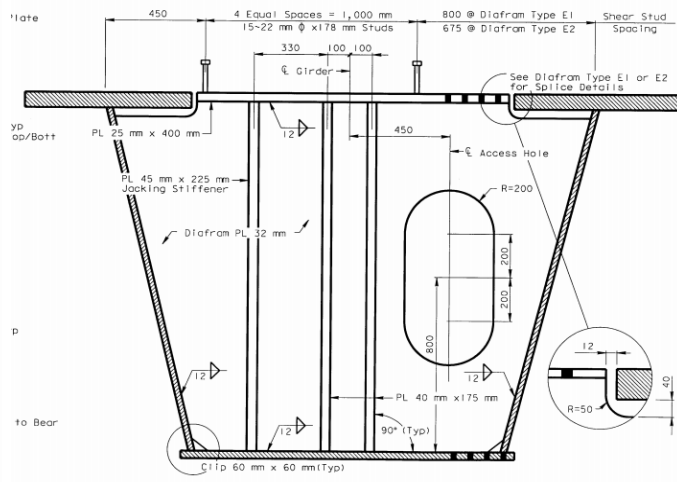
A1 Web Fillets are 1,500 mm Deep (Vertically)

TABLE OF VARIABLE GIRDER DIMENSIONS(METERS)													
GIRDER	A	B	C	D	E	F	G	H	I	J	K	L	M
1	124.752	41.633	45.549	37.113	29.819	7.517	4.097	4.496	8.516	9.725	4.375	8.481	24.253
2	127.955	42.648	46.454	38.616	30.431	8.153	4.164	4.469	8.663	20.170	4.452	8.628	25.536

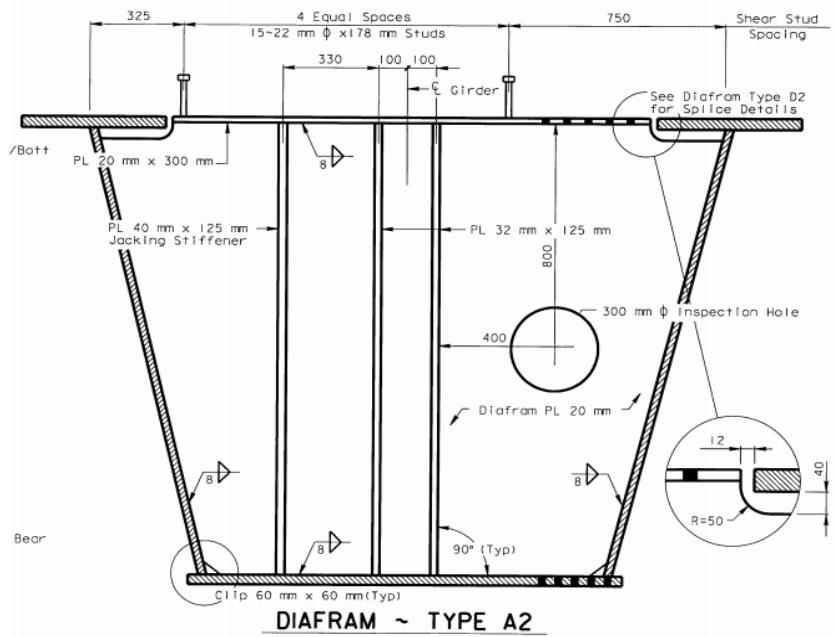




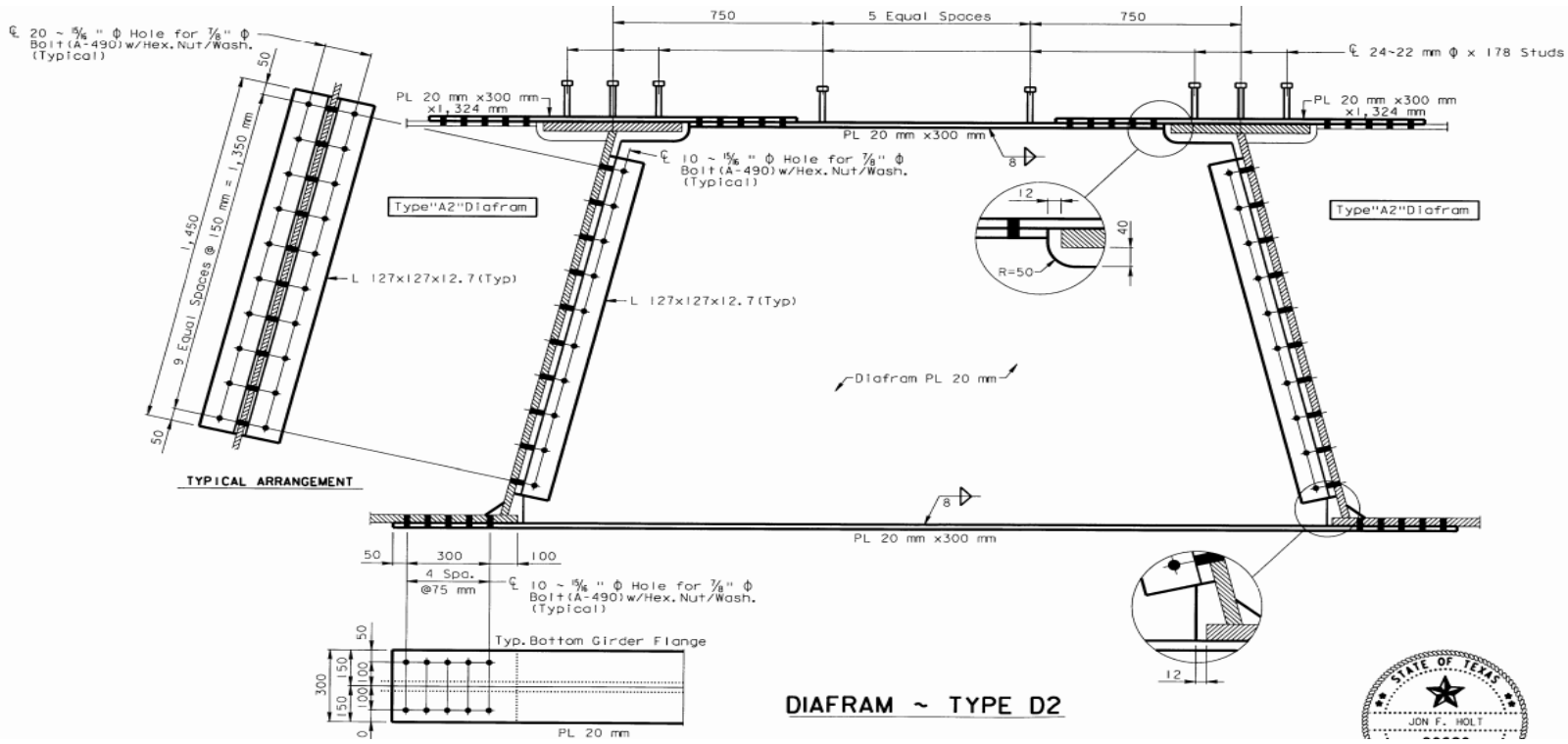
DIAFRAM ~ TYPE AI

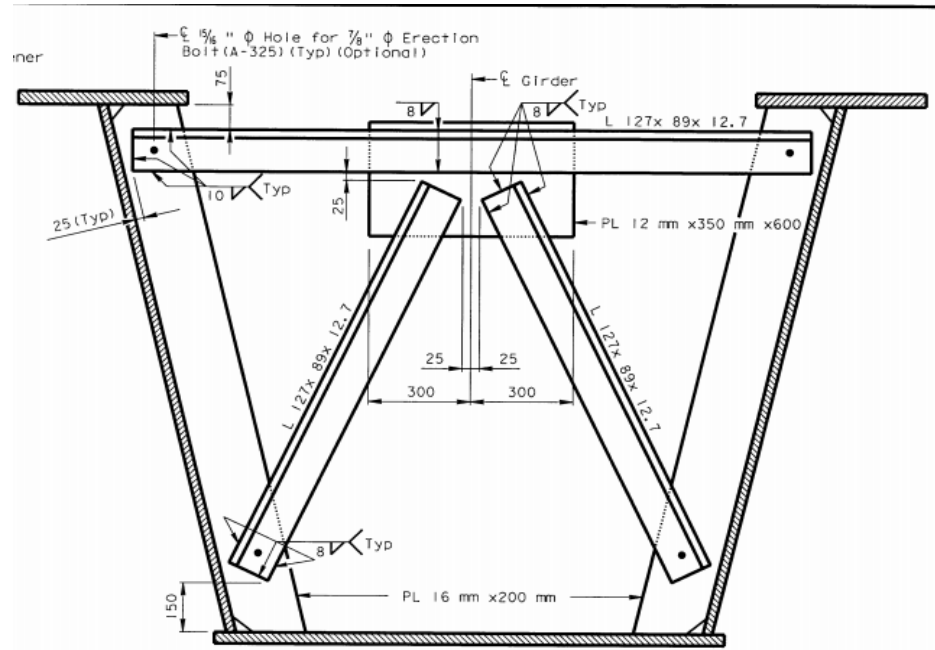


DIAFRAM ~ TYPE C



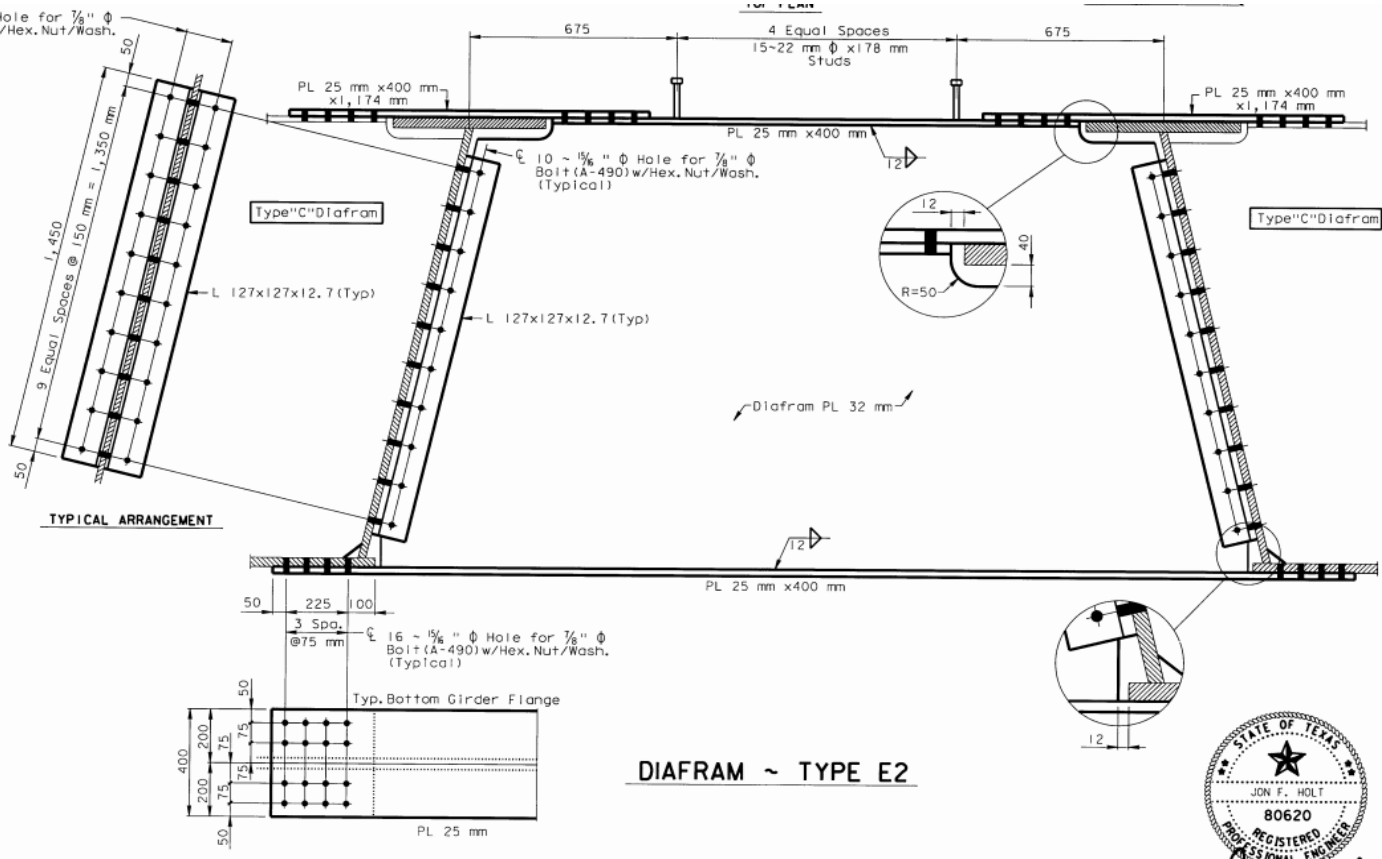
DIAFRAM ~ TYPE A2





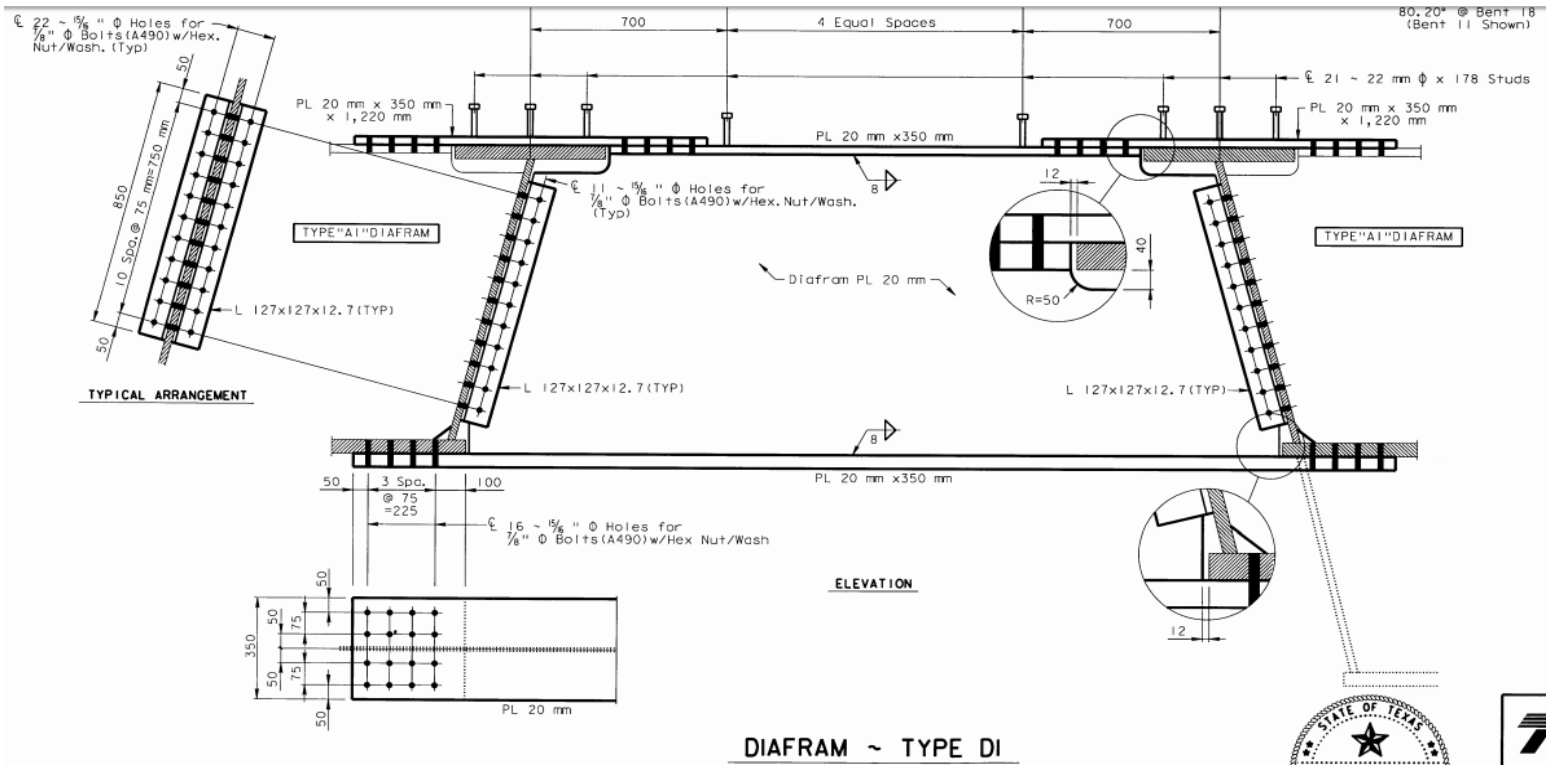
DIAFRAM ~ TYPE B
 Note: All Angles Placed with Long Leg Vertical (Typ)

\varnothing 20 - $\frac{5}{16}$ " \varnothing Hole for $\frac{7}{8}$ " \varnothing Bolt (A-490) w/Hex. Nut/Wash. (Typical)

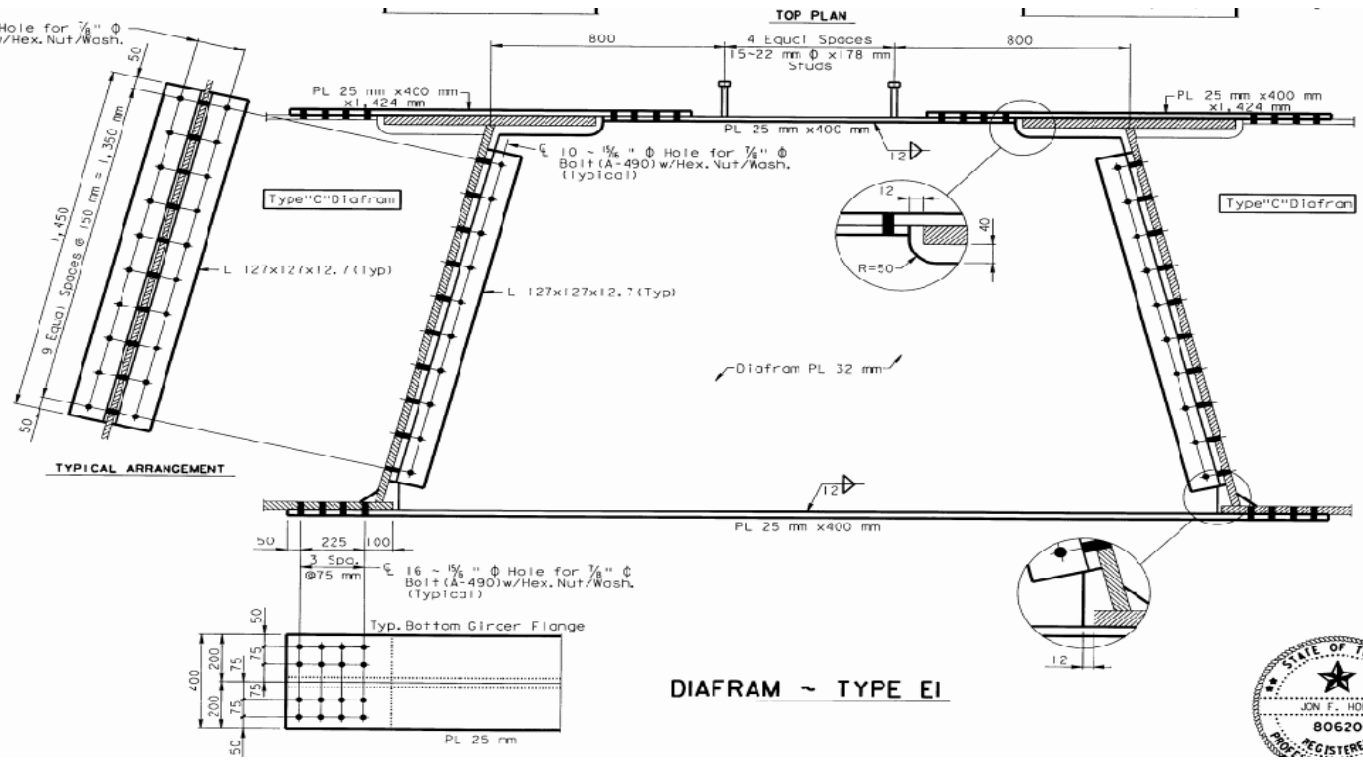


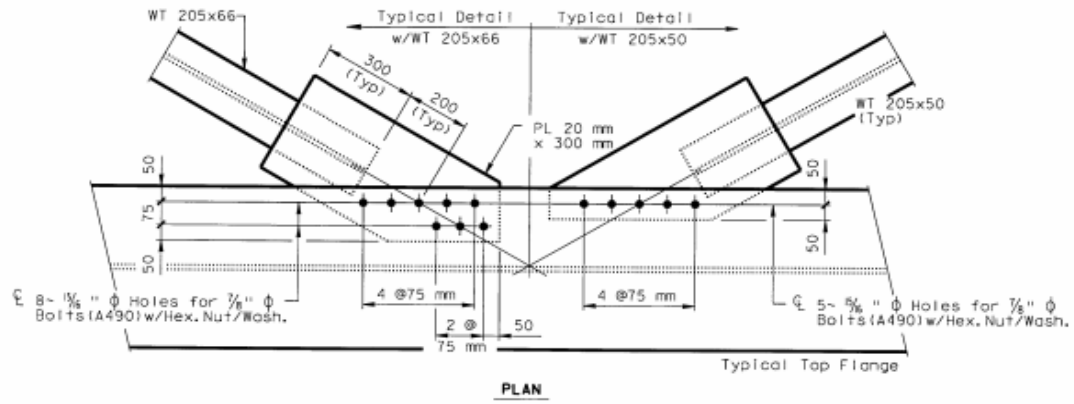
DIAFRAM ~ TYPE E2





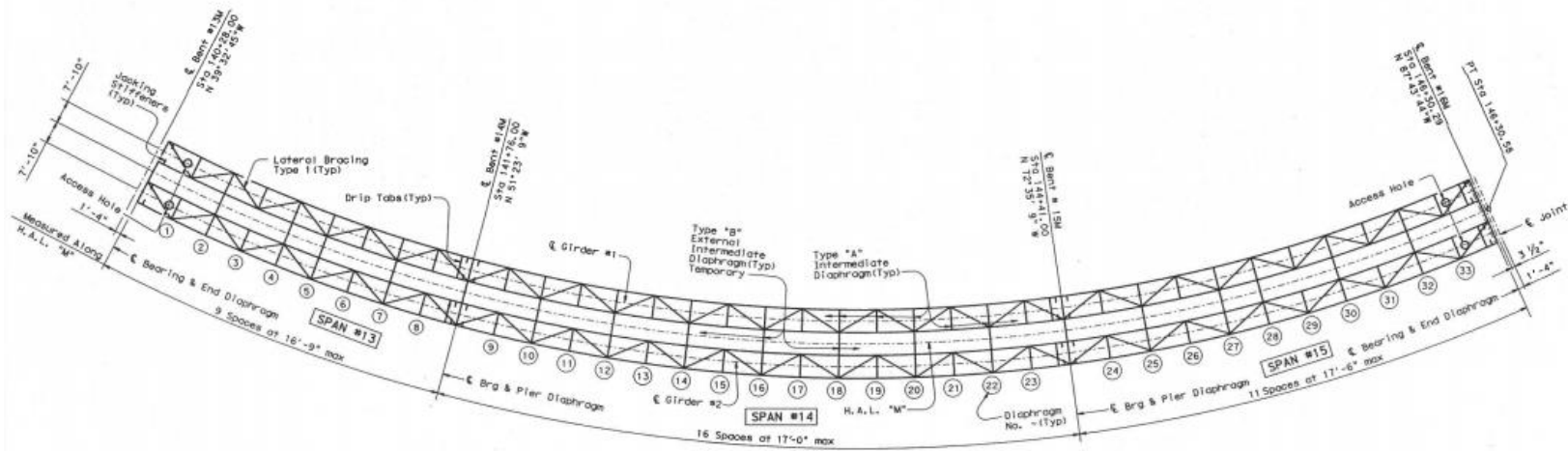
ϕ 20 ~ 3/4" ϕ Hole for 7/8" ϕ Bolt (A-490) w/Hex. Nut/Wash. (Typical)

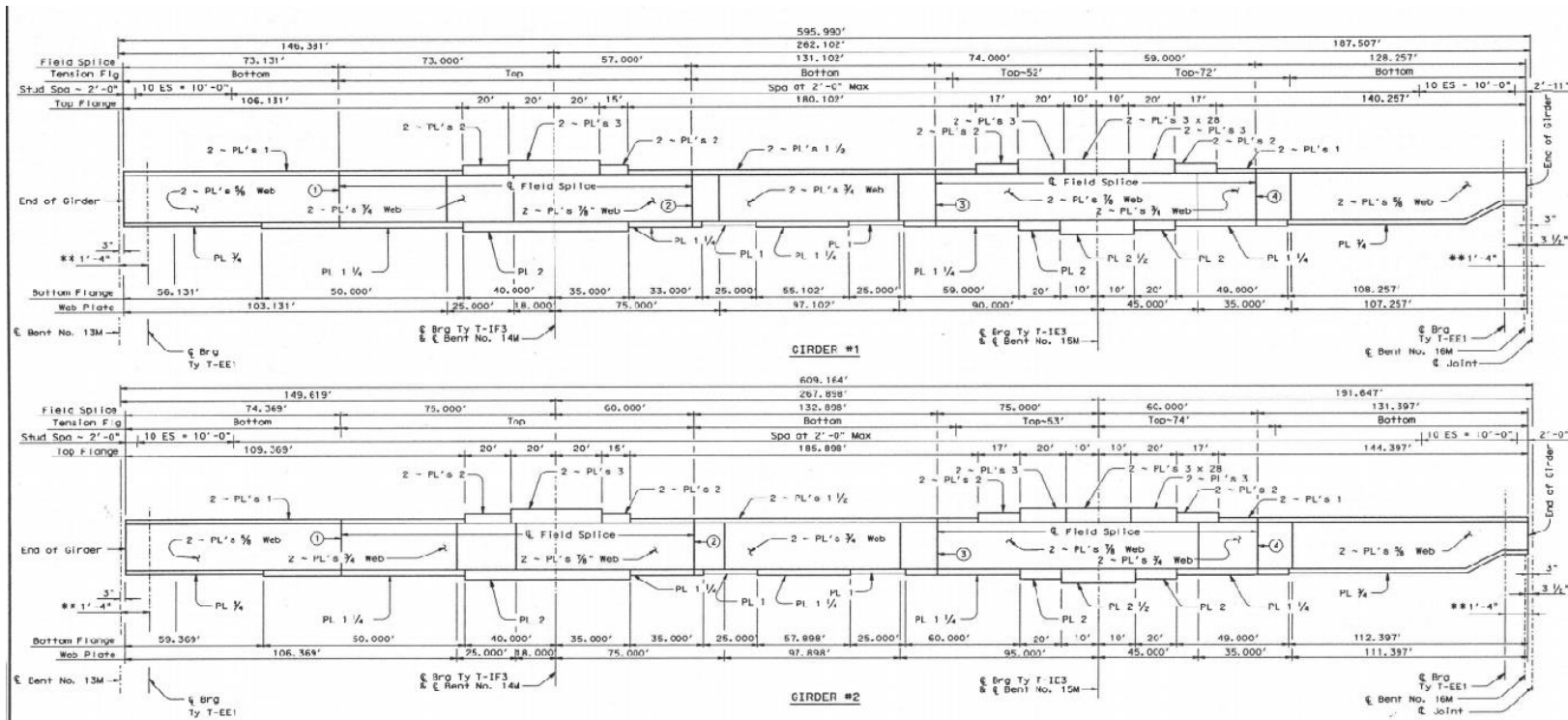


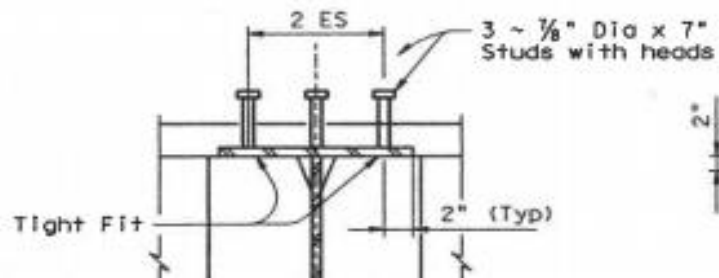
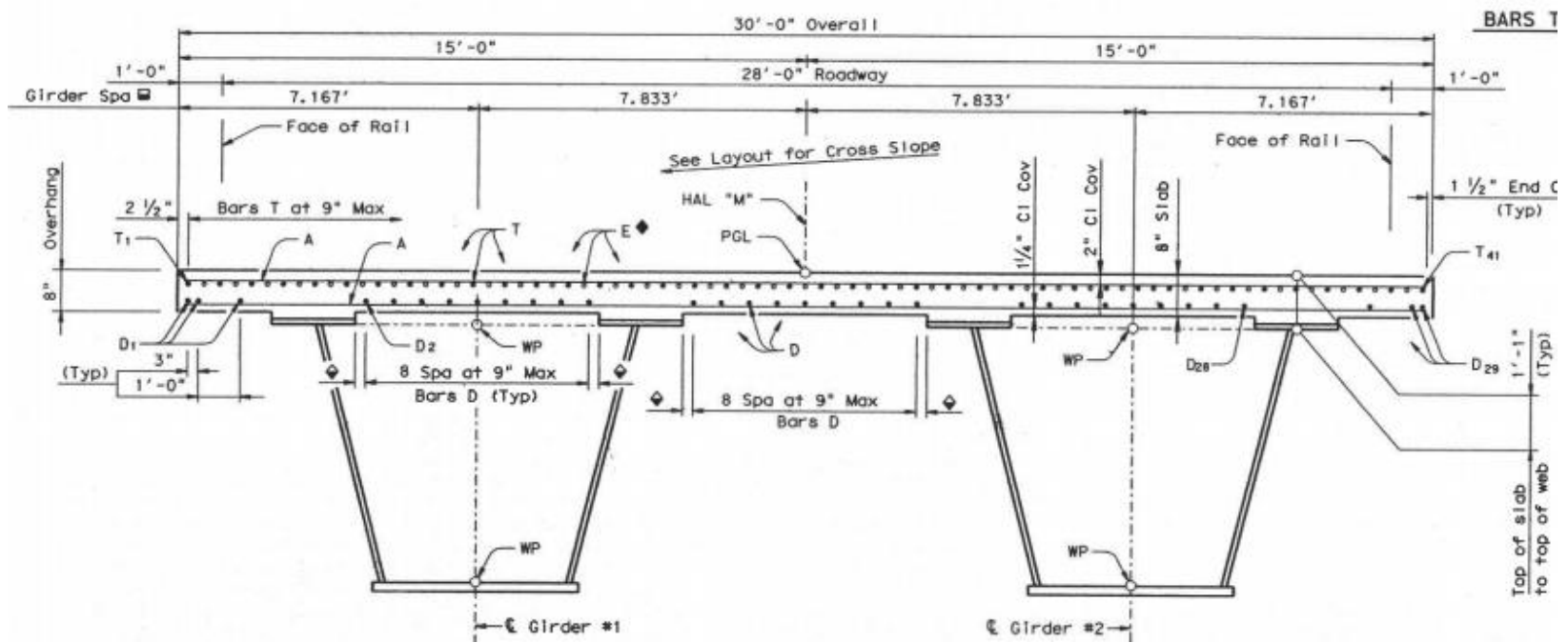


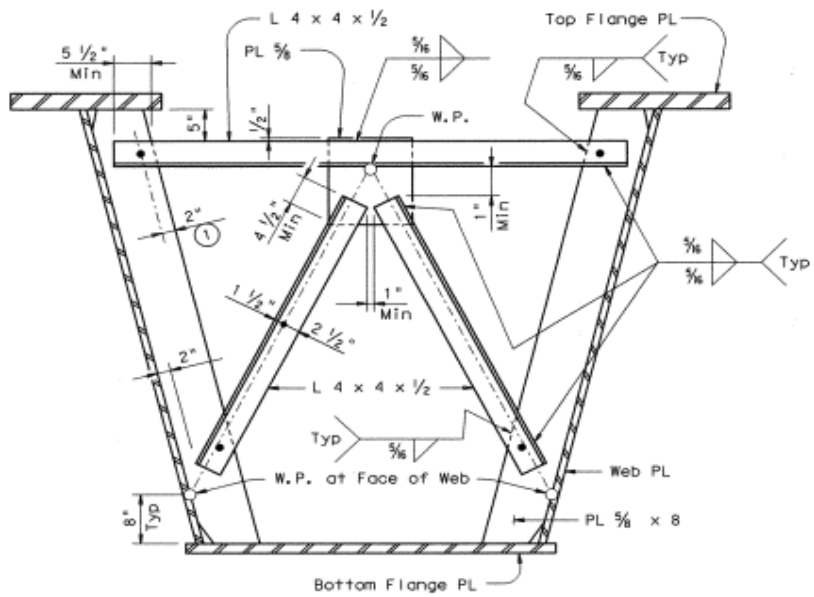
BRIDGE 10: 14-227-0-0015-13-450

⊕ G Girder #2] 724.030
 * Measured at top of web



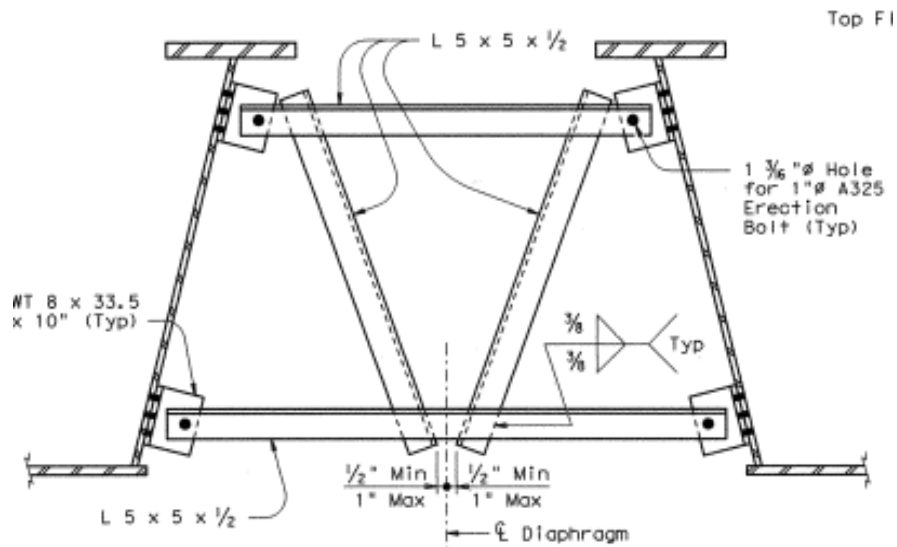




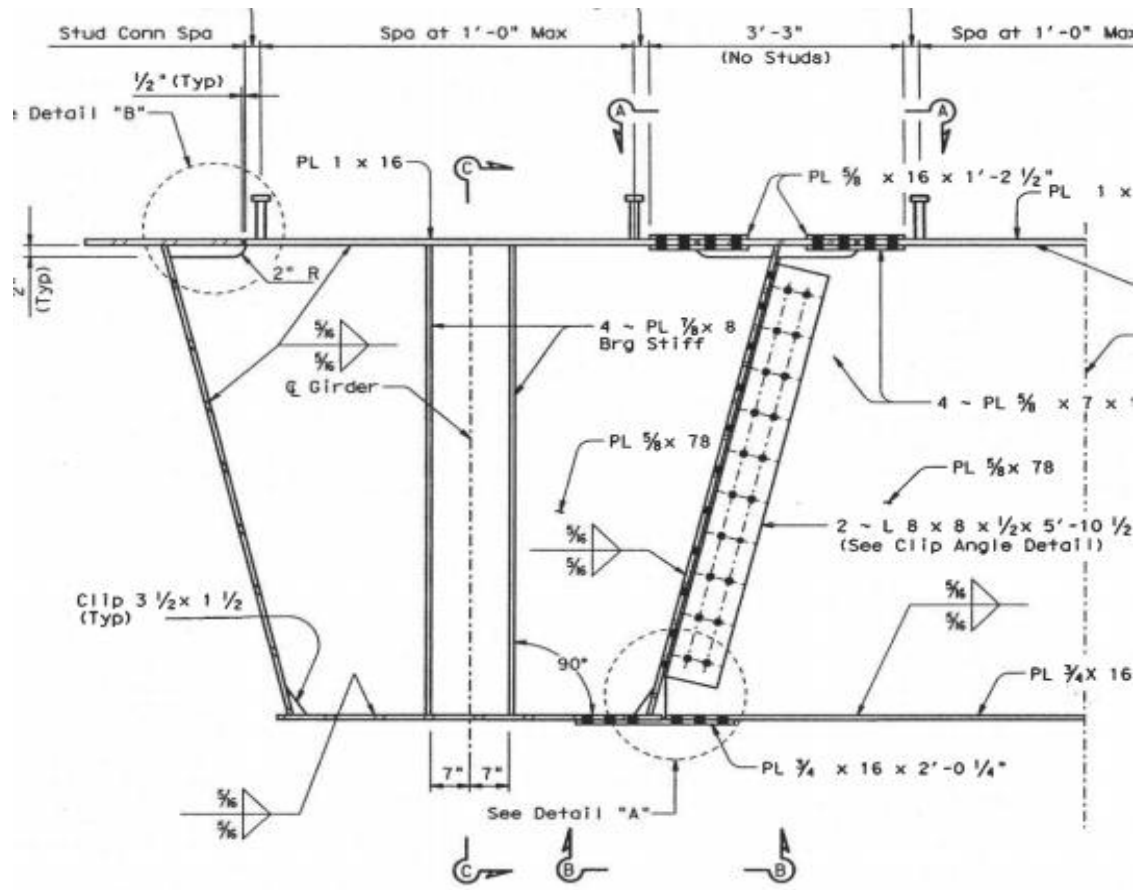


**TYPICAL SECTION AT TYPE "A"
INTERNAL INTERMEDIATE DIAPHRAGM**

To be fully installed in the shop.



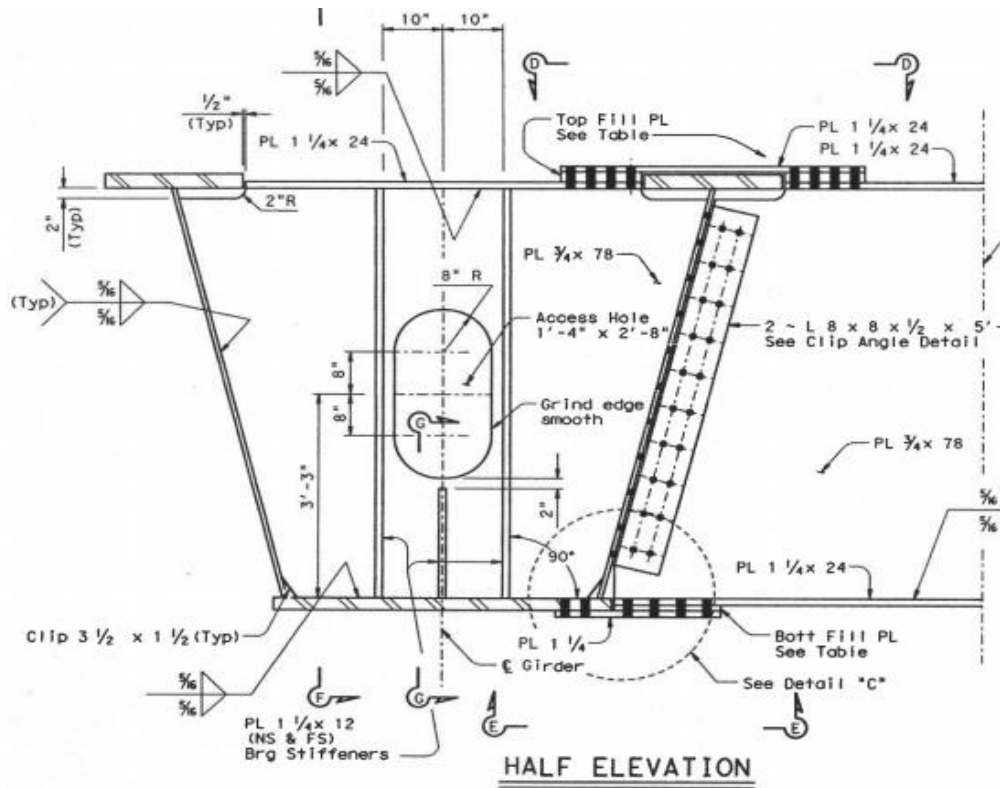
TYPICAL SECTION AT TYPE "B" EXTERNAL INTERMEDIATE DIAPHRAGM (TEMPORARY)



HALF ELEVATION

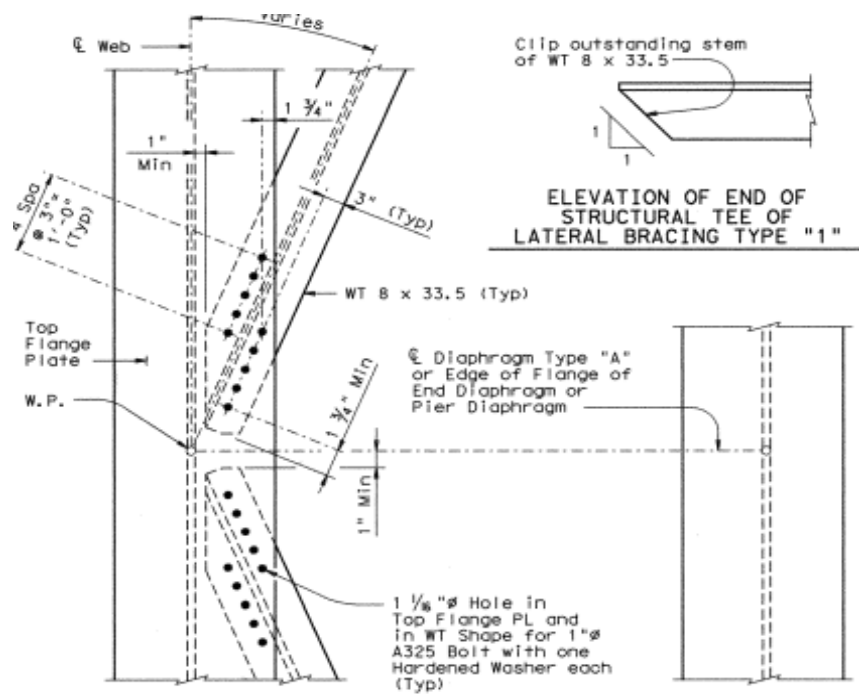
END DIAPHRAGM DETAILS

(At Bent No. 13M)



PIER DIAPHRAGM DETAILS

(At Bent Nos. 14M & 15M)

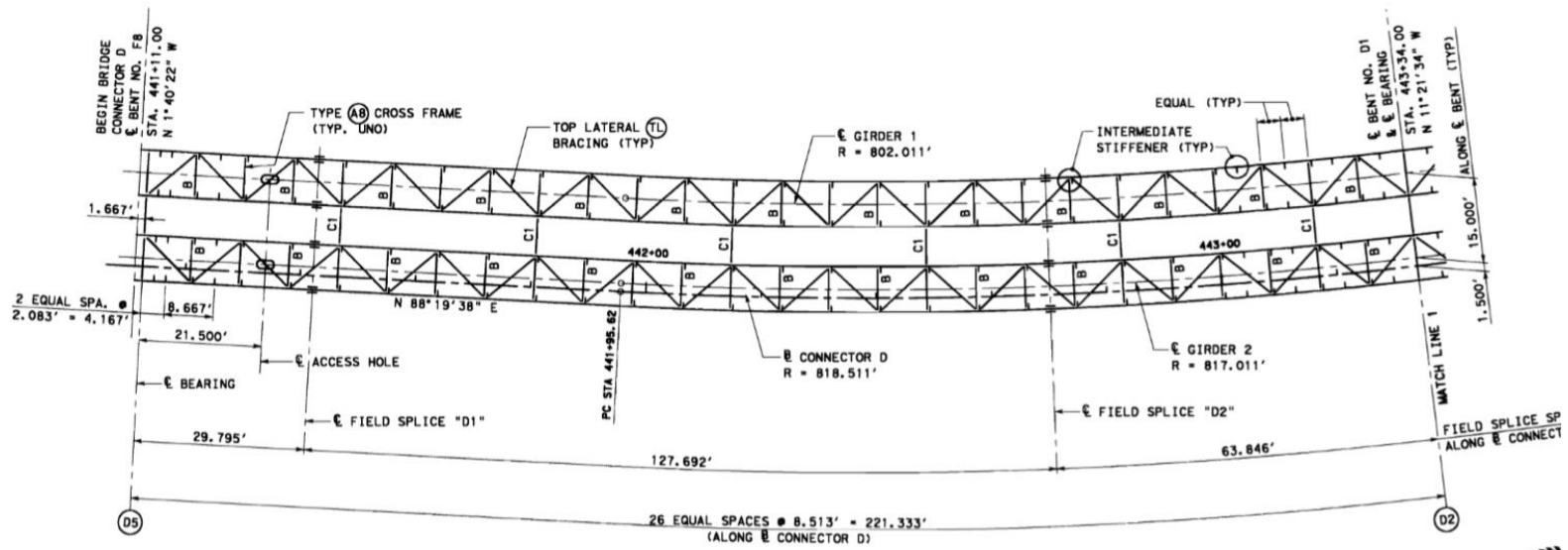


TYPICAL PLAN VIEW OF LATERAL BRACING TYPE "1"

Installed in shop except at locations spanning a field splice, which shall be installed in the field.

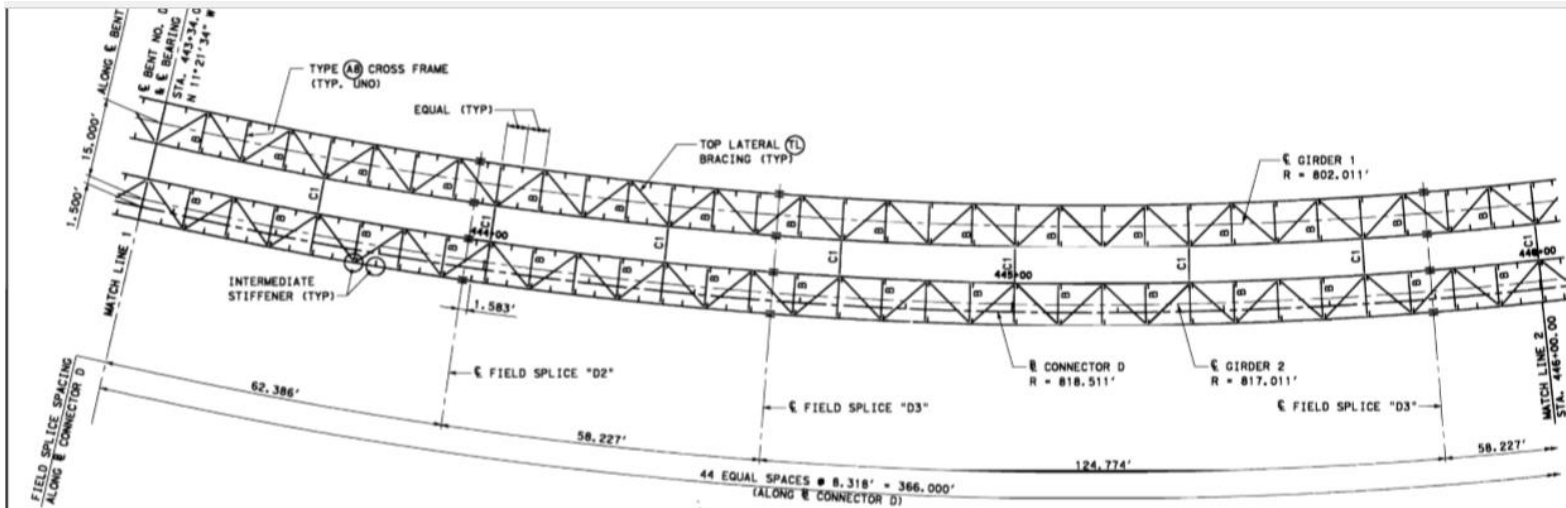
BRIDGE 11: 12-102-0271-07-593

NOTE: GIRDER RADIUS 1
AT TOP OF BOX



SPAN 1





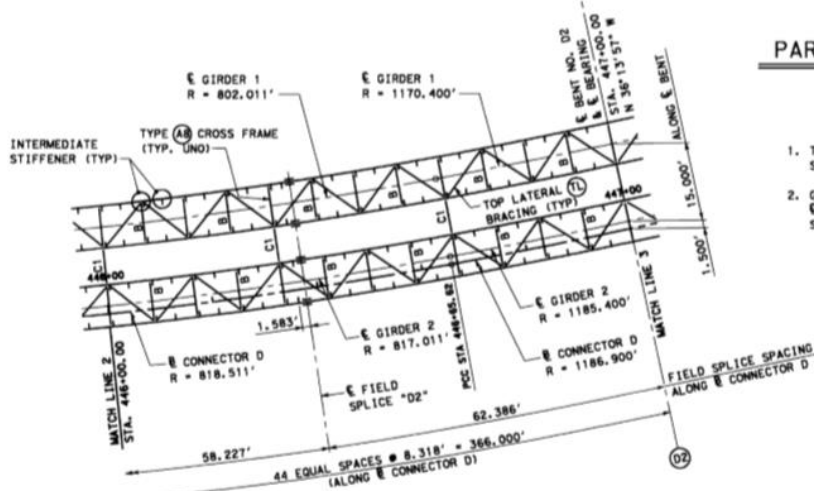
PARTIAL SPAN 2

NOTES

1. THE CONTRACTOR SHALL LOCATE PICK-UP POINTS SO ERECTION STRESSES DO NOT EXCEED ALLOWABLE STRESSES.
2. GIRDER DIMENSIONS SHOWN ARE MEASURED HORIZONTALLY ALONG GIRDERS AT TOP OF WEB UNLESS NOTED OTHERWISE. THE CONTRACTOR SHALL MAKE ADJUSTMENTS FOR GRADE AND CAMBER.

ABBREVIATIONS

- (AB) = TYPE AB CROSS FRAME
- B = TOP STRUT ONLY (L6x6x $\frac{1}{4}$)
- C1 = TYPE C1 TEMPORARY EXTERNAL CROSS FRAME
- (D2) = TYPE D2 DIAPHRAGM
- (TL) = TOP LATERAL BRACING (WT9x71.5)



PARTIAL SPAN 2



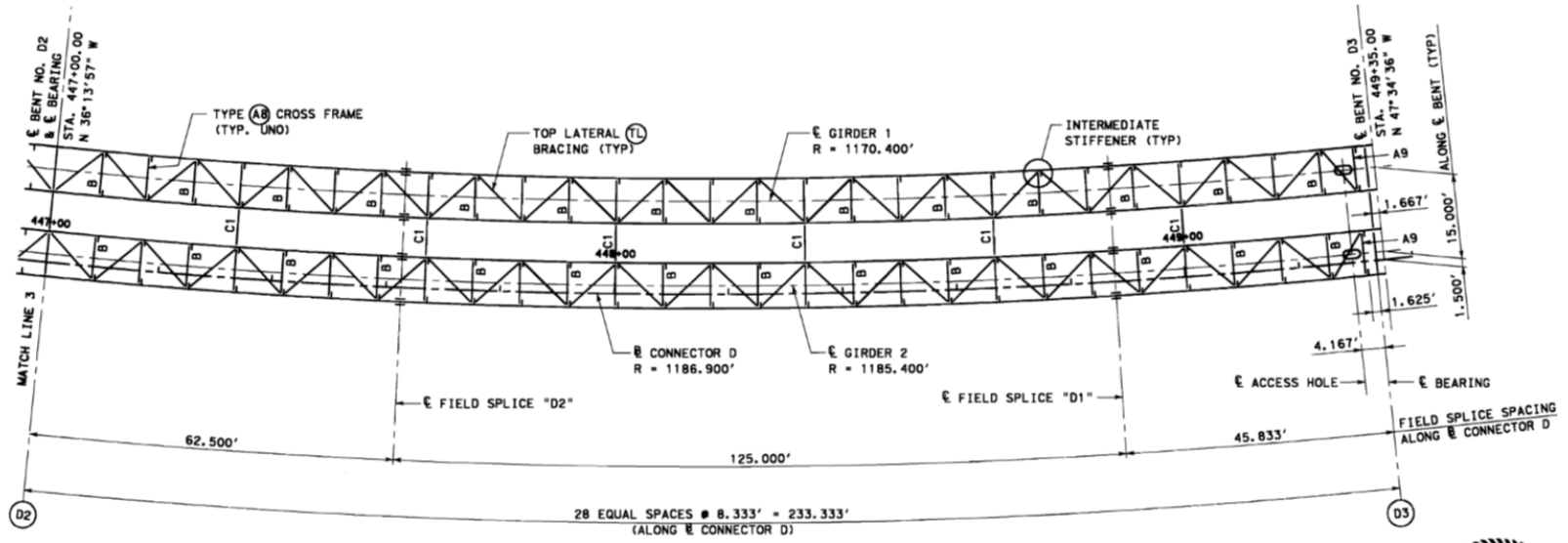
ASME
4/15/11

Texas Department of Transportation
8004 7407

URS
8801 WESTHEIMER, SUITE 500
HOUSTON, TEXAS 77042
713.914.8899

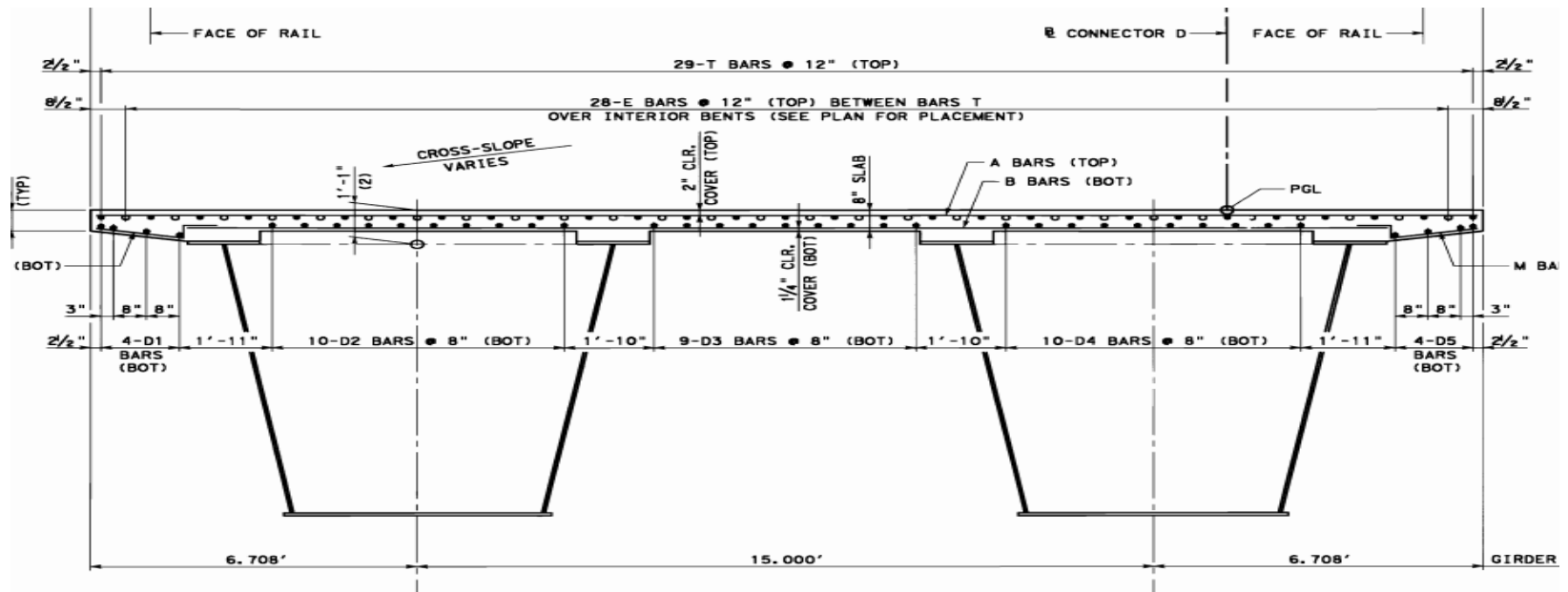
**KATY FREEWAY
RECONSTRUCTION PROG
DIRECT CONNECTOR *
UNIT D1
FRAMING PLAN**

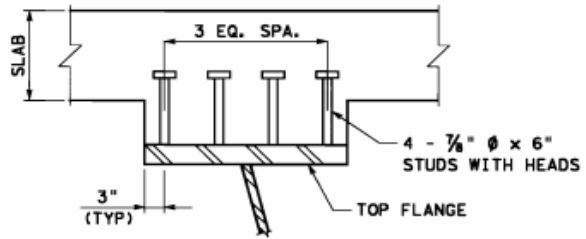
DESIGN LEADER		DESIGN		CHECK		APPROVE	
DATE	BY	DATE	BY	DATE	BY	DATE	BY
STATE OF TEXAS				COUNTY OF HARRIS			
12 HARRIS 0271				07			



SPAN 3

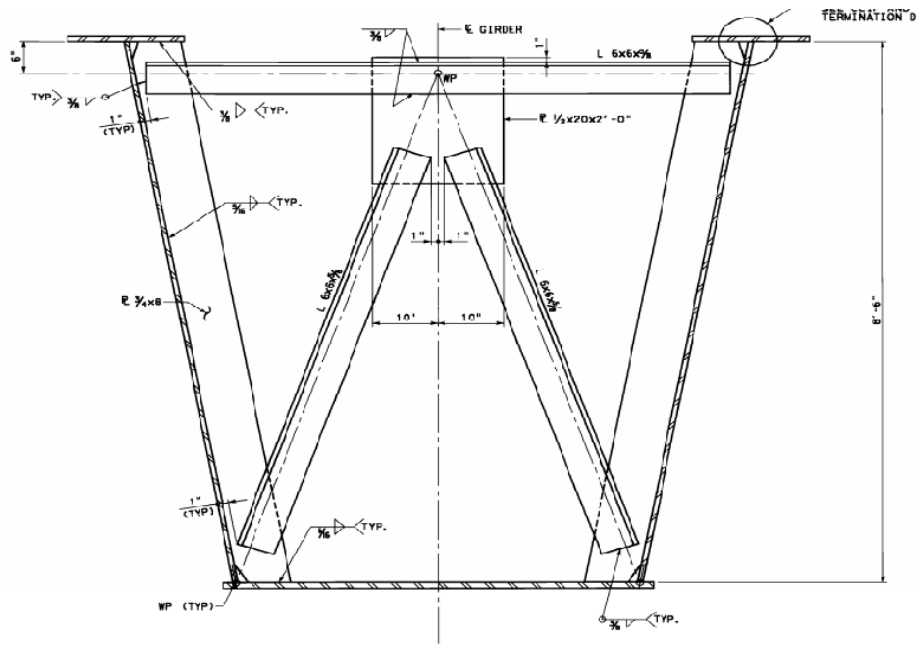




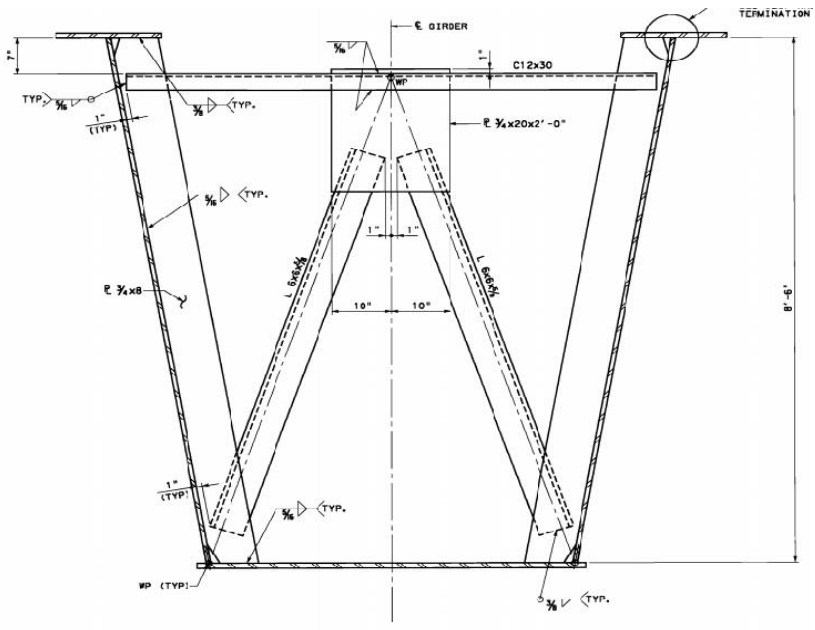


SHEAR CONNECTOR STUD DETAIL

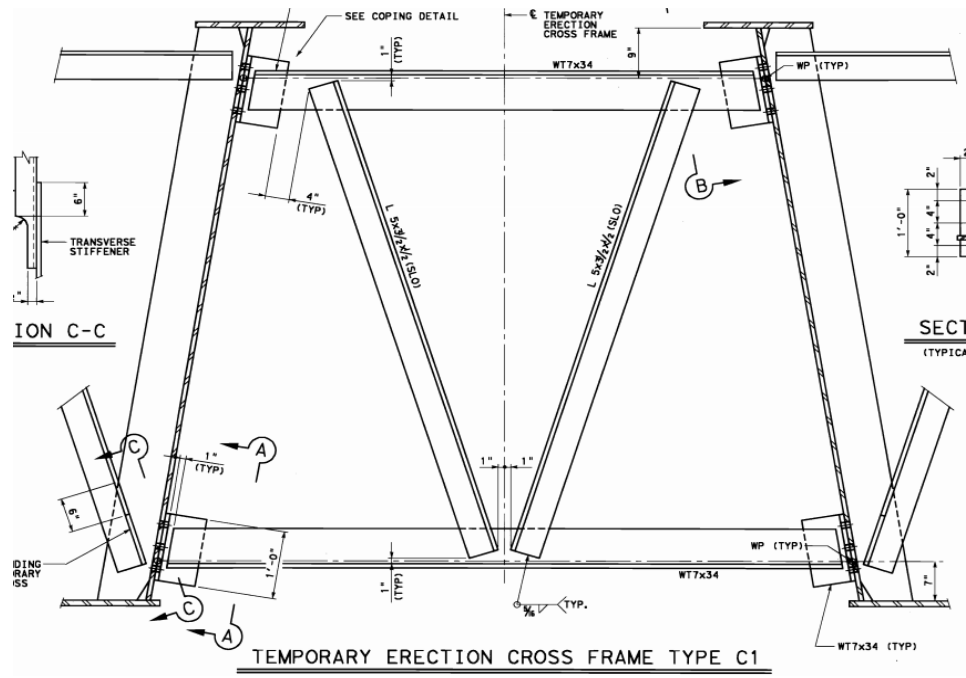
STUDS SHALL BE ELECTRIC ARC END WELDED
TO THE FLANGES WITH COMPLETE FUSION.
(SEE GIRDER ELEVATIONS FOR SPACING ALONG GIRDER)

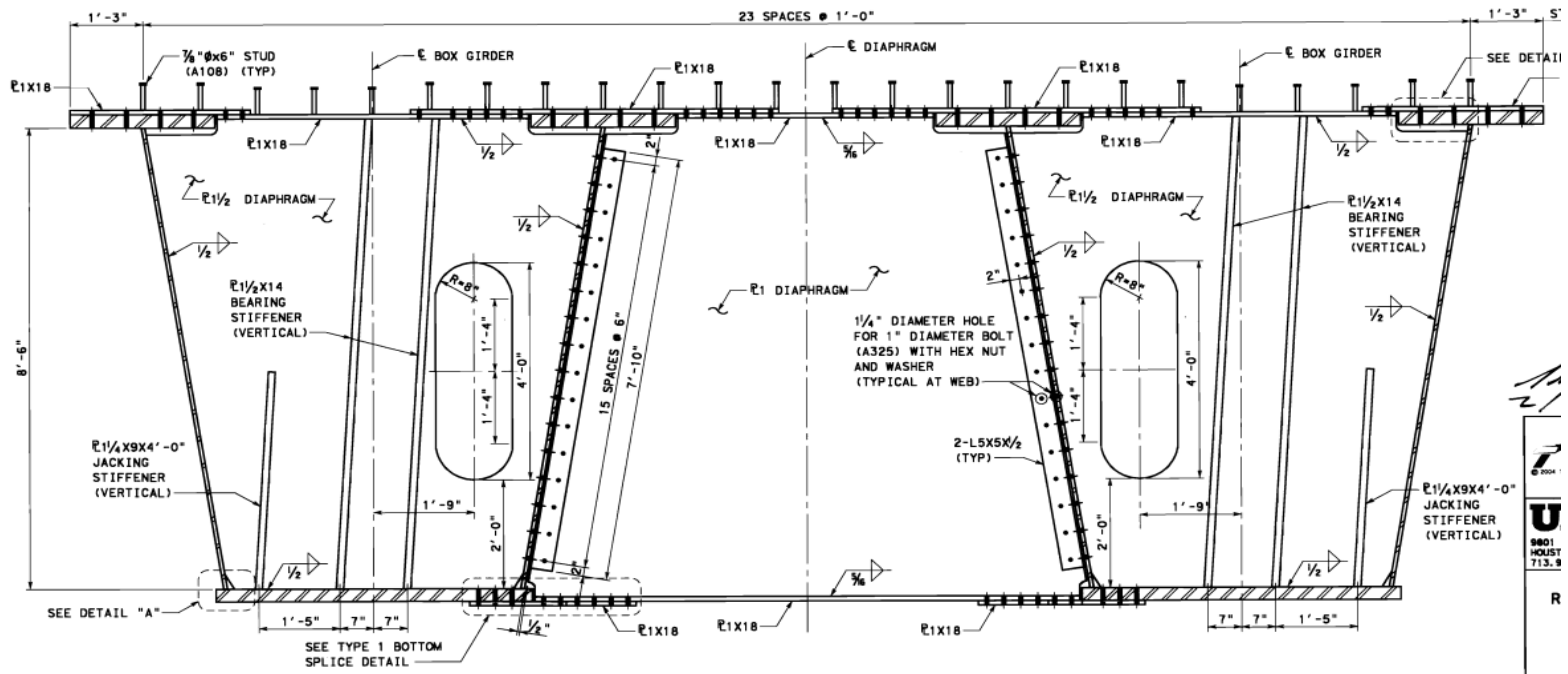


CROSS FRAME - TYPE AB

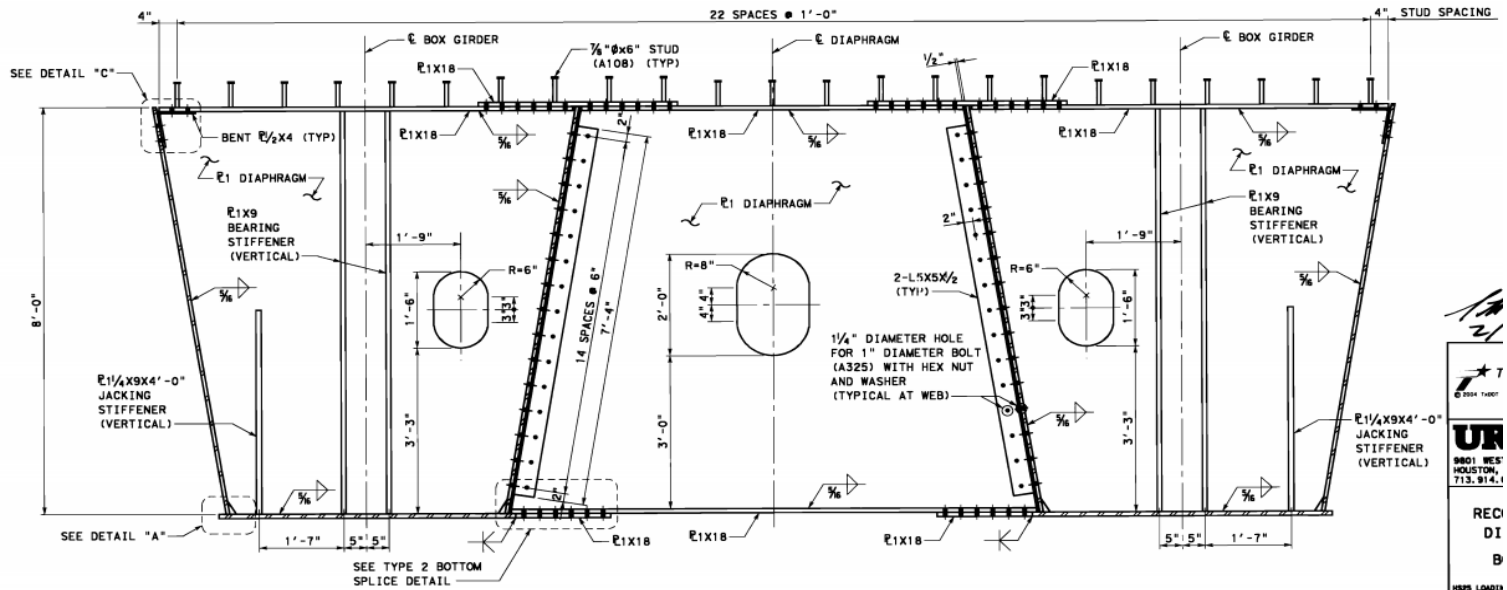


CROSS FRAME - TYPE A9



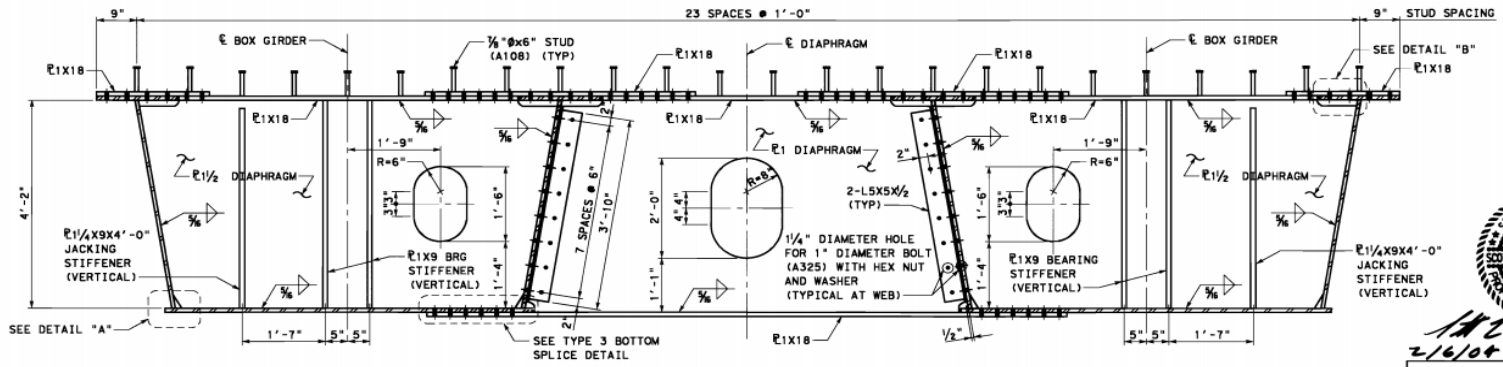


DIAPHRAGM - TYPE D2




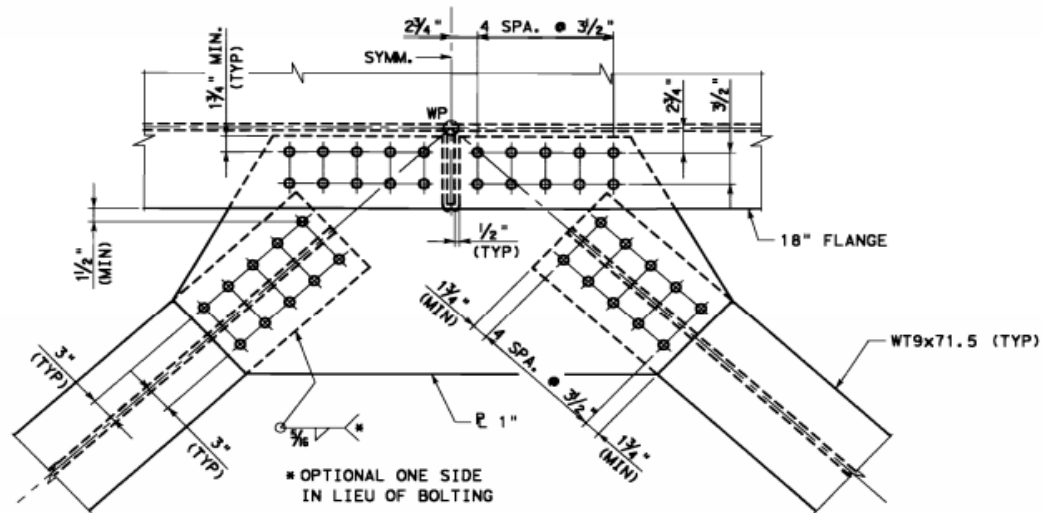
DIAPHRAGM - TYPE D3


 © 2004 TADP
UR
 9801 WES
 HOUSTON,
 TX 77036-1141
 REC'D
 DI
 B
 HRS LOADS
 10/11/13



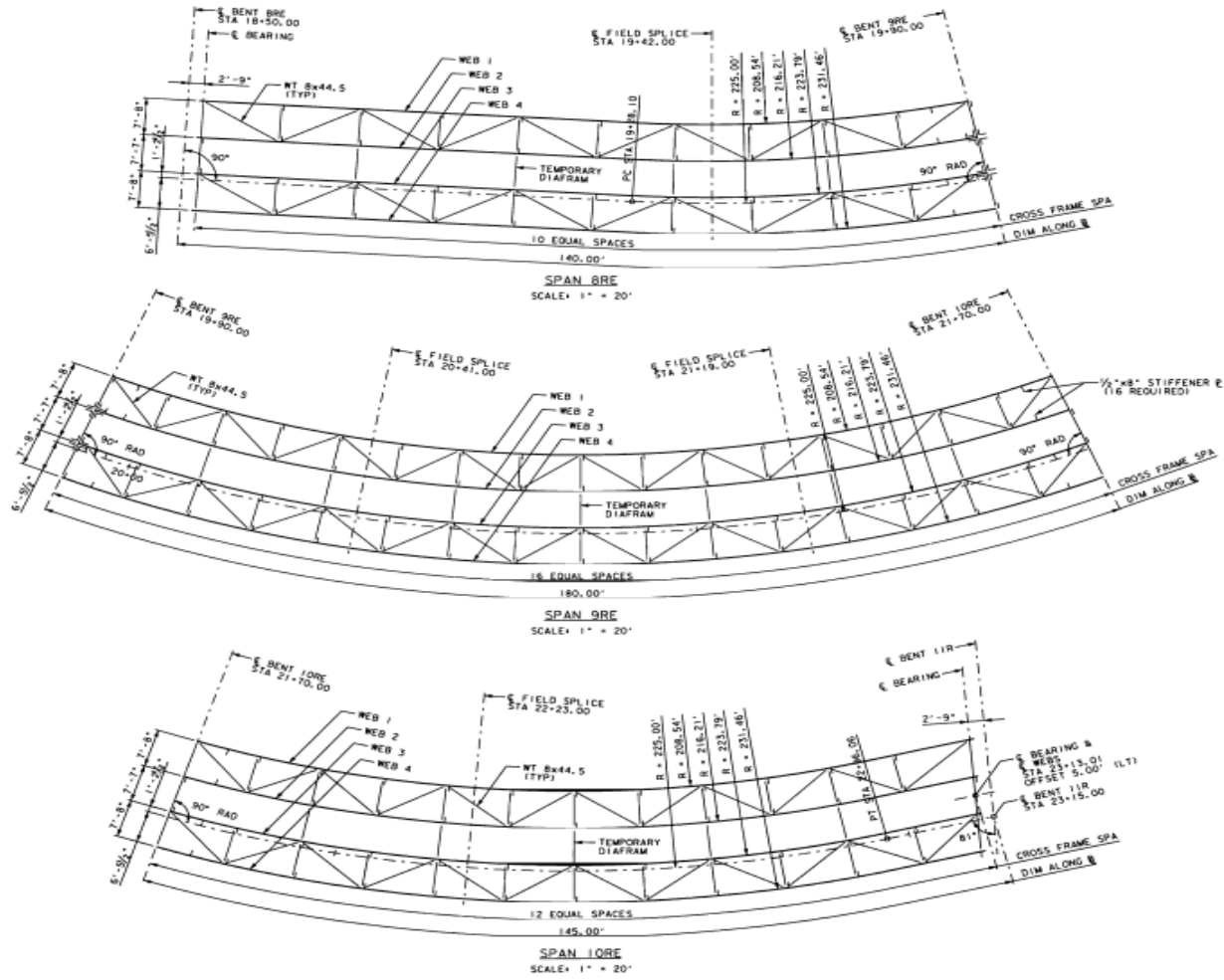
DIAPHRAGM - TYPE D5


 2/16/04
 Texas Dept

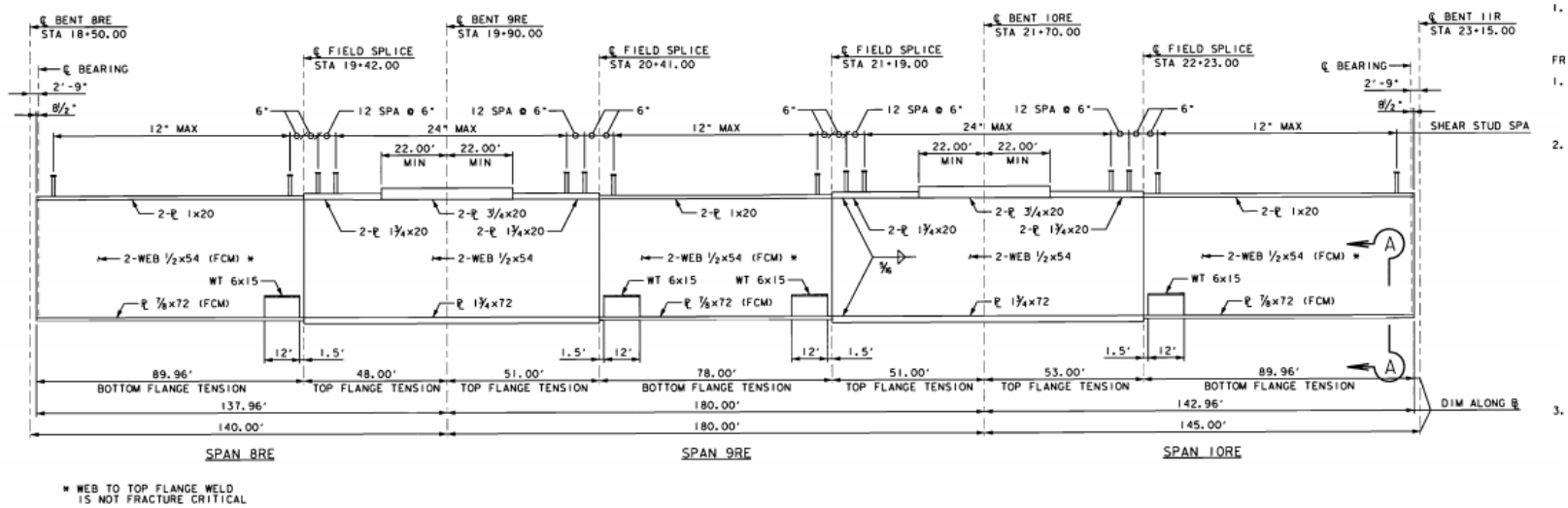


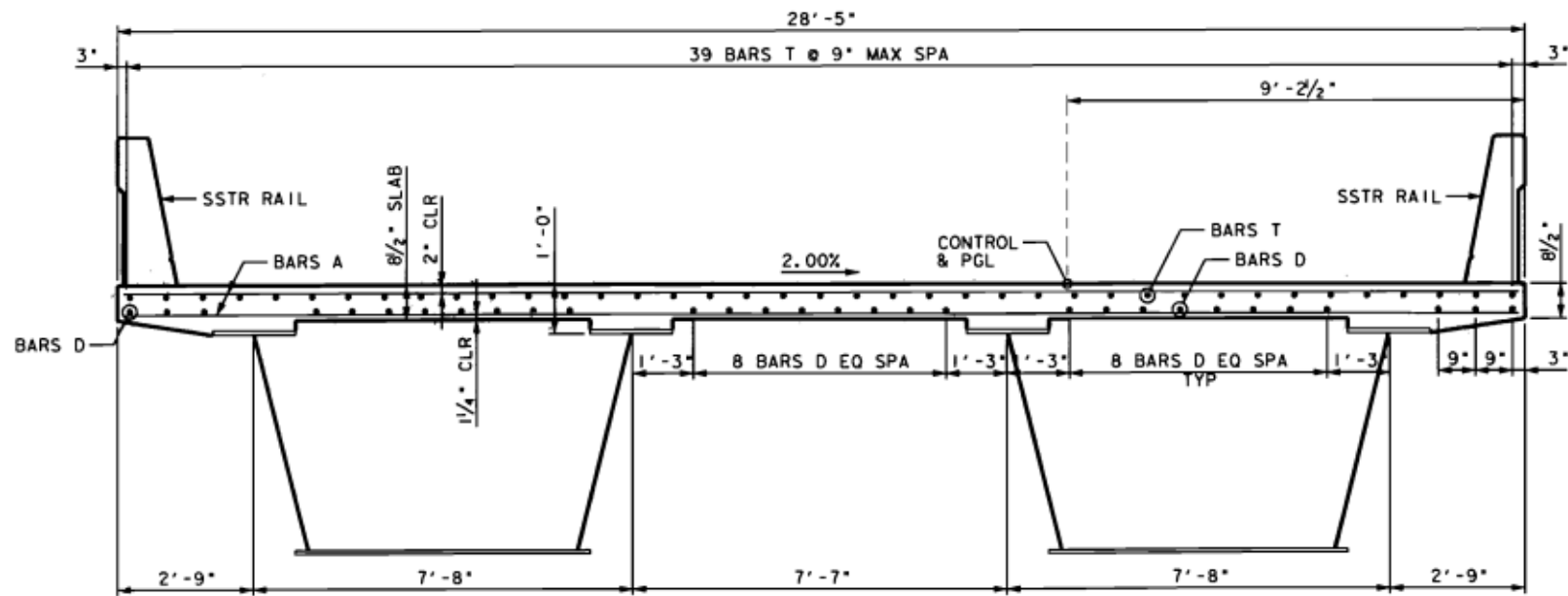
TOP LATERAL BRACING CONNECTION
DETAIL - UNIT D1
 (18" TOP FLANGE)

BRIDGE 12: 12-102-0271-07-639



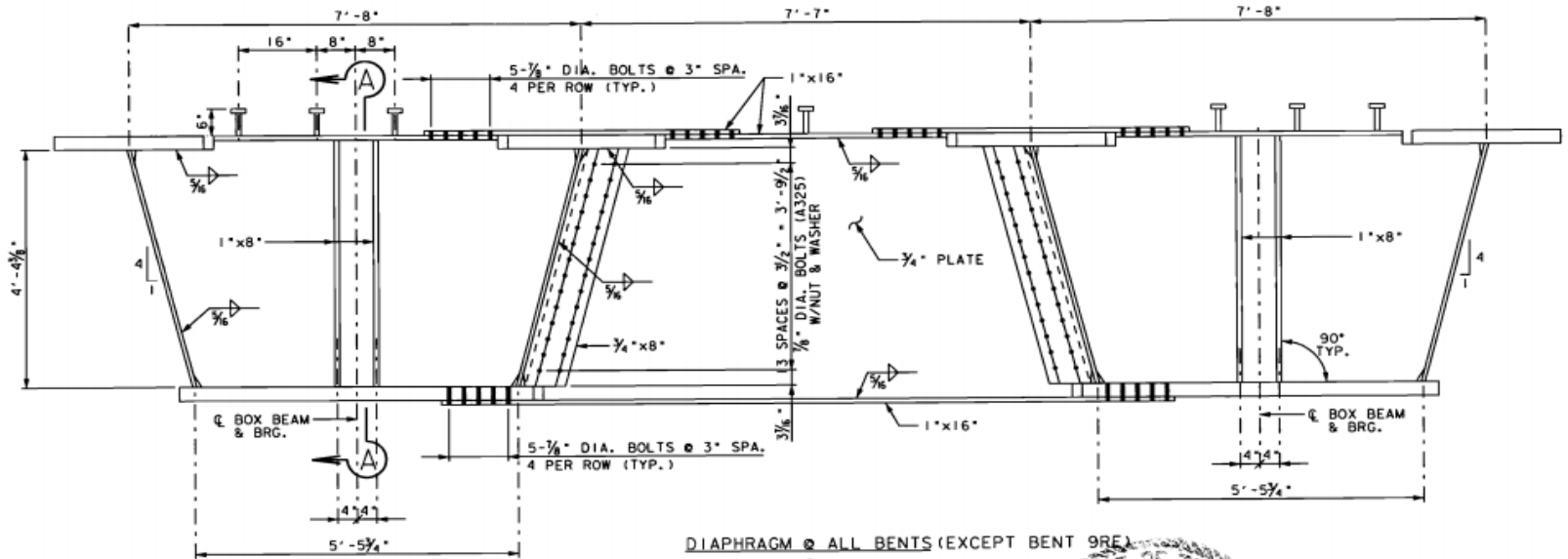
14
SA
C





TYPICAL SECTION

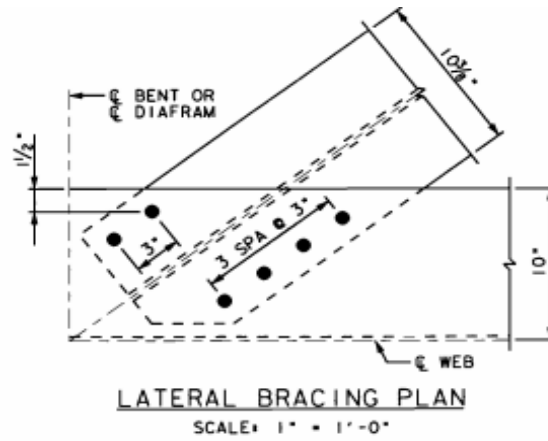
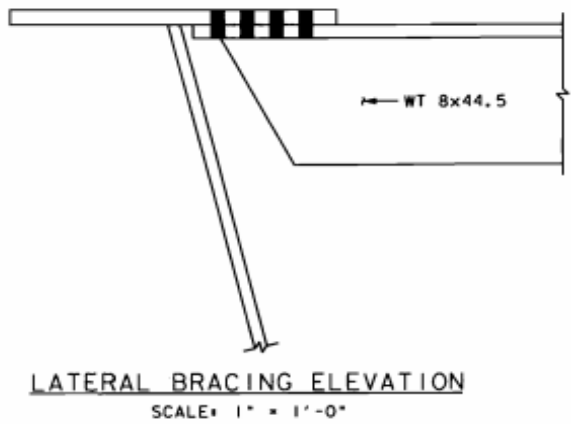
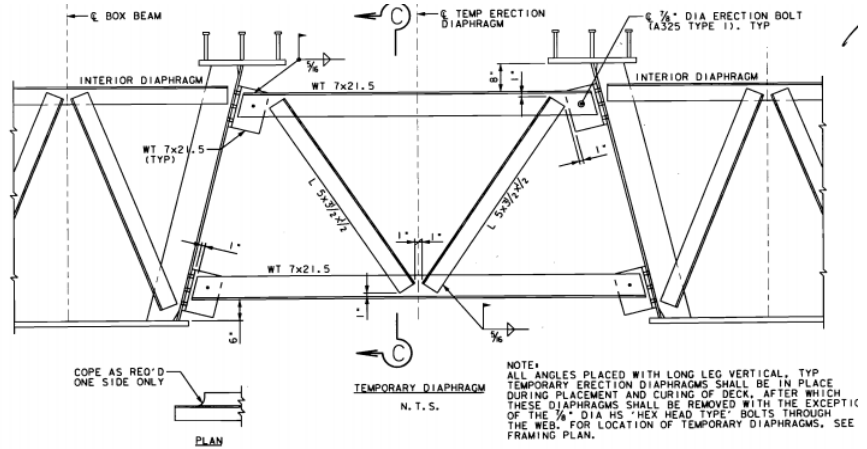
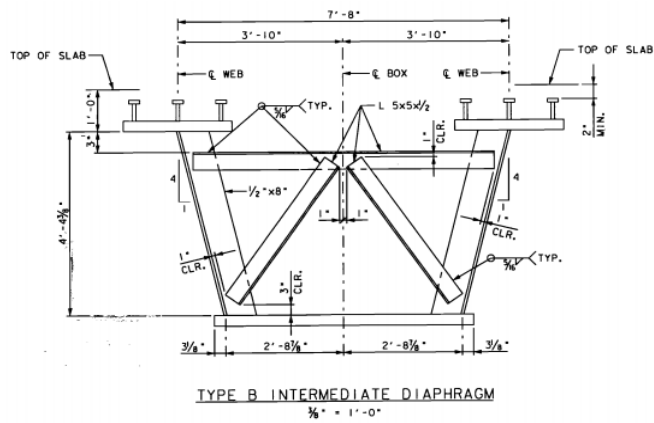
SCALE: 1/4" = 1'



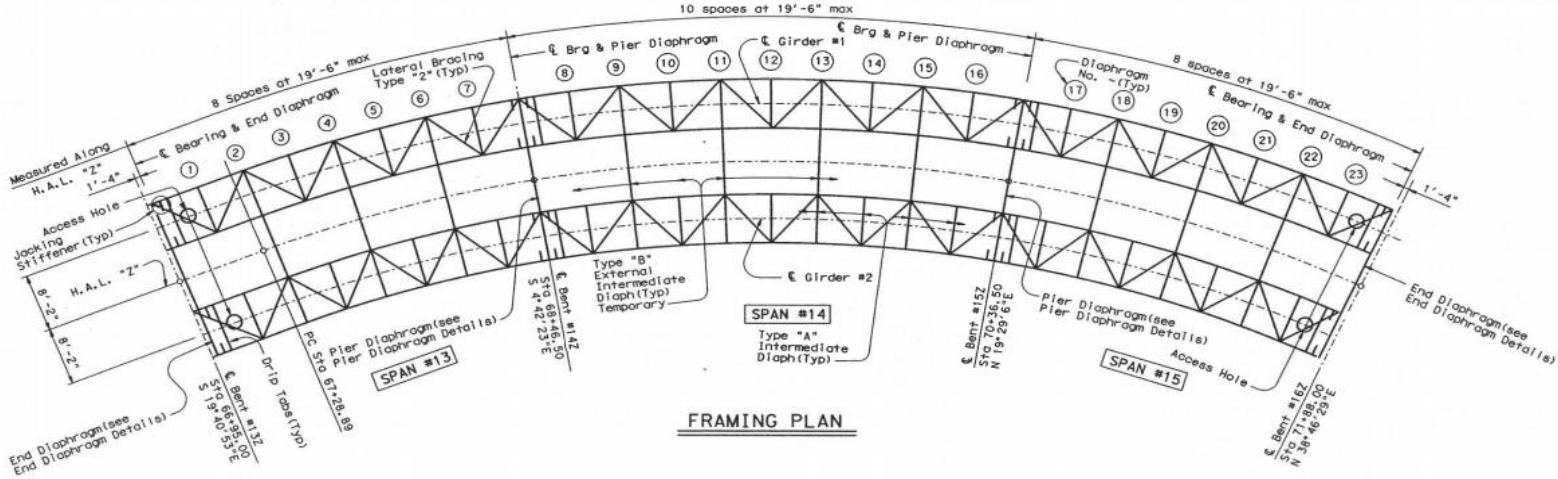
DIAPHRAGM @ ALL BENTS (EXCEPT BENT 9RE)

SCALE: 3/8" = 1'

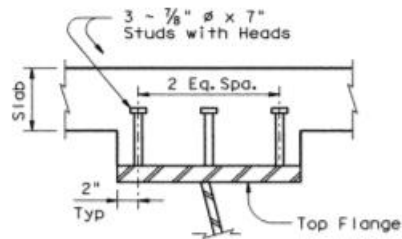
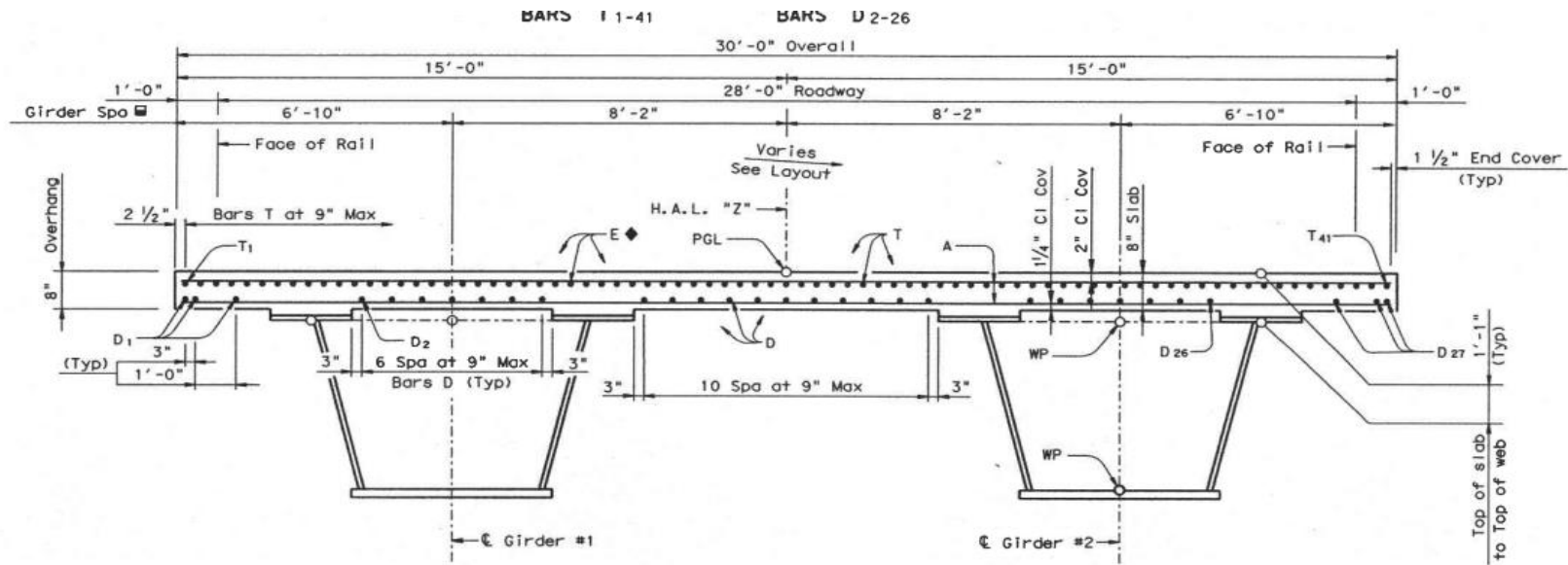




BRIDGE 13: 14-227-0-0015-13-452

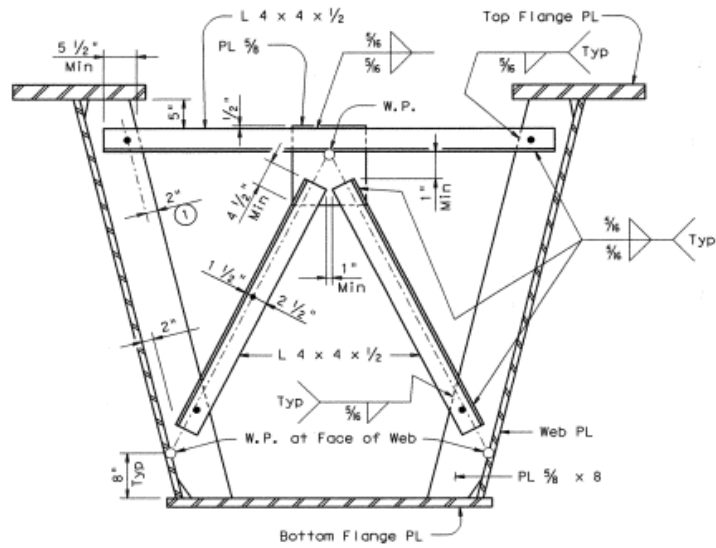


FRAMING PLAN



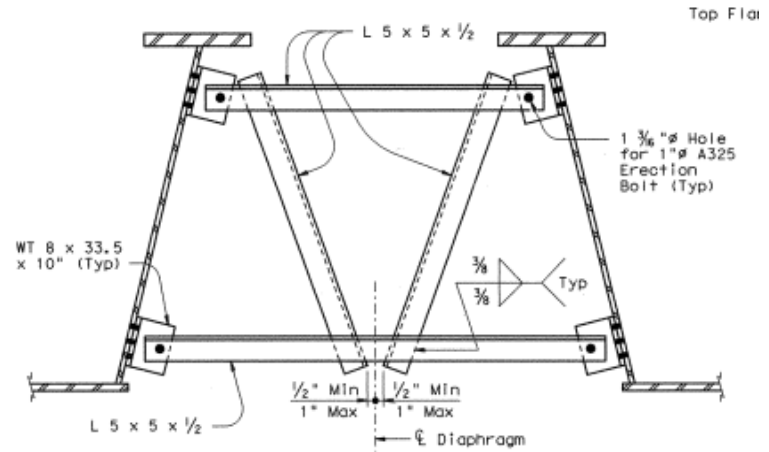
SHEAR CONNECTOR STUD DETAIL

Studs shall be Electric arc end-welded to the flanges with complete fusion. (See Span details for spacing along girder.)

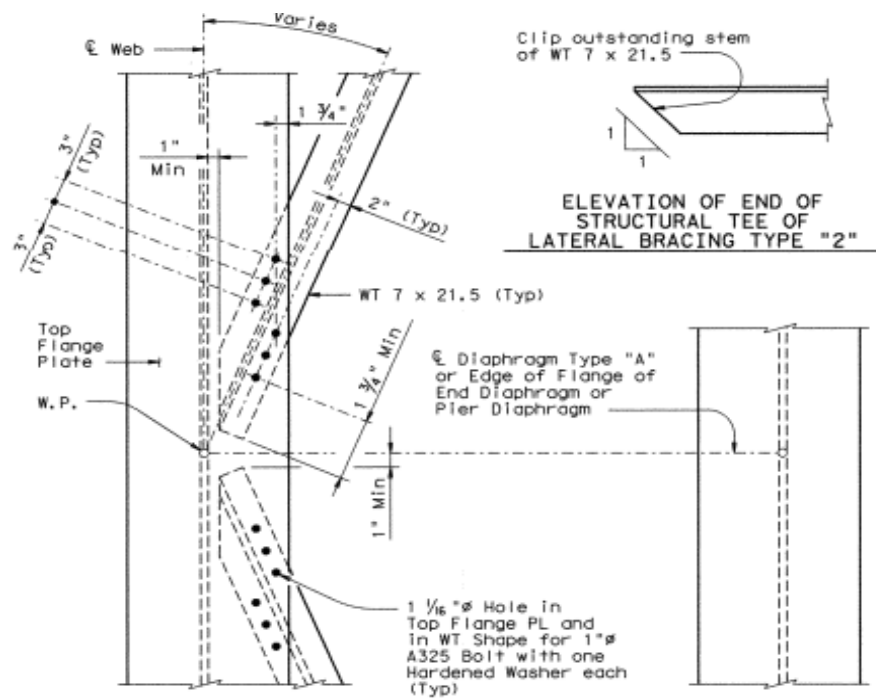


**TYPICAL SECTION AT TYPE "A"
INTERNAL INTERMEDIATE DIAPHRAGM**

To be fully installed in the shop.



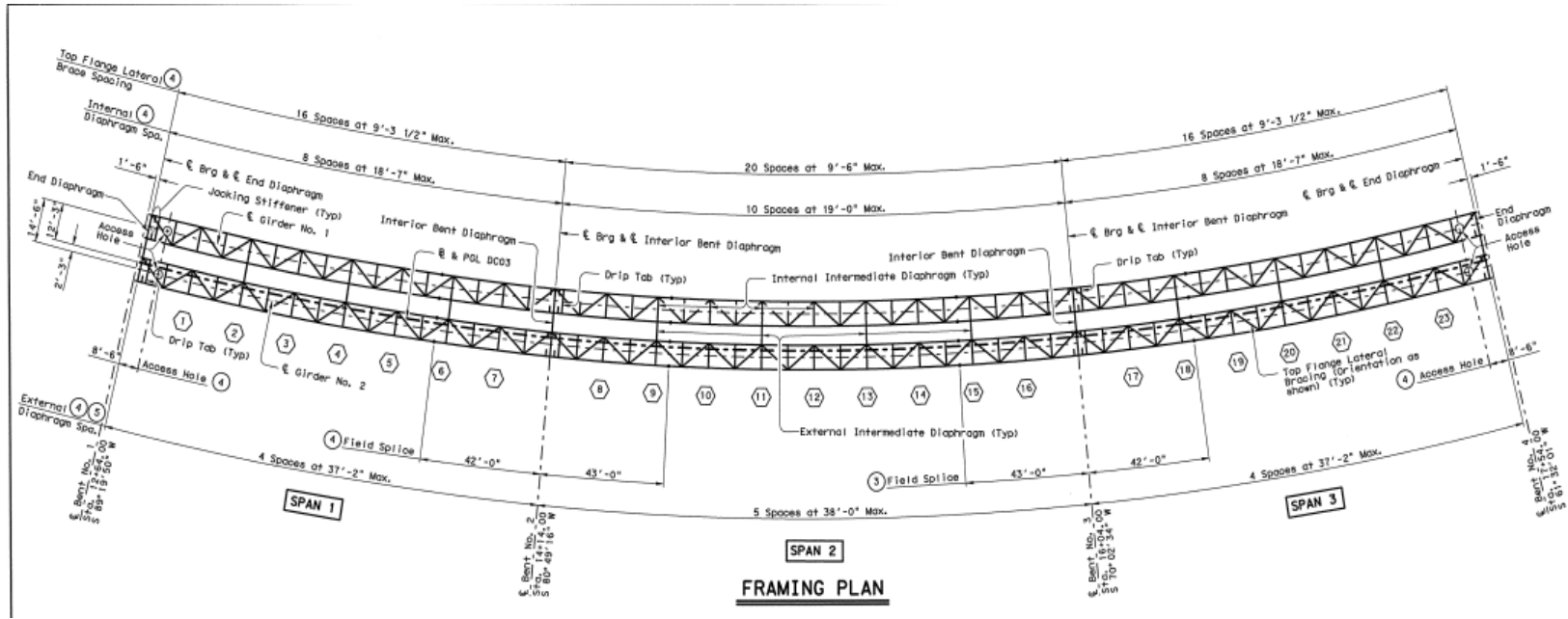
**TYPICAL SECTION AT TYPE "B" EXTERNAL
INTERMEDIATE DIAPHRAGM (TEMPORARY)**

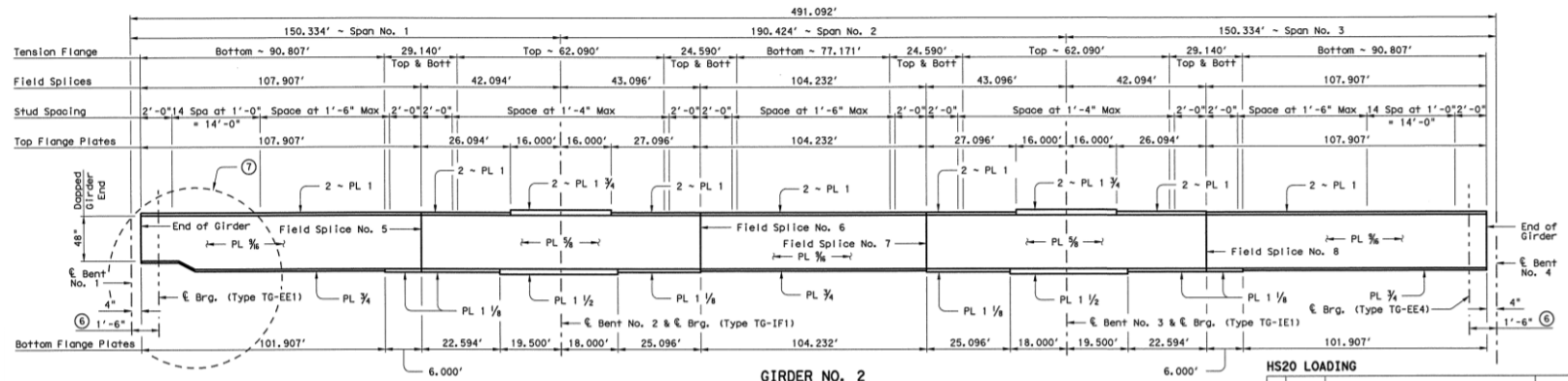
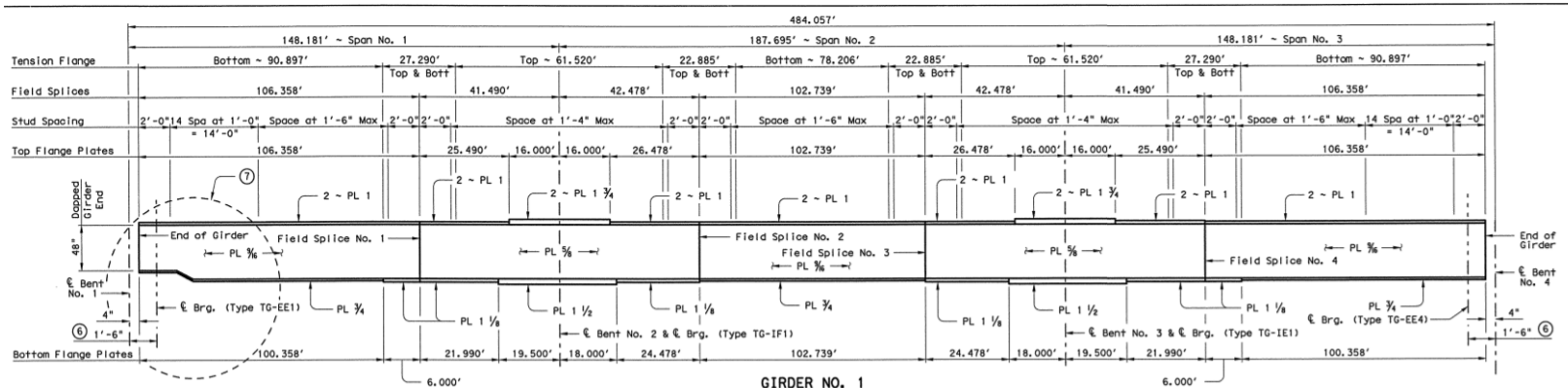


TYPICAL PLAN VIEW OF LATERAL BRACING TYPE "2"

Installed in shop except at locations spanning a field splice, which shall be installed in the field.

BRIDGE 14: 18-057-0-0009-11-460





⑥ Measured horizontally at bottom of web along centerline of girder.

⑦ See TRAPEZOIDAL STEEL BOX GIRDER DETAILS, Sheet 3 of 4 for Dapped Girder End Details.

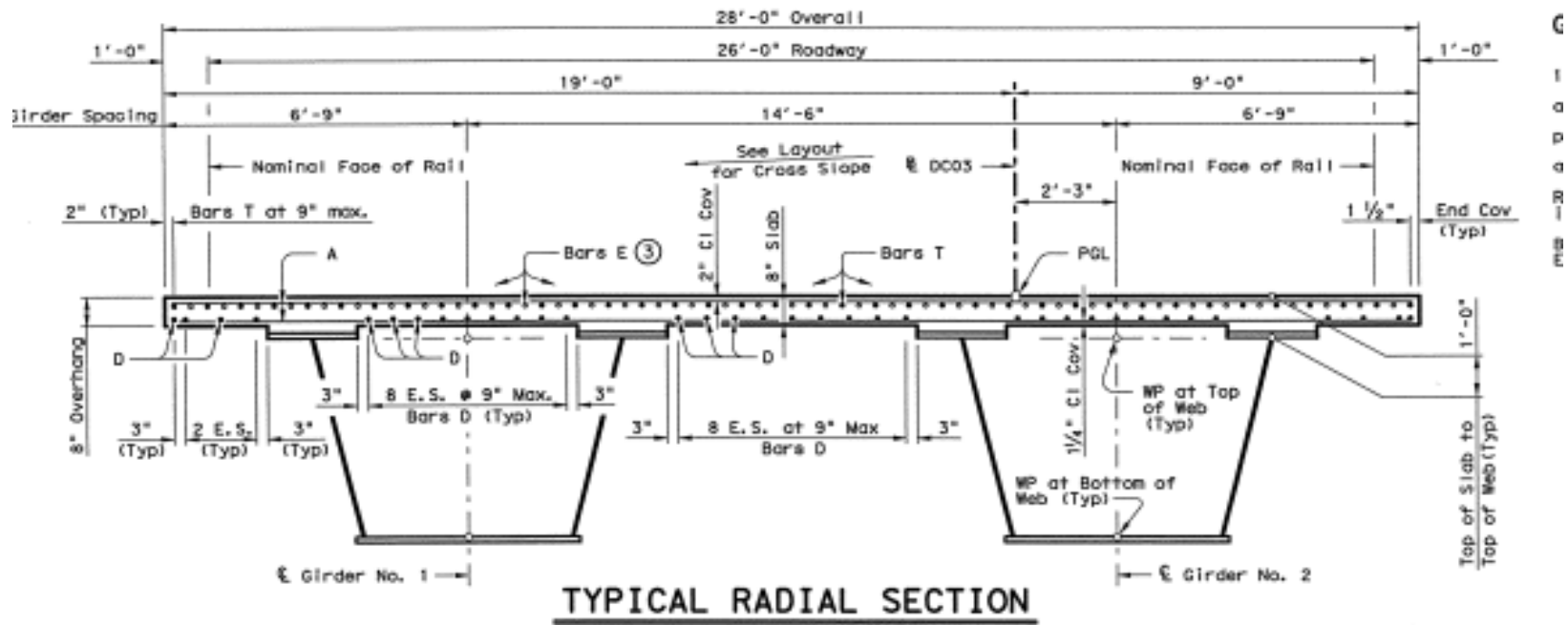
GIRDER ELEVATION

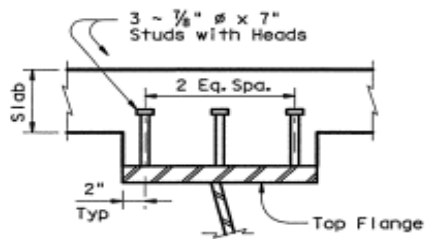
All Web Plates are 60" deep except at dapped ends. Web depths are measured perpendicular to flanges. All Top Flange Plates are 22" wide. All Bottom Flange Plates are 70" wide except at dapped ends.

HS20 LOADING

NO.	DATE	REVISION	APPROVED

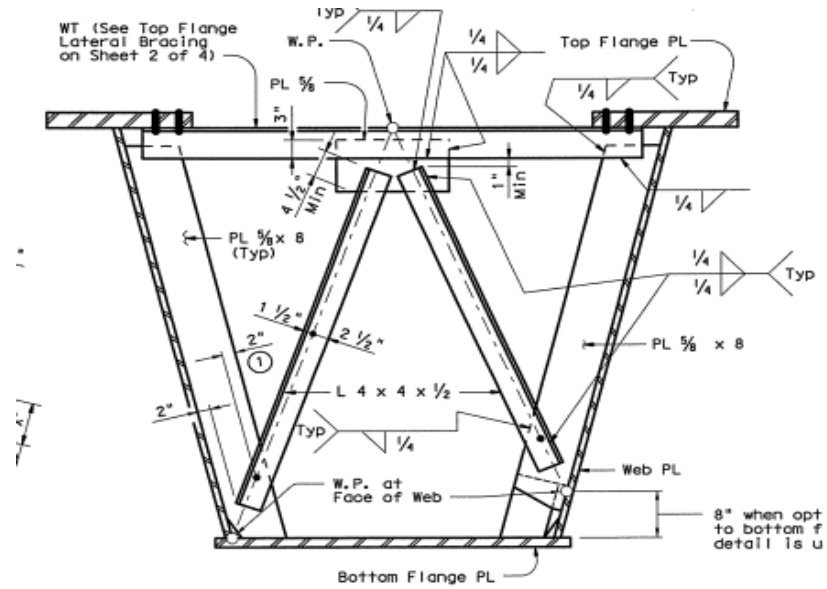
HDR HDR Engineering, Inc.
17111 Preston Road, Suite 200
Dallas, Texas 75248-1229





SHEAR CONNECTOR STUD DETAIL

Studs shall be Electric arc end-welded to the flanges with complete fusion. (See Span details for spacing along girder.)

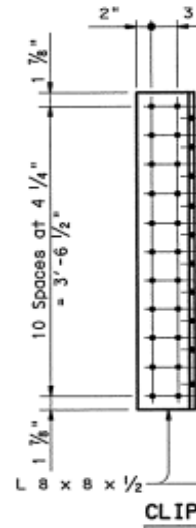
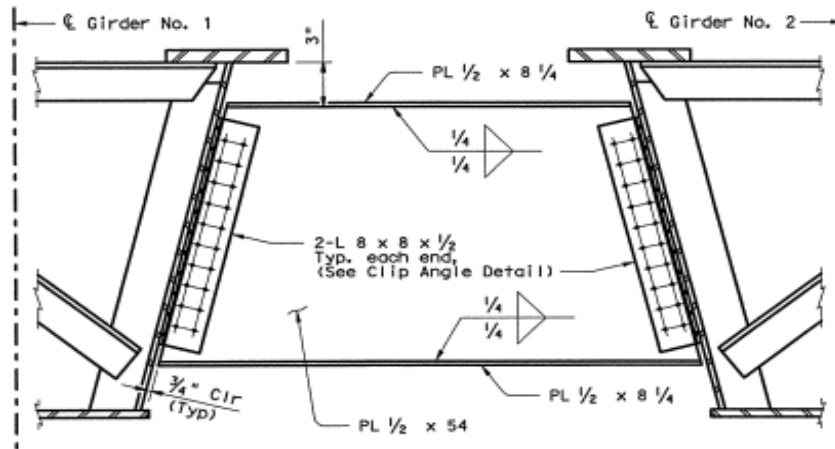


TYPICAL SECTION AT INTERNAL INTERMEDIATE DIAPHRAGM

To be fully installed in the shop.



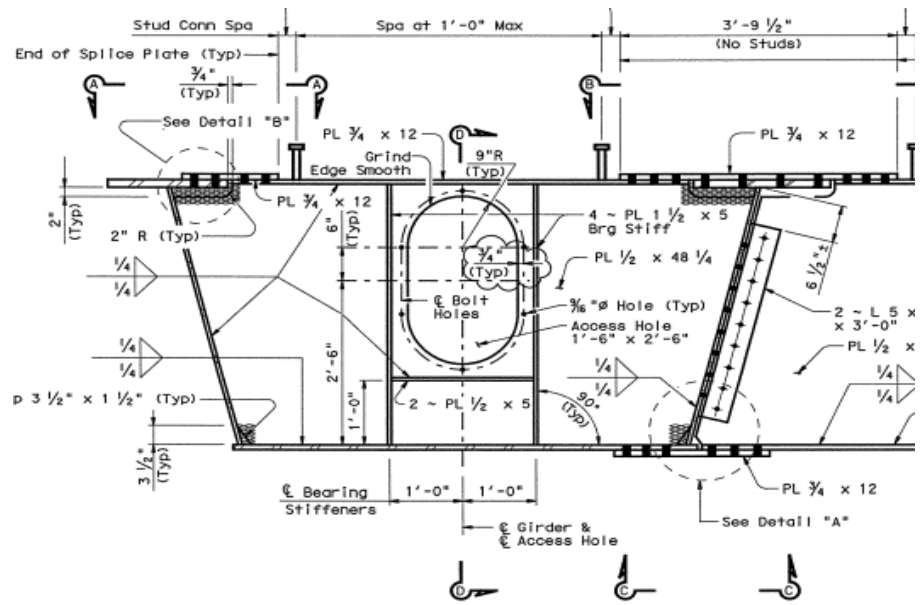
Note: Apply silicon bead uniformly around edge of access hole cover plate before securing



TYPICAL SECTION

CLIP

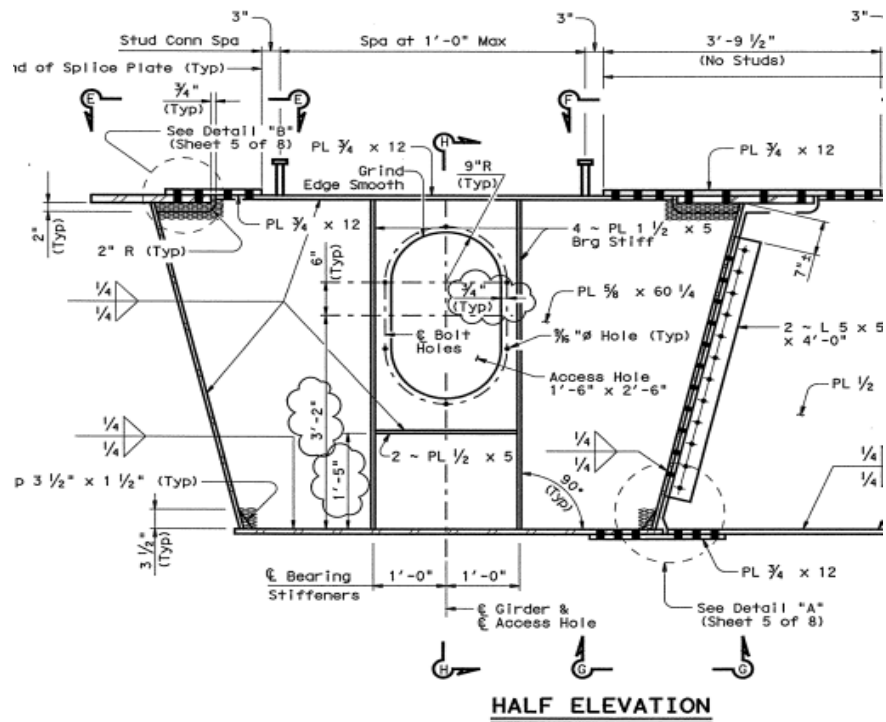
EXTERNAL INTERMEDIATE DIAPHRAGM



HALF ELEVATION

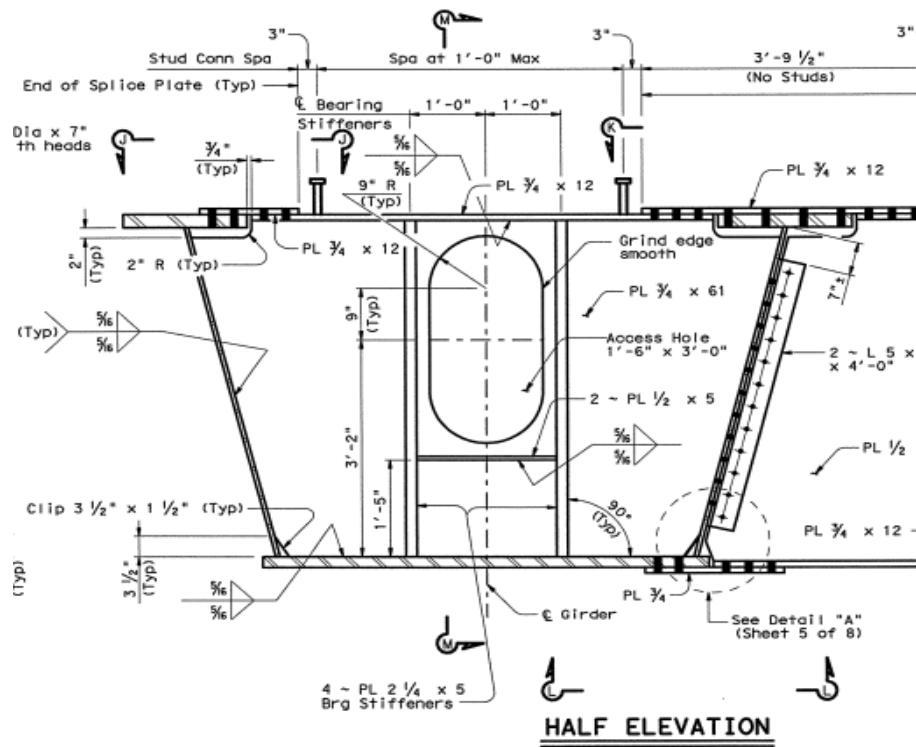
TRAGM DETAILS - BENT NO. 1

TRAPEZOIDAL STEEL BOX GIRDER DETAILS
 and Diaphragm Access Hole Cover Plate
 to be installed at each End Diaphragm

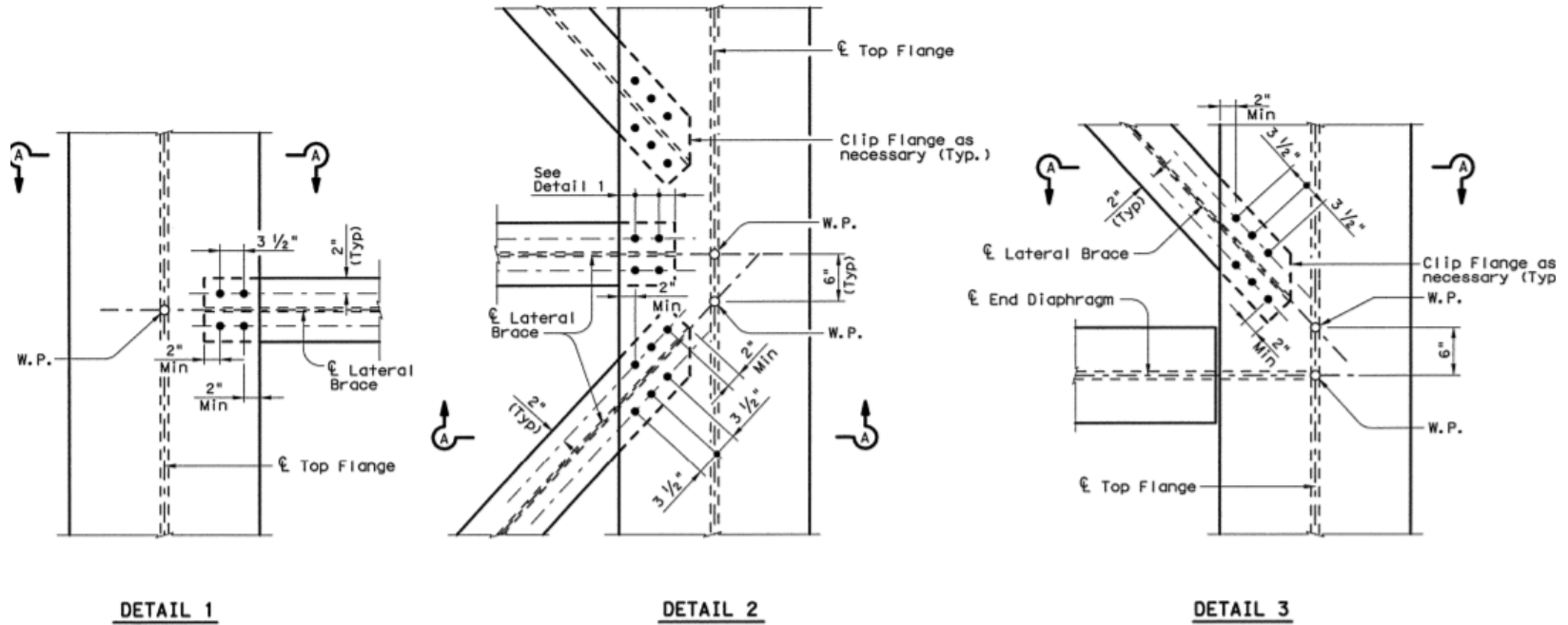


TRAP DETAILS - BENT NO. 4

TRAPEZOIDAL STEEL BOX GIRDER DETAILS
 Diaphragm Access Hole Cover Plate
 Installed at each End Diaphragm



INTERIOR BENT DIAPHRAGM DETAILS



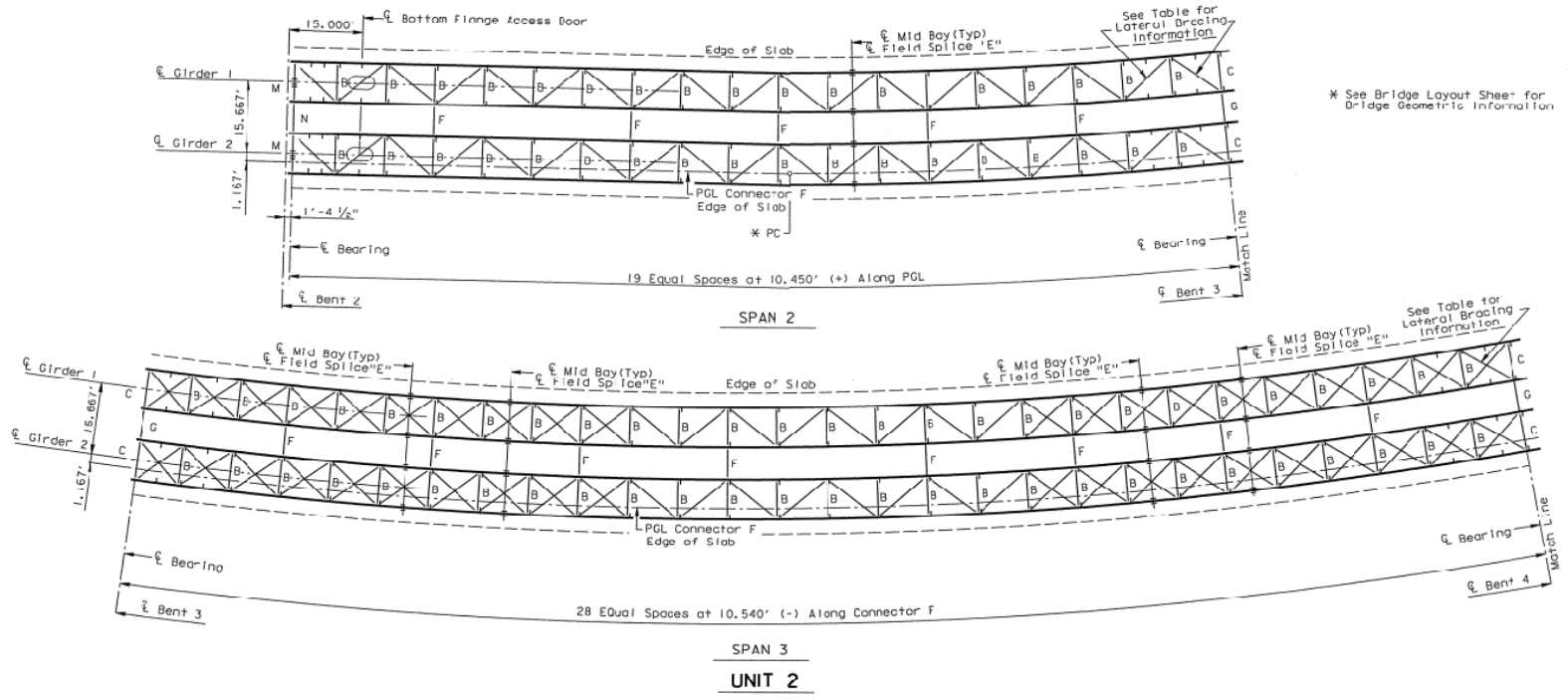
LATERAL BRACING CONNECTION DETAILS

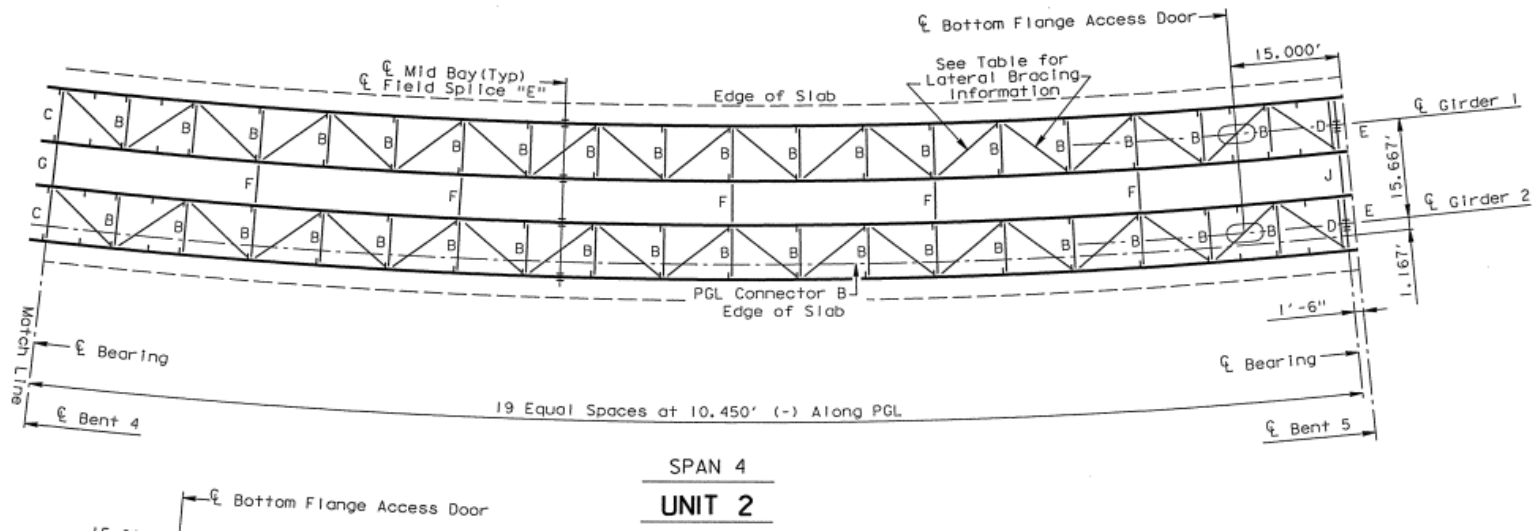
Provide 1/16" Dia Hole in Top Flange PL and in WT Shape at spacing shown for 1" Dia A325 Type 3 Bolt with one Hardened Washer each (typ.)

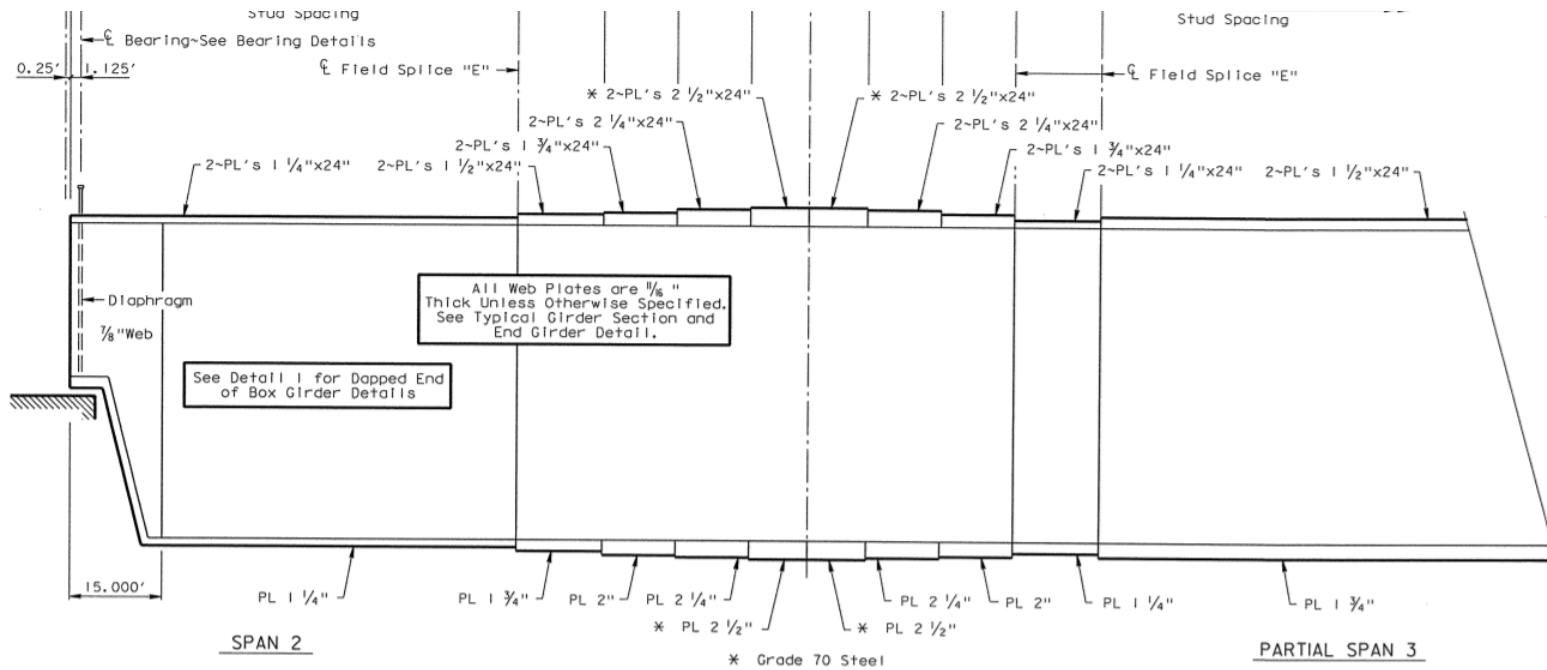
LOCATION	DIAGONAL BRACE	HORIZONTAL STRUT
DC02 - 326.00' UNIT	WT 7 X 30.5	WT 5 X 16.5
DC03 - 490.00' UNIT	WT 7 X 21.5	WT 5 X 16.5
DC03 - 360.00' UNIT	WT 7 X 34	WT 5 X 16.5
DC03 - 310.00' UNIT	WT 7 X 24	WT 5 X 16.5
DC03 - 340.00' UNIT	WT 7 X 34	WT 5 X 16.5
DC04 - 345.00' UNIT	WT 7 X 21.5	WT 5 X 16.5
DC04 - 330.00' UNIT	WT 7 X 21.5	WT 5 X 16.5
DC04 - 663.00' UNIT	WT 7 X 30.5	WT 5 X 16.5

LATERAL BRACING MEMBER SIZES

BRIDGE 15: 12-102-0271-06-689

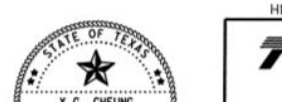
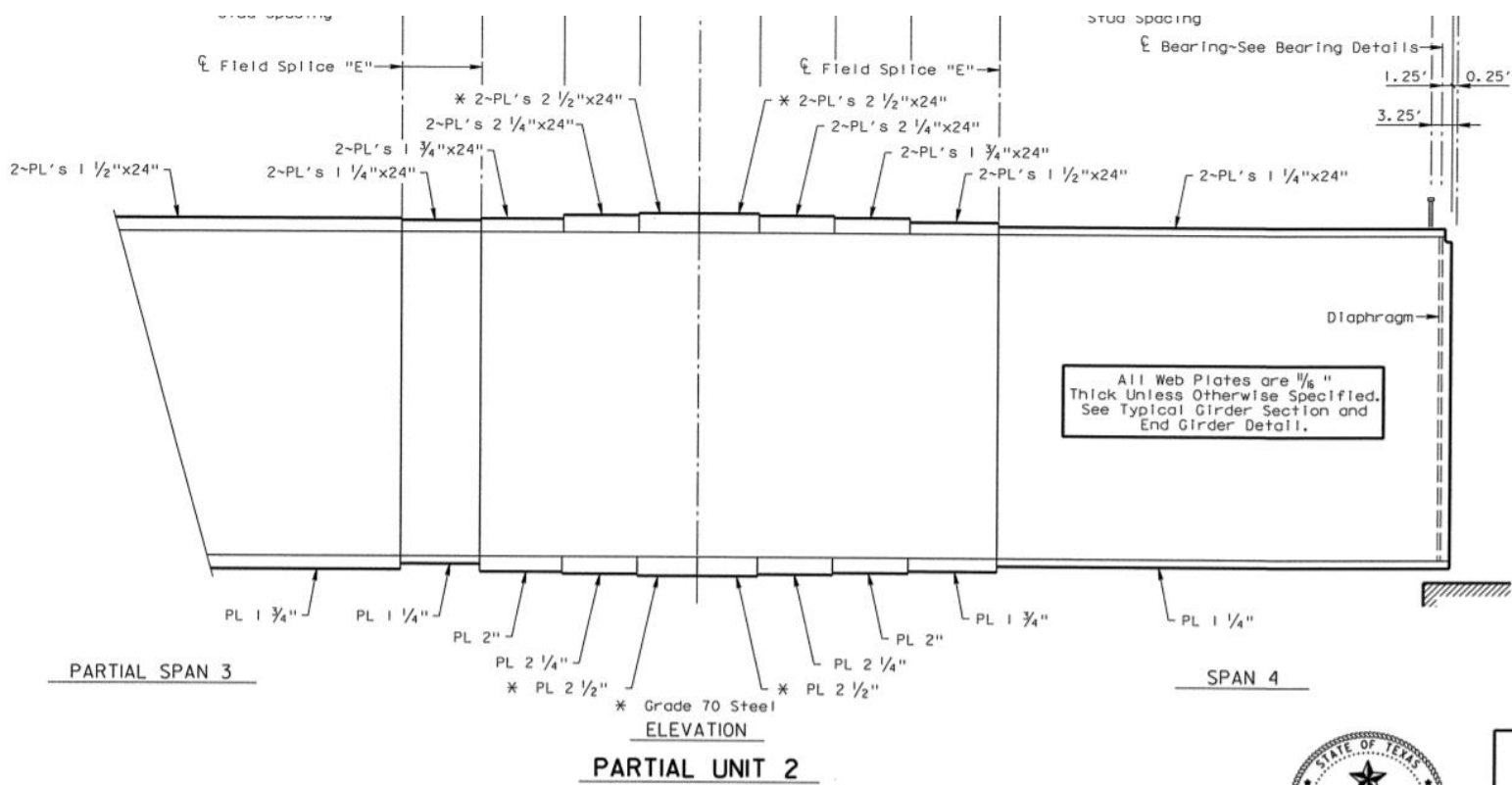


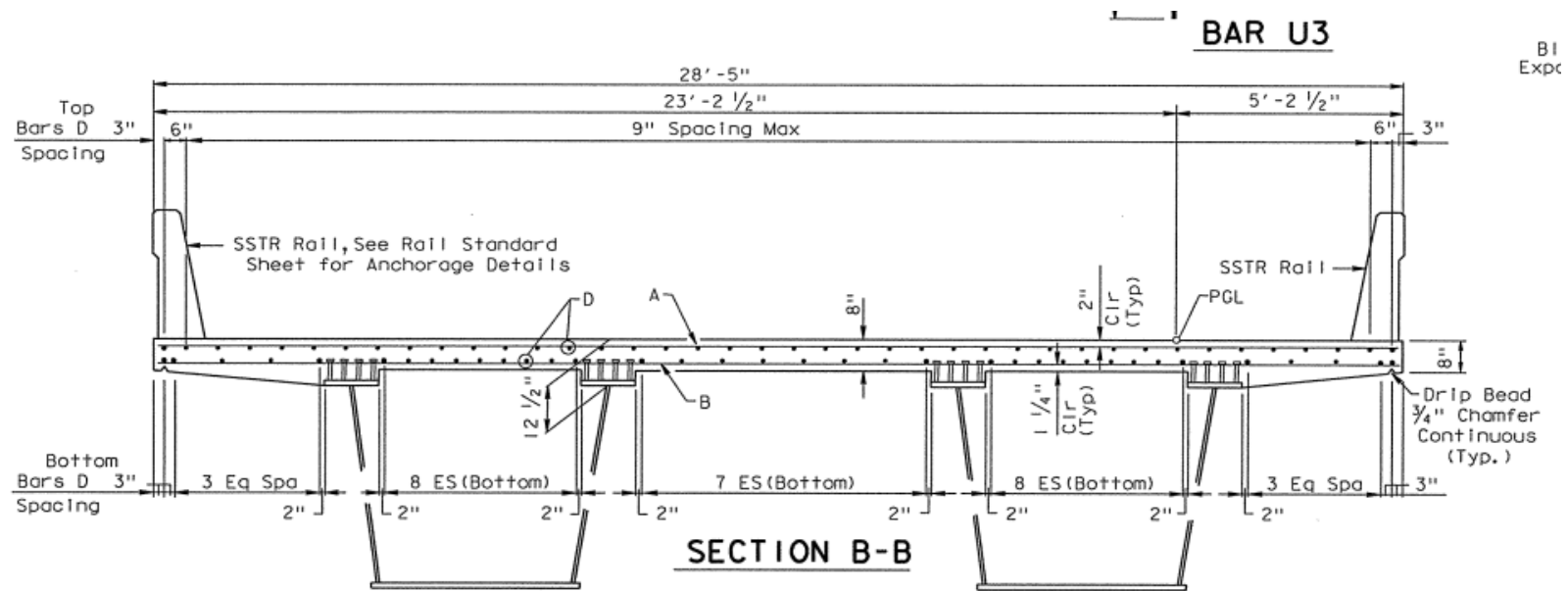


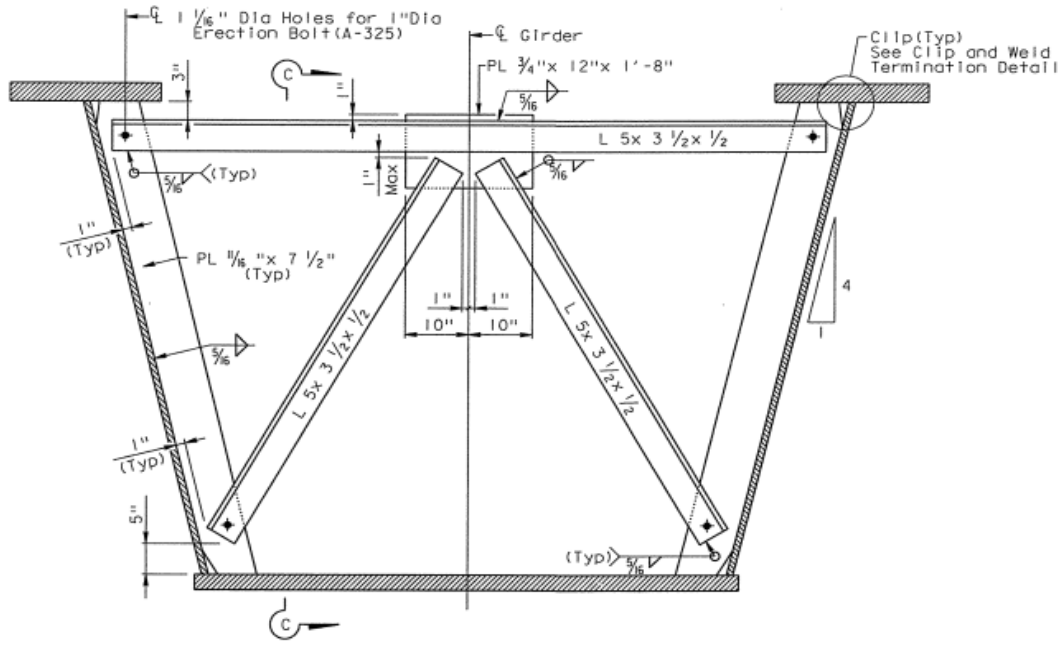


* Grade 70 Steel
 ELEVATION
PARTIAL UNIT 2

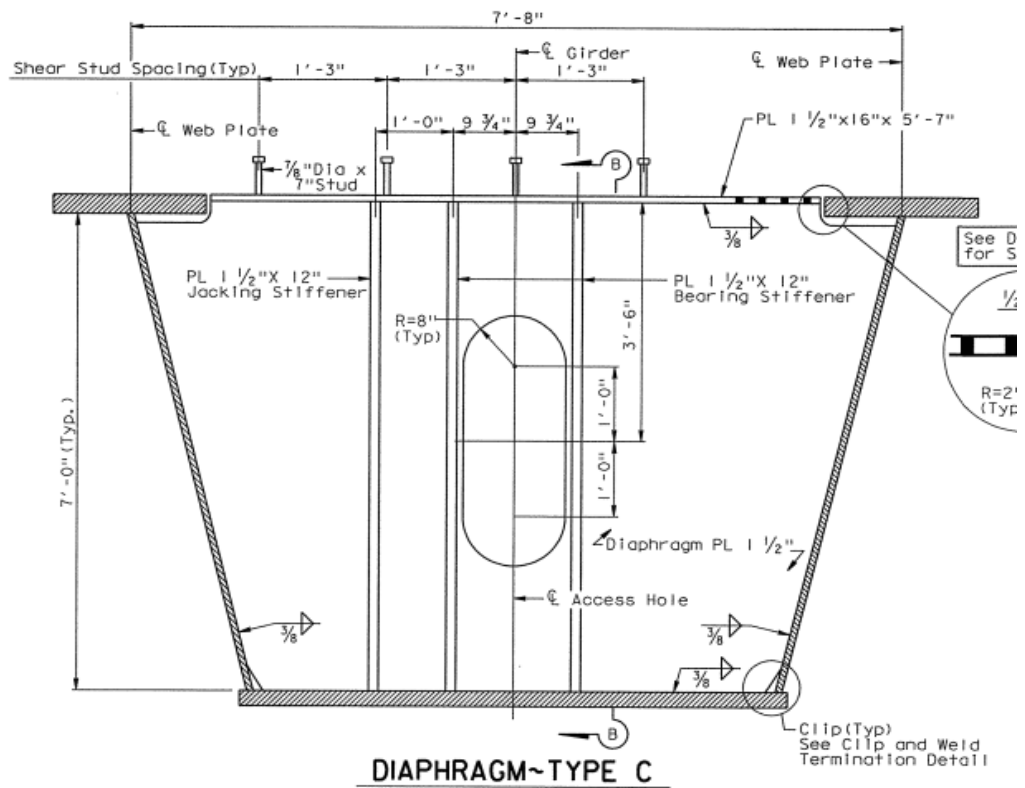


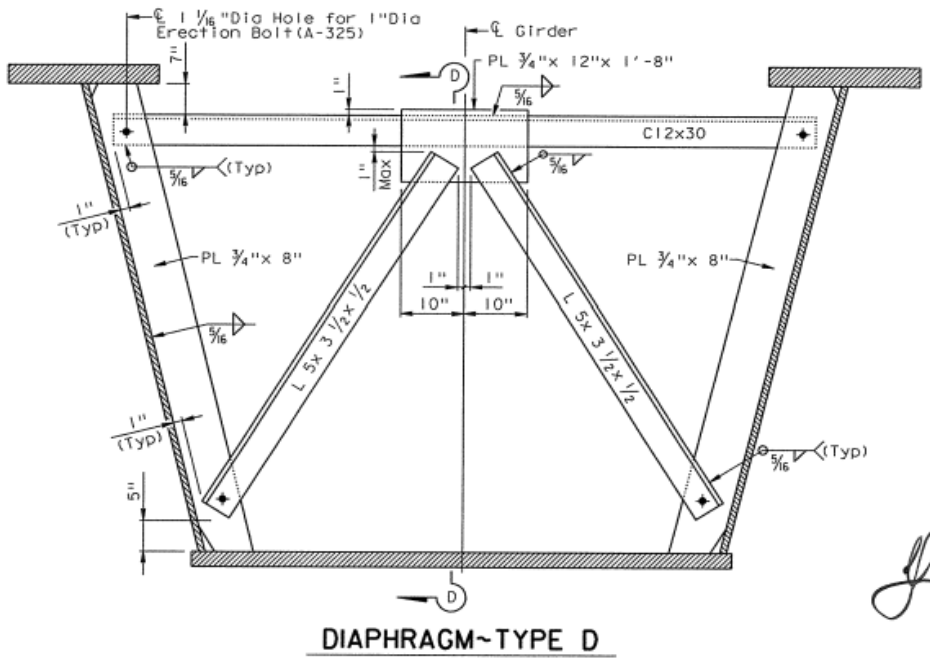


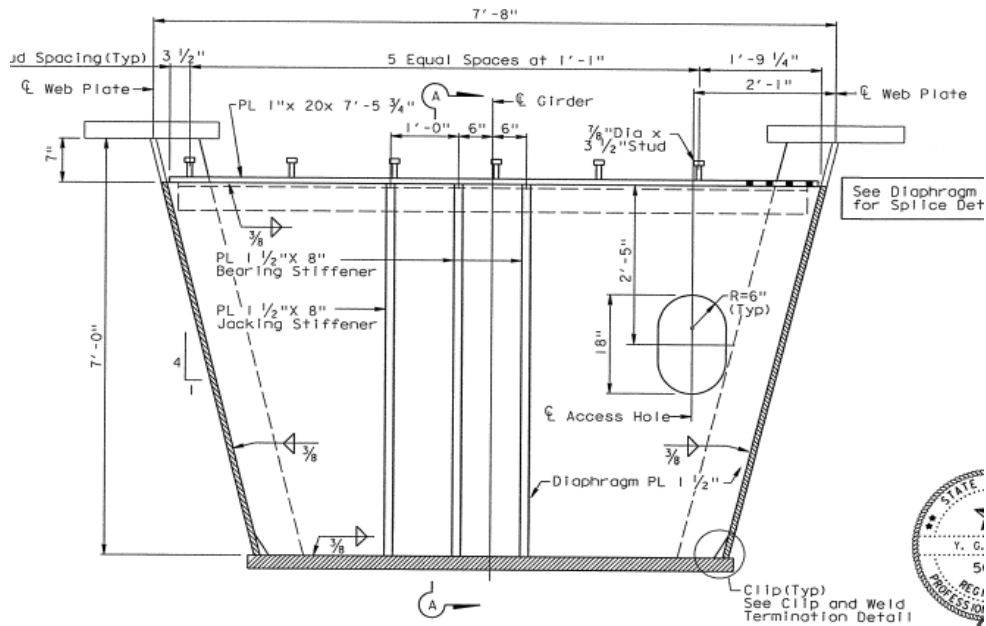




DIAPHRAGM~TYPE B





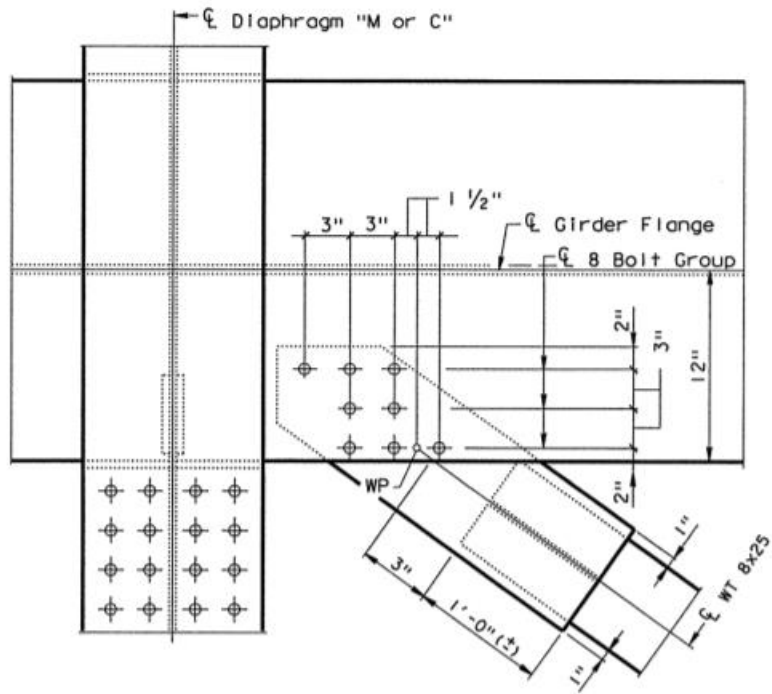


ELEVATION

DIAPHRAGM~TYPE E



J.G. Clark
4/4/1



LATERAL BRACING CONNECTION DETAIL "4"

APPENDIX B
GRILLAGE HINGE PROPERTIES

Bridge 1: Hinge and Section Data

	Long. Ext. 1.1		Long. Int. 1.1		Long. Ext. 2.1		Long. Int. 2.1	
	<i>M</i>	<i>C</i>	<i>M</i>	<i>C</i>	<i>M</i>	<i>C</i>	<i>M</i>	<i>C</i>
Positive SF	325620	5.8E-05	301909	0.00019	409992	6E-05	382836	0.0002
Negative SF	198418	5.8E-05	203118	6.4E-05	267269	6E-05	272043	6.7E-05
Normalized Moment Curvature	-1.36	-35	-1.38	-35	-1.36	-35	-1.38	-35
	-1.36	-23	-1.38	-23	-1.36	-23	-1.38	-23
	-1	-1	-1	-1	-1	-1	-1	-1
	-0.75	-0.56	-0.8	-0.56	-0.7	-0.56	-0.8	-0.56
	0	0	0	0	0	0	0	0
	0.92	0.56	0.87	0.19	0.95	0.56	0.91	0.25
	1	1	1	1	1	1	1	1
	1	3	1	3	1	3	1	3
1	13	1	13	1	13	1	13	
	Frac. Ext. 1.1		Frac. Int. 1.1		Trans.		Trans.End	
	<i>M</i>	<i>C</i>	<i>M</i>	<i>C</i>	<i>M</i>	<i>C</i>	<i>M</i>	<i>C</i>
Positive SF	12736	1.14E-04	1730	2.42E-03	1910	0.00187	371	0.00187
Negative SF	1915	5.15E-04	2066	5.37E-04	1640	0.00187	316	0.00187
Normalized Moment Curvature	-1	-35	-1	-20	-1	-30	-1	-30
	-1	-23	-1	-10	-1	-22	-1	-22
	-1	-1	-1	-5	-1	-1	-1	-1
	-0.91	-0.22	-1	-1	-0.76	-0.22	-0.76	-0.22
	0	0	0	0	0	0	0	0
	1	1	0.88	0.22	0.76	0.22	0.77	0.14
	1	3	1	1	1	1	1	1
	1	5	1	5	1	3	1	3
1	15	1	15	1	13	1	13	

Note: M=Moment (kip-in.) and C=Curvature (1/in.)

Section	Start (ft)	End (ft)
1.1	0	47
2.1	47	166
1.1	166	220

Bridge 2: Hinge and Section Data

	Long. Ext. 1.1		Long. Int. 1.1		Frac. Ext. 1.1		Frac. Int. 1.1	
	<i>M</i>	<i>C</i>	<i>M</i>	<i>C</i>	<i>M</i>	<i>C</i>	<i>M</i>	<i>C</i>
Positive SF	250798	5.96E-05	221238	0.000154	13209	1.05E-04	1130	2.45E-3
Negative SF	144085	5.96E-05	142720	6.91E-05	1844	7.36E-04	1611	5.44E-4
Normalized Moment Curvature	-1.35	-35	-1.38	-35	-1	-35	-1	-20
	-1.35	-25	-1.38	-25	-1	-22	-1	-10
	-1	-1	-1	-1	-1	-1	-1	-1
	-0.72	-0.56	-0.8	-0.56	-0.76	-0.36	-1	-1
	0	0	0	0	0	0	0	0
	0.91	0.56	0.955	0.45	1	1	0.98	0.56
	1	1	1	1	1	3	1	1
	1	3	1	3	1	5	1	5
1	13	1	13	1	15	1	15	
	Trans.		Trans.End					
	<i>M</i>	<i>C</i>	<i>M</i>	<i>C</i>				
Positive SF	1970	0.00168	1367	0.00168				
Negative SF	1598	0.00168	1104	0.00168				
Normalized Moment Curvature	-1.1	-25	-1.1	-25				
	-1.1	-15	-1.1	-15				
	-1	-1	-1	-1				
	-0.76	-0.22	-0.76	-0.22				
	0	0	0	0				
	0.76	0.22	0.76	0.22				
	1	1	1	1				
	1	3	1	3				
1	13	1	13					

Note: M=Moment (kip-in.) and C=Curvature (1/in.)

Section	Start (ft)	End (ft)
<i>1.1</i>	0	115

Bridge 3: Hinge and Section Data

	Long. Ext. 1.1		Long. Int. 1.1		Long. Ext. 2.1		Long. Int. 2.1	
	<i>M</i>	<i>C</i>	<i>M</i>	<i>C</i>	<i>M</i>	<i>C</i>	<i>M</i>	<i>C</i>
Positive SF	469639	7.72E-05	454024	0.000203	556185	7.86E-05	539178	0.00016
Negative SF	303757	4.96E-05	314564	5.22E-05	407572	5.05E-05	417493	5.3E-05
Normalized Moment Curvature	-1.36	-35	-1.37	-35	-1.37	-35	-1.38	-35
	-1.36	-23	-1.37	-23	-1.37	-23	-1.38	-23
	-1	-1	-1	-1	-1	-1	-1	-1
	-0.75	-0.56	-0.8	-0.56	-0.7	-0.56	-0.8	-0.56
	0	0	0	0	0	0	0	0
	0.88	0.36	0.85	0.14	0.91	0.36	0.96	0.33
	1	1	1	1	1	1	1	1
	1	3	1	3	1	3	1	3
1	13	1	13	1	13	1	13	
	Long. Ext. 3.1		Long. Int. 3.1		Frac. Ext. 3.1		Frac. Int. 3.1	
	<i>M</i>	<i>C</i>	<i>M</i>	<i>C</i>	<i>M</i>	<i>C</i>	<i>M</i>	<i>C</i>
Positive SF	720943	5.36E-05	707906	0.000125	13389	1.30E-4	2978	1.99E-3
Negative SF	528265	5.36E-05	540368	5.62E-05	2402	5.84E-4	2835	4.43E-4
Normalized Moment Curvature	-1.37	-35	-1.38	-35	-1	-35	-1	-20
	-1.37	-23	-1.38	-23	-1	-23	-1	-10
	-1	-1	-1	-1	-1	-1	-1	-3
	-0.7	-0.56	-0.8	-0.56	-0.9	-0.22	-1	-1
	0	0	0	0	0	0	0	0
	0.91	0.36	0.91	0.25	1	1	0.86	0.22
	1	1	1	1	1	3	1	1
	1	3	1	3	1	5	1	5
1	13	1	13	1	15	1	15	

Note: M=Moment (kip-in.) and C=Curvature (1/in.)

	Trans		Trans End	
	<i>M</i>	<i>C</i>	<i>M</i>	<i>C</i>
Positive SF	2325	0.002166	2166	0.002166
Negative SF	1937	0.002166	1814	0.002166
Normalized Moment Curvature	-1.12	-30	-1.15	-30
	-1.12	-13	-1.15	-20
	-1	-1	-1	-1
	-0.76	-0.22	-0.76	-0.22
	0	0	0	0
	0.77	0.14	0.77	0.14
	1	1	1	1
	1	3	1	3
	1	13	1	13

Note: M=Moment (kip-in.) and C=Curvature (1/in.)

Section	Start (ft)	End (ft)
<i>1.1</i>	0	17
<i>2.1</i>	17	38
<i>3.1</i>	38	185
<i>2.1</i>	185	206
<i>1.1</i>	206	230

Bridge 4: Hinge and Section Data

	Long. Ext. 1.1		Long. Int. 1.1		Long. Ext. 2.2		Long. Int. 2.2	
	<i>M</i>	<i>C</i>	<i>M</i>	<i>C</i>	<i>M</i>	<i>C</i>	<i>M</i>	<i>C</i>
Positive SF	190121	8.16E-05	163477	0.000285	265333	4.94E-05	242505	0.00016
Negative SF	97566	8.16E-05	102225	9.49E-05	143129	8.89E-05	147628	0.0001
Normalized Moment Curvature	-1.35	-35	-1.35	-35	-1.4	-30	-1.4	-30
	-1.35	-25	-1.35	-25	-1.4	-20	-1.4	-20
	-1	-1	-1	-1	-1	-1	-1	-1
	-0.7	-0.56	-0.8	-0.56	-0.86	-0.56	-0.92	-0.56
	0	0	0	0	0	0	0	0
	0.95	0.56	0.89	0.19	0.54	0.4	0.94	0.36
	1	1	1	1	1	1	1	1
	1	3	1	3	1	3	1	3
1	13	1	13	1	13	1	13	
	Long. Ext. 3.2		Long. Int. 3.2		Frac. Ext. 1.1		Frac. Int. 1.1	
	<i>M</i>	<i>C</i>	<i>M</i>	<i>C</i>	<i>M</i>	<i>C</i>	<i>M</i>	<i>C</i>
Positive SF	269552	8.63E-05	248898	0.00022	11005	1.04E-4	1361	2.26E-3
Negative SF	199102	8.63E-05	201214	9.89E-05	1607	4.66E-4	1740	5.03E-4
Normalized Moment Curvature	-1.35	-35	-1.35	-35	-1	-35	-1	-20
	-1.35	-25	-1.35	-25	-1	-25	-1	-10
	-1	-1	-1	-1	-1	-1	-1	-3
	-0.7	-0.56	-0.89	-0.56	-0.92	-0.22	-1	-1
	0	0	0	0	0	0	0	0
	0.95	0.56	0.93	0.25	1	1	1	1
	1	1	1	1	1	3	1	3
	1	3	1	3	1	5	1	5
1	13	1	13	1	15	1	15	

Note: M=Moment (kip-in.) and C=Curvature (1/in.)

	Trans		Trans End 1		Trans End 2		Trans Pier	
	<i>M</i>	<i>C</i>	<i>M</i>	<i>C</i>	<i>M</i>	<i>C</i>	<i>M</i>	<i>C</i>
Positive SF	2107	0.00152	1971	0.00152	1325	0.00152	3400	0.00152
Negative SF	1745	0.00152	1633	0.00152	1094	0.00152	2822	0.00152
Normalized Moment Curvature	-1.2	-25	-1.2	-25	-1.2	-25	-1.2	-25
	-1.2	-15	-1.2	-15	-1.2	-15	-1.2	-15
	-1	-1	-1	-1	-1	-1	-1	-1
	-0.76	-0.22	-0.76	-0.22	-0.76	-0.22	-0.76	-0.22
	0	0	0	0	0	0	0	0
	0.76	0.22	0.76	0.22	0.76	0.22	0.76	0.22
	1	1	1	1	1	1	1	1
	1	3	1	3	1	3	1	3
1	13	1	13	1	13	1	13	

Note: M=Moment (kip-in.) and C=Curvature (1/in.)

Section	Start (ft)	End (ft)
<i>1.1</i>	0	80
<i>2.2</i>	80	108
<i>3.2</i>	108	154
<i>2.2</i>	154	182
<i>1.1</i>	182	260

Bridge 5: Hinge and Section Data

	Long. Ext. 1.1		Long. Int. 1.1		Long. Ext. 2.2		Long. Int. 2.2	
	<i>M</i>	<i>C</i>	<i>M</i>	<i>C</i>	<i>M</i>	<i>C</i>	<i>M</i>	<i>C</i>
Positive SF	130422	0.000132	126415	0.000343	177826	0.000141	175804	0.000284
Negative SF	80979	8.46E-05	84913	8.83E-05	115300	9.08E-05	120784	9.48E-05
Normalized Moment Curvature	-1.35	-35	-1.35	-35	-1.35	-35	-1.35	-35
	-1.35	-25	-1.35	-25	-1.35	-25	-1.35	-25
	-1	-1	-1	-1	-1	-1	-1	-1
	-0.7	-0.56	-0.8	-0.56	-0.7	-0.56	-0.8	-0.56
	0	0	0	0	0	0	0	0
	0.97	0.64	0.85	0.14	0.936	0.36	0.85	0.14
	1	1	1	1	1	1	1	1
	1	3	1	3	1	3	1	3
	1	13	1	13	1	13	1	13
	Long. Ext. 3.2		Long. Int. 3.2		Long. Ext. 4.2		Long. Int. 4.2	
	<i>M</i>	<i>C</i>	<i>M</i>	<i>C</i>	<i>M</i>	<i>C</i>	<i>M</i>	<i>C</i>
Positive SF	180799	0.000138	178975	0.00027	204632	0.000139	203853	0.000278
Negative SF	136766	8.88E-05	139570	9.23E-05	161921	8.93E-05	164301	9.26E-05
Normalized Moment Curvature	-1.35	-35	-1.38	-35	-1.4	-35	-1.42	-35
	-1.35	-25	-1.38	-25	-1.4	-25	-1.42	-25
	-1	-1	-1	-1	-1	-1	-1	-1
	-0.7	-0.56	-0.8	-0.56	-0.7	-0.56	-0.8	-0.56
	0	0	0	0	0	0	0	0
	0.936	0.36	0.85	0.14	0.936	0.36	0.85	0.14
	1	1	1	1	1	1	1	1
	1	3	1	3	1	3	1	3
	1	13	1	13	1	13	1	13

Note: M=Moment (kip-in.) and C=Curvature (1/in.)

	Frac. Ext. 1.1		Frac. Int. 1.1		Trans/Trans Pier		Trans End 1&2	
	<i>M</i>	<i>C</i>	<i>M</i>	<i>C</i>	<i>M</i>	<i>C</i>	<i>M</i>	<i>C</i>
Positive SF	5557	2.32E-4	1612	2.61E-3	1876	0.00168	890	0.00168
Negative SF	1615	5.81E-4	1868	5.80E-4	1513	0.00168	714	0.00168
Normalized Moment Curvature	-1	-35	-1	-20	-1.1	-25	-1.1	-25
	-1	-20	-1	-10	-1.1	-15	-1.1	-15
	-1	-1	-1	-1	-1	-1	-1	-1
	-0.83	-0.4	-1	-1	-0.76	-0.22	-0.76	-0.22
	0	0	0	0	0	0	0	0
	1	1	0.84	0.22	0.76	0.22	0.76	0.22
	1	3	1	1	1	1	1	1
	1	5	1	5	1	3	1	3
1	15	1	15	1	13	1	13	

Note: M=Moment (kip-in.) and C=Curvature (1/in.)

Section	Start (ft)	End (ft)
<i>1.1</i>	0	91
<i>2.2</i>	91	112
<i>3.2</i>	112	126
<i>4.2</i>	126	147
<i>3.2</i>	147	161
<i>2.2</i>	161	182
<i>1.1</i>	182	280

Bridge 6: Hinge and Section Data

	Long. Ext. 1.1		Long. Int. 1.1		Long. Ext. 2.2		Long. Int. 2.2	
	<i>M</i>	<i>C</i>	<i>M</i>	<i>C</i>	<i>M</i>	<i>C</i>	<i>M</i>	<i>C</i>
Positive SF	326511	6.38E-05	300556	0.000159	473215	7.08E-05	438043	8.05E-05
Negative SF	175770	6.38E-05	178676	7.16E-05	226048	7.08E-05	232720	8.05E-05
Normalized Moment Curvature	-1.37	-35	-1.38	-35	-1.4	-35	-1.45	-35
	-1.37	-25	-1.38	-25	-1.4	-20	-1.45	-17
	-1	-1	-1	-1	-1	-1	-1	-1
	-0.7	-0.56	-0.8	-0.56	-0.7	-0.56	-0.8	-0.56
	0	0	0	0	0	0	0	0
	0.97	0.64	0.85	0.14	0.936	0.36	0.85	0.14
	1	1	1	1	1	1	1	1
	1	3	1	3	1	3	1	3
1	13	1	13	1	13	1	13	
	Long. Ext. 3.2		Long. Int. 3.2		Frac. Ext. 1.1		Frac. Int. 1.1	
	<i>M</i>	<i>C</i>	<i>M</i>	<i>C</i>	<i>M</i>	<i>C</i>	<i>M</i>	<i>C</i>
Positive SF	481552	6.91E-05	451631	0.000121	15849	1.23E-4	1915	2.55E-3
Negative SF	294883	6.91E-05	302235	7.76E-05	2130	5.55E-4	1139	3.96E-3
Normalized Moment Curvature	-1.38	-35	-1.36	-35	-1	-35	-1	-20
	-1.38	-20	-1.36	-19	-1	-20	-1	-12
	-1	-1	-1	-1	-1	-1	-1	-2
	-0.7	-0.56	-0.8	-0.56	-0.83	-0.56	-1	-1
	0	0	0	0	0	0	0	0
	0.936	0.36	0.85	0.14	1	1	0.97	0.56
	1	1	1	1	1	1	1	1
	1	3	1	3	1	5	1	5
1	13	1	13	1	15	1	15	

Note: M=Moment (kip-in.) and C=Curvature (1/in.)

	Trans/Trans Pier		Trans End 1&2	
	<i>M</i>	<i>C</i>	<i>M</i>	<i>C</i>
Positive SF	2422	0.0016	1211	0.0016
Negative SF	2023	0.0016	1011	0.0016
Normalized Moment Curvature	-1.15	-25	-1.15	-25
	-1.15	-15	-1.15	-15
	-1	-1	-1	-1
	-0.76	-0.22	-0.76	-0.22
	0	0	0	0
	0.76	0.22	0.76	0.22
	1	1	1	1
	1	3	1	3
	1	13	1	13

Note: M=Moment (kip-in.) and C=Curvature (1/in.)

Section	Start (ft)	End (ft)
<i>1.1</i>	0	98
<i>2.2</i>	98	119
<i>3.2</i>	119	154
<i>2.2</i>	154	175
<i>1.1</i>	175	280

Bridge 7: Hinge and Section Data

	Long. Ext. 1.1		Long. Int. 1.1		Long. Ext. 2.1		Long. Int. 2.1	
	<i>M</i>	<i>C</i>	<i>M</i>	<i>C</i>	<i>M</i>	<i>C</i>	<i>M</i>	<i>C</i>
Positive SF	213076	7.09E-05	188227	0.000244	354649	7.85E-05	323880	0.000141
Negative SF	121565	7.09E-05	120700	8.12E-05	226366	7.85E-05	225805	9.03E-05
Normalized Moment Curvature	-1.35	-35	-1.37	-35	-1.35	-35	-1.35	-35
	-1.35	-25	-1.37	-25	-1.35	-25	-1.35	-20
	-1	-1	-1	-1	-1	-1	-1	-1
	-0.7	-0.56	-0.8	-0.56	-0.7	-0.56	-0.8	-0.56
	0	0	0	0	0	0	0	0
	0.97	0.64	0.87	0.19	0.936	0.36	0.93	0.36
	1	1	1	1	1	1	1	1
	1	3	1	3	1	3	1	3
	1	13	1	13	1	13	1	13
	Long. Ext. 3.1		Long. Int. 3.1		Long. Ext. 3.2		Long. Int. 3.2	
	<i>M</i>	<i>C</i>	<i>M</i>	<i>C</i>	<i>M</i>	<i>C</i>	<i>M</i>	<i>C</i>
Positive SF	297884	7.57E-05	265857	0.000194	298366	7.57E-05	266127	0.000136
Negative SF	180976	7.57E-05	179504	8.71E-05	187592	7.57E-05	187181	8.71E-05
Normalized Moment Curvature	-1.35	-35	-1.38	-35	-1.35	-35	-1.38	-35
	-1.35	-25	-1.38	-25	-1.35	-25	-1.38	-21
	-1	-1	-1	-1	-1	-1	-1	-1
	-0.7	-0.56	-0.8	-0.56	-0.7	-0.56	-0.8	-0.56
	0	0	0	0	0	0	0	0
	0.936	0.36	0.977	0.45	0.936	0.36	0.977	0.45
	1	1	1	1	1	1	1	1
	1	3	1	3	1	3	1	3
	1	13	1	13	1	13	1	13

Note: M=Moment (kip-in.) and C=Curvature (1/in.)

	Long. Ext. 4.1		Long. Int. 4.1		Long. Ext. 4.2		Long. Int. 4.2	
	<i>M</i>	<i>C</i>	<i>M</i>	<i>C</i>	<i>M</i>	<i>C</i>	<i>M</i>	<i>C</i>
Positive SF	297327	7.47E-05	266825	0.000187	297795	7.47E-05	268404	0.000187
Negative SF	210110	7.47E-05	209302	8.43E-05	214882	7.47E-05	214860	8.43E-05
Normalized Moment Curvature	-1.35	-35	-1.36	-35	-1.35	-35	-1.37	-35
	-1.35	-25	-1.36	-25	-1.35	-25	-1.37	-25
	-1	-1	-1	-1	-1	-1	-1	-1
	-0.7	-0.56	-0.8	-0.56	-0.7	-0.56	-0.8	-0.56
	0	0	0	0	0	0	0	0
	0.936	0.36	0.85	0.14	0.936	0.36	0.85	0.14
	1	1	1	1	1	1	1	1
	1	3	1	3	1	3	1	3
	1	13	1	13	1	13	1	13
	Long. Ext. 5.2		Long. Int. 5.2		Long. Ext. 6.1		Long. Int. 6.1	
	<i>M</i>	<i>C</i>	<i>M</i>	<i>C</i>	<i>M</i>	<i>C</i>	<i>M</i>	<i>C</i>
Positive SF	437012	7.92E-05	409104	0.000138	225491	7.18E-05	198753	0.000183
Negative SF	355101	7.92E-05	354835	8.86E-05	127166	7.18E-05	126139	8.25E-05
Normalized Moment Curvature	-1.36	-35	-1.38	-35	-1.36	-35	-1.38	-35
	-1.36	-25	-1.38	-25	-1.36	-25	-1.38	-25
	-1	-1	-1	-1	-1	-1	-1	-1
	-0.7	-0.56	-0.8	-0.56	-0.7	-0.56	-0.8	-0.56
	0	0	0	0	0	0	0	0
	0.936	0.36	0.85	0.14	0.936	0.36	0.88	0.25
	1	1	1	1	1	1	1	1
	1	3	1	3	1	3	1	3
	1	13	1	13	1	13	1	13

Note: M=Moment (kip-in.) and C=Curvature (1/in.)

	Frac. Ext. 2.1		Frac. Int. 2.1		Frac. Ext. 6.1		Frac. Int. 6.1	
	<i>M</i>	<i>C</i>	<i>M</i>	<i>C</i>	<i>M</i>	<i>C</i>	<i>M</i>	<i>C</i>
Positive SF	11389	1.26E-4	1288	3.22E-3	11389	1.26E-4	1288	3.22E-3
Negative SF	2220	5.66E-4	1999	4.60E-4	2220	5.66E-4	1999	4.60E-4
Normalized Moment Curvature	-1	-35	-1	-20	-1	-35	-1	-20
	-1	-20	-1	-10	-1	-20	-1	-10
	-1	-1	-1	-5	-1	-1	-1	-5
	-0.86	-0.22	-1	-1	-0.86	-0.22	-1	-1
	0	0	0	0	0	0	0	0
	1	1	0.93	0.36	1	1	0.93	0.36
	1	3	1	1	1	3	1	1
	1	5	1	5	1	5	1	5
	1	15	1	15	1	15	1	15
	Trans		Trans End 1		Trans End 2		Trans Pier	
	<i>M</i>	<i>C</i>	<i>M</i>	<i>C</i>	<i>M</i>	<i>C</i>	<i>M</i>	<i>C</i>
Positive SF	1683	0.00168	1938	0.00168	1810	0.00168	3844	0.00168
Negative SF	1341	0.00168	1546	0.00168	1443	0.00168	3076	0.00168
Normalized Moment Curvature	-1.06	-25	-1.09	-25	-1.09	-25	-1.09	-25
	-1.06	-15	-1.09	-15	-1.09	-15	-1.09	-15
	-1	-1	-1	-1	-1	-1	-1	-1
	-0.76	-0.22	-0.76	-0.22	-0.76	-0.22	-0.76	-0.22
	0	0	0	0	0	0	0	0
	0.76	0.22	0.76	0.22	0.76	0.22	0.76	0.22
	1	1	1	1	1	1	1	1
	1	3	1	3	1	3	1	3
	1	13	1	13	1	13	1	13

Note: M=Moment (kip-in.) and C=Curvature (1/in.)

Section	Start (ft)	End (ft)
<i>1.1</i>	0	18.5
<i>2.1</i>	18.5	137.5
<i>3.1</i>	137.5	144.5
<i>3.2</i>	144.5	165.5
<i>4.2</i>	165.5	186.5
<i>5.2</i>	186.5	244
<i>4.2</i>	244	272
<i>4.1</i>	272	286
<i>6.1</i>	286	377
<i>1.1</i>	377	409

Bridge 8: Hinge and Section Data

	Long. Ext. 1.1		Long. Int. 1.1		Long. Ext. 2.1		Long. Int. 2.1	
	<i>M</i>	<i>C</i>	<i>M</i>	<i>C</i>	<i>M</i>	<i>C</i>	<i>M</i>	<i>C</i>
Positive SF	370539	5.49E-05	349445	0.000133	403697	5.59E-05	382149	0.000135
Negative SF	233674	5.49E-05	243588	5.98E-05	257589	5.59E-05	267853	6.09E-05
Normalized Moment Curvature	-1.37	-35	-1.37	-35	-1.37	-35	-1.38	-35
	-1.37	-25	-1.37	-25	-1.37	-25	-1.38	-23
	-1	-1	-1	-1	-1	-1	-1	-1
	-0.7	-0.56	-0.8	-0.56	-0.7	-0.56	-0.8	-0.56
	0	0	0	0	0	0	0	0
	0.91	0.56	0.87	0.19	0.915	0.56	0.98	0.7
	1	1	1	1	1	1	1	1
	1	3	1	3	1	3	1	3
1	13	1	13	1	13	1	13	
	Long. Ext. 3.1		Long. Int. 3.1		Long. Ext. 4.2		Long. Int. 4.2	
	<i>M</i>	<i>C</i>	<i>M</i>	<i>C</i>	<i>M</i>	<i>C</i>	<i>M</i>	<i>C</i>
Positive SF	466905	5.82E-05	439859	0.000099	435027	5.73E-05	414385	0.000139
Negative SF	287156	5.82E-05	298668	6.36E-05	273090	5.73E-05	289604	6.27E-05
Normalized Moment Curvature	-1.38	-35	-1.39	-35	-1.35	-35	-1.39	-35
	-1.38	-25	-1.39	-25	-1.35	-25	-1.39	-25
	-1	-1	-1	-1	-1	-1	-1	-1
	-0.7	-0.56	-0.8	-0.56	-0.7	-0.56	-0.8	-0.56
	0	0	0	0	0	0	0	0
	0.924	0.56	0.97	0.64	0.936	0.36	0.96	0.45
	1	1	1	1	1	1	1	1
	1	3	1	3	1	3	1	3
1	13	1	13	1	13	1	13	

Note: M=Moment (kip-in.) and C=Curvature (1/in.)

	Long. Ext. 5.2		Long. Int. 5.2		Long. Ext. 6.2		Long. Int. 6.2	
	<i>M</i>	<i>C</i>	<i>M</i>	<i>C</i>	<i>M</i>	<i>C</i>	<i>M</i>	<i>C</i>
Positive SF	471122	5.72E-05	450807	0.000138	538066	5.84E-05	513367	9.83E-05
Negative SF	333928	5.72E-05	348645	6.21E-05	396561	5.84E-05	411494	6.32E-05
Normalized Moment Curvature	-1.37	-35	-1.38	-35	-1.37	-35	-1.38	-35
	-1.37	-25	-1.38	-25	-1.37	-25	-1.38	-25
	-1	-1	-1	-1	-1	-1	-1	-1
	-0.7	-0.56	-0.8	-0.56	-0.7	-0.56	-0.8	-0.56
	0	0	0	0	0	0	0	0
	0.936	0.36	0.85	0.14	0.932	0.56	0.88	0.25
	1	1	1	1	1	1	1	1
	1	3	1	3	1	3	1	3
	1	13	1	13	1	13	1	13
	Long. Ext. 7.1		Long. Int. 7.1		Frac. Ext. 3.1		Frac. Int. 3.1	
	<i>M</i>	<i>C</i>	<i>M</i>	<i>C</i>	<i>M</i>	<i>C</i>	<i>M</i>	<i>C</i>
Positive SF	531378	5.93E-05	506462	0.0001	10423	1.04E-4	1636	2.39E-3
Negative SF	356981	5.93E-05	368277	6.45E-05	1661	7.3E-4	2162	5.3E-4
Normalized Moment Curvature	-1.37	-35	-1.39	-35	-1	-35	-1	-20
	-1.37	-25	-1.39	-25	-1	-22	-1	-10
	-1	-1	-1	-1	-1	-1	-1	-5
	-0.7	-0.56	-0.8	-0.56	-0.77	-0.36	-1	-1
	0	0	0	0	0	0	0	0
	0.932	0.56	0.97	0.64	1	1	0.83	0.22
	1	1	1	1	1	3	1	1
	1	3	1	3	1	5	1	5
	1	13	1	13	1	15	1	15

Note: M=Moment (kip-in.) and C=Curvature (1/in.)

	Frac. Ext. 7.1		Frac. Int. 7.1		Trans/Trans Pier		Trans End 1	
	<i>M</i>	<i>C</i>	<i>M</i>	<i>C</i>	<i>M</i>	<i>C</i>	<i>M</i>	<i>C</i>
Positive SF	10423	1.04E-4	1636	2.39E-3	1970	0.00168	857	0.00163
Negative SF	1661	7.3E-4	2162	5.3E-4	1598	0.00168	697	0.00163
Normalized Moment Curvature	-1	-35	-1	-20	-1.09	-30	-1.09	-30
	-1	-22	-1	-10	-1.09	-22	-1.09	-20
	-1	-1	-1	-5	-1	-1	-1	-1
	-0.77	-0.36	-1	-1	-0.76	-0.22	-0.76	-0.22
	0	0	0	0	0	0	0	0
	1	1	0.83	0.22	0.76	0.22	0.76	0.22
	1	3	1	1	1	1	1	1
	1	5	1	5	1	3	1	3
	1	15	1	15	1	13	1	13
	Trans End 2							
	<i>M</i>	<i>C</i>						
Positive SF	1112	0.00168						
Negative SF	900	0.00168						
Normalized Moment Curvature	-1.09	-25						
	-1.09	-15						
	-1	-1						
	-0.76	-0.22						
	0	0						
	0.76	0.22						
	1	1						
	1	3						
1	13							

Note: M=Moment (kip-in.) and C=Curvature (1/in.)

Section	Start (ft)	End (ft)
<i>1.1</i>	0	20.5
<i>2.1</i>	20.5	62.5
<i>3.1</i>	62.5	139.5
<i>2.1</i>	139.5	174.5
<i>4.2</i>	174.5	202.5
<i>5.2</i>	202.5	223.5
<i>6.2</i>	223.5	300.5
<i>4.2</i>	300.5	335.5
<i>2.1</i>	335.5	363.5
<i>3.1</i>	363.5	384.5
<i>7.1</i>	384.5	489.5
<i>3.1</i>	489.5	524.5
<i>1.1</i>	524.5	560

Bridge 9: Hinge and Section Data

	Long. Ext. 1.1		Long. Int. 1.1		Long. Ext. 1.2		Long. Int. 1.2	
	<i>M</i>	<i>C</i>	<i>M</i>	<i>C</i>	<i>M</i>	<i>C</i>	<i>M</i>	<i>C</i>
Positive SF	207692	7.21E-05	183132	0.000249	207889	7.21E-05	184293	0.000249
Negative SF	119209	7.21E-05	121462	8.29E-05	124631	7.21E-05	127592	8.29E-05
Normalized Moment Curvature	-1.35	-35	-1.37	-35	-1.35	-35	-1.38	-35
	-1.35	-24	-1.37	-23	-1.35	-23	-1.38	-23
	-1	-1	-1	-1	-1	-1	-1	-1
	-0.7	-0.56	-0.8	-0.56	-0.7	-0.56	-0.8	-0.56
	0	0	0	0	0	0	0	0
	0.91	0.56	0.87	0.19	0.92	0.56	0.98	0.52
	1	1	1	1	1	1	1	1
	1	3	1	3	1	3	1	3
1	13	1	13	1	13	1	13	
	Long. Ext. 2.2		Long. Int. 2.2		Long. Ext. 3.2		Long. Int. 3.2	
	<i>M</i>	<i>C</i>	<i>M</i>	<i>C</i>	<i>M</i>	<i>C</i>	<i>M</i>	<i>C</i>
Positive SF	236543	7.43E-05	210295	0.000191	270759	7.59E-05	242600	0.000195
Negative SF	137495	7.43E-05	140681	0.000086	168541	7.59E-05	171669	8.78E-05
Normalized Moment Curvature	-1.38	-35	-1.39	-35	-1.35	-35	-1.39	-35
	-1.38	-25	-1.39	-25	-1.35	-25	-1.39	-25
	-1	-1	-1	-1	-1	-1	-1	-1
	-0.7	-0.56	-0.8	-0.56	-0.7	-0.56	-0.8	-0.56
	0	0	0	0	0	0	0	0
	0.93	0.56	0.97	0.64	0.939	0.56	0.96	0.45
	1	1	1	1	1	1	1	1
	1	3	1	3	1	3	1	3
1	13	1	13	1	13	1	13	

Note: M=Moment (kip-in.) and C=Curvature (1/in.)

	Frac. Ext. 3.1		Frac. Int. 3.1		Trans		Trans Pier 1&2	
	<i>M</i>	<i>C</i>	<i>M</i>	<i>C</i>	<i>M</i>	<i>C</i>	<i>M</i>	<i>C</i>
Positive SF	10410	1.20E-4	1386	2.45E-3	1970	0.00168	1588	0.00163
Negative SF	1613	8.37E-4	1628	5.45E-4	1598	0.00168	1291	0.00163
Normalized Moment Curvature	-1	-35	-1	-20	-1.09	-30	-1.1	-30
	-1	-22	-1	-10	-1.09	-22	-1.1	-20
	-1	-1	-1	-5	-1	-1	-1	-1
	-0.8	-0.36	-1	-1	-0.76	-0.22	-	-0.22
	0	0	0	0	0	0	0	0
	1	1	0.875	0.22	0.76	0.22	0.76	0.22
	1	3	1	1	1	1	1	1
	1	5	1	5	1	3	1	3
	1	15	1	15	1	13	1	13
	Trans End 1&2							
	<i>M</i>	<i>C</i>						
Positive SF	985	0.00163						
Negative SF	799	0.00163						
Normalized Moment Curvature	-1.09	-30						
	-1.09	-20						
	-1	-1						
	-0.76	-0.22						
	0	0						
	0.76	0.22						
	1	1						
	1	3						
1	13							

Note: M=Moment (kip-in.) and C=Curvature (1/in.)

Section	Start (ft)	End (ft)
<i>1.1</i>	0	77
<i>1.2</i>	77	91
<i>2.2</i>	91	119
<i>3.2</i>	119	145.5
<i>2.2</i>	145.5	173.5
<i>1.1</i>	173.5	243.5
<i>2.2</i>	243.5	271.5
<i>3.2</i>	271.5	298
<i>2.2</i>	298	326
<i>1.2</i>	326	333
<i>1.1</i>	333	417

Bridge 10: Hinge and Section Data

	Long. Ext. 1.1		Long. Int. 1.1		Long. Ext. 2.2		Long. Int. 2.2	
	<i>M</i>	<i>C</i>	<i>M</i>	<i>C</i>	<i>M</i>	<i>C</i>	<i>M</i>	<i>C</i>
Positive SF	217603	9.71E-05	212466	0.000254	278214	0.000103	270328	0.000208
Negative SF	140128	6.24E-05	142863	6.53E-05	179860	0.000066	183001	6.94E-05
Normalized Moment Curvature	-1.36	-35	-1.37	-35	-1.35	-35	-1.38	-35
	-1.36	-24	-1.37	-23	-1.35	-23	-1.38	-23
	-1	-1	-1	-1	-1	-1	-1	-1
	-0.7	-0.56	-0.8	-0.56	-0.7	-0.56	-0.8	-0.56
	0	0	0	0	0	0	0	0
	0.966	0.64	0.84	0.14	0.92	0.56	0.98	0.52
	1	1	1	1	1	1	1	1
	1	3	1	3	1	3	1	3
	1	13	1	13	1	13	1	13
	Long. Ext. 3.1		Long. Int. 3.1		Long. Ext. 3.2		Long. Int. 3.2	
	<i>M</i>	<i>C</i>	<i>M</i>	<i>C</i>	<i>M</i>	<i>C</i>	<i>M</i>	<i>C</i>
Positive SF	296612	0.000104	286104	0.000157	298104	0.000104	288148	0.000157
Negative SF	178276	6.71E-05	181632	7.05E-05	188232	6.71E-05	191464	7.05E-05
Normalized Moment Curvature	-1.38	-35	-1.39	-35	-1.37	-35	-1.39	-35
	-1.38	-25	-1.39	-25	-1.37	-25	-1.39	-25
	-1	-1	-1	-1	-1	-1	-1	-1
	-0.7	-0.56	-0.8	-0.56	-0.7	-0.56	-0.8	-0.56
	0	0	0	0	0	0	0	0
	0.97	0.64	0.97	0.64	0.885	0.36	0.96	0.45
	1	1	1	1	1	1	1	1
	1	3	1	3	1	3	1	3
	1	13	1	13	1	13	1	13

Note: M=Moment (kip-in.) and C=Curvature (1/in.)

	Long. Ext. 4.2		Long. Int. 4.2		Long. Ext. 5.2		Long. Int. 5.2	
	<i>M</i>	<i>C</i>	<i>M</i>	<i>C</i>	<i>M</i>	<i>C</i>	<i>M</i>	<i>C</i>
Positive SF	384584	0.000108	375509	0.000113	392385	0.000105	383816	0.000156
Negative SF	281405	6.95E-05	284502	7.28E-05	320221	6.73E-05	322860	7.01E-05
Normalized Moment Curvature	-1.37	-35	-1.39	-35	-1.38	-35	-1.39	-35
	-1.37	-25	-1.39	-23	-1.38	-25	-1.39	-23
	-1	-1	-1	-1	-1	-1	-1	-1
	-0.7	-0.56	-0.8	-0.56	-0.7	-0.56	-0.8	-0.56
	0	0	0	0	0	0	0	0
	0.885	0.36	0.96	0.45	0.885	0.36	0.96	0.45
	1	1	1	1	1	1	1	1
	1	3	1	3	1	3	1	3
	1	13	1	13	1	13	1	13
	Long. Ext. 6.2		Long. Int. 6.2		Long. Ext. 7.2		Long. Int. 7.2	
	<i>M</i>	<i>C</i>	<i>M</i>	<i>C</i>	<i>M</i>	<i>C</i>	<i>M</i>	<i>C</i>
Positive SF	409398	0.000106	402775	0.000158	40078	0.000109	393203	0.00115
Negative SF	331376	6.81E-05	333892	7.09E-05	289823	7.03E-05	293010	7.36E-05
Normalized Moment Curvature	-1.38	-35	-1.38	-35	-1.38	-35	-1.38	-35
	-1.38	-25	-1.38	-23	-1.38	-23	-1.38	-23
	-1	-1	-1	-1	-1	-1	-1	-1
	-0.7	-0.56	-0.8	-0.56	-0.7	-0.56	-0.8	-0.56
	0	0	0	0	0	0	0	0
	0.885	0.36	0.96	0.45	0.919	0.36	0.96	0.45
	1	1	1	1	1	1	1	1
	1	3	1	3	1	3	1	3
	1	13	1	13	1	13	1	13

Note: M=Moment (kip-in.) and C=Curvature (1/in.)

	Long. Ext. 8.1		Long. Int. 8.1		Long. Ext. 8.2		Long. Int. 8.2	
	<i>M</i>	<i>C</i>	<i>M</i>	<i>C</i>	<i>M</i>	<i>C</i>	<i>M</i>	<i>C</i>
Positive SF	311592	0.000106	300765	0.000111	314537	0.000106	306241	0.000159
Negative SF	186784	6.81E-05	190210	7.15E-05	196656	6.81E-05	199977	7.15E-05
Normalized Moment Curvature	-1.38	-35	-1.38	-35	-1.38	-35	-1.38	-35
	-1.38	-23	-1.38	-23	-1.38	-23	-1.38	-23
	-1	-1	-1	-1	-1	-1	-1	-1
	-0.7	-0.56	-0.8	-0.56	-0.7	-0.56	-0.8	-0.56
	0	0	0	0	0	0	0	0
	0.88	0.36	0.96	0.45	0.88	0.36	0.977	0.64
	1	1	1	1	1	1	1	1
	1	3	1	3	1	3	1	3
	1	13	1	13	1	13	1	13
	Long. Ext. 9.1		Long. Int. 9.1		Long. Ext. 10.1		Long. Int. 10.1	
	<i>M</i>	<i>C</i>	<i>M</i>	<i>C</i>	<i>M</i>	<i>C</i>	<i>M</i>	<i>C</i>
Positive SF	286913	0.000103	276390	0.000155	267679	0.000102	257893	0.000152
Negative SF	172623	6.64E-05	175858	6.96E-05	164251	6.53E-05	167380	6.85E-05
Normalized Moment Curvature	-1.38	-35	-1.38	-35	-1.38	-35	-1.38	-35
	-1.38	-23	-1.38	-23	-1.38	-23	-1.38	-23
	-1	-1	-1	-1	-1	-1	-1	-1
	-0.7	-0.56	-0.8	-0.56	-0.7	-0.56	-0.8	-0.56
	0	0	0	0	0	0	0	0
	0.88	0.36	0.955	0.45	0.87	0.36	0.955	0.45
	1	1	1	1	1	1	1	1
	1	3	1	3	1	3	1	3
	1	13	1	13	1	13	1	13

Note: M=Moment (kip-in.) and C=Curvature (1/in.)

	Long. Ext. 11.2		Long. Int. 11.2		Long. Ext. 12.2		Long. Int. 12.2	
	<i>M</i>	<i>C</i>	<i>M</i>	<i>C</i>	<i>M</i>	<i>C</i>	<i>M</i>	<i>C</i>
Positive SF	321647	0.000103	312965	0.000207	462765	0.00011	460216	0.000164
Negative SF	238811	6.06E-05	241427	6.89E-05	368211	7.05E-05	371099	7.36E-05
Normalized Moment Curvature	-1.38	-35	-1.38	-35	-1.38	-35	-1.38	-35
	-1.38	-23	-1.38	-23	-1.38	-23	-1.38	-23
	-1	-1	-1	-1	-1	-1	-1	-1
	-0.7	-0.56	-0.8	-0.56	-0.7	-0.56	-0.8	-0.56
	0	0	0	0	0	0	0	0
	0.87	0.36	0.955	0.45	0.93	0.36	0.955	0.45
	1	1	1	1	1	1	1	1
	1	3	1	3	1	3	1	3
	1	13	1	13	1	13	1	13
	Frac. Ext. 1.1		Frac. Int. 1.1		Frac. Ext. 2.2		Frac. Int. 2.2	
	<i>M</i>	<i>C</i>	<i>M</i>	<i>C</i>	<i>M</i>	<i>C</i>	<i>M</i>	<i>C</i>
Positive SF	4870	2.69E-4	1288	3.14E-3	7056	2.69E-4	1597	2.02E-3
Negative SF	1882	6.73E-4	1963	4.48E-4	2966	6.73E-4	2950	4.48E-4
Normalized Moment Curvature	-1	-35	-1	-20	-1	-35	-1	-20
	-1	-20	-1	-10	-1	-20	-1	-10
	-1	-1	-1	-3	-1	-1	-1	-5
	-0.86	-0.4	-1	-1	-0.7	-0.4	-1	-1
	0	0	0	0	0	0	0	0
	1	1	0.93	0.36	1	1	0.88	0.56
	1	3	1	1	1	3	1	1
	1	5	1	5	1	5	1	5
	1	15	1	15	1	15	1	15

Note: M=Moment (kip-in.) and C=Curvature (1/in.)

	Frac. Ext. 3.1		Frac. Int. 3.1		Trans		Trans End 1&2	
	<i>M</i>	<i>C</i>	<i>M</i>	<i>C</i>	<i>M</i>	<i>C</i>	<i>M</i>	<i>C</i>
Positive SF	4870	2.69E-4	1288	3.14E-3	1683	0.00163	1810	0.00163
Negative SF	1882	6.73E-4	1963	4.48E-4	1341	0.00163	1443	0.00163
Normalized Moment Curvature	-1	-35	-1	-20	-1.09	-30	-1.09	-30
	-1	-20	-1	-10	-1.09	-22	-1.09	-20
	-1	-1	-1	-3	-1	-1	-1	-1
	-0.86	-0.4	-1	-1	-0.76	-0.22	-0.76	-0.22
	0	0	0	0	0	0	0	0
	1	1	0.93	0.36	0.76	0.22	0.76	0.22
	1	3	1	1	1	1	1	1
	1	5	1	5	1	3	1	3
	1	15	1	15	1	13	1	13
	Trans Pier 1&2							
	<i>M</i>	<i>C</i>						
Positive SF	2573	0.00168						
Negative SF	2056	0.00168						
Normalized Moment Curvature	-1.1	-30						
	-1.1	-20						
	-1	-1						
	-0.76	-0.22						
	0	0						
	0.76	0.22						
	1	1						
	1	3						
1	13							

Note: M=Moment (kip-in.) and C=Curvature (1/in.)

Section	Start (ft)	End (ft)
<i>1.1</i>	0	53
<i>2.2</i>	53	95
<i>3.2</i>	95	102
<i>4.2</i>	102	116
<i>5.2</i>	116	123
<i>6.2</i>	123	161.5
<i>7.2</i>	161.5	175.5
<i>8.2</i>	175.5	210.5
<i>9.1</i>	210.5	217.5
<i>10.1</i>	217.5	238.5
<i>3.1</i>	238.5	294.5
<i>10.1</i>	294.5	315.5
<i>9.1</i>	315.5	322.5
<i>8.1</i>	322.5	343.5
<i>8.2</i>	343.5	364.5
<i>11.1</i>	364.5	378.5
<i>6.2</i>	378.5	399.5
<i>12.2</i>	399.5	424
<i>6.2</i>	424	438
<i>11.2</i>	438	459
<i>3.2</i>	459	494
<i>1.1</i>	494	603

Bridge 11: Hinge and Section Data

	Long. Ext. 1.1		Long. Int. 1.1		Long. Ext. 1.2		Long. Int. 1.2	
	<i>M</i>	<i>C</i>	<i>M</i>	<i>C</i>	<i>M</i>	<i>C</i>	<i>M</i>	<i>C</i>
Positive SF	447209	5.19E-05	408675	9.05E-05	448318	5.19E-05	411855	9.05E-05
Negative SF	247199	5.19E-05	250474	5.82E-05	255876	5.19E-05	259154	5.82E-05
Normalized Moment Curvature	-1.38	-35	-1.39	-35	-1.38	-35	-1.38	-35
	-1.38	-24	-1.39	-23	-1.38	-23	-1.38	-23
	-1	-1	-1	-1	-1	-1	-1	-1
	-0.7	-0.56	-0.8	-0.56	-0.7	-0.56	-0.8	-0.56
	0	0	0	0	0	0	0	0
	0.91	0.56	0.86	0.36	0.9	0.56	0.96	0.64
	1	1	1	1	1	1	1	1
	1	3	1	3	1	3	1	3
1	13	1	13	1	13	1	13	
	Long. Ext. 2.2		Long. Int. 2.2		Long. Ext. 3.2		Long. Int. 3.2	
	<i>M</i>	<i>C</i>	<i>M</i>	<i>C</i>	<i>M</i>	<i>C</i>	<i>M</i>	<i>C</i>
Positive SF	530622	5.46E-05	472660	6.18E-05	539602	5.22E-05	508662	8.94E-05
Negative SF	293839	5.46E-05	296990	6.18E-05	387820	5.22E-05	390551	5.75E-05
Normalized Moment Curvature	-1.38	-35	-1.37	-35	-1.37	-35	-1.39	-35
	-1.38	-23	-1.37	-21	-1.37	-23	-1.39	-25
	-1	-1	-1	-1	-1	-1	-1	-1
	-0.7	-0.56	-0.8	-0.56	-0.7	-0.56	-0.8	-0.56
	0	0	0	0	0	0	0	0
	0.92	0.56	0.91	0.56	0.92	0.56	0.96	0.45
	1	1	1	1	1	1	1	1
	1	3	1	3	1	3	1	3
1	13	1	13	1	13	1	13	

Note: M=Moment (kip-in.) and C=Curvature (1/in.)

	Long. Ext. 4.2		Long. Int. 4.2		Long. Ext. 5.1		Long. Int. 5.1	
	<i>M</i>	<i>C</i>	<i>M</i>	<i>C</i>	<i>M</i>	<i>C</i>	<i>M</i>	<i>C</i>
Positive SF	802228	5.61E-05	774300	9.56E-05	535682	5.36E-05	494752	9.34E-05
Negative SF	624428	5.61E-05	626681	6.14E-05	326054	5.36E-05	329068	0.00006
Normalized Moment Curvature	-1.37	-35	-1.4	-35	-1.37	-35	-1.36	-35
	-1.37	-23	-1.4	-23	-1.37	-23	-1.36	-23
	-1	-1	-1	-1	-1	-1	-1	-1
	-0.7	-0.56	-0.8	-0.56	-0.7	-0.56	-0.8	-0.56
	0	0	0	0	0	0	0	0
	0.92	0.56	0.977	0.64	0.92	0.56	0.977	0.64
	1	1	1	1	1	1	1	1
	1	3	1	3	1	3	1	3
	1	13	1	13	1	13	1	13
	Long. Ext. 5.2		Long. Int. 5.2		Long. Ext. 6.1		Long. Int. 6.1	
	<i>M</i>	<i>C</i>	<i>M</i>	<i>C</i>	<i>M</i>	<i>C</i>	<i>M</i>	<i>C</i>
Positive SF	537206	5.36E-05	498665	9.34E-05	539611	0.000053	503906	9.17E-05
Negative SF	335055	5.36E-05	338073	0.00006	351542	0.000053	354478	0.000059
Normalized Moment Curvature	-1.37	-35	-1.39	-35	-1.37	-35	-1.39	-35
	-1.37	-23	-1.39	-23	-1.37	-23	-1.39	-23
	-1	-1	-1	-1	-1	-1	-1	-1
	-0.7	-0.56	-0.8	-0.56	-0.7	-0.56	-0.8	-0.56
	0	0	0	0	0	0	0	0
	0.92	0.56	0.977	0.64	0.92	0.56	0.977	0.64
	1	1	1	1	1	1	1	1
	1	3	1	3	1	3	1	3
	1	13	1	13	1	13	1	13

Note: M=Moment (kip-in.) and C=Curvature (1/in.)

			Trans Pier 2	
			<i>M</i>	<i>C</i>
Positive SF			1556	0.00168
Negative SF			1239	0.00168
Normalized Moment Curvature	-	1.05	-30	
	-	1.05	-22	
	-1	-1		
	-	0.76	-0.22	
	0	0		
	0.76	0.22		
	1	1		
	1	3		
	1	13		

Note: M=Moment (kip-in.) and C=Curvature (1/in.)

Section	Start (ft)	End (ft)
<i>1.1</i>	0	62.5
<i>1.2</i>	62.5	118.5
<i>2.2</i>	118.5	153.5
<i>3.2</i>	153.5	167.5
<i>4.2</i>	167.5	245
<i>3.2</i>	245	280
<i>5.2</i>	280	315
<i>5.1</i>	315	336
<i>6.1</i>	336	462
<i>5.1</i>	462	490
<i>5.2</i>	490	518
<i>3.2</i>	518	553
<i>4.2</i>	553	629.5
<i>3.2</i>	629.5	650.5
<i>2.2</i>	650.5	678.5
<i>1.2</i>	678.5	734.5
<i>1.1</i>	734.5	824

Bridge 12: Hinge and Section Data

	Long. Ext. 1.1		Long. Int. 1.1		Long. Ext. 2.2		Long. Int. 2.2	
	<i>M</i>	<i>C</i>	<i>M</i>	<i>C</i>	<i>M</i>	<i>C</i>	<i>M</i>	<i>C</i>
Positive SF	177808	8.01E-05	150041	0.000279	265809	4.91E-05	242338	0.00016
Negative SF	91919	8.01E-05	95191	9.29E-05	148519	8.83E-05	152662	0.000103
Normalized Moment Curvature	-1.38	-35	-1.36	-35	-1.39	-35	-1.38	-35
	-1.38	-24	-1.36	-23	-1.39	-21	-1.38	-19
	-1	-1	-1	-1	-1	-1	-1	-1
	-0.7	-0.56	-0.8	-0.56	-0.7	-0.56	-0.8	-0.56
	0	0	0	0	0	0	0	0
	0.93	0.56	0.89	0.19	0.54	0.4	0.91	0.56
	1	1	1	1	1	1	1	1
	1	3	1	3	1	3	1	3
	1	13	1	13	1	13	1	13
	Long. Ext. 3.2		Long. Int. 3.2		Frac. Ext. 1.1		Frac. Int. 1.1	
	<i>M</i>	<i>C</i>	<i>M</i>	<i>C</i>	<i>M</i>	<i>C</i>	<i>M</i>	<i>C</i>
Positive SF	271522	8.54E-05	249832	0.000216	9162	1.04E-4	1291	3.40E-3
Negative SF	206366	8.54E-05	208809	9.71E-05	1456	1.04E-4	1448	4.86E-4
Normalized Moment Curvature	-1.35	-35	-1.37	-35	-1	-35	-1	-20
	-1.35	-23	-1.37	-23	-1	-22	-1	-11
	-1	-1	-1	-1	-1	-5	-1	-5
	-0.7	-0.56	-0.8	-0.56	-1	-1	-1	-1
	0	0	0	0	0	0	0	0
	0.92	0.56	0.96	0.45	1	1	0.86	0.14
	1	1	1	1	1	3	1	1
	1	3	1	3	1	5	1	5
	1	13	1	13	1	15	1	15

Note: M=Moment (kip-in.) and C=Curvature (1/in.)

	Trans		Trans End 1		Trans End 2		Trans Pier 1	
	<i>M</i>	<i>C</i>	<i>M</i>	<i>C</i>	<i>M</i>	<i>C</i>	<i>M</i>	<i>C</i>
Positive SF	2107	0.00152	1053	0.00152	1836	0.00152	1836	0.00152
Negative SF	1745	0.00152	872	0.00152	1522	0.00152	1522	0.00152
Normalized Moment Curvature	-1.12	-30	-1.12	-30	-1.13	-30	-1.13	-30
	-1.12	-22	-1.12	-21	-1.13	-21	-1.13	-21
	-1	-1	-1	-1	-1	-1	-1	-1
	-0.76	-0.22	-0.76	-0.22	-0.76	-0.22	-0.76	-0.22
	0	0	0	0	0	0	0	0
	0.76	0.22	0.76	0.22	0.76	0.22	0.76	0.22
	1	1	1	1	1	1	1	1
	1	3	1	3	1	3	1	3
	1	13	1	13	1	13	1	13
	Trans Pier 2							
	<i>M</i>	<i>C</i>						
Positive SF	2618	0.00152						
Negative SF	2172	0.00152						
Normalized Moment Curvature	-1.13	-30						
	-1.13	-21						
	-1	-1						
	-0.76	-0.22						
	0	0						
	0.76	0.22						
	1	1						
	1	3						
1	13							

Note: M=Moment (kip-in.) and C=Curvature (1/in.)

Section	Start (ft)	End (ft)
<i>1.1</i>	0	84
<i>2.2</i>	84	112
<i>3.2</i>	112	153
<i>2.2</i>	153	181
<i>1.1</i>	181	258
<i>2.2</i>	258	286
<i>3.2</i>	286	336.5
<i>2.2</i>	336.5	364.5
<i>1.1</i>	364.5	465

Bridge 13: Hinge and Section Data

	Long. Ext. 1.1		Long. Int. 1.1		Long. Ext. 2.1		Long. Int. 2.1	
	<i>M</i>	<i>C</i>	<i>M</i>	<i>C</i>	<i>M</i>	<i>C</i>	<i>M</i>	<i>C</i>
Positive SF	141226	0.000132	137479	0.000344	131426	0.00013	127379	0.000338
Negative SF	94747	0.000085	96545	8.84E-05	89122	8.37E-05	90702	0.000087
Normalized Moment Curvature	-1.38	-35	-1.38	-35	-1.39	-35	-1.4	-35
	-1.38	-24	-1.38	-23	-1.39	-23	-1.4	-23
	-1	-1	-1	-1	-1	-1	-1	-1
	-0.7	-0.56	-0.8	-0.56	-0.7	-0.56	-0.8	-0.56
	0	0	0	0	0	0	0	0
	0.97	0.64	0.89	0.19	0.88	0.36	0.91	0.56
	1	1	1	1	1	1	1	1
	1	3	1	3	1	3	1	3
1	13	1	13	1	13	1	13	
	Long. Ext. 3.2		Long. Int. 3.2		Long. Ext. 4.2		Long. Int. 4.2	
	<i>M</i>	<i>C</i>	<i>M</i>	<i>C</i>	<i>M</i>	<i>C</i>	<i>M</i>	<i>C</i>
Positive SF	183037	0.000141	181343	0.000282	206928	9.14E-05	204910	0.000285
Negative SF	127072	9.04E-05	130833	9.41E-05	154578	9.14E-05	158006	0.000095
Normalized Moment Curvature	-1.36	-35	-1.37	-35	-1.36	-35	-1.37	-35
	-1.36	-23	-1.37	-23	-1.36	-23	-1.37	-23
	-1	-1	-1	-1	-1	-1	-1	-1
	-0.7	-0.56	-0.8	-0.56	-0.8	-0.56	-0.83	-0.56
	0	0	0	0	0	0	0	0
	0.93	0.36	0.97	0.52	0.93	0.56	0.96	0.33
	1	1	1	1	1	1	1	1
	1	3	1	3	1	3	1	3
1	13	1	13	1	13	1	13	

Note: M=Moment (kip-in.) and C=Curvature (1/in.)

	Long. Ext. 5.2		Long. Int. 5.2		Frac. Ext. 2.1		Frac. Int. 2.1	
	<i>M</i>	<i>C</i>	<i>M</i>	<i>C</i>	<i>M</i>	<i>C</i>	<i>M</i>	<i>C</i>
Positive SF	255210	9.29E-05	251558	0.000214	4670	2.45E-4	1313	3.58E-3
Negative SF	206924	9.29E-05	209171	9.61E-05	1517	1.10E-4	1654	5.11E-4
Normalized Moment Curvature	-1.36	-35	-1.39	-35	-1	-35	-1	-20
	-1.36	-23	-1.39	-23	-1	-18	-1	-10
	-1	-1	-1	-1	-1	-1	-1	-5
	-0.85	-0.56	-0.83	-0.56	-0.84	-0.22	-1	-1
	0	0	0	0	0	0	0	0
	0.95	0.56	0.97	0.45	1	1	0.95	0.36
	1	1	1	1	1	3	1	1
	1	3	1	3	1	5	1	5
1	13	1	13	1	15	1	15	
	Trans		Trans End 1&2		Trans Pier 1&2			
	<i>M</i>	<i>C</i>	<i>M</i>	<i>C</i>	<i>M</i>	<i>C</i>		
Positive SF	1683	0.00168	523	0.00168	2430	0.00168		
Negative SF	1341	0.00168	415	0.00168	1946	0.00168		
Normalized Moment Curvature	-1.06	-30	-1.05	-30	-1.06	-30		
	-1.06	-22	-1.05	-21	-1.06	-21		
	-1	-1	-1	-1	-1	-1		
	-0.76	-0.22	-0.76	-0.22	-0.76	-0.22		
	0	0	0	0	0	0		
	0.76	0.22	0.76	0.22	0.76	0.22		
	1	1	1	1	1	1		
	1	3	1	3	1	3		
1	13	1	13	1	13			

Note: M=Moment (kip-in.) and C=Curvature (1/in.)

Section	Start (ft)	End (ft)
<i>1.1</i>	0	12.75
<i>2.1</i>	12.75	89.75
<i>1.1</i>	89.75	96.75
<i>3.2</i>	96.75	124.75
<i>4.2</i>	124.75	131.75
<i>5.2</i>	131.75	162.5
<i>4.2</i>	162.5	169.5
<i>3.2</i>	169.5	197.5
<i>1.1</i>	197.5	204.5
<i>2.1</i>	204.5	281.5
<i>1.1</i>	281.5	288.5
<i>3.2</i>	295.5	316.5
<i>4.2</i>	316.5	323.5
<i>5.2</i>	323.5	354.5
<i>4.2</i>	354.5	361.25
<i>3.2</i>	361.5	389.25
<i>1.1</i>	389.25	396.25
<i>2.1</i>	396.25	473.25
<i>1.1</i>	473.25	439

Bridge 14: Hinge and Section Data

	Long. Ext. 1.1		Long. Int. 1.1		Long. Ext. 2.1		Long. Int. 2.1	
	<i>M</i>	<i>C</i>	<i>M</i>	<i>C</i>	<i>M</i>	<i>C</i>	<i>M</i>	<i>C</i>
Positive SF	173059	0.000077	141867	0.000273	212111	8.09E-05	179280	0.000215
Negative SF	92595	0.000077	95620	9.09E-05	105407	8.09E-05	111621	9.69E-05
Normalized Moment Curvature	-1.34	-35	-1.36	-35	-1.39	-35	-1.35	-35
	-1.34	-23	-1.36	-23	-1.39	-23	-1.35	-21
	-1	-1	-1	-1	-1	-1	-1	-1
	-0.7	-0.56	-0.8	-0.56	-0.7	-0.56	-0.8	-0.56
	0	0	0	0	0	0	0	0
	0.92	0.56	0.87	0.19	0.95	0.56	0.91	0.25
	1	1	1	1	1	1	1	1
	1	3	1	3	1	3	1	3
		13	13	1	13	1	13	
	Long. Ext. 3.2		Long. Int. 3.2		Long. Ext. 4.2		Long. Int. 4.2	
	<i>M</i>	<i>C</i>	<i>M</i>	<i>C</i>	<i>M</i>	<i>C</i>	<i>M</i>	<i>C</i>
Positive SF	216831	8.15E-05	185714	0.000271	250576	8.53E-05	222027	0.000161
Negative SF	117869	8.15E-05	122621	9.75E-05	123737	8.53E-05	131276	0.000103
Normalized Moment Curvature	-1.36	-35	-1.37	-35	-1.39	-35	-1.37	-35
	-1.36	-23	-1.37	-23	-1.39	-21	-1.37	-19
	-1	-1	-1	-1	-1	-1	-1	-1
	-0.7	-0.56	-0.8	-0.56	-0.8	-0.56	-0.83	-0.56
	0	0	0	0	0	0	0	0
	0.95	0.56	0.97	0.45	0.98	0.56	0.96	0.33
	1	1	1	1	1	1	1	1
	1	3	1	3	1	3	1	3
		13	13	1	13	1	13	

Note: M=Moment (kip-in.) and C=Curvature (1/in.)

	Long. Ext. 5.2		Long. Int. 5.2		Frac. Ext. 1.1		Frac. Int. 1.1	
	<i>M</i>	<i>C</i>	<i>M</i>	<i>C</i>	<i>M</i>	<i>C</i>	<i>M</i>	<i>C</i>
Positive SF	254768	8.39E-05	226322	0.000221	9168	1.04E-4	1220	2.28E-3
Negative SF	162599	8.39E-05	166674	9.96E-05	1539	1.04E-4	1522	5.06E-4
Normalized Moment Curvature	-1.35	-35	-1.38	-35	-1	-35	-1	-20
	-1.35	-23	-1.38	-23	-1	-23	-1	-10
	-1	-1	-1	-1	-1	-5	-1	-5
	-0.85	-0.56	-0.83	-0.56	-1	-1	-1	-1
	0	0	0	0	0	0	0	0
	0.98	0.56	0.97	0.45	1	1	0.88	0.22
	1	1	1	1	1	3	1	1
	1	3	1	3	1	5	1	5
1	13	1	13	1	15	1	15	
	Trans		Trans End 1&2		Trans Pier 1&2			
	<i>M</i>	<i>C</i>	<i>M</i>	<i>C</i>	<i>M</i>	<i>C</i>		
Positive SF	1683	0.00168	297	0.002611	2192	0.00168		
Negative SF	1341	0.00168	216	0.00168	1750	0.00168		
Normalized Moment Curvature	-1.06	-30	-1	-30	-1.06	-30		
	-1.06	-22	-1	-21	-1.06	-21		
	-1	-1	-1	-1	-1	-1		
	-0.76	-0.22	-0.76	-0.22	-0.76	-0.22		
	0	0	0	0	0	0		
	0.76	0.22	0.77	0.14	0.76	0.22		
	1	1	1	1	1	1		
	1	3	1	3	1	3		
1	13	1	13	1	13			

Note: M=Moment (kip-in.) and C=Curvature (1/in.)

Bridge 15: Hinge and Section Data

	Long. Ext. 1.1		Long. Int. 1.1		Long. Ext. 1.2		Long. Int. 1.2	
	<i>M</i>	<i>C</i>	<i>M</i>	<i>C</i>	<i>M</i>	<i>C</i>	<i>M</i>	<i>C</i>
Positive SF	323409	5.78E-05	293107	0.000147	323958	5.78E-05	295102	0.000147
Negative SF	203763	5.78E-05	207149	6.61E-05	212854	5.78E-05	216195	6.61E-05
Normalized Moment Curvature	-1.36	-35	-1.38	-35	-1.36	-35	-1.38	-35
	-1.36	-23	-1.38	-23	-1.36	-23	-1.38	-23
	-1	-1	-1	-1	-1	-1	-1	-1
	-0.7	-0.56	-0.8	-0.56	-0.7	-0.56	-0.8	-0.56
	0	0	0	0	0	0	0	0
	0.91	0.56	0.87	0.19	0.91	0.56	0.87	0.19
	1	1	1	1	1	1	1	1
	1	3	1	3	1	3	1	3
	1	13	1	13	1	13	1	13
	Long. Ext. 2.1		Long. Int. 2.1		Long. Ext. 2.2		Long. Int. 2.2	
	<i>M</i>	<i>C</i>	<i>M</i>	<i>C</i>	<i>M</i>	<i>C</i>	<i>M</i>	<i>C</i>
Positive SF	384229	5.99E-05	350980	0.000153	385000	5.99E-05	350195	0.000107
Negative SF	246757	5.99E-05	250145	6.88E-05	256878	5.99E-05	260221	6.88E-05
Normalized Moment Curvature	-1.36	-35	-1.38	-35	-1.36	-35	-1.38	-35
	-1.36	-23	-1.38	-23	-1.36	-23	-1.38	-23
	-1	-1	-1	-1	-1	-1	-1	-1
	-0.7	-0.56	-0.8	-0.56	-0.7	-0.56	-0.8	-0.56
	0	0	0	0	0	0	0	0
	0.95	0.56	0.91	0.25	0.95	0.56	0.91	0.25
	1	1	1	1	1	1	1	1
	1	3	1	3	1	3	1	3
	1	13	1	13	1	13	1	13

Note: M=Moment (kip-in.) and C=Curvature (1/in.)

	Long. Ext. 3.2		Long. Int. 3.2		Long. Ext. 4.2		Long. Int. 4.2	
	<i>M</i>	<i>C</i>	<i>M</i>	<i>C</i>	<i>M</i>	<i>C</i>	<i>M</i>	<i>C</i>
Positive SF	415986	6.06E-05	383112	0.000155	448197	0.000061	411657	0.000108
Negative SF	285021	6.06E-05	288302	6.96E-05	326085	0.000061	329189	6.95E-05
Normalized Moment Curvature	-1.36	-35	-1.38	-35	-1.37	-35	-1.39	-35
	-1.36	-23	-1.38	-23	-1.37	-23	-1.39	-23
	-1	-1	-1	-1	-1	-1	-1	-1
	-0.7	-0.56	-0.8	-0.56	-0.8	-0.56	-0.83	-0.56
	0	0	0	0	0	0	0	0
	0.95	0.56	0.97	0.45	0.98	0.56	0.96	0.33
	1	1	1	1	1	1	1	1
	1	3	1	3	1	3	1	3
	1	13	1	13	1	13	1	13
	Long. Ext. 5.2		Long. Int. 5.2		Frac. Ext. 1.1		Frac. Int. 1.1	
	<i>M</i>	<i>C</i>	<i>M</i>	<i>C</i>	<i>M</i>	<i>C</i>	<i>M</i>	<i>C</i>
Positive SF	582446	4.79E-05	550752	9.82E-05	12087	1.15E-4	1347	2.12E-3
Negative SF	469228	8.62E-05	471302	9.82E-05	2126	8.06E-4	2067	4.72E-4
Normalized Moment Curvature	-1.24	-35	-1.25	-35	-1	-35	-1	-20
	-1.24	-19	-1.25	-17	-1	-23	-1	-10
	-1	-1	-1	-1	-1	-1	-1	-5
	-0.85	-0.56	-0.96	-0.56	-0.78	-0.36	-1	-1
	0	0	0	0	0	0	0	0
	0.55	0.4	0.96	0.56	1	1	0.77	0.22
	1	1	1	1	1	3	1	1
	1	3	1	3	1	5	1	5
	1	13	1	13	1	15	1	15

Note: M=Moment (kip-in.) and C=Curvature (1/in.)

	Frac. Ext. 2.1		Frac. Int. 2.1		Trans		Trans End 1&2	
	<i>M</i>	<i>C</i>	<i>M</i>	<i>C</i>	<i>M</i>	<i>C</i>	<i>M</i>	<i>C</i>
Positive SF	12087	1.15E-4	1347	2.12E-3	1970	0.00168	1588	0.00168
Negative SF	2126	8.06E-4	2067	4.72E-4	1598	0.00168	1291	0.00168
Normalized Moment Curvature	-1	-35	-1	-20	-	-	-	-
	-1	-23	-1	-10	1.06	-30	1.11	-30
	-1	-1	-1	-5	-	-	-	-
	-0.78	-0.36	-1	-1	1.06	-22	1.11	-22
	0	0	0	0	-1	-1	-1	-1
	1	1	0.77	0.22	-	-	-	-
	1	3	1	1	0.76	-0.22	0.76	-0.22
	1	5	1	5	0	0	0	0
1	15	1	15	0	0	0	0	
	Trans Pier 1&2							
	<i>M</i>	<i>C</i>						
Positive SF	2701	0.00168						
Negative SF	2193	0.00168						
Normalized Moment Curvature	-1.09	-30						
	-1.09	-21						
	-1	-1						
	-0.76	-0.22						
	0	0						
	0.76	0.22						
	1	1						
	1	3						
1	13							

Note: M=Moment (kip-in.) and C=Curvature (1/in.)

Section	Start (ft)	End (ft)
<i>1.1</i>	0	100
<i>2.1</i>	100	114
<i>2.2</i>	114	135
<i>3.2</i>	135	156
<i>4.2</i>	156	177
<i>5.2</i>	177	207.5
<i>4.2</i>	207.5	228.5
<i>3.2</i>	228.5	249.5
<i>1.2</i>	249.5	256.5
<i>1.1</i>	256.5	277.5
<i>2.1</i>	277.5	410.5
<i>1.1</i>	410.5	424.5
<i>1.2</i>	424.5	431.5
<i>3.2</i>	431.5	452.5
<i>4.2</i>	452.5	473.5
<i>5.2</i>	473.5	504
<i>4.2</i>	504	525
<i>3.2</i>	525	546
<i>2.2</i>	546	567
<i>1.1</i>	567	695

APPENDIX C

GRILLAGE DESIGN EXAMPLES*

* Part of this chapter is reprinted with permission from “Analysis Guidelines and Examples for Fracture Critical Steel Twin Tub Girder Bridges” 0-6937-P1 by Hurlebaus S., Mander J., Terzioglu T., Boger N., Fatima A., 2018. Texas A&M Texas Transportation Institute, 26-48, 60-82, 99-123, Copyright 2018 by Texas A&M Texas Transportation Institute

Grillage Analysis Example of Bridge 2

1. Gather Bridge Geometry and Material Information.

Steel Tub Properties ($f_y=50$ ksi)						
Location ft	Top Flange		Web		Bottom Flange	
	Width in.	Thickness in.	Width in.	Thickness in.	Width in.	Thickness in.
0-115	18	1.00	79	0.625	50	1.00

Location	Parameter	Description/Value
Bridge	Location	Harris County, I610
	Year Designed/Year Built	2002/2004
	Design Load	HS25
	Length, ft	115
	Spans, ft	115
	Radius of Curvature, ft	1909.86
Deck	Width, ft	26.417
	Thickness, in.	8
	Haunch, in.	4
	Rail Type	SSTR
Rebar	# of Bar Longitudinal Top Row (#5)	40
	# of Bar Longitudinal Bottom Row (#5)	32
	Transverse Spacing Top Row (#5)	5
	Transverse Spacing Bottom Row (#5)	5
	Rebar Strength (ksi)	60
Girder	CL of Bridge to CL of Girder (in.)	79.5
	CL of Top Flange to CL of Top Flange (in.)	86

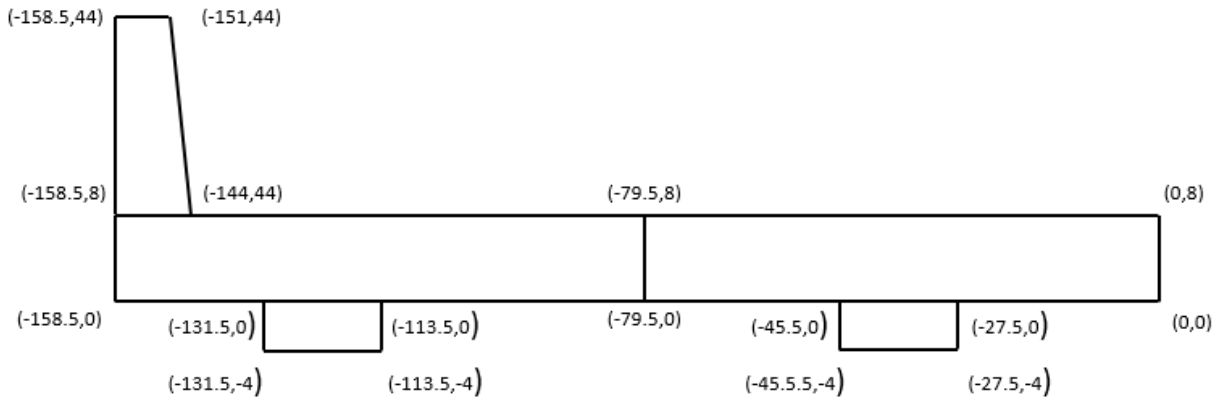
2. Material constitutive behavior

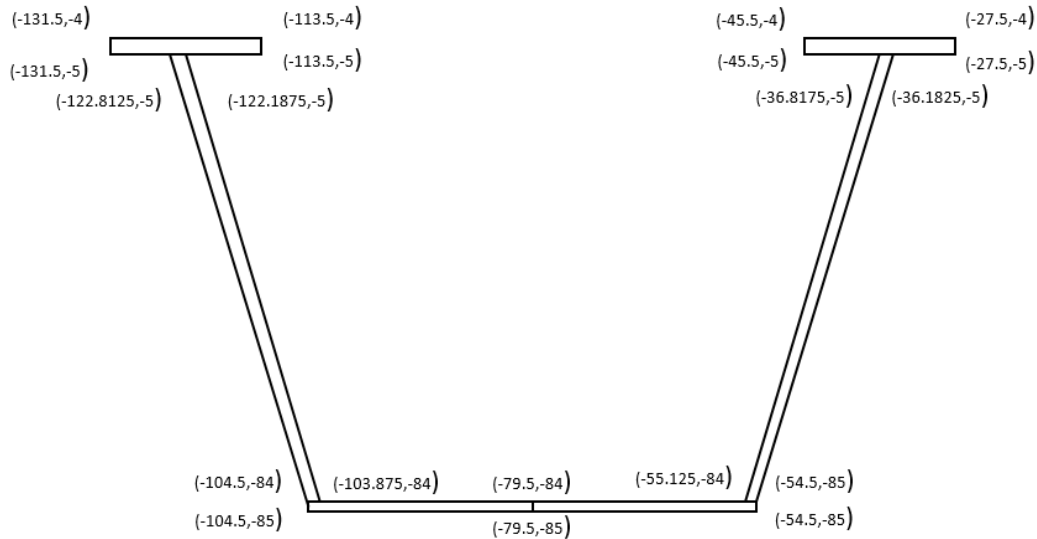
Stress (ksi)	Strain (1/in)
-4	-3.79E-03
-4	-3.56E-03
-4	-2.69E-03
-4	-1.78E-03
-3.8205	-1.40E-03
-2.8718	-8.69E-04
-0.6403	-1.78E-04
0	0
0.378	1.06E-04
0.378	1.16E-03

Stress (ksi)	Strain (1/in)
-87.9	-0.095
-87.9	-0.0944
-86.6	-0.0761
-78	-0.0386
-60.7	-9.80E-03
-60.3	-2.08E-03
0	0
60.3	2.08E-03
60.7	9.80E-03
78	0.0386
86.6	0.0761
87.9	0.0944
87.9	0.095

Stress (ksi)	Strain (1/in)
-71.6	-0.1
-71.6	-0.097
-71.6	-0.095
-71.6	-0.0946
-70.3	-0.0764
-62.5	-0.039
-50	-0.0196
-50	-1.72E-03
0	0
50	1.72E-03
50	0.0196
62.5	0.039
70.3	0.0764
71.6	0.0946
71.6	0.095
71.6	0.097
71.6	0.1

3. Create a Coordinate system for half width of the span





4. Create a cylindrical coordinate system for the curved bridge assuring that the middle transverse divisions are 7 ft, as this will aid in applying the HS20 truck load whose axels are separated by 14 ft.
 - a. # of Segments = $\left(\frac{\text{Length (ft)} * 12}{84 \text{ in (7ft)}}\right)$ rounded to nearest even number
 - i. # of Segments = $\left(\frac{115 * 12}{84}\right) = 16.428$ so 14 was selected
 - b. End Segment Length = $\left(\frac{(\text{Length} * 12) - (\# \text{ of Segments} * 84)}{2}\right)$
 - i. End Segment Length = $\frac{((115 * 12) - (14 * 84))}{2} = 102 \text{ in.}$
 - c. $\text{Theta} = \frac{\text{Length}}{\text{Radius}}$
 - i. $\text{Theta} = \frac{115}{1909.86} = 0.0602 \text{ rad or } 3.450 \text{ degrees}$
 - d. Determine the radial offsets using the outside edge, the outside flange, the inner flange and centerline of the bridge.

Offsets (in.)	
Edge	158.5
Outside Flange	122.5
Inner Flange	36.5
CL of Bridge	0

Radial Spacing (in.)		
A	23077.3	CL+Edge
B	23041.3	CL+OF
C	22955.3	CL+IF
Center Line	22918.8	or 1909.86 (ft)
D	22882.3	CL-IF
E	22796.3	CL-OF
F	22760.3	CL-Edge

a. The Longitudinal or spacing along theta is determined by converting the longitudinal segment lengths into degrees.

i. The first and last segments are 102 in. and the intermediate segments are 84 in. The total length is 115 ft or 1380 in.

ii. $Radial\ Spacing\ (rad) = \frac{Long.Spacing}{Radius}$

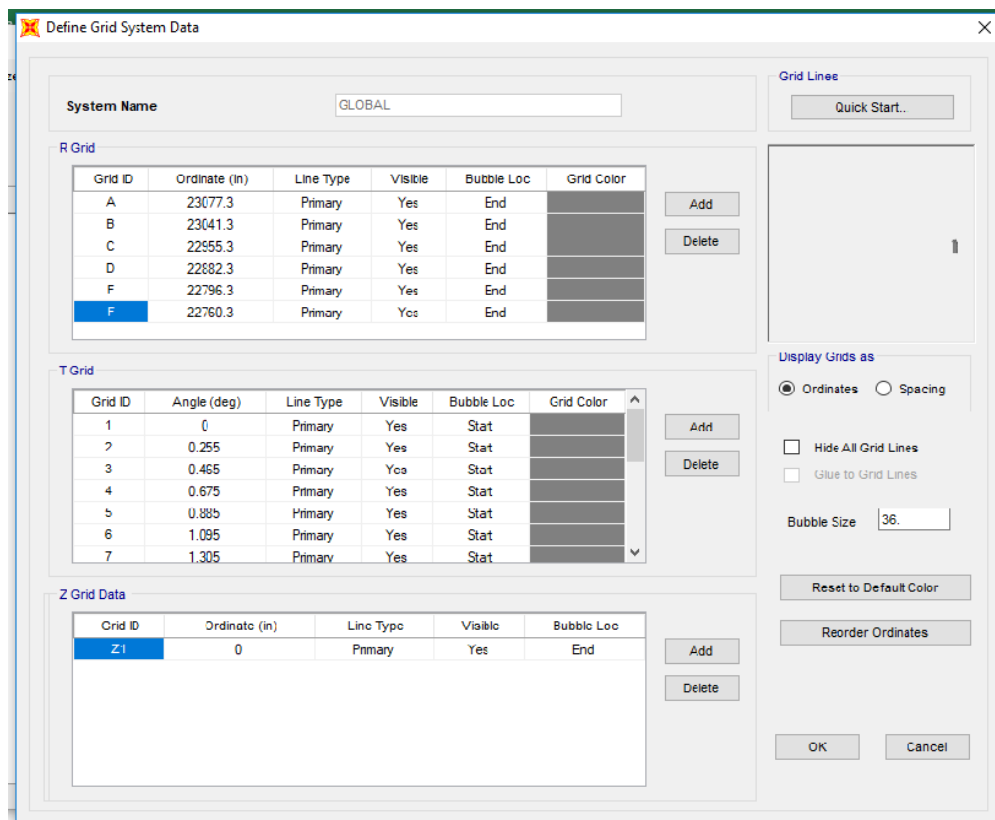
iii. $Radial\ Spacing\ (degree) = Radial\ Spacing\ (rad) * \frac{180}{\pi}$

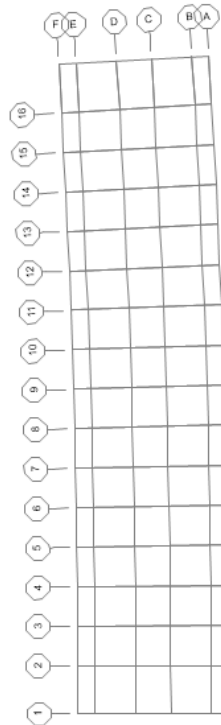
Long. Spacing (in.)	Radial Spacing (rad.)	Radial Spacing (degrees)
0	0.0000	0.000
102	0.0045	0.255
186	0.0081	0.465
270	0.0118	0.675
354	0.0154	0.885
438	0.0191	1.095
522	0.0228	1.305
606	0.0264	1.515
690	0.0301	1.725
774	0.0338	1.935
858	0.0374	2.145
942	0.0411	2.355
1026	0.0448	2.565
1110	0.0484	2.775
1194	0.0521	2.985
1278	0.0558	3.195
1380	0.0602	3.450

iv. *Int. Transverse Element width = 84 in.*

$$v. \text{ End Transverse Element} = 102 - \left(\frac{84}{2}\right) = 60 \text{ in.}$$

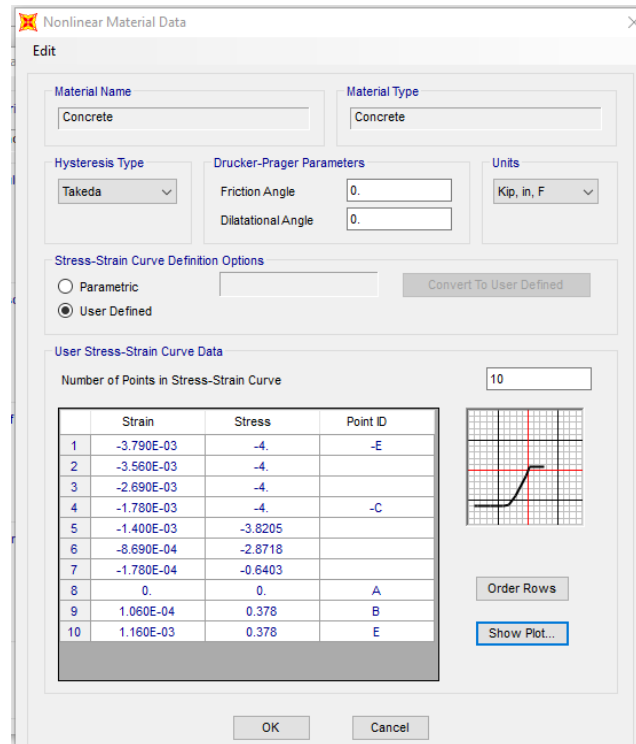
5. Inputting the coordinate system into SAP2000
 - a. Select File -> New Model -> Blank model (making sure units are in kips and inches)
 - b. Right click on the blank workspace and select Edit Grid Data-> Modify/Show System->Quick Start->Cylindrical.
 - i. In the Number of Grid Lines panel set “Along Z=1”
 - ii. In the Grid Spacing panel set “Along Z=1”
 - iii. Select OK.
 - iv. Delete all R and T Coordinates that were generated
 - c. Add correct coordinates for R
 - i. All radial coordinates (A, B, C, D, E, and F).
 - d. Add correct coordinates for T
 - i. All theta coordinates for T (0 to 1380 in.)
 - ii. Click OK
 - e. The Grid System is now formed.





6. Defining Material in SAP200

- a. Click Define-> Materials->Add New Material->Material Type (Steel, Concrete, or Rebar)->Standard (User)->OK
- b. At the bottom of the window select the box which states “Switch to Advanced Properties”
- c. In the open window name the material “Concrete” “Steel” or “Rebar” depending on which material is being defined. Then click “Modify/Show Material Properties”
- d. On the Material Property Data window click “Nonlinear Material Data” icon.
- e. In the Nonlinear Material Data window select the “Convert to User Defined” icon.
- f. Input the number of number of data points for the stress strain behavior (10 for concrete, 13 for rebar, 17 for steel)
- g. Input the data points for the stress strain behavior.
- h. Select “OK”
- i. Repeat this process again for the remaining materials.

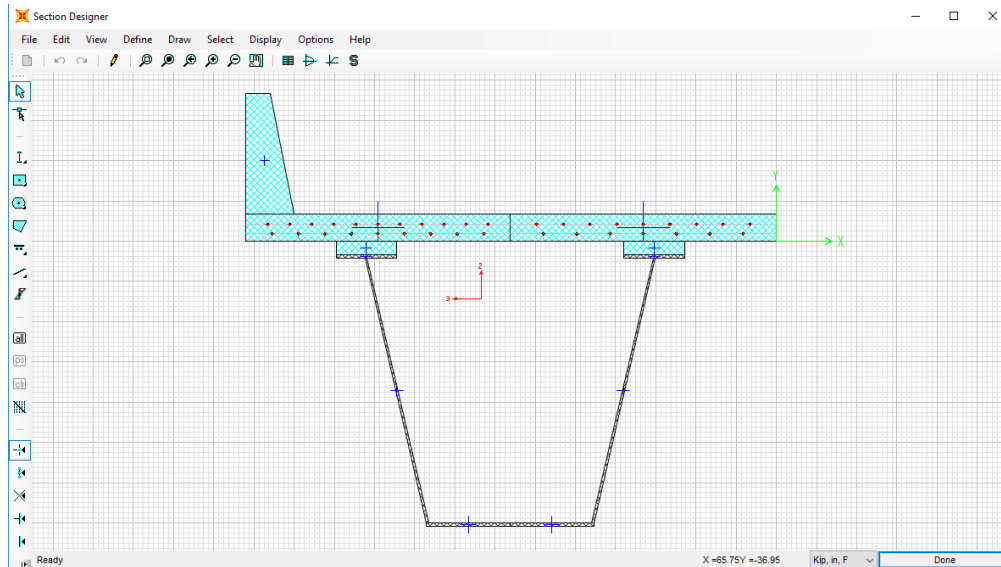


7. Defining Frame Cross Sections in SAP2000.

- a. Click Define->Section Properties->Frame Sections->Add New Properties
- b. In the Frame Section Properties Drop down box select "Other" and click Section Designer. In the SD Section Designer Window name the section B2Long click the "Section Designer" Icon.
- c. Using the Polygon feature draw the features of the half width of the bridge from Step 3. This includes: one rail, two concrete deck pieces, to concrete haunches, two top flanges, two webs, and two pieces of the bottom flange.
 - i. To change material types for the polygons right click on the polygon and select the desired material type from the material drop down menu.
 - ii. To change the coordinates of the polygon's nodes use the Reshaper tool to change the coordinates.
- d. Add in the longitudinal rebar to both concrete deck elements by using the Line Bar from the Draw Reinforcing Shape tool. From the design drawings it can be determined that there are 11 #5 top bars and 9 #5 bottom bars in the outer concrete deck element and 9 #5 top bars and 7 #5 bottom bars in the inner concrete element. With a 2 inch top cover and transvers reinforcement the top bars are located at 5.0625 inches and with

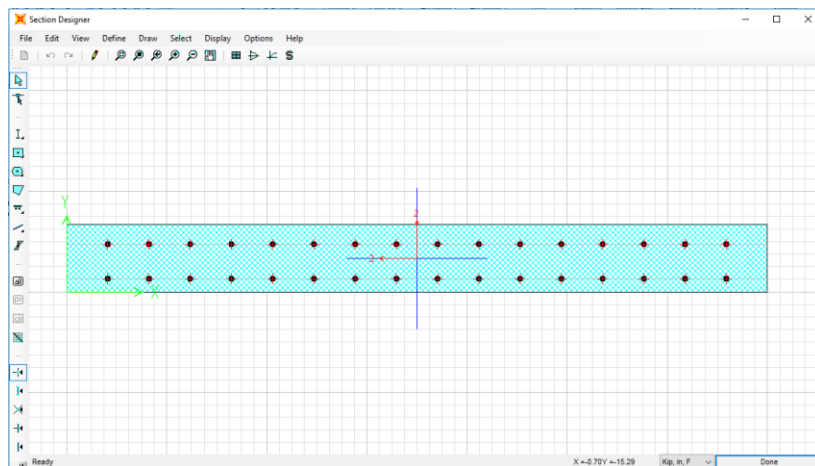
a 1.25 inch bottom cover and transverse reinforcement are located at 2.1875.

e. Click Done



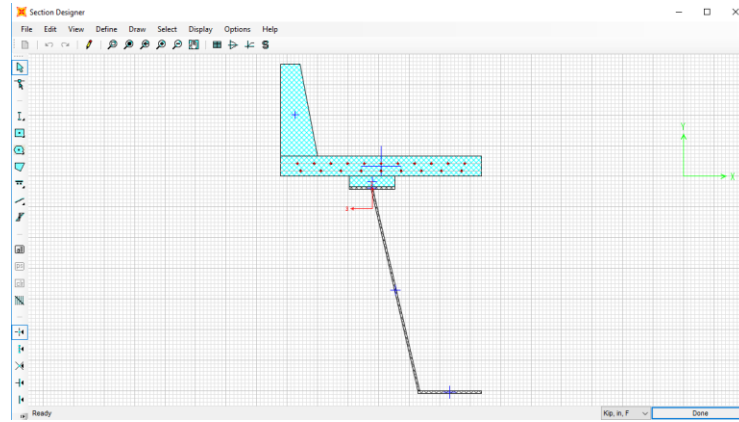
f. Repeat this process for the transverse elements

- i. At the SD Section Designer Window select Modifiers and set Mass and Weight to 0, as to not double count the dead weight.
- ii. The interior transverse members are 84 inches wide (end members are 60 in. wide) with #5 rebar at 5 inch spacing at 5.6875 in. and 1.5625 in.

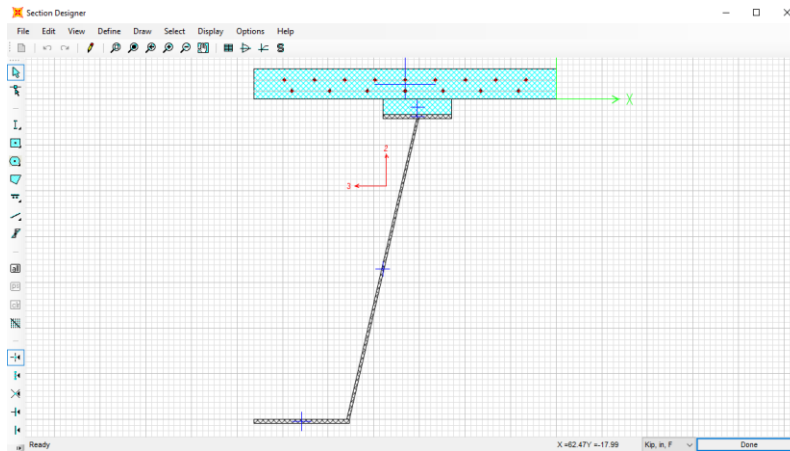


g. To generate and exterior longitudinal member and an interior longitudinal member. Make two copies of the B2Long section. Label one LongOut and on LongInt.

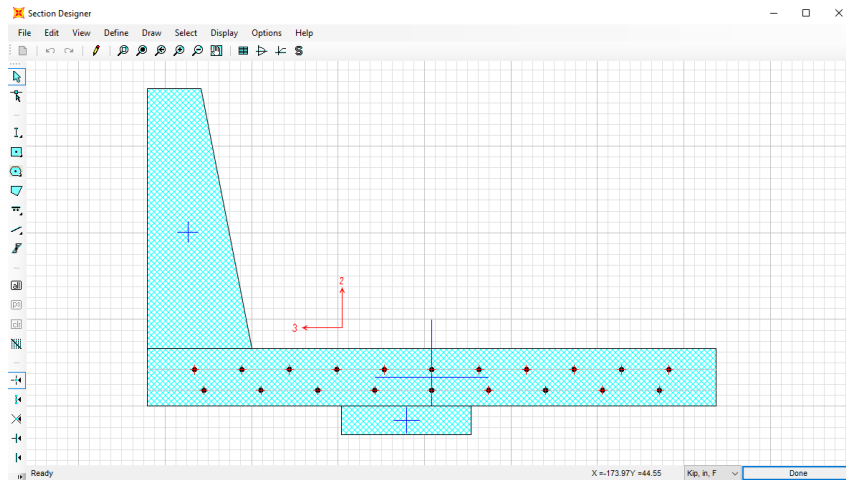
- i. For the LongOut delete every element right of the centerline.



- ii. For the LongInt delete every element left of the centerline.

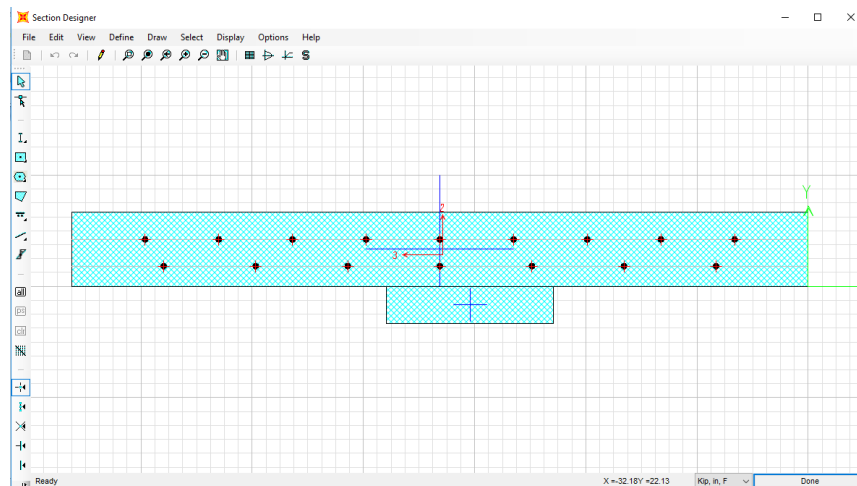


- h. To generate a simulated fracture section make copies of LongOut and LongInt.
 - i. Name the copy of LongOut FracOut.
 1. Delete the bottom flange, web, and top flange of the steel tub.



ii. Name the copy of LongInt FracInt.

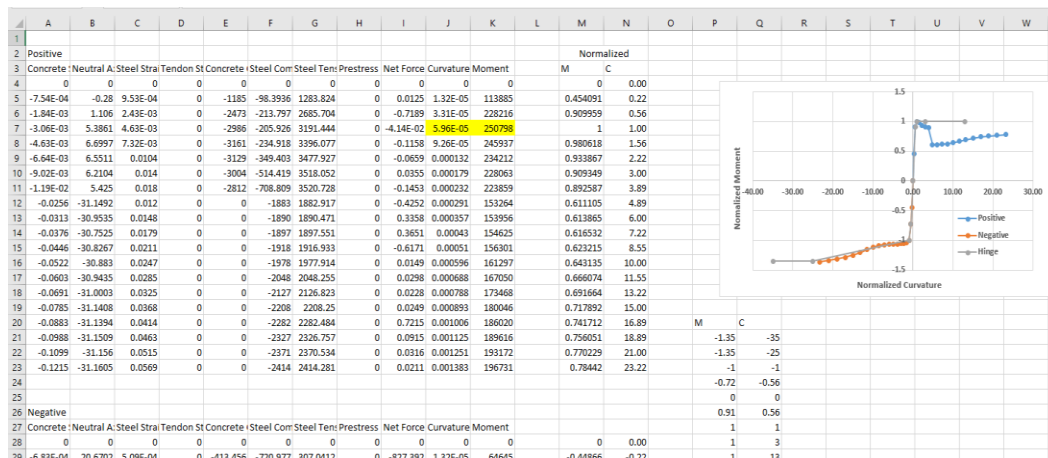
1. Delete the bottom flange, web, and top flange of the steel tub.



8. Generating plastic hinges for frame elements in SAP2000.

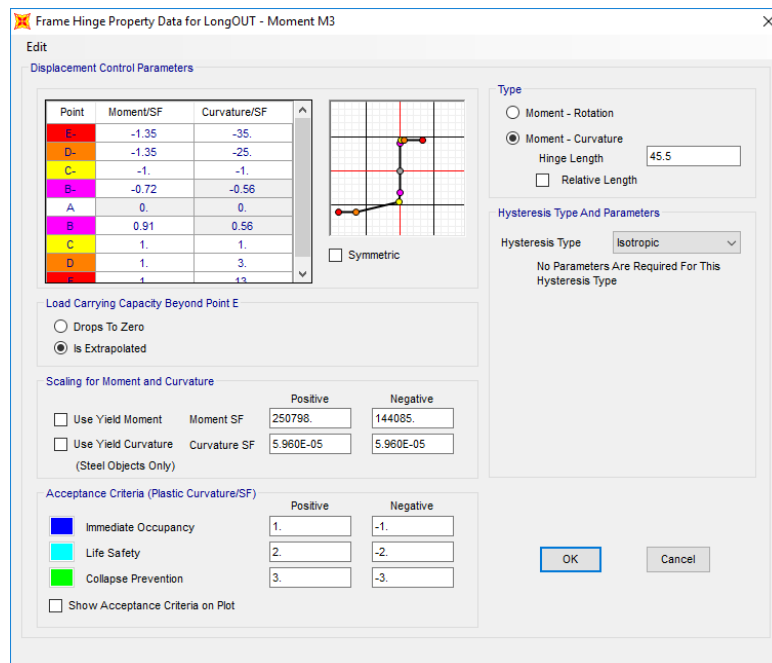
- a. Define->Section Properties->Frame Sections
- b. Select the desired cross section. Hinges will need to be made for the LongOut, LongInt, FracOut, FracInt, Trans, and TransEnd.
- c. Once selected, click Modify/Show Property->Section Designer
- d. Once in the section designer select the Moment Curvature Curve tool.
- e. In the Moment Curvature Curve window select Details.
 - i. Copy the moment curvature data to an Excel file.
 - ii. Select OK.
- f. In the Moment Curvature Curve window change the Angle (deg) to 180 then select Details

- i. Copy the moment curvature data to the same Excel file as previous.
 - ii. Select OK.
- g. Generate a Normalized Moment Curvature Diagram
- i. Normalize the Moments by dividing each of the positive moments by the maximum positive moment and the negative moment by the maximum negative moment. And divide the curvatures by the curvatures corresponding to the maximum and negative moments.
 - ii. Plot the normalized positive and negative moment curvatures on a chart.
 - iii. Create a hinge moment curvature plot on the same chart with 4 positive moment points and 4 negative moment points without generating a negative slope.



- h. Define Hinge Length
- i. The hinge length is one half of the section depth.
 1. $Hinge_{long} = 0.5 * (Deck\ thickness + haunch\ height + top\ flange\ thickness + web\ height + bottom\ flange\ thickness)$
 - a. $Hinge_{long} = 45.5\ in.$
 2. $Hinge_{Frac} = 0.5 * (Deck\ thickness + haunch\ height)$
 - a. $Hinge_{Frac} = 6\ in.$
 3. $Hinge_{Trans} = 0.5 * (Deck\ thickness)$
 - a. $Hinge_{Trans} = 4\ in.$
 - i. Making the plastic hinge in SAP200.
 - i. Select Define->Section Properties-> Hinge Properties->Add New Properties
 - ii. In the Type window select moment curvature and input the corresponding correct Hinge Length.

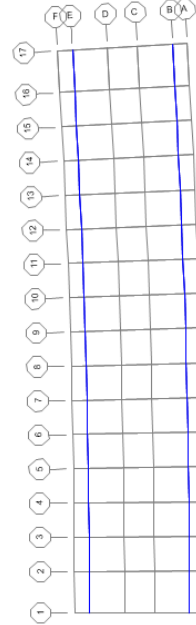
- iii. In the Moment Curvature table insert the 4 positive and 4 negative normalized moment curvatures and the zero point.
- iv. Uncheck the symmetric box and select the Is Extrapolated option in the “Load Carrying Capacity beyond Point E” window.
- v. In the “Scaling for Moment and Curvature” window insert the maximum positive moment and corresponding curvature as well as the maximum negative curvature and corresponding curvature.
- vi. In the Acceptance Criteria use the values 1,2, and 3 for Immediate Occupancy, Life Safety, and Collapse Prevention in the positive column and -1, -2, and -3 for the negative column.
- vii. Repeat for all remaining Frame Sections (LongOut, LongInt, FracOut, FracInt, Trans, and TransOut)



9. Assign Frame Members to Grid.

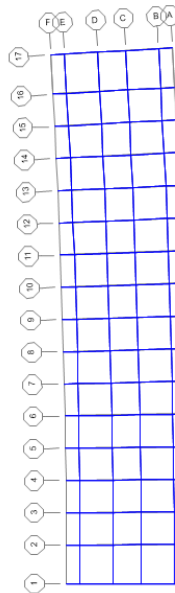
- a. Select the Draw tab->Quick Draw Frame/Cable/Tendon
- b. In the Section drop down menu select LongOut.
- c. Then click on every grid segment on second to last longitudinal grids (B & E).

Properties of Object	
Line Object Type	Straight Frame
Section	LongOUT
Moment Releases	Continuous
XY Plane Offset Normal	0.



- d. Change the Section to LongInt and repeat step c but for the two interior longitudinal grids (C & D).
- e. Change the Section to TransEnd and repeat step c but for the end transvers grids (1 & 17).
- f. Change the Section to Trans and repeat step c but for all other transverse grids (2 to 16).

Properties of Object	
Line Object Type	Straight Frame
Section	Trans
Moment Releases	Continuous
XY Plane Offset Normal	0.



10. Assign Hinges to Frame Elements

- a. The Longitudinal Hinges are placed at the ends of the longitudinal frame elements or at a relative distance of 0 and 1.
- b. The Transvers hinges are placed at a distance of half a top flange width away from the node.

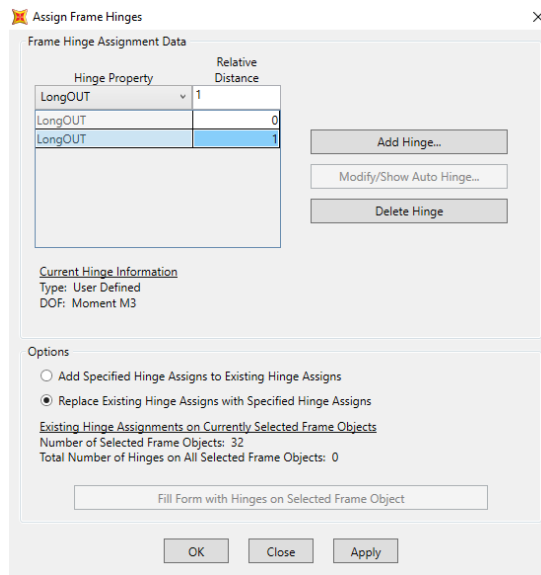
i. $Hinge\ Loc_{F\ to\ E} = \frac{half\ flange\ width}{Element\ Width} = 1 - \frac{18/2}{36} = 0.75$

ii. $Hinge\ Loc_{E\ to\ D\ and\ C\ to\ B} = \frac{half\ flange\ width}{Element\ Width} = \frac{18/2}{86} = 0.1046\ and\ (1 - 0.1046)\ or\ 0.8954$

iii. $Hinge\ Loc_{D\ to\ C} = \frac{half\ flange\ width}{Element\ Width} = \frac{18/2}{73} = 0.1233\ and\ (1 - 0.1046)\ or\ 0.8767$

iv. $Hinge\ Loc_{B\ to\ A} = \frac{half\ flange\ width}{Element\ Width} = \frac{18/2}{36} = 0.25$

- c. In SAP2000 assign the hinges to corresponding frame elements.
- i. Select the desired frame elements you wish to assign hinges to such as LongOut. (The elements will turn from blue to yellow).
 - ii. In SAP2000 select the Assign tab->Frame->Hinges
 1. From the drop down menu select LongOut and set relative distance to 0 and click ADD.
 2. From the drop down menu select LongOut and set relative distance to 1 and click ADD.
 3. Then click OK.



- iii. Repeat Step ii. for all other frame elements.



11. Assigning Loads to the Frame Elements

a. HS20 Wheel Axel Loads

- i. HS20 Axel Loads will be placed at distances of 36 in., 108 in., 180 in., and 252 in. from the outside of the curved edge.
- ii. One line of the 16 kip axels will be placed at the half way point of the bridge or transverse grid 9 with the second line 14 feet away at transverse grid number 7. One line of 4 kip axels will be placed 14 feet away from the first line of axels at grid line 11.
- iii. In SAP2000 the loads have to be placed at a relative distance so this value needs to be calculated.

$$1. \text{HS20}_{Axel 1 \text{ Loc } (B-A)} = \frac{L_1 - 36}{L_1} = \frac{36 - 36}{36} = 0$$

$$2. \text{HS20}_{Axel 2 \text{ Loc } (C-B)} = \frac{L_1 + L_2 - 108}{L_2} = \frac{36 + 86 - 108}{86} = 0.1628$$

$$3. \text{HS20}_{Axel 3 \text{ Loc } (D-C)} = \frac{L_1 + L_2 + L_3 - 180}{L_3} = \frac{36 + 86 + 73 - 180}{73} = 0.2055$$

$$4. \text{HS20}_{Axel 4 \text{ Loc } (E-D)} = \frac{L_1 + L_2 + L_3 + L_4 - 252}{L_4} = \frac{36 + 86 + 73 + 86 - 252}{86} = 0.3372$$

b. Lane Loads

- i. Lane Loads are line loads of 0.640 kip/ft (0.05333 kip/in.) centered at a distance of 96 in. and 240 in. from outside of the curved edge.
- ii. These lane loads will be placed on the longitudinal frame elements. They will be assigned to elements along the B, C, D,

and E longitudinal elements according to the appropriate tributary distance.

$$1. LaneLoad_B = \left(\frac{L_1 + L_2 - 96}{L_2} \right) * laneload = \left(\frac{36 + 86 - 96}{86} \right) * 0.05333 = 0.016124 \frac{kip}{in}.$$

$$2. LaneLoad_C = laneload - laneload_B = 0.05333 - 0.016124 = 0.037209 \frac{kip}{in}.$$

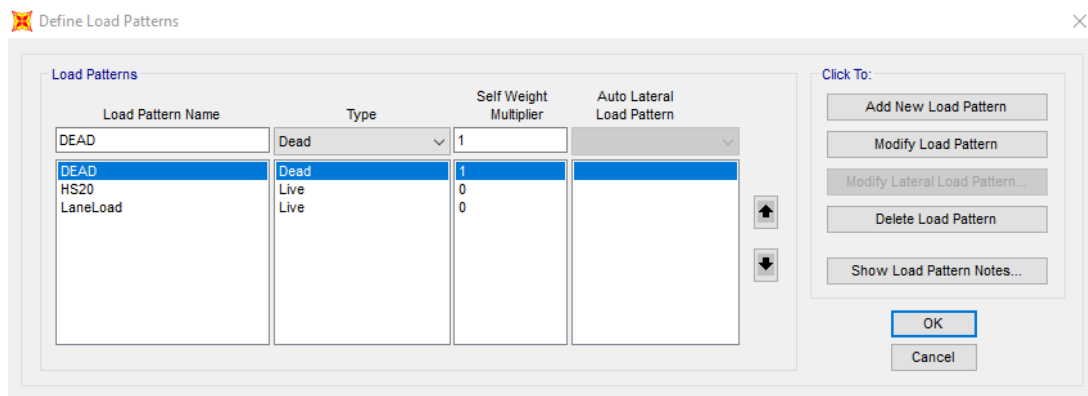
$$3. LaneLoad_D = \left(\frac{L_1 + L_2 + L_3 + L_4 - 240}{L_4} \right) * laneload = \left(\frac{36 + 86 + 73 + 86 - 240}{86} \right) * 0.05333 = 0.025426 \frac{kip}{in}.$$

$$4. LaneLoad_E = laneload - laneload_D = 0.05333 - 0.025426 = 0.027907 \frac{kip}{in}.$$

c. In SAP2000 the load patterns must be first be defined.

i. Select the Define tab->Load Patterns.

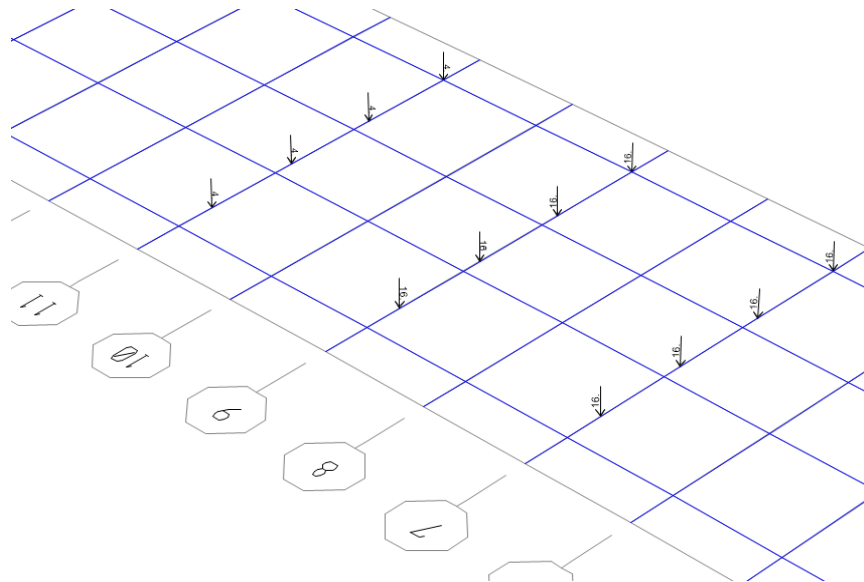
1. Under the Load Pattern Name enter HS20 and change the type in the drop down menu to Live. The self-weight multiplier should be set to 0. Then click Add New Load Pattern.
2. Under the Load Pattern Name enter LaneLoad and change the type in the drop down menu to Live. The self-weight multiplier should be set to 0. Then click Add New Load Pattern.
3. Then click OK.



ii. Assigning the HS20 wheel loads in SAP2000.

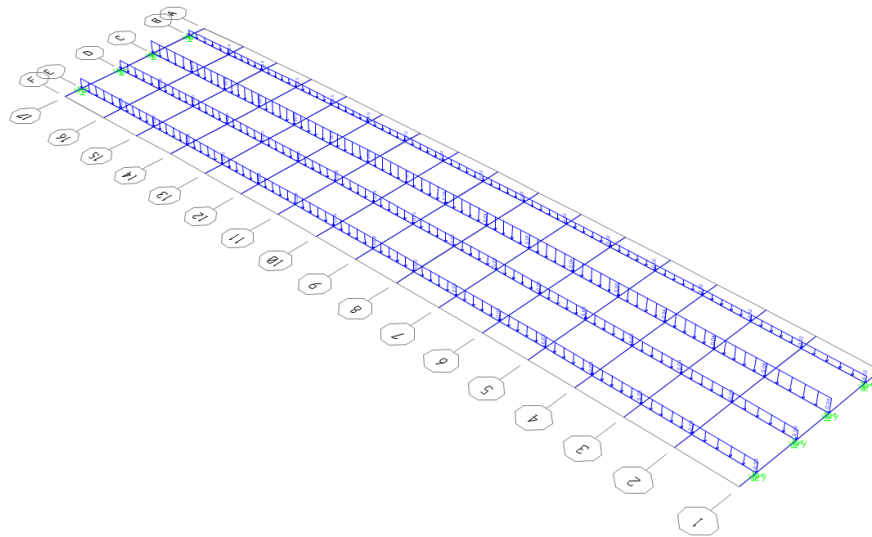
1. Select the exterior transverse element of grid line 9 and 7.
2. Click Assign->Frame Loads->Point

3. From the Load Pattern drop down menu select HS20 and verify that the Coordinate System is set to Global, the Load Direction is Gravity, and the Load Type is Force.
4. In column 1 enter a Relative Distance of 0 (HS20 Axel 1 Loc. B-A) and Load of 16 kips.
5. Click OK.
6. Repeat for grid line 11 to assign the 4 kip load.
7. Repeat Steps 1-6 for HS20 Axel 2,3,4 Loc. C-B, D-C, and E-D.



iii. Assigning the Lane Load in SAP2000.

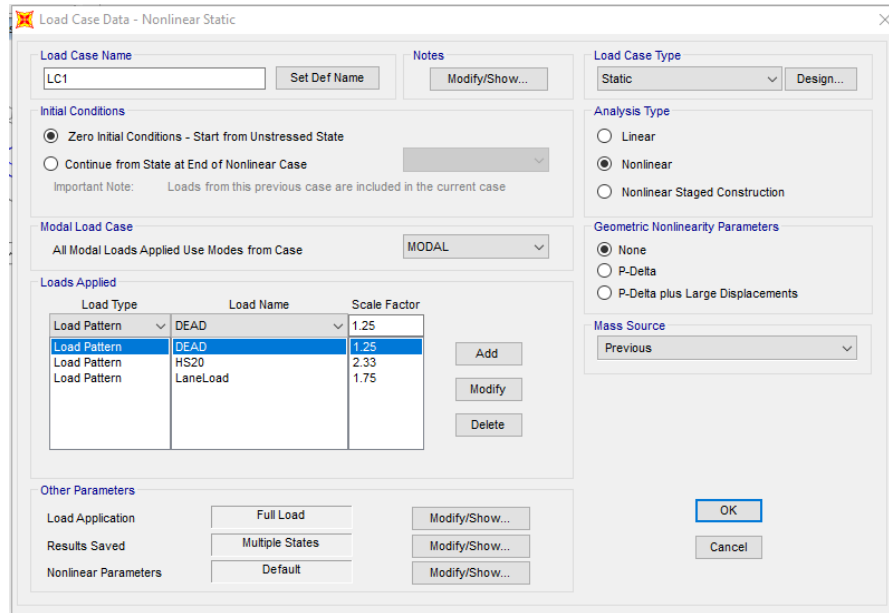
1. Select all exterior longitudinal frame elements along grid line B.
2. Click Assign->Frame Loads->Distributed
3. From the Load Pattern drop down menu select Lane Load and verify that the Coordinate System is set to Global, the Load Direction is Gravity, and the Load Type is Force.
4. In the Uniform Load box enter 0.016124 (Lane Load B).
5. Click OK.
6. Repeat Steps 1-5 for all of the longitudinal elements along gridlines C, D, and E.



12. Defining Load Cases

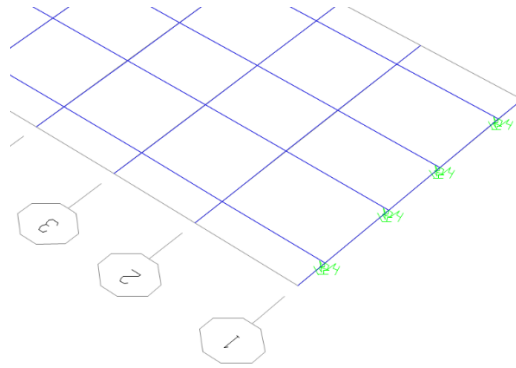
- a. The Load Case being used to determine redundancy is $1.25DL + 1.75(LL + IM)$. Where DL=Dead Load, LL= Live Load, and IM= Impact Load. When substituting in the HS20 truck load and the Lane Load the preceding equation reduces to $1.25DL + 1.75LaneLoad + 2.33HS20$
- b. Generating Load Cases in SAP2000.
 - i. Click Define->Load Cases->Add New Load Case
 - ii. In the Load Case Name Panel name the load case "LC1"
 - iii. In the Analysis Type select "Non-Linear"
 - iv. For the LC1 Load Case in the Stiffness to use panel select "Zero Initial Conditions"
 - v. In the Loads Applied panel leave the Load Type "Load Pattern" in the drop down Load Name menu select DEAD and change the Scale Factor to 1.25. Click Add. Change the Load Name menu select HS20 and change the Scale Factor to 2.33. Click ADD. Change the Load Name menu select Lane Load and change the Scale Factor to 1.75. Click ADD.
 - vi. In the Other Parameters panel in the Results Saved section click Modify/Show.
 - vii. In the Results Saved for Nonlinear Static Load Cases window change the Results Saved to Multiple States and in the For Each Stage panel change the Minimum Number of Saved Steps and the Maximum Number of Saved Steps to 20. Click OK.
 - viii. Then Click the OK on the Load Case Data Window.
 - ix. Repeat Steps i.-viii. to create an LC2, LC3, and LC4. However, in the Initial Conditions Window select Continue from State at End

of Nonlinear Case and from the drop down menu select the preceding load case. (For LC2 the Nonlinear Case LC1 would be selected).



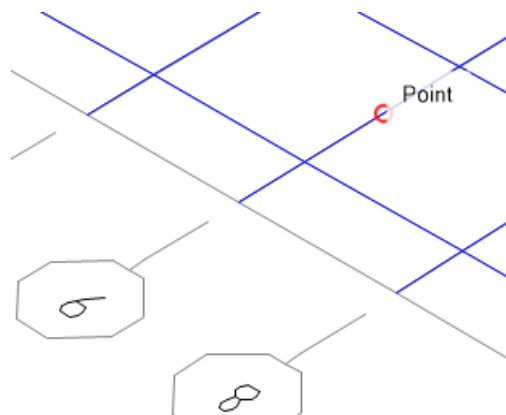
13. Defining End Supports

- a. The elastomeric bearing pad for each girder have lateral stiffness of 12 kip/in. and a vertical stiffness of 6100 kip/in. Since the tub girders are divided in half, the lateral stiffness will be 6 kip/in. and the vertical stiffness will be 3050 kip/in.
- b. Assigning spring supports in SAP2000.
 - i. Select the 8 nodes at the very end of the longitudinal members.
 - ii. Click Assign->Joint->Springs
 - iii. In the Assign Joint Springs window in the Simple Springs Stiffness panel enter 6 for Translation 1&2 and 3050 for Translation 3.
 - iv. Click OK.



14. Defining Centerline Data Acquisition Points at Mid-Span of Girder

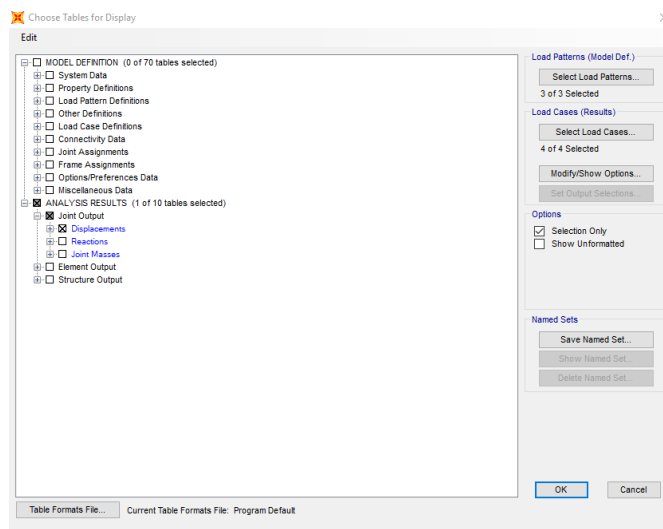
- a. Select the transverse frame elements between B&C as well as D&E at Mid-Span (Gridline 9).
- b. Click Edit->Edit Lines->Divide Frames
- c. In the Divide into Specified Number of Frames window enter 2 for Number of Frames.
- d. Click OK.



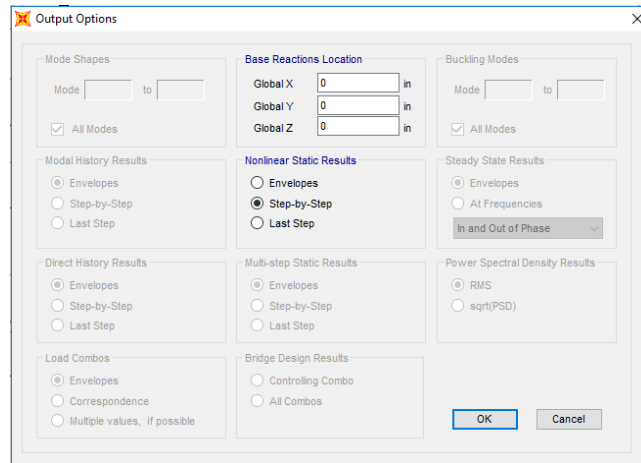
15. Analyzing the Non-Fracture Structure for Dead Load Only

- a. In SAP2000 click Analyze->Run Analysis
- b. In the Set Load Cases to Run window click the Run/Do Not Run All button until every Action is Do Not Run.
- c. Select DEAD then click Run/Do Not Run Case until the Action is Run.
- d. Then click Run Now. Let SAP2000 Run the Load Cases until the screen says the Analysis is Complete.
- e. Once the analysis is complete, select the spring reactions.
- f. Click Display->Show Tables

- g. In the Choose Table for Display window click the + symbol beside Joint output and select the square box beside Reactions.
 - h. In the Output Options window in the Nonlinear Static Results panel select Last Step.
 - i. Select and copy the information from the F3 column.
 - j. The sum of the F3 values is the dead load.
 - k. Then click Done.
 - l. Unlock the structure.
16. Analyzing the Non-Fractured Structure
- a. In SAP2000 click Analyze->Run Analysis
 - b. In the Set Load Cases to Run window click the Run/Do Not Run All button until every Action is Do Not Run.
 - c. Select LC1, LC2, LC3, and LC4 then click Run/Do Not Run Case until the Action for all 4 is Run.
 - d. Then Click Run Now.
 - e. Let SAP2000 Run the Load Cases until the scree says the Analysis is Complete.
 - f. Once the analysis is complete, select the data collection point on the transverse member on the outside girder (C-B).
 - g. Click Display->Show Tables
 - h. In the Choose Table for Display window click the + symbol beside Joint output and select the square box beside Displacements



- i. Click the Modify/Show Options button.
- j. In the Output Options window in the Nonlinear Static Results panel select Step-by-Step.



- k. Click OK.
- l. Select and copy the information from the Output Case, StepNum Unitless, and the U3 in. column and paste them into an Excel worksheet. These columns represent Load Case, Step Number, and Deflection for the Outside Girder respectively.

Joint Text	OutputCase	Case Type Text	Step Type Text	StepNum Unitless	U1 in	U2 in	U3 in	R1 Radians	R2 Radians	R3 Radians
103	LC1	NonStatic	Step	0	0	0	0	0	0	0
103	LC1	NonStatic	Step	1	0.002545	7.7E-05	-0.087926	-2.681E-06	0.000169	5.324E-08
103	LC1	NonStatic	Step	2	0.00509	0.000154	-0.175851	-5.363E-06	0.000338	1.065E-07

- m. Then click Done.
- n. Select the data collection point on the transverse member on the inside girder (E-D) and repeat Steps g-l. However, on Step 1 there is no need to copy Output Case, Step Num Unitless again.
- o. Select the joint on the transverse member on the outside girder at transverse element 9 (at longitudinal element B) and repeat Steps g-l. This information goes into the Delta 4 column. However, on Step 1 there is no need to copy Output Case, Step Num Unitless again.
- p. Select the joint on the transverse member on the outside girder at transverse element 9 (at longitudinal element C) and repeat Steps g-l. This information goes into the Delta 3 column. However, on Step 1 there is no need to copy Output Case, Step Num Unitless again.
- q. Select the joint on the transverse member on the inside girder at transverse element 9 (at longitudinal element D) and repeat Steps g-l. This information goes into the Delta 2 column. However, on Step 1 there is no need to copy Output Case, Step Num Unitless again.

- r. Select the joint on the transverse member on the outside girder at transverse element 9 (at longitudinal element E) and repeat Steps g-l. This information goes into the Delta 1 column. However, on Step 1 there is no need to copy Output Case, Step Num Unitless again.

	A	B	C	D	E	F	G	H	I	J	K	L	M	V	X	Y	Z	AA	AB	AC	AD
1	Intact			OG-CL	IG-CL			Point 4	Point 3	Point 2	Point 1			Applied Load (kip)	OG	IG					
2	Load Case	Load Step	Ω	Delta (in)	Chord (rad)	Delta (in)	Chord (rad)	Delta (in)	Delta (in)	Delta (in)	Delta (in)	α 23 (rad)	α 32 (rad)	Ω (cal)	Delta (in)	Chord (deg)	Delta (in)	Chord (deg)	α 23 (deg)	α 32 (deg)	
3	LC1	0	0	0	0.00000	0	0.00000	0	0	0	0	0	0	0	0.00	0.00	0.00000	0.00	0.00000	0	0
4	LC1	1	0.05	-0.1037	0.00015	-0.087926	0.00013	-0.10541	-0.10129	-0.0942	-0.07905	7.89E-05	4.94E-05	66	0.05	0.10	0.00861	0.09	0.00730	0.004522	0.002831
5	LC1	2	0.1	-0.2074	0.00030	-0.175851	0.00025	-0.21081	-0.20259	-0.18839	-0.15809	0.000158	9.88E-05	132	0.10	0.21	0.01722	0.18	0.01460	0.009043	0.005662

- s. Once all of the data is collected unlock the model by selecting the Lock tool on the left hand side of SAP2000 screen.

17. Analyzing the Fractured Structure

- a. At Mid-Span along grid line 9, replace the hinges of the outside longitudinal element (gridline B) with FracOUT hinges according to Step 10.
- b. At Mid-Span, along gridline 9, replace the hinges of the first interior longitudinal element (gridline C) with FracInt hinges according to Step 10.



- c. Repeat Step 15 for the Fractured Case and collect the data accordingly.

18. Post Processing of the Data

- a. In the Excel Sheet the following values need to be calculated for each step.
- i. Omega (Ω)

$$1. \Omega_i = \Omega_{i-1} + \left(\frac{1}{\# \text{ of Steps in Load case}} \right)$$

ii. Longitudinal Chord Rotation of Interior and Exterior Girder

$$1. \text{ Chord Rot.}_{single span} = -1 * \left(\frac{\delta_{CL}}{0.5 * L} \right) \text{ (rad)}$$

iii. Transverse Deck Rotation

$$1. \alpha_{2-3} = \left(\frac{\delta_3 - \delta_2}{s} \right) - \left(\frac{\delta_2 - \delta_1}{w} \right) \text{ (rad)}$$

$$2. \alpha_{2-3} = \left(\frac{\delta_3 - \delta_2}{s} \right) - \left(\frac{\delta_2 - \delta_1}{w} \right) \text{ (rad)}$$

3. Where s=spacing between the interior top flanges of the inside and outside girders and w=spacing between the top flanges of the same girder.

iv. Applied Load

1. Calculate unit applied load or applied load at 1 Ω .

$$2. \text{ Unit Applied Load}_{single span} = 1.25 *$$

$$\text{Total Reactions from Dead Load Case} + 2 * (2.33 * \text{HS20 truck} + 1.75 * \text{Lane Load})$$

$$3. \text{ Applied Load} = \text{Unit Applied Load} * \Omega$$

b. Repeat Step A for the Fractured Case.

c. Calculate the initial stiffness for intact bridge and instantaneous stiffness for fractured bridge.

i. For the Non-Fractured condition (Intact Bridge) find the absolute displacement for the Outside Girder at an Ω value of 0.4.

$$1. \text{ Initial Stiffness} = \frac{0.4}{\text{Absolute Displacement OG (at } \Omega=0.4)}$$

ii. For the Fractured case add an additional column labeled stiffness

$$1. \text{ Instantaneous Stiffness}_{OG-Frac. i} = \frac{\Omega_i - \Omega_{i-1}}{\delta_i - \delta_{i-1}}$$

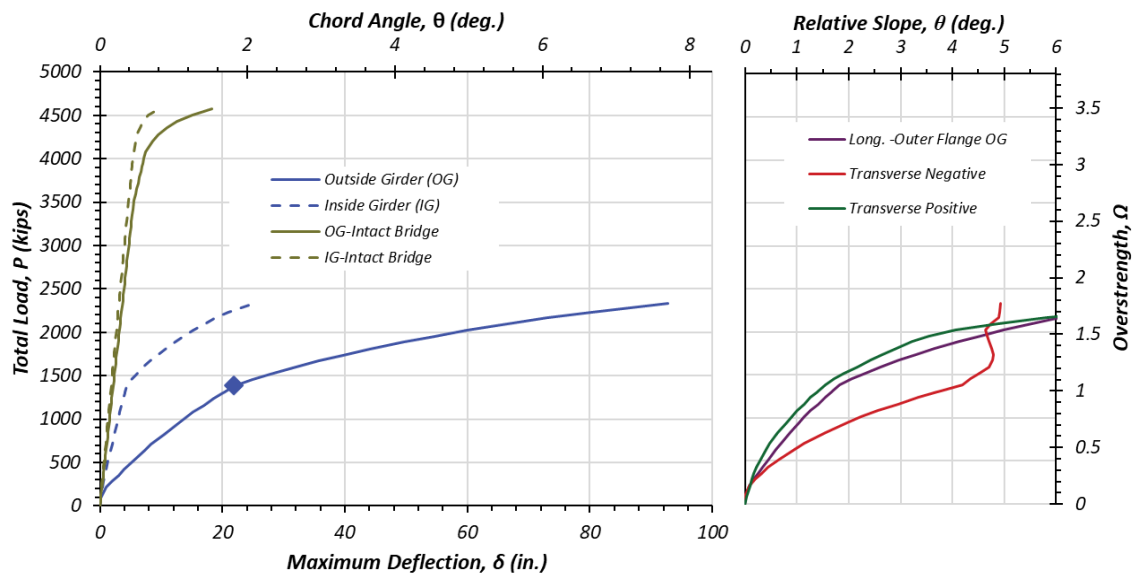
d. Failure of the structure occurs at the Ω of the Fractured Bridge at the first of the following criteria.

i. The instantaneous stiffness for the fractured outside girder is less than 5% of the initial stiffness of the intact outside girder.

ii. The chord angle of the outside girder for a simple spans or interior spans is greater than 2°. The chord angle for exterior spans of multi-span bridges is greater than 3°.

iii. The transverse deck rotation is greater than 5°.

e. On a chart plot the Non-Fractured Outside and Inside Girder as well as the Fractured Outside and Inside Girder with displacement on the primary x axis and the Total Force on the primary y axis and Ω on the secondary y-axis



Grillage Analysis Example of Bridge 5

1. Gather Bridge Geometry and Material Information.

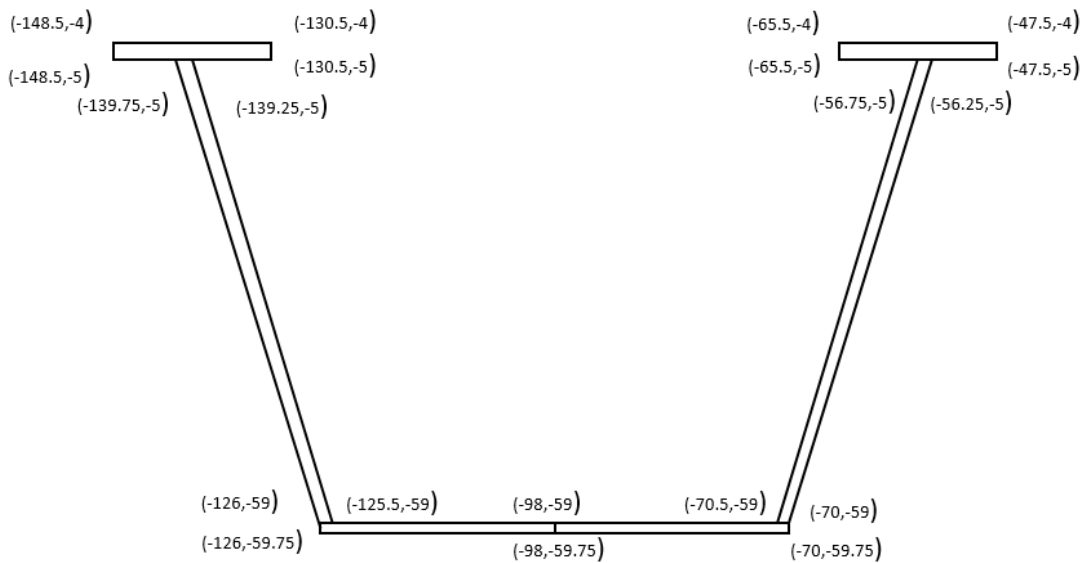
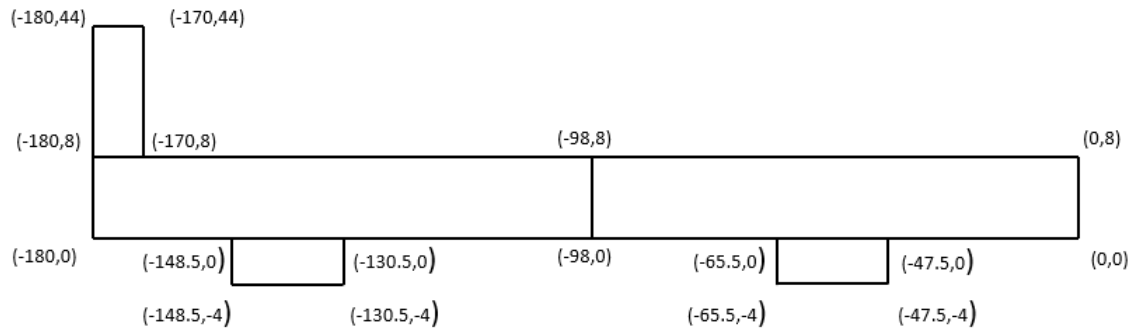
Location ft	Top Flange		Web		Bottom Flange	
	Width in.	Thickness in.	Width in.	Thickness in.	Width in.	Thickness in.
0-105	18	1.00	54	0.5	56	0.75
105-122	18	1.00	54	0.5625	56	1.250
122-140	18	1.75	54	0.5625	56	1.250
140-157	18	1.75	54	0.5625	56	1.250
157-174	18	1.57	54	0.5625	56	1.250
174-192	18	1.00	54	0.5625	56	0.75
192-280	18	1.00	54	0.5	56	0.75

Location	Parameter	Description/Value
Bridge	Location	Travis County, I35
	Year Designed/Year Built	1998/2002
	Design Load	HS20
	Length, ft	279.58
	Spans, ft	140, 139.58
	Radius of Curvature, ft	450
Deck	Width, ft	30
	Thickness, in.	8
	Haunch, in.	4
	Rail Type	T4(S)
Rebar	# of Bar Longitudinal Top Row (#4)	40
	# of Bar Longitudinal Bottom Row (#5)	36
	# of Bar Longitudinal Top Row (#4) @support	41
	# of Bar Longitudinal Top Row (#5) @support	40
	# of Bar Longitudinal Bottom Row (#5) @support	36
	Transverse Spacing Top Row (#5), in.	5
	Transverse Spacing Bottom Row (#5), in.	5
	Girder	CL of Bridge to CL of Girder (in.)
CL of Top Flange to CL of Top Flange (in.)		83

2. Material constitutive behavior

Concrete (4 ksi)		Rebar (60 ksi)		Steel (50 ksi)	
Stress (ksi)	Strain (1/in)	Stress (ksi)	Strain (1/in)	Stress (ksi)	Strain (1/in)
-4	-3.79E-03	-87.9	-0.095	-71.6	-0.1
-4	-3.56E-03	-87.9	-0.0944	-71.6	-0.097
-4	-2.69E-03	-86.6	-0.0761	-71.6	-0.095
-4	-1.78E-03	-78	-0.0386	-71.6	-0.0946
-3.8205	-1.40E-03	-60.7	-9.80E-03	-70.3	-0.0764
-2.8718	-8.69E-04	-60.3	-2.08E-03	-62.5	-0.039
-0.6403	-1.78E-04	0	0	-50	-0.0196
0	0	60.3	2.08E-03	-50	-1.72E-03
0.378	1.06E-04	60.7	9.80E-03	0	0
0.378	1.16E-03	78	0.0386	50	1.72E-03
		86.6	0.0761	50	0.0196
		87.9	0.0944	62.5	0.039
		87.9	0.095	70.3	0.0764
				71.6	0.0946
				71.6	0.095
				71.6	0.097
				71.6	0.1

3. Create a Coordinate system for half width of the span for each cross section in 1. An example of the first cross section is show below.



4. Create a cylindrical coordinate system for the curved bridge assuring that the middle transverse divisions are 7 ft, as this will aid in applying the HS20 truck load whose axels are separated by 14 ft.

a. # of Segments_{per span} =

$$\left(\frac{\text{Length (ft)} * 12}{84 \text{ in (7ft)}} \right) \text{ rounded to nearest even number}$$

i. # of Segments_{Span 1&2} = $\left(\frac{140 * 12}{84} \right) = 20$

b. End Segment Length = $\left((\text{Length} * 12) - (\# \text{ of Segments} * 84) \right) / 2$

- i. $End\ Segment\ Length = \frac{((140*12)-(14*84))}{2} = 0\ in.$
- ii. Therefore, the end segments are also equal to 84 in.
- c. $Theta = \frac{Total\ Length}{Radius}$
- i. $Theta = \frac{280}{450} = 0.6222\ rad\ or\ 36.65\ degrees$
- d. Determine the radial offsets using the outside edge, the outside flange, the inner flange and centerline of the bridge.

Offsets (in.)	
Edge	180
Outside Flange	139.5
Inner Flange	56.5
CL of Bridge	0

Radial Spacing (in.)		
A	5580	CL+Edge
B	5539.5	CL+OF
C	5456.5	CL+IF
Center Line	5400	or 450 (ft)
D	5343.5	CL-IF
E	5260.5	CL-OF
F	5220	CL-Edge

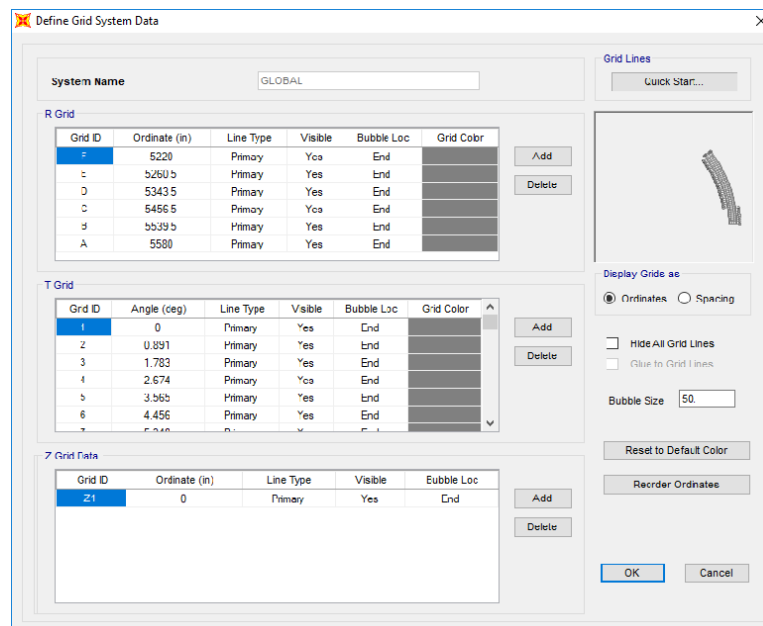
- b. The Longitudinal or spacing along theta is determined by converting the longitudinal segment lengths into degrees.
- i. All segments are 84 in. The total length is 280 ft or 3360 in.
- ii. $Radial\ Spacing\ (rad) = \frac{Long.Spacing}{Radius}$
- iii. $Radial\ Spacing\ (degree) = Radial\ Spacing\ (rad) * \frac{180}{\pi}$

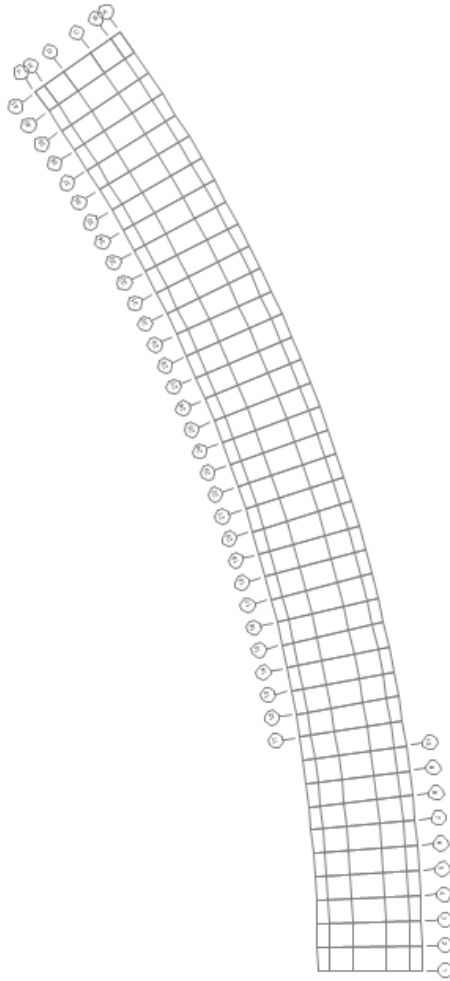
Long. Spacing (in.)	Radial Spacing (rad.)	Radial Spacing (deg.)	Cross Section
0	0.0000	0.000	Long1
84	0.0156	0.891	Long1
168	0.0311	1.783	Long1
252	0.0467	2.674	Long1

336	0.0622	3.565	Long1
420	0.0778	4.456	Long1
504	0.0933	5.348	Long1
588	0.1089	6.239	Long1
672	0.1244	7.130	Long1
756	0.1400	8.021	Long1
840	0.1556	8.913	Long1
924	0.1711	9.804	Long1
1008	0.1867	10.695	Long1
1092	0.2022	11.586	Long1
1176	0.2178	12.478	Long2
1260	0.2333	13.369	Long2
1344	0.2489	14.260	Long2
1428	0.2644	15.152	Long3
1512	0.2800	16.043	Long3
1596	0.2956	16.934	Long4
1680	0.3111	17.825	Long4
1764	0.3267	18.717	Long4
1848	0.3422	19.608	Long3
1932	0.3578	20.499	Long3
2016	0.3733	21.390	Long2
2100	0.3889	22.282	Long2
2184	0.4044	23.173	Long2
2268	0.4200	24.064	Long1
2352	0.4356	24.955	Long1
2436	0.4511	25.847	Long1
2520	0.4667	26.738	Long1
2604	0.4822	27.629	Long1
2688	0.4978	28.521	Long1
2772	0.5133	29.412	Long1
Long. Spacing (in.)	Radial Spacing (rad.)	Radial Spacing (deg.)	Cross Section
2856	0.5289	30.303	Long1
2940	0.5444	31.194	Long1
3024	0.5600	32.086	Long1
3108	0.5756	32.977	Long1

3192	0.5911	33.868	Long1
3276	0.6067	34.759	Long1
3360	0.6222	35.651	Long1

- iv. *Int. Transverse Element width = 84 in.*
 - v. *End Transverse Element = $84 - \left(\frac{84}{2}\right) = 42 \text{ in.}$*
 - vi. *Peir Tansvers Element = $84 + 84 - 84 = 84 \text{ in.}$*
5. Inputting the coordinate system into SAP2000
- a. Select File -> New Model -> Blank model (making sure units are in kips and inches)
 - b. Right click on the blank workspace and select Edit Grid Data-> Modify/Show System->Quick Start->Cylindrical.
 - i. In the Number of Grid Lines panel set “Along Z=1”
 - ii. In the Grid Spacing panel set “Along Z=1”
 - iii. Select OK.
 - iv. Delete all R and T Coordinates that were generated
 - c. Add correct coordinates for R
 - i. All radial coordinates (A, B, C, D, E, and F).
 - d. Add correct coordinates for T
 - i. All theta coordinates for T (0 to 3360 in.)
 - ii. Click OK
 - e. The Grid System in now formed.

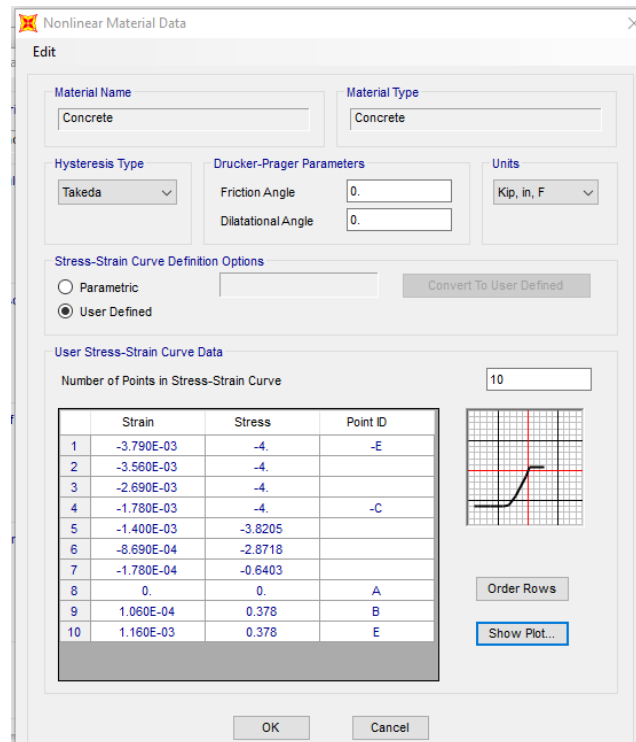




6. Defining Material in SAP200

- a. Click Define-> Materials->Add New Material->Material Type (Steel, Concrete, or Rebar)->Standard (User)->OK
- b. At the bottom of the window select the box which states “Switch to Advanced Properties”
- c. In the open window name the material “Concrete” “Steel” or “Rebar” depending on which material is being defined. Then click “Modify/Show Material Properties”
- d. On the Material Property Data window click “Nonlinear Material Data” icon.
- e. In the Nonlinear Material Data window select the “Convert to User Defined” icon.
- f. Input the number of number of data points for the stress strain behavior (10 for concrete, 13 for rebar, 17 for steel)

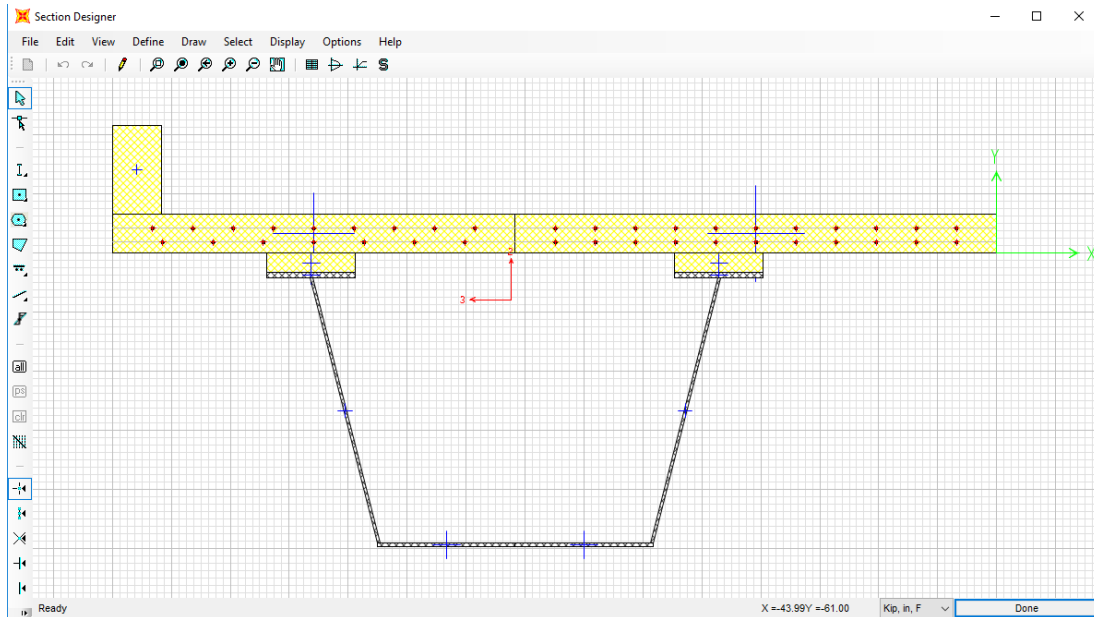
- g. Input the data points for the stress strain behavior.
- h. Select “OK”
- i. Repeat this process again for the remaining materials.



- a. Click Define->Section Properties->Frame Sections->Add New Properties
- b. In the Frame Section Properties Drop down box select “Other” and click Section Designer. In the SD Section Designer Window name the section B5Long1 click the “Section Designer” Icon.
- c. Using the Polygon feature draw the features of the half width of the bridge from Step 3. This includes: one rail, two concrete deck pieces, to concrete haunches, two top flanges, two webs, and two pieces of the bottom flange.
 - i. To change material types for the polygons right click on the polygon and select the desired material type from the material drop down menu.
 - ii. To change the coordinates of the polygon’s nodes use the Reshaper too to change the coordinates.
- d. Add in the longitudinal rebar to both concrete deck elements by using the Line Bar from the Draw Reinforcing Shape tool. From the design drawings it can be determined that there are 7 #4 top bars and 9 #5 bottom bars in the outer concrete deck element and 11 #4 top bars and 11

#5 bottom bars in the inner concrete element. At the pier support 9 additional #5 top bars are added to the top of the outer concrete deck and 10 additional #5 top bars are added to the inner concrete deck. With a 2 inch top cover and transverse reinforcement the top bars are located at 5.0625 inches and with a 1.25 inch bottom cover and transverse reinforcement are located at 2.1875.

e. Click Done (Below is an example of the 1st cross section).

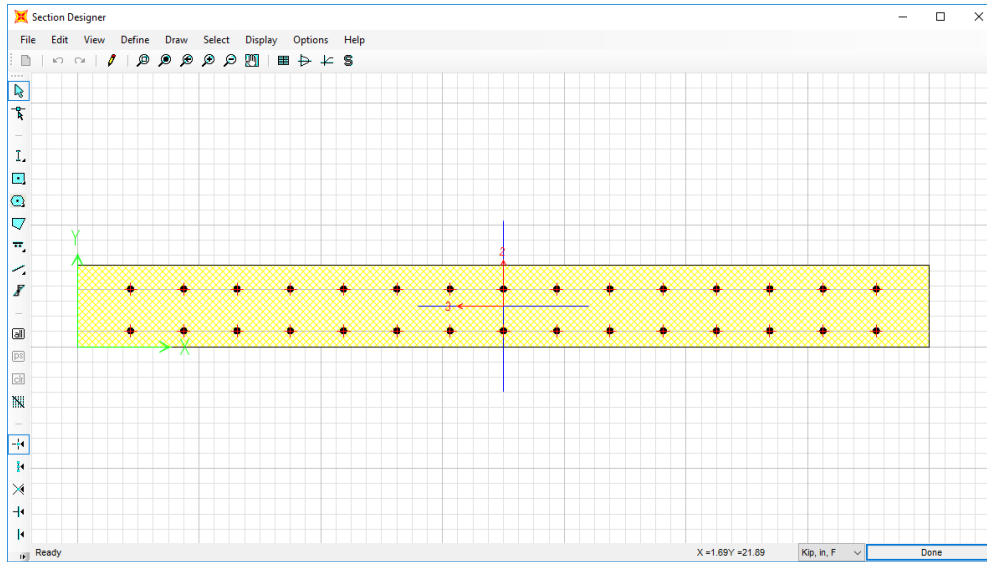


f. Repeat this process for the remaining longitudinal elements.

g. Repeat the process for the transverse elements.

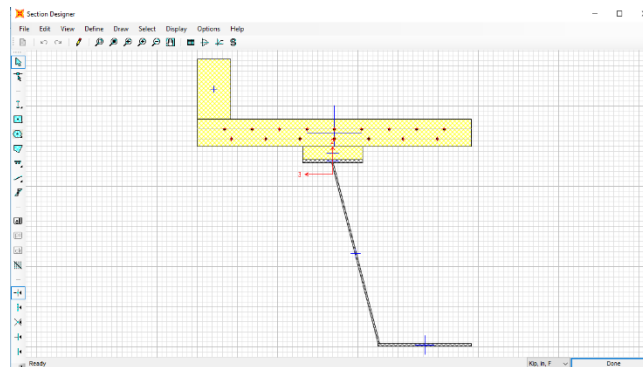
i. At the SD Section Designer Window select Modifiers and set Mass and Weight to 0, as to not double count the dead weight.

ii. The interior transverse members are 84 inches wide (end members are 42 in. wide) with #5 rebar at 5 inch spacing at 5.6875 in. and 1.5625 in.

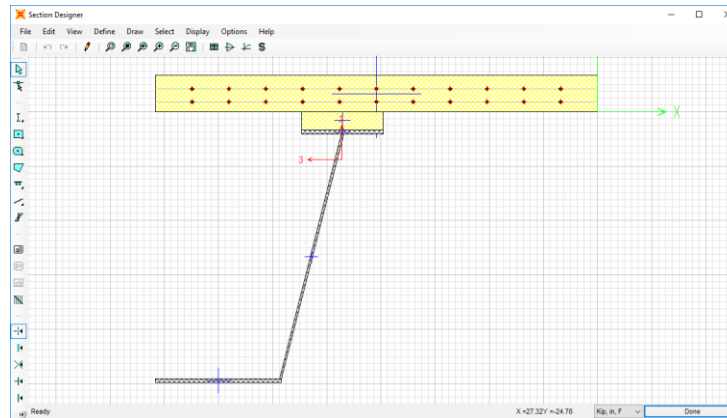


- h. To generate an exterior longitudinal member and an interior longitudinal member. Make two copies of the B5Long1 section. Label one Long1Out and on Long1Int.

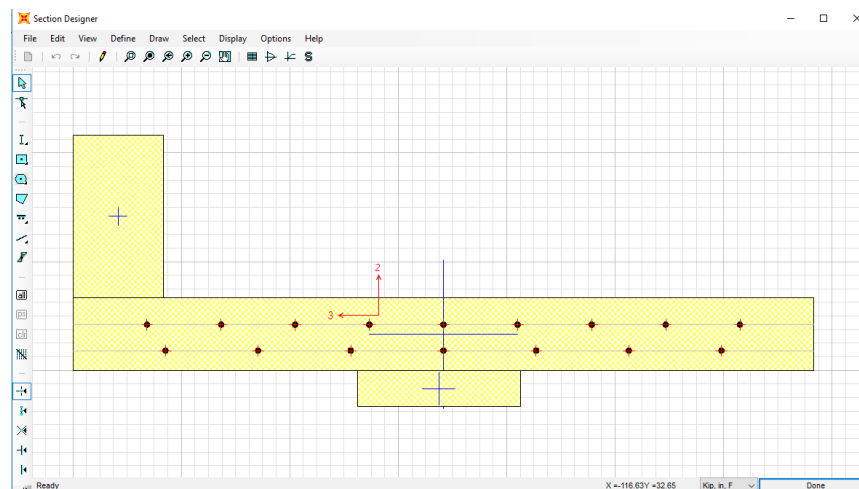
- i. For the Long1Out delete every element right of the centerline.



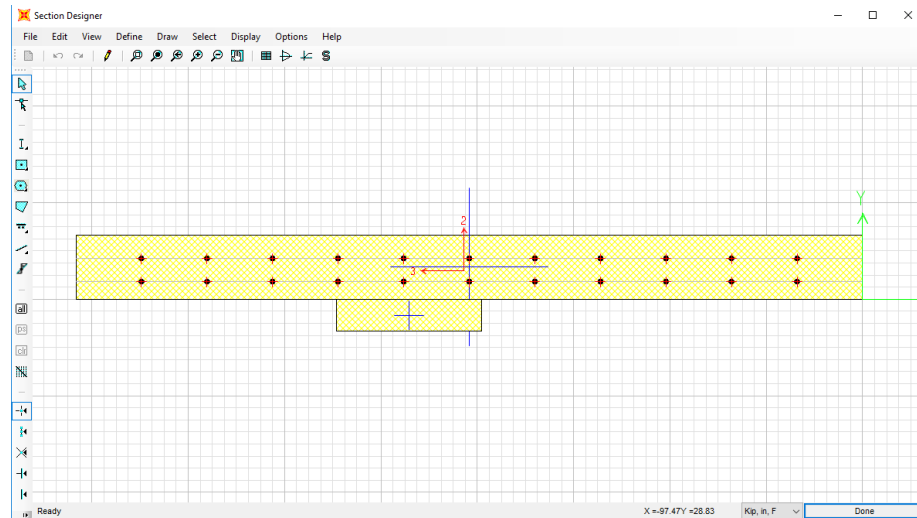
- ii. For the Long1Int delete every element left of the centerline.



- iii. Repeat this process for all cross sections.
- i. To generate a simulated fracture section make copies of Long1Out and Long1Int.
 - i. The reason Long1Out and Long1Int are chosen for the fractured section is because the fracture occurs at $0.4*L$ or 672 inches. Which from the radial spacing table Long1 is the section used at 672 in.
 - ii. Name the copy of Long1Out Frac1Out.
 - 1. Delete the bottom flange, web, and top flange of the steel tub.

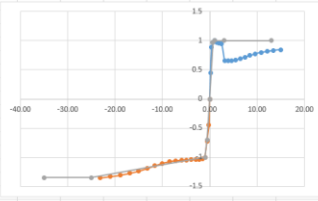


- iii. Name the copy of LongInt FracInt.
 - 1. Delete the bottom flange, web, and top flange of the steel tub.



8. Generating plastic hinges for frame elements in SAP2000.
 - a. Define->Section Properties->Frame Sections
 - b. Select the desired cross section. Hinges will need to be made for the Long(1-4)Out, Long(1-4)Int, FracOut, FracInt, Trans, and TransEnd.
 - c. Once selected, click Modify/Show Property->Section Designer
 - d. Once in the section designer select the Moment Curvature Curve tool.
 - e. In the Moment Curvature Curve window select Details.
 - i. Copy the moment curvature data to an Excel file.
 - ii. Select OK.
 - f. In the Moment Curvature Curve window change the Angle (deg) to 180 then select Details
 - i. Copy the moment curvature data to the same Excel file as previous.
 - ii. Select OK.
 - g. Generate a Normalized Moment Curvature Diagram
 - i. Normalize the Moments by dividing each of the positive moments by the maximum positive moment and the negative moment by the maximum negative moment. And divide the curvatures by the curvatures corresponding to the maximum and negative moments.
 - ii. Plot the normalized positive and negative moment curvatures on a chart.
 - iii. Create a hinge moment curvature plot on the same chart with 4 positive moment points and 4 negative moment points without generating a negative slope.

	A	B	C	D	E	F	G	H	I	J	K	L	M	N	O	P	Q	R	S	T	U	V	W	
2	Positive																							
3	Concrete	Neutral A	Steel Str	Tendon St	Concrete	Steel Com	Steel Ten	Prestress	Net Force	Curvature	Moment		M	C										
4	0	0	0	0	0	0	0	0	0	0	0	0	0	0	0	0	0	0	0	0	0	0	0	0
5	-6.42E-04	-0.0653	9.56E-04	0	-849.525	-71.5223	921.2336	0	0.1867	1.86E-05	56261		0.447094	0.14										
6	-1.53E-03	1.4924	2.46E-03	0	-1.758	-130.476	1888.462	0	-0.0221	4.66E-05	111681		0.887505	0.36										
7	-2.49E-03	4.6917	4.70E-03	0	-2119	-90.6898	2208.794	0	-5.01E-01	8.39E-05	121852		0.968332	0.64										
8	-3.67E-03	6.2978	7.52E-03	0	-2351	-110.929	2462.295	0	0.0775	0.000191	125893		1	1.00										
9	-5.21E-03	6.4308	0.0108	0	-2439	-154.905	2593.535	0	-0.0456	0.000186	121679		0.966957	1.43										
10	-7.04E-03	6.4221	0.0145	0	-2495	-209.435	2703.974	0	-0.4069	0.000252	119891		0.952748	1.93										
11	-9.17E-03	6.2948	0.0188	0	-2537	-256.469	2793.547	0	-0.0143	0.000326	119168		0.947003	2.50										
12	-0.0225	-20.3633	0.0127	0	0	-1461	1460.759	0	-0.0104	0.00041	82471		0.65538	3.14										
13	-0.0275	-20.1838	0.0157	0	0	-1465	1465.611	0	0.1893	0.000503	82810		0.658074	3.86										
14	-0.0329	-19.9925	0.019	0	0	-1470	1470.333	0	0.2082	0.000606	83150		0.660775	4.64										
15	-0.0393	-20.4119	0.0222	0	0	-1494	1493.947	0	0.0502	0.000718	84541		0.671829	5.50										
16	-0.0464	-20.868	0.0256	0	0	-1533	1533.258	0	0.0173	0.000839	86803		0.689805	6.43										
17	-0.0537	-20.9742	0.0294	0	0	-1590	1590.45	0	0.3643	0.000969	90046		0.715576	7.43										
18	-0.0615	-21.0802	0.0336	0	0	-1653	1653.258	0	0.0119	0.001109	93606		0.743867	8.50										
19	-0.07	-21.2377	0.0379	0	0	-1718	1718.782	0	0.3503	0.001258	97263		0.772928	9.64										
20	-0.0786	-21.1113	0.0428	0	0	-1771	1771.636	0	0.1748	0.001416	100205		0.796308	10.85										
21	-0.0875	-20.8117	0.0484	0	0	-1816	1815.259	0	0.1105	0.001584	102095		0.816095	12.14	-1.35	-35								
22	-0.0973	-20.8379	0.0537	0	0	-1849	1849.515	0	0.1005	0.001761	104568		0.83098	13.49	-1.35	-25								
23	-0.1077	-20.877	0.0593	0	0	-1883	1882.613	0	0.0149	0.001948	106436		0.845824	14.93	-1	-1								
24															-0.7	-0.56								
25															0	0								
26	Negative																							
27	Concrete	Neutral A	Steel Str	Tendon St	Concrete	Steel Com	Steel Ten	Prestress	Net Force	Curvature	Moment													
28	0	0	0	0	0	0	0	0	0	0	0		0	0.00	1	1								
29	-7.09E-04	13.106	4.99E-04	0	-341.349	-577.707	235.8451	0	-683.211	1.86E-05	35333		-0.44896	-0.22	1	13								



h. Define Hinge Length

i. The hinge length is one half of the section depth.

1. $Hinge_{long} = 0.5 * (Deck\ thickness + haunch\ height + top\ flange\ thickness + web\ height + bottom\ flange\ thickness)$

- a. $Hinge_{long} = 30\ in.$

2. $Hinge_{Frac} = 0.5 * (Deck\ thickness + haunch\ height)$

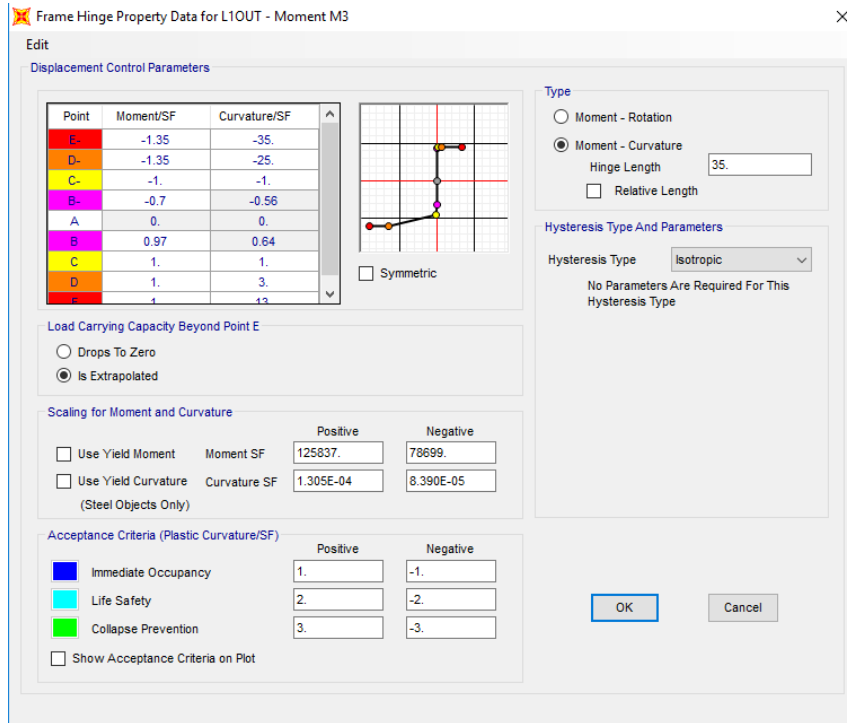
- a. $Hinge_{Frac} = 6\ in.$

3. $Hinge_{Trans} = 0.5 * (Deck\ thickness)$

- a. $Hinge_{Trans} = 4\ in.$

i. Making the plastic hinge in SAP200.

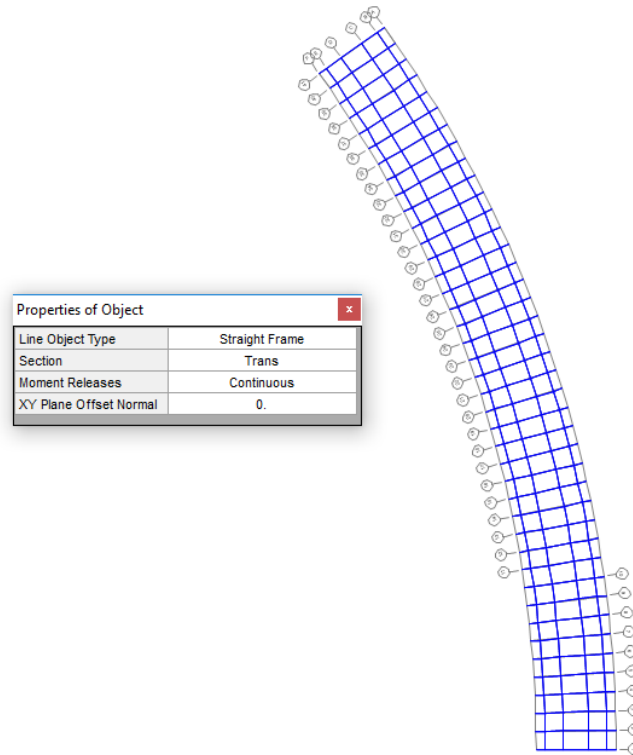
- i. Select Define->Section Properties-> Hinge Properties->Add New Properties
- ii. In the Type window select moment curvature and input the corresponding correct Hinge Length.
- iii. In the Moment Curvature table insert the 4 positive and 4 negative normalized moment curvatures and the zero point.
- iv. Uncheck the symmetric box and select the Is Extrapolated option in the “Load Carrying Capacity beyond Point E” window.
- v. In the “Scaling for Moment and Curvature” window insert the maximum positive moment and corresponding curvature as well as the maximum negative curvature and corresponding curvature.
- vi. In the Acceptance Criteria use the values 1,2, and 3 for Immediate Occupancy, Life Safety, and Collapse Prevention in the positive column and -1, -2, and -3 for the negative column.
- vii. Repeat for all remaining Frame Sections (Long(1-4)Out, Long(1-4)Int, FracOut, FracInt, Trans, and TransEnd)



9. Assign Frame Members to Grid.

- a. Select the Draw tab->Quick Draw Frame/Cable/Tendon
- b. In the Section drop down menu select Long1Out.
- c. Then click on every grid segment on second to last longitudinal grids (B & E) from transverse girds (1-15) and (28-41).
- d. Change the Section to Long1Int and repeat step c but for the two interior longitudinal grids (C & D).
- e. In the Section drop down menu select Long2Out.
- f. Then click on every grid segment on second to last longitudinal grids (B & E) from transverse girds (15-18) and (25-28).
- g. Change the Section to Long2Int and repeat step e but for the two interior longitudinal grids (C & D).
- h. In the Section drop down menu select Long3Out.
- i. Then click on every grid segment on second to last longitudinal grids (B & E) from transverse girds (18-20) and (23-25).
- j. Change the Section to Long3Int and repeat step i but for the two interior longitudinal grids (C & D).
- k. In the Section drop down menu select Long4Out.
- l. Then click on every grid segment on second to last longitudinal grids (B & E) from transverse girds (20-23).
- m. Change the Section to LongInt and repeat step l but for the two interior longitudinal grids (C & D).

- n. Change the Section to TransEnd and repeat step c but for the end transvers grids (1 & 41).
- o. Change the Section to Trans and repeat step c but for all other transverse grids (2 to 40).



10. Assign Hinges to Frame Elements

- a. The Longitudinal Hinges are placed at the ends of the longitudinal frame elements or at a relative distance of 0 and 1.
- b. The Transvers hinges are placed at a distance of half a top flange width away from the node.

- i. $Hinge\ Loc_{F\ to\ E} = \frac{half\ flange\ width}{Element\ Width} = 1 - \frac{18/2}{40.5} = 0.7778$

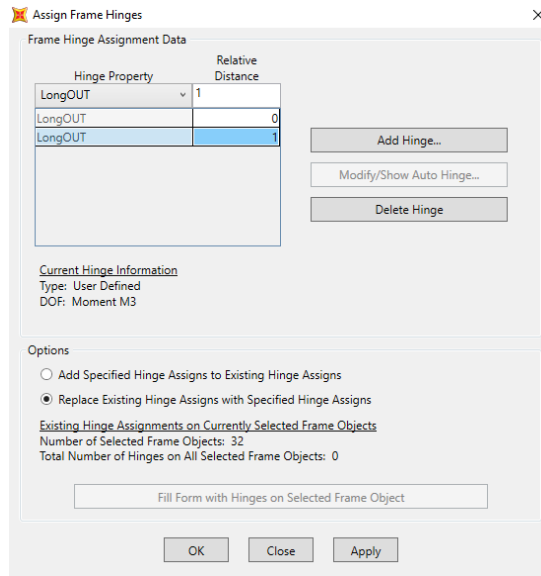
- ii. $Hinge\ Loc_{E\ to\ D\ and\ C\ to\ B} = \frac{half\ flange\ width}{Element\ Width} = \frac{18/2}{83} = 0.1084\ and\ (1 - 0.1084)\ or\ 0.8916$

- iii. $Hinge\ Loc_{D\ to\ C} = \frac{half\ flange\ width}{Element\ Width} = \frac{18/2}{113} = 0.0796\ and\ (1 - 0.0796)\ or\ 0.9204$

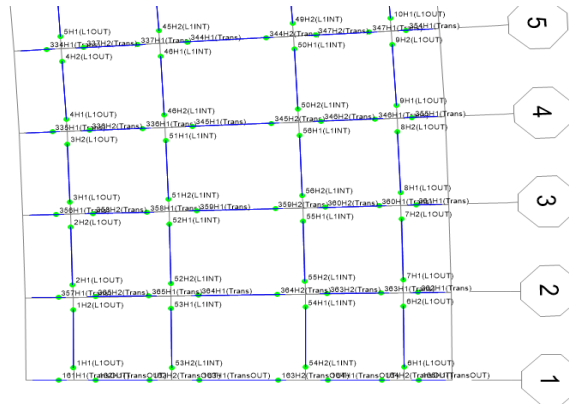
- iv. $Hinge\ Loc_{B\ to\ A} = \frac{half\ flange\ width}{Element\ Width} = \frac{18/2}{40.5} = 0.2222$

- c. In SAP2000 assign the hinges to corresponding frame elements.
 - i. Select the desired frame elements you wish to assign hinges to such as Long1Out. (The elements will turn from blue to yellow).

- ii. In SAP2000 select the Assign tab->Frame->Hinges
 1. From the drop down menu select Long1Out and set relative distance to 0 and click ADD.
 2. From the drop down menu select Long1Out and set relative distance to 1 and click ADD.
 3. Then click OK.



- iii. Repeat Step ii. for all other frame elements.



11. Assigning Loads to the Frame Elements

a. HS20 Wheel Axel Loads

- i. HS20 Axel Loads will be placed at distances of 36 in., 108 in., 180 in., and 252 in. from the outside of the curved edge.
- ii. One line of the 16 kip axels will be placed at the 0.4L point of the bridge or transverse grid 9 with the second line 14 feet away at

transverse grid number 7. One line of 4 kip axels will be placed 14 feet away from the first line of axels at grid line 11.

- iii. In SAP2000 the loads have to be placed at a relative distance so this value needs to be calculated.

$$\begin{aligned}
 1. \quad HS20_{Axel\ 1\ Loc\ (B-A)} &= \frac{L_1 - 36}{L_1} = \frac{40.5 - 36}{40.5} = 0.1111 \\
 2. \quad HS20_{Axel\ 2\ Loc\ (C-B)} &= \frac{L_1 + L_2 - 108}{L_2} = \frac{40.5 + 83 - 108}{83} = 0.1867 \\
 3. \quad HS20_{Axel\ 3\ Loc\ (D-C)} &= \frac{L_1 + L_2 + L_3 - 180}{L_3} = \frac{40.5 + 83 + 113 - 180}{113} = \\
 &0.5 \\
 4. \quad HS20_{Axel\ 4\ Loc\ (E-D)} &= \frac{L_1 + L_2 + L_3 + L_4 - 252}{L_4} = \\
 &\frac{40.5 + 83 + 113 + 83 - 252}{83} = 0.8133
 \end{aligned}$$

b. Lane Loads

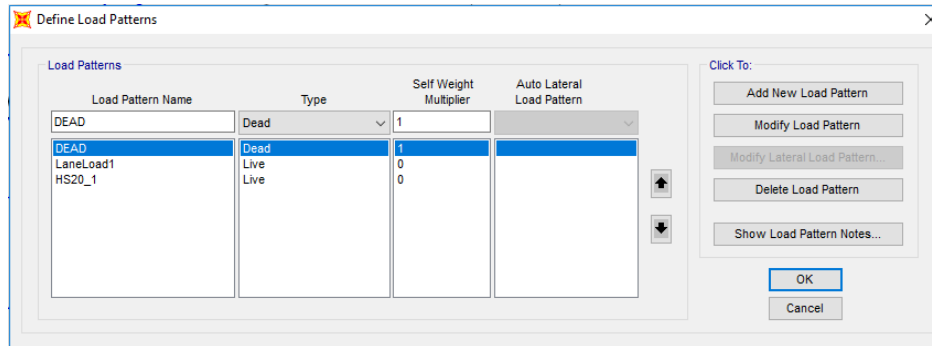
- i. Lane Loads are line loads of 0.640 kip/ft (0.05333 kip/in.) centered at a distance of 96 in. and 240 in. from outside of the curved edge.
- ii. These lane loads will be placed on the longitudinal frame elements. They will be assigned to elements along the B, C, D, and E longitudinal elements according to the appropriate tributary distance.

$$\begin{aligned}
 1. \quad LaneLoad_B &= \left(\frac{L_1 + L_2 - 96}{L_2} \right) * laneload = \left(\frac{40.5 + 83 - 96}{83} \right) * \\
 &0.05333 = 0.017671 \frac{kip}{in}. \\
 2. \quad LaneLoad_C &= laneload - laneload_B = 0.05333 - \\
 &0.017671 = 0.035663 \frac{kip}{in}. \\
 3. \quad LaneLoad_D &= \left(\frac{L_1 + L_2 + L_3 + L_4 - 240}{L_4} \right) * laneload = \\
 &\left(\frac{40.5 + 83 + 113 + 83 - 240}{83} \right) * 0.05333 = 0.051084 \frac{kip}{in}. \\
 4. \quad LaneLoad_E &= laneload - laneload_D = 0.05333 - \\
 &0.051084 = 0.002249 \frac{kip}{in}.
 \end{aligned}$$

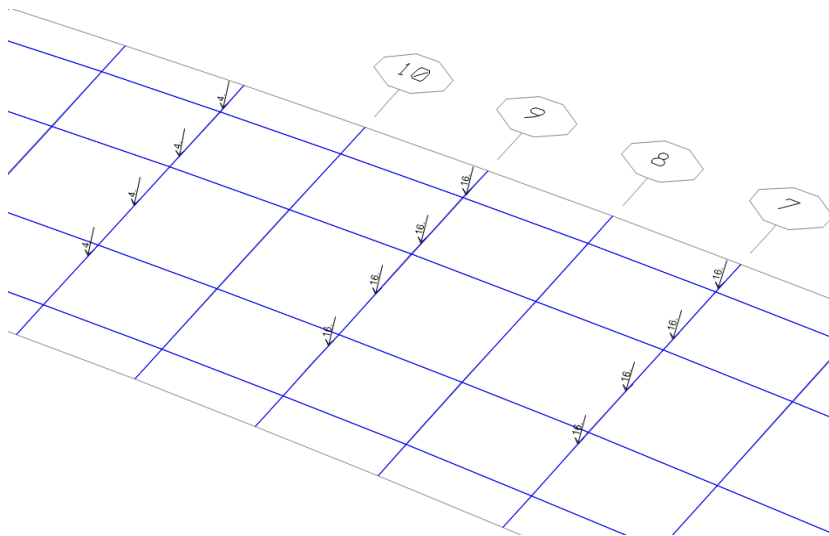
c. In SAP2000 the load patterns must be first be defined.

- i. Select the Define tab->Load Patterns.
 1. Under the Load Pattern Name enter HS20_1 and change the type in the drop down menu to Live. The self-weight multiplier should be set to 0. Then click Add New Load Pattern.
 2. Under the Load Pattern Name enter LaneLoad1 and change the type in the drop down menu to Live. The self-

- weight multiplier should be set to 0. Then click Add New Load Pattern.
- Then click OK.

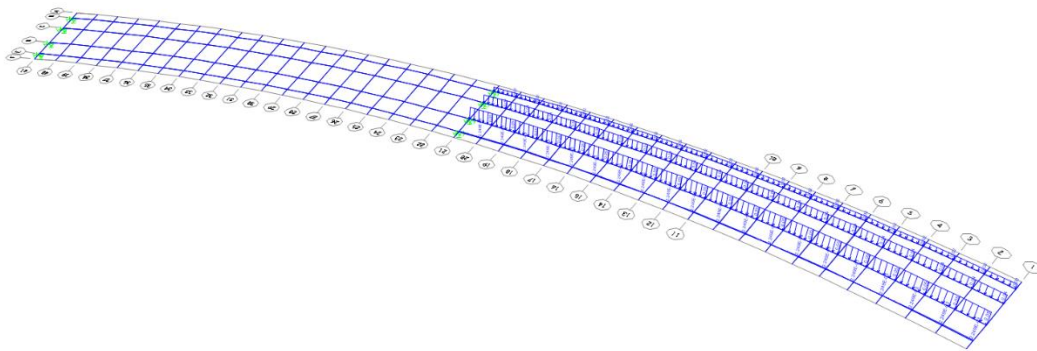


- Assigning the HS20 wheel loads in SAP2000.
 - Select the exterior transverse element of grid line 9 and 7.
 - Click Assign->Frame Loads->Point
 - From the Load Pattern drop down menu select HS20 and verify that the Coordinate System is set to Global, the Load Direction is Gravity, and the Load Type is Force.
 - In column 1 enter a Relative Distance of 0 (HS20 Axle 1 Loc. B-A) and Load of 16 kips.
 - Click OK.
 - Repeat for grid line 11 to assign the 4 kip load.
 - Repeat Steps 1-6 for HS20 Axle 2,3,4 Loc. C-B, D-C, and E-D.



- Assigning the Lane Load in SAP2000.

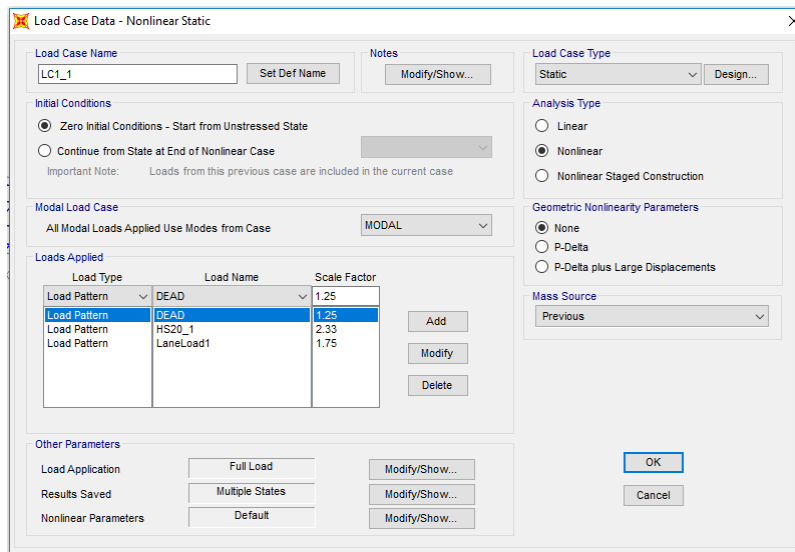
1. Select all exterior longitudinal frame elements along grid line B.
2. Click Assign->Frame Loads->Distributed
3. From the Load Pattern drop down menu select Lane Load and verify that the Coordinate System is set to Global, the Load Direction is Gravity, and the Load Type is Force.
4. In the Uniform Load box enter 0.016124 (Lane Load B).
5. Click OK.
6. Repeat Steps 1-5 for all of the longitudinal elements along gridlines C, D, and E.



12. Defining Load Cases

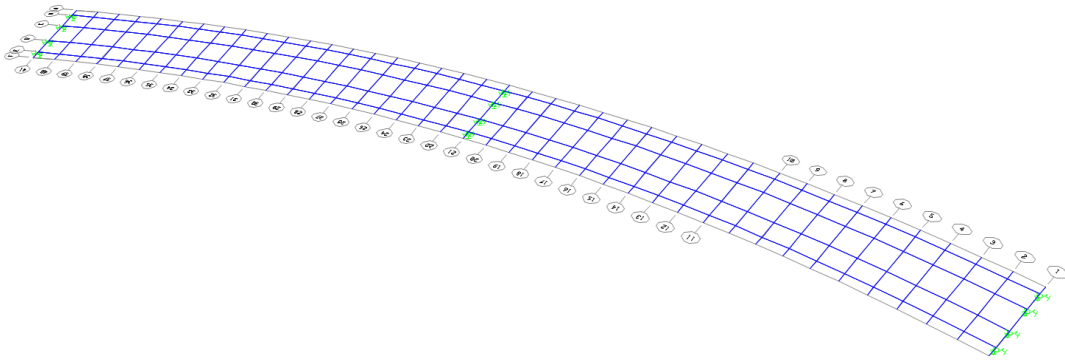
- a. The Load Case being used to determine redundancy is $1.25DL + 1.75(LL + IM)$. Where DL=Dead Load, LL= Live Load, and IM= Impact Load. When substituting in the HS20 truck load and the Lane Load the preceding equation reduces to $1.25DL + 1.75LaneLoad + 2.33HS20$
- b. Generating Load Cases in SAP2000.
 - i. Click Define->Load Cases->Add New Load Case
 - ii. In the Load Case Name Panel name the load case "LC1_1"
 - iii. In the Analysis Type select "Non-Linear"
 - iv. For the LC1_1 Load Case in the Stiffness to use panel select "Zero Initial Conditions"
 - v. In the Loads Applied panel leave the Load Type "Load Pattern" in the drop down Load Name menu select DEAD and change the Scale Factor to 1.25. Click Add. Change the Load Name menu select HS20 and change the Scale Factor to 2.33. Click ADD. Change the Load Name menu select Lane Load and change the Scale Factor to 1.75. Click ADD.
 - vi. In the Other Parameters panel in the Results Saved section click Modify/Show.

- vii. In the Results Saved for Nonlinear Static Load Cases window change the Results Saved to Multiple States and in the For Each Stage panel change the Minimum Number of Saved Steps and the Maximum Number of Saved Steps to 20. Click OK.
- viii. Then Click the OK on the Load Case Data Window.
- ix. Repeat Steps i.-viii. to create an LC2_1, LC3_1, and LC4_1. However, in the Initial Conditions Window select Continue from State at End of Nonlinear Case and from the drop down menu select the preceding load case. (For LC2_1 the Nonlinear Case LC1_1 would be selected).



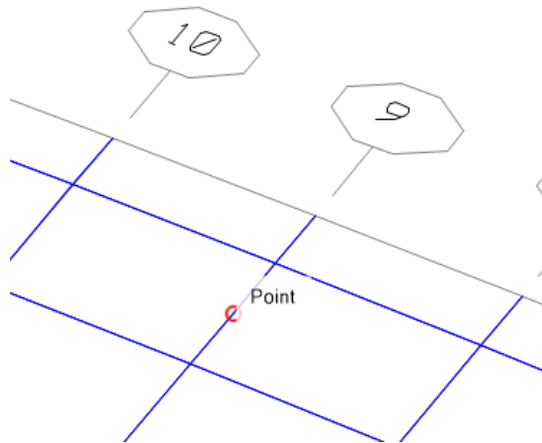
13. Defining End Supports

- a. The elastomeric bearing pad for each girder have lateral stiffness of 12 kip/in. and a vertical stiffness of 6100 kip/in. Since the tub girders are divided in half, the lateral stiffness will be 6 kip/in. and the vertical stiffness will be 3050 kip/in.
- b. Assigning spring supports in SAP2000.
 - i. Select the 12 nodes, 8 at the very end of the longitudinal members, 4 at the location of the pier.
 - ii. Click Assign->Joint->Springs
 - iii. In the Assign Joint Springs window in the Simple Springs Stiffness panel enter 6 for Translation 1&2 and 3050 for Translation 3.
 - iv. Click OK.



14. Defining Centerline Data Acquisition Points at Mid-Span of Girder

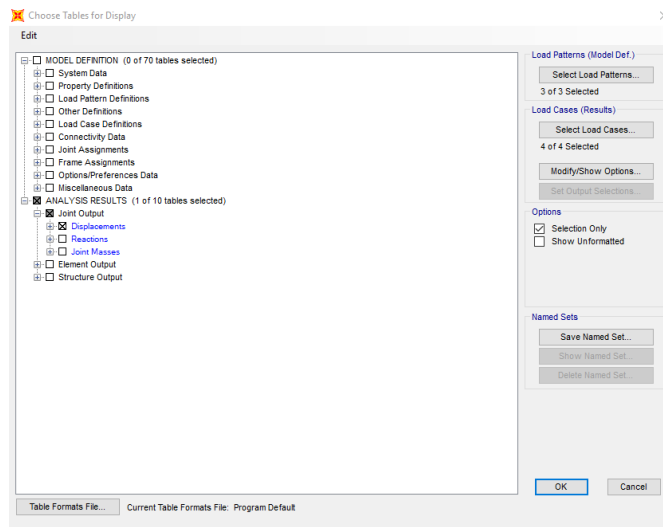
- a. Select the transverse frame elements between B&C as well as D&E at 0.4L (Gridline 9).
- b. Click Edit->Edit Lines->Divide Frames
- c. In the Divide into Specified Number of Frames window enter 2 for Number of Frames.
- d. Click OK.



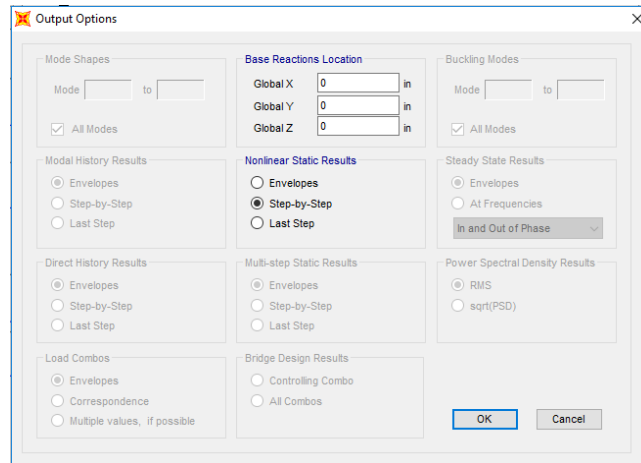
15. Analyzing the Non-Fracture Structure for Dead Load Only

- a. In SAP2000 click Analyze->Run Analysis
- b. In the Set Load Cases to Run window click the Run/Do Not Run All button until every Action is Do Not Run.
- c. Select DEAD then click Run/Do Not Run Case until the Action is Run.
- d. Then click Run Now. Let SAP2000 Run the Load Cases until the screen says the Analysis is Complete.
- e. Once the analysis is complete, select the spring reactions.

- f. Click Display->Show Tables
 - g. In the Choose Table for Display window click the + symbol beside Joint output and select the square box beside Reactions.
 - h. In the Output Options window in the Nonlinear Static Results panel select Last Step.
 - i. Select and copy the information from the F3 column.
 - j. The sum of the F3 values is the dead load.
 - k. Then click Done.
 - l. Unlock the structure.
16. Analyzing the Non-Fractured Structure
- a. In SAP2000 click Analyze->Run Analysis
 - b. In the Set Load Cases to Run window click the Run/Do Not Run All button until every Action is Do Not Run.
 - c. Select LC1_1, LC2_1, LC3_1, and LC4_1 then click Run/Do Not Run Case until the Action for all 4 is Run.
 - d. Then Click Run Now.
 - e. Let SAP2000 Run the Load Cases until the screen says the Analysis is Complete.
 - f. Once the analysis is complete, select the data collection point on the transverse member on the outside girder (C-B).
 - g. Click Display->Show Tables
 - h. In the Choose Table for Display window click the + symbol beside Joint output and select the square box beside Displacements



- i. Click the Modify/Show Options button.
- j. In the Output Options window in the Nonlinear Static Results panel select Step-by-Step.



- k. Click OK.
- l. Select and copy the information from the Output Case, StepNum Unitless, and the U3 in. column and paste them into an Excel worksheet. These columns represent Load Case, Step Number, and Deflection for the Outside Girder respectively.

Joint Text	Output Case	Case Type	Step Type	Step Num Unitless	U1 in	U2 in	U3 in	R1 Radians	R2 Radians	R3 Radians
103	LC1	NonStatic	Step	0	0	0	0	0	0	0
103	LC1	NonStatic	Step	1	0.002545	7.7E-05	-0.087926	-2.681E-06	0.000169	5.324E-08
103	LC1	NonStatic	Step	2	0.00509	0.000154	-0.175851	-5.363E-06	0.000338	1.065E-07

- m. Then click Done.
- n. Select the data collection point on the transverse member on the inside girder (E-D) and repeat Steps g-l. However, on Step 1 there is no need to copy Output Case, Step Num Unitless again.
- o. Select the joint on the transverse member on the outside girder at transverse element 9 (at longitudinal element B) and repeat Steps g-l. This information goes into the Delta 4 column. However, on Step 1 there is no need to copy Output Case, Step Num Unitless again.
- p. Select the joint on the transverse member on the outside girder at transverse element 9 (at longitudinal element C) and repeat Steps g-l. This information goes into the Delta 3 column. However, on Step 1 there is no need to copy Output Case, Step Num Unitless again.
- q. Select the joint on the transverse member on the inside girder at transverse element 9 (at longitudinal element D) and repeat Steps g-l. This information goes into the Delta 2 column. However, on Step 1 there is no need to copy Output Case, Step Num Unitless again.

- r. Select the joint on the transverse member on the outside girder at transverse element 9 (at longitudinal element E) and repeat Steps g-l. This information goes into the Delta 1 column. However, on Step 1 there is no need to copy Output Case, Step Num Unitless again.

	A	B	C	D	E	F	G	H	I	J	K	L	M	V	X	Y	Z	AA	AB	AC	AD
1	Intact			OG-CL		IG-CL		Point 4	Point 3	Point 2	Point 1			Applied Load (kip)	Ω (cal)	Delta (in)	Chord (deg)	IG			
2	Load Case	Load Step	Ω	Delta (in)	Chord (rad)	Delta (in)	Chord (rad)	Delta (in)	Delta (in)	Delta (in)	α 23 (rad)	α 32 (rad)			Ω (cal)	Delta (in)	Chord (deg)	Delta (in)	Chord (deg)	α 23 (deg)	α 32 (deg)
3	LC1	0	0	0	0.00000	0	0.00000	0	0	0	0	0	0	0	0.00	0.00	0.00000	0.00	0.00000	0	0
4	LC1	1	0.05	-0.1037	0.00015	-0.087926	0.00013	-0.10541	-0.10129	-0.0942	-0.07905	7.89E-05	4.94E-05	66	0.05	0.10	0.00861	0.09	0.00730	0.004522	0.002831
5	LC1	2	0.1	-0.2074	0.00030	-0.175851	0.00025	-0.21081	-0.20259	-0.18839	-0.15809	0.000158	9.88E-05	132	0.10	0.21	0.01722	0.18	0.01460	0.009043	0.005662

19. Once all of the data is collected unlock the model by selecting the Lock tool on the left hand side of SAP2000 screen.

17. Analyzing the Fractured Structure

- At Mid-Span along grid line 9, replace the hinges of the outside longitudinal element (gridline B) with FracOUT hinges according to Step 10.
- At Mid-Span, along gridline 9, replace the hinges of the first interior longitudinal element (gridline C) with FracInt hinges according to Step 10.



- Repeat Step 15 for the Fractured Case and collect the data accordingly.

18. Post Processing of the Data

- In the Excel Sheet the following values need to be calculated for each step.
 - Omega (Ω)

$$1. \Omega_i = \Omega_{i-1} + \left(\frac{1}{\# \text{ of Steps in Load case}} \right)$$
 - Longitudinal Chord Rotation of Interior and Exterior Girder

$$1. \text{ Chord Rot.}_{single\ span} = -1 * \left(\frac{\delta_{CL}}{0.5*L} \right) \text{ (rad)}$$

iii. Transverse Deck Rotation

$$1. \alpha_{2-3} = \left(\frac{\delta_3 - \delta_2}{s} \right) - \left(\frac{\delta_2 - \delta_1}{w} \right) \text{ (rad)}$$

$$2. \alpha_{2-3} = \left(\frac{\delta_3 - \delta_2}{s} \right) - \left(\frac{\delta_2 - \delta_1}{w} \right) \text{ (rad)}$$

3. Where s=spacing between the interior top flanges of the inside and outside girders and w=spacing between the top flanges of the same girder.

iv. Applied Load

1. Calculate unit applied load or applied load at 1 Ω .

$$2. \text{ Unit Applied Load}_{single\ span} = 1.25 * \text{ Total Reactions from Dead Load Case} + 2 * (2.33 * \text{ HS20 truck} + 1.75 * \text{ Lane Load})$$

$$3. \text{ Applied Load} = \text{ Unit Applied Load} * \Omega$$

b. Repeat Step A for the Fractured Case.

c. Calculate the initial stiffness for intact bridge and instantaneous stiffness for fractured bridge.

i. For the Non-Fractured condition (Intact Bridge) find the absolute displacement for the Outside Girder at an Ω value of 0.4.

$$1. \text{ Initial Stiffness} = \frac{0.4}{\text{Absolute Displacement OG (at } \Omega=0.4)}$$

ii. For the Fractured case add an additional column labeled stiffness

$$1. \text{ Instantaneous Stiffness}_{OG-Frac. i} = \frac{\Omega_i - \Omega_{i-1}}{\delta_i - \delta_{i-1}}$$

d. Failure of the structure occurs at the Ω of the Fractured Bridge at the first of the following criteria.

i. The instantaneous stiffness for the fractured outside girder is less than 5% of the initial stiffness of the intact outside girder.

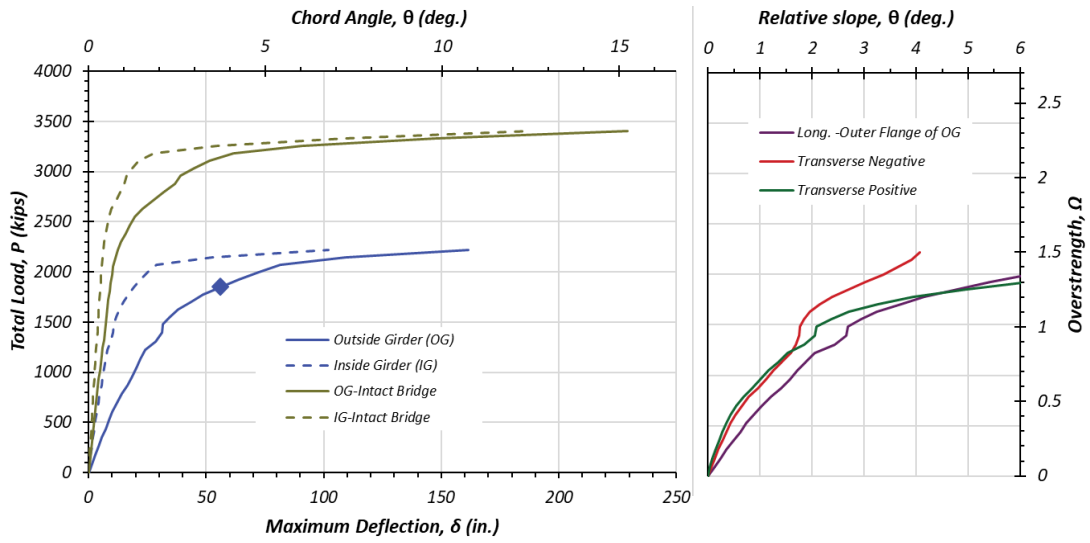
ii. The chord angle of the outside girder for a simple spans or interior spans is greater than 2°. The chord angle for exterior spans of multi-span bridges is greater than 3°.

iii. The transverse deck rotation is greater than 5°.

e. On a chart plot the Non-Fractured Outside and Inside Girder as well as the Fractured Outside and Inside Girder with displacement on the primary x axis and the Total Force on the primary y axis and Ω on the secondary y-axis

19. Repeat Steps 11-18 for Span 2.

a. However, since Span 1 and Span 2 are both 140 feet long. No repetition need.



Grillage Analysis Example of Bridge 10

1. Gather Bridge Geometry and Material Information.

Loc. ft	Top Flange		Web		Bottom Flange		Sec. Type	
	W in.	T in.	W in.	T in.	W in.	T in.	Sect.	Rebar
0-50	24	1.00	78	0.625	59	0.750	1	Reg.
50-98	24	1.00	78	0.625	59	1.250	2	Pier
98-131	24	2.00	78	0.75	59	2.000	3	Pier
131-181	24	3.00	78	0.875	59	2.000	4	Pier
181-230	24	1.00	78	0.875	59	1.250	5	Pier
230-247	24	1.00	78	0.75	59	1.000	6	Reg.
247-297	24	1.00	78	0.75	59	1.250	7	Reg.
297-330	24	1.00	78	0.75	59	1.000	8	Reg.
330-380	24	1.00	78	0.875	59	1.250	5	Pier
380-396	24	2.00	78	0.875	59	1.250	5	Pier
396-430	24	3.00	78	0.875	59	2.000	9	Pier
430-447	24	3.00	78	0.875	59	2.000	9	Pier
447-464	24	2.00	78	0.75	59	1.250	10	Pier
464-499	24	1.00	78	0.75	59	1.250	10	Pier
499-602	24	1.00	78	0.625	59	0.750	1	Reg.

Location	Parameter	Description/Value
Bridge	Location	Harris County, IH10
	Year Designed/Year Built	1998/2002
	Design Load	HS20
	Length, ft	602.58
	Spans, ft	148, 265, 189.58
	Radius of Curvature, ft	716.2
Deck	Width, ft	30
	Thickness, in.	8
	Haunch, in.	5
	Rail Type	T4(s)
Rebar	# of Bar Longitudinal Top Row (#4)	42
	# of Bar Longitudinal Bottom Row (#5)	32
	# of Bar Longitudinal Top Row (#4) @support	42
	# of Bar Longitudinal Top Row (#5) @support	40
	# of Bar Longitudinal Bottom Row (#5) @support	32
	Transverse Spacing Top Row (#5), in.	6
	Transverse Spacing Bottom Row (#5), in.	6
Grider	CL of Bridge to CL of Girder (in.)	45
	CL of Top Flange to CL of Top Flange (in.)	96

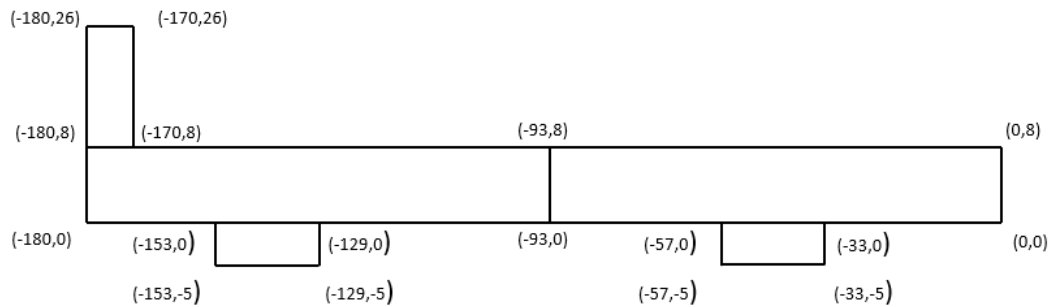
2. Material constitutive behavior

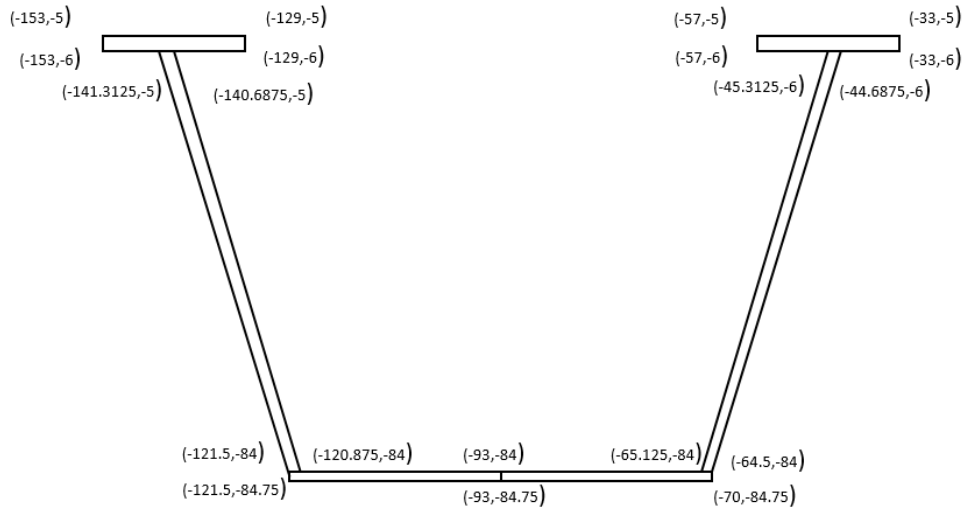
Concrete (4 ksi)	
Stress (ksi)	Strain (1/in)
-4	-3.79E-03
-4	-3.56E-03
-4	-2.69E-03
-4	-1.78E-03
-3.8205	-1.40E-03
-2.8718	-8.69E-04
-0.6403	-1.78E-04
0	0
0.378	1.06E-04
0.378	1.16E-03

Rebar (60 ksi)	
Stress (ksi)	Strain (1/in)
-87.9	-0.095
-87.9	-0.0944
-86.6	-0.0761
-78	-0.0386
-60.7	-9.80E-03
-60.3	-2.08E-03
0	0
60.3	2.08E-03
60.7	9.80E-03
78	0.0386
86.6	0.0761
87.9	0.0944
87.9	0.095

Steel (50 ksi)	
Stress (ksi)	Strain (1/in)
-71.6	-0.1
-71.6	-0.097
-71.6	-0.095
-71.6	-0.0946
-70.3	-0.0764
-62.5	-0.039
-50	-0.0196
-50	-1.72E-03
0	0
50	1.72E-03
50	0.0196
62.5	0.039
70.3	0.0764
71.6	0.0946
71.6	0.095
71.6	0.097
71.6	0.1

3. Create a Coordinate system for half width of the span for each cross section. An example of the first cross section is show below.





4. Create a cylindrical coordinate system for the curved bridge assuring that the middle transverse divisions are 7 ft, as this will aid in applying the HS20 truck load whose axels are separated by 14 ft.

a. # of Segments_{per span} =

$$\left(\frac{\text{Length (ft)} * 12}{84 \text{ in (7ft)}} \right) \text{ rounded to nearest even number}$$

i. # of Segments_{Span 1} = $\left(\frac{148 * 12}{84} \right) = 21.428$ or 18

ii. # of Segments_{Span 2} = $\left(\frac{265 * 12}{84} \right) = 37.857$ or 36

iii. # of Segments_{Span 3} = $\left(\frac{190 * 12}{84} \right) = 27.143$ or 24

b. End Segment Length = $\left((\text{Length} * 12) - (\# \text{ of Segments} * 84) \right) / 2$

i. End Segment Length_{Span 1} = $\frac{((148 * 12) - (18 * 84))}{2} = 132 \text{ in.}$

ii. End Segment Length_{Span 2} = $\frac{((265 * 12) - (36 * 84))}{2} = 78 \text{ in.}$

iii. End Segment Length_{Span 3} = $\frac{((190 * 12) - (24 * 84))}{2} = 132 \text{ in.}$

c. $\text{Theta} = \frac{\text{Total Length}}{\text{Radius}}$

i. $\text{Theta} = \frac{603}{716.2} = 0.84194 \text{ rad}$ or 48.24 degrees

- d. Determine the radial offsets using the outside edge, the outside flange, the inner flange and centerline of the bridge.

Offsets (in.)	
Edge	180
Outside Flange	141
Inner Flange	45
CL of Bridge	0

Radial Spacing (in.)		
A	8774.4	CL+Edge
B	8735.4	CL+OF
C	8639.4	CL+IF
Center Line	8594.4	or 450 (ft)
D	8549.4	CL-IF
E	8453.4	CL-OF
F	8414.4	CL-Edge

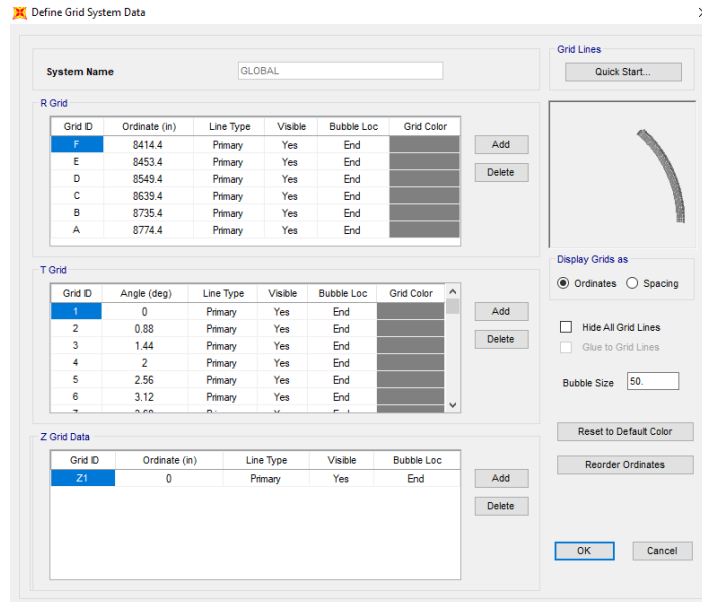
- c. The Longitudinal or spacing along theta is determined by converting the longitudinal segment lengths into degrees.
- i. The segments vary in length. The total length is 603 ft or 7236 in.
 - ii. $Radial\ Spacing\ (rad) = \frac{Long.Spacing}{Radius}$
 - iii. $Radial\ Spacing\ (degree) = Radius\ Spacing\ (rad) * \frac{180}{\pi}$

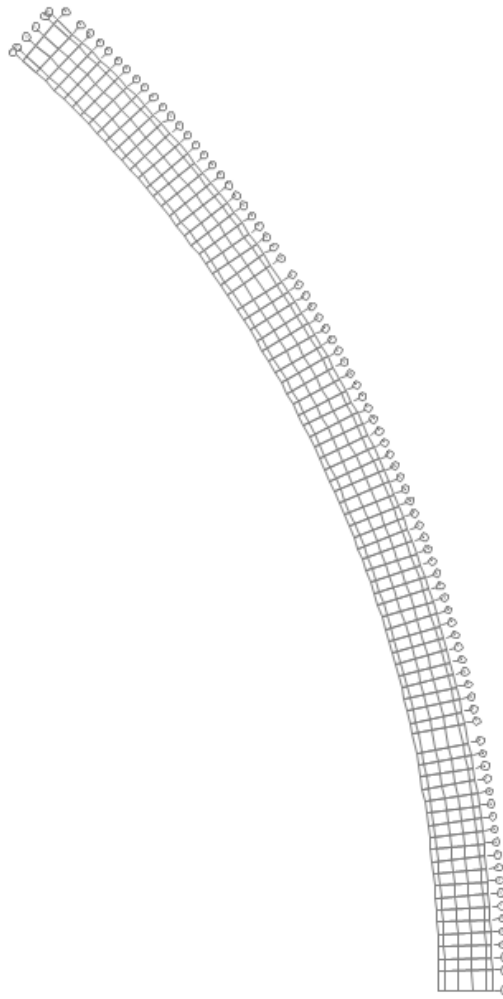
Long. Spacing (in.)	Radial Spacing (rad.)	Radial Spacing (deg.)
0	0.0000	0.000
132	0.0154	0.880
216	0.0251	1.440
300	0.0349	2.000
384	0.0447	2.560
468	0.0545	3.120
552	0.0642	3.680
636	0.0740	4.240
720	0.0838	4.800
804	0.0935	5.360
888	0.1033	5.920
972	0.1131	6.480
1056	0.1229	7.040

Long. Spacing (in.)	Radial Spacing (rad.)	Radial Spacing (deg.)
1140	0.1326	7.600
1224	0.1424	8.160
1308	0.1522	8.720
1392	0.1620	9.280
1476	0.1717	9.840
1560	0.1815	10.400
1644	0.1913	10.960
1776	0.2066	11.840
1854	0.2157	12.360
1938	0.2255	12.920
2022	0.2353	13.480
2106	0.2450	14.040
2190	0.2548	14.600
2274	0.2646	15.160
2358	0.2744	15.720
2442	0.2841	16.280
2526	0.2939	16.840
2610	0.3037	17.400
2694	0.3135	17.960
2778	0.3232	18.520
2862	0.3330	19.080
2946	0.3428	19.640
3030	0.3526	20.200
3114	0.3623	20.760
3198	0.3721	21.320
3282	0.3819	21.880
3366	0.3917	22.440
3450	0.4014	23.000
3534	0.4112	23.560
3618	0.4210	24.120
3702	0.4307	24.680
3786	0.4405	25.240
3870	0.4503	25.800
3954	0.4601	26.360
4038	0.4698	26.920
4122	0.4796	27.480

Long. Spacing (in.)	Radial Spacing (rad.)	Radial Spacing (deg.)
4206	0.4894	28.040
4290	0.4992	28.600
4374	0.5089	29.160
4458	0.5187	29.720
4542	0.5285	30.280
4626	0.5383	30.840
4710	0.5480	31.400
4794	0.5578	31.960
4878	0.5676	32.520
4956	0.5767	33.040
5088	0.5920	33.920
5172	0.6018	34.480
5256	0.6116	35.040
5340	0.6213	35.600
5424	0.6311	36.160
5508	0.6409	36.720
5592	0.6507	37.280
5676	0.6604	37.840
5760	0.6702	38.400
5844	0.6800	38.960
5928	0.6898	39.520
6012	0.6995	40.080
6096	0.7093	40.640
6180	0.7191	41.200
6264	0.7288	41.760
6348	0.7386	42.320
6432	0.7484	42.880
6516	0.7582	43.440
6600	0.7679	44.000
6684	0.7777	44.560
6768	0.7875	45.120
6852	0.7973	45.680
6936	0.8070	46.240
7020	0.8168	46.800
7104	0.8266	47.360
7236	0.8419	48.240

- iv. *Int. Transverse Element width = 84 in.*
 - v. *End Transverse Element = $132 - \left(\frac{84}{2}\right) = 90 \text{ in.}$*
 - vi. *Peir Tansvers Element = $132 + 78 - 84 = 126 \text{ in.}$*
5. Inputting the coordinate system into SAP2000
- a. Select File -> New Model -> Blank model (making sure units are in kips and inches)
 - b. Right click on the blank workspace and select Edit Grid Data-> Modify/Show System->Quick Start->Cylindrical.
 - i. In the Number of Grid Lines panel set “Along Z=1”
 - ii. In the Grid Spacing panel set “Along Z=1”
 - iii. Select OK.
 - iv. Delete all R and T Coordinates that were generated
 - c. Add correct coordinates for R
 - i. All radial coordinates (A, B, C, D, E, and F).
 - d. Add correct coordinates for T
 - i. All theta coordinates for T (0 to 7236 in.)
 - ii. Click OK
 - e. The Grid System in now formed.

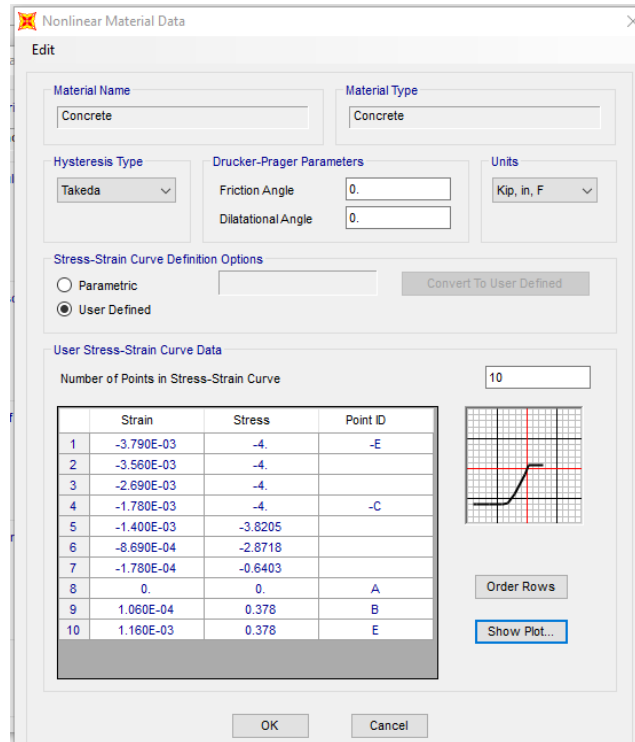




6. Defining Material in SAP200

- a. Click Define-> Materials->Add New Material->Material Type (Steel, Concrete, or Rebar)->Standard (User)->OK
- b. At the bottom of the window select the box which states “Switch to Advanced Properties”
- c. In the open window name the material “Concrete” “Steel” or “Rebar” depending on which material is being defined. Then click “Modify/Show Material Properties”
- d. On the Material Property Data window click “Nonlinear Material Data” icon.
- e. In the Nonlinear Material Data window select the “Convert to User Defined” icon.
- f. Input the number of number of data points for the stress strain behavior (10 for concrete, 13 for rebar, 17 for steel)

- g. Input the data points for the stress strain behavior.
- h. Select “OK”
- i. Repeat this process again for the remaining materials.

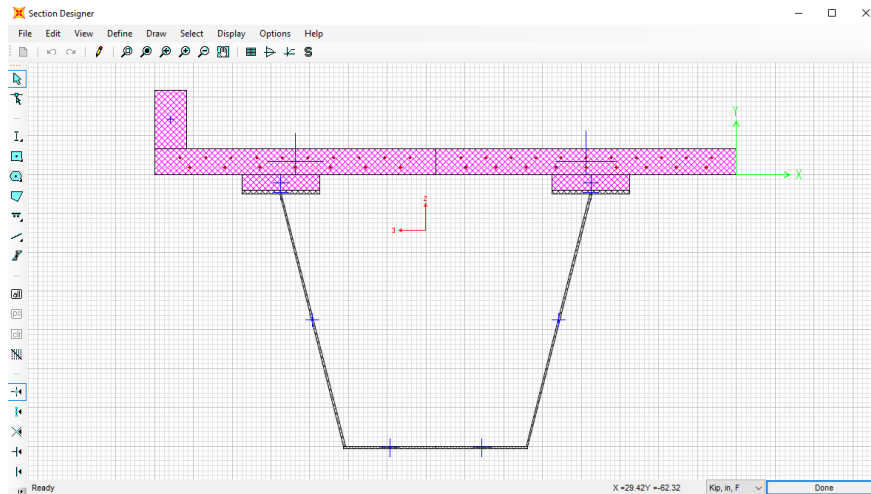


7. Defining Frame Cross Sections in SAP2000.

- a. Click Define->Section Properties->Frame Sections->Add New Properties
- b. In the Frame Section Properties Drop down box select “Other” and click Section Designer. In the SD Section Designer Window name the section B5Long1 click the “Section Designer” Icon.
- c. Using the Polygon feature draw the features of the half width of the bridge from Step 3. This includes: one rail, two concrete deck pieces, to concrete haunches, two top flanges, two webs, and two pieces of the bottom flange.
 - i. To change material types for the polygons right click on the polygon and select the desired material type from the material drop down menu.
 - ii. To change the coordinates of the polygon’s nodes use the Reshaper too to change the coordinates.
- d. Add in the longitudinal rebar to both concrete deck elements by using the Line Bar from the Draw Reinforcing Shape tool. From the design drawings it can be determined that there are 10 #4 top bars and 7 #5 bottom bars in the outer concrete deck element and 11 #4 top bars and 9

#5 bottom bars in the inner concrete element. At the pier supports 10 additional #5 top bars are added to the top of the outer concrete deck and 10 additional #5 top bars are added to the inner concrete deck. With a 2 inch top cover and transverse reinforcement the top bars are located at 5.0625 inches and with a 1.25 inch bottom cover and transverse reinforcement are located at 2.1875.

e. Click Done (Below is an example of the 1st cross section).

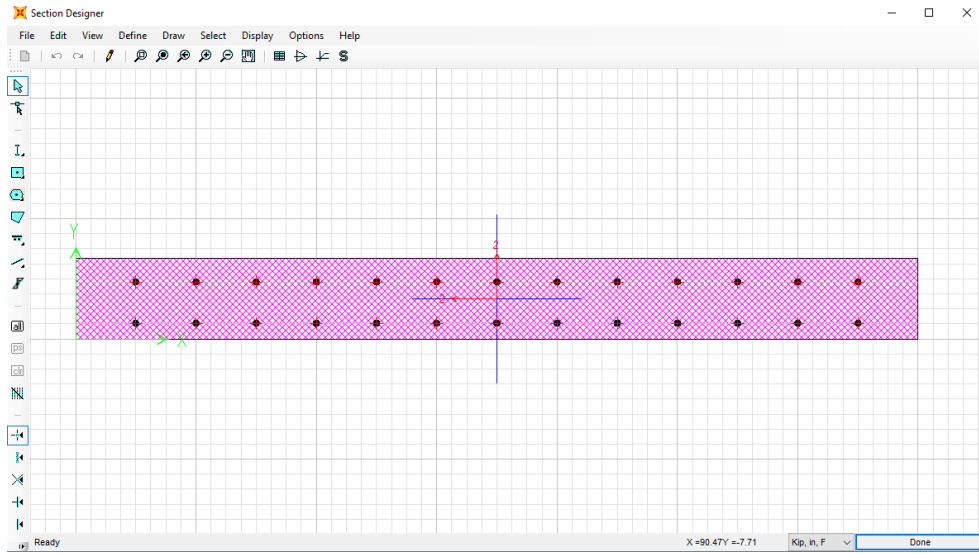


f. Repeat this process for the remaining longitudinal elements.

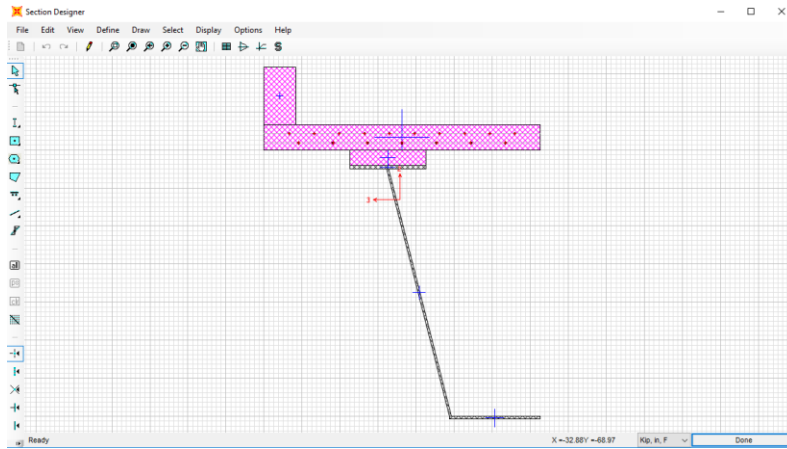
g. Repeat the process for the transverse elements.

i. At the SD Section Designer Window select Modifiers and set Mass and Weight to 0, as to not double count the dead weight.

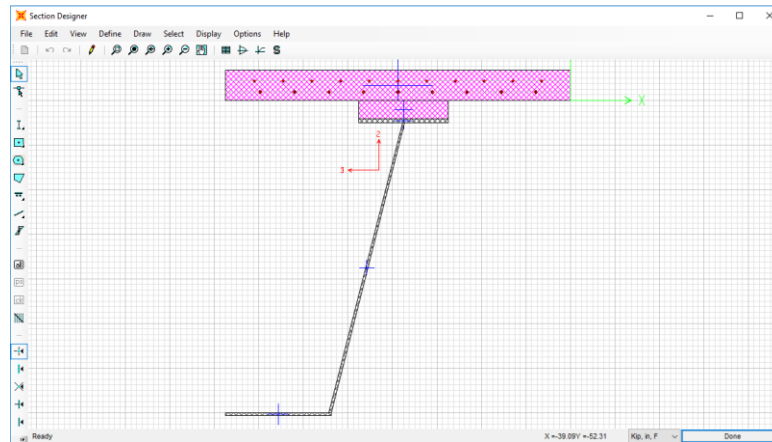
ii. The interior transverse members are 84 inches wide (end members are 90 in. wide and pier members are 126 in.) with #5 rebar at 5 inch spacing at 5.6875 in. and 1.5625 in.



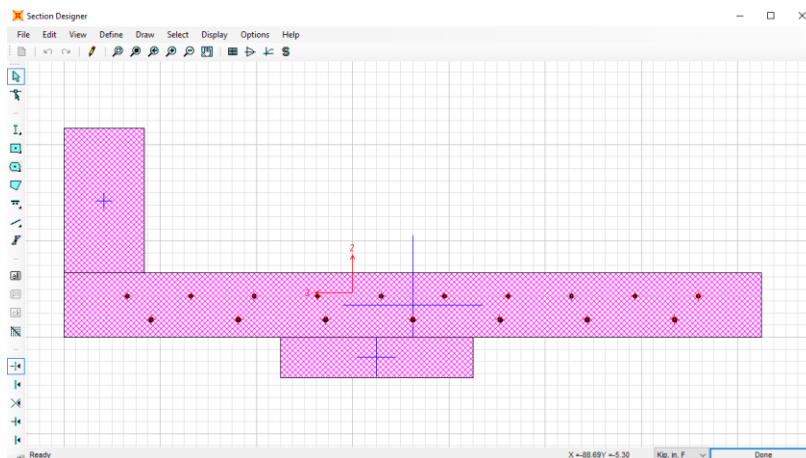
- h. To generate an exterior longitudinal member and an interior longitudinal member. Make two copies of the B10Long1.1 section. Label one Long1Out and one Long1Int.
 - i. For the L1.1Out delete every element right of the centerline.



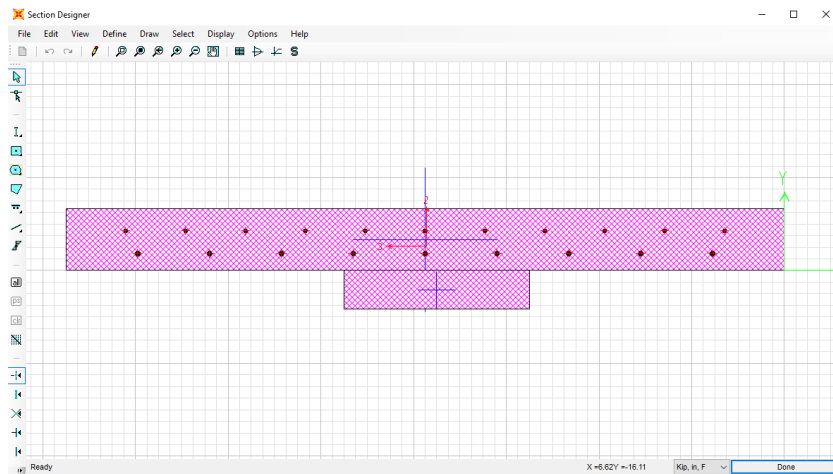
- ii. For the L1.1Int delete every element left of the centerline.



- iii. Repeat this process for all cross sections.
- i. To generate a simulated fracture section make copies of Long1Out and Long1Int.
 - i. The reason Long1Out and Long1Int are chosen for the fractured section is because the fracture occurs at $0.4*L$ or 710 inches. Which from the radial spacing table L1.1 is the section used at 710 in.
 - ii. Name the copy of L1.1Out FracInt1.1.
 - 1. Delete the bottom flange, web, and top flange of the steel tub.

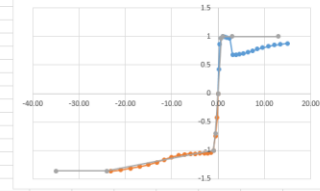


- iii. Name the copy of L1.1Int to FracInt1.1.
 - 1. Delete the bottom flange, web, and top flange of the steel tub.



8. Generating plastic hinges for frame elements in SAP2000.
 - a. Define->Section Properties->Frame Sections
 - b. Select the desired cross section. Hinges will need to be made for all of the necessary cross sections.
 - c. Once selected, click Modify/Show Property->Section Designer
 - d. Once in the section designer select the Moment Curvature Curve tool.
 - e. In the Moment Curvature Curve window select Details.
 - i. Copy the moment curvature data to an Excel file.
 - ii. Select OK.
 - f. In the Moment Curvature Curve window change the Angle (deg) to 180 then select Details
 - i. Copy the moment curvature data to the same Excel file as previous.
 - ii. Select OK.
 - g. Generate a Normalized Moment Curvature Diagram
 - i. Normalize the Moments by dividing each of the positive moments by the maximum positive moment and the negative moment by the maximum negative moment. And divide the curvatures by the curvatures corresponding to the maximum and negative moments.
 - ii. Plot the normalized positive and negative moment curvatures on a chart.
 - iii. Create a hinge moment curvature plot on the same chart with 4 positive moment points and 4 negative moment points without generating a negative slope.

	A	B	C	D	E	F	G	H	I	J	K	L	M	N	O	P	Q	R	S	T	U	V	W	
2	Positive																							
3	Concrete	Neutral A:	Steel Strai	Tendon St	Concrete	Steel Com	Steel Tens	Prestress	Net Force	Curvature	Moment		M	C										
4	0	0	0	0	0	0	0	0	0	0	0	0	0	0	0	0	0	0	0	0	0	0	0	
5	-5.83E-04	-0.202	9.54E-04	0	-1023	-134.148	1137.457	0	0.6999	1.39E-05	92327		0.424291	0.14										
6	-1.39E-03	1.8021	2.46E-03	0	-2182	-278.572	2460.218	0	-0.5396	3.47E-05	188832		0.868683	0.36										
7	-2.20E-03	6.5568	4.72E-03	0	-2709	-258.87	2968.071	0	-4.31E-02	6.24E-05	210140		0.965704	0.64										
8	-3.16E-03	9.2404	7.66E-03	0	-3022	-189.735	3211.843	0	-0.0135	9.21E-05	219769		1	1.00										
9	-4.38E-03	10.2529	0.011	0	-3170	-162.774	3332.986	0	0.022	0.000139	216983		0.997174	1.43										
10	-5.91E-03	10.2344	1.48E-02	0	-3162	-221.373	3383.742	0	0.4763	0.000187	213039		0.979026	1.93										
11	-7.71E-03	10.0496	1.92E-02	0	-3122	-281.487	3403.438	0	-0.0672	0.000243	210855		0.968989	2.50										
12	-0.0198	-22.9408	0.014	0	0	-1854	1854.169	0	-0.0301	0.000305	148132		0.680744	3.14										
13	-0.0242	-22.8196	0.0173	0	0	-1838	1838.773	0	0.3035	0.000175	148358		0.682702	3.86										
14	-0.0292	-22.9173	0.0208	0	0	-1871	1871.122	0	0.052	0.000451	149608		0.687527	4.64										
15	-0.0349	-23.6182	0.0242	0	0	-1906	1906.511	0	0.1244	0.000534	152481		0.70073	5.50										
16	-0.0411	-24.0453	0.028	0	0	-1961	1960.493	0	-9.66E-02	0.000624	156827		0.720702	6.43										
17	-0.0476	-24.1875	0.0323	0	0	-2034	2033.797	0	0.0141	0.000722	162696		0.747674	7.43										
18	-0.0546	-24.3215	0.0369	0	0	-2115	2115.214	0	0.015	0.000826	169211		0.777613	8.50										
19	-0.0618	-24.2485	0.0419	0	0	-2189	2189.226	0	0.1694	0.000937	175107		0.804709	9.64										
20	-0.0693	-23.9243	0.0475	0	0	-2249	2249.521	0	0.0233	0.001055	179894		0.826707	10.86										
21	-0.0772	-23.6615	0.0534	0	0	-2307	2306.81	0	0.2443	0.001179	184442		0.847608	12.14										
22	-0.0859	-23.727	0.0593	0	0	-2351	2350.667	0	0.0432	0.001311	187939		0.863678	13.50										
23	-0.0951	-23.7901	0.0655	0	0	-2395	2394.726	0	0.0178	0.00145	191454		0.878932	14.93										
24																								
25	Negative																							
26	Concrete	Neutral A:	Steel Strai	Tendon St	Concrete	Steel Com	Steel Tens	Prestress	Net Force	Curvature	Moment													
27	0	0	0	0	0	0	0	0	0	0	0	0	0	0	0	0	0	0	0	0	0	0	0	
28	-7.27E-04	16.5861	5.20E-04	0	-374.912	-698.732	323.5235	0	-750.12	1.39E-05	59719		-0.42617	-0.22										



h. Define Hinge Length

i. The hinge length is one half of the section depth.

1. $Hinge_{long} = 0.5 * (Deck\ thickness + haunch\ height + top\ flange\ thickness + web\ height + bottom\ flange\ thickness)$

a. $Hinge_{long} = 45\ in.$

2. $Hinge_{Frac} = 0.5 * (Deck\ thickness + haunch\ height)$

a. $Hinge_{Frac} = 7\ in.$

3. $Hinge_{Trans} = 0.5 * (Deck\ thickness)$

a. $Hinge_{Trans} = 4\ in.$

i. Making the plastic hinge in SAP200.

i. Select Define->Section Properties-> Hinge Properties->Add New Properties

ii. In the Type window select moment curvature and input the corresponding correct Hinge Length.

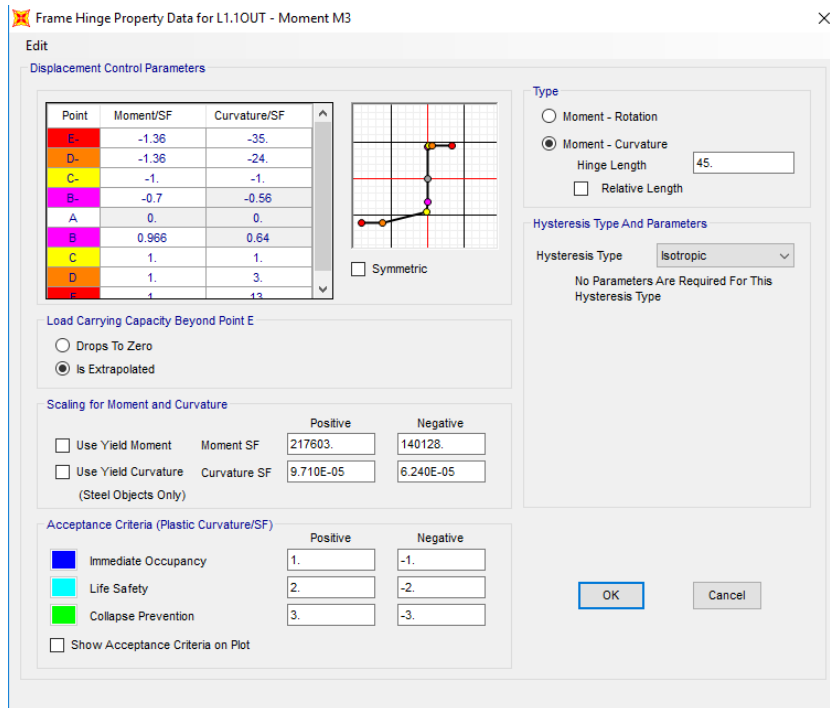
iii. In the Moment Curvature table insert the 4 positive and 4 negative normalized moment curvatures and the zero point.

iv. Uncheck the symmetric box and select the Is Extrapolated option in the “Load Carrying Capacity beyond Point E” window.

v. In the “Scaling for Moment and Curvature” window insert the maximum positive moment and corresponding curvature as well as the maximum negative curvature and corresponding curvature.

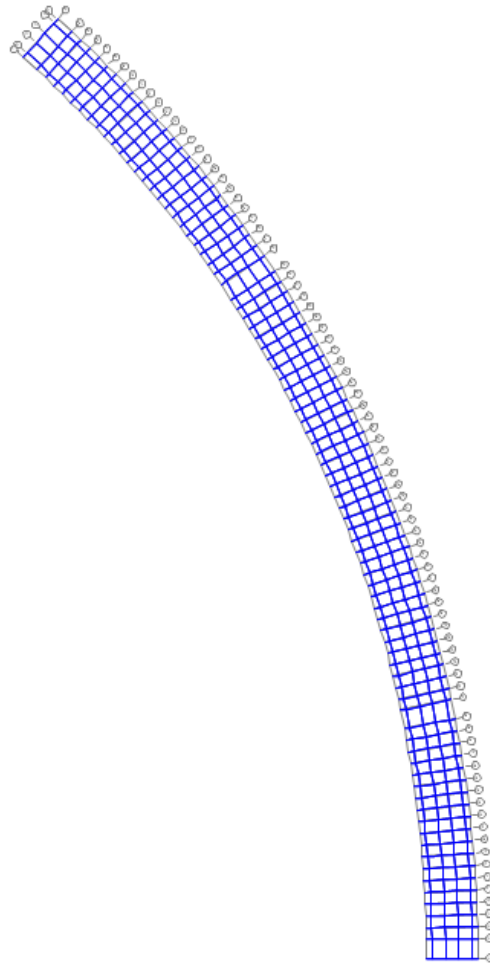
vi. In the Acceptance Criteria use the values 1,2, and 3 for Immediate Occupancy, Life Safety, and Collapse Prevention in the positive column and -1, -2, and -3 for the negative column.

vii. Repeat for all remaining Frame Sections.



9. Assign Frame Members to Grid.

- a. Select the Draw tab->Quick Draw Frame/Cable/Tendon
- b. In the Section drop down menu select the appropriate cross section and click on the grid grillage grid member.



10. Assign Hinges to Frame Elements

- a. The Longitudinal Hinges are placed at the ends of the longitudinal frame elements or at a relative distance of 0 and 1.
- b. The Transvers hinges are placed at a distance of half a top flange width away from the node.

- i. $Hinge\ Loc_{F\ to\ E} = \frac{half\ flange\ width}{Element\ Width} = 1 - \frac{24/2}{39} = 0.6923$

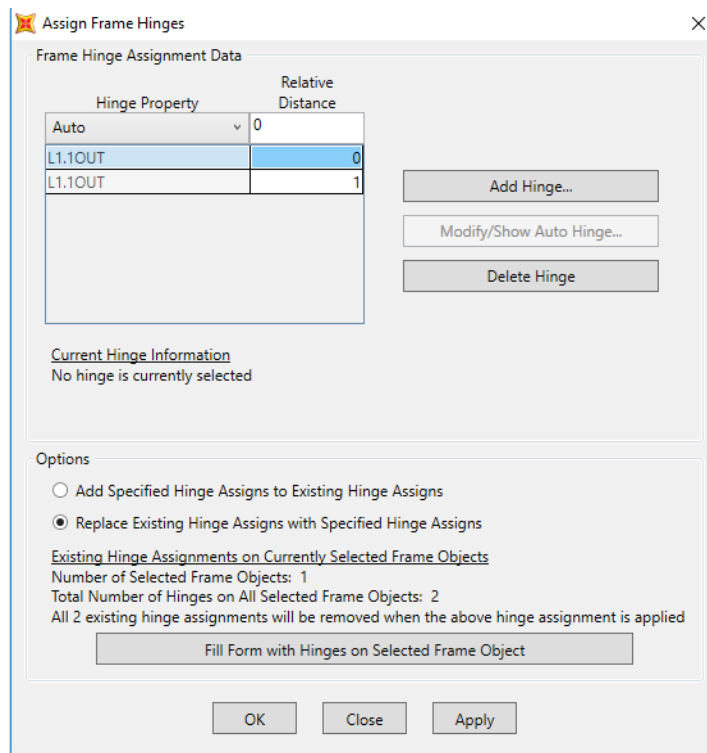
- ii. $Hinge\ Loc_{E\ to\ D\ and\ C\ to\ B} = \frac{half\ flange\ width}{Element\ Width} = \frac{24/2}{96} = 0.125\ and\ (1 - 0.125)\ or\ 0.875$

- iii. $Hinge\ Loc_{D\ to\ C} = \frac{half\ flange\ width}{Element\ Width} = \frac{24/2}{90} = 0.1333\ and\ (1 - 0.1333)\ or\ 0.8667$

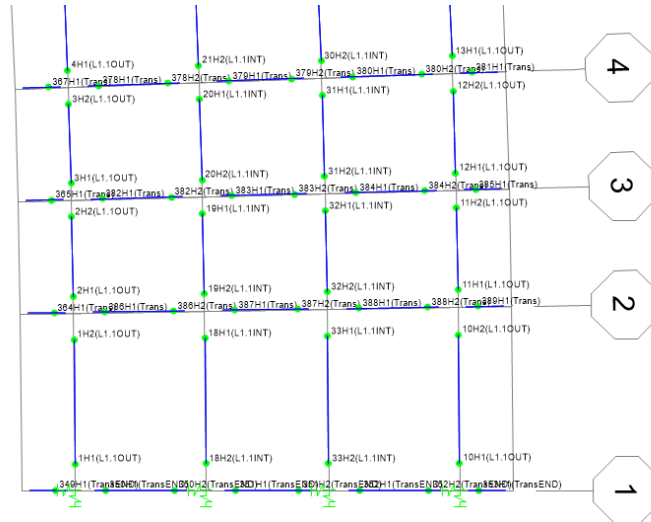
- iv. $Hinge\ Loc_{B\ to\ A} = \frac{half\ flange\ width}{Element\ Width} = \frac{24/2}{39} = 0.3077$

- c. In SAP2000 assign the hinges to corresponding frame elements.

- i. Select the desired frame elements you wish to assign hinges to such as Long1Out. (The elements will turn from blue to yellow).
- ii. In SAP2000 select the Assign tab->Frame->Hinges
 1. From the drop down menu select Long1Out and set relative distance to 0 and click ADD.
 2. From the drop down menu select Long1Out and set relative distance to 1 and click ADD.
 3. Then click OK.



- iii. Repeat Step ii. for all other frame elements.



11. Assigning Loads to the Frame Elements

a. HS20 Wheel Axel Loads

- i. HS20 Axle Loads will be placed at distances of 36 in., 108 in., 180 in., and 252 in. from the outside of the curved edge.
- ii. One line of the 16 kip axels will be placed at the 0.4L point of the bridge or transverse grid 9 with the second line 14 feet away at transverse grid number 7. One line of 4 kip axels will be placed 14 feet away from the first line of axels at grid line 11.
- iii. In SAP2000 the loads have to be placed at a relative distance so this value needs to be calculated.

$$1. HS20_{Axel 1 Loc (B-A)} = \frac{L_1 - 36}{L_1} = \frac{39 - 36}{39} = 0.0792$$

$$2. HS20_{Axel 2 Loc (C-B)} = \frac{L_1 + L_2 - 108}{L_2} = \frac{39 + 96 - 108}{96} = 0.2813$$

$$3. HS20_{Axel 3 Loc (D-C)} = \frac{L_1 + L_2 + L_3 - 180}{L_3} = \frac{39 + 96 + 90 - 180}{90} = 0.5$$

$$4. HS20_{Axel 4 Loc (E-D)} = \frac{L_1 + L_2 + L_3 + L_4 - 252}{L_4} = \frac{39 + 96 + 90 + 96 - 252}{90} = 0.7188$$

b. Lane Loads

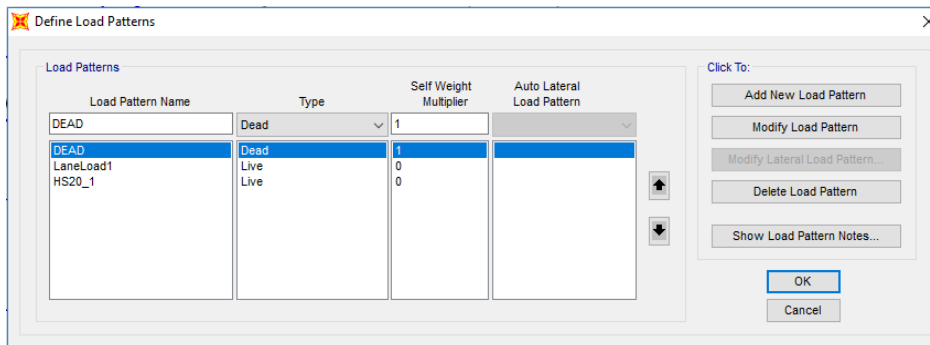
- i. Lane Loads are line loads of 0.640 kip/ft (0.05333 kip/in.) centered at a distance of 96 in. and 240 in. from outside of the curved edge.
- ii. These lane loads will be placed on the longitudinal frame elements. They will be assigned to elements along the B, C, D, and E longitudinal elements according to the appropriate tributary distance.

1. $LaneLoad_B = \left(\frac{L_1 + L_2 - 96}{L_2} \right) * laneload = \left(\frac{39 + 96 - 96}{96} \right) * 0.05333 = 0.021667 \frac{kip}{in}$.
2. $LaneLoad_C = laneload - laneload_B = 0.05333 - 0.021667 = 0.031667 \frac{kip}{in}$.
3. $LaneLoad_D = \left(\frac{L_1 + L_2 + L_3 + L_4 - 240}{L_4} \right) * laneload = \left(\frac{39 + 96 + 90 + 96 - 240}{96} \right) * 0.05333 = 0.045 \frac{kip}{in}$.
4. $LaneLoad_E = laneload - laneload_D = 0.05333 - 0.045 = 0.00833 \frac{kip}{in}$.

c. In SAP2000 the load patterns must be first be defined.

i. Select the Define tab->Load Patterns.

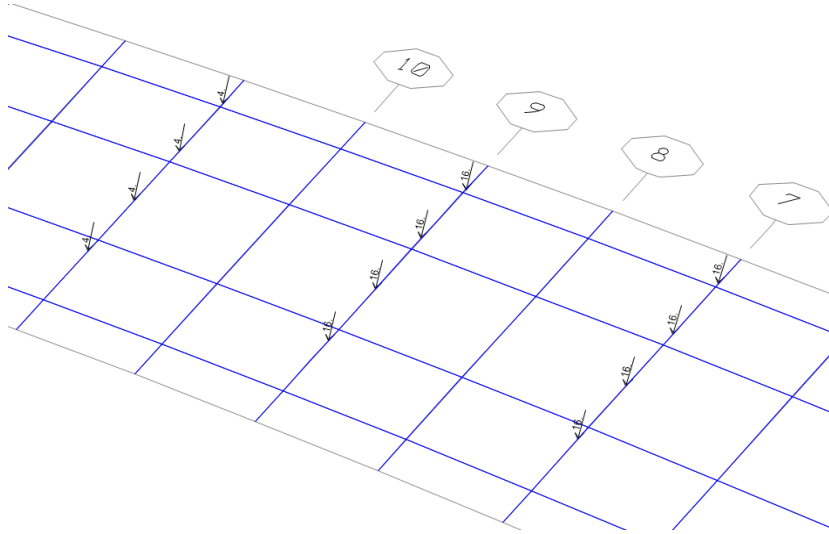
1. Under the Load Pattern Name enter HS20_1 and change the type in the drop down menu to Live. The self-weight multiplier should be set to 0. Then click Add New Load Pattern.
2. Under the Load Pattern Name enter LaneLoad1 and change the type in the drop down menu to Live. The self-weight multiplier should be set to 0. Then click Add New Load Pattern.
3. Then click OK.



ii. Assigning the HS20 wheel loads in SAP2000.

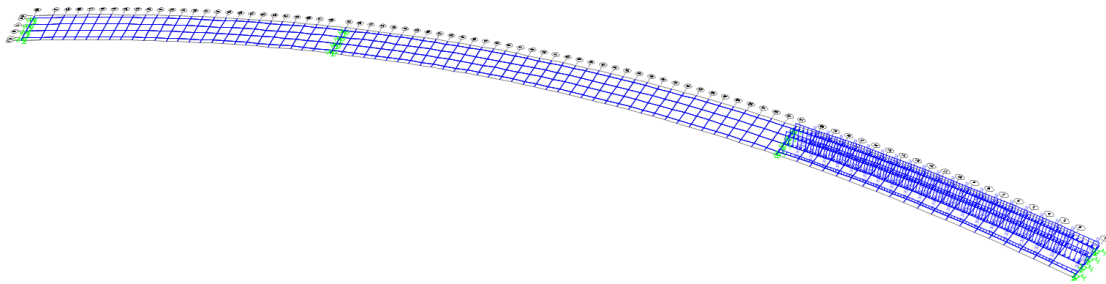
1. Select the exterior transverse element of grid line 9 and 7.
2. Click Assign->Frame Loads->Point
3. From the Load Pattern drop down menu select HS20 and verify that the Coordinate System is set to Global, the Load Direction is Gravity, and the Load Type is Force.
4. In column 1 enter a Relative Distance of 0 (HS20 Axel 1 Loc. B-A) and Load of 16 kips.
5. Click OK.

6. Repeat for grid line 11 to assign the 4 kip load.
7. Repeat Steps 1-6 for HS20 Axle 2,3,4 Loc. C-B, D-C, and E-D.



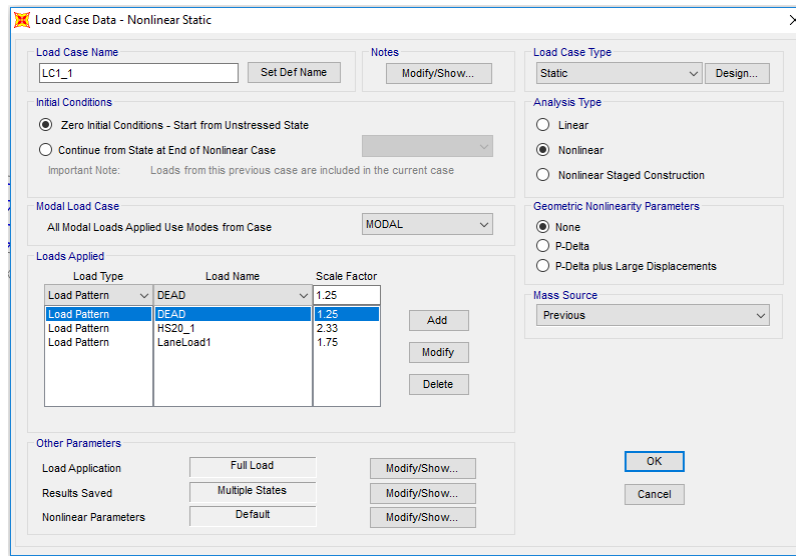
iii. Assigning the Lane Load in SAP2000.

1. Select all exterior longitudinal frame elements along grid line B.
2. Click Assign->Frame Loads->Distributed
3. From the Load Pattern drop down menu select Lane Load and verify that the Coordinate System is set to Global, the Load Direction is Gravity, and the Load Type is Force.
4. In the Uniform Load box enter 0.021667 (Lane Load B).
5. Click OK.
6. Repeat Steps 1-5 for all of the longitudinal elements along gridlines C, D, and E.



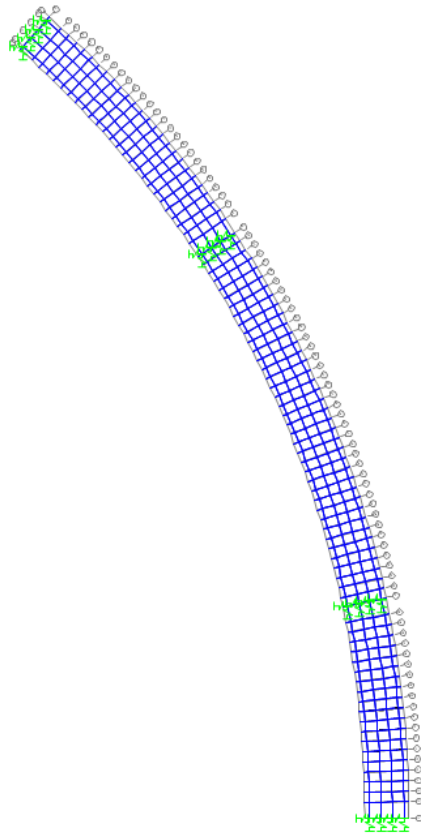
12. Defining Load Cases

- a. The Load Case being used to determine redundancy is $1.25DL + 1.75(LL + IM)$. Where DL=Dead Load, LL= Live Load, and IM= Impact Load. When substituting in the HS20 truck load and the Lane Load the preceding equation reduces to $1.25DL + 1.75LaneLoad + 2.33HS20$
- b. Generating Load Cases in SAP2000.
 - i. Click Define->Load Cases->Add New Load Case
 - ii. In the Load Case Name Panel name the load case "LC1_1"
 - iii. In the Analysis Type select "Non-Linear"
 - iv. For the LC1_1 Load Case in the Stiffness to use panel select "Zero Initial Conditions"
 - v. In the Loads Applied panel leave the Load Type "Load Pattern" in the drop down Load Name menu select DEAD and change the Scale Factor to 1.25. Click Add. Change the Load Name menu select HS20 and change the Scale Factor to 2.33. Click ADD. Change the Load Name menu select Lane Load and change the Scale Factor to 1.75. Click ADD.
 - vi. In the Other Parameters panel in the Results Saved section click Modify/Show.
 - vii. In the Results Saved for Nonlinear Static Load Cases window change the Results Saved to Multiple States and in the For Each Stage panel change the Minimum Number of Saved Steps and the Maximum Number of Saved Steps to 20. Click OK.
 - viii. Then Click the OK on the Load Case Data Window.
 - ix. Repeat Steps i.-viii. to create an LC2_1, LC3_1, and LC4_1. However, in the Initial Conditions Window select Continue from State at End of Nonlinear Case and from the drop down menu select the preceding load case. (For LC2_1 the Nonlinear Case LC1_1 would be selected).
 - x. Repeat Step ix. to create LC(1-4)_2 for Span 2 and LC(1-4)_3 for Span 3.

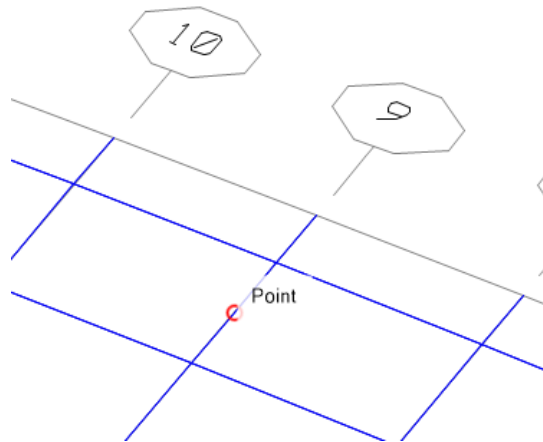


13. Defining End Supports

- a. The elastomeric bearing pad for each girder have lateral stiffness of 12 kip/in. and a vertical stiffness of 6100 kip/in. Since the tub girders are divided in half, the lateral stiffness will be 6 kip/in. and the vertical stiffness will be 3050 kip/in.
- b. Assigning spring supports in SAP2000.
 - i. Select the 16 nodes, 8 at the very end of the longitudinal members, 8 at the location of the piers.
 - ii. Click Assign->Joint->Springs
 - iii. In the Assign Joint Springs window in the Simple Springs Stiffness panel enter 6 for Translation 1&2 and 3050 for Translation 3.
 - iv. Click OK.

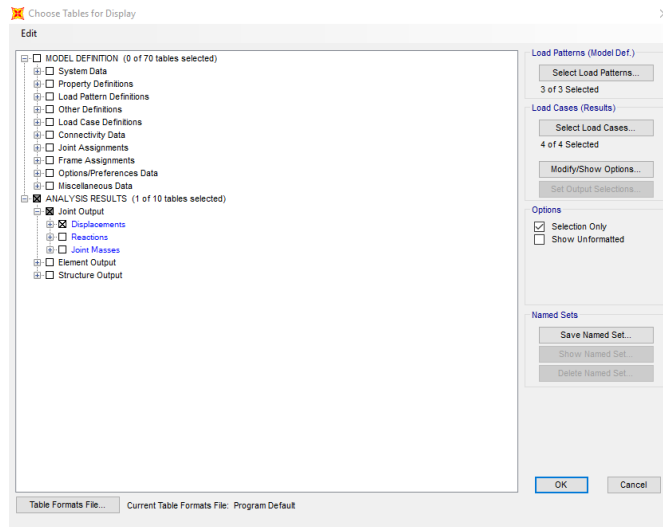


14. Defining Centerline Data Acquisition Points at Mid-Span of Girder
 - a. Select the transverse frame elements between B&C as well as D&E at 0.4L (Gridline 9).
 - b. Click Edit->Edit Lines->Divide Frames
 - c. In the Divide into Specified Number of Frames window enter 2 for Number of Frames.
 - d. Click OK.

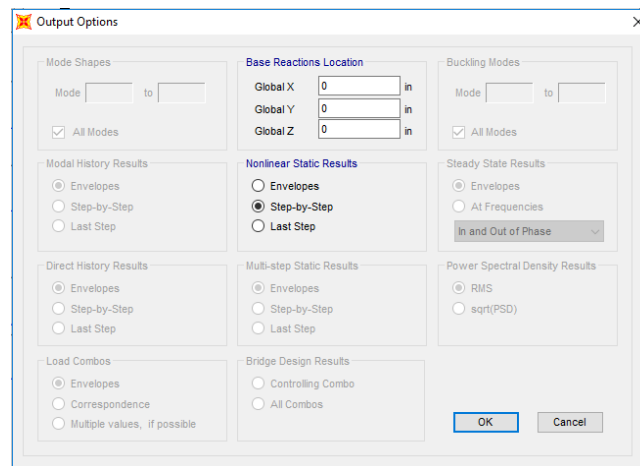


15. Analyzing the Non-Fracture Structure for Dead Load Only
 - a. In SAP2000 click Analyze->Run Analysis
 - b. In the Set Load Cases to Run window click the Run/Do Not Run All button until every Action is Do Not Run.
 - c. Select DEAD then click Run/Do Not Run Case until the Action is Run.
 - d. Then click Run Now. Let SAP2000 Run the Load Cases until the screen says the Analysis is Complete.
 - e. Once the analysis is complete, select the spring reactions.
 - f. Click Display->Show Tables
 - g. In the Choose Table for Display window click the + symbol beside Joint output and select the square box beside Reactions.
 - h. In the Output Options window in the Nonlinear Static Results panel select Last Step.
 - i. Select and copy the information from the F3 column.
 - j. The sum of the F3 values is the dead load.
 - k. Then click Done.
 - l. Unlock the structure.
16. Analyzing the Non-Fractured Structure
 - a. In SAP2000 click Analyze->Run Analysis
 - b. In the Set Load Cases to Run window click the Run/Do Not Run All button until every Action is Do Not Run.
 - c. Select LC1_1, LC2_1, LC3_1, and LC4_1 then click Run/Do Not Run Case until the Action for all 4 is Run.
 - d. Then Click Run Now.
 - e. Let SAP2000 Run the Load Cases until the screen says the Analysis is Complete.

- f. Once the analysis is complete, select the data collection point on the transverse member on the outside girder (C-B).
- g. Click Display->Show Tables
- h. In the Choose Table for Display window click the + symbol beside Joint output and select the square box beside Displacements



- i. Click the Modify/Show Options button.
- j. In the Output Options window in the Nonlinear Static Results panel select Step-by-Step.



- k. Click OK.
- l. Select and copy the information from the Output Case, StepNum Unitless, and the U3 in. column and paste them into an Excel worksheet. These columns represent Load Case, Step Number, and Deflection for the Outside Girder respectively.

Joint Displacements

File View Edit Format-Filter-Sort Select Options

Units: As Noted Joint Displacements

Filter:

Joint Text	OutputCase	CaseType Text	StepType Text	StepNum Unitless	U1 in	U2 in	U3 in	R1 Radians	R2 Radians	R3 Radians
103	LC1	NonStatic	Step	0	0	0	0	0	0	0
103	LC1	NonStatic	Step	1	0.002545	7.7E-05	-0.087926	-2.681E-06	0.000169	5.324E-08
103	LC1	NonStatic	Step	2	0.00509	0.000154	-0.175851	-5.363E-06	0.000338	1.065E-07

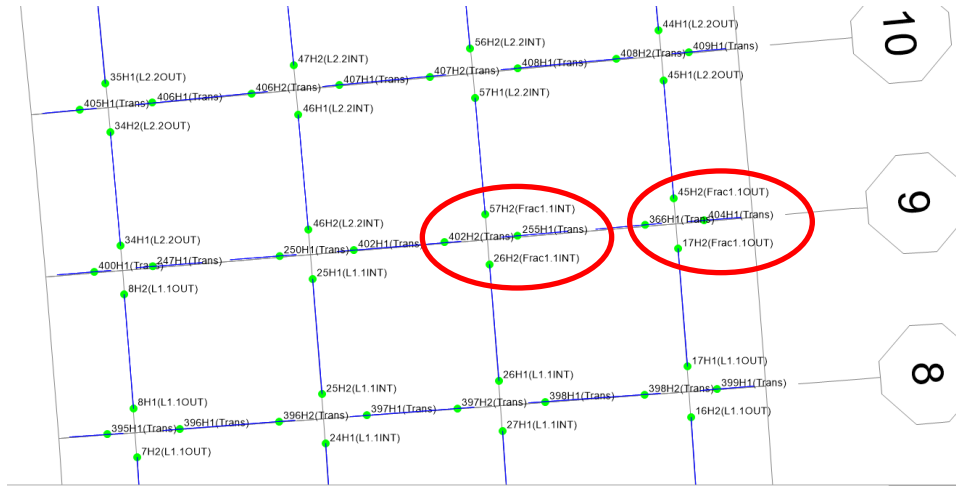
- m. Then click Done.
- n. Select the data collection point on the transverse member on the inside girder (E-D) and repeat Steps g-l. However, on Step 1 there is no need to copy Output Case, Step Num Unitless again.
- o. Select the joint on the transverse member on the outside girder at transverse element 9 (at longitudinal element B) and repeat Steps g-l. This information goes into the Delta 4 column. However, on Step 1 there is no need to copy Output Case, Step Num Unitless again.
- p. Select the joint on the transverse member on the outside girder at transverse element 9 (at longitudinal element C) and repeat Steps g-l. This information goes into the Delta 3 column. However, on Step 1 there is no need to copy Output Case, Step Num Unitless again.
- q. Select the joint on the transverse member on the inside girder at transverse element 9 (at longitudinal element D) and repeat Steps g-l. This information goes into the Delta 2 column. However, on Step 1 there is no need to copy Output Case, Step Num Unitless again.
- r. Select the joint on the transverse member on the outside girder at transverse element 9 (at longitudinal element E) and repeat Steps g-l. This information goes into the Delta 1 column. However, on Step 1 there is no need to copy Output Case, Step Num Unitless again.

	A	B	C	D	E	F	G	H	I	J	K	L	M	V	X	Y	Z	AA	AB	AC	AD
1	Intact			OG-CL		IG-CL		Point 4	Point 3	Point 2	Point 1			Applied Load (kip)			OG	IG			
2	Load Case	Load Step	0	Delta (in)	Chord (rad)	Delta (in)	Chord (rad)	Delta (in)	Delta (in)	Delta (in)	Delta (in)	α 23 (rad)	α 32 (rad)	0	Ω (cal)	Delta (in)	Chord (deg)	Delta (in)	Chord (deg)	α 23 (deg)	α 32 (deg)
3	LC1		0	0	0.00000	0	0.00000	0	0	0	0	0	0	0	0.00	0.00	0.00000	0.00	0.00000	0	0
4	LC1	1	0.05	-0.1037	0.00015	-0.087926	0.00013	-0.10541	-0.10129	-0.0942	-0.07905	7.89E-05	4.94E-05	66	0.05	0.10	0.00861	0.09	0.00730	0.004522	0.002831
5	LC1	2	0.1	-0.2074	0.00030	-0.175851	0.00025	-0.21081	-0.20259	-0.18839	-0.15809	0.000158	9.88E-05	132	0.10	0.21	0.01722	0.18	0.01460	0.009043	0.005662

20. Once all of the data is collected unlock the model by selecting the Lock tool on the left hand side of SAP2000 screen.

17. Analyzing the Fractured Structure

- a. At Mid-Span along grid line 9, replace the hinges of the outside longitudinal element (gridline B) with FracOUT hinges according to Step 10.
- b. At Mid-Span, along gridline 9, replace the hinges of the first interior longitudinal element (gridline C) with FracInt hinges according to Step 10.



c. Repeat Step 15 for the Fractured Case and collect the data accordingly.
 18. Post Processing of the Data

a. In the Excel Sheet the following values need to be calculated for each step.

i. Omega (Ω)

$$1. \Omega_i = \Omega_{i-1} + \left(\frac{1}{\# \text{ of Steps in Load case}} \right)$$

ii. Longitudinal Chord Rotation of Interior and Exterior Girder

$$1. \text{Chord Rot.}_{\text{single span}} = -1 * \left(\frac{\delta_{CL}}{0.5 * L} \right) \text{ (rad)}$$

iii. Transverse Deck Roataion

$$1. \alpha_{2-3} = \left(\frac{\delta_3 - \delta_2}{s} \right) - \left(\frac{\delta_2 - \delta_1}{w} \right) \text{ (rad)}$$

$$2. \alpha_{2-3} = \left(\frac{\delta_3 - \delta_2}{s} \right) - \left(\frac{\delta_2 - \delta_1}{w} \right) \text{ (rad)}$$

3. Where s=spacing between the interior top flanges of the inside and outside girders and w=spacing between the top flanges of the same girder.

iv. Applied Load

1. Calculate unit applied load or applied load at 1 Ω .

$$2. \text{Unit Applied Load}_{\text{single span}} = 1.25 * \text{Total Reactions from Dead Load Case} + 2 * (2.33 * \text{HS20 truck} + 1.75 * \text{Lane Load})$$

$$3. \text{Applied Load} = \text{Unit Applied Load} * \Omega$$

b. Repeat Step A for the Fractured Case.

c. Calculate the initial stiffness for intact bridge and instantaneous stiffness for fractured bridge.

- i. For the Non-Fractured condition (Intact Bridge) find the absolute displacement for the Outside Girder at an Ω value of 0.4.
 1. $Initial\ Stiffness = \frac{0.4}{Absolute\ Displacement\ OG\ (at\ \Omega=0.4)}$
- ii. For the Fractured case add an additional column labeled stiffness
 1. $Instantaneous\ Stiffness_{OG-Frac.\ i} = \frac{\Omega_i - \Omega_{i-1}}{\delta_i - \delta_{i-1}}$
- d. Failure of the structure occurs at the Ω of the Fractured Bridge at the first of the following criteria.
 - i. The instantaneous stiffness for the fractured outside girder is less than 5% of the initial stiffness of the intact outside girder.
 - ii. The chord angle of the outside girder for a simple spans or interior spans is greater than 2° . The chord angle for exterior spans of multi-span bridges is greater than 3° .
 - iii. The transverse deck rotation is greater than 5° .
- e. On a chart plot the Non-Fractured Outside and Inside Girder as well as the Fractured Outside and Inside Girder with displacement on the primary x axis and the Total Force on the primary y axis and Ω on the secondary y-axis

19. Repeat Steps 11-18 for Span 2 and 3. (Span 1 is pictured below)

